Study of an intermittent regenerative cycle for solar cooling

Adam B. Harvey

A dissertation submitted for the degree of Doctor of Philosophy

Department of Engineering
University of Warwick, Coventry, U.K.

January 1990

Text cut off in original

PAGE NUMBERING AS ORIGINAL

Table of Contents

Acknowledgements

The research reported here has been undertaken under the supervision of Dr. R. E. Critoph, whose guidance and encouragement has been invaluable. The author is indebted also Dr. S. P. Subramaniam, Acting Chief of the Fisheries Research Office, Zambia, for the advice and support given during implementation studies, to Sidi Sokoni for the companionship and insights he provided in different parts of Zambia, and also to Colin Major, Geoffrey Robinson, and Paul Hedley in the Engineering Workshops at Warwick University, Department of Engineering, for their skill and interest in the construction of experimental units.

Summary

The study presented here is focused on the use of aqua-ammonia solution in a novel solar-powered refrigeration cycle intended to be suitable for use in the rural areas of developing countries. The cycle is referred to as a "intermittent regenerative" (IR) cycle, the term regenerative meaning in this context to the use of heat recovery or recuperation.

The first chapter describes the three better known cycles which may be considered for this application. The IR cycle is introduced as a hybrid development of these which offers the significant advantages of high efficiency while minimising complexity. Chapter 1 provides a methodology by which the novel aqua-ammonia system can be evaluated in comparison with existing systems. The second chapter surveys previous experimental work on solar driven aqua-ammonia cycles.

Chapter 3 consists of a detailed design study of the new IR cycle based on computer modelling techniques. The study serves as an analysis of the cycle and allows the performance of the cycle, together with design features and component sizes, to be simulated in a variety of metereological conditions. A number of original design proposals are evaluated through the modelling exercise. Chapter 4 summarises the results of a second separate modelling exercise which investigates the absorption phase of the cycle.

Chapters 5 and 6 describe experimental work. The results of laboratory tests are compared with the predictions of the computer model, and in the event serve to validate the theoretical characterisation made in chapter 3 of the performance of key components of the system. The energy efficiency of the system as measured by experiment is proved to correspond to theoretical prediction, so representing a significant advance on the performance of alternative systems.

Chapter 7 addresses itself to the wider question of the social and economic validity of a device with the performance and cost of the IR device. A case study is undertaken which explores the potential role of the device in the fish trading economy of Zambia. The study provides data valuable in assessing the usefulness of the technology in helping to stimulate the under-capitalised rural economy of a developing country and in improving local food resource utilisation.

Chapter 8 draws together the conclusions of the various chapters and provides an overall conclusion and comment on the value of the IR system. It is proved to have a high efficiency but not to have the robustness nor portability demanded for widespread application in remote locations. Nevertheless the likely life-time cost-effectiveness of the system is judged to be an improvement on existing alternatives and suggestions are made for further improvement.

Nomenclature

Abbreviations

IB	intermittent basic (non regenerative) cycle
CP	continuous cycle with externally powered pump
IR	intermittent regenerative cycle
DA	diffusion-absorption or "Platen-Munters" cycle (used by the Electrolux and Sibir companies)
FVR	fixed volume reservoir (variation of IR cycle)
VVR	variable volume reservoir (variation of IR cycle)

Roman symbols

$A_{component}$	area of component	m^2
COP	coefficient of performance	
Solar COP	coefficient of performance as ratio of cooling energy to energy absorbed by solar collector	
Internal/cycle COP	coeffiecient of performance as ratio of cooling energy to energy absorbed by boiler	
CR	ratio of rich solution mass flow to vapour mass flow at station 6	
CR′	ratio of rich solution mass flow to condensate yield rate	
CR_v	ratio of volume flows at stations 1 and 6	
$c_{p(component)}$	specific heat capacity of fluid contained in component	joules/kg K
$c_{p(st)}$	specific heat capacity of steel of container	joules/ kg K

E	internal energy	joules
EFF_{she}	effectiveness of the solution heat exchanger	
eff(she)	synonomous with EFF_{she}	
$h_{Liquid\ or\ vapour,\ x}$	specific enthalpy of fluid at numbered station (vapour: "v"; liquid:"l" or "L")	joules/kg
k	heat transfer characteristic	watts/$m^2K^{1.25}$
$\dot{G}$	instaneous rate of incident solar irradiation	watts/m^2
Gr	Grashof number	
Gz	Graetz number	
$L_{component}$	length of component	m
$M_{Liquid\ or\ vapour,\ default\ Liquid}$	mass (vapour: "v"; liquid:"l" or "L")	kg
M_{rec}	mass of refrigerent in receiver	kg
$M_{st(component)}$	mass of steel in component	kg
$\dot{m}_{Liquid\ or\ vapour,\ x}$	instantaneous rate of mass flow past numbered station (vapour: "v"; liquid:"l" or "L")	kg/s
$\dot{m}_{sep}$	rate of decrease of mass of liquid in separator	kg/s
Nu	Nusselt number	
Δp	pressure difference causing solution circulation	bar absolute
P_{phase}	uniform system pressure	bar absolute
Pr	Prandtl number	
$q_{component}$	energy flow across component boundry integrated with respect to time	joules
$\dot{q}_{component}$	heat flow rate across component boundry per unit mass refrigerent generated	watts/kg
Q	where context indicates, volume flow	m^3/s
$Q_{component}$	energy flow crossing component boundry integrated with respect to time	joules
$\dot{Q}_{component}$	heat flow crossing component boundry	watts
$\dot{Q}_b$	heat flow rate into boiler	watts
Re	Reynolds number	
T_x	temperature at numbered station	degC

T_{ab}	temperature in absorber at end of absorption phase	degC
T_{gen}	temperature in boiler at the end of desorption phase (IB system) or during desorption (IR, CP, DA systems)	degC
U	internal energy	joules
$U_{component}$	heat transfer value	watts/m^2K
VCR	ratio of condensate yield to vapour produced at station 6	
VCR′	ratio of condensate yield rate to vapour mass flow at station 6	
WR	ratio of minimum initial solution charge to condensate yielded	
$x_{Liquid\ or\ vapour}$	concentration: mass fraction of ammonia in binary solution (vapour: "v"; liquid:"l" or "L")	kg/kg
yield	refrigerent condensed during generation phase	kg
z_{xy}	piezometric height between stations x and y	m

Greek symbols

Δt_I	duration of phase I	s
Δt_{day}	period between surise and sunset	s
$\eta_{component}$	efficiency of component	
η_i	internal efficiency, or COP in artificial case where boiler heat input steady	
η_{solar}	overall system efficiency with collectors included or, or solar COP in artificial case where solar heat input constant	
ν	specific volume of fluid	m^3/kg
ρ_{xy}	bulk density of fluid assumed uniform between numbered stations	kg/m^3

Subscripts

she/SHE	solution heat exchanger
hpc/HPC	heat pipe condenser
rec	receiver
ab	absorption
st	steel
L or l	liquid
v	vapour

Chapter 1: Review of techniques

1.1. Introduction

The present chapter describes three well known aqua-ammonia refrigerator cycles, referred to respectively as the basic intermittent cycle (IB), the continuous pumped (CP), and the diffusion-absorption (DA) cycles. The chapter first outlines the primary criteria whereby the matching of various sorption systems to the specified end-use conditions can be assessed. Following this the IB and CP cycles are described in some detail, firstly to provide an introduction to the analysis of the intermittent regenerative (IR) cycle, and secondly in order to to develop a common methodology whereby the matching of solar power to various sorption systems can be evaluated. Quantitative solutions for relative performance are obtained for a common set of operating conditions. The IR cycle is introduced.

1.1.1. Specification

The desirability of novel techniques for the preservation of agricultural, fisheries, and dairy products in remote tropical locations of the world has been pointed out by several authors (Brinkworth, 1972; National Academy of Sciences, 1978; International Institution of Refrigeration, 1976). The absence in such areas of grid electricity and the inadequacy of transport and other infrastructural services has meant that their capacity for export food production is severely limited, both through non-use of potentially fertile land area and through the occurence of high post-harvest yield losses. Both these conditions may be alleviated by the introduction of preservation techniques which are capable of being mounted and supported in remote environments.

The present study is limited to refrigerating techniques which are capable of ice-making, since packing of produce with ice is a proven method of providing simple refrigerated transport and storage in remote regions. Traditional passive ice-making techniques, as practised

historically in Asia Minor, are not discussed. It is taken for granted that thermal energy is more immediately available to power active devices than mechanical energy or electricity, and that the conversion of thermal energy to mechanical will be more costly and inconvenient than direct use of thermal power. Accordingly attention has focused on sorption cycle refrigeration. A number of studies (Haseler, 1978, Mansoori and Patel, 1979) have investigated novel liquid absorption pairs for sub-zero cooling, and have found that the well-known aqua-ammonia pair is still to be recommended in terms of cycle efficiency. It has been chosen as the working pair for the present research because of these findings and because its properties are well known, so that it has been possible to orientate the present study around system design and system matching to remote applications with less uncertainty as to solution properties.

The primary characteristics of ice-making devices suitable for remote use can be listed as follows. They are expressed as qualitative indicators of suitability to remote application rather than as economic costs since their weighting in terms of economic cost is dependent on widely varying conditions throughout the world. The criteria form the basis of a comparative study of aqua-ammonia systems which is the subject of this chapter, and also form the rationale for the study of a novel aqua-ammonia system which follows in succeeding chapters. The systems examined in chapter 1 are the basic intermittent cycle ("IB"), the conventional continuous pumped system ("CP"), and the thermosyphoned diffusion -absorption system ("DA"). The improved novel system proposed as a result of the examination is the intermittent regenerative system ("IR"). These are described by the schematic diagrams presented in figures 1.2.1, 1.3.1, 1.4.1, and 3.1.1 respectively. The proposed indicators are

a) **Supportability.** The matching of design to the support and maintenance environment is an essential requirement. Supportability can be interpreted as a labour and infrastructure-related criterion of the suitability a device for remote application, expressing whether or not necessary skills are available to a degree which will keep a device functioning, and whether necessary supply lines exist. A further aspect of support is the degree of acceptance that the device attracts from its immediate users, and the skill and effort, or consumed time, required in daily attendance. The present study takes the approach that the device should be

in the greater part manufacturable within a less developed country, and require a minimum of imported parts. It should be designed to operate without any technical maintenance procedures or expectation of parts replacement.

b) **Transportability and safety.** The use of ice-makers in remote locations may imply a requirement that weight and size is minimised. Certainly this critereon has a bearing in cases where a crop is not geographically fixed, as is the case where fishing operations move seasonally. There may be a capital utilisation imperative dictating that the machinery move from one location to another following seasonal variations in agricultural harvests, possibly moving from crop preservation to a non-agricultural application. Equally it is possible that in some applications transportability is not relevant and a large and heavy device is fully acceptable, possibly having the advantage of not being easily stolen.

Where a device is weighty because it contains a large solution charge of a toxic fluid such as aqua-ammonia, then it will present also a safety hazard, and be subject to safety restrictions. This also poses problems with respect to the transport to site and the cost of a fresh charge should maintenance procedures or repairs require one. Associated with large ammonia charges are the safety risks associated with operation in a non-industrial environment.

c) **Power cost.** The primary contender as a fuel source for remote location coolers will often be conventional fossil fuel. This is because the use of ice makers for commercial agricultural purposes will often be associated with internal combustion powered vehicles providing a fuel transport facility and presupposing a dependency on this fuel. Despite this there are a number of arguments for the encouragement of alternative fuels. The income generated for the local community by agricultural produce will be higher if the fuel cost of preservation is set by the producer rather than the purchaser. The design of devices suitable for non-fossil fuels may therefore promote rural incomes by allowing cold storage to be a local economic function. There will certainly be benefits to a national economy if economic indigenous fuels are found, and since thermal refrigerators are powered by external combustion their use with locally available fuels such as plant alcohols and agrowastes is feasible. (Saunier,

1986). It is likely that stoves designed for low calorific fuels such as these will have a lower maintenance requirement than those designed for high calorific fuels, so better satisfying the supportability critereon described above. They are likely to be more flexible to use with a variety of fuels depending on availability.

The direct use of solar energy as thermal power has gathered considerable interest (Heywood, 1953, Brinkworth, 1972). It is often available just when cooling is needed, although it has the unfortunate disadvantage of being costly to collect because of its low concentration of energy with respect to area irradiated. Collection is necessarily by passive devices of relatively large area and therefore high cost if they are to be durable and comprising materials capable of limiting heat losses. In previous studies of solar driven refrigerating devices (Exell, 1984, Shiran, 1982) the cost penalty of the collector component has been found to be more than half the overall cost. Accordingly the overall cost of the refrigerator is significantly reduced if the cycle efficiency is high. The cycle efficiency is often referred to as the coefficient of performance (COP); it is the ratio of energy used to cooling energy produced. The present study focuses exclusively on the use of solar energy, and emphasises the importance of COP as an indicator of system cost, since high COP leads to savings in collector size and therefore in cost.

Clearly the relatively high cost of solar collection implies that careful study of the availiability and reliability of supply of alternative indigenuous fuels is necessary before adoption of the solar option.

A second disadvantage of the solar option is the variability of solar energy. The required insolation varies in three ways: firstly, with the time of day, secondly, with season, and thirdly, with cloud cover, the latter being itself often a function of both location and season. The bulk energy collected daily will vary, and also the rate at which it arrives varies. An appraisal of the usefulness of the solar power source must take these variations into account. A refrigerator design well matched to solar power will respond flexibly to the varying insolation rate. The present study develops a method for estimating yearly performance in varying representative locations in order to allow a full appraisal. The occurence

of long periods of low-level irradiation may require that hold-over cold storage is provided; the storage of ice itself forms a convenient medium for this.

Other meteorological conditions will effect the performance of a solar cooler, especially with respect to the sink temperatures available for absorption and condenser cooling. A well matched solar cooler design will respond flexibly to the expected variations in ambient temperature, not tending to fall off in performance unduly at off design conditions.

Solar collectors may have disadvantages with respect to the fragility of glass and evacuated enclosures, and with the need for cleaning of absorbing surfaces, collecting surfaces, and reflectors. They may be awkward to transport, and inconveniently large, possibly giving rise to a land usage cost.

Despite these problems the matching of solar power to cooling has attracted attention because it has two advantageous features. The first is that solar energy is very often abundantly available where and when it is needed. The second relates to the requirement for a low-maintenance sorption cycle. The simplest form of sorption cycle is intermittent, the only complex control action needed being the requirement that the power source cycles from the off to on state. Since simplicity satisfies the supportability critereon, the intermittent cycle is immediately of interest, and since the sun automatically cycles the remaining complexity is removed. It may additionally be an advantage in some conditions of application, for instance vaccine cooling, that the collection of the energy source is necessarily passive, so that a cooler can be imagined to function independently of any operator input. Where ice making is considered as a commercial process, some operator input is implicit, so a limited non-critical operator input is acceptable in the present context.

The proposed IR cycle is intermittent, taking advantage of the diurnal cycling of the solar source. An evaluation of this feature is made in the present chapter by comparative consideration of two continuous cycles.

d) **Further component cost.** Beyond the size and cost of the power source, the sizes of other heat exchangers, and the number and costs of intricate components require attention. The thermodynamic process employed will govern the size of components such as heat

exchangers; although two processes may provide similar COPs the transfer of more heat either internally or in relation to the surroundings will entail more expensive components. In the case of solar powered absorption cycles the first example of this is the degree to which high generation temperatures force up the size of the collector, because of the inducement of increased collector loss, and will also require larger generator to collector interface areas. (The "generator" is the term which collectively describes all the components which act to generate - or desorb, or boil off - refrigerant from an absorbent-refrigerant solution. The generator is that part of the device which rises in temperature, and is always therefore insulated to ensure heat is directed toward the boiling of solution). The component cost divides into two aspects, firstly the cost of manufacture and retail, comprising the purchase cost, and secondly the cost of replacement parts, in so far as this can be separated from the question of feasibility of maintenance, covered by the supportability critereon mentioned above.

The investigation that follows of each of three aqua-ammonia systems can be read in the light of these four indicators of suitability for remote use. Table 1.5.1 concludes the chapter by grouping the investigative findings under the headings of the four indicators. The weighting attached to each indicator is left as a mute subject, since it is specific to any particular intended area of implementation.

The IB, or non-regenerative system, is examined in some detail because it provides a useful introduction to the later analysis of the IR system. Some detailed attention is paid also to the continuous pumped system, for the same reason, and because it provides a reference, since it is a well known system, whereby the potential performance of the IR system can be assessed.

1.1.2. Ammonia and aqua-ammonia equilibrium property data

In accordance with the Gibbs phase rule the state properties of the aqua-ammonia solution at equilibrium conditions are each functions of any two other state properties. The computer code described here makes use of the following bivariate functions (the subscript "L" referring to the liquid state, and "v" to the vapour state):

$$P=function(x_L,T)$$

$$x_v=function(x_L,T)$$

$$h_L=function(x_L,T)$$

$$h_v=function(x_L,T)$$

$$T=function(x_L,P)$$

$$\rho_L=function(x_L,T)$$

Experimental data was presented by Scratchard et al (1947) in a series of tables. In order to allow these data to be accessible in a computer code some manipulation was necessary. Firstly, a computer code was devised which converted the $P=f(x_L,T)$ table into $x_L=f(P,T)$ form by performing quadratic interpolations on the original data. A further alogarithm then allowed the simulation programme to access any of the tables by locating nine relevant points in the table required and applying quadratic equations across them. The function determining temperature operates by a similar application of linear interpolation across four relevant points. The resulting functions gave values matching the original data with sufficient accuracy, some problems being encountered with values obtained from data near the edges of the tables. These problems led to the adoption of other functions where necessary.

Macriss (1964) at the Institute of Gas Technology published experimental data and these were converted into 5th order bivariate polynomials by Crees (1986). Crees' equations are used by the programme in one case where the interpolative method is inadequate, in the case where $x_L=f(P,T)$ when $x_L>0.9$.

Problems were experienced with the interpolative method for vapour concentration (as function of x_L and T) and the equation proposed by Crees for this also found to be inadequate. Consequently use was made of the equation developed by Jain and Gable (1971); this was also based on tabulated data collected by Macriss (1964).

1.2. The intermittent basic system (IB)

A simple means of implementing the NH_3/H_2O absorption cycle is illustrated on figure 1.2.1.

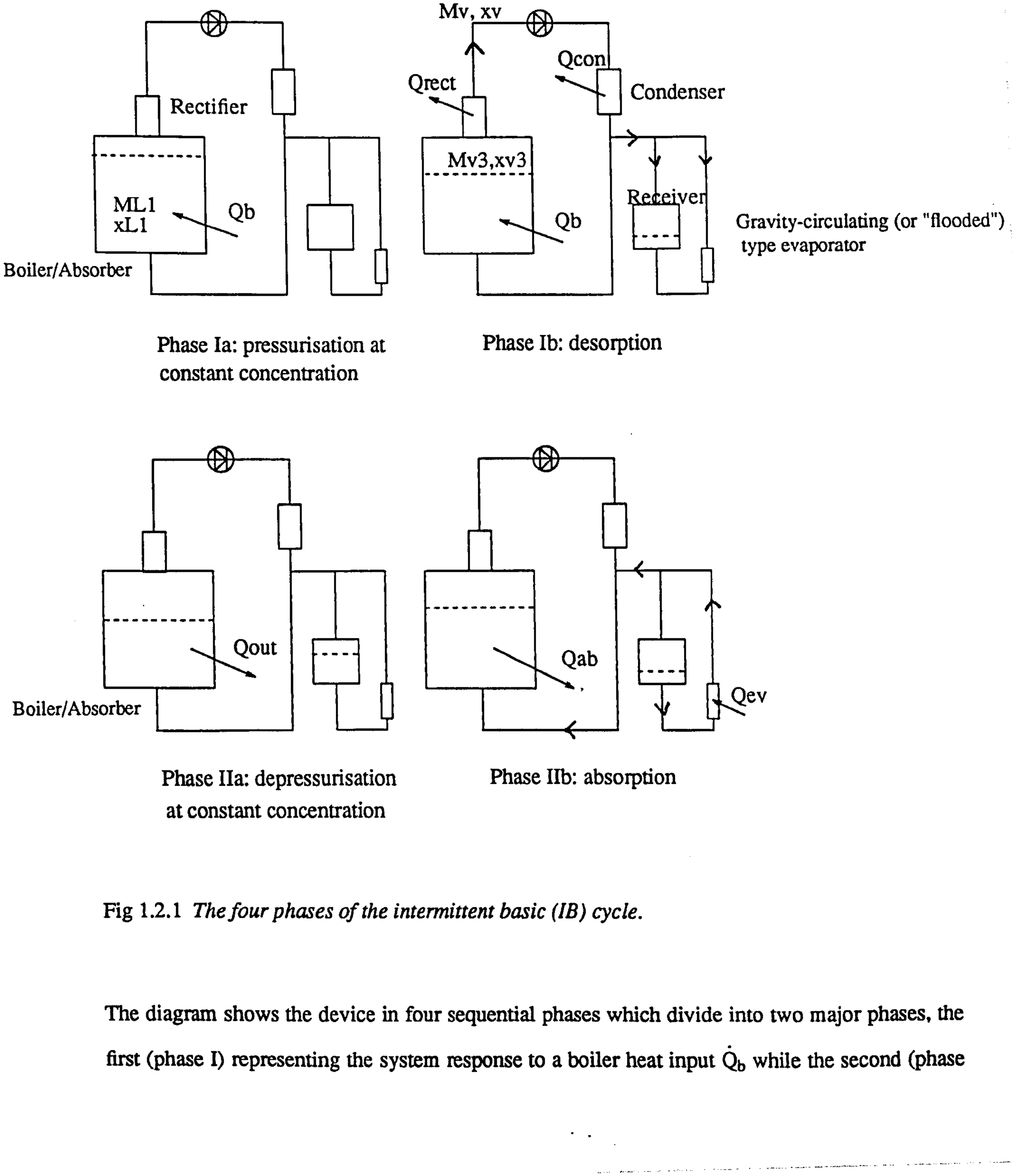

Fig 1.2.1 *The four phases of the intermittent basic (IB) cycle.*

The diagram shows the device in four sequential phases which divide into two major phases, the first (phase I) representing the system response to a boiler heat input $\dot{Q}_b$ while the second (phase

II) represents the system response with $\dot{Q}_b$ removed. The early part of phase I represents the sensible heating of solution and the pressurisation of the system. The later part represents the period during which vapour is desorbed from the solution and collected in the receiver vessel. This process, phase Ib, begins soon after the pressure reaches its saturation value for vapour cooled to sink temperature by contact with the walls of the condenser, which are initially in equilibrium with the sink medium. The sink is assumed here to be ambient air. A slight rise in pressure allows condensation to occur at an elevated temperature (T_{con}) causing heat to flow from the condenser ($\dot{Q}_{con}$). A similar process occurs in the reflux condenser or rectifier, such that vapour leaving the boiler at concentration x_{v3} is purified to the value x_v.

The check valve shown is adjusted to allow vapour to flow with a negligible pressure drop from the boiler to the condenser; when a reverse pressure difference exists, as in Phase IIb, it diverts a vapour flow from the evaporator through the pipework leading to the lower portion of the boiler. The reason for this is discussed in section 4.2.

A convenient illustration of the cycle can be given on a plot of temperature against concentration for NH_3/H_2O. A schematic representation of this plot is given as fig 1.2.2. Phase I is shown on part (a) of the diagram and phase II, which is described below, on part (b). The purpose of dividing the two graphs is to demonstrate that the cycle does not in practice necessarily close, although further discussion will assume that it does. Phase Ia, sensible heating of full strength solution, begins at point 1 and ends at point 11, where the isostere representing the initial solution concentration x_{L1} meets the isobar (P_i) representing a dew point temperature for refrigerant just exceeding the sink temperature. The process is indicated by a dashed line since it represents solution in a non-saturated state. The isostere is nominal: in practice the change in pressure will alter the concentration, although for the sake of clarity it can be considered isosteric.

Between points 11 and 2 the temperature at which condensation occurs rises, and sensible heating continues together with desorption, until the rate of desorption balances the rate of condensation heat removal. Further desorption and sensible heating then follows the isobar P_{gen} representing a stable condensing temperature, until point 3 is reached, and the desorption phase (Ib) is ended. This point either represents the limiting temperature of the heat source ($T_{gen(max)}$),

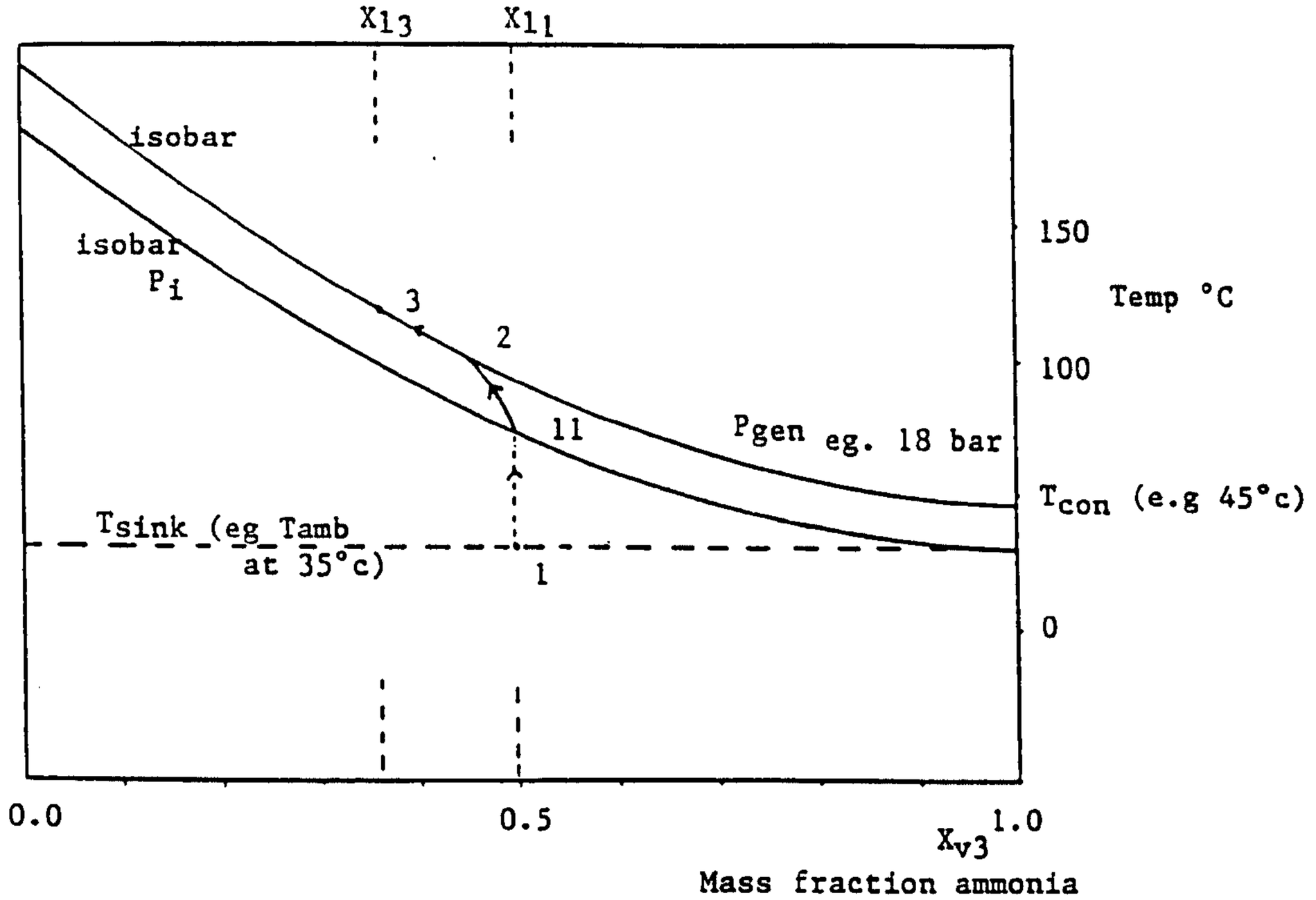

Fig. 1.2.2(a). Phase I of the intermittent basic (IB) cycle plotted schematically against solution concentration (ammonia : water mass fraction) and temperature.

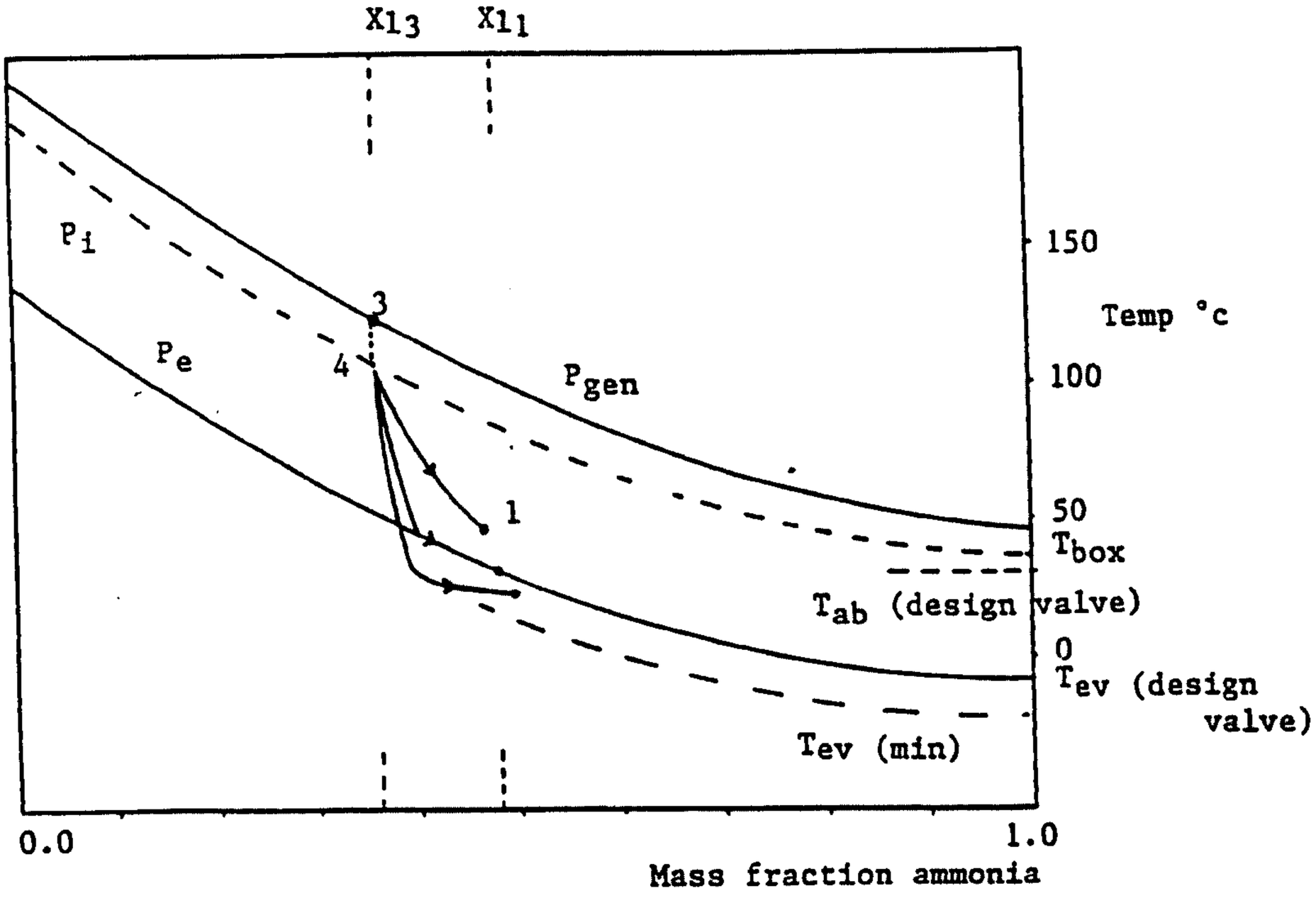

Fig. 1.2.2(b). Phase II of the IB cycle plotted as above against solution concentration and temperature.

since further desorption implies an increase in the solution equilibrium temperature at the prevailing system pressure, or it implies that the heat source $\dot{Q}_b$ is removed or reduced in magnitude so that its limiting temperature falls below the previously obtained boiling temperature.

The condenser is assumed to cool to air, although a cheaper form of condenser cooling may be the immersion of a condenser coil in a still water reservoir. This forms a sink of finite capacity the temperature of which will rise as heat of condensation is accumulated. In this case the pressure of the system in the process 2 to 3 rises together with rising condensation temperature. A water cooled condenser is subject to to the danger of a lost water supply with the attendent safety risk of excessive pressures developing in the system.

The following phase, IIa, consists of depressurisation of the system while the solution in the boiler rejects heat ($\dot{Q}_{out}$). The solution concentration (x_{L3}) remains nominally constant (in practice depressurisation is associated with some de-sorption) at the strength determined by the value of $T_{gen(max)}$ in the previous phase. The process is one of subcooling of the weakened solution and so is represented by a dashed line. The point at which the solution begins to re-absorb refrigerant vapour from the cold box depends on the loading conditions in the cold box. It may, for instance, have been freshly charged during phase I with water at ambient temperature due for freezing, in which case the temperature at which the cold box contents will tend to equilibriate will approximate to ambient temperature. Alternatively the cold box may contain residual ice and reach a lower temperature. It is assumed that the evaporator is arranged so that condensation of refrigerant in the cold box during phase I does not occur to a significant degree. In either case, at point 3, immediately that external heating of the solution stops, the temperature of the refrigerant approximates to a value considerably lower than T_{con} which is marked on the p-t-x plot as T_{box}. The refrigerant is therefore in a sub-cooled state, having a vapour pressure of an intermediate value P_i, as shown. Heat removal from the solution during phase IIa then allows the system pressure to approach P_i. The check valve shown in fig 1.2.1 remains open so equalising the pressures in the boiler and receiver. (Continued boiling of solution while self cooling in the process 3 to 4 will aid the depressurisation process and continue to weaken the solution so that the process is not strictly isostereic as shown). At the intersection of the solution isostere and the intermediate

isobar the check valve closes and the refrigerant vapour can begin to expand forcing solution against the hydrostatic head h, since the solution pressure continues to reduce below P_i. Evaporation of the refrigerant occurs so reducing T_{box} and the temperature of the refrigerant. When solution pressure reaches the value (P_i–h) the reabsorption process (phase IIb) begins as represented by the point 4. At this point the boiler vessel becomes an absorber vessel.

During reabsorption the temperature of the solution is raised by the heat of sorption, and the magnitude of $\dot{Q}_{out}$ must be sufficient to ensure that the system pressure continues to decrease so that useful evaporating temperatures can be obtained. $\dot{Q}_{out}$ is determined by the size of the absorber heat exchanger $(UA)_{ab}$ and the temperature difference between the solution and the sink, which is likely to be closely related to ambient temperature at night, when absorption takes place. The additional effects of wind cooling and radiative loss can be neglected in this context:

$$\dot{Q}_{out}=(UA)_{ab}(T_{ab}-T_{sink})$$

If $\dot{Q}_{out}$ is small, evaporation at high temperature and pressure implies a very low rate of cooling in the cold box, so that undesirably long durations will be required for the absorption phase in order to meet a specific cooling duty. The period available for absorption is predetermined by meteorological conditions in the case of a diurnal solar driven intermittent cycle, which has the important implication that low evaporation rates can lead to inadequate cooling. In contrast the achievement of full absorption within a period shorter than that between sunset and sunrise implies that the absorber heat exchanger is unnecessarily large and uneconomic. The optimum value of Q_{out} is that which results in full use being made of the finite absorption period available. The practical achievement of this optimum will depend on the extent to which environmental conditions such as ambient temperature vary, and the extent to which the system can be regulated to take account of such variations.

To illustrate the situation the p-t-x plot of fig 1.2.2 shows three alternative paths for absorption, the upper path corresponding to a low value of $\dot{Q}_{out}$ and the lower path to a high one. The central one shows a constant pressure process. If a single heat exchanger size is assumed then these paths may represent high and low night sink temperatures respectively. The upper path shows the danger of obtaining inadequate evaporator temperatures and final solution

concentration, while the lower path shows that low evaporator temparatures are obtainable and high final solution concentrations.

It is useful to see that the minimum evaporating temperature is effected by the maximum solution temperature produced by the heat source. It is seen that the greater the weakening of the solution the lower the T_{ev} that can be obtained if $\dot{Q}_{out}$ is large.

If a valve is included in the circuit to divide the receiver and absorber vessels greater control over the process can be exercised. Firstly, closure of the valve during phase IIa can be used to prolong the phase so ensuring that absorption starts at low pressure and minimum evaporating temperature. Secondly the valve can be used to regulate the process. The use of automatic self regulating valves in this way is referred to as "dry expansion evaporation". If no valve is used an evaporator arrangement as shown in Fig 1.2.1 can be used.This is referred to as a gravity circulating evaporator. The relative merits of these options are described in chapter 4, one disadvantage, for instance, of the use of a gravity circulating evaporator in an aqua-ammonia system being that it causes water to accumulate in the evaporator, so demanding that some means for periodic purging is provided.

The performance of the device can be estimated in terms of the efficiency with which it converts energy absorbed at the boiler to energy extracted usefully by the evaporator. This ratio is identical to the internal cycle COP of the refrigerator for a given rate of energy absorption in the boiler. In the case of a solar driven device this rate ($\dot{Q}_b$) necessarily fluctuates, so that a meaningful value of COP can only be obtained at the end of a twenty-four hour cycle in terms of the ratio of bulk cooling obtained to the bulk heat input, or integral of $\dot{Q}_b$ with respect to time. The situation is further complicated by the fact that the device does not necessarily make use of all the available solar insolation available. In the case of the IB system the generation of vapour continues only in so far as the solution temperature continues to rise. As the rate of solar insolation declines on a clear day after midday, this condition becomes increasingly hard to satisfy. A twenty-four hour definition of the solar COP allows theoretical or actual benefits, in terms of useful economic output, of one solar refrigerator design to be compared more effectively with another, and allows a more effective measure of performance of a given system given design

changes or parameter changes. An estimate of yearly COP can be made on the basis of representative 24 hour values for the different seasons. The twenty-four hour solar COP of the device is:

$$COP_{24,solar}=\frac{Q_{ev}}{\int_{t=dawn}^{t=dusk}\dot{G}A_{coll}dt}$$

where Q_{ev} represents the energy extracted by the evaporator during absorption, and $\dot{G}$ represents the rate of incident irradiation. Given uniform operating conditions over successive cycles the cooling effect will tend toward the value

$$Q_{ev}=M_v\Delta h=M_v(h_{v(T_{ev},x_v)})-h_{l(T_{box},x_L)})$$

where M_v is the mass of vapour condensed during the generation phase and the useful enthalpy rise of the refrigerant (Δh) is expressed in terms of a constant value of T_{ev} on the assumption of constant pressure absorption. T_{box} is the temperature of the cold box contents at the start of the absorption phase. A 24-hour internal cycle COP can also be defined in order to evaluate the refrigeration cycle performance independently from the solar collector performance. This constitutes:

$$COP_{24,cycle}=\frac{Q_{ev}}{\int_{t=dawn}^{t=dusk}\dot{Q}_b dt}$$

where the relationship between the solar and cycle COP is given by the efficiency of the solar collector (η_{coll}), itself a function of solar insolation rate:

$$\dot{Q}_b=\eta_{coll}\dot{G}\dot{A}_{coll}$$

$\dot{Q}_b$ and $\dot{G}$ throughout phase I, which is taken as having a duration Δt_I, and so define the system's performance in terms of a nominal internal and a solar efficiency:

$$\eta_i=\frac{Q_{ev}}{Q_b\Delta t_I}=\frac{Q_{ev}}{Q_b}$$

$$\eta_{solar}=\eta_i\eta_{coll}$$

With reference to the state points numbered on the p-t-x diagram, the equation for conservation of energy in the boiler integrated over the complete generation period is

$$Q_b=(M_{L3}-M_{v3})h_{L3}-M_{L1}h_{L1}+\int_1^3 h_{v3}dm$$

given that the specific enthalpy of liquid solution is approximately equal to its specific internal energy. M_{v3} here is the vapour produced directly by the boiler, before entry to the rectifier section. The rectifier acts to differentially condense the vapour, such that the ammonia concentration of the vapour progressing to the condenser is enhanced; the magnitude of M_{v3} is clearly greater than that of M_v, the difference being made up by the return of the rectifier condensate to the boiler. The remaining integral can be solved by Simpson's rule but for further manipulation of the equation in the present context it can be approximately solved:

$$Q_b=(M_{L3}-M_{v3})h_{L3}-M_{L1}h_{L1}+M_{v3}h_{v3} \qquad (1.2.1)$$

Chinnappa (1961) calculates that errors of less than 2% result from this simplification in the conditions considered. Since the refrigerant yield is in practice the dependent variable the equation can be expressed:

$$M_{v3}=\frac{Q_b-M_{L1}(h_{L3}-h_{L1})}{(h_{v3}-h_{L3})} \qquad (1.2.2)$$

Eqn 1.2.1 can be expressed in terms of unit yield:

$$\dot{q}_b=\frac{1}{R}(h_{L3}-h_{L1})-(h_{v3}-h_{L3}) \qquad (1.2.3)$$

where R is the ratio of initial solution charge to condensate yield, defined by the mass balance:

$$M_{v3}=M_{L1}\left[\frac{x_{L1}-x_{L3}}{x_{v3}-x_{L3}}\right]=M_{L1}R \qquad (1.2.4)$$

The conditions at the end of the generation phase are determined by both the maximum generation temperature $T_{gen(max)}$ and the system pressure P_{gen}. The pressure is a function of the temperature of condensation, T_{con}, which is determined by the physical characteristics of the condenser and the vapour production rate. T_{con} is taken here as invariate such that pressure becomes a function only of vapour concentration. The initial concentration x_{L1} is determined by the preceeding absorption phase and by the sink temperature, as described in section 3.3. Fig 1.2.3 describes the calculation procedure adopted for solution of the IB cycle performance. The calculation is

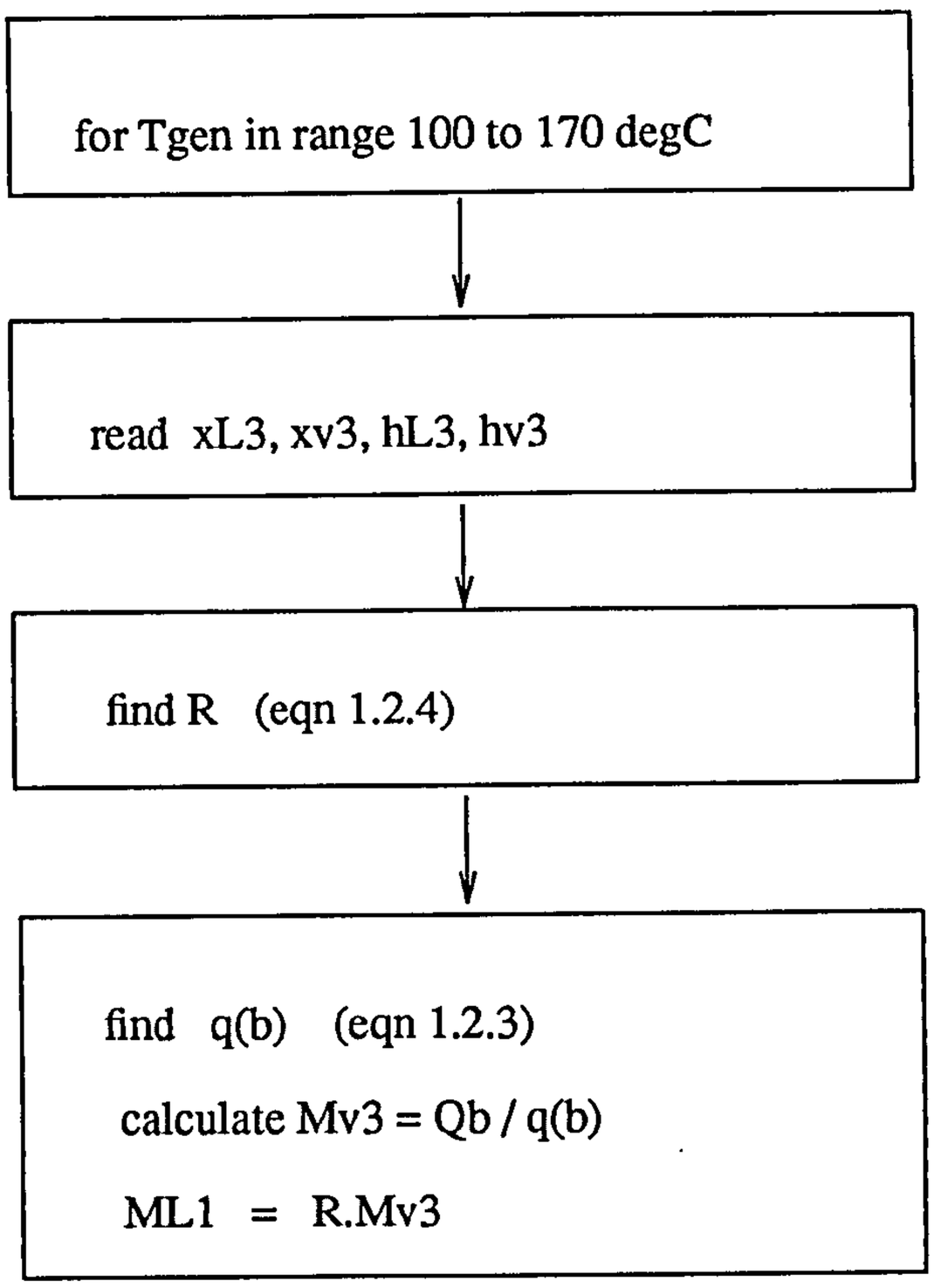

Fig 1.2.3 *Calculation procedure used to solve for IB cycle performance; results presented graphically in figs 1.2.4, 1.2.6, and 1.2.7.* T_{exit} *is the temperature of the vapour leaving the rectifier.*

performed for the set of input parameters listed on table 1.2.1. The pressure at which generation proceeds is calculated to be 17.8 bar absolute and the initial solution concentration is 0.45. Fig 1.2.4 plots the cycle performance with respect to the final solution concentration, x_{L3}, in order to facilitate comparison with the enthalpy-concentration plot for aqua-ammonia prepared by Merkel and Bosnjakovic (Bosnjakovic, 1937) reproduced as fig 1.2.5. Fig 1.2.4 (a) shows the variation of Tgen with x_{L3}, and the variation of solution charge (M_{L1}) implied. Clearly a conflict of interest exists between the desirability of minimising charge (so reducing overall weight, bulk, and cost) and minimising generating temperature in order to obtain high collector efficiencies or to be able

to use low-cost collectors. It may be remarked that this problem is unlikely to effect a non-solar IB system, where the optimum temperature is more easily obtained, with the result that less bulky units can be realized.

$\dot{Q}_b$	300	watts	T_{ev}	-10	degC
T_{con}	45	degC	T_{ab}	30	degC
T_{exit}	75	degC	M_{steel}	0	kg
T_{amb}	35	degC	Δt_I	8	hours

Table 1.2.1 *Values adopted for input parameters in calculating the performance of the IB cycle; graphical results given in figs 1.2.4, 1.2.6, and 1.2.7*

The mass of ammonia vapourised is the product of the concentration x_{v3} and mass of the mixed vapour generated, M_{v3}. This mass is shown on fig 1.2.4 (b) to peak at a solution concentration of 0.25 and a generating temperature of 135 degC, clearly the optimum for the operating conditions listed in table 1.2.1. Reference to the enthalpy-concentration plot reproduced on figure 1.2.5 shows that this is the minimum concentration at which the vapour enthalpy remains closely related to vapour enthalpy of pure ammonia; at reduced concentrations the heat of desorption is diverted heavily into vapourisation of water, as indicated on the h-x plot by falling vapour concentration. Figs (c) and (d) show the calculated specific enthalpies. At greater final solution concentrations, due to an insufficiently optimised value of final generating temperature, decreasing values of specific enthalpy lift (h_{L3}–h_{L1}) are required (fig (e)) but the rise in solution mass results nevertheless in a rise in the proportion of heat of desorption devoted to the sensible heating of liquid ($M_{L1}(h_{L3}–h_{L1})$) on figure 1.2.4(f)). Q_b has the value 8.64 MJ. Consequently less heat is available for vapourisation just as (hv3-hl3) rises; the net effect is that the mass of vapour yielded declines.

Equilibrium can be assumed to exist throughout the rectifier as elsewhere. The mass of vapour entering the rectifier is found by taking mass balances to be

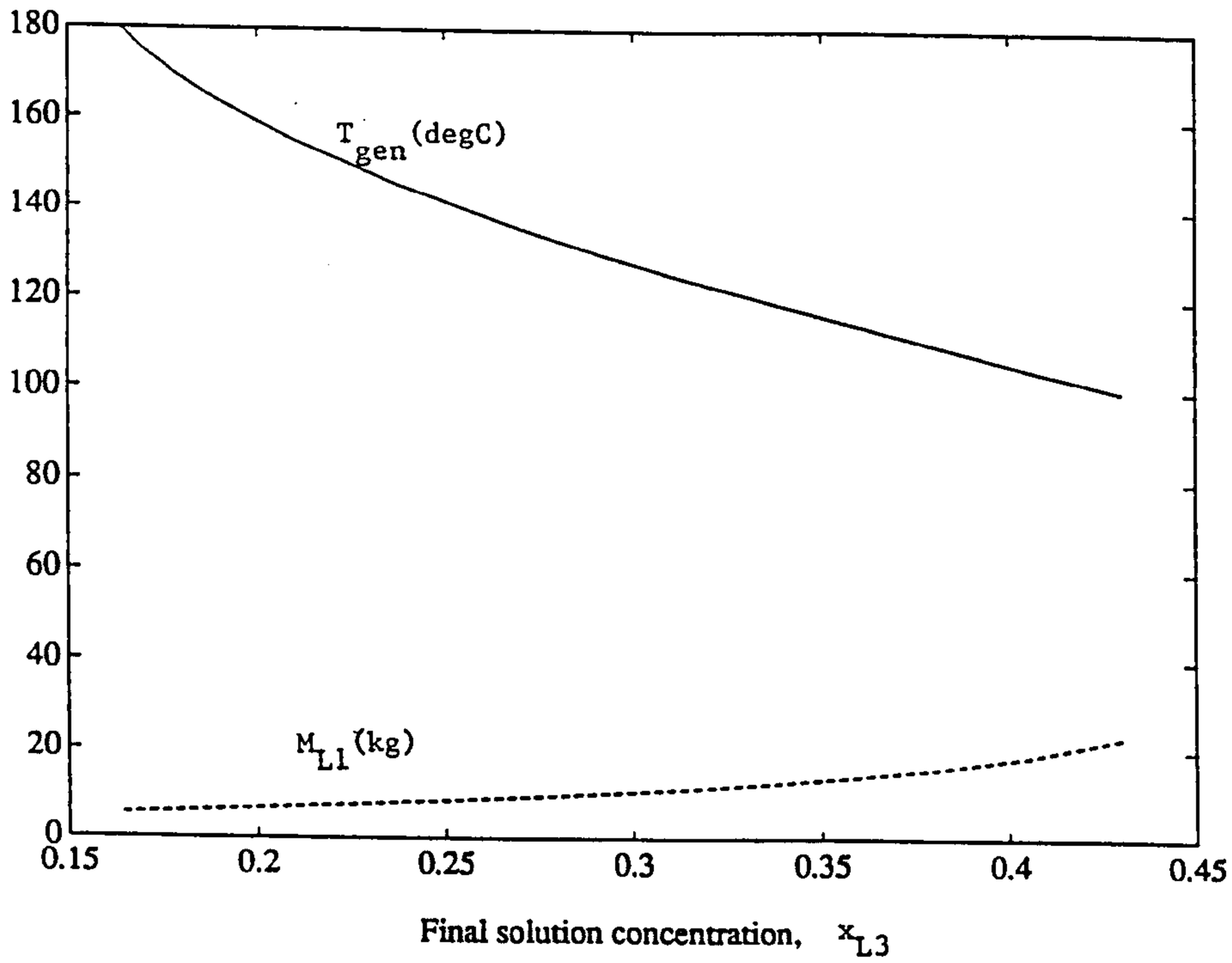

Fig. 1.2.4(a). Final generating temperature (T_{gen}) and initial solution charge (M_{L1}) plotted for the intermittent basic (IB) cycle against final solution concentration (X_{L3}). The IB cycle is illustrated in Figures 1.2.1 and 1.2.2. Parameter values used for the calculation (Figure 1.2.3) are presented on Table 1.2.1. Initial solution concentration (X_{L1}) is calculated to be 0.45 and generating pressure is 17.8 bar abs. The variation in X_{L3} is due to changes in the initial solution charge.

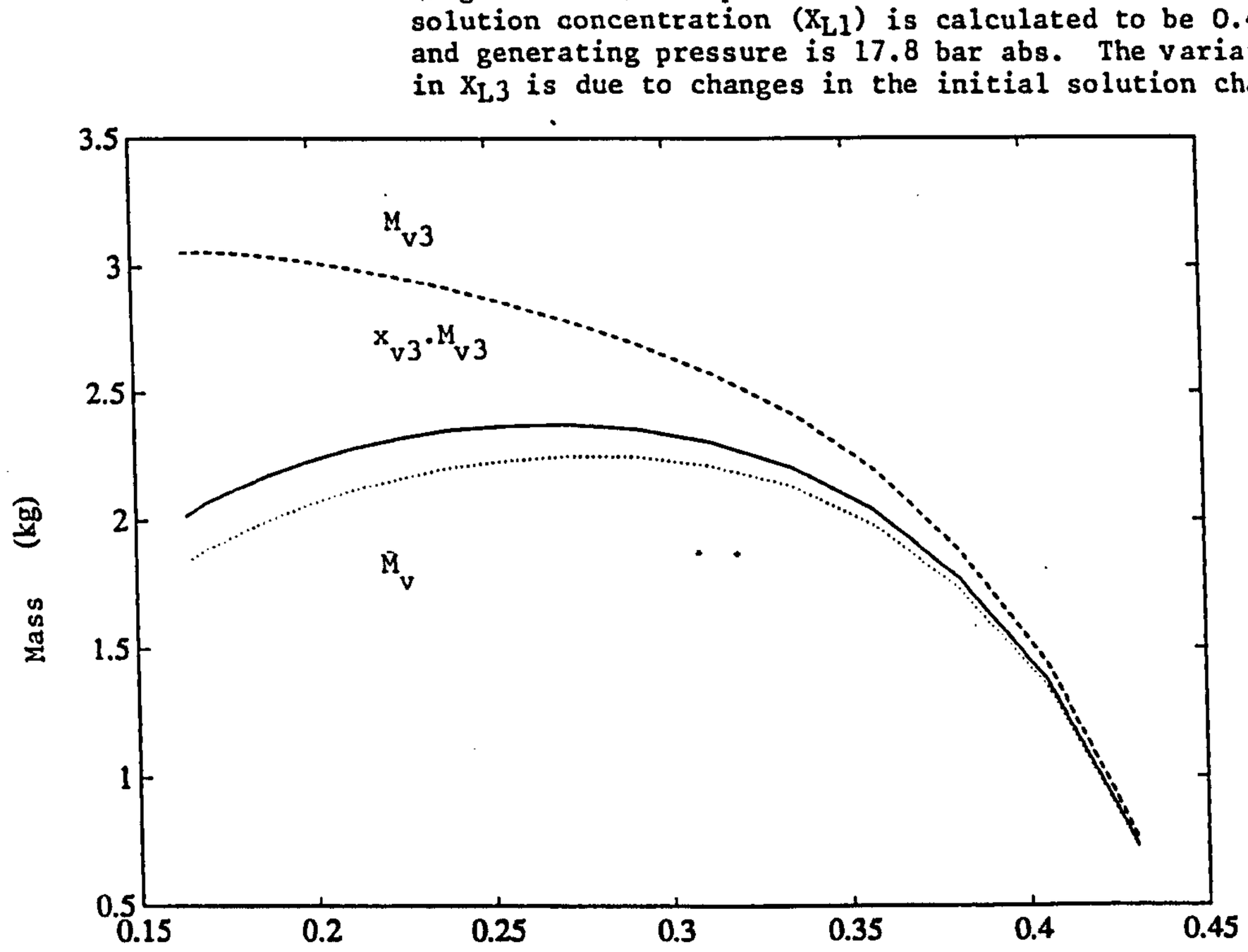

Fig. 1.2.4(b). IB cycle, as described in caption to Fig. 1.2.4(a), showing intermediate parameters illustrated for Figure 1.2.1 plotted against final solution concentration. $X_{v3}.M_{v3}$ is the total mass of ammonia which enters the rectifier during desorption. M_{v3} is the mass of water and ammonia mix which enters the rectifier and M_v is the mass of vapour which enters the condenser.

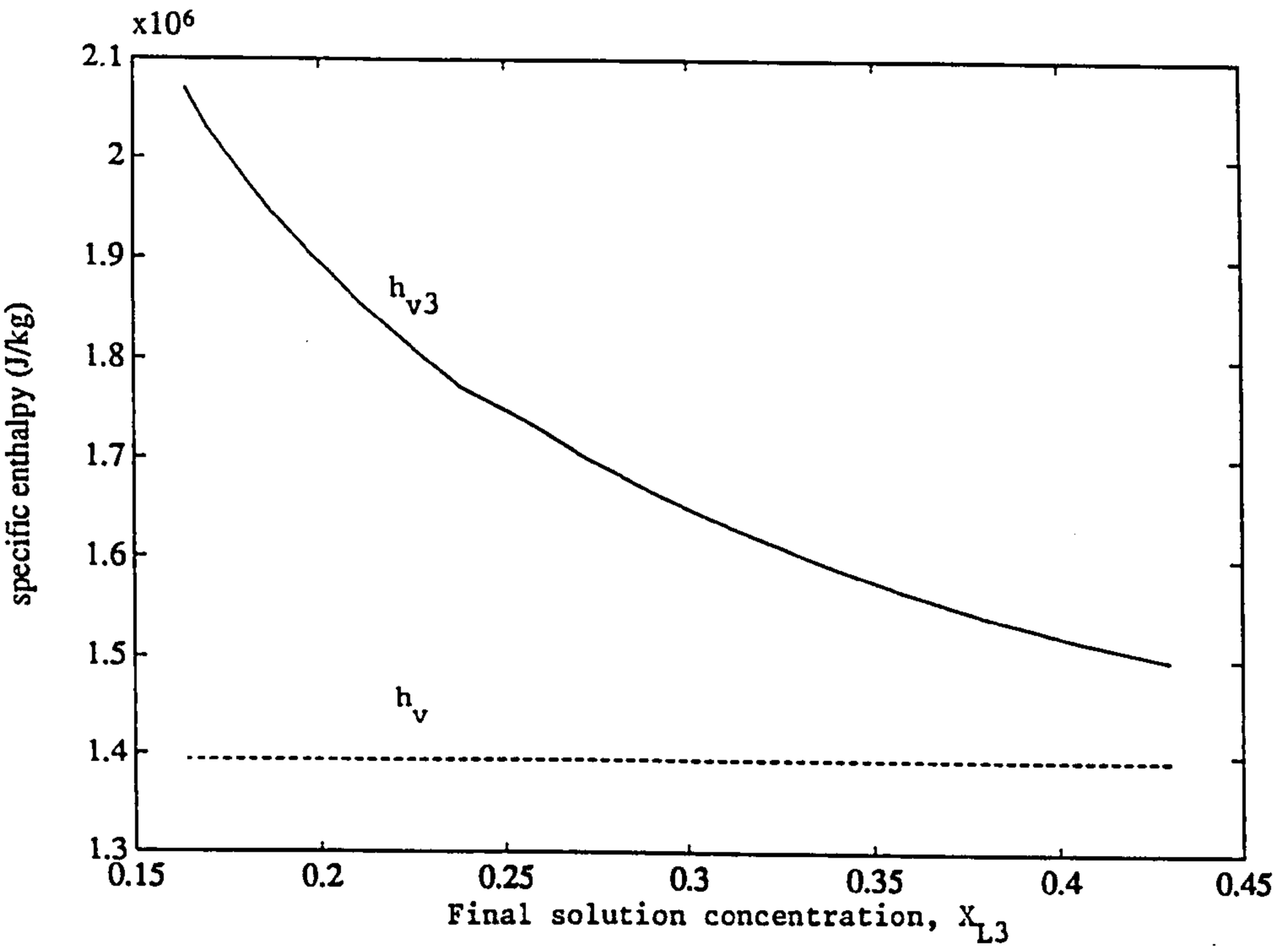

Fig. 1.2.4(c) 1B cycle desorption phase. h_{v3} is the enthalpy of vapour which enters the rectifier, while h_v is the enthalpy of vapour which leaves the rectifier. Final solution concentration varies with changing quantities of initial solution charge (M_{L1})

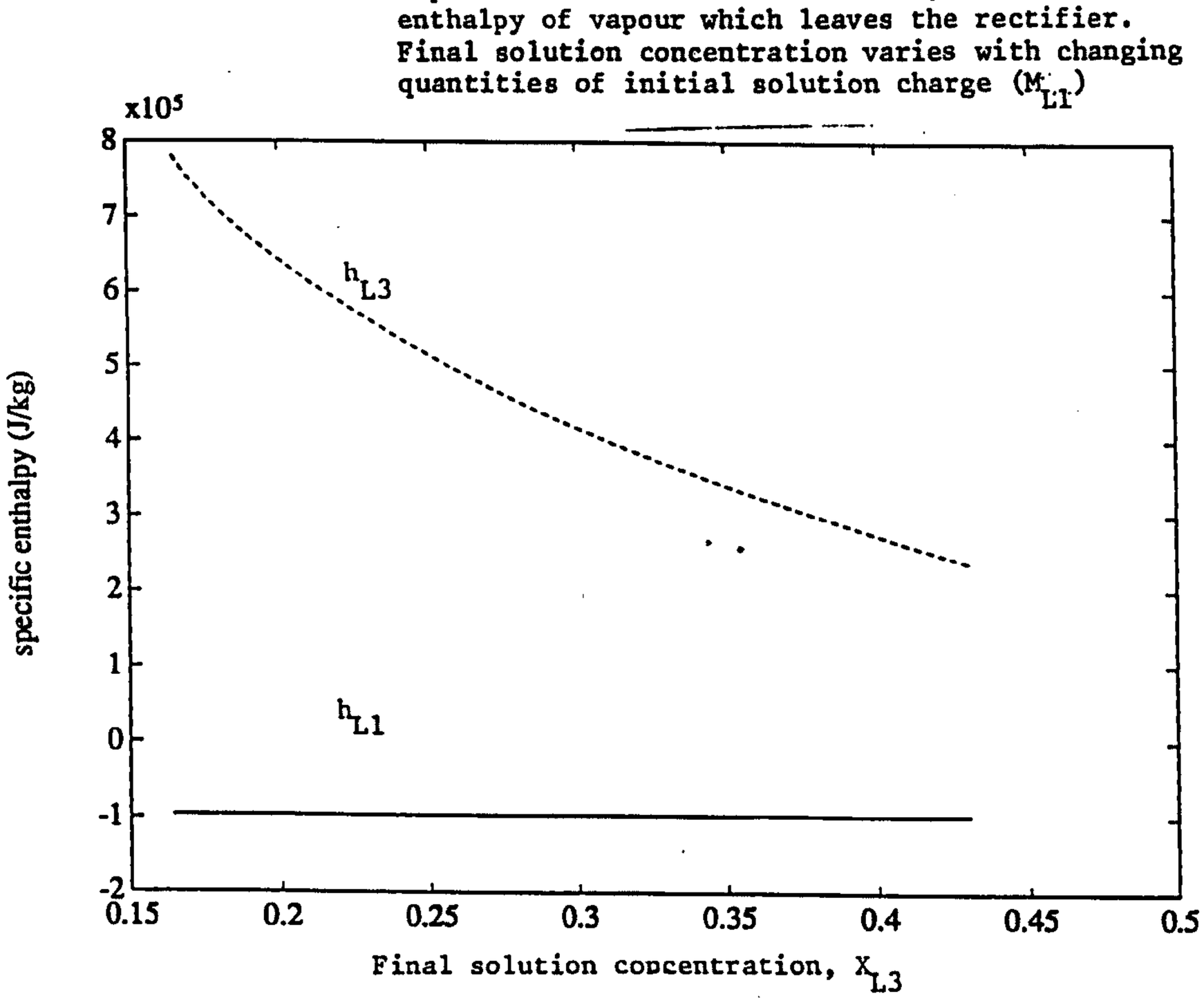

Fig. 1.2.4(d). 1B cycle desorption phase. h_{L3} is the enthalpy of liquid remaining in the boiler at the end of the desorption phase, while h_{L1} is the original enthalpy of liquid in the boiler before the start of desorption.

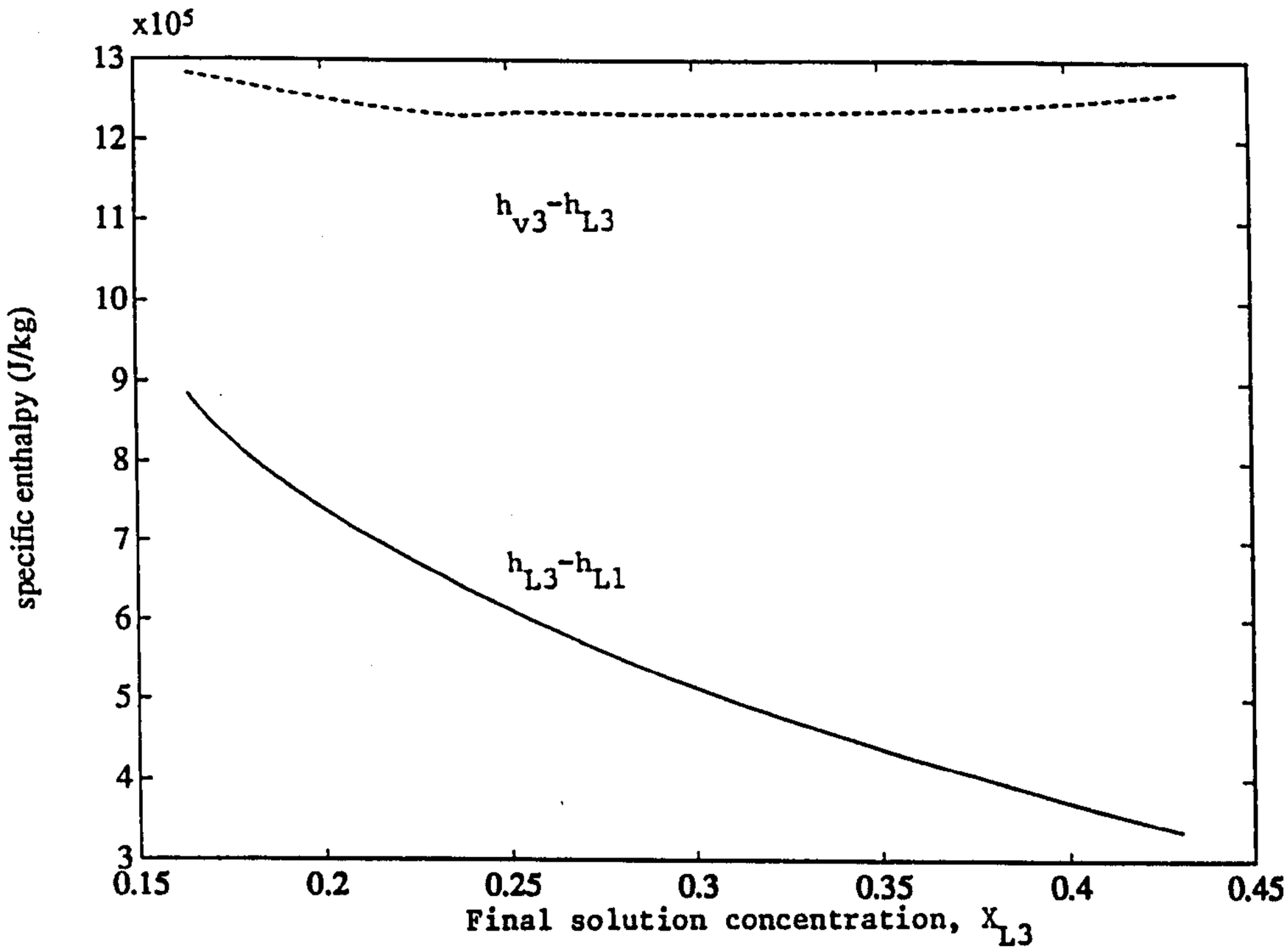

Fig. 1.2.4(e). 1B cycle, desorption phase under operating conditions described in caption to Fig. 1.2.4(a). The plotted enthalpy lift values refer to equation 1.2.2.

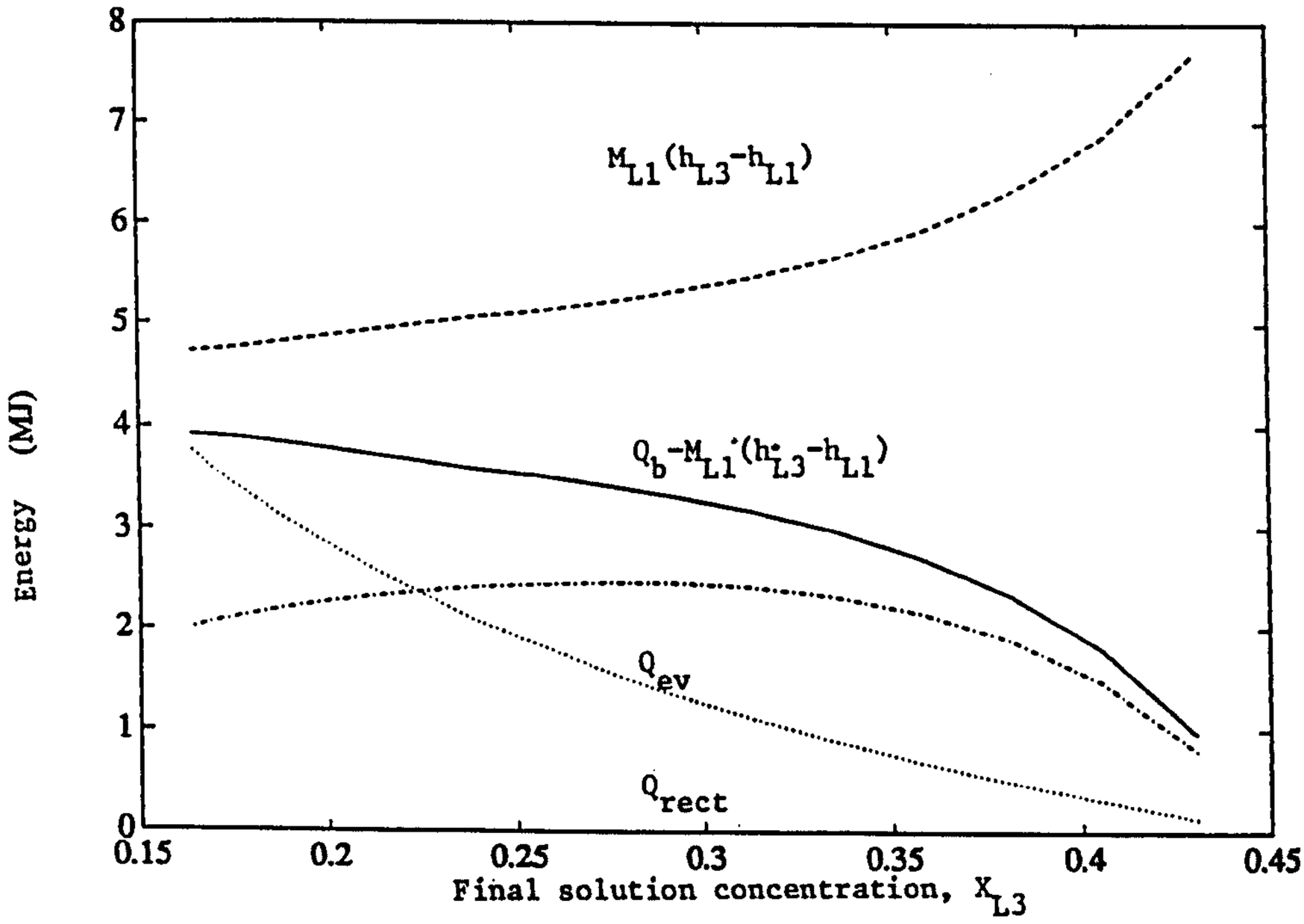

Fig. 1.2.4(f). 1B cycle, desorption phase. The plotted energy values refer to equation 1.2.2. Q_{ev} and Q_{rect} are indicated on Fig. 1.2.1.

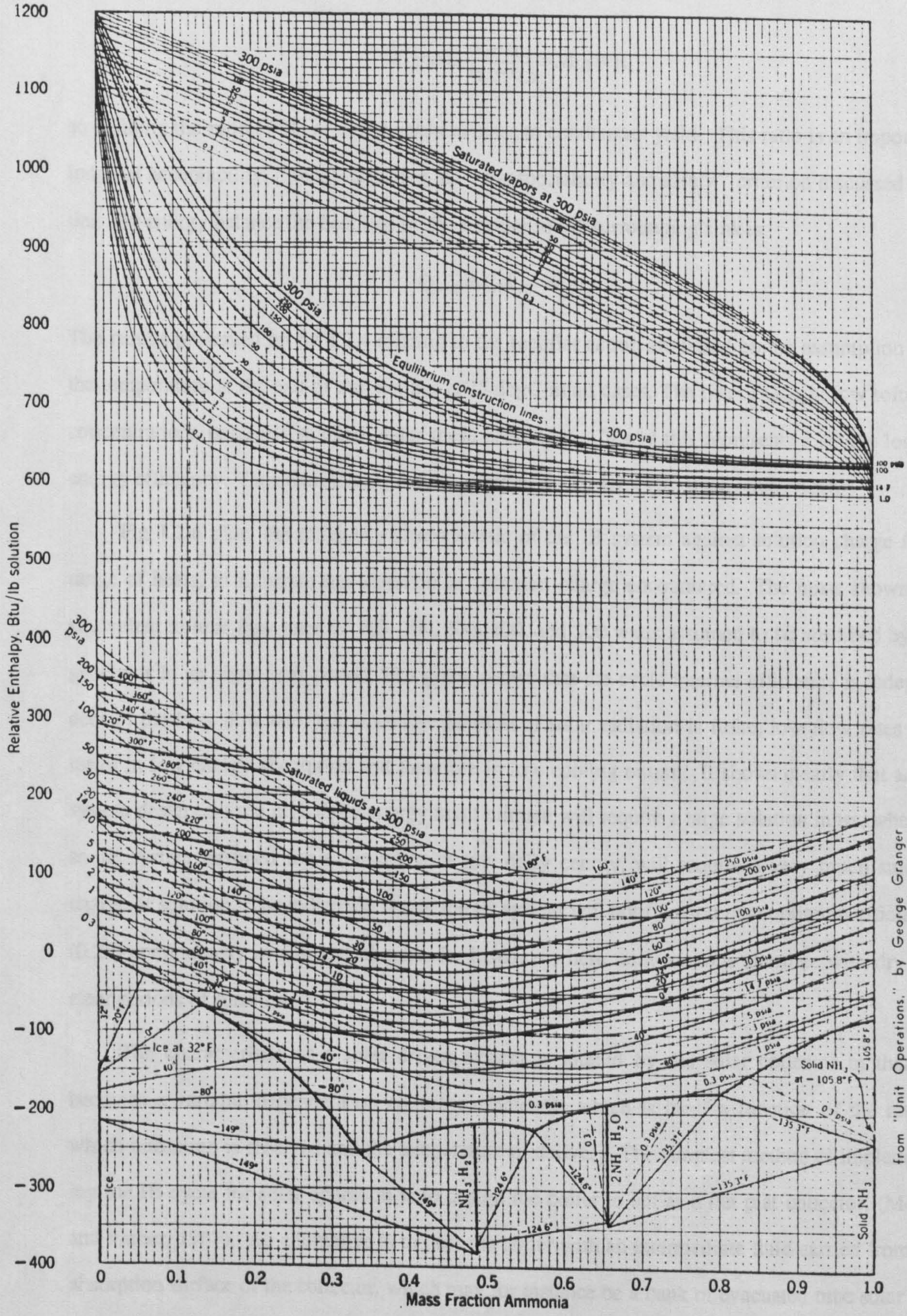

Fig 1.2.5 ENTHALPY-CONCENTRATION DIAGRAM FOR AMMONIA-WATER COMBINATION

$$M_{L1}=M_v\frac{x_v-x_{L3}}{x_{L1}-x_{L3}}=M_{L1}WR$$

so defining the ratio (WR) of initial solution mass to condensate yield. This ratio is an important index of acceptability, directly affecting the ''transportability and safety'' criterion discussed earlier. By energy balance the heat lost by the rectifier to the surrounding sink is

$$Q_{rect}=M_{v3}h_{v3}-M_vh_v$$

The results presented on fig 1.2.4 relating to the rectifier action are based on the assumption that the temperature at the exit of the rectifier is 75 degC in all cases. The rise of Q_{rect} at low solution concentrations is clearly marked under these conditions. Clearly this represents a severe loss in energy efficiency. The condensate yield, M_v, plotted on fig 1.2.4 (b), shows this effect.

Fig 1.2.6 plots the efficiency characteristic of the IB system against solution charge for a range of heats, to illustrate the variation in optimum charge encountered. The heats shown are equivalent to heat flow rates of 100, 200, 300, 400, and 500 watts assumed to be absorbed by the generator in an eight hour period. The graph shows that the cycle internal efficiency is independent of the heat flow rate, but since the duration of solar radiation is finite, low flow rates will result in low energy absorption and therefore in low cooling output. It shows clearly that an IB system designed for a high daily energy input climate will require a large solution mass, whereas an IB system destined for a climate with low daily energy, will require a very much smaller charge of solution. The indication is that the IB system will not function near optimum efficiency (0.28) continuously in a mixed climate, for instance where rainy seasons alternate with dry and clear periods of sunshine.

The characteristic of a solar driven system is altered by the solar collector in that Q_b becomes a variable dependent on collector efficiency, which is itself a function of the rate at which insolation is received and the temperature of delivery. The simplest method of implementing the IB cycle for solar operation is to design the boiler to act as a flat plat collector. (Moore and Farber, 1967). An alternative is to heat the boiler with an intermediate fluid carried from the absorption surface of the collector, which may for instance be a bank of evacuated tube solar collectors. In order to simplify a comparison of the performance of the IB system with that of the IR

system considered in the following chapters this latter path is chosen and use is made of the collector characteristic discussed in section 3.5.2 for the IB performance results calculated here. Solar insolation is assumed to arrive at a constant rate ($\dot{G}$) for the period Δt_I, which is taken as 8 hours again as in the study of internal efficiency above. Fig 1.2.7 (a) shows the relationship of solution charge to performance for a unit absorbing solar radiation at different rates. The plot confirms the conclusion reached in investigation of the internal efficiency (Fig. 1.2.6) in that the IB system holding any particular solution charge will not maintain optimum efficiency under varying daily insolation levels. The additional observation is made that lower isolation levels give rise to lower peak efficiency values. The reason for this is that collector efficiency reduces at low isolation levels, because losses rise in proportion to the heat transferred. Fig. 1.2.7(b) shows the variation in collector efficiency due to decreasing insolation. It also shows that collector efficiency drops with decreasing solution charge, because small charges result in high boiler temperatures and so greater collector loss. In practice an IB device will contain a fixed solution charge while daily insolation varies with season. Fig. 1.2.7(c) essentially repeats the information given in figure 1.2.7(a) in order to clarify. Three fixed charge devices are shown. The 10 Kg device is clearly suitable where insolation levels tend to fluctuate between 500 and 900 watts/m^2. The 5Kg device is suitable at a lower range of insolation valves. Application of fixed size devices to a climate where seasons are characterised by distinctively variant mean insolation levels will require careful balancing of the bulk yearly performance expected and weight of solution charge. A cooler designed to operate in a cloudy season or place will be inefficient in clear periods. If efficient in clear skies it will have too high a cut off point for use on cloudy days.

Variations of insolation level within a day are also of importance. The decline of insolation rate during the afternoon has the important effect of causing the basic system to stop generating altogether, since the generating temperature is unable to continue to rise. In practice any drop in ambient air temperature may reduce condensing temperature sufficiently to offset this effect to an extent. The experimental evidence obtained by Exell (1981) demonstrates this effect, visible on the plot of fig 2.2.4.3 in chapter 2. An additional problem associated with the basic device is that the sensible heating of the complete solution mass will not be compensated for by full vapourisation if the cumulative clear insolation period of the day falls short of design expectations. The

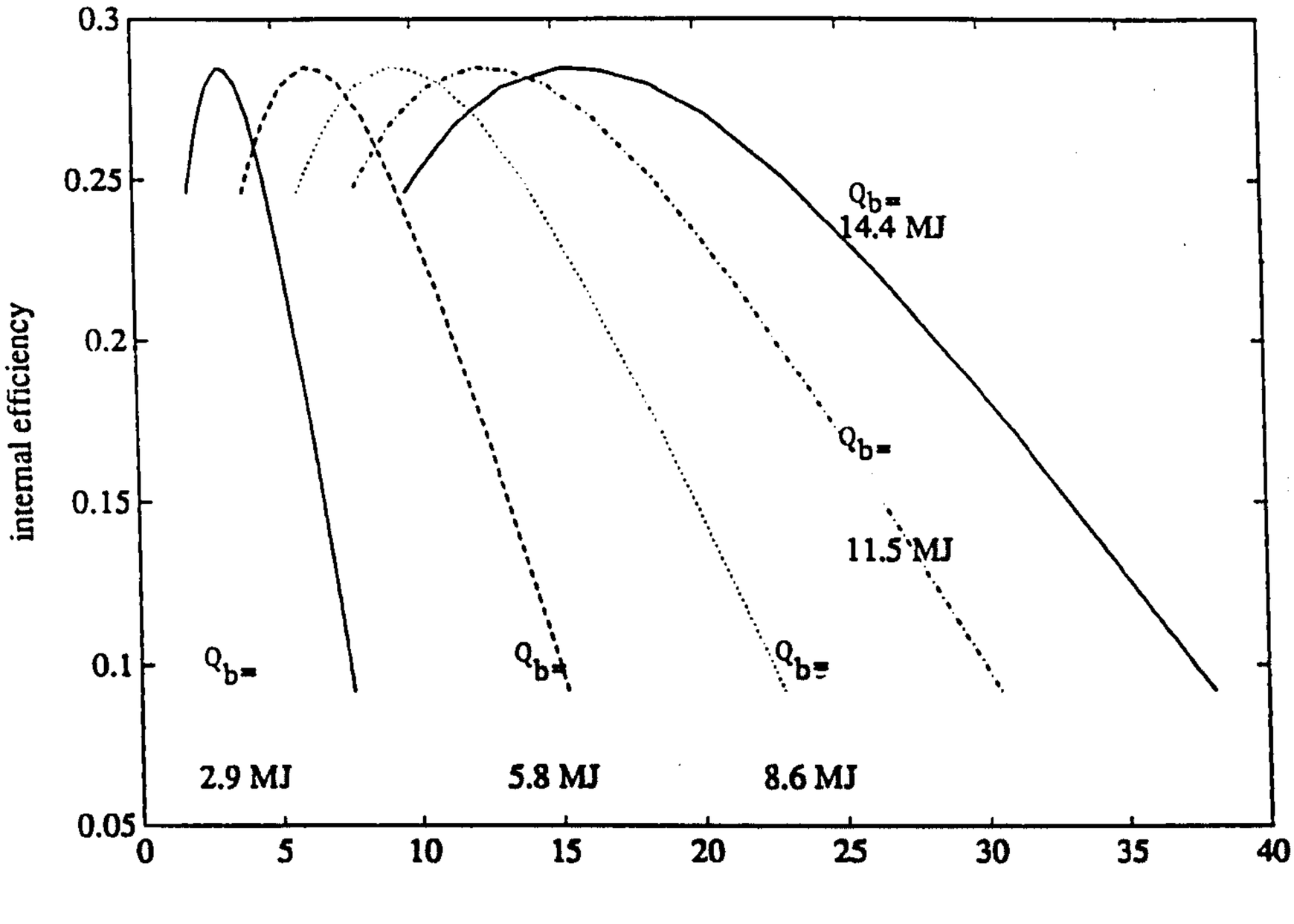

Fig. 1.2.6. The internal efficiency (η_i) of the 1B cycle is plotted against different initial solution charge values (M_{L1}), at constant boiler heat input values of 100, 200, 300, 400 and 500 watts. Since the heat is assumed to flow for eight hours, the boiler heat input (Q_b) is expressed as an energy input in each case. Input parameters value are listed on Table 1.2.1 with the exception of Q_b which in this case is varied.

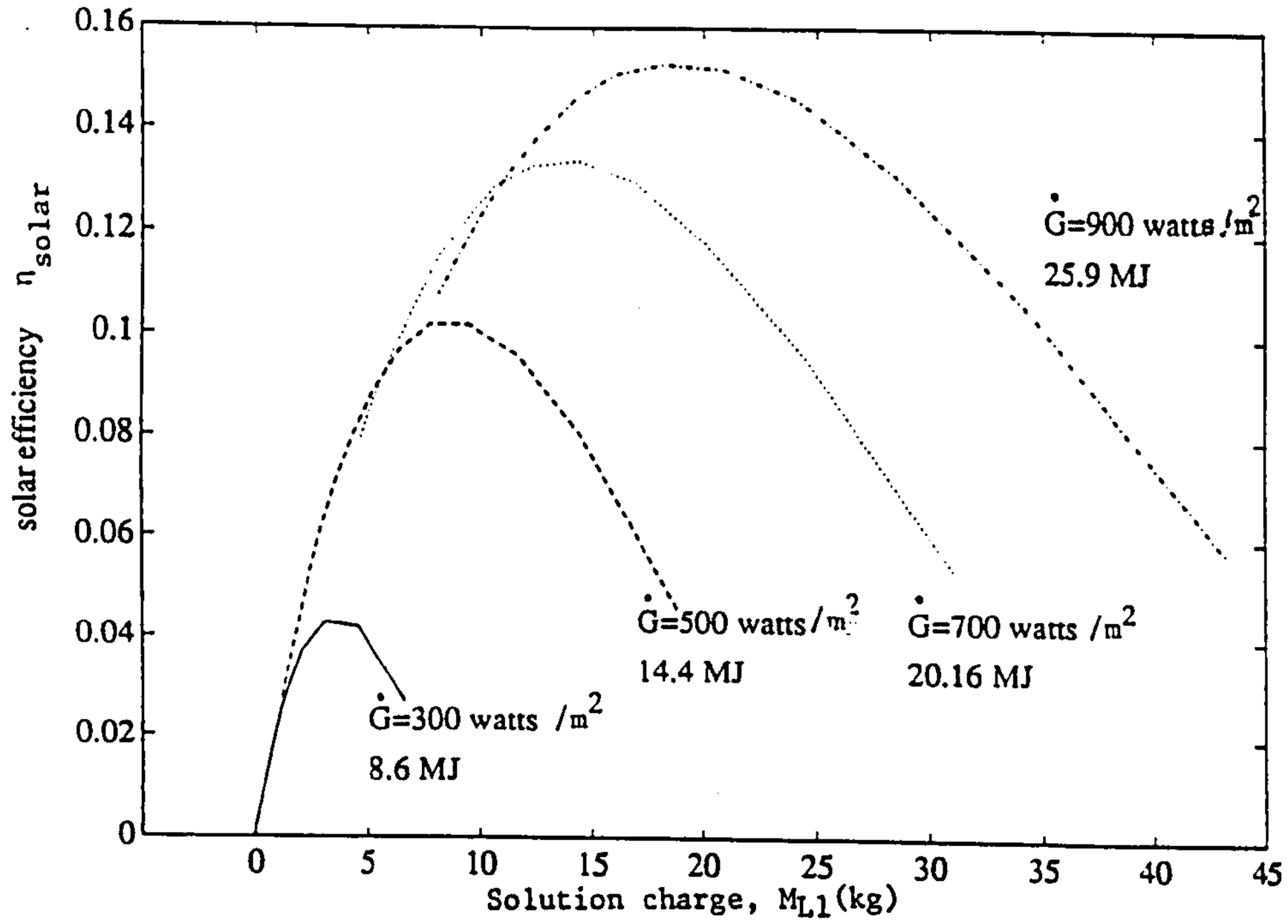

Fig. 1.2.7(a). The solar efficiency (η_{solar}) of the 1B cycle is plotted against different initial solution charges. Solar insolation is assumed at arrive at constant wattage on a collector of 1m^2 area, for an eight hour period. Solar efficiency curves result each of which represents a different amount of energy absorbed by the collector daily. Input parameter values are listed on Table 1.2.1.

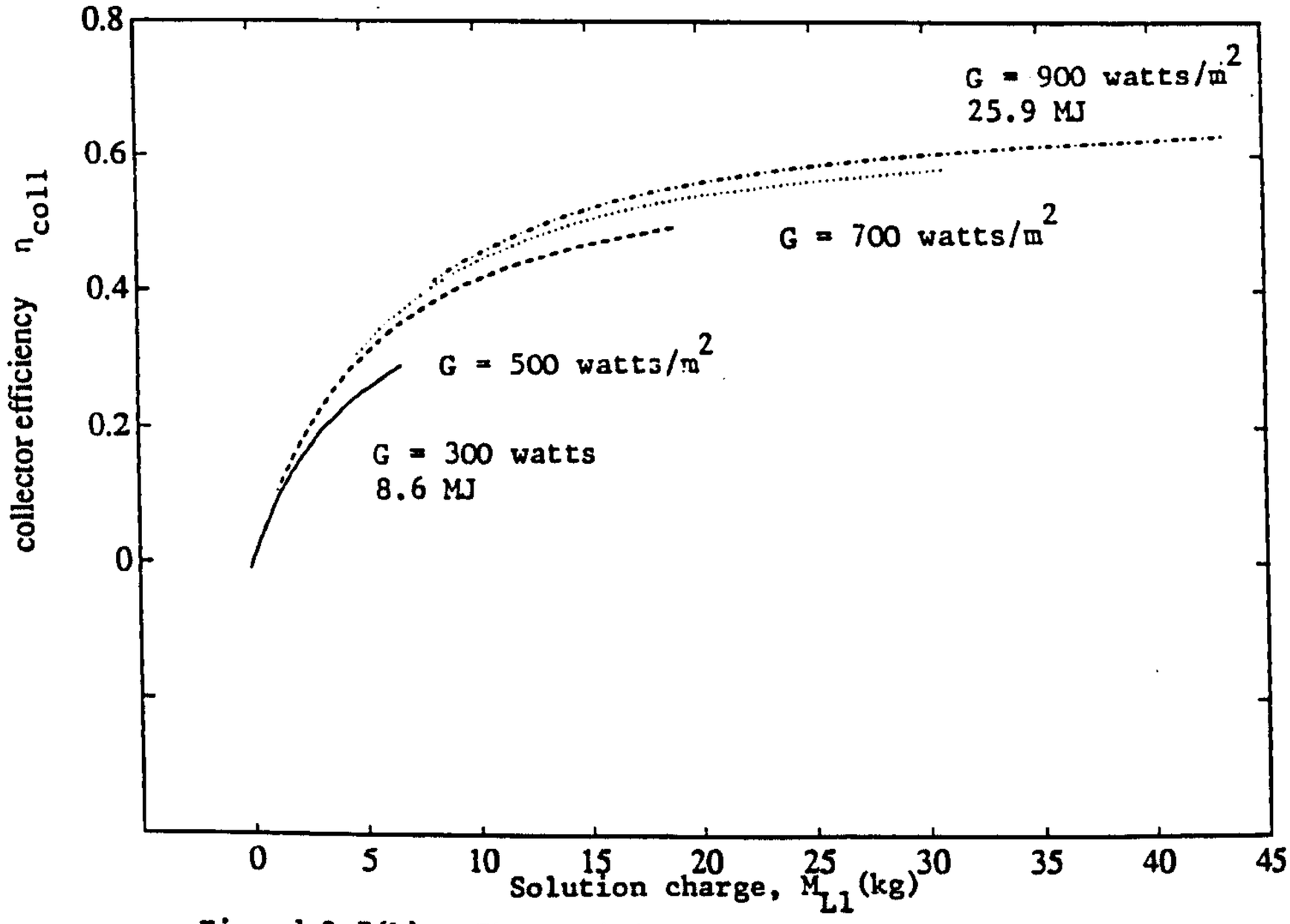

Fig. 1.2.7(b). The efficiency of the collector in the 1B cycle is plotted against different initial solution charges, for the same range of values of constant insolation rate taken in Figure 1.2.7(a) above. Input parameterd are listed in Table 1.2.1.

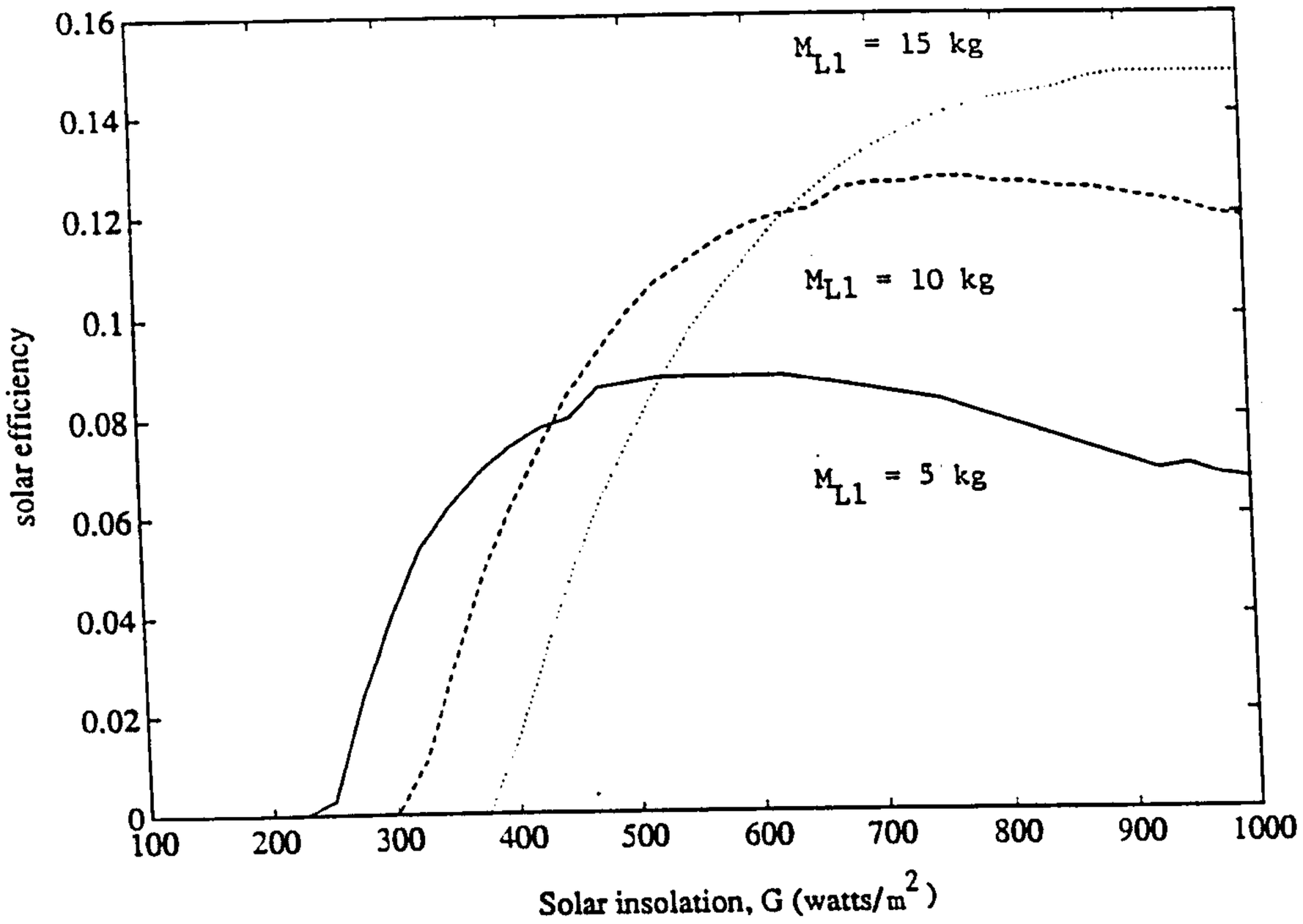

Fig. 1.2.7(c). Solar efficiency of the 1B cycle plotted against steady state insolation for 3 1B devices charged with 5, 10 or 15kg of solution respectively. Input parameter values are listed on Table 1.2.1.

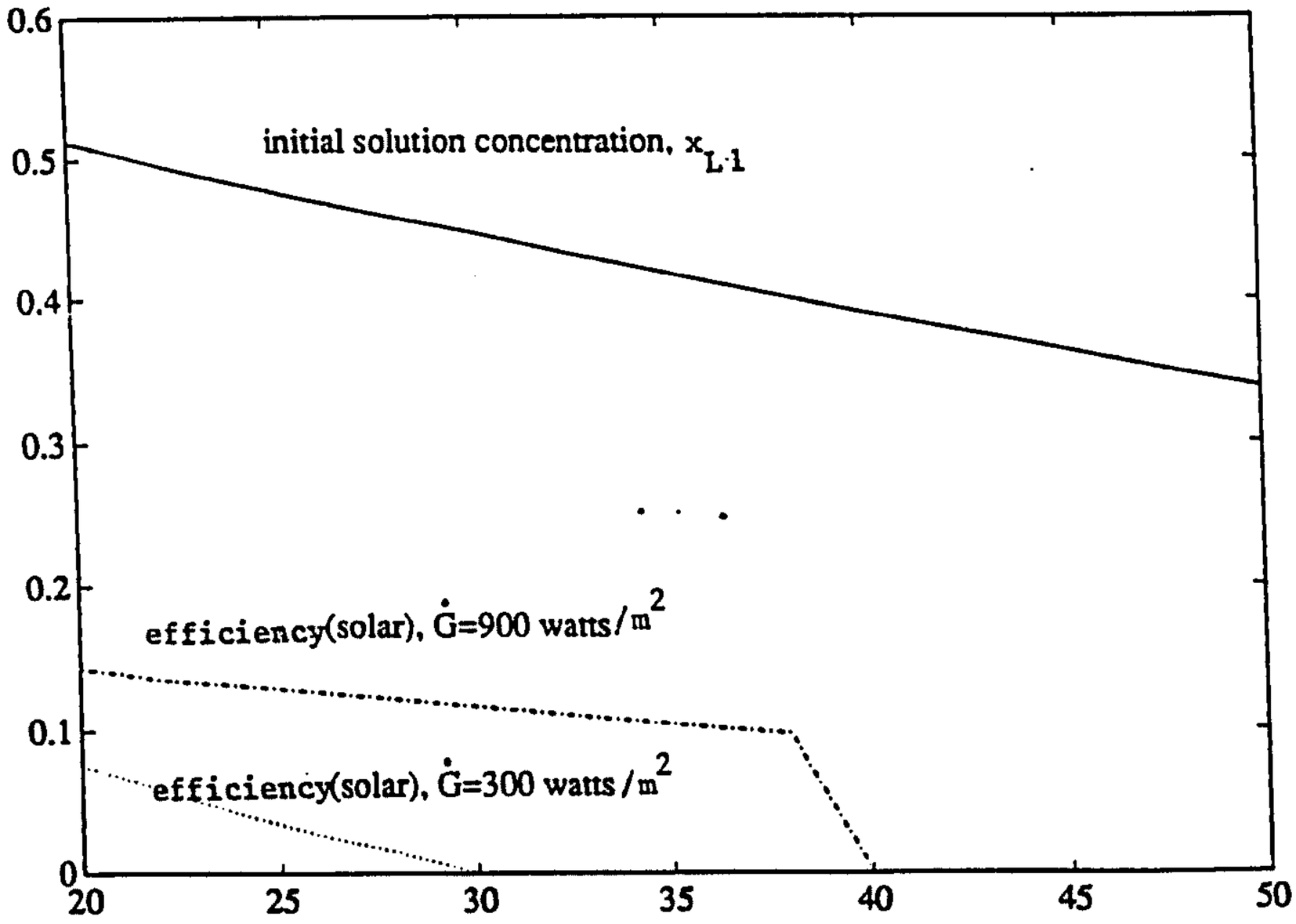

Fig. 1.2.8. The solar efficiency of the 1B cycle plotted against final absorber temperature, T_{ab}. Efficiency$_2$ is shown for steady insolation of 900 and 300 watts/m^2 to allow comparison with Figure 1.2.7(a). The effect of T_{ab} on initial solution concentration, x_{L1}, is also shown, since the sensitivity of the system to absorber temperature is due to the effect of absorber temperature on initial concentration.

wet seasons of many tropical countries are often characterised by days of predominantly diffuse and dull insolation interspersed with short clear periods.

Table 1.2.1 indicates that the final temperature (T_{ab}) at the end of the absorption phase is assumed to be 30 degC. This temperature is represented by point "1" on fig. 1.2.2 (b). The value of T_{ab} actually achieved in a real situation will depend on night-time conditions which vary considerably from region to region. The effect of low or high values of T_{ab} on the IB cycle performance is significant, since the solution concentration (x_{L1}) at the start of the desorption phase is determined by T_{ab}. Fig. 1.2.8 shows how x_{L1} varies with change in T_{ab}, and shows also how increase in x_{l1}, increases the solar efficiency of the cycle. The figure also indicates that zero output can be expected if T_{ab} is allowed to rise too high. This provides important design information, since it is clearly indicated the absorber must be sized large enough to lose sufficient heat so that T_{ab} always remains within the indicated limits.

1.3. The continuous pumped system (CP)

Most commercial ammonia water absorption coolers are designed to allow desorption and absorption phases to run concurrently, as shown in the schematic diagram of fig 1.3.1. In this case the solution is actively circulated by an pump which provides the full difference between condensing and evaporating pressures. Concurrent phasing has the advantage of dispensing with the need for a reservoir of rich solution, which is inconveniently large in the case of diurnal cycle IB units. Actively pumped systems (as opposed to thermosyphoned versions which are surveyed in the following sections) have the disadvantage of requiring a parasitic power supply and additional maintenance. Their performance in tropical conditions is investigated here given the external parameters applied to the IB system previously.

Two refinements often included in the design of continuous pumped systems (CP systems) are the the analysing column and the rectifier heat reclaimer, options not open to the IB system. The efficiency gains resulting from the use of these components are calculated approximately here.

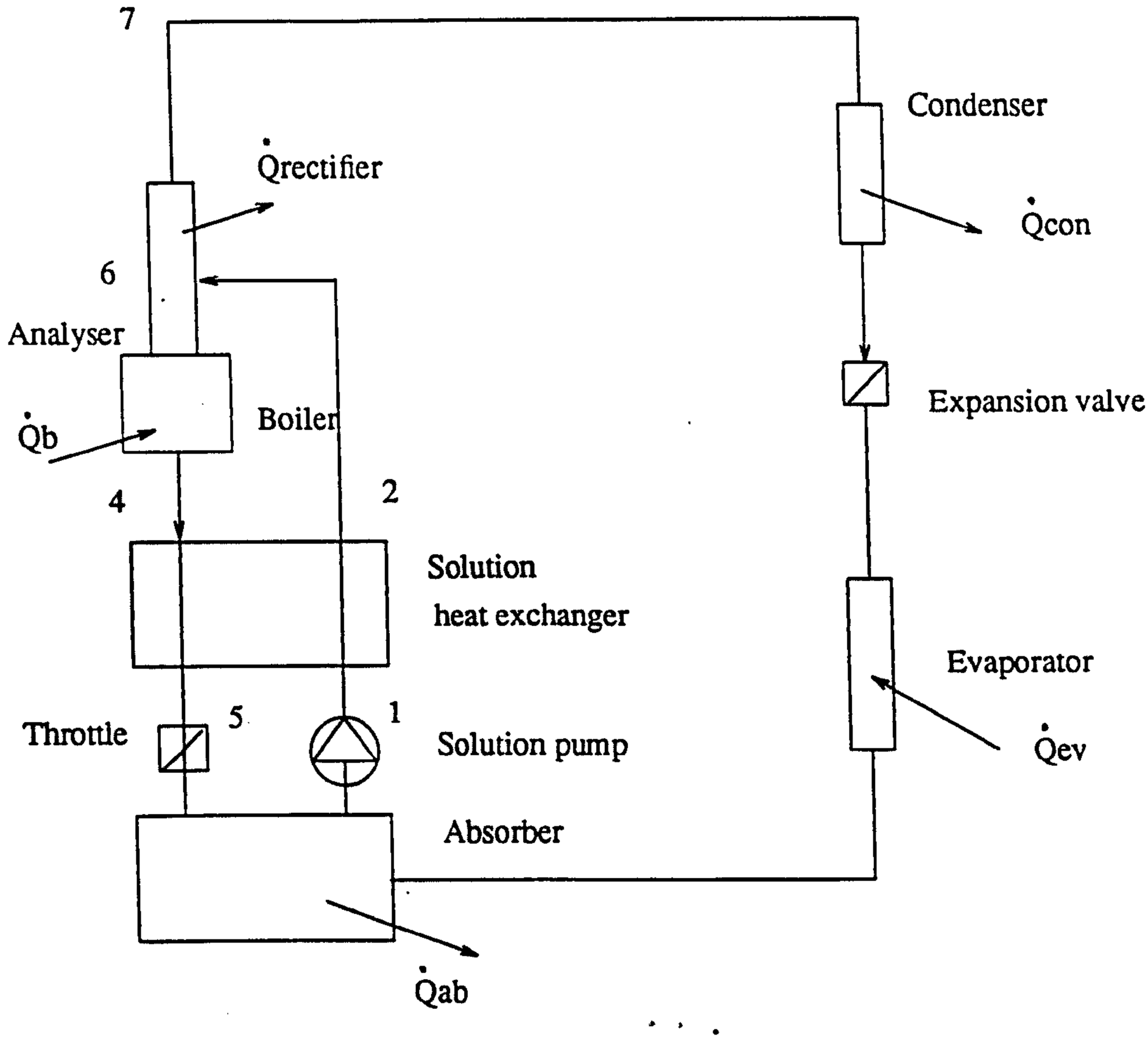

Fig 1.3.1 *The continuous pumped (CP) system. Absorption and desorption phases occur concurrently. An external power supply is required to drive the solution pump.*

In the IB system the energy lost to the vapourisation of absorbent increases as the desorption proceeds. In a continuous system, a portion of this energy can be reclaimed by an analysing column which allows the relatively cool incoming rich liquid to condense the vapour stream, while itself being partly stripped of a portion of its ammonia component by the hot vapour. If the

area of contact of the streams is large enough equilibrium of temperature between the opposing streams can be approached at the point at which rich liquid enters the analyser. The vapour then leaves the analyser at a concentration determined by the temperature and concentration of the incoming liquid. Effectively the rectification process has been largely internalised and the energy lost to vapourisation of absorbent largely reclaimed.

A quantitative comparison of the CP system performance can be made for the CP system with and without an analyser. Variation in the value of absorption temperature and maximum generating temperature is also considered. A mass balance over the control volume 1-5-7 allows the ratio of feed liquid flow rate to condensate yield rate (CR′) to be evaluated:

$$CR' = \frac{\dot{m}_{L1}}{\dot{m}_{v7}} = \frac{x_{v7} - x_{L4}}{x_{L1} - x_{L4}}$$

An energy balance over the same control volume gives:

$$q_b + CR' h_{L1} = (CR' - 1) h_{L5} + h_{v7} + q_r$$

where q refers to heat transferred per unit mass of condensate yield. The energy equation is rearranged to give:

$$q_b - q_r = CR'(h_{L5} - h_{L1}) + (h_{v7} - h_{L5})$$

Given an identical purity of condensate and the same operating conditions

$\dot{Q}_b$	300	watts	EFF_{she}	0.875	watts/m^2
$\dot{m}_{L1}$	na	mg/sec	M_{st}	na	kg
T_{con}	45	degC	Δt_I	na	hours
T7	75	degC	T1	na	degC
T_{amb}	35	degC	T_{ab}	30	degC
T_{ev}	-10	degC	A_{coll}	1	m^2

Table 1.3.1 *Values adopted for input parameters in calculating the performance of the CP cycle; results are given in fig 1.3.2.*

the net specific heat of generation expressed by the equation is always the same whatever the nature of the components within the control volume. It can be anticipated therefore that the system containing an analyser will require smaller values of both q_b and q_r. Table 1.3.1 specifies the same set of operating conditions that was used in investigation of the IB system. A solution heat exchanger effectiveness of 0.875 is specified. No account is taken here of the loss of energy to sensible heating of a CP device at the start of the day, so implying that the performance limits calculated here are optimistic to a marginal degree, the error being in the order of 3% if a liquid mass of 2.5 kg is assumed present in the generator at the start of the day. The weight ratio, WR, is estimated as being approximately 2.5. (The weight ratio is defined in the previous section; it is the ratio of solution charge to daily refrigerant yield).

A mass balance over the rectifier control volume 6-7 reveals that the ratio of vapour produced at point 6 to the condensate yield (VCR′) can be written:

$$VCR' = \frac{m_{v6}}{m_{v7}} = \frac{x_{v7} - x_{L6}}{x_{v6} - x_{L6}}$$

The corresponding energy balance allows the rectification heat loss to be expressed:

$$q_r = VCR' h_{v6} - (VCR' - 1) h_{L6} - h_{v7}$$

In the case of the system without an analyser the calculation of the heats is straightforward, as conditions at point 6 are identical to the specified conditions of point 4. In the case of the analyser, conditions at 6 are identical to conditions at 2, such that it is necessary to calculate T2 by calculating the heat absorbed on the feed side of the solution heat exchanger. The situation is complicated if the solution leaving the feed side of the solution heat exchanger is boiling; in the present calculation this does not occur. It is observed that the analyser improves the efficiency of the system by only 3%. Perfect rectification heat reclaim is calculated as improving efficiency by 7%. These figures are in agreement with the findings of Stoecker (1971) and Shiran (1982). Shiran, using a calculation method based on that proposed by Stoecker, shows that rectifier heat reclaim can add approximately 6% to optimum COP values, the saving being greater at higher generating temperatures and less at lower generating temperatures. The calculation is based on adoption of rectifier exit temperatures having values midway between the specified condensing

temperature and the generating temperature. The option of rectifier heat reclaim, with attendent cost of of installation, is open to all the systems considered here with the exception of basic, or non-circulating, systems. Neither this nor the analysing column are given any consideration in the folowing discussion.

Fig 1.3.2 shows the performance of the CP system calculated for a range of values of boiler temperature T_{gen}, given a boiler heat input rate of 300 watts. The indication that optimum generator temperature is in the order of 115 degC, considerably less than in that for the IB system, is in agreement with Stoecker, Whitlow (1976), and Mansoori (1979), as is the indication that obtainable COPs are of the order of 0.5. These results are calculated for the standard value taken for absorption temperature, 30 degC. The sensitivity of the system to the value of absorption temperature (T_{ab}) is illustrated in fig 1.3.3. It is clear that the availiability of low temperature cooling sinks is of great importance. The CP system necessarily absorbs concurrently with generation, so implying that direct air cooling of the absorber will give rise to absorption temperatures of the same order of magnitude as that specified for the condenser (45 degC). Under these conditions it can be seen that the CP system is under a severe disadvantage compared to systems which make use of a reduced night temperature, where climatic conditions supply this. Clearly the CP system is normally designed to have condenser and absorber cooling supplied by a pumped jacket water system. The provision of water cooling for the absorber will give rise to cost penalties and difficulties associated with scaling. (Whitlow, 1976).

The weight of working fluid is considerably less in the CP system, so implying greater portability, safety, and reduced cost.

Fig 1.3.4 shows the CP system in response to varying insolation rates, taking steady operation only into account. In comparison with figure 1.2.7(a) the system can operate at twice the solar efficiency of the IB system, 0.3 as opposed 0.15. This increase in efficiency is due to the recuperation of sensible heat in the solution heat exchanger. Clearly an optimum characteristic for solution flow rate would be one which maintained high efficiency throughout. An evaluation of the benefit in providing for flow regulation can be made by comparing the net yield of a system with ideal regulation with that of an unregulated system. The cost of providing control to the

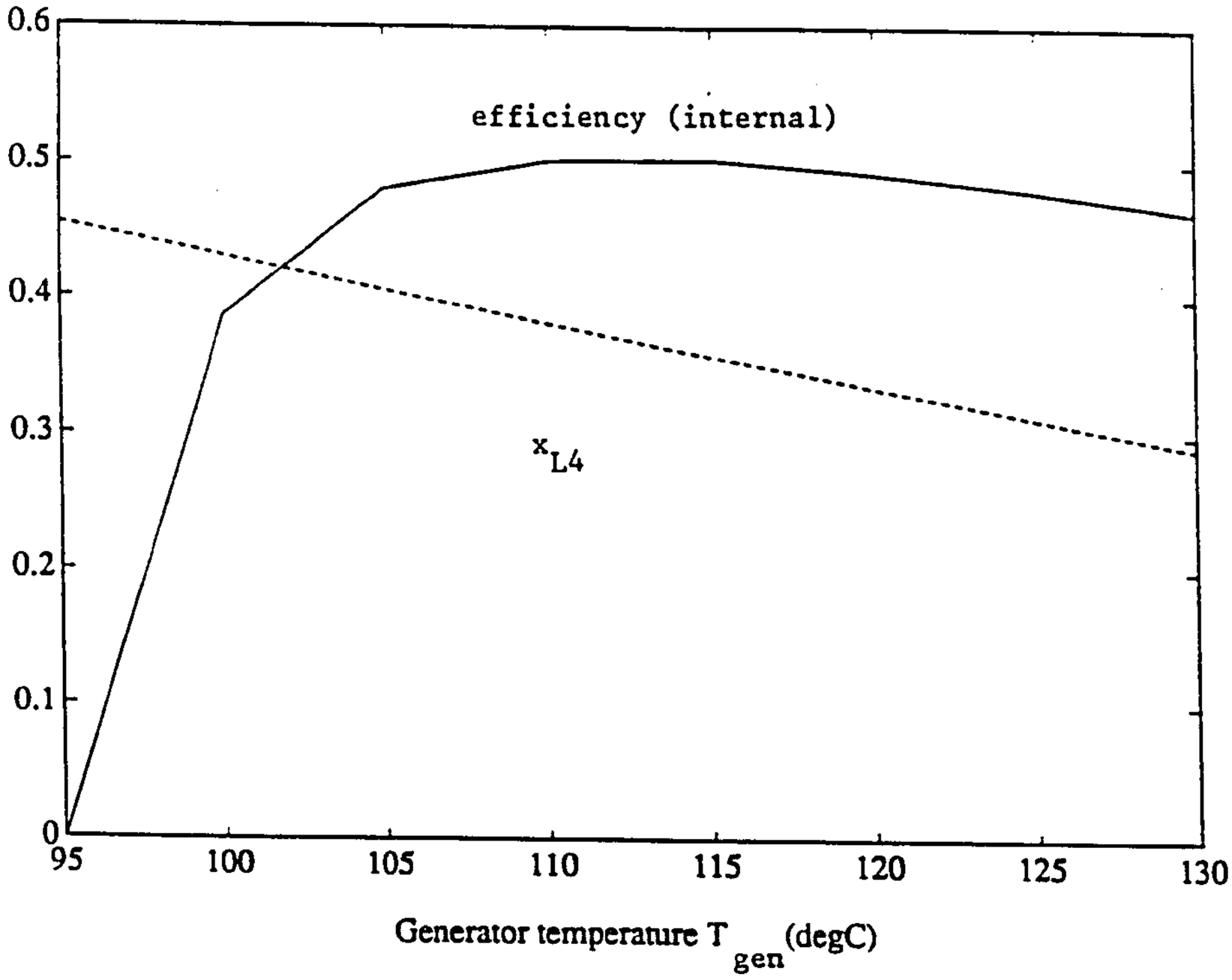

Fig. 1.3.2 The internal efficiency of the continuous pumped (CP) system plotted against boiler or generator temperature. Generator temperature occurs at point 4 on Figure 1.3.1 which illustrates the CP cycle. Parameters for the calculation are given on Table 1.3.1. The plot shows also the variation of final solution concentration, x_{L4}, with boiler temperature T_{gen}.

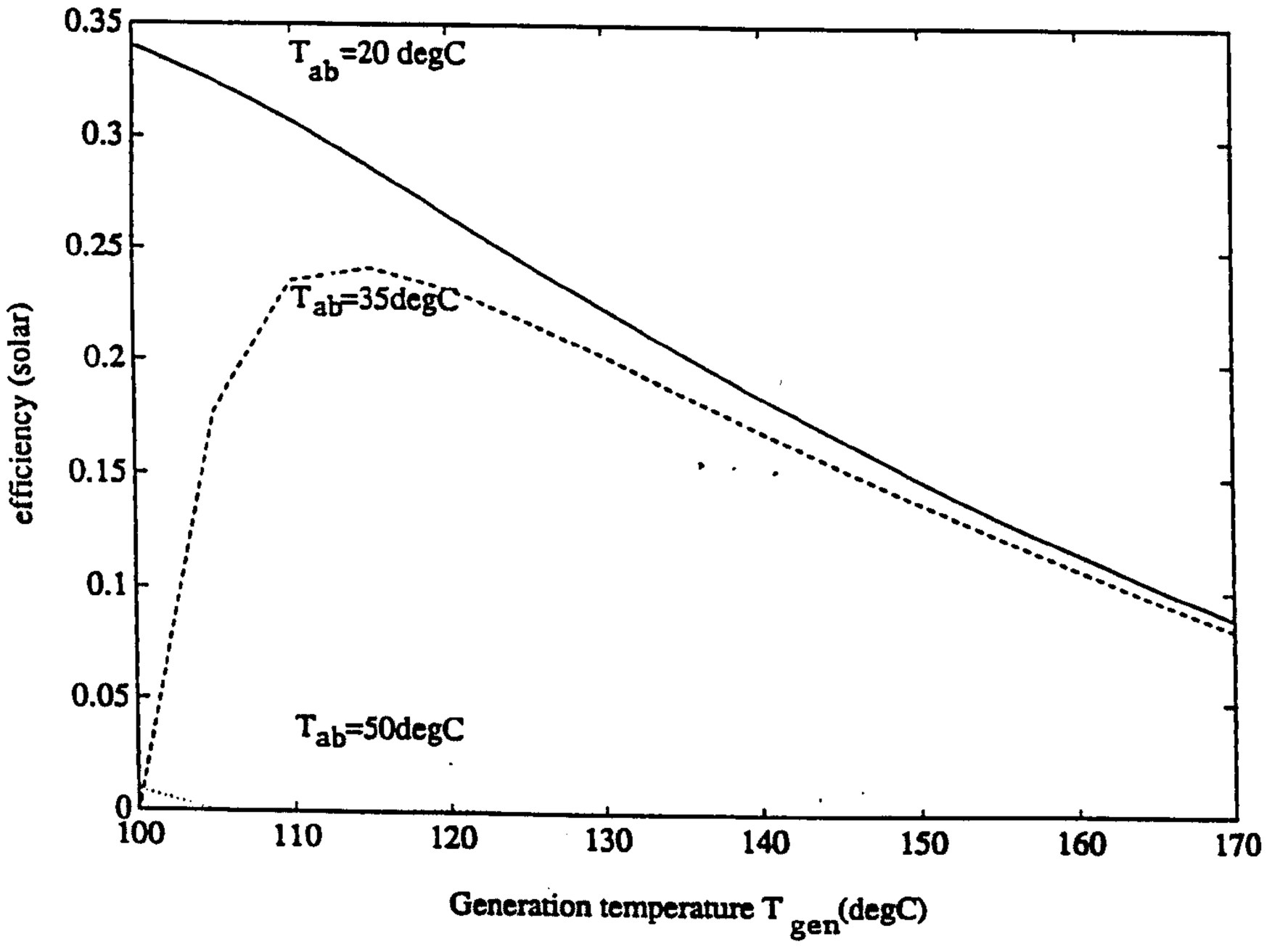

Fig. 1.3.3. The solar efficiency of the CP cycle against boiler temperature T_{gen}, for a range of values of absorption temperature (T_{ab}). Since in the CP system the absorber operates during the day, when low absorber temperatures are more difficult to achieve, this plot illustrates an important disadvantage of the system. Parameter values are given on Table 1.3.1.

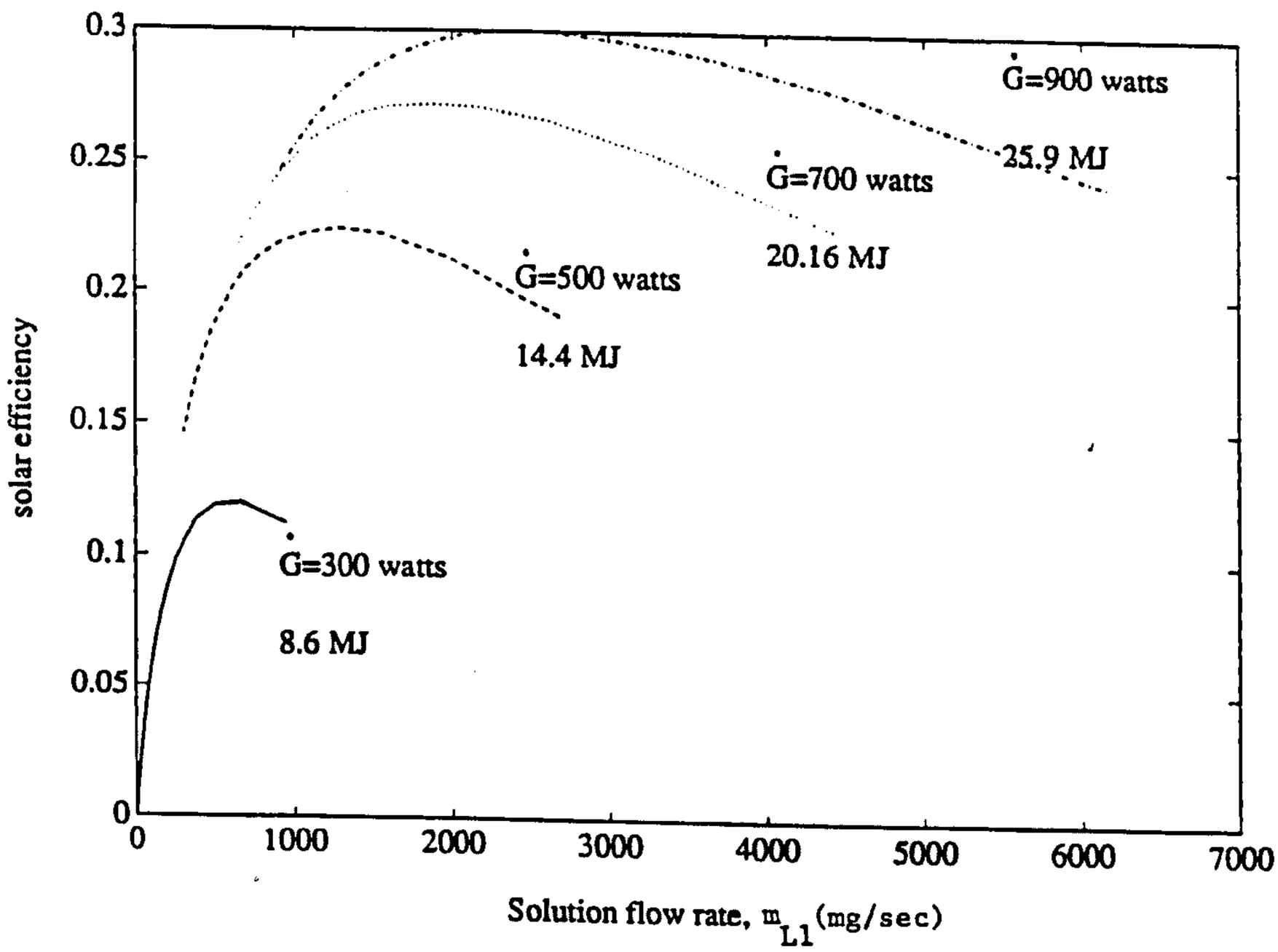

Fig. 1.3.4. The solar efficiency of the CP system against varied solution flow rate. The plot illustrates that different flow rates are required to produce optimum efficiency at different levels of constant solar insolation (assumed absorbed for a period of eight hours). Parameters for the calculation are given in Table 1.3.1.

pumped flow must also be borne in mind, though it may be that where solar energy is used as the source of pump power via photo-voltaic conversion a certain amount of 'built-in' regulation will exist. No study has yet been made of the possible benefit of flow regulation in response to varying ambient temperature, although this may have significance in an air-cooled continuous system, since absorption temperature will be affected. It is noticeable that the CP system does not offer any immediately convenient method of responding to changed rich solution concentration, which will tend to change the value of the optimum flow rate.

The CP system can be designed to respond more flexibly to the expected variations in solar insolation. It can continue to operate at declining generator temperature in the afternoon of a clear day, and its thermal mass is low so that its response to very short durations of usable irradiation is adequately fast.

1.4. The diffusion-absorption system

The "Platen-Munters" or diffusion-absorption system (DA system) is also a continuous system, and like the pumped system the temperature of absorption is likely to be adversely affected by day-time ambient temperatures. A schematic version of the DA circuit is given in fig 1.4.1; it can be seen that analyser and rectification heat reclaim components can be incorporated. The diagram does not show the need for careful levelling of the various components of the low pressure circuit in relation to each other, which is necessary to maintain liquid seals confining the third fluid. The DA system is of very great importance in the development of autonomous and low-maintenance refrigeration systems, since the introduction of a third fluid into the absorption side of the circuit leads to the complete removal of all moving parts. In the province of non-solar applications it is already a successful device meeting precisely this specification with widespread application. The third fluid is an inert gas such as hydrogen or helium and allows a low partial pressure of refrigerant in the evaporator and absorber to exist while total system pressures on either side are balanced. The inert gas is prevented from entering the generator side by liquid seals. The pumping requirement is reduced to a small hydrostatic head which is met by thermosyphon effect vapour produced in the generator or in the pipe work leading into the generator.

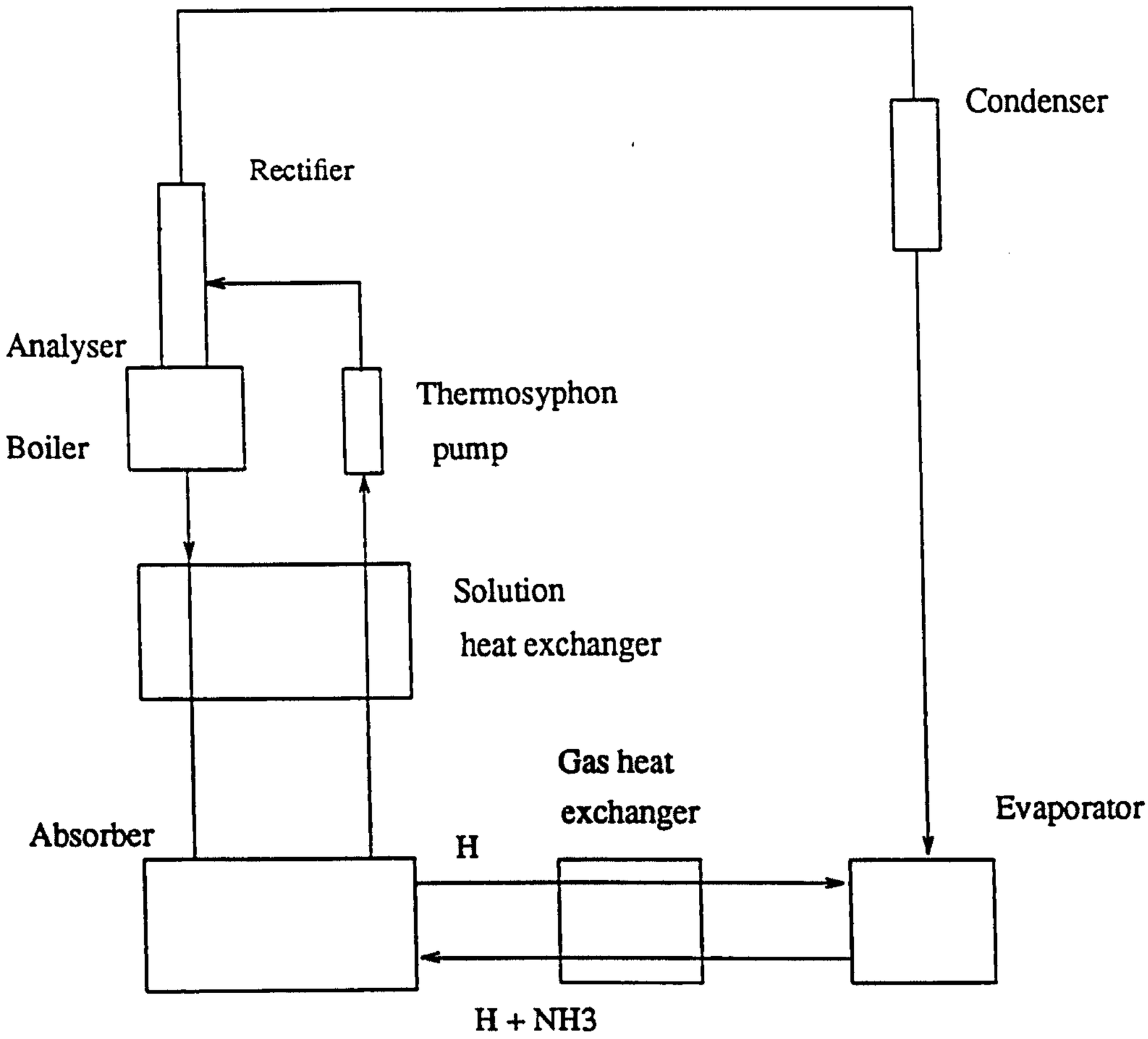

Fig 1.4.1 *The diffusion absorption (DA) or Platen-Munters system.*

Desorption and absorption phases occur concurrently.

The pumping effect, and therefore the circulation rate of the solution on the generator side, is induced by the same heat source which is operating the boiler, and will therefore vary with variations in the input heat. Some studies of the potential for conversion have been made, although at the present time no fully engineered solar DA systems are reported to exist. Hinotani (1984) has shown that the dependency of solution flow on the heat input rate can improve the operation of a generator powered by solar energy. Little study has been made of the effects of varying vapourisation rate and solution flow on the effectiveness of the evaporator, but the experiments of Hinotani and Guttierez (1988) show that it may prove difficult to avoid severe difficulties in this

respect. The indication is that fundamental redesign of all components the DA system is necessary to develop an effective solar version, as in the work of Svensson (1979) and Perrson (1982), and Hinotani (1984). Most practical studies have to date have been limited to partial redesign and conversion, as in the work of Guttierez (1988).

The inclusion into the circuit of a third fluid has detrimental effects on the overall efficiency of the cycle. Cooling in the evaporator is accomplished by diffusion of the refrigerant into the inert gas stream and is therefore limited by the transport capability of the gas. This is a function of its mass flow rate, the extent to which it is loaded with refrigerant on entry to the evaporator, and its temperature. These factors are in turn dependent on the conditions under which absorption is taking place, and the effectiveness of the gas heat exchanger. Cooling by diffusion is inherently less efficient due to the greater practical pressure drops experienced in the gas transport process and the undesirable heat flow from the absorber to the evaporator due to the gas circulation. The difficulties referred to above caused by varying vapourisation rate and solution flow in the absorber tend to push the the operating conditions of the cooling circuit out of its already narrow efficiency band. The DA system is intrinsically not ideal for ice-making because the basic evaporator design induces a widely varying temperature differential along its length, a limitation which will tend to be accentuated by operation at off-design conditions.

A summary of experimental work is made in chapter 2, which indicates that solar DA systems can produce at design conditions internal efficiencies of the order of 0.2 and solar efficiencies of the order of 0.1. These findings correspond to the experience of the manufacturers of conventional DA units; Electrolux expect design COPs of 0.2, and laboratory tests of refined units developed by Sibir, which feature analysis and heat reclaim components, produce COPs of 0.3 at best. (Green, 1985). The effect of inflexibilities to solar power indicate reductions in COP of more than 50%. The very great attractiveness of the DA system as a system devoid of any moving parts, and as a compact system, since no solution reservoir is required, is therefore offset by a high collector and condenser cost. In addition the DA system, as a continuous system, must reject heat of absorption during the day, when sink temperatures in many parts of the world are likely to be higher than at night. Provision of cooling water for this purpose will introduce

expense, a requirement for maintenance, and an element of unreliability. As in the case of all continuous systems, simultaneous rejection of absorption and condensation heat will require larger cooling surface areas than demanded when the heat flows are out of phase, as in an intermittent system, where the same surface can be shared.

1.5. Tabulated summary

The choice of a suitable system for remote cooling will depend on the weighting given to each of the criterea shown on table 1.5.1, which summarises the findings of the present chapter. If high reliability and low maintenance are strict requirements then the choice is narrowed to the DA and IB systems, particularly the DA system which has the additional advantage of greater compactness and fast response. Where auxiliary power sources can complement the solar source then low efficiency and inflexible devices such as these are of greater interest. In practice the use of auxiliary power sources may invite a higher level of complexity overall and lead to the use of cooling devices of higher efficiency.

Chapter 2 reviews the experimental and theoretical evidence collected by researchers which bears directly on the present comparison of systems. Certain other novel and hybrid systems have been devised to provide solar cooling, with an emphasis on the removal of the solution pump in the CP system while obtaining high efficiencies. Some of these have been chosen for review in the next chapter, since they constitute attempts to develop systems with a minimum of active and intricate parts.

1.6. The intermittent regenerative system

The proposal for a hybrid system which combined the advantages of a circulating solution in the generator, allowing reclaim of sensible heat, and the simplicity of an intermittent system, requiring a minimum of intricate parts and no active solution pump, was first made by Trombe and Foex (1957). A version of the IR system, which included the use of a flat plate collector, was built and tested by Van Paasen (1986).

A schematic diagram of the system in the form developed here is given in figure 1.6.1. This design differs in some fundamental respects from the designs considered by Trombe and Van Paassen. The operation of the system can be described as follows. Sufficient solution is stored in

System	Supportability	Solar COP	Component cost	Weight
IB	active components: check valve, valve for nightly release of absorption heat (manual or automatic) expansion valve or drain valve depending on type of evaporator	less than 0.12 since not flexible to variations in $\dot{G}$	Aab low since integral collector and absorber reduced cooling surface since Qcon and Qab out of phase	WR=7
CP	active components: solution pump expansion valve regulating expansion valve if dry expansion evaporator used evap purging if gravity circulating evaporator used day and night running possible with auxiliary heat source	0.2 day absorption at high temperature no self regulation of flow	separate pump power supply larger cooling surface since Qcon and Qab in phase	WR=2.5 less solution charge cost
DA	No active components day and night running possible with auxiliary heat source	less than 0.07 since evaporator matching suspect uneven Tev may limit application	additional component: gas heat exchanger plumbing more complex larger cooling surface since Qcon and Qab in phase	WR=2.5 less solution charge cost

Table 1.5.1 *Summary of conclusions reached in review of intermittent basic (IB), continuous pumped (CP), and diffusion-absorption (DA) cycles.*

the reservoir to allow generation of refrigerant to continue throughout the day, implying the IR system suffers the disadvantage of any intermittent system in requiring a large solution charge. The solution is boiled in the tube between the points 2 and 3 where the associated reduction in bulk density creates a thermosyphonic pressure head which draws rich solution from the upper part of the reservoir and returns weak solution to the lower part. Counter-flow heat exchange can be arranged in a solution heat exchanger, allowing reclaim of liquid sensible heat. Vapour

formed in the boiler is differentially condensed in the rectifier and then passed to the condenser, finally collecting in the receiver. A dry expansion evaporator is shown connected to the receiver, through which evaporated refrigerant passes during the absorption phase before re-absorption in the lower portion of the reservoir.

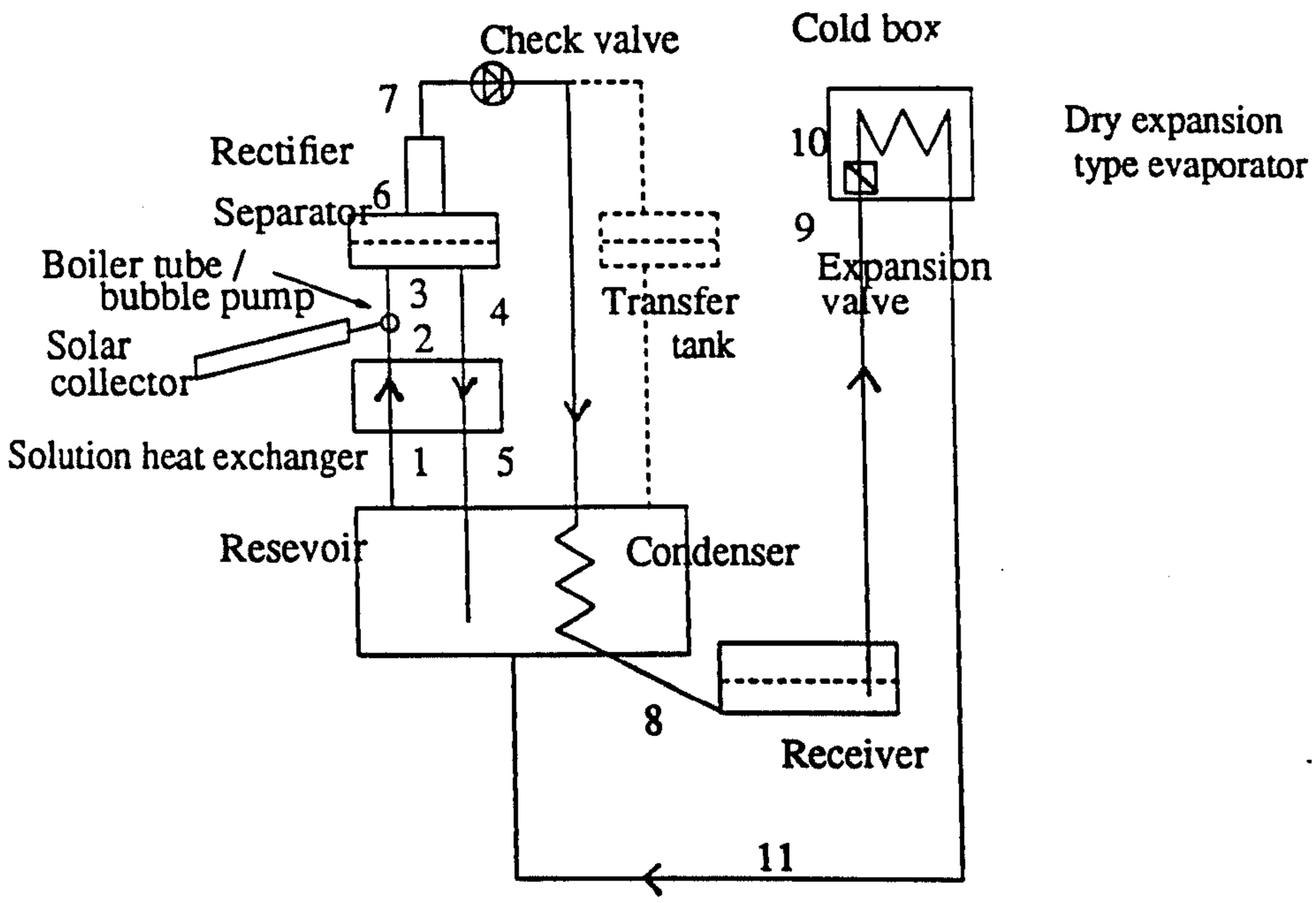

Fig 1.6.1 *The intermittent regenerative system (IR) in the novel form proposed in this study. The transfer tank is an optional component.*

In the design schematic the condenser is immersed in the reservoir in order that the heat of condensation as well as the heat of absorption can be removed from the reservoir by the same cooling circuit; the reservoir cooling circuit is not shown. In the absence of a transfer tank (shown by broken lines) the progressive depletion of solution mass during the desorption phase is accomodated by the separator vessel. The shorthand label "FVR" (fixed volume reservoir) is used to describe this arrangement. Harvey (1987) suggested that performance could be significantly improved with a reduction in size of the separator. Accordingly the alternative arrangement proposed here is that the change of solution mass can in the major part be accomodated by the addition of a transfer tank. In this case the separator becomes a small container which allows liquid to enter (carried by vapour) and leave at its base while vapour rises through an upper exit. It does

	Support	Solar COP	Component cost	Weight
IR	Similar to IB	better than CP, since absorption governed by lower night temperature desorption phase flexible to variations in $\dot{G}$	reduced cooling surface area since Qcon and Qab out of phase	WR: similar to IB

Table 1.6.1 *Summary of potential advantages of the IR system, to provide comparison with table 1.5.1.*

not need to be large enough to store a mass of solution corresponding to the mass of refrigerant that is expected to collect in the receiver during the desorption phase, as is the case with the FVR circuit. The small separator can nevertheless be depicted in exactly the same way as the FVR separator in the schematic diagram of fig 1.6.1, the only difference being capacity. A transfer tank is then placed at the same elevation as this small separator. The tank can in fact be the uppper portion of the reservoir, or can be a discreet tank connected by pipework to the reservoir as shown. The transfer tank has enough storage volume to accomodate the loss in solution mass due to refrigerant collection in the receiver. It is a "squat" tank with low height relative to diameter, as shown. This shape causes the fall in liquid level associated with a given refrigerant yield to be small. This in turn ensures that the liquid level reduction in the separator is small so that the height required of the separator container is minimised. The separator then acts in a manner very similar to that of a conventional continuous machine, either a continuous pumped or a bubble-pumped diffusion-absorption machine. A difference remains in that the separator level reduces during the desorption period, but since this can be limited to a fall of two or three centimetres, it is possible to build into the bubble pump/boiler unit cost-saving and efficiency-raising features (for instance, analysis, and rectification heat reclaim) which are developed already for continuous machines.

The transfer tank liquid surface is separated from the vapour above it by an impermeable membrane, such as a rubber bellows. This bellows can contract as the level drops. The vapour above the bellows is plumbed in contact with the vapour in the pipework connecting the separator

to the condenser. The resulting equalisation of pressures in the transfer tank and separator ensures that the liquid surface level in the transfer tank corresponds to the separator liquid surface level. As desorption proceeds the separator always remains partially filled with liquid, so eliminating the danger of circulation stopping due to drying out of the separator. The transfer tank acts as a gravity pump filling the separator at all times. The major advantage of this arrangement is that the mass of liquid in the transfer tank can remain cold. In the FVR system the equivalent mass of liquid absorbs a portion of the energy input in sensible heating.

If the transfer tank is seen as part of or as an appendage to the reservoir it removes the constraint of reservoir fixed volume, and the system incorporating the transfer tank is accordingly labelled the ""VVR" (variable volume reservoir) system.

The thermosyphonic pumping principle introduces to the hybrid IR system the advantage of 'built in' flow regulation to absorb variations in solar intensity and day-time sink temperature, without the attendent disadvantages of concurrent absorption noted with respect to the CP and DA systems. The hybrid is described as an intermittent regenerative system (IR) since the term regenerative signifies sensible heat reclaim or recuperation. The circuit considered here is fundamentally advanced in relation to the devices investigated by Trombe and Foex (1957) and Van Paassen (1985). The transfer tank has the effect of reducing the generator thermal mass, leading to faster response and higher efficiency at off-design conditions. The novel circuit allows the IR system to be refined with the addition of rectifier heat reclaim and analysis components. Low thermal mass collectors are integrated into the design, and the cost effectiveness of the heat removal process as a whole has been increased by the rationalised design described in Chapter 4 and Appendix A. Table 1.6.1 compares the IR system qualitatively with the systems already reviewed. Subsequent chapters form a study of the IR system which seeks to establish whether it can fulfill the promise it shows in relation to the other systems.

Chapter 2: Literature Survey

2.1. Introduction

A large literature now exists on the subject of solar refrigeration. A summary of the contents of a number of research papers is given here, most of the papers chosen being ones which describe experimental work on the systems described in chapter 1. The present chapter provides a reference which is useful in validating the analytical approach developed in chapters 1 and 3. It has the function also of assembling data on practical difficulties met with in the implementation of solar refrigerator designs, which is informative in an attempt to produce more advanced designs. It has been necessary to describe the operating conditions under which tests have been conducted in some detail because of the sensitivity of solar refrigerator performance to a number of parameters. Performance results are nevertheless summarised in table 2.7 and provide a context for evaluating the experimental results obtained for the IR system as given in chapter 6.

2.2. Intermittent basic (IB) systems with aqua-ammonia

2.2.1. University of Wisconsin, USA

Williams et al (1957) report on theoretical and experimental studies made on solar absorption cooling possibilities. The studies encompass a comparison of the suitability of various absorbent-refrigerant pairs, out of which a preference for ammonia-water emerges. The authors are firstly concerned to meet a need for small domestic coolers producing about 1 MJ of cooling per day, not necessarily at freezing temperatures, but indicate that their study can progress to an investigation of the design of larger units for ice making. Later the study is reported again by Chung and Duffie (1961) with the addition of more detailed proposals on the design of a unit sized to produce 66 kg of ice per day, as described below in section 4.1.

The design of the domestic cooler is approached by maximising durability and inexpense, and is to a large extent a solar modification of the portable "Icy-ball" (or "La Frigor") cooler. Figs 2.2.1.1 and 2.2.1.2 illustrate the design of the generator. No attempt is made to avoid manual operating procedures, while the absence of moving parts and parasitic power requirements is maintained. It is recognised that the cost of solar collection is high, and that therefore a system which frees the use of the solar collector for other purposes will reduce the effective cost. It is proposed that parabolic reflecting shells are used, and sized relative to the refrigerator so that the generation phase requires less than 2 hours, allowing the remaining 22 hours in a day cycle to be devoted to evaporation and absorption. Given the offset in the collector cost, this approach has the advantage of minimising the heat transfer duties of the evaporator and absorber, so reducing their cost or improving their performance in unfavourable operating conditions. Once generation is completed the user removes the generator from the collector and places it in a water cooling bath which then acts to absorb the heat of re-mixing of refrigerant and absorbent. Simultaneously the condenser is removed from a cooling water bath and placed in the cold space where it acts as an evaporator. Air-cooling can also be considered. The drawing presented of the generator shows the use of a liquid seal component. The device is described below in section 4.2; it prevents absorption of pure ammonia onto the solution surface in the generator/absorber during absorption. Were this to happen, the absorption pressure would be too high to allow evaporation at the desired temperatures. Instead the the vapour stream is conducted into the liquid-filled portion of the vessel.

The cycle analysis adopted (developed by Linge in 1929) defines internal efficiency (η_i) as the ratio of heat absorbed by refrigerant during refrigeration (Q_{ev}) to the heat absorbed by the generator contents during generation (Q_{gen}). A solar heating ratio is then defined as the ratio of Q_{gen} to radiation incident on the collector. Internal efficiency is calculated as a function of five important input parameters: rich solution concentration (x_{L1}), absorption temperature ($T_{gen(max)}$), condensation temperature (T_{con}), and evaporation temperature (T_{ev}). The results are reproduced in figs 2.2.1.3 and 2.2.1.4. At a condensing temperature of 30 degC, a T_{ev} of -4 degC, a T_{ab} of 27 degC (corresponding to a solution charge concentration of 0.5), internal efficiency optimises at

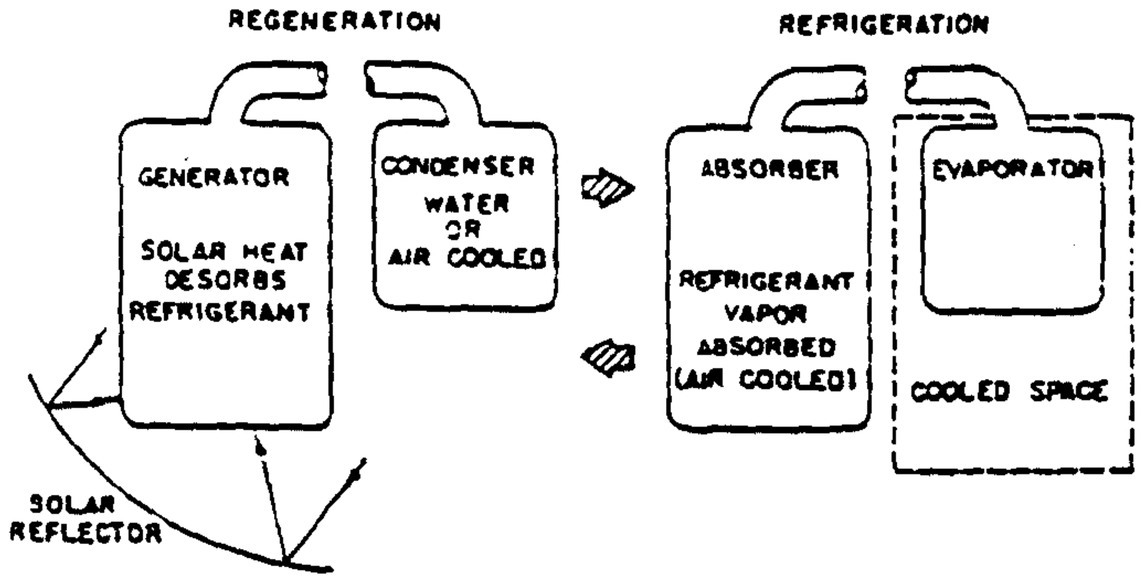

Diagram of a simple intermittent cooler. Each of the two vessels has dual functions: during regeneration as shown on the left, generator-absorber acts as generator and condenser-evaporator acts as condenser: during refrigeration as shown on right, the generator-absorber acts as absorber and the condenser-evaporator acts as evaporator

Fig. 2.2.1.1 from Williams (1957, 1958)

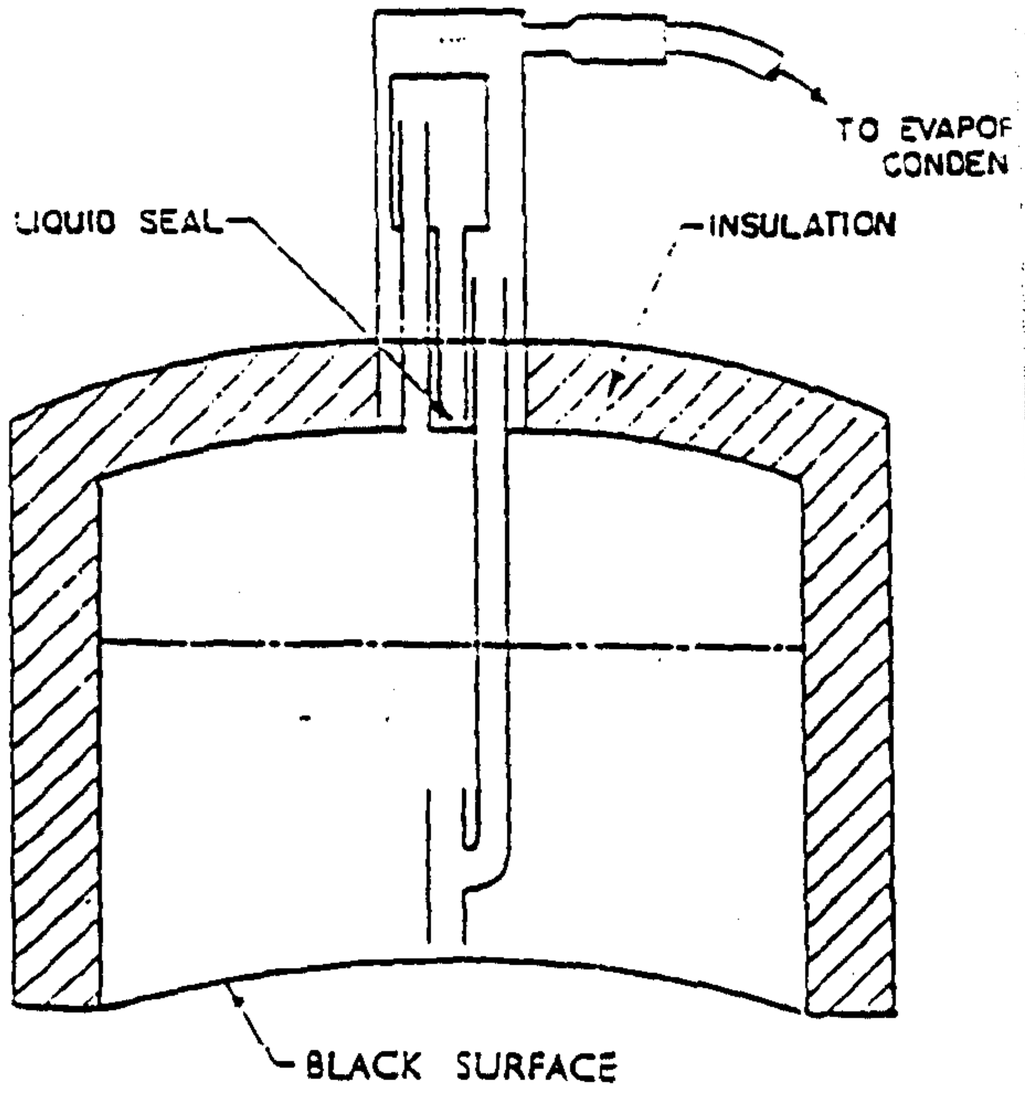

Fig. 2.2.1.2 from Williams (1957, 195

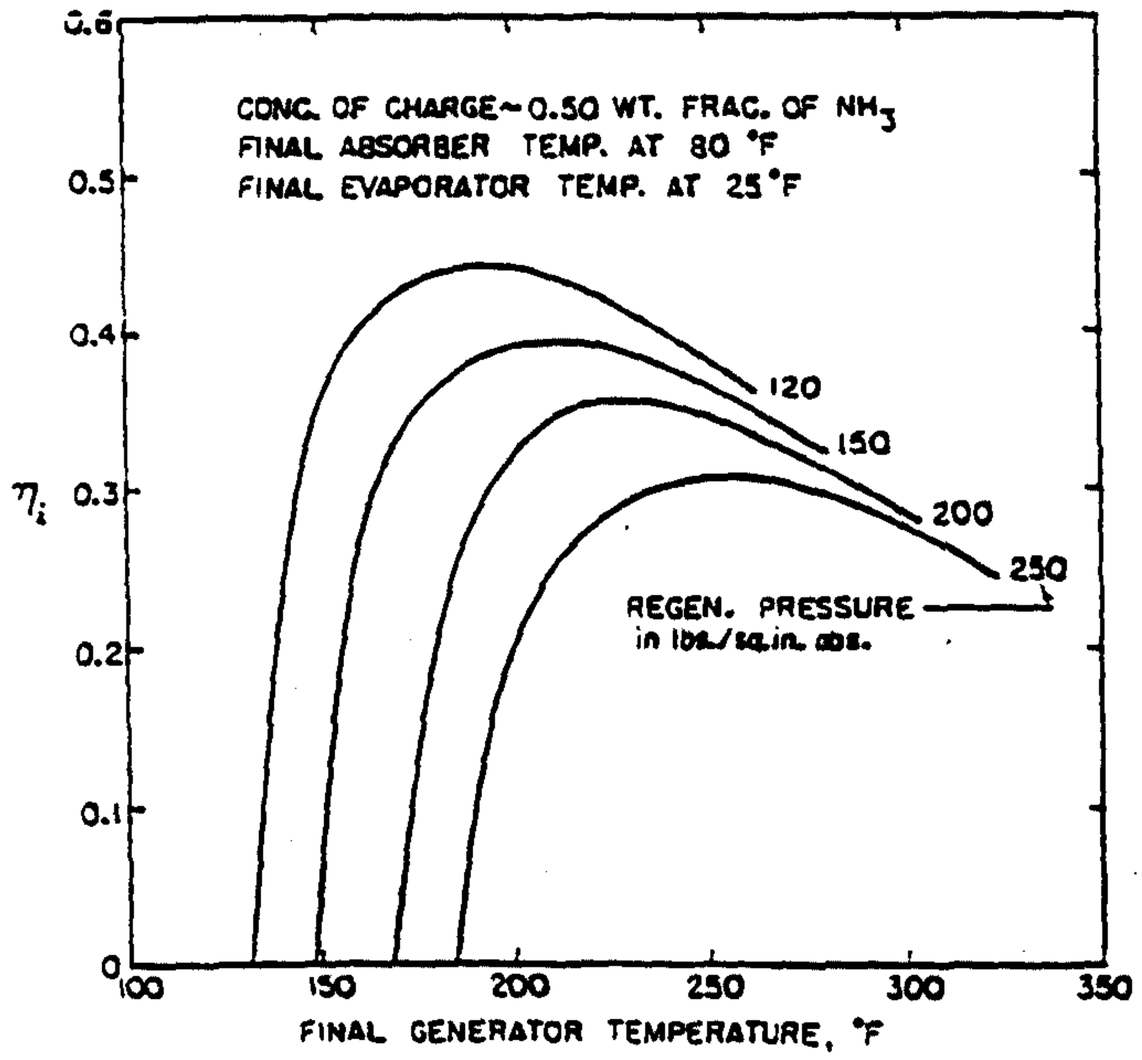

Fig 2.2.1.3 from Williams (1957, 1958)

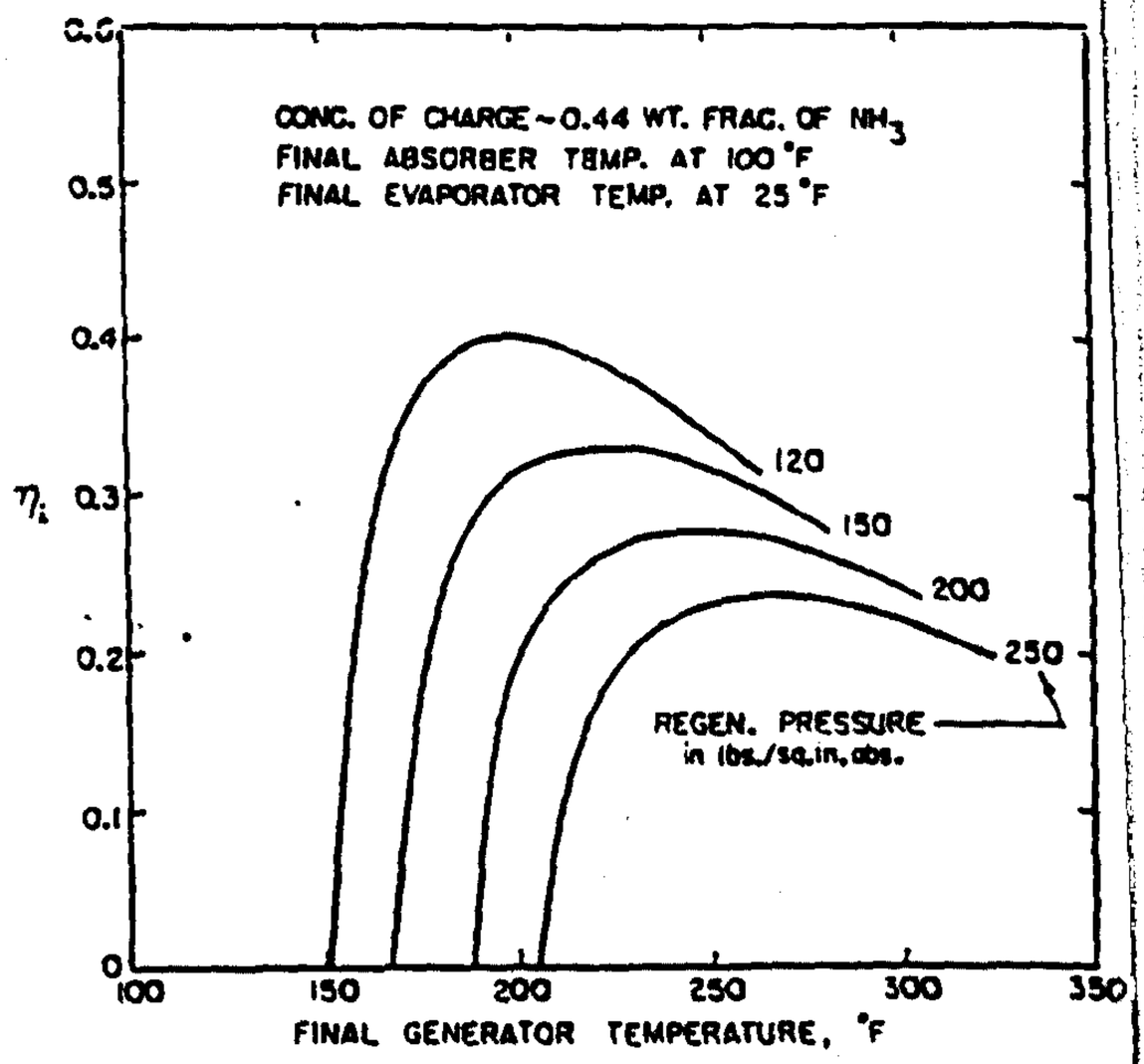

Fig. 2.2.1.4 from Williams (1957, 195

0.37 when $T_{gen(max)}$ is 100 degC. Above this temperature internal efficiency falls off and sensible heating of the weak solution takes an increasing amount of the available energy. Chung and Duffie (1961) also report on the theoretical study and mention that the calculation fixes the differential condensation taking place in the rectifier as 10% by weight of the vapour leaving the generator. The later paper also shows the result of varying this ratio, an optimum value of 9.5% being found to exist given parameter values of $T_{gen(max)}$=121, T_{con}=26, T_{ab}=38, T_{ev}=4 degC.

Williams explains that the reduction in COP due to rising T_{con} (at a given $T_{gen(max)}$) is due to the higher equilibrium concentration found at higher generating pressures, which causes a greater proportion of the generation heat to be devoted to sensible heating of the solution. Put another way, one can say that the concentration swing is restricted and that therefore less vapour is generated while sensible heating of a greater mass of liquid to the same final temperature must nevertheless be accomplished. When the final absorption temperature is raised to 38 degC, such that x_{L1} becomes 0.44, the optimum internal efficiency falls to 0.32, while the corresponding $T_{gen(max)}$ rises to 107 decC.

Results for a practical test are given. Internal efficiencies of the order of 0.36 are obtained experimentally with T_{con}=28 degC, T_{ev} approximately 0 degC, initial concentration 0.44, $T_{gen(max)}$= 121 degC. The COP is calculated by modelling the solar energy flow to comprise four components, the optical loss (scattering due to reflector imperfections and dust, and imperfect absorption) consuming 33%, the convective loss due to imperfect insulation of the generator and reflector consuming 24%, sensible heating of the steel consuming 3%, and finally the remaining 40% being utilised by the internal cycle. Overall solar COP in the range 0.14 to 0.16 were obtained. By use of a flexible connection to the evaporator, allowing its mass to be continuously monitored, the rate of heat extraction from the cold box could be measured. This was found to be proportional to the evaporator surface area and to the temperature difference between the the cold box interior and the evaporator interior raised to power 1.25. A modification was made to the heat absorbing surface of the generator, whereby its original convex shape was altered to become concave. No comment is given on the effect of this, but no attributable improvement in performance can be detected in the listing provided of test results.

2.2.2. University of Florida

Eisenstadt (1959) conducted studies very similar to those being undertaken at Wisconsin, but with more of an emphasis on airconditioning applications of solar absorption cooling, and with more readiness to accept designs including electrically operated pumps. They accepted the value of the ammonia- water pair and first considered the basic cycle with no recovery of solution sensible heat. They observed that the basic cycle was bounded by the values of $T_{gen(max)}$, T_{con}, and T_{ab}, and so built an experimental unit (fig 2.2.2.1) which allowed measurement of the effect of these variables on four system parameters. These were yield (M_{ref}), cooling rate, COP, and minimum T_{ev}. Their results are reproduced on fig 2.2.2.2 In the case of COP it is "probable COP" that must be read as the actual curves were erroneous due to imperfect design of the evaporator allowing liquid entrainment into the absorber. Their experiment differed from that of Williams in that T_{con} and T_{ab} could be maintained externally as constants, and they took relatively low values of $T_{gen(max)}$ as the range permitted by use of flat plate collectors. The trends shown are in accordance with theory, but the observation that cooling rate declines as x_{L1} rises is of interest, since it implies that large absorber and evaporator heat exchangers are needed. So whereas in air-conditioning applications high T_{ev}s are acceptable and higher overall efficiency can be obtained, nevertheless some extra cost is incurred.

In order to provide airconditioning Eisenstadt suggests a quasi-continuous system, whereby two intermittent systems are run out of phase with each other. Eisenstadt makes the reservation that temperature control difficulties will tend to be encountered in applications of the basic intermittent cycle.

Moore and Farber (1967) report on the design of a combined generator and solar collector. Tests on the unit constructed established the feasibility of the design and showed therefore that heat loss occuring between the collector and generator of a solar refrigeration system could be eliminated.

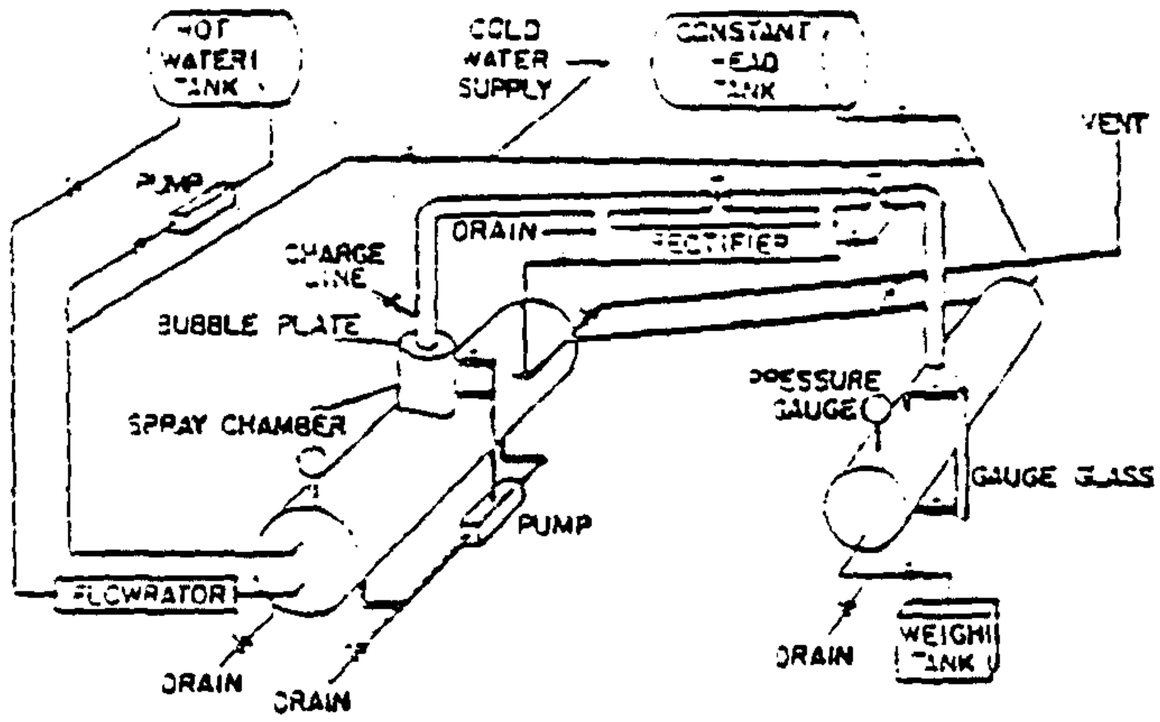

Fig. 2.2.2.1 from Eisenstadt (1960)

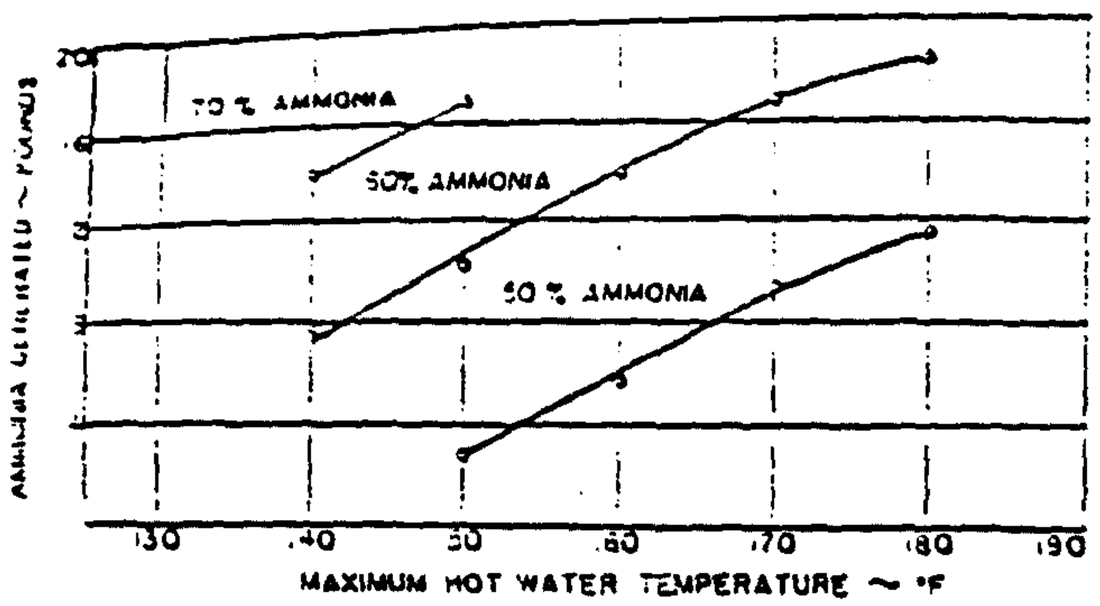

(a) Weight of ammonia

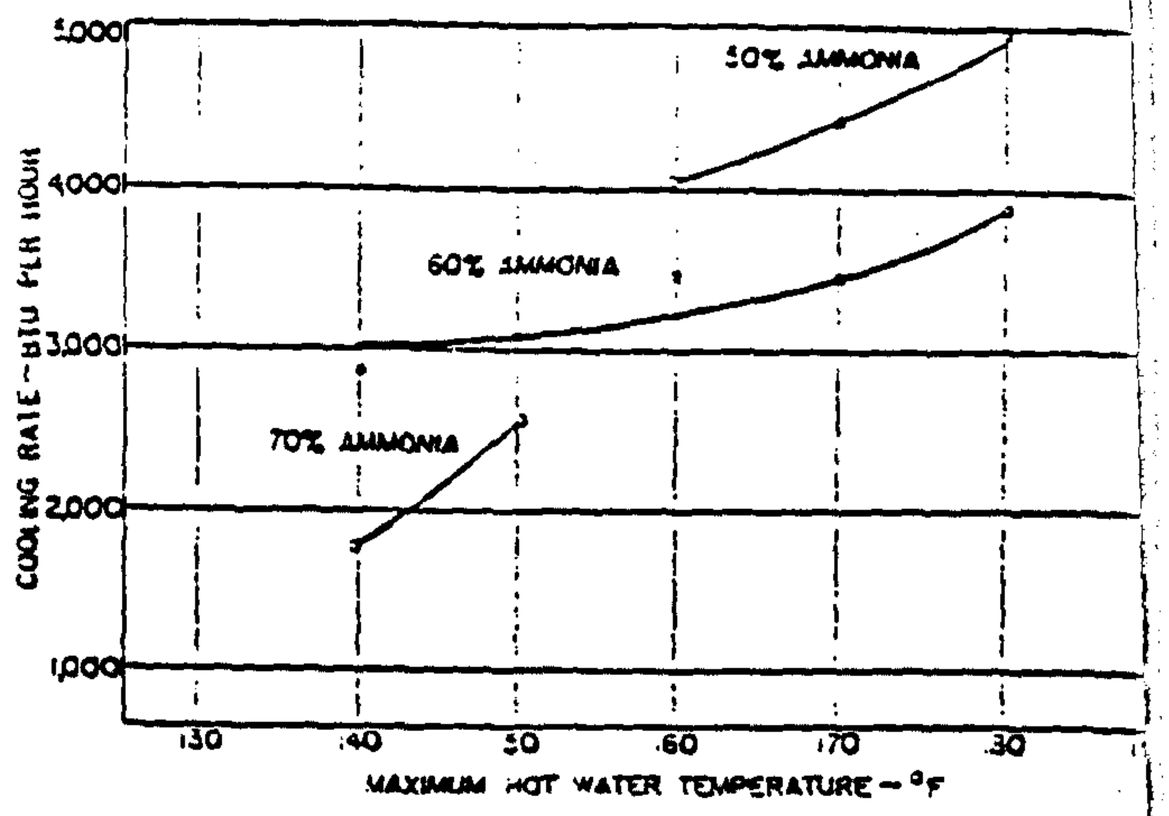

(b) Cooling Rate

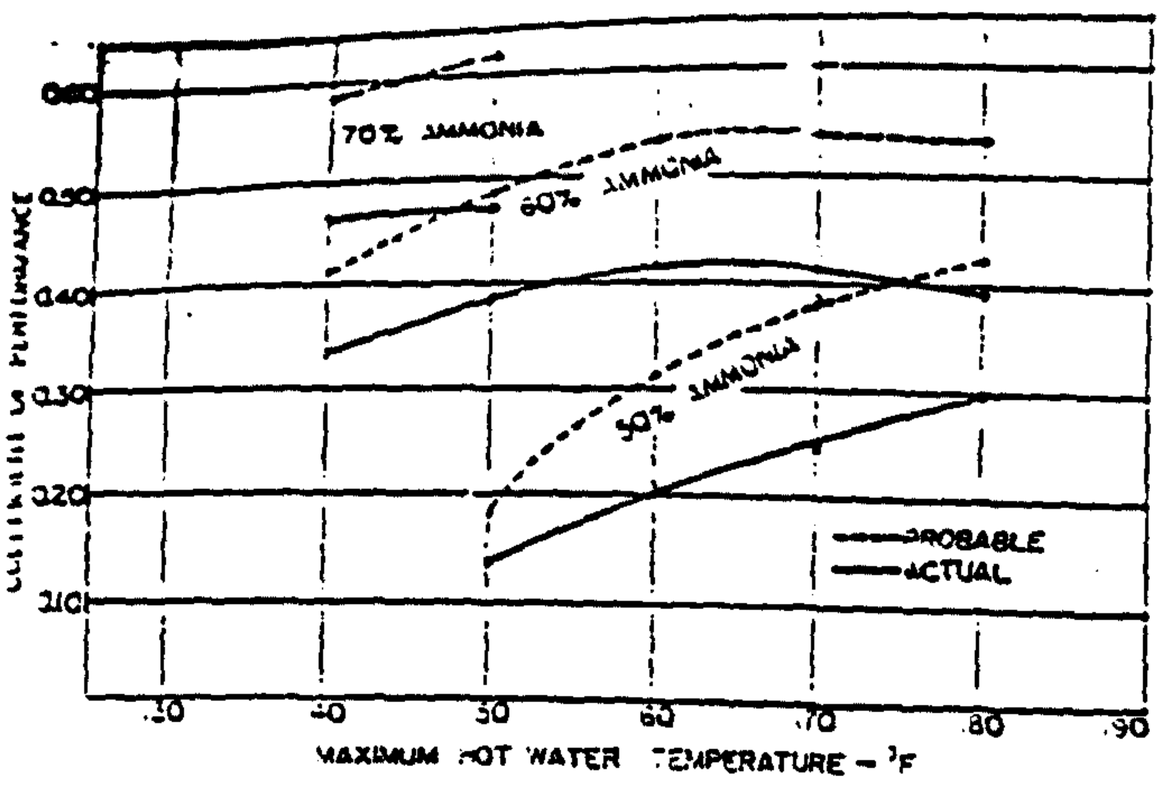

(c) COP

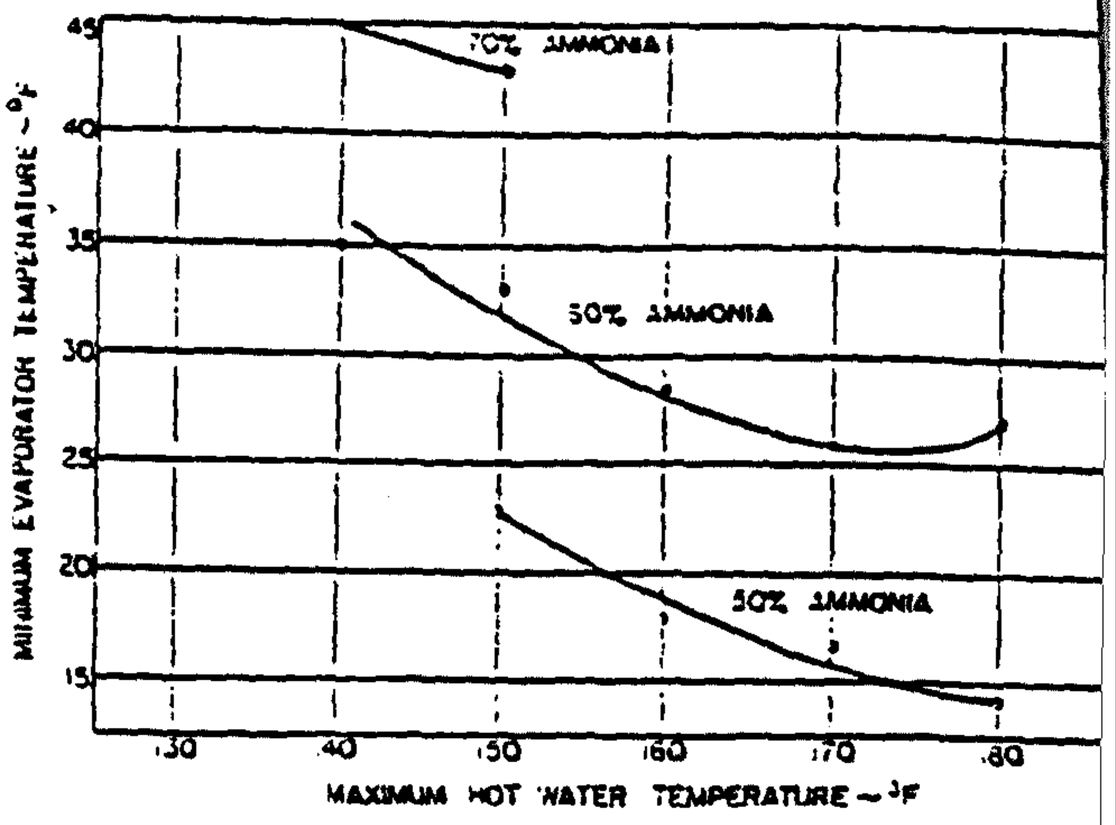

(d) Minimum Tev

Fig. 2.2.2.2 from Eisenstadt (1960)

2.2.3. University of Sri Lanka, Colombo

Detailed results on experiments with solar driven aqua-ammonia cycles were also presented by Chinnappa (1961), together with a theoretical investigation following the approach of Williams. He first conducted laboratory experiments (1961) and later built a solar refrigerator (1962). This refrigerator included a generator/collector component through which the solution circulated by means of thermosyphon and bubble-pumping action, as shown in fig 2.2.3.1. A reservoir contains an unspecified proportion of the solution. It is not clear whether the length of the generation period is determined by the emptying time of the header, but since this would correspond to his use of a bulk-heat analysis, it is likely. In the course of four test runs, he records solar COP values in the range 5.4% to 6.0%. The minimum evaporating temperatures are in the range -13 to -9 degC. Initial concentration is 0.46, condensing temperature is 36 degC, and final generating temperatures are in the range 93 to 100 degC. The overall efficiency of the collector is estimated to be 21%, which includes a 13% loss of solar radiation in sensible heating of the collector and generator materials.

Whereas the theoretical values of cycle COP are calculated to be between 27% and 32% for test conditions, actual values were 24% to 28%. The major reason for the discrepancy was that condensation took place at a higher temperature than allowed for theoretically, resulting in less concentration shift in the solution at the maximum temperatures obtainable by the collector.

In fact the discrepancy found here to some extent repeated the results of Chinnappa's earlier laboratory tests (1961), where theoretical and actual COPs were compared. The major finding of the laboratory experiment was that insufficient condenser surface area would seriously effect the performance of the refrigerator, as excessive temperature differences would occur between the cooling medium and the condensate. This would raise final solution concentration and reduce yield (M_{ref}). Chinnappa points out that the gain from increased heat input (as would be found at high insolation levels) in his experiment was offset by a factor of 0.6 because of this effect. In general for all laboratory tests practical COP values lagged 5 to 15% below theoretical values, partly for this reason, but also because the theory had not allowed for the sensible cooling required each cycle of the container which doubled as an evaporator and condenser. Further, he

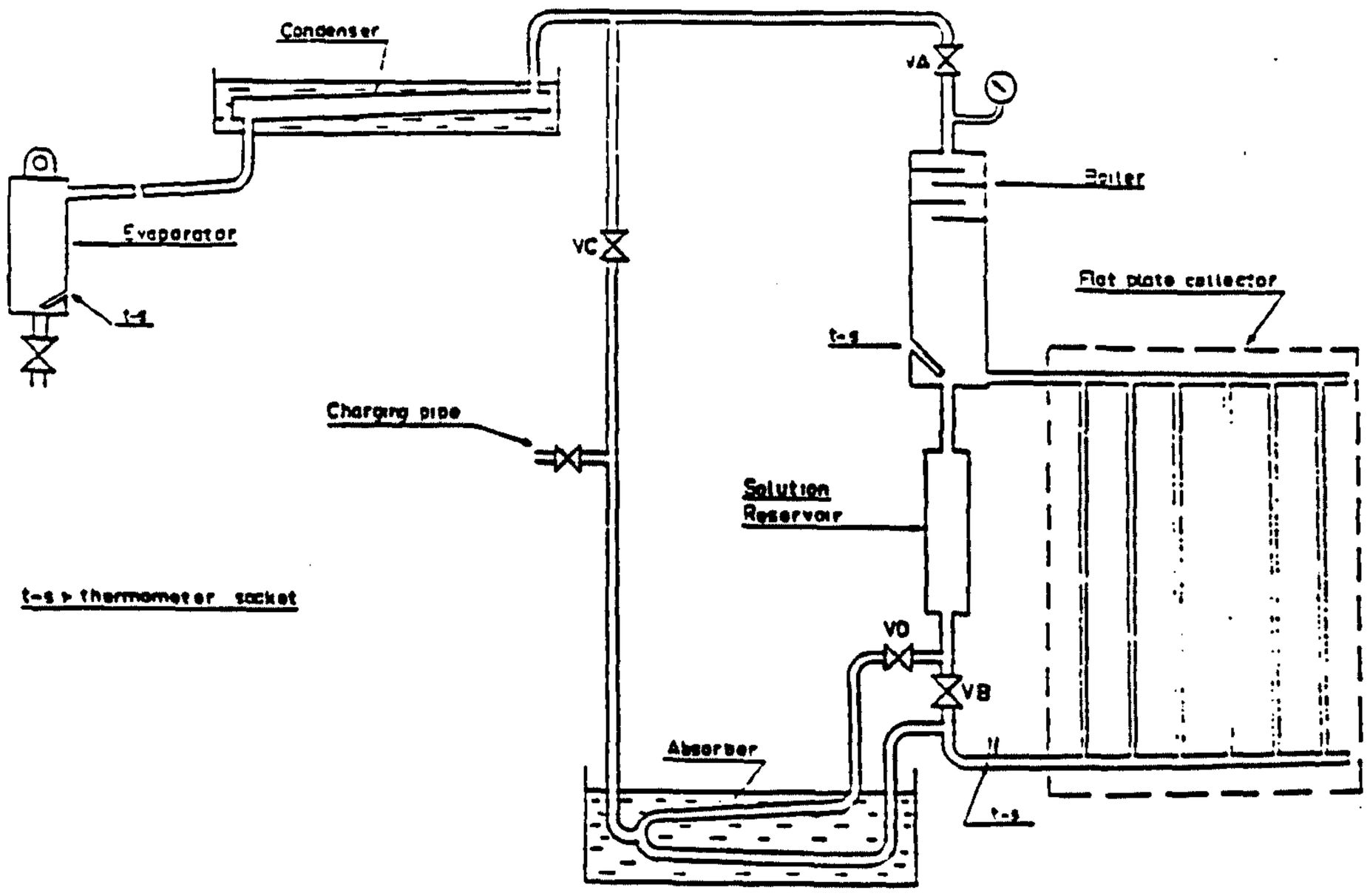

t-s = thermometer socket

Fig. 2.2.3.1 from Chinnappa (1961)

had theoretically assumed perfect rectification, which was not attained. He noted another practical effect, which was that a pressure difference was needed to drive refrigerant vapour into the solution during absorption, so raising the minimum temperature of the distillate in relation to the theoretically assumed value. Chinnappa's analytical work caused him to point out that cycle COP increases with increasing initial concentration, because this causes generation to start at lower temperatures giving rise to a greater concentration swing to achieve the same maximum generator temperature at the same condensing pressure.

Chinnappa comments on the possible use of a heat exchanger to recover sensible heat, and estimates that solar COP could be raised by about 50% to values of 8 or 9% by such a refinement. He does not give details of how this estimate is made. In the present context it is worth attempting an estimate based on Chinnappa's collector and cycle performance. A heat exchanger of high effectiveness would at worst increase the loss of solar radiation to sensible heating of materials to 18% from the original 13%. Collector efficiency would then reduce from 21% to 16%. The regenerator would double the cycle COP, so that the net effect would be a 50% increase in solar COP just as Chinnappa estimates. It is then a fair conclusion that attempts to improve the overall COP should be addressed as much to reduction of hot side thermal mass as to cycle refinements such as the introduction of a solution heat exchanger.

Chinnappa does not mention the advantages of the circulating generator with respect to maximising mean performance over periods containing days of low and high solar energy availability.

2.2.4. Asian Institute of Technology, Thailand

Exell (1978) constructed an aqua-ammonia prototype solar refrigerator incorporating the collector/generator design recommended by Moore and Farber (1967) scaled to form a collecting area of 1.44m^2. An auxiliary plane mirror was used to augment the captured radiation by manual readjustment of its position each hour, first on the western edge of the collector in the morning, then on the eastern edge in the afternoon. This had the effect of increasing the captured insolation on a typical bright day from 28.2 MJ to 38.6 MJ. Temperatures measured showed that the heat of

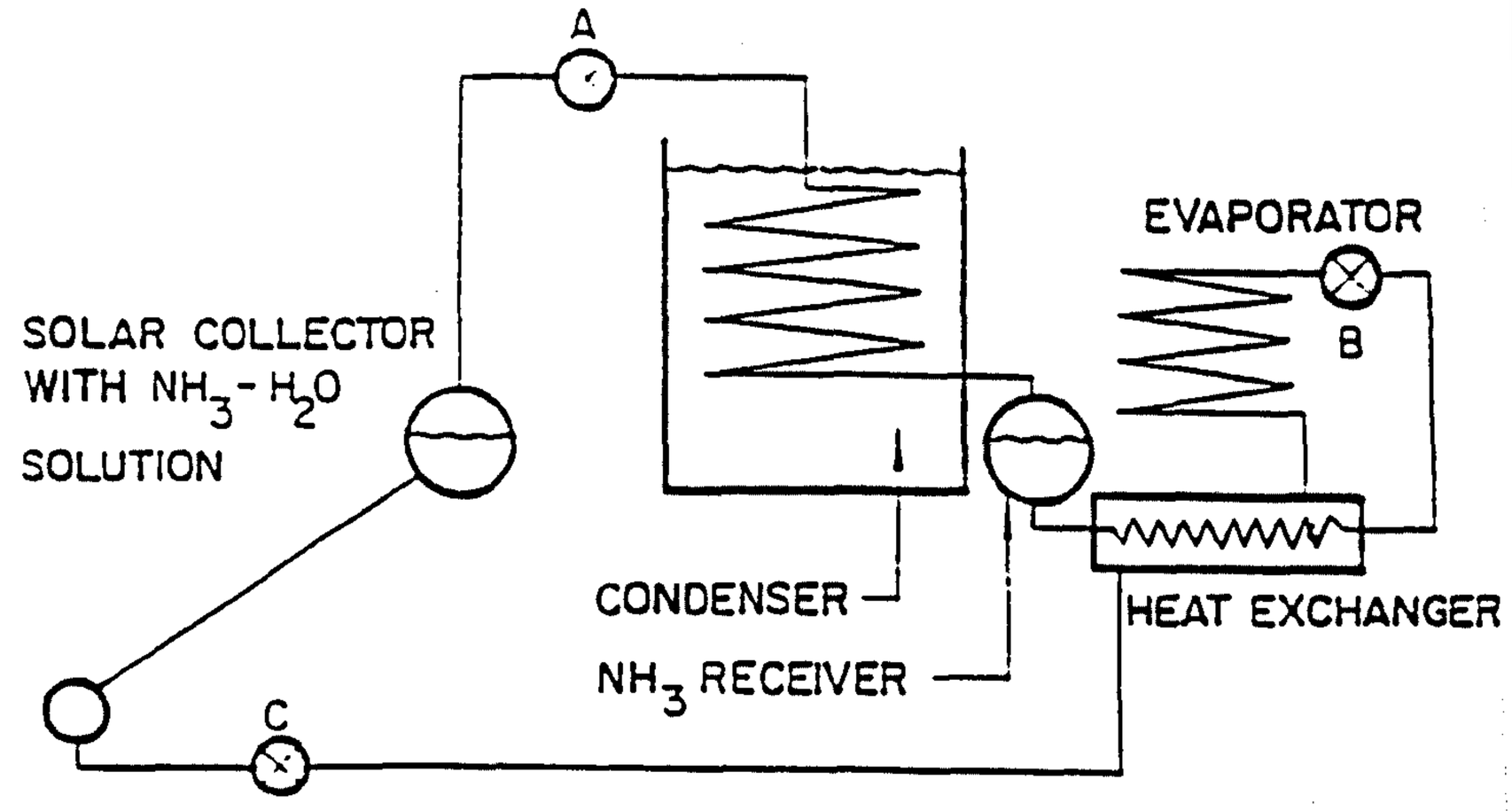

Model I

Fig. 2.2.4.1 from Exell (1981)

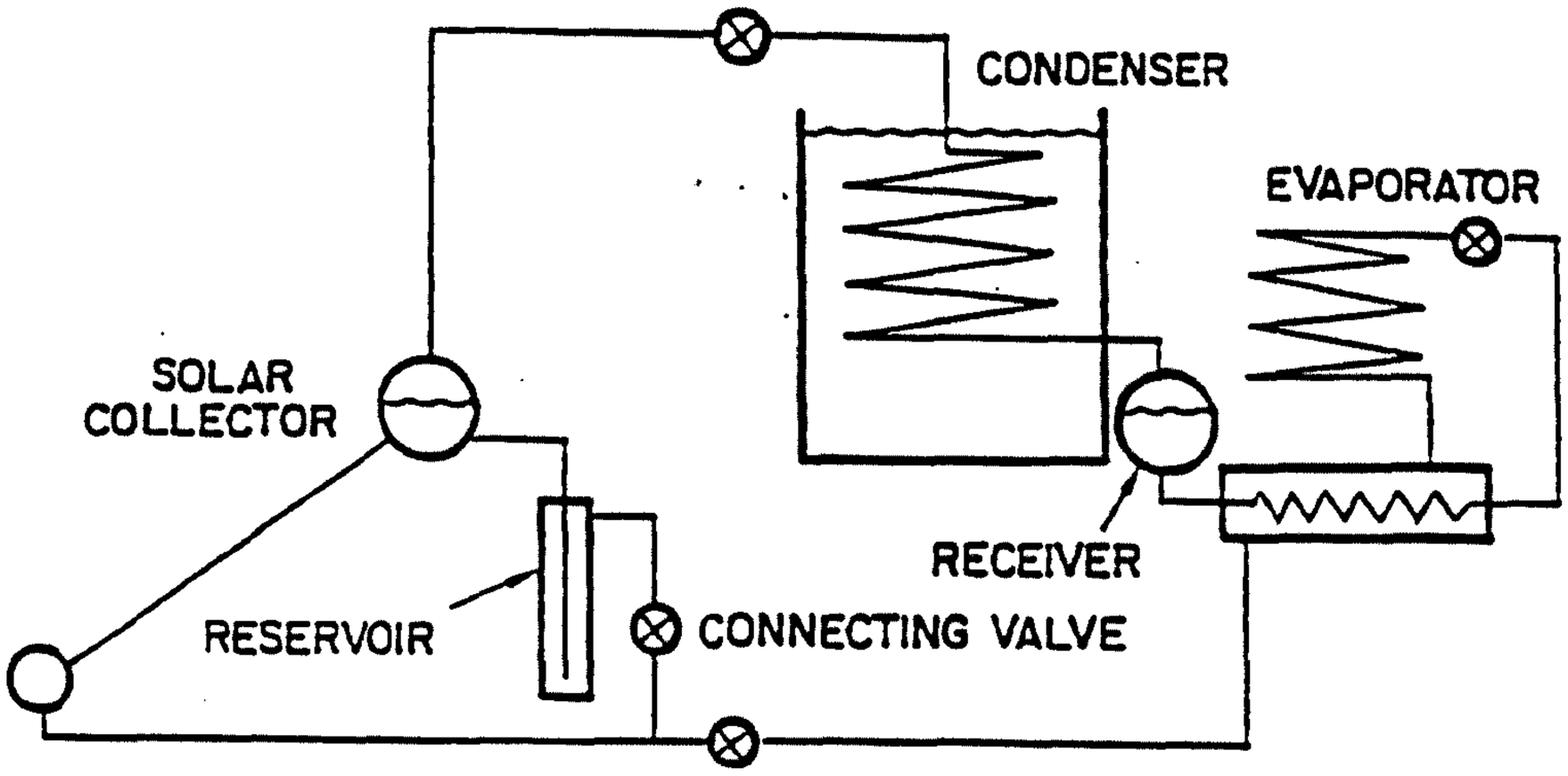

Model II

Fig. 2.2.4.2 from Exell (1981

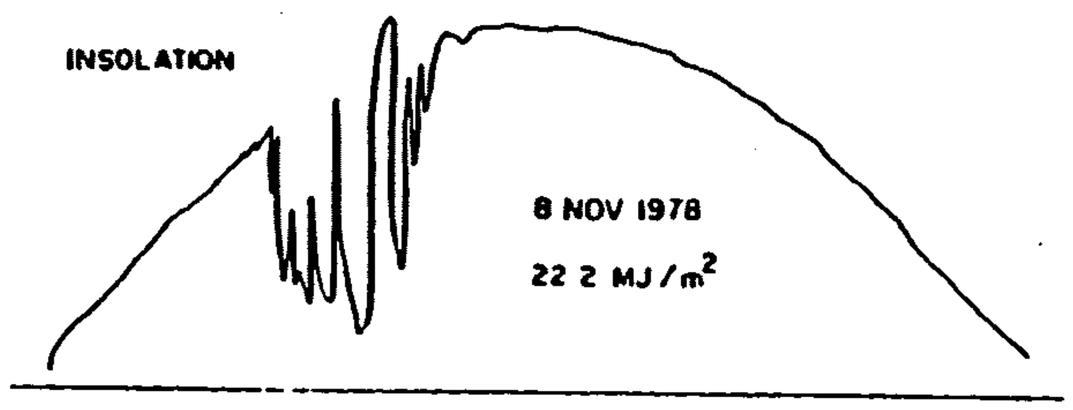

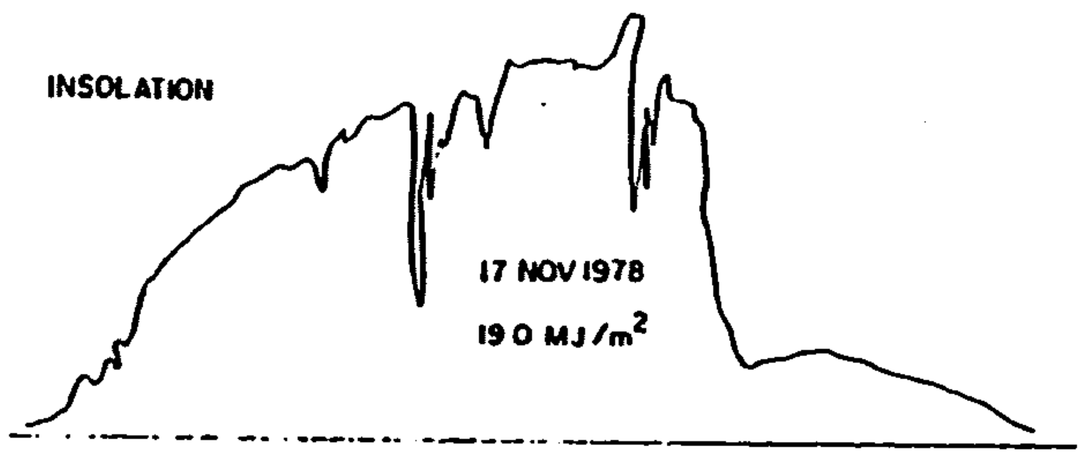

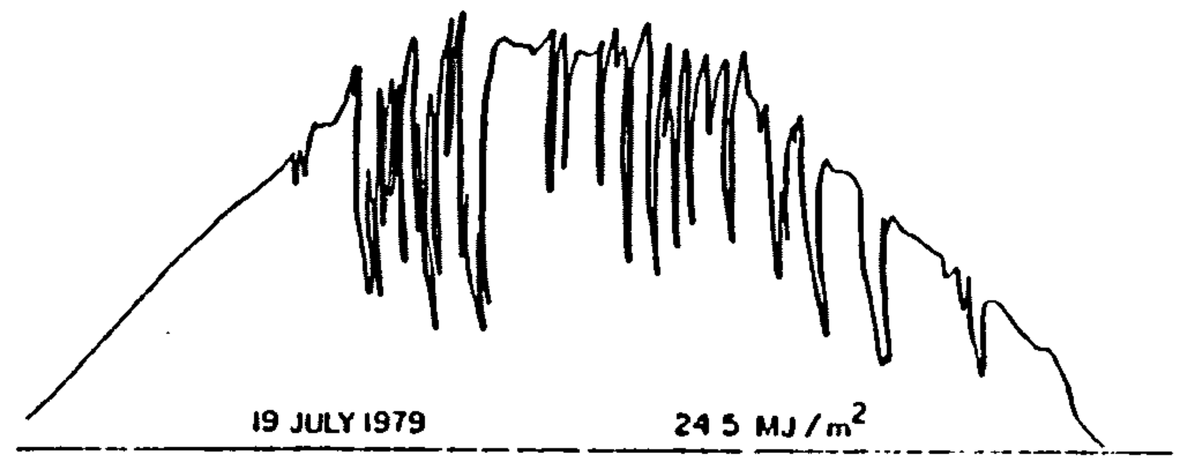

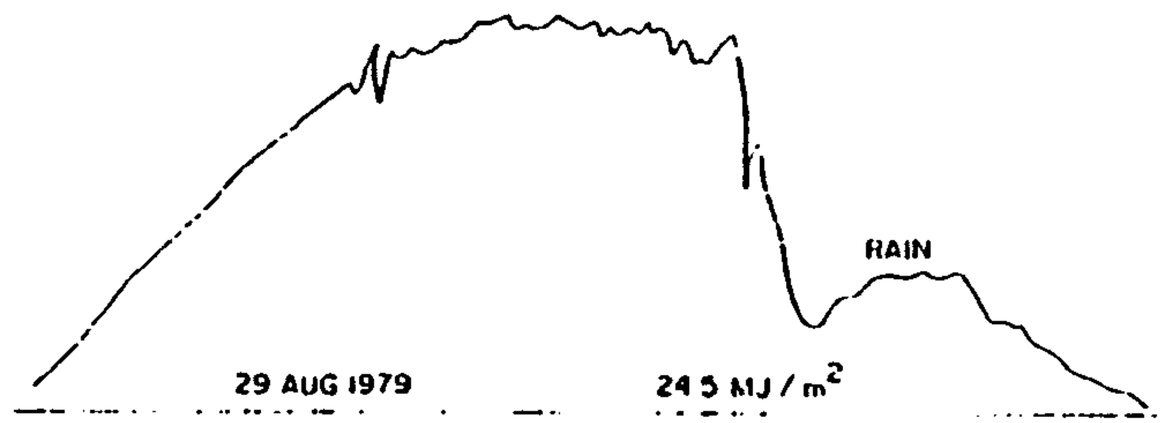

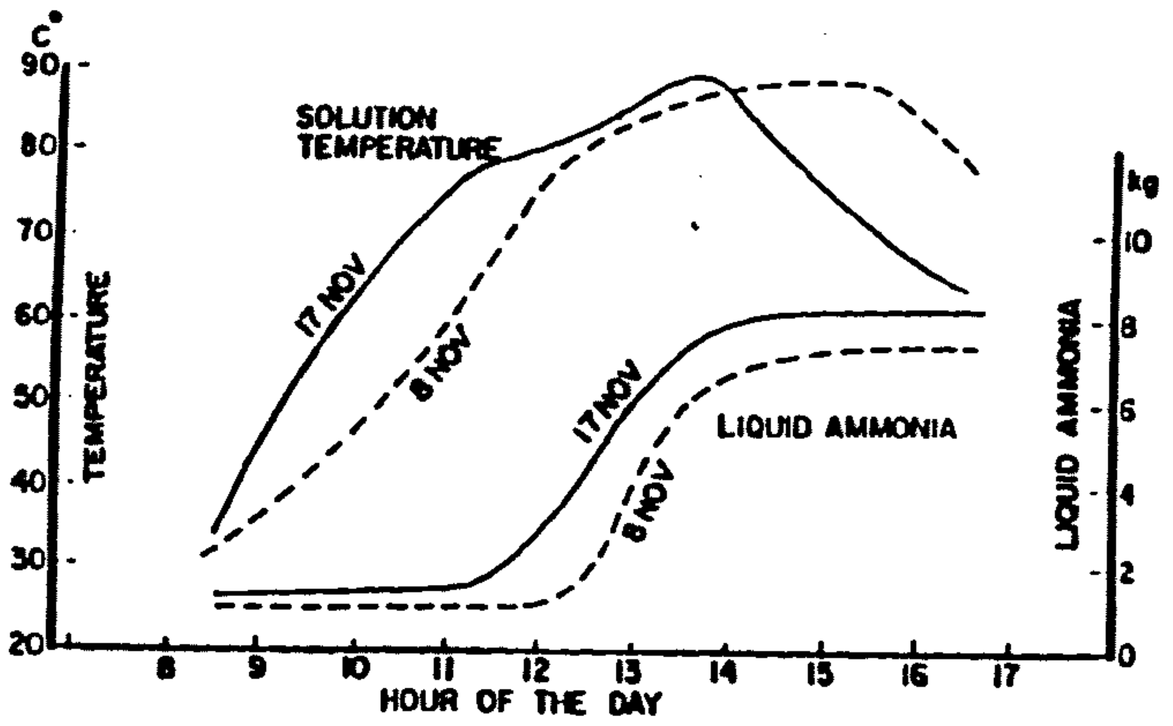

Results of a test on model 1
without auxiliary mirrors

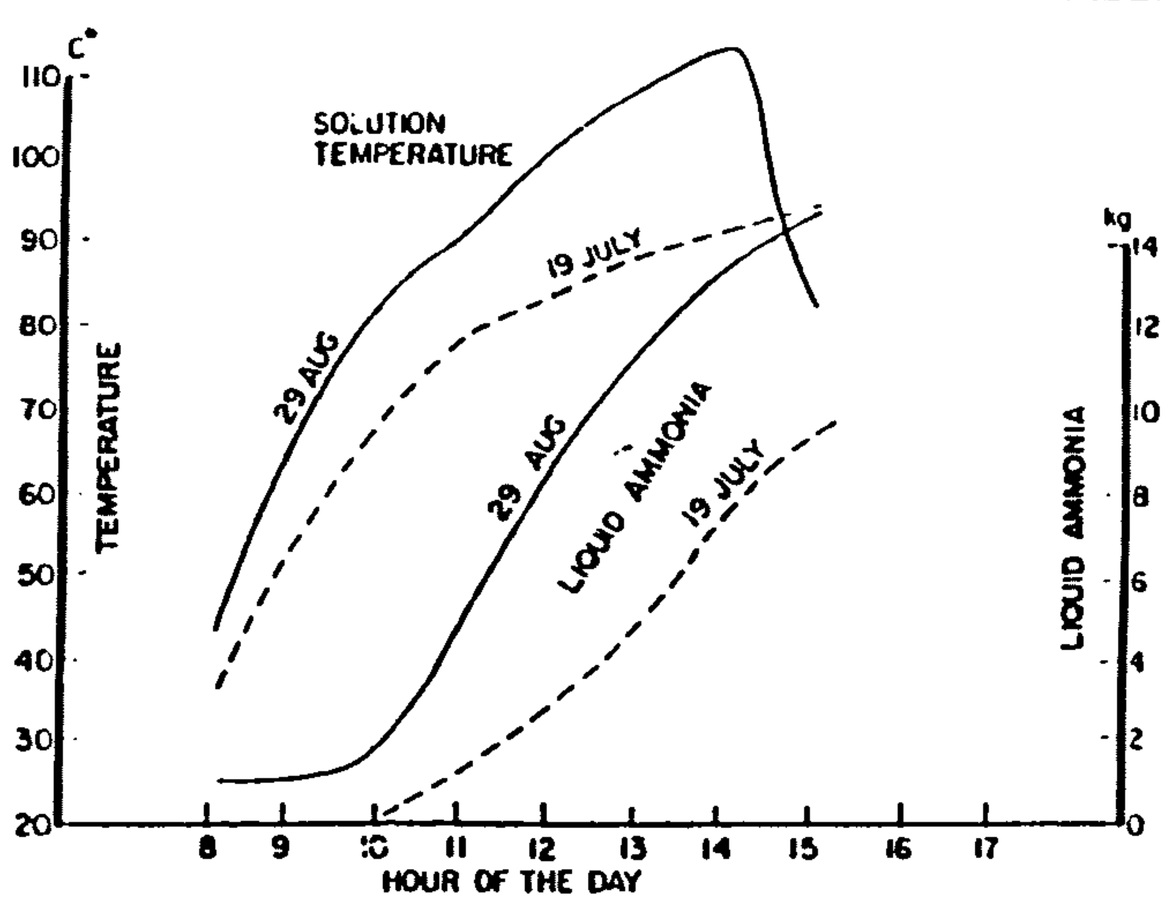

Results of test on Model 1
with mirrors

Fig. 2.2.4.3 from Exell (1981)

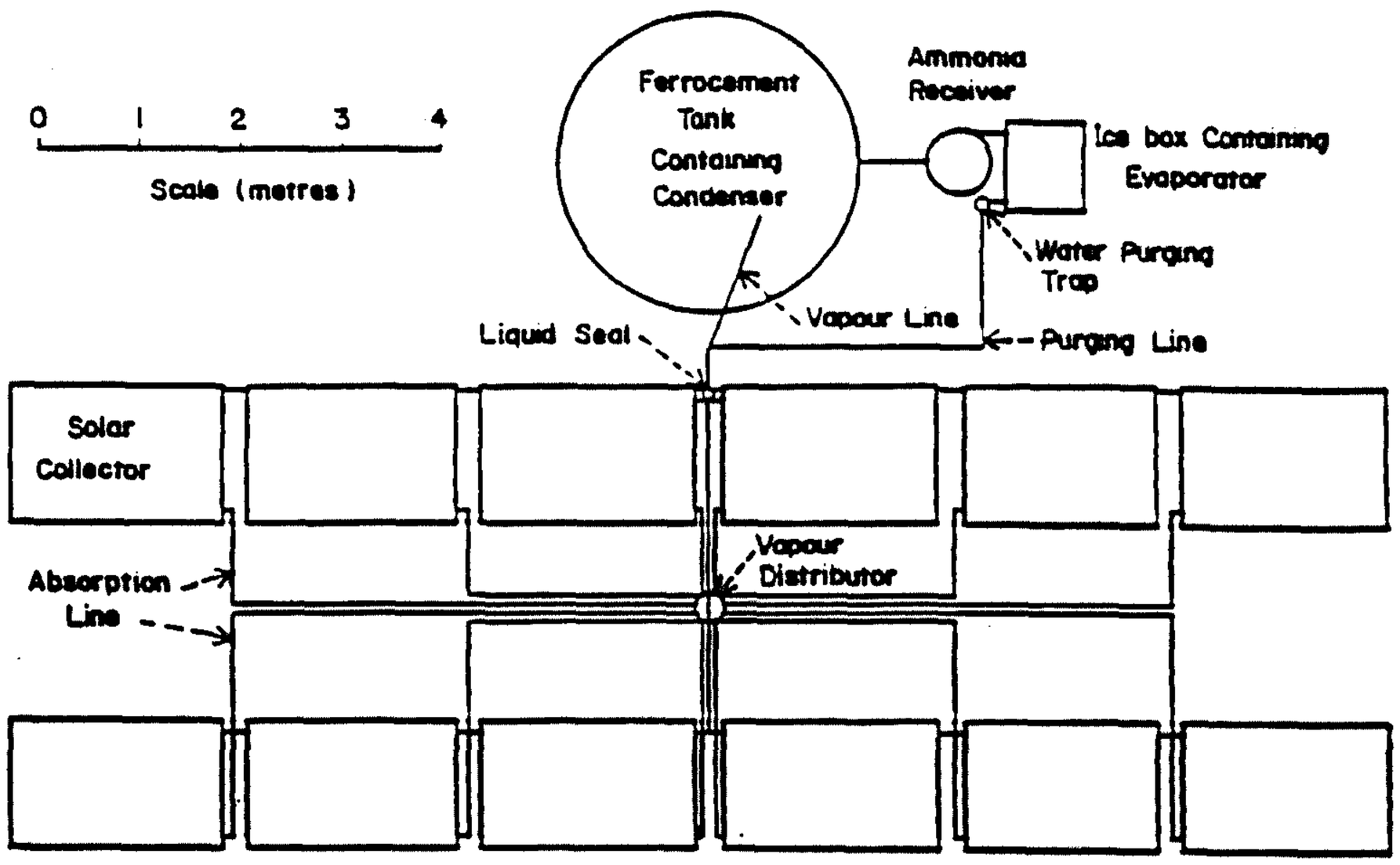

Plan view of village-size solar refrigeration system

Fig. 2.2.4.4. from Exell (1984)

generation on the same day was 10.8 MJ implying a collector efficiency of 28%. The cycle COP achieved was 0.26, the solar COP being 0.07. Ice production on a good day was 4.2 kg/m^2. The prototype was charged with 19 kg of solution and on a good day would start generating at approximately 11 a.m. A precooler heat exchanger was incorporated which was calculated to improve performance by 4%. Condensation heat rejection was to a tank of stagnant water which was kept at close to night temperatures by the removal of insulation during the night and replacement during the day. The heat of absorption was rejected by removal of the collector's glass cover during the night. The cycle was controlled by three manual valves.

Exell (1981) then constructed two test units, one (model 1) with a tube-in-sheet collector like that of the early prototype, and one with non-focusing cylindrical concentrating reflectors positioned below finned riser tubes (model 2), as illustrated on figs 2.2.4.1. and 2.2.4.2. Model 2 therefore featured a collector/generator with half the thermal mass of the flat plate design of model 1. To provide sufficient solution for a full day's operation model 2 was also fitted with a reservoir from which fresh solution was to be supplied to the collector during generation. Both models had total collecting areas of 5 m^2 which were augmented with flat mirrors hinged to the east and west edges of the collectors. With hourly repositioning the mirrors could effectively double the received insolation. Condensation cooling was accomplished as in the early prototype, and a precooler (providing heat exchange between the gas leaving the evaporator and the liquid entering) designed to improve performance by 8% was fitted to each unit. Both units used dry evaporator designs whereby evaporation rate was controlled manually by a hand valve which in practice was continuously and carefully manipulated in order to achieve the measured results. Absorption in both units was by opening of slots in the sides of the collectors to allow heat transfer by natural convection.

Both units were charged with 65-67 kg of solution at a concentration of 0.46. Performance measurements showed considerable sensitivity to the distribution pattern of solar radiation, primarily because the reflecting mirrors became less effective during periods of low direct and high diffuse radiation. This effect is shown in figure 2.2.4.3.

On a consistently bright day model 1 could generate 14 kg of NH_3, and 25 kg of ice from water initially at 28 degC. This represented a solar COP in the order of 0.14, if the $5m^2$ area of glass is taken as determining power input, or 0.07 if the total collection area is taken. Fig 2.2.4.3 shows that in contrast a day of similar total insolation but with greater diffuse component reduces COP from 0.14 to 0.09. The heat capacity of the collector was 155 kJ/degC, implying a mass of 344 kg of steel to contain 65 kg of solution. On good days generation started at 10 a.m., some four hours after sunrise, and maximum generation temperatures were reached at 3 or 4 p.m. Fig 2.2.4.3 shows this, and also indicates that effective yield production ceases at around 1.30 pm. Clearly some solar capacity is lost through this characteristic of the device. Sensible heating of liquid consumed 42% of the total energy consumption of about 48 MJ, the steel took 22%, and vapourisation took 36%. The collector operated at an efficiency of around 0.39, given the improvement due to hourly adjustment of the mirrors. The range of daily irradiation values during testing was between 17 and 25 MJ/m^2, over which range output varied approximately linearly with irradiation, such that solar COP remained near 0.1, although considerable scatter occured, probably due to the varying distribution of direct and diffuse radiation. Practical precooler efficiency is not recorded.

The performance of model 2 was consistently worse than that of model 1, by an order of 1 or 2%. The fabrication costs of the two units are given as Thai Bahts spent in 1978, when the conversion rate was 45 Bahts to the pound sterling. At this conversion, the price of model 2 was £ 788 as opposed to £ 933 for model 1.

No saving of thermal mass was expected in this design with the reservoir connected in the circuit, but an improvement in COP of 12.5% was expected, presumeably due to the reclaim of sensible heat in the heat exchanger portion of the reservoir. It should be noted that with the reservoir not connected the refrigerator contains too small a solution charge for full use of the available insolation. The report attributes the low efficiency of model 2 to the use of less expensive mirrors, in this case being stainless steel sheets, but the loss involved is not quantified. The decision was made to give no further consideration to the development of model 2.

Returning to model 1 Exell calculates that the cost of ice produced is roughly twice the city price, an indication that the device is viable economically in rural areas. 60% of the cost is in collector components. Certain improvements are identified as necessary for further development. Firstly, the skilled manual manipulation of the expansion valve is not feasible in a commercial unit. Secondly, the use of slots to cool the absorber is not sufficient to reject absorption heat because the large headers are not properly exposed to convective cooling by this method, and because dust is allowed to enter and impair the absorber surface.

Exell (1984) reports on the testing of a further design of solar refrigerator which features many of the improvements listed above. The refrigerator is sized to produce 100 kg of ice per day, sufficient to satisfy the needs of a typical village in Thailand. The collector design is shown in fig 2.2.4.4; in this design the bulk of the solution is contained in reservoir tubes placed to either side of the solar window so that the portion of thermal mass exposed to insolation is reduced. Circulation of liquid into the window area is by thermosyphon and vapour lift action. The problem of the expansion valve is solved by a return to a flooded evaporator design, and the requirement for an automatic valve system for switching from generation to absorption mode is solved by the incorporation of the liquid seal used in the work reported by Williams. Exell gives a description of the operating principle of the liquid seal. The refrigerator now required only one valve, provided for the periodic purging of water from the evaporator.

The collector comprised twelve flat plate panels with a total area of 25 m^2. During the absorption phase vapour was distributed evenly to the panels with the aid of specially designed distributor component, the critical part of which was a carefully levelled horizontal disc divided into twelve segments each drilled for fluid passage. It is commented that during absorption this component released a sizeable portion of the heat of absorption. The major mode of release of absorption heat was by convection from the underside of the panels, where the insulation was manually removed for the duration of the night.

The design of the solar collector allowed for the use of auxiliary mirrors although these were not in fact used during tests. Measurements were taken of the performance of the collector which allowed the efficiency characteristic to be written as

$$\eta_{coll}=0.68-5.3\frac{\Delta T}{G}$$

The condenser consisted of 60 meters of 1/2 inch nominal diameter stainless steel pipe cooled by a water bath and divided into 12 parallel sections in order to maintain the pressure drop at a manageable level. This design was based on guidance provided in the ASHRAE data book suggesting a heat transfer coefficient from steel to water of 170 W/m^2K. 10 m^3 of cooling water were held in a ferrocement tank.

The evaporator was of the gravity circulation type and was designed to pass 51 kg of refrigerant during the night, and to freeze five 20 litre ice cans. The design was based on a coefficient of 56 W/m^2, a value selected from King (1971) for the heat transfer into the evaporator tube. 30 coils of 1/2 inch tube, each 3.2 meters long, provided a total area of 3.4 m^2.

Test results revealed that the refrigerant yield rates were satisfactory, the measured solar COP of the device being in the order of 0.11. The evaporator did not succeed in making use of all the yield available, ice production being in general 60% of the desired target value. This was seen to be due to the presence of greater thermal resistance in the evaporator than expected, and an enlargement of the evaporator surface area to 6 m^2 is recommended.

The maintenance of the liquid seal proved troublesome, and the use of check valves is recommended, with the proviso that a system incorporating two check valves immersed in liquid would be worth investigation.

. . .

2.3. Continuous pumped (CP) systems

2.3.1. The Netherlands and Sudan

Theoretical investigations were undertaken by Haverthals in association with Stolk at Delft University of Technology into the feasibility of fully solar-driven agricultural coolers suitable for use in the Sudanese climate. Aqua-ammonia absorption coolers were envisaged, utilising solution pumps powered by photovoltaic cells. A comparison between dual stage and single stage systems revealed that dual stage system had certain advantages for the intended application, mostly

resulting from the very much wider concentration swing possible in a dual system. Because of the wide swing the device was capable of tolerating ambient temperature fluctuations which would otherwise impose severe limits on the operating range of a single stage system. It also acted to reduce the mass flow of solution required for a given duty, so reducing the size and energy consumption of the solution pump. A costing exercise revealed that the solar collection components would constitute more than half of the total system cost.

A practical demonstration was then conducted and is reported on by Sloetjes (1988). This comprised a single stage system designed to produce 13 KW of cooling continuously for 5.5 sunshine hours, or a 3KW mean over 24 hours. Conventional power sources for pumps were used and cooling water at 20 degC was circulated. Collector efficiencies in the range 0.5 to 0.6 were achieved and solar efficiencies in the range 0.08 to 0.15.

2.4. Solar conversion of the Diffusion-Absorption (DA)/Platen Munters cycle

2.4.1. Mexico

Gutierrez (1988) reports on an investigation into the conversion of a diffusion-absorption type refrigerator to solar power. The investigation is needed because many communities in Mexico are without utilities and services and therefore require an autonomous solar driven cooler which has no parasitic power requirements and a minimum of service requirements. An intermittent absorption cycle is considered unsuitable because it involves the use of externally operated valves. A conventional continuous absorption device is ruled out because of the need to power a pump capable of maintaining a substantial pressure difference. The Platen Munters cycle is considered suitable because no switching operations are required and service can be reduced to the task of keeping the collector dust free, although it is recognised that the circulation of a third gas causes the cycle efficiency to be inherently lower than that of other absorption devices.

The unit chosen for conversion was a 250 litre capacity Servel designed for operation with a gas burner producing a generator temperature of 160 degC. The expected design COP for this type of device is in the order of 0.28 - 0.32. The burner and solution boiler was replaced by a flat

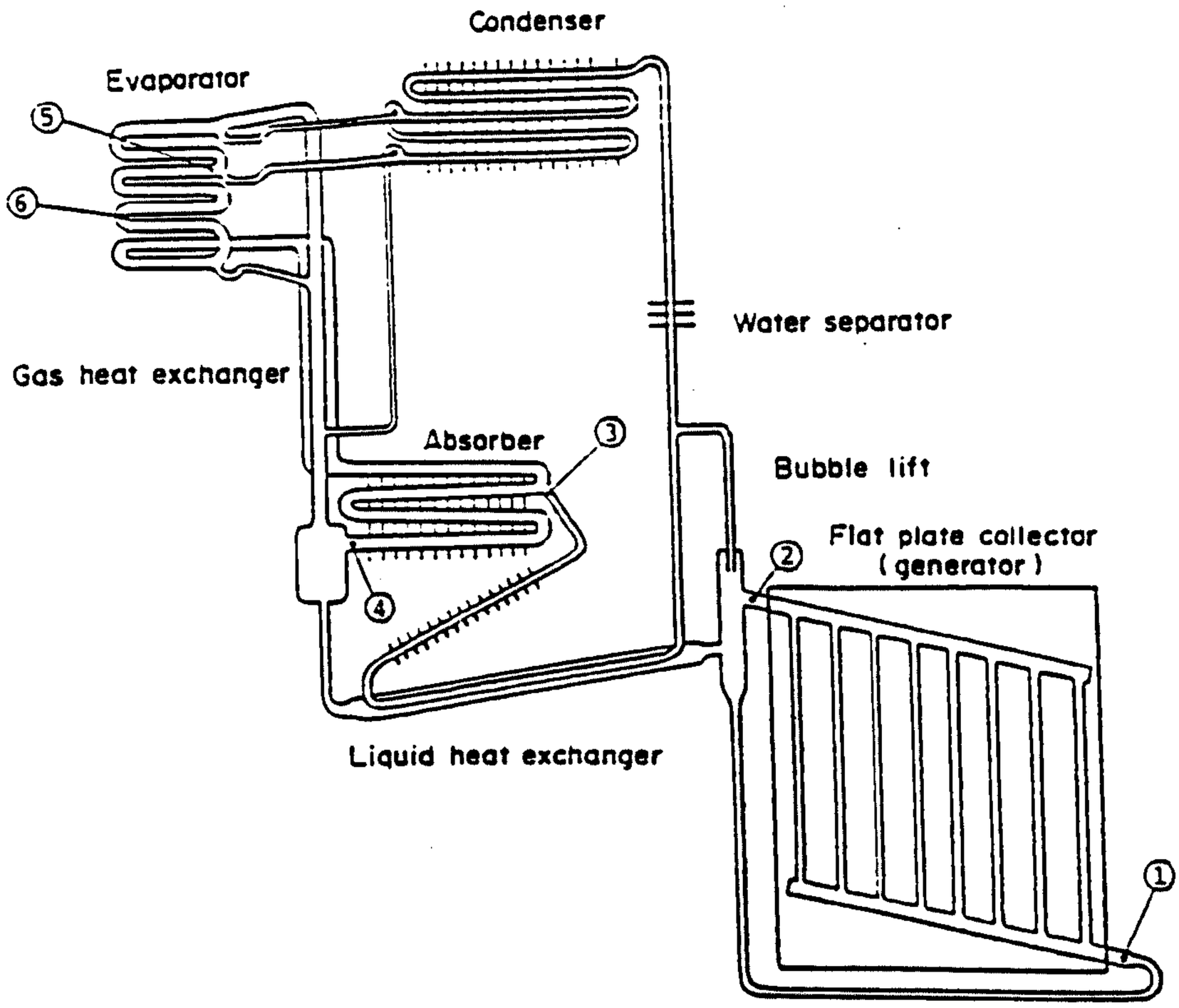

Schematic view of the solar refrigerator. The temperature measuring points are indicated with numbers. 1 = collector inlet, 2 = collector outlet, 3 = absorber liquid entrance, 4 = absorber liquid exit, 5 = evaporator inlet, 6 = evaporator middle section.

Fig. 2.4.1.1 from Gutierrez (1988)

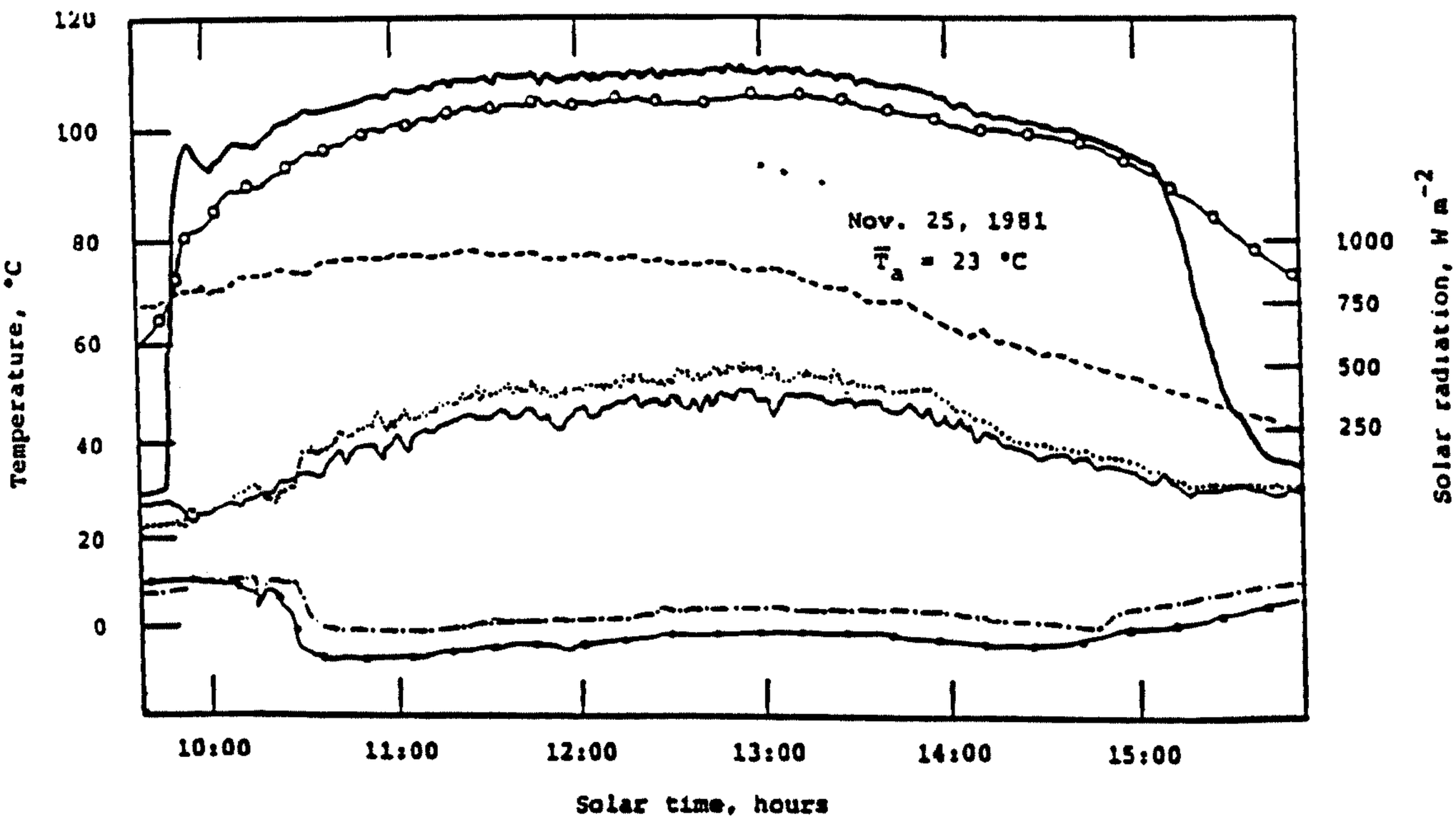

Fig. 2.4.1.2 from Gutierrez (1988)

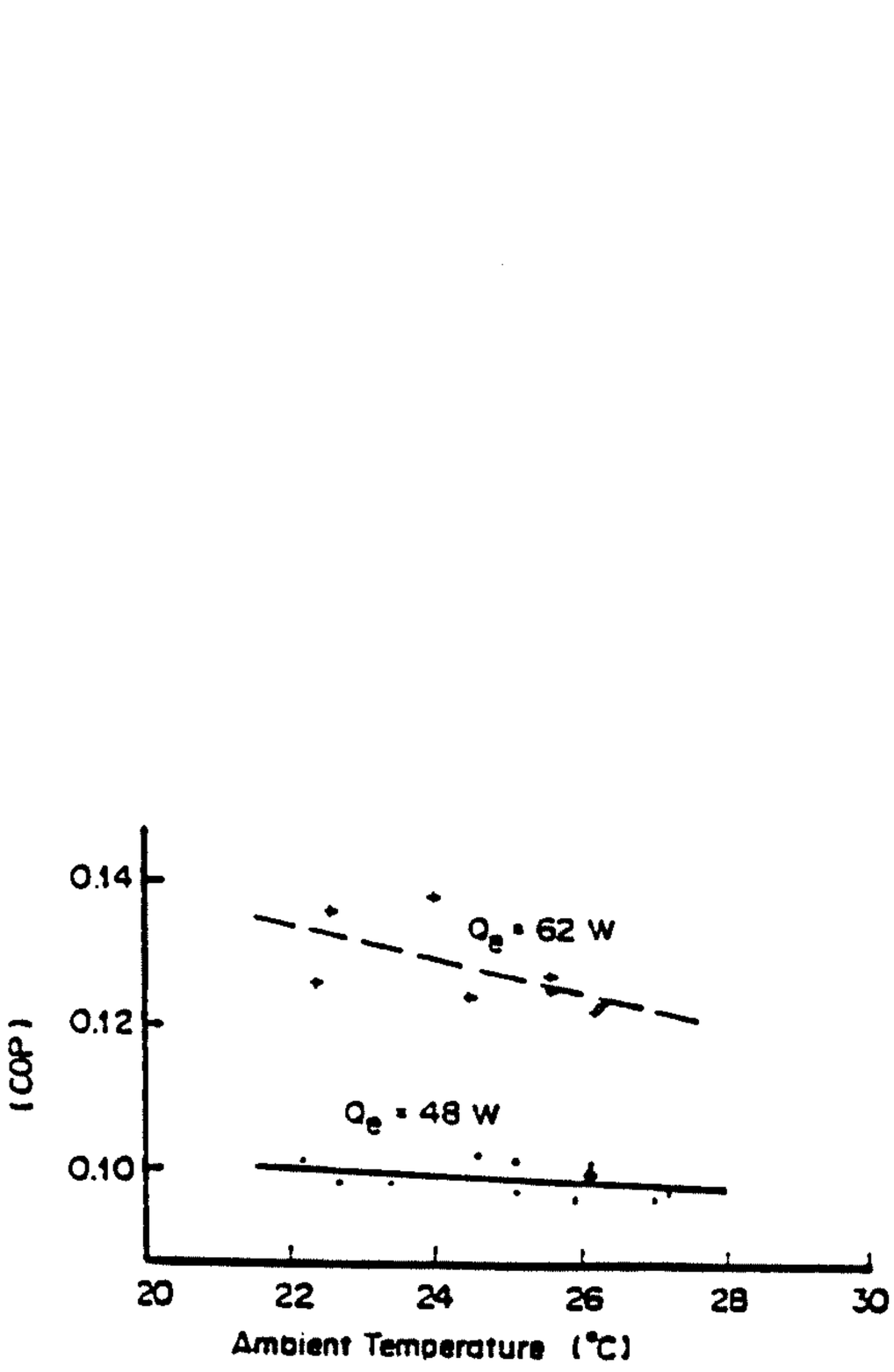

Fig. 2.4.1.3 from Gutierrez (1988)

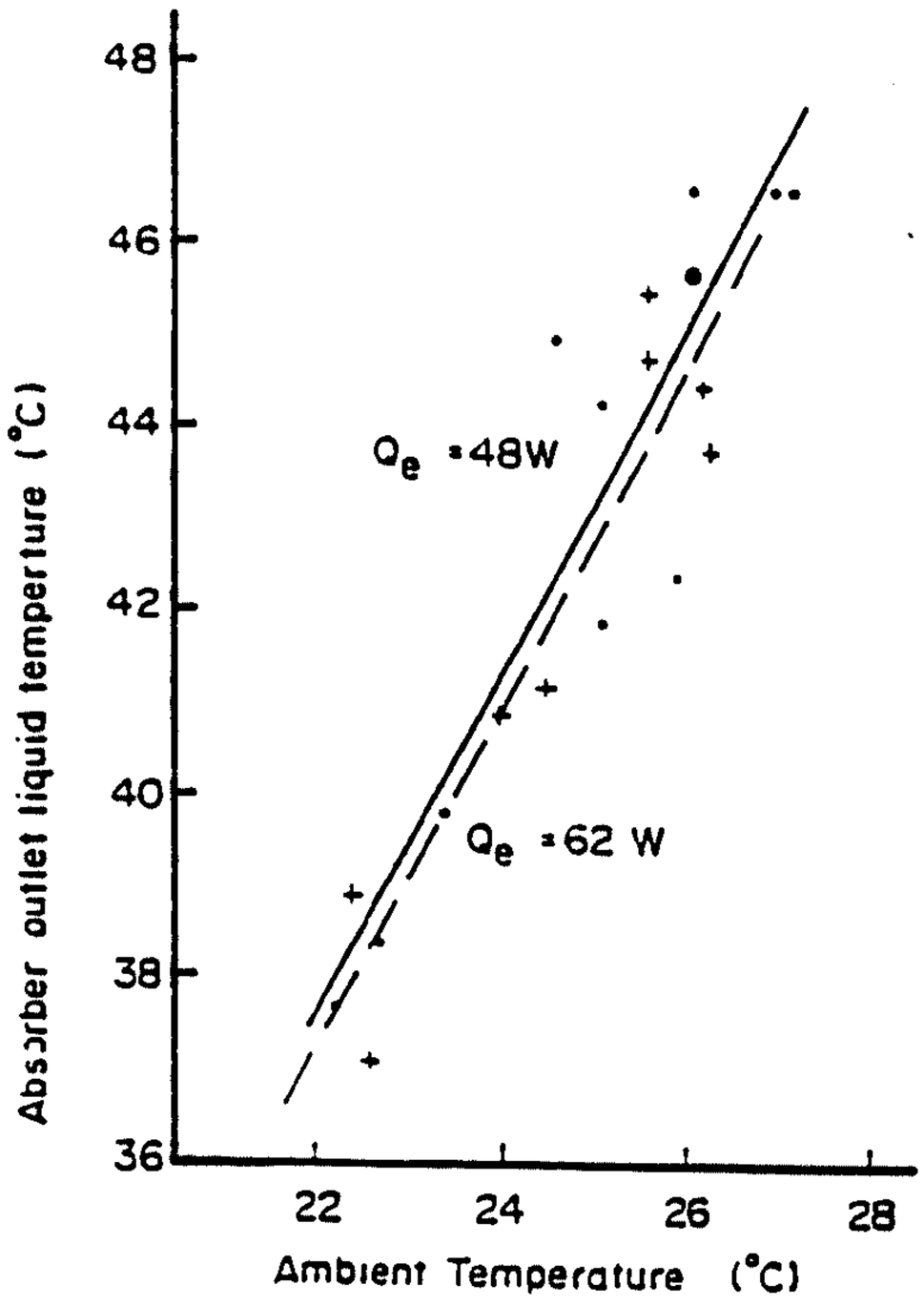

Fig. 2.4.1.4 from Gutierrez (1988)

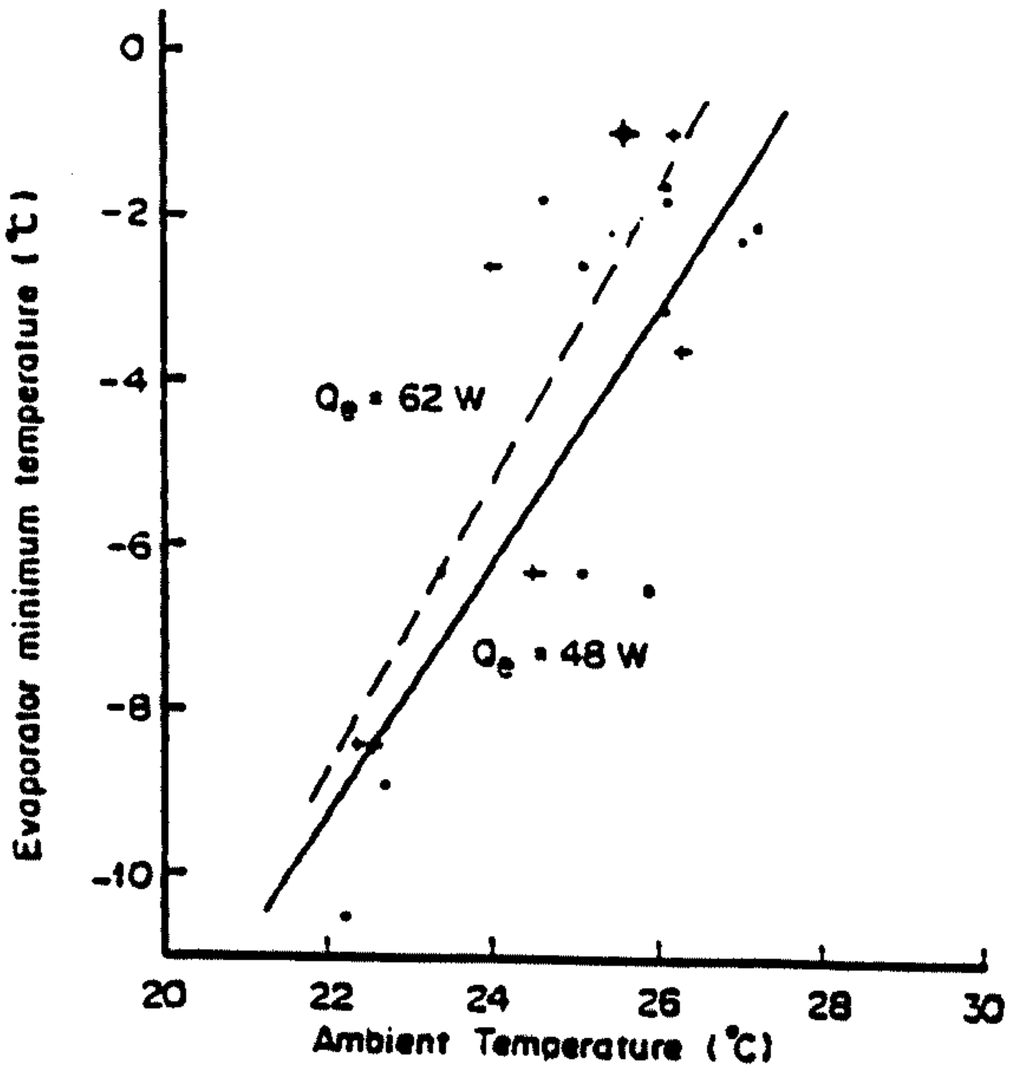

Fig. 2.4.1.5 from Gutierrez (1988)

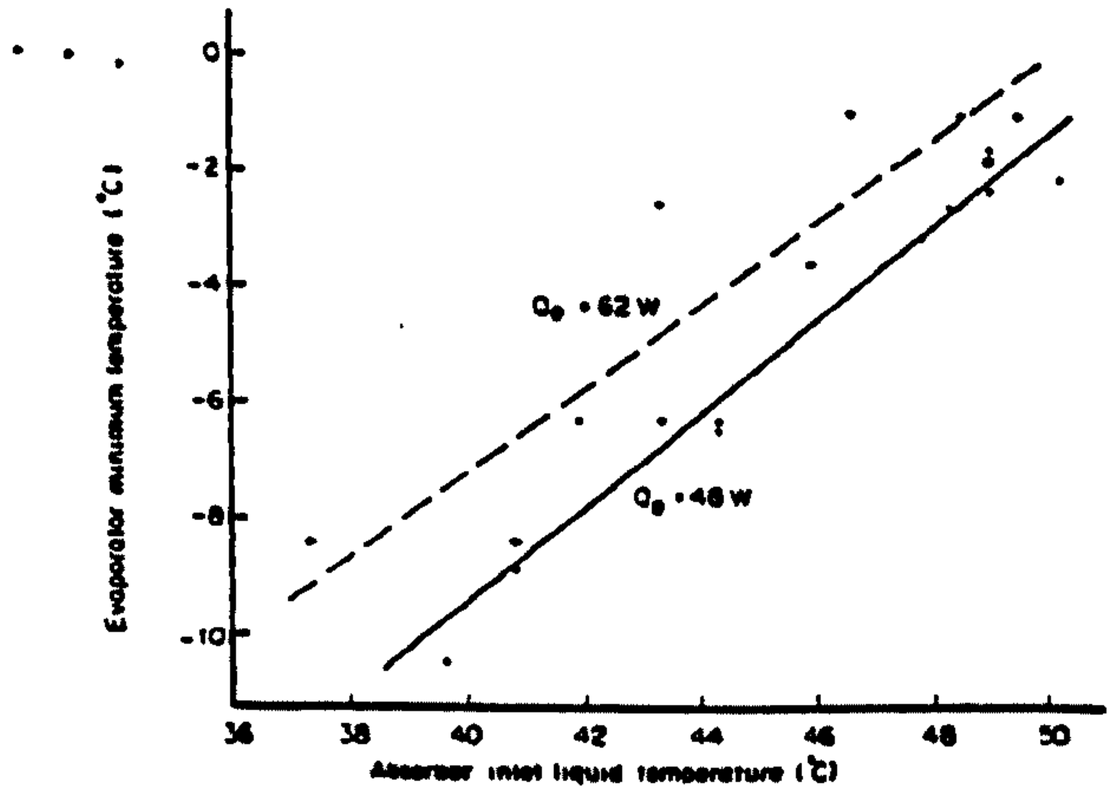

Fig. 2.4.1.6 from Guttierrez (1988)

plate collector with an area of $2.5m^2$ as shown in fig 2.4.1.1. No comment is made by Gutierrez on the original layout of boiler and bubble pump; it must be assumed that the boiler preceded the bubble pump in the original design as in the converted design. The solution concentration is raised from 32% to 42% to allow boiling at the reduced generator temperature of 105 degC. The new circulation ratio (weak solution circulated per unit mass refrigerant generated) is expected to be almost 5 times larger than the original ratio, such that the solution heat exchanger is replaced with a larger version to ensure that absorption takes place at the original temperature. No mention is made of alteration to the original bubble pump, while it is stated that the absorber is maintained unchanged.

The performance of the converted unit is shown in fig 2.4.1.2, but no mention is made of evaporator loading conditions during this and other similar tests. Controlled experiments are also conducted with the aid of a solar simulator. During these both solar input and evaporator loading are held constant so that the overall system COP at steady state conditions is held constant. Fig 2.4.1.3 shows simulation results at an insolation rate of 850 watts/m^2. The reduction of cycle efficiency with rising T_{amb} is attributed to reduced collector efficiency and reduced heat rejection performance. Fig 2.4.1.4 shows the effect of rising T_{amb} on absorber exit temperature. The resulting increase in system pressure (and the decrease in rich solution concentration which is implied) lowers cycle efficiency. Fig 2.4.1.5 shows that the evaporator temperature is very sensitive to ambient temperature, possibly because of high pressure in the evaporator and the circulation of unabsorbed ammonia vapour tending to impede the diffusion rate. Fig 2.4.1.6 plots the measured absorber inlet temperature against minimum evaporator temperature. High ambient temperature contributes to high absorber inlet temperature. One indication of the experiments is that the absorber size is not adequate for the duty.

Variation of generation efficiency with changing T_{amb}, and with insolation rate, is not documented. Gutierrez concludes that freezing temperatures are obtainable for five hours of the day, so long as the ambient temperature does not rise beyond 28 degC. Fig 2.4.1.2 indicates that insolation rates below 500 watts/m^2 also raise evaporating temperature above freezing. Gutierrez points out that actual day-long COP values are therefore lower than those shown for the steady

state conditions.

2.4.2. Sanyo Electric Co Ltd, Japan

Hinotani (1984) reports on the testing of an experimental diffusion-type refrigerator designed specifically for solar operation. The collector adopted for the purpose is a high efficiency evacuated tube collector, enclosing a parabolic mirror providing a concentration ratio of 1.5. The generator incorporates a bubble lift pump of a triple tube design similar to that used in Electrolux refrigerators. The bubble-lift action takes place in an inner tube, which is surrounded by an annulus which forms the boiler component. This design causes the pumping action to consume only a portion of the input heat, and to operate at a lower temperature so ensuring that rich solution leaves the mouth of the pump, where an analysing (or stripping) effect occurs in relation to the vapour leaving the boiler.

The aim of Hinotani's experiment was to observe whether a diffusion type cycle could operate successfully with the varying generator heat inputs expected when operating with a solar input. In the tests he conducted Hinotani varied the area of the solar collector while maintaining a constant simulated insolation rate. The test results shown in table 2.4.2.1 show that it was possible to achieve high generator temperatures while collector efficiencies remained high, and that these temperatures were maintained despite variations in heat input rate. The rate of heating of the generator was calculated from the measured value of simulated insolation, the generator temperature, and the collector characteristic curve which was obtained in a separate series of experiments. Fig 2.4.2.1 shows that for the conditions listed in the table the generator output temperature is 15 to 20 degrees lower than the generator temperature. The heat transfer area between collector condenser and generator tube is described as a cylinder of 100 to 125 mm length and 19 mm diameter, the overall length of heated tube being 875 mm. The dilute solution concentration values listed in the table were obtained from measurements taken of the dilute solution temperature, which was closely related to generator output temperature, and system pressure. Because they remained relatively constant while heat input varied, Hinotani concludes that the generator design adopted is successful in pumping the solution at an optimised rate matching the level of

incoming insolation.

An evaporator temperature below -15 degC was measured during most of the cycle as indicated on the plot given of a field test in fig 2.4.2.1. It can be presumed that this temperature was obtained at the cold end of the evaporator. A cold cabinet temperature of 0 degC is recorded. The rise in evaporator temperature between 11 am and 12 am is explained as the response to a high level of generator heat absorption. It is reaffirmed that the flow regulating effect of the generator is nevertheless working. The loss of cooling effect, and the failure of cooling effect to rise with rising insolation, is explained as being due to insufficient circulation of hydrogen gas in the evaporator. Although more ammonia is available for evaporation at higher insolation rates, it cannot diffuse at the greater rate required because the transport medium has already reached its limiting flow rate. It is not commented whether the range of operation of the device can be broadened with further design of the hydrogen circuit.

Fig 2.4.2.2 shows measurements of cooling power calculated from the drop in temperature of water in an insulated jacket fitted to the evaporator. It can be presumed from the figure that the trials were run with the varying degrees of initial water temperature, and that higher powers were achieved when greater temperature differences existed. For refrigeration purposes the solar COP obtained at water temperatures below 5 degC is of interest, and it can be seen that this is demonstrated to be less than 0.05 in Hinotani's experiment.

The value of Hinotani's work is very great. The demonstration of a generator design producing solution flow rates which maintain an optimum concentration shift at varying insolation levels is of interest to the present investigation. The experiment is also rare in devoting attention to the design of all aspects of the diffusion-absorption cycle with respect to solar power, since it has been evident that conversion of only the generator of a standard unit is insufficient. Unfortunately it is clear that discussion of inherent limits posed by the use of a third gas and improvements to the design of the hydrogen circuit is outside the scope of Hinotani's paper.

Hour	Insolation W m	Collector efficiency	Inout heat of generator W	Total system pressure Moa	Temoer-ature of generator C	dilute so-lution con-centration W%
12:00	9 0 7	0.48	4 3 5	2.78	1 5 7	2 5
13:00	3 7 2	0.46	2 3 3	2.46	1 6 1	2 0
15:00	6 4 4	0.38	1 4 0	2.40	1 5 7	2 2

Input heat of generator and dilute solution concentration

Table 2.4.2.1 from Hinotani (1983)

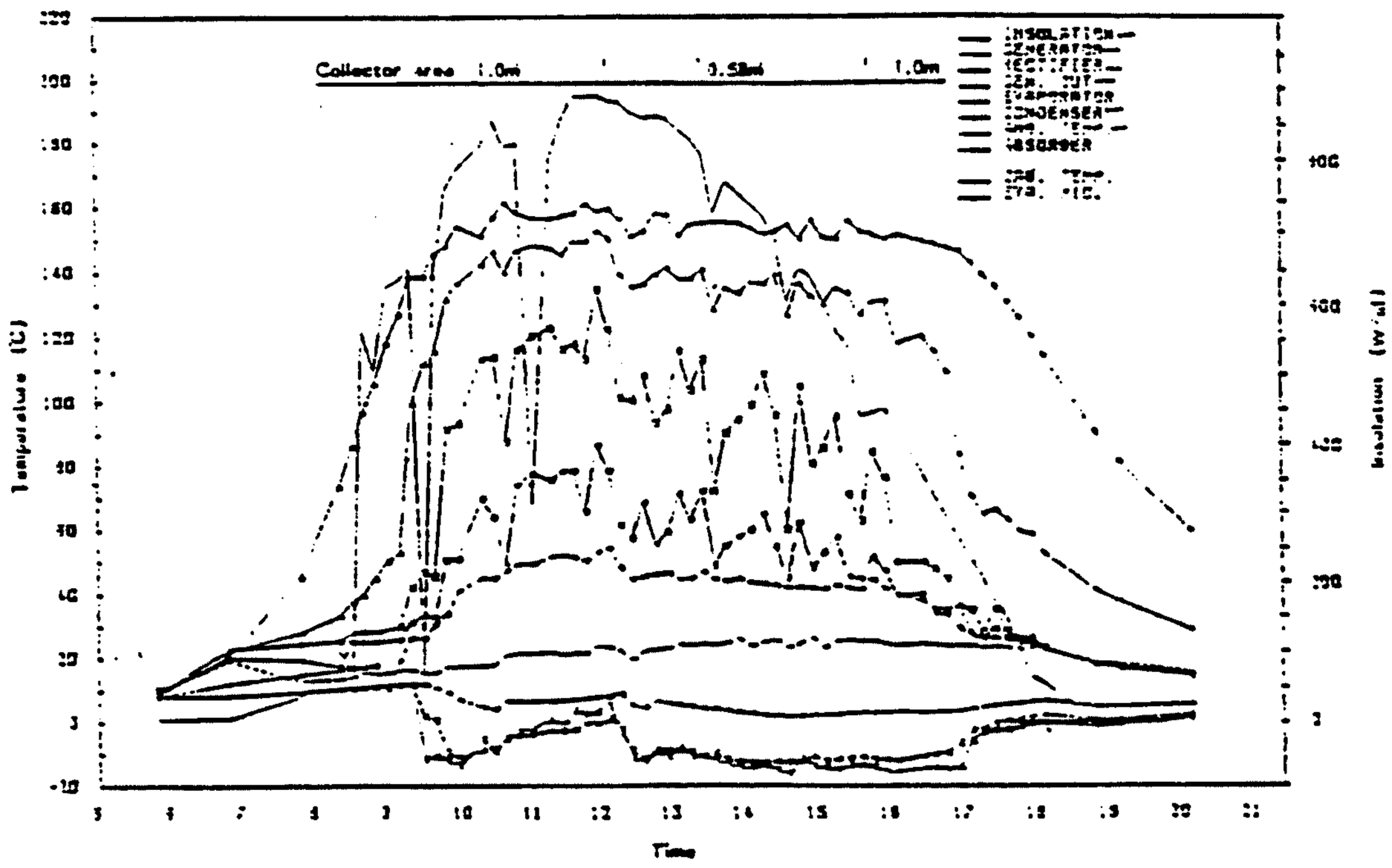

Performance of the test unit

Fig. 2.4.2.1 from Hinotani (1983)

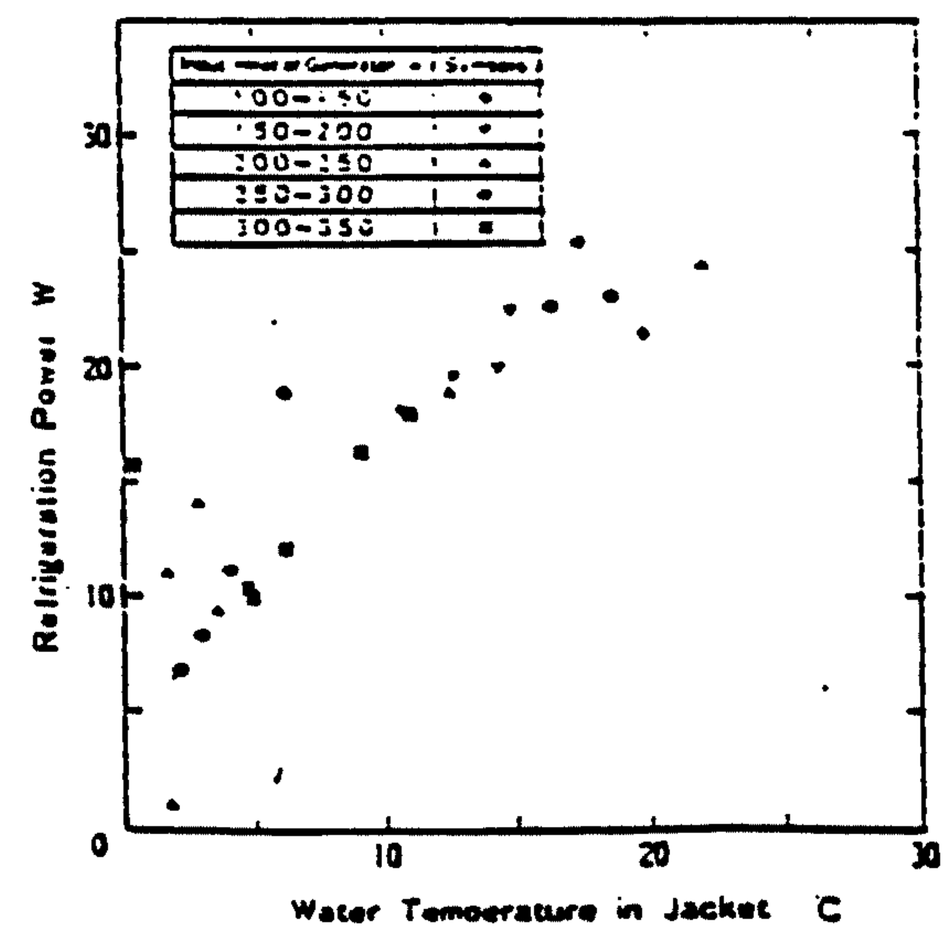

Refrigeration power of the test unit

Fig. 2.4.2.2 from Hinotani (1983)

2.5. Pumpless continuous systems

2.5.1. University of Wisconsin, USA

Chung and Duffie (1961) propose a unit capable of making 66 kg of ice per day. Their schematic diagram of the system is shown in figure 2.5.1.1. Because the unit is larger than the small domestic unit that they first considered, so implying great expense in solar collection costs, and because the production of ice requires lower values of T_{ev} and is therefore susceptible to poor efficiency, they consider the introduction of some complexity to improve COP to be justified.

To set the scene for an appreciation of their design the authors first consider a number of approaches to the problem. They continue to be interested in designs which maximise the length of the refrigeration phase of the cycle in order to reduce the costs of evaporator and absorber heat transfer components. They are particularly interested in doing this by devising means whereby the generation and refrigeration phases can run simultaneously. This is because the reduction of collector cost demands that generation also is extended over as long a period as possible. They first note that the suggestion of Eisenstadt mentioned above accomplishes this. The suggestion was that two basic intermittent units were run out of phase to provide approximately continuous refrigeration. Chung and Duffie consider the use of indirect heating from the solar collector for such a system, such that the generators are driven by a heat store. This would allow the collector to operate usefully for a maximum length of time. No comments are made on the promise of this approach, nor is it pursued further.

Turning their attention to alternatives, Chung and Duffie suggest two methods of increasing cycle efficiency in order to reduce the collector cost:

1) The tendency of T_{ev} to rise during the absorption phase in a flooded evaporator design could be made use of by dividing the process of cooling water and freezing it into two phases. In one cycle the latter part of the evaporation phase is devoted to sensible cooling of fresh water at high T_{ev}, and in the next cycle the first part is used to freeze the precooled batch of water. This would allow the final T_{ev} value to be much higher, so that COP is higher. The authors calculate an 18% improvement in COP.

2) T_{ab} can be lowered if the otherwise wasted sensible heat in the weak solution of a basic unit is used to generate refrigerant in a secondary unit which cools the absorber of the first unit. The secondary unit would be charged with a higher concentration so that it would operate at low $T_{gen(max)}$ and high T_{ev} relatively, but would be capable of increasing the COP of the main unit by 15%.

A third approach to improving efficiency is to adopt the refinements conventionally used in continuous systems, primarily the the solution heat exchanger and the fractionater column. The authors suggest a circuit to do this while avoiding the inclusion of a pump, as shown in fig 2.5.1.1. Because the diagram and text are short of detail some elaboration is needed to describe the principle of operation. A generator reservoir (marked "absorbent storage") containing rich solution is arranged to feed the generator continuously by gravity. The condensate is continuously passed through an expansion valve into the evaporator. Together with a corresponding expansion valve in the weak solution line this maintains the absorber and evaporator at low pressure. The absorber also has storage capacity and fills progressively with rich solution while generation proceeds. The two storage vessels are large enough to allow generation to make use of all the sunshine hours. When generation ends or the generator reservoir is exhausted, it is isolated from the high pressure side of the circuit and connected to the absorber. The contents of the absorber then drain into it by gravity so that it is ready for the succeeding generation phase. The authors maintain that this arrangement allows refrigeration to proceed almost continuously for the full 24 hours, only being interrupted for a period of minutes while the solution transfer takes place. They presumeably mean this to occur in conjunction with collector heat storage allowing generation also to proceed for nearly 24 hours. It is remarked that the prolongation of absorption like this takes advantage of low night temperatures. (It may remarked in addition that generation would proceed with the advantage of lower condensing temperature during cool nights, although $T_{gen(max)}$ may also decline).

A theoretical calculation of the system performance in terms of $T_{gen(max)}$ is made for the following operating conditions: T_{ev}=-4 degC or below, T_{con}=38 degC, T_{ab}=38 (x_{L1}=0.44). An optimum solar COP of just over 0.2 is predicted at a $T_{gen(max)}$ value of 95 degC. An internal

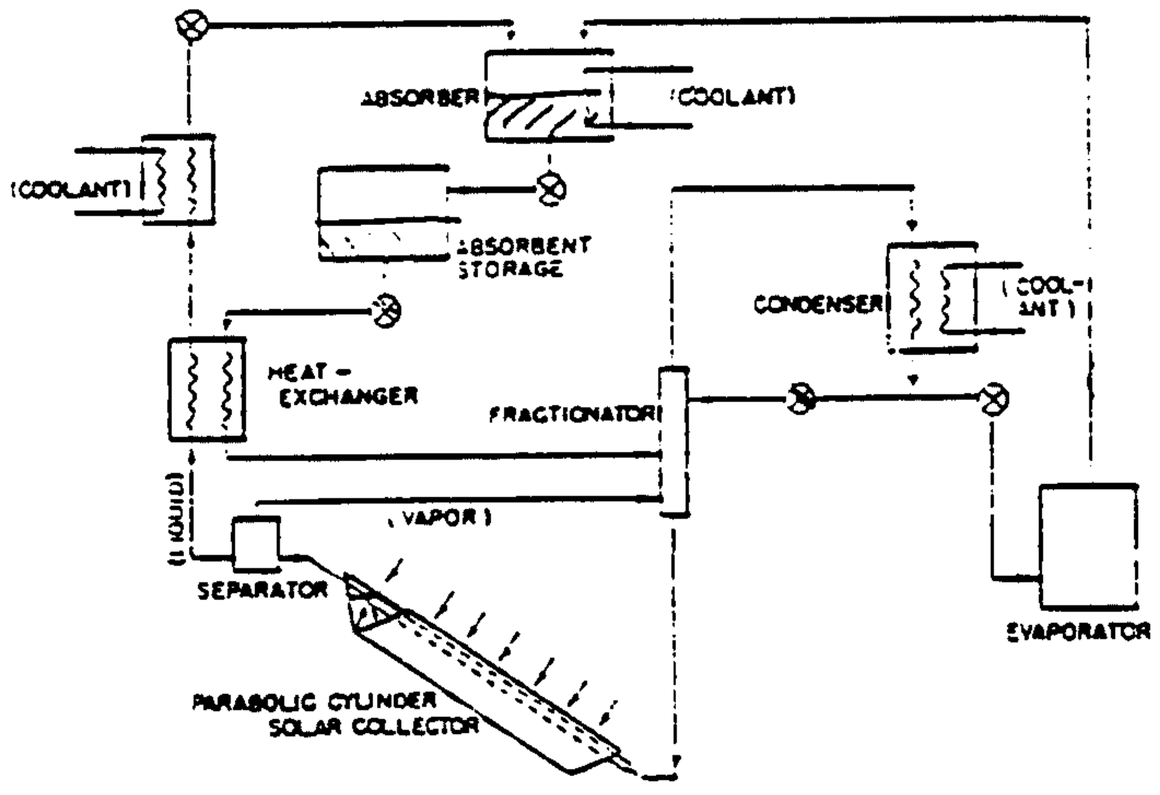

Fig. 2.5.1.1 from Chung (1961)

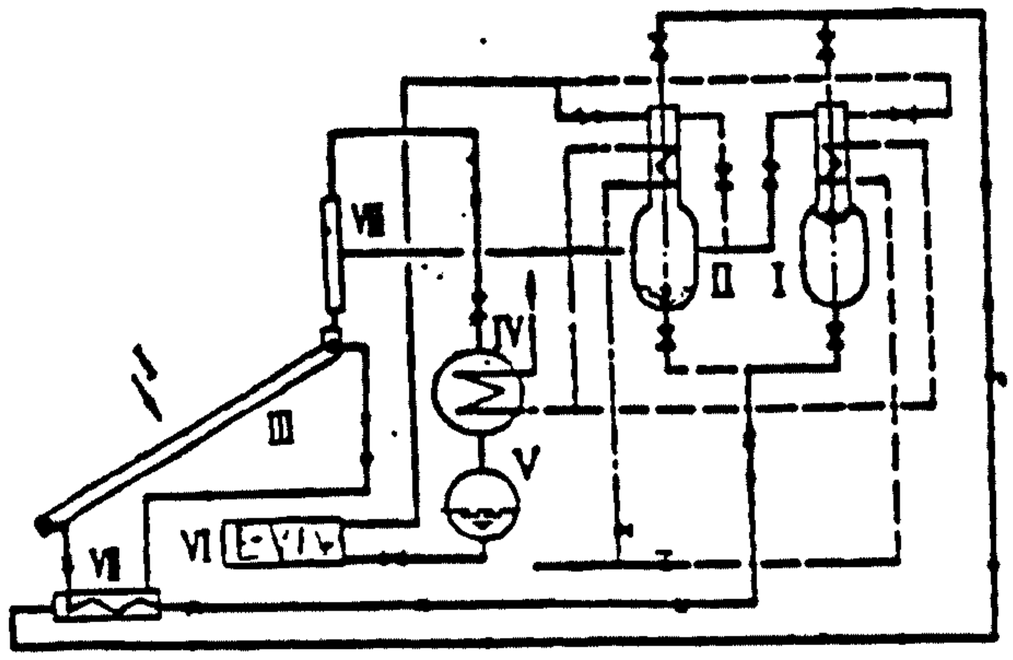

Fig. 2.5.2.1 from Zhang (1982)

I.II absorber
III heat accumulator
IV condenser
V storage liquid
VI evaporator
VII heat exchanger
VIII separate condenser (rectifier)

cycle COP of 0.47 is achieved at temperatures above 100 degC, and the solar heating ratio is in the order of 0.45 at optimum performance conditions. If the reflecting parabolic collector envisaged for this device has a length of 12 feet and an aperture of 6.19 feet, with a reflectivity of 0.76, and insolation is a daily beam radiation of 22.7 MJ/m^2 then the daily ice production is 66 kg. The effectiveness expected of the solution heat exchanger in the calculation is not mentioned.

2.5.2. China

Zhang Zhi-jing (1982) argues that the intermittent system is inherently limited by two things, firstly the tendency of progressive weakening of the solution to push up generating temperature and pressure, and secondly the tendency of the absorption process to raise the evaporating temperature and pressure. He proposes a continuous cycle which does not have these problems and furthermore does not require either a conventional or a bubble pump for its operation.

Fig 2.5.2.1 shows a diagram presented by Zhang. Two twin-mode vessels operate out of phase with each other, one absorbing generated vapour into the weak solution return stream at low pressure, while the other is switched into the high pressure generator circuit. The high pressure vessel acts to feed the generator with rich solution, the flow being partly the result of a gravity head, and partly the result of a pressure differential which is caused by the introduction of a small amount of rectified vapour into the vapour space above the liquid surface. This causes a thin layer of ammonia-rich and warm solution to form on the liquid surface. The absorption heat generated is only slowly conducted away, since the vessel walls are insulated, and only slowly convected away because of the inhibiting effect of density stratification. Diffusion is also inhibited. The existence of the high temperature layer is confirmed with measurements. A finite amount of ammonia vapour is required to form the layer until equilibrium is reached, the proportion of yield drawn off in this way being about 10% of the total generated vapour. The loss can be minimised by increasing the circulation period (tests were run at periods of between 1.6 and 2.5 hours) and by increasing the height to diameter ratio of the twin-mode vessels. We are told that "the degree and violence of, and time taken by, the exchange of heat and mass, effect the reliability and economy of the system". No reason is given by Zhang as to why the gravity head is insufficient by

itself for circulation of solution. There is no discussion as to the head needed to raise the weak solution to the absorbing vessel. The method envisaged for automatic switching of the two twin-mode vessels is not described. Absorption is by spray-mixing.

It may be commented that in order for a gravity feed system to work a pressure equalising line is needed, so that the formation of a ammonia-rich layer is in practice unavoidable. It is possible to revise the geometry of Zhang's diagram such that the additional pressure created by the rich layer in the feed vessel provides an additional head, present in a generator stand-pipe (which would be large enough to accommodate vapour flow and be well-insulated), sufficient to cause the weak solution to flow into the absorbing vessel.

Zhang makes use of a collector area of 2.4 m^2 in his experiment, with an efficiency given as

$$0.73 - 5.2\frac{\Delta T}{G}$$

and runs some 100 tests. The solution heat exchanger effectiveness is not given. Evaporating temperatures of -3 to -6 degC are obtained such that ice production varies between 12 and 20 kg/day. Absorption and condensation temperatures are similar, the measured COP varying between 0.12 and 0.18 as they vary between 25 and 29 degC, while the theoretical COP is between 0.15 and 0.18. Rich solution concentration is between 0.49 and 0.52, maximum generating temperatures being between 60 and 76 degC.

2.5.3. Indian Institute of Technology, Madras

Chinnappa and Kok (1986) report on the development of a continuous cycle ice plant in which the pump is replaced by a hydraulically operated transfer tank. Whereas similar systems had already been commercialised (Merrick, 1960) utilising electrically operated transfer tanks, the introduction of automatic transfer was unique in that the complete cycle now required only a source of heat for its operation. The circuit is close to the one suggested by Chung and Duffie (1961) with the exception of being automatic and cycling more rapidly. Chinnappa's system comprised flat plate collectors acting in series with tracking CPCs and auxiliary gas heating, and included rectifier heat reclaim and a solution heat exchanger. A reproduction of the diagram

provided is shown figure 2.5.3.1. The device operates in two phases, first with valve A open and B closed, the second with a closed and B open. The cycle has low and high pressure sides separated by two expansion valves and by the valves A,B,C1,C2, which allow the transfer tank pressure to oscillate. In the first phase the transfer tank is filling from the absorption reservoir and the absorber, since A allows equalisation of pressure between the two vessels, and a gravity head can open check valve C1. In the second phase B allows the generator reservoir to be filled by the contents of the transfer tank. The switching of A and B is controlled by a float which senses transfer tank level. When transfer into the generator reservoir is completed the opening of B causes high pressure vapour to pass into the absorber vapour. A portion of this passes through a blow-down valve into the bottom of the absorber, until pressures are equalised and lowered to a value suitable for absorption. It can be supposed that this is accomplished because the ammonia-rich vapour absorbs into residual solution in the absorber so that after a delay the vapour in the two tanks is in equilibrium with solution only marginally richer than previously, and only marginally warmer. It can also be presumed that were the blow-down line not present the vapour would form a rich liquid layer on the top surface of the absorber liquid, so inhibiting a pressure reduction and inhibiting the action of the two expansion valves feeding the absorber.

Chinnappa estimates rich solution concentration during his tests to be 0.42 to 0.43 and achieves measured solar COP values of 0.133, and 0.145, in the two tests reported in which only solar heat was used. Comparative tests where a conventional pump replaced the transfer tank gave better results; the use of the transfer tank was estimated to reduce system efficiency by 30%. The theoretical cycle COPs for the same two tests were 0.394, and 0.374. The tests were conducted between 11 a.m. and 2 p.m. on clear days, the total insolation arriving on the 10.86 m^2 collector area being 81.9 and 83.5 MJ, with collector efficiencies of 0.355 and 0.329 respectively. Condensing temperature was in the order of 27 to 29 degC and 25 to 27 respectively, with absorption temperature being very similar; generating temperatures were 104 and 105 degC. Evaporating temperatures were -6 and -8 degC.

Chinnappa does not comment on the cause of the transfer tank inefficiency. One possibility is that yield is lost by absorption into the tank, an effect which would perhaps be marked if the

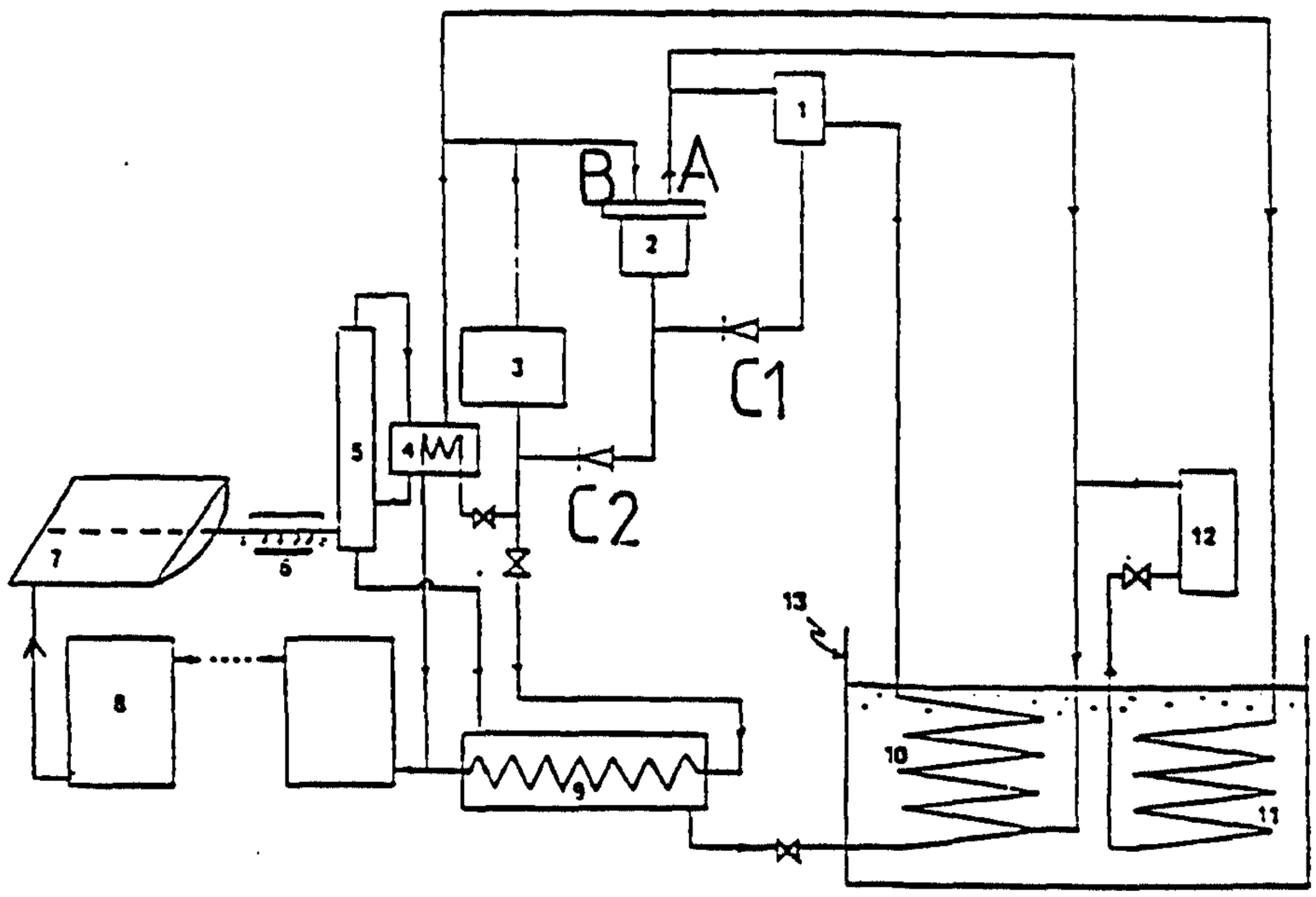

Schematic Flow Diagram. 1 - absorber reservoir;
2 - transfer tank; 3 - generator res.;
4 - rectifier; 5 - separator; 6 - gas heater;
7 - conc, collectors; 8 - flat plate collectors;
9 - heat exch.; 10 - absorber coils;
11 - condenser coils; 12 - evaporator;
13 - cooling water tank.

Fig. 2.5.3.1 from Chinnappa (1984)

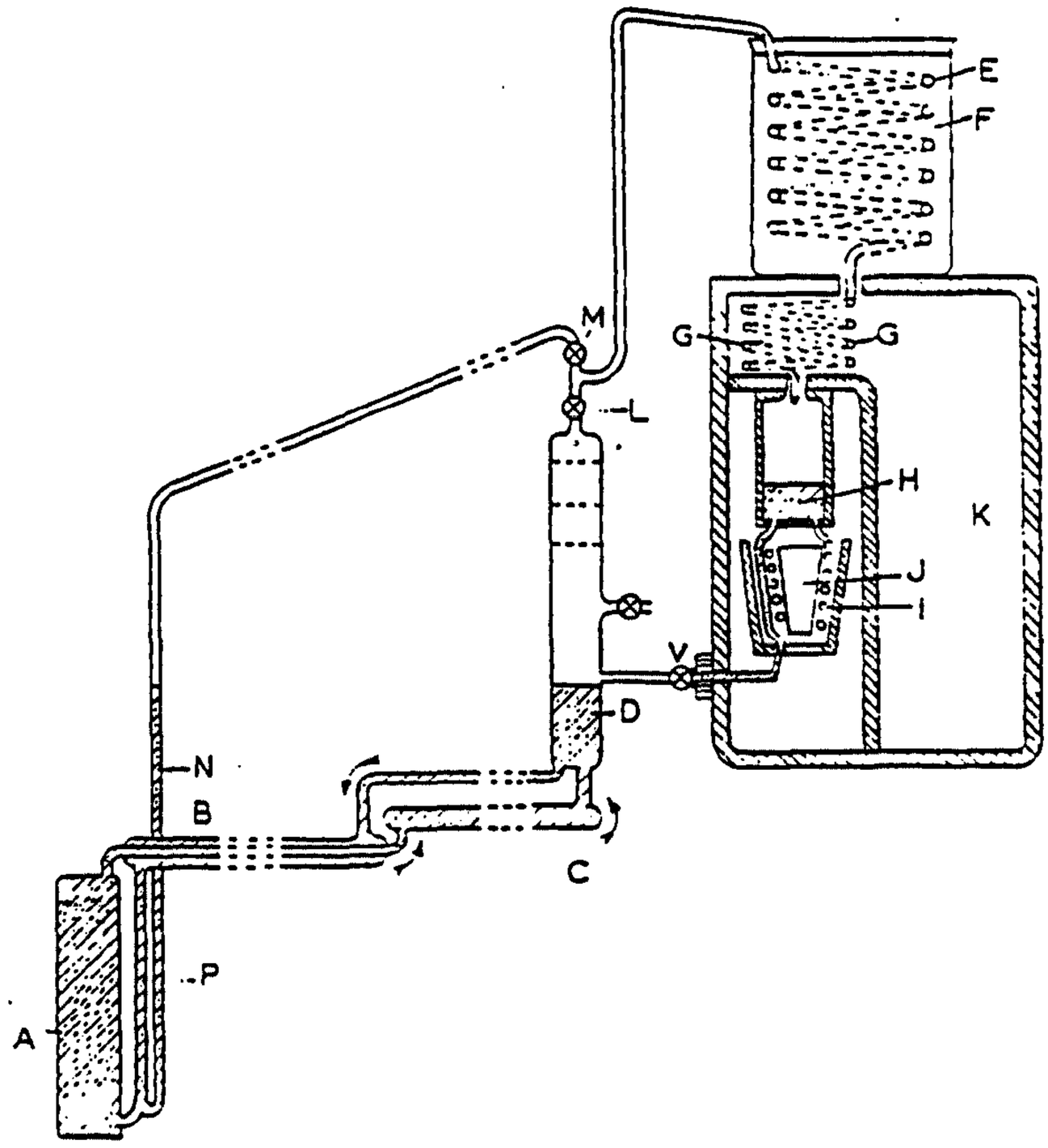

Fig. 2.6.1.1 from Trombe and Foex (1957)

transfer action is not gentle. It would be interesting to know whether the inefficiency resulting can be controlled by the use of a very small diameter connecting line. Cycle COPs are rather lower than one would expect considering the use of rectification heat reclaim and a solution heat exchanger. Chinnappa does not provide any information on the effectiveness of the solution heat exchanger, nor on the relative flow rates between the rectification heat reclaimer and which are plumbed in parallel.

This system is like other continuous systems in not requiring any method of cooling the hot side components, and in not requiring large and heavy solution reservoirs, implying the possibility of portability. Another advantage is that the whole day's insolation is made use of. The setting of solution flow rate is not a function of heat input as is the case in bubble-pumped systems. Its disadvantages would appear to be that several more discreet vessels are needed, and four automatic valves must work reliably. Low night temperatures are not made use of in the absorption phase.

2.6. Hybrid intermittent and regenerative systems

2.6.1. Mont-Louis solar energy research center, Pyrenees, France

Trombe and Foex (1957) propose the circuit shown in fig 2.6.1.1. It includes a reservoir that remains substantially at ambient temperature throughout the twenty-four hour cycle. During generation the lower part of the reservoir (A) contains the weak concentration liquid returned from the generator, while the upper part contains the unused strong solution. It is anticipated that the effect of density stratification will be to inhibit mixing. A cylindro-parabolic reflecting collector, the inclination of which can be manually adjusted, concentrates solar energy onto a generator tube (C). Inside the tube bubbles form to provide a vapour lift effect capable of circulating the solution in the direction shown by the arrows on the diagram. A separator (D) is sized so that it can contain enough solution to allow circulation to continue throughout the desired generation period. The condenser is to be cooled by a stagnant water tank which is insulated against solar energy during the day but allowed to cool to ambient temperature during the night. The circuit

also comprises manually operated valves to allow it to be switched between generation and absorption phases, and a valve to allow the evaporator to be periodically purged of water.

In order for evaporation to take place at low temperature the separator temperature must be substantially reduced. Trombe and Foex do not point out that this is a difficult demand on the circuit as shown, because the separator is insulated and decoupled from the rest of the liquid circuit by the solution heat exchanger. Since manual manipulation of valves L and M is required to switch phases, it can be supposed that the removal of the separator insulation manually is also practical, but no mention is made of this. They explain that once L is closed and M opened bubbles will appear in the pipe O which cause a circulation of solution in the opposite direction of the arrows (the authors write that it is in the direction of the arrows) by means of a vapour lift effect. This circulation accelerates the cooling of the separator which has already commenced at an earlier stage, presumeably either by leakage through the insulation or by removal of the insulation. It may be commented that if the separator is presumed empty, as it ideally would be after generation, the effect of the solution heat exchanger is to retain separator heat for less time than if it contains appreciable residual solution, assuming the solution heat exchanger remains insulated. If the circulation rate is rapid then the delay in cooling is decreased. The source of gas is the evaporator which is presumeably functioning at high temperature during this delay, while the refrigerant cools itself or cools cold box contents if they are initially at ambient temperature. No comment is made as to whether this vapour mass will be sufficient at all times to cool the separator. The authors comment that the refrigeration efficiency varies little between the beginning of absorption and the end. They draw attention to the advantage of the arrangement that the vapour in O is mixing with weak solution being drawn out of the reservoir. This implies that their design does not experience a sharp drop in evaporator temperature at the start of absorption as enriched solution is always present in the tube O. It can be seen that the pipe O may be designed to provide the necessary heat transfer for absorption heat rejection; the danger of failure of heat rejection is evident as transfer of absorption heat to the separator will cause a rise in evaporating pressure and temperature.

The authors point out that an advantage of their circuit is that is that it has low thermal inertia and most sensible heat is recovered by the solution heat exchanger. It also has the advantage of requiring no pumps and no power inputs other than solar.

Tests on two prototypes are given a very brief mention. One prototype is reported to produce 6 kg of ice per day with a collector area of 1.5 m^2 while the other produces 95 kg per day with a collector area of 18 m^2. The sensible preheating period is 1.5 hours while generation is for 4.5 to 5.5 hours. The COPs are not reported, but it is noted that the COP of the large cooler was greater than that of the small. It can be quickly surmised that if solar insolation was in the range 20 to 25 MJ/m^2day during testing, and 1 MJ of cooling produced 2 kg of ice, then the small unit would have had a COP of 0.08 to 0.1 and the large unit a COP of 0.1 to 0.13. Unfortunately the efficiencies of the collectors are not reported which leaves the internal cycle COPs unknown.

2.6.2. Technical University of Delft, Netherlands

Fig 2.6.2.2 illustrates the circuit of an intermittent regenerative solar refrigerator designed by Van Paassen (1986) to satisfy the WHO specification for vaccine preservation. Fig 2.6.2.1 shows a drawing of the refrigerator, which was developed and constructed at Delft. Tests were undertaken in Botswana in 1985 and 1986 and reported on by Van Paassen (1986). The collector/generator is a flat plate type with an absorption area of 1.6 m^2. It incorporates a counterflow tube-in-tube solution heat exchanger the dimensions of which are not given. The design has similarities with that of Trombe and Foex, some differences being that a check valve allows it to function automatically, the absorption path differs, and the evaporator design differs. An automatic expansion valve is included which eliminates the need for a valve to purge water from the evaporator. Vapour lift pumping is accomplished in the generator. The separator has an internal volume of 8 litres, the reservoir 30 litres, and the receiver 7 litres. Van Paassen makes the point that the correct sizing of the receiver is of great importance, as an undersized receiver could lead to liquid filling the condenser and so causing a dangerous rise in system pressure.

Test data collected on 23 June 1985 are used to describe the generation phase behaviour. Some of the results recorded are reproduced in figs 2.6.2.3(a) to (c). At 8.15 a.m. the solution

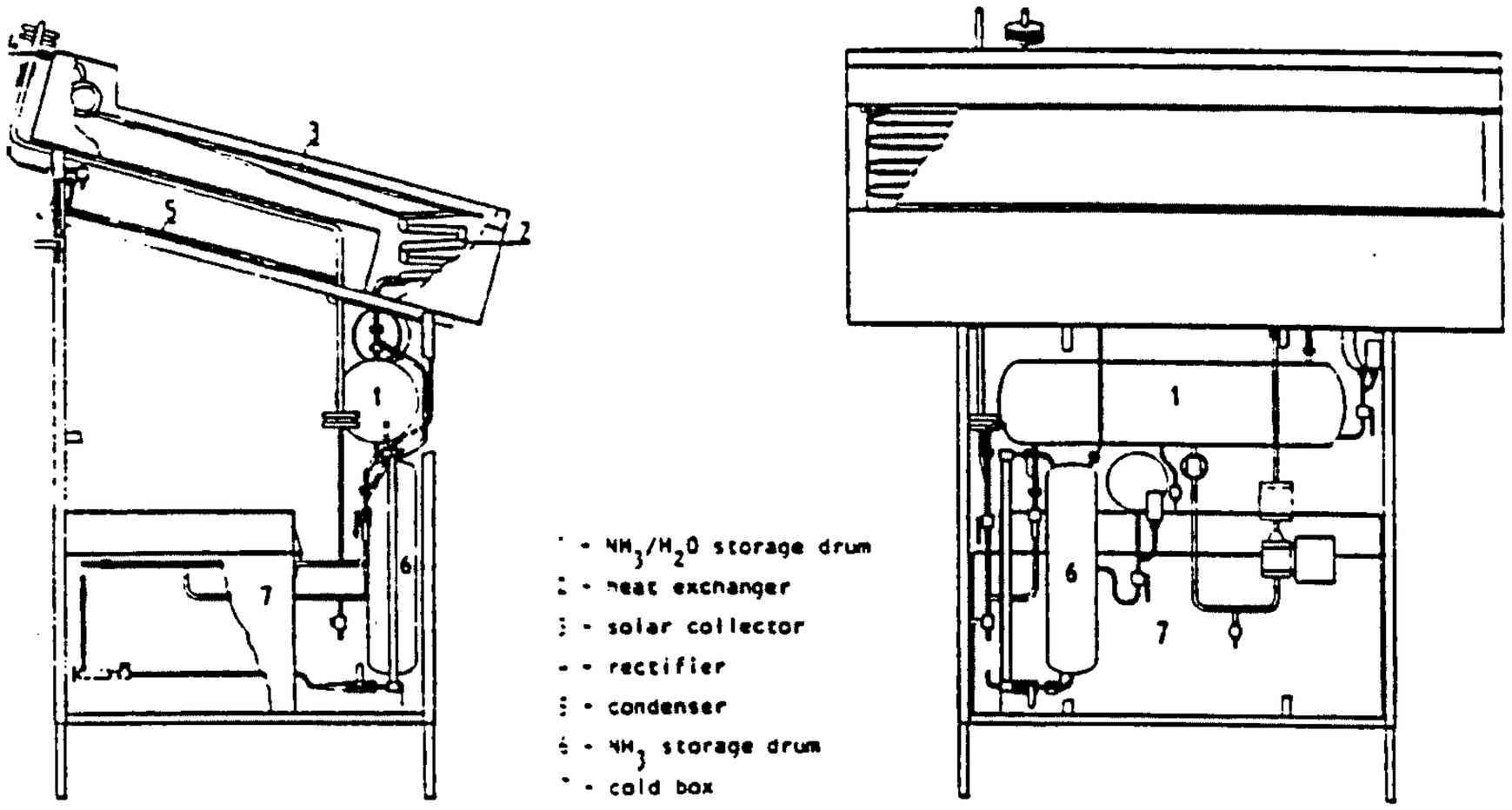

Fig. 2.6.2.1 from Van Paasen (1986)

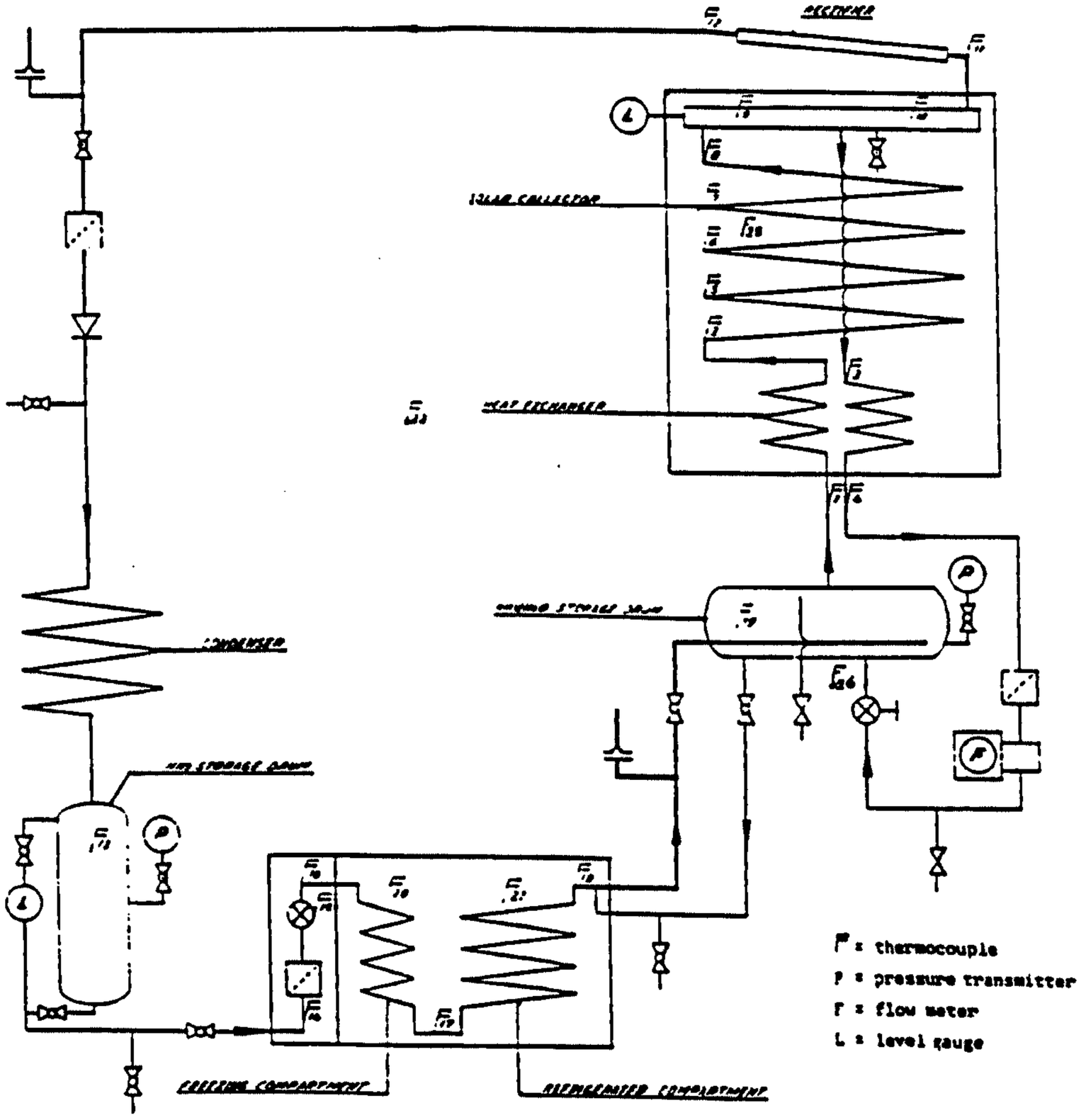

Fig. 2.6.2.2 from Van Paasen (1986)

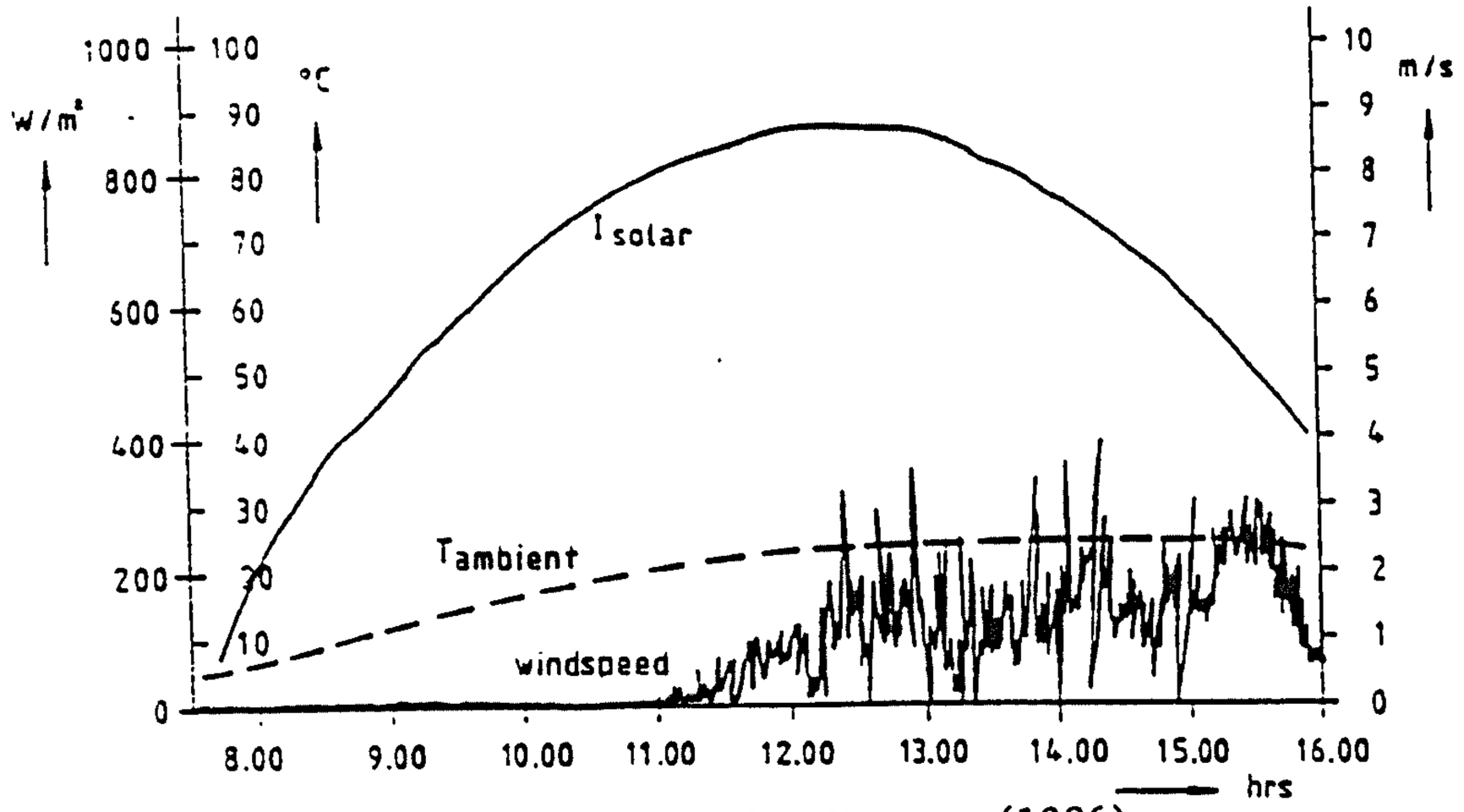

Fig. 2.6.2.3 (a) from Van Paasen (1986)

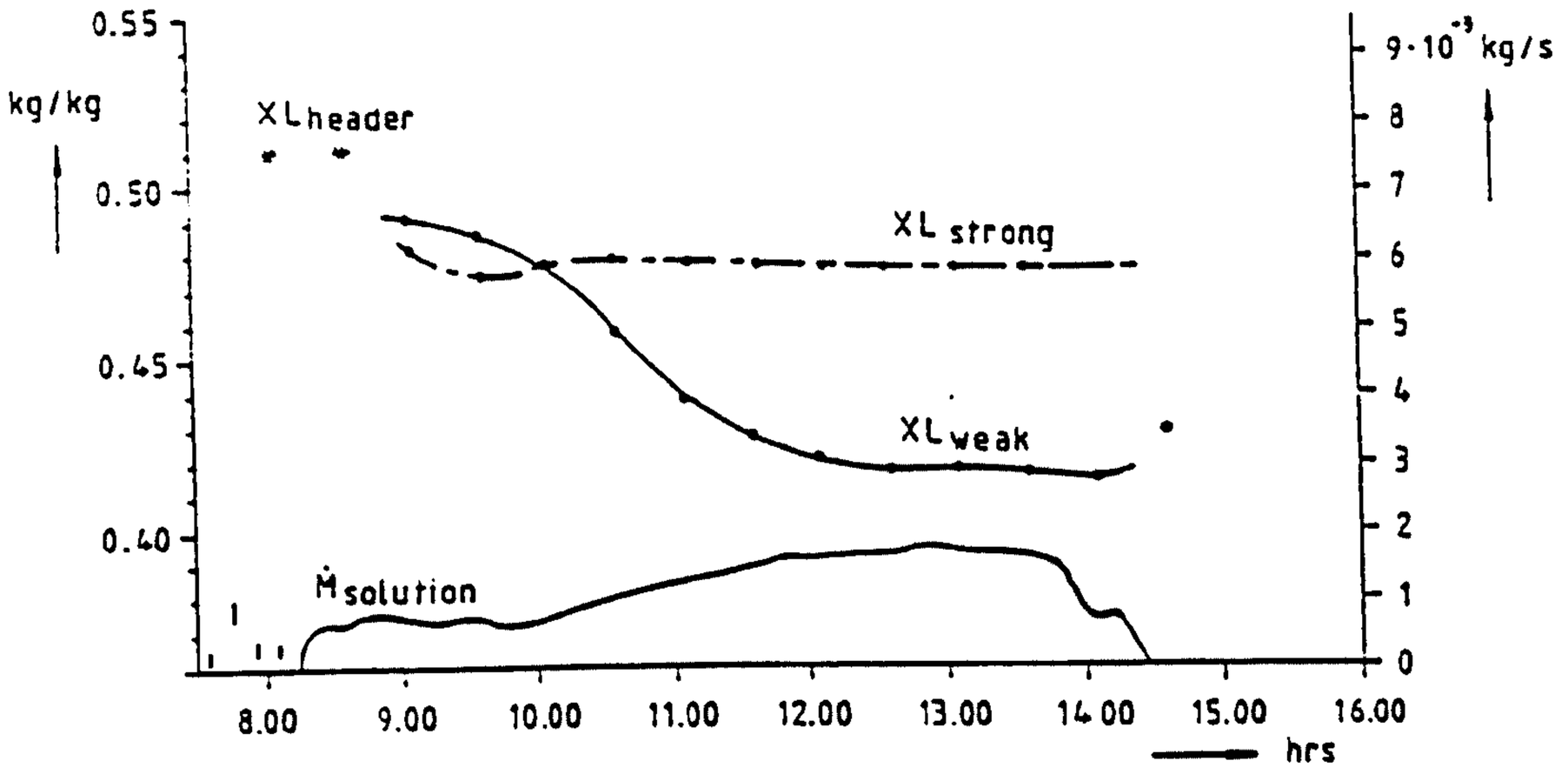

Fig. 2.6.2.3 (b) from Van Paasen (1986)

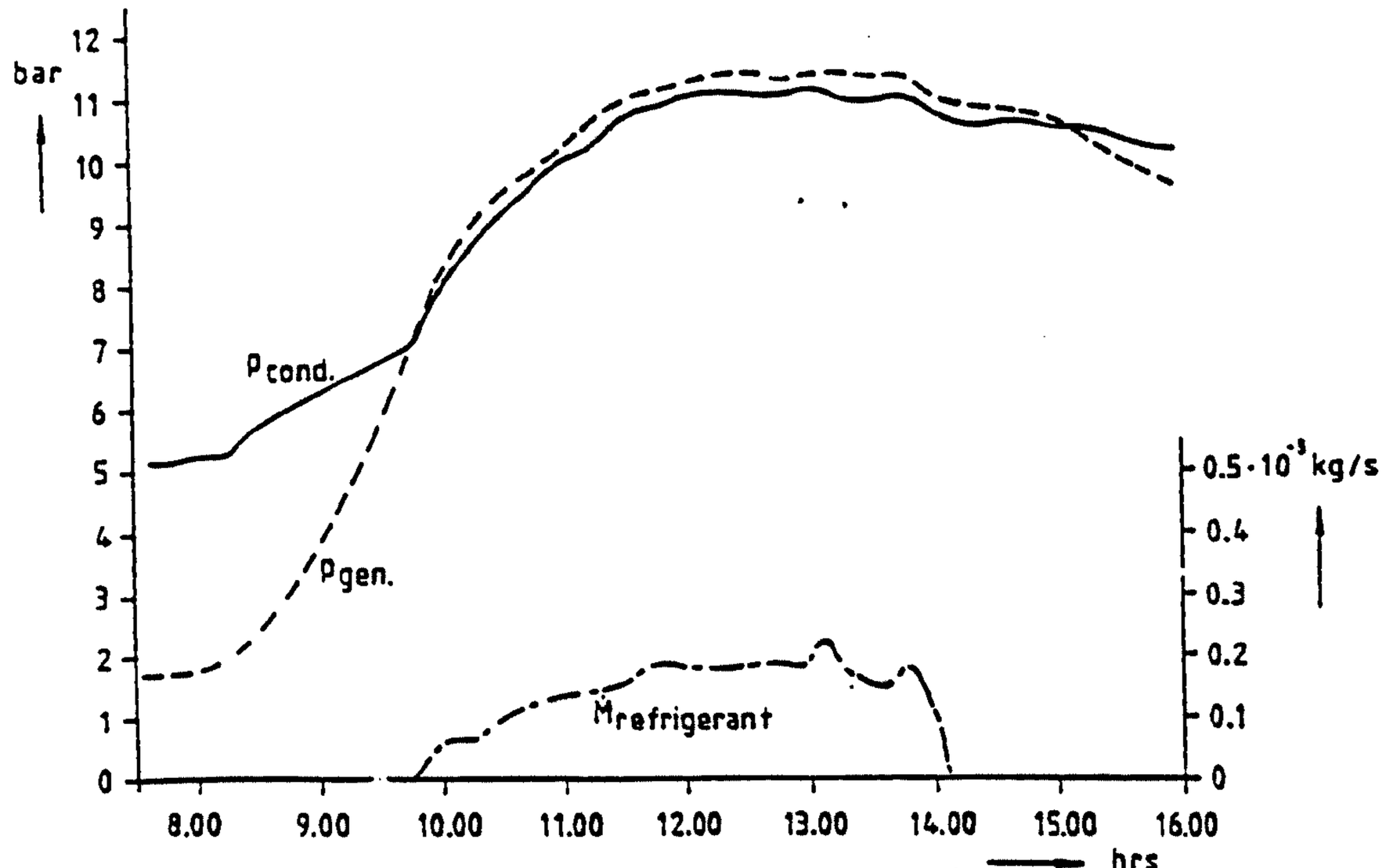

Fig. 2.6.2.3 (c) from Van Paasen (1986)

flow begins, implying that solar insolation below 300 W/m^2 has little effect. The condensate collection rate is measurable at 9.45 a.m, when the generating pressure has risen to match the receiver pressure. The separator is observed to run dry just after 2.00 p.m. 2.2 kg of refrigerant having been collected by this time. The feed solution concentration is monitored throughout generation, maintaining its initial concentration of 0.48 throughout. The reservoir contents are fully cycled by the end of the period, so indicating that the density stratification principle proposed by Trombe and Foex is successful.

Weak and rich solution flow rates were separately measured. Total mass and energy transfers for the for the generation period (07:35 to 14:05) are calculated. 25.12 MJ of solar energy are received, 17.62 MJ of which are lost optically or as heat leakage to ambient. This implies a collector efficiency of 0.3. 1.38 MJ of the remaining 7.5 MJ is stored as sensible heat in the collector/generator materials, where these are taken as excluding the solution heat exchanger. It is not stated whether the figure includes sensible heat storage in the separator vessel and any residual liquid inside it, but this can be presumed to be the case. Of the 5.43 MJ recovered from the weak solution flow only 4.64 MJ are absorbed in the solution heat exchanger by the rich solution flow. It might be commented that the total loss in sensible heating, if heat leakage is considered only in terms of collector efficiency, was 2.17 MJ, constituting 17% of the energy available (7.5 MJ from the collector and 5.43 MJ from the weak stream). Whereas the solution heat exchanger loses 14% in this manner the generator and separator lose 18%. It is apparent that the solution heat exchanger is contributing 43% of the remaining useful energy (4.64 MJ as a fraction of 10.75 MJ), and therefore cannot be faulted. Its effectiveness is calculated from the four end temperatures to be typically in the order of 0.8 as a day average, stabilising at 0.86 in the hottest period of the day. From measurements taken periodically of vapour concentration, it was observed that rectification was successful and an adequately pure refrigerant was produced. The refrigerating capacity can be based on the the useful latent heat of the refrigerant which is 1160 kJ/KG, so implying a capacity of 2.6 MJ and a solar COP of 0.1.

It is useful to attempt to draw from these results an indication of how a modified version of the circuit might perform. If, for instance, the thermal mass of the collector/generator was

eliminated altogether, the internal cycle COP for the whole generation period is 0.49 rather than the 0.35 indicated above. If a more efficient collector is also postulated, for instance one capable of an efficiency of 0.5 in these conditions, then a solar COP of nearer 0.24 might be sought after. In the report Van Paassen does point to low collector and generator efficiencies as the cause of the low solar COP.

Absorption is designed to take place primarily in the generator, the collector acting as a night radiator. The refrigerant gas is first passed through the reservoir where a limited portion is absorbed, the remainder passing into the generator tubing and causing circulation by a combination of thermosyphon and vapour lift effects. In practice an unexpectedly large proportion of the refrigerant mass absorbed in the reservoir, only 14% passing into the generator. It was found that heat rejection from the collector was unsatisfactory and that high concentrations appeared in the separator. System pressure rose during absorption so hindering the refrigeration process; this is explained to be both the result of rising temperature in the reservoir due to it not being designed specifically to reject heat, and due to failure of the generator to absorb. It is commented with reference to a particular absorption process that the generator circuit would ideally have been at ambient temperature such that its pressure would have been 2.1 bar lower; the indication was of failure of heat rejection from the absorber or possibly of artificially high pressure being maintained by a layer of rich solution in the separator.

The 3.38 MJ rejected by the reservoir during the absorption process of 27 June implies a heat rejection rate of 80 watts if a full 12 hours of absorption is postulated. The reservoir is a horizontal cylinder of length to diameter ratio of 4.3, and although free of encumbrances, it is not finned or in any way equipped for heat transfer to ambient. Van Paassen states that 3 MJ of cooling is accomplished. The ambient temperature during a similar process fell from 25 to 15 degC by 20:00 hours, while reservoir temperature rose to 30 degC and then declined toward 25 degC. If the night temperature is taken as 15 degC and the reservoir temperature as 28 degC, the emissivity of the drum surface as 0.25, and the surface area (A) of the drum as 0.8 m^2, then assuming that all the surface can transfer heat by radiation to sinks at ambient, the radiative loss from the drum is in the order of 15 watts. The remaining 65 watts of loss can be assumed to transfer by

natural convection according to the relation:

$$\dot{Q}amb=kA\Delta T^{1.25}$$

where "k" is the heat transfer constant defined by the relation. The value of k is therefore 3.3, which is larger than expected; it is conceivable that the night may have become colder than 15 degC and the action of the regulating valve in maintaining the absorber pressure would have led to a higher average value of ΔT and greater radiative loss, and so a lower value of k.

Comments are made on each of the components in turn. The check valve did not work satisfactorily mounted in a horizontal position but gave no problems when mounted vertically. The air-cooled condenser functioned consistently well with a temperature drop of 7.5 degC. The expansion valve used was of a design which did not respond to the temperature of the evaporator alone, but was also responsive to the receiver pressure. Since ambient temperature underwent large fluctuations this led to inadequate regulation of evaporator temperature. It was recommended that a different type of expansion valve is adopted in further work, in particular one which responds only to downstream pressure.

The cold box comprised two compartments, a freezer capable of holding 8 ice packs of dimensions 80mm 190mm 30mm, and a cold storage space of 40 litre capacity. The cold storage space was surrounded by a jacket containing 12 kg of water. The evaporator pipework arrangement is not described. Tests were undertaken which showed that the ice packs, containing approximately 3.6 kg of water, required 8 hours to freeze completely when the wall temperature surrounding them was held at -10 degC.

Field testing of the cold box revealed that temperature regulation of the cold storage compartment could not be maintained. The water jacket contents would freeze completely after a series of clear days and the cold storage temperature would drop below 0 degC. The performance of the evaporator was evaluated during a six day period in August 1985. The average solar COP during this time is calculated as 0.09. The freezing compartment was filled with cold water in ice packs only once at the start of the test, whereas new water at ambient temperature was placed in the cold storage chamber each day. The water jacket was fully frozen at the start of the period. The energy consumed in freezing water was calculated to be on average 1830 KJ per day, while

the average evaporation rate was 2.75 kg per day of refrigerant. The useful energy extraction was therefore 665 KJ/kg ammonia, or 2 kg of ice per kg of ammonia.

Tests were conducted also to measure the hold-over performance of the cold box, which was insulated with 100 mm thick polystyrene walls. The lid was kept shut during the test. The ambient temperature cycled between average day and night values of approximately 20 and 13 degrees. A temperature of below 0 degC was held for nearly five days and did not rise to 8 degC for a total of 6 days. The average insulation loss was therefore 9 watts, or 800 KJ/day.

Certain problems are mentioned with respect to the reliability of operation of the test unit. Stratification in the separator header is mentioned as a problem. The expansion valve is considered inadequate and further design aimed at combining a capillary tube with a an expansion valve is proposed. The unit is described as being not adequate for year round operation as the achieved efficiencies are often too low.

2.7. Summary

The discussion above has reported on the experience of various researchers in prediction and measurement of the characteristics of the intermittent basic (IB), continuous pumped (CP), diffusion-absorption (DA), and intermittent regenerative (IR) type devices, as well as a further variant, the ''pumpless continuous'' systems. Their work helps us to check the validity of the IR design examined in later chapters, and to check the validity of the presumptions made in chapter 1 as to its potential improved performance.

The intermittent basic (IB) system is built in different forms by Williams, Chinnappa, and Exell. Solar COP values ranging between 0.09 and 0.15 are obtained in practical tests, as listed on table 2.7. Component costs are not presented and analysed generally. Exell's work establishes that in the economic conditions of Thailand a COP of this order represents a production cost of remotely made ice which is twice the urban retail price, suggesting that commercial viability, given reliable operation, is within reach. Certain observations as to constraints on IB performance can be made. With the exception of Williams', the systems makes use of flat-plate collectors, and all demonstrate collector efficiencies of the order of 0.3 or 0.4 during clear sunny periods.

Response during diffuse periods is very low, and even on a clear day desorption starts after a considerably delay, and stops in early afternoon. The indication is that an increase in collector efficiency and a reduction in both solution and collector/generator thermal masses could raise solar COP considerably. Both Exell's and Chinnappa's design show attempts to introduce solution circulation in order to reduce collector/generator thermal masses, but these have not had very significant effects, because the flat plate collectors have necessarily contained relatively large masses of steel and liquid. The intended advantage of the flat plate collector/generator is that it also serves as an absorption heat radiator. In the most highly developed of the IB systems, Exell's 100 kg ice/day unit, this is arranged successfully by manual removal of heat insulation covers from the back of the collectors each night.

Very little data on practical results obtained in solar driven continuous pumped (CP) tests are available. Although considerably greater complexity and expense were involved in the reported experiment by Sloetjes, solar COP values did not exceed those achieved by the IB systems. The theoretical analysis of Chapter 1 suggests a value of 0.2 is obtainable. The use of evacuated tube collectors increased collector efficiency to 0.5 and above, implying that cycle efficiencies, despite the presence of a solution heat exchanger, were lower than those of the IB systems. No information is given which might help explain this.

Hinotani's work on the diffusion-absorption (DA) system is revealing. He establishes through experiments that the solution flow rate varies with boiler heat input in such a way that optimum desorption efficiency is maintained while insolation rate varies. This is due to the thermosyphonic ''bubble pump'' action. He then discovers that the advantage of this feature is lost because the circulation rate of hydrogen in the evaporator and absorber does not undergo a corresponding variation. Although refrigerant is produced efficiently at all times by the generator, the evaporator fails to make use of it because the evaporation rate depends on a hydrogen circulation rate which is inflexible. Solar COP values of the order of 0.05 are reported. Nevertheless with respect to the proposed IR system Hinotani demonstrates that the design and construction of a self-regulating generator is possible. Since the IR system does not depend on a separate fluid circulation system in the evaporator, this is a strong indication in favour of the IR system.

Hinotani also clearly marks the way for future researchers on solar driven DA systems, demonstrating that the evaporator/absorber circuit is the major constraint to efficient performance.

Some attempts to develop refined ''semi-continuous'' (SC) systems are also made, by Chung, Zhang, and Chinnappa. In all three cases considerable complexity and expense is involved implying that solar COP values of the order of 0.2 must be achieved if these systems are to be improvements on the cost-effectiveness of the IB system. In practice solar COPs up to 0.15 are obtained.

Two realisations of the IR system are reported. The earliest version, conceived by Trombe and Foex, has been important in stimulating further ideas, but their paper contains no detail on practical performance. The later design by Van Paassen was tested in the field and is fully documented. This design centred around the use of a flat plate collector, the intention beting that the collector would double an absorption heat radiator during the night. No manual or automatic valve was considered necessary to transfer from desorption to absorption phase, other than the check valve. In all Van Paassen's design comprised only two moving parts, the check valve and the expansion valve feeding refrigerant into the evaporator. Its operation was intended to be fully automatic. In the event the solution circulation required for absorption did not take place and the absorption heat rejection rate acheived in the collector was inadequate. The penalty paid for adopting a flat plate collector/absorber approach, was that collector efficiency was low, measurements indicating a collector efficiency of 0.3. In addition the overall liquid and steel thermal mass of the collector was high, leading to delay in achieving desorption temperatures and a loss of energy stored as sensible heat. The design did not incorporate any kind of transfer tank, so that an inefficiency resulted from the separator containing a fixed mass of liquid. On clear days the separator would run dry and the desorption process would stop, such that the remaining solar energy was not made use of. The solar COP achieved under the best conditions was 0.1. An analysis shows that the solution heat exchanger operated effectively.

The IR design examined in the following chapters seeks to overcome the constraints identified in reading these reports. High efficiency collectors are adopted, and a low thermal mass generator design, consisting only of a bubble pump tube together with a separator and

solution heat exchanger. The separator size is minimised in the transfer tank version, which is referred to as the variable volume reservoir (VVR) version. In these two ways the proposed IR design approximates to the CP and DA systems powered by evacuated tube collectors. The bubble pump operation of the DA system, which was demonstrated by Hinotani as allowing the generator to be self-regulating to varying boiler heat input, is adopted in the new IR cycle.

	Reference Section	COP theoretical	COP practical	Description
IB	Williams (57) 2.2.1	int 0.37	int 0.36 sol 0.15	non-dedicated collector considerable manipulation no moving parts minimum complexity domestic scale
	Chinnappa (61) 2.2.3	int 0.3	int 0.26	
	Exell (81) 2.2.4		sol 0.09-0.14	flat plate collectors hourly adjustment of mirrors 60% of cost in collectors small scale
	Exell (84) 2.2.4		sol 0.11	scaled for 100 kg ice per day automatic except for water purging
CP	Sloetjes (88) 2.3.1		sol 0.08-0.15	3 KW continuous (24 hr) cooling rate pumped cooling water collectors: ETCs
DA	Hinotani (83) 2.4.2		sol 0.05	fully automatic collectors: ETCs
SC	Chung (61) 2.5.1	int 0.47 sol 0.2		continuous for 23 hours manual transfer switching complex
	Zhang (82) 2.5.2	sol 0.17	sol 0.15	pumped cooling water complex
	Chinnappa (84) 2.5.3	int 0.39	sol 0.13 η_{coll} 0.35	fully automatic complex
IR	Van Paassen (86) 2.6.2	int 0.6	sol 0.1	fully automatic problems with expansion valve inefficient flat plate collector excessive thermal mass

Table 2.7 *Summary of COP figures reported by various researchers.*
Key: int = internal ; sol = solar.
ETC = Evaccuated tube collector. SC = semi-continuous systems

Chapter 3: Modelling of the intermittent regenerative (IR) system

3.1. Introduction

The intermittent regenerative (IR) cycle is introduced in Chapter 1, section 1.6. It is illustrated here in fig 3.1.1. It can be described as a combination of the continuous pumped (CP) and intermittent basic (IB) systems. These two cycles are depicted in figures 1.2.1 and 1.3.1 respectively. It contains also elements of the diffusion-absorption (DA) system; in the IR system the solution feed pump shown in the CP system is replaced by a circulation thermosyphon pump as used in the DA system. This pump provides only just enough pressure difference to circulate solution through the heat exchanger, boiler, and separator (see fig 3.1.1). These three components are the only components of the IR system to rise significantly in temperature during desorption, and can be collectively referred to as the "generator" of the system. Unlike the CP system, a low pressure is not maintained on the absorber and evaporator side of the system, and therefore no weak solution throttle is needed. Desorption pressure pervades the circuit as a whole during the desorption phase, as in the IB system described in section 1.2. Similarly, absorption pressure pervades the circuit as a whole during the absorption phase, just as in the IB system, if a gravity circulating evaporator is used. The phases are intermittent, operating on a diurnal cycle, incoming solar energy causing high pressures and desorption to occur during the day, while the absence of incoming solar energy at night causes the absorption phase to occur. During desorption thermosyphonic circulation of the solution is automatic, by virtue of the incoming solar energy being fed into one leg of the feed pipe to the separator (points 2 to 3 on fig 3.1.1), so that vapourisation of solution causes a density reduction and a bubble-pumping effect in that leg, while denser and single-phase solution descends in the return leg.

The desorption and absorption phases are preceeded by pressurisation and depressurisation phases respectively. In this respect the IR cycle follows a pattern similar to the IB system and the

description given in section 1.2 can be returned to for an indication of the phase pattern followed by the IB and IR systems. The essential difference between the two cycles is that the IR cycle allows the sensible heat of boiled solution to be reclaimed in a heat exchanger. This means that it promises to provide double the COP of the IB system, since the CP system is known to offer this improvement through the use of solution heat exchanger. It does this without the need for an externally powered pump, as used in the CP system. It also does this in a diurnal cycle which allows absorption to occur at night, so taking advantage of climates where night time ambient temperatures are lower than daytime. The brief study made in Chapter 1 of the effect of absorption temperature on cycle efficiency indicates that this constitutes a significant advantage of the IR system over the CP system. An additional advantage of the intermittent cycle over the continuous one is that the rejection of heat of absorption is not required to occur simultaneously with the rejection of heat of condensation. Since the devices considered are intended for use in remote locations with minimal technical supervision the use of air-cooled heat exchangers or radiators is preferred to the use of water-cooled heat exchangers. This implies that a major component of the cost of the device is in radiator area. The IR system offers the possibility of both absorption and condensation heat being rejected through the same radiator area, whereas in the case of the concurrent-phase CP system this is impossible, so implying that an IR system would have significantly lower cost. A method of sharing radiator area is discussed in Chapter 4 and Appendix A.

A fourth feature of the IR system distinguishes it from both the IB and CP systems. Because the solution is circulated by thermosyphonic action which is a positive function of the intensity of incoming solar energy, the solution flow rate will tend to increase as solar intensity increases. The parametric study of the CP system (see fig. 1.3.4) indicated flow regulation of this sort would be an advantage to allow the CP system to maintain optimum efficiency in the face of changing solar intensity. The IR system operating principle suggests that this kind of flow regulation will occur automatically and the system will self-match, or self-tune, itself to climatic conditions. Bulk yearly COP should therefore be greater in the case of an IR system for this additional reason.

The purpose of this chapter and the remainder of the study is to examine the IR system in detail in order to test the validity of these projections.

The present chapter develops a computer model of the IR cycle. The desorption phase, equivalent to phase Ib as described by figure 1.2.1, is examined in detail for steady state operating conditions. The simulation includes an allowance for transient effects due to variations in boiler heat input and to take account of the pressurisation phase Ia.

The development of a model is justified in several ways. Firstly , it was found in Chapter 1 that the three existing aqua-ammonia cycles each have shortcomings with respect to use with solar collectors as their sole energy sources. Some ways in which the proposed IR system promises to avoid these shortcomings, and so lead a significantly more cost-effective system, are mentioned above. The first purpose of the model is to put these promises to the test in quantitive rather than purely qualitative terms. By applying the same operating conditions, or input parameters, as were applied to the reference systems in Chapter 1, quantitive comparisons can be made as to COP, self-regulation with respect to variations in solar intensity, and response to absorption temperature. The usefulness of the novel IR system can be evaluated. No model of the proposed IR system already exists.

Secondly the model allows extensive parametric study of the system to be made. The effect on performance of condenser size, evaporator temperature, and solution heat exchanger size, can be studied. This also means that the model is useful in sizing and predicting the system performance in a variety of different climatic conditions, for instance under different diurnal temperature regimes.

Thirdly, the model is based on the fundamental equations governing the cycle operation. It therefore functions as an analysis of the operating principles of the cycle.

Fourthly the model is a design tool. It allows the solution heat exchanger size to be optimised, the condenser temperature to be chosen, and the frictional resistance to fluid flow of the solution circuit to be set for optimum performance. It determines the quantity of solution required, and the concentration required, for given climatic conditions and a given cooling duty.

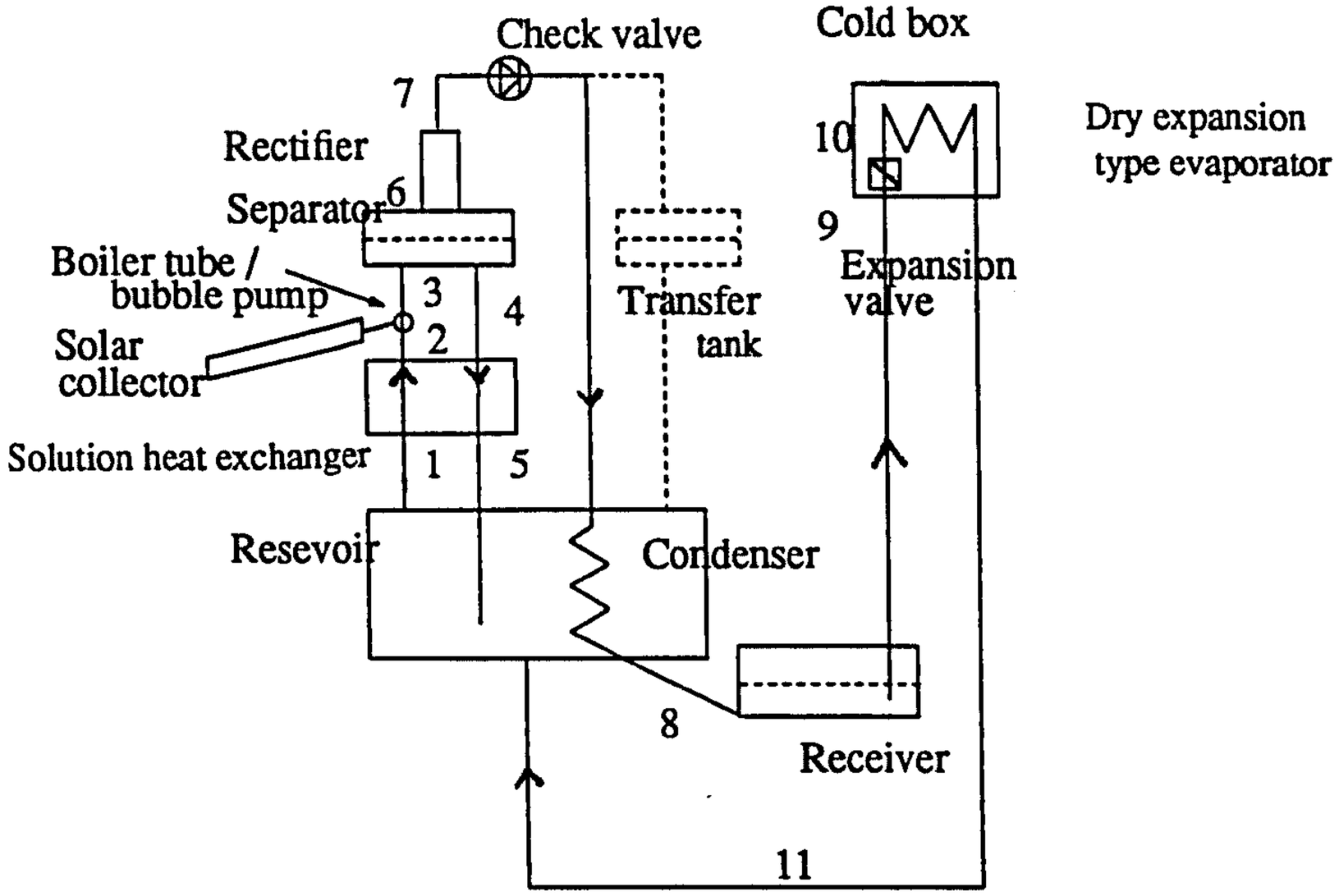

Fig 3.1.1 *The intermittent regenerative (IR) system in the novel form proposed for this study. Without the transfer tank in circuit, the cycle is referred to as the fixed volume reservoir (FVR) cycle. With the transfer tank in circuit, the cycle is referred to as the variable volume reservoir (VVR) cycle.*

In order to allow the simulation to function as an analysis of the complete cycle an approximate solution is adopted for the refrigerating effect of phase IIb. A closer examination of phase IIb is then made in chapter 4 and Appendix A.

The IR circuit is considered in two forms, both shown in figure 3.1.1. The simpler form makes use of a reservoir of fixed volume (the FVR circuit), and does not include the transfer tank component shown by the dashed line. The refined form of the IR circuit differs in that the separator component is significantly smaller and in making use of a variable volume reservoir which is accomplished by the use of a transfer tank as shown. This is referred to as the VVR circuit. An explanation of the distinctive operating principles of these circuits is given in chapter 1, section 1.6.

Sections 2 and 3 of the present chapter present the first law equations governing the components of the generator, and number those expressions which form the basis of a computerised solution for steady state conditions. The computer model is described in section 4. The model is applied to the task of sizing and optimising various components in the circuit (the solution heat exchanger, and the air-cooled condenser). In addition the potential for self-regulation of flow in the IR system is investigated and a method determined for the adjustment of the circuit pressure drop in order to obtain optimum performance in varying climatic conditions. Finally the model of steady state performance is developed as a step-wise dynamic simulation in order to establish the performance limitations of the device more precisely.

Certain assumptions are made which idealise the cycle, the most important of which is the assumption of phase equilibrium in the rectifier, separator and boiler. These act to separate and to combine vapour and liquid solution and so require finite differences in both pressure and temperature to accomplish mass and heat transfers respectively. A second assumption is that one pressure pertains at any instant throughout the system during generation. In practice the mass flows in the pipework imply the existence of finite pressure differences between the system components.

3.2. System pressure

The pressure at which generation takes place is governed predominantly by the temperature at which the refrigerant vapour is condensed. The condensing temperature is dependent on the rate at which heat is removed from the condenser, and so is a function of the heat removal characteristics of the condenser and the sink temperature, and the rate at which refrigerant is produced by the generator ($\dot{m}v7$ in figure 3.4.1). The system pressure is also a function of effectiveness of the rectifier since the greater the water content the less the pressure at which condensation occurs. The concentration of the vapour leaving the rectifier can be assumed to be the outcome of equilibrium conditions existing at the exit, so is a direct function of the temperature of the rectifier exit and the system pressure.

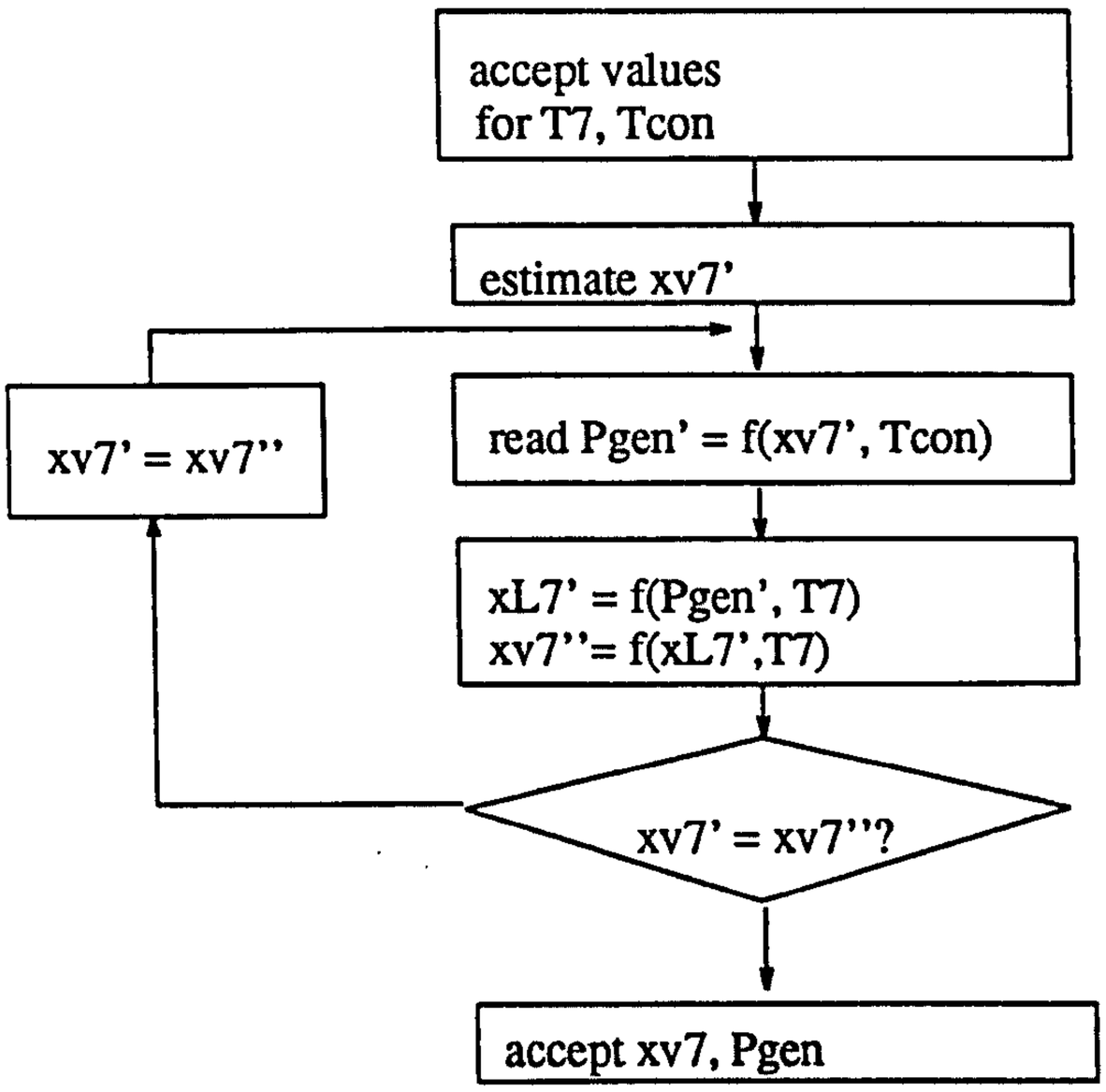

Fig 3.2.1 *The iterative solution used by the computer model, to establish the concentration of vapour leaving the rectifier* (x_{v7}) *and desorption (or generation) pressure* (P_{gen})*, given values for condensation temperature* (T_{con}) *and rectifier exit temperature (T7). Nomenclature is easier understood by referring to the station points marked on figures 3.1.1 and 3.4.1 and to the nomenclature listing. Successive iterations are indicated by apostrophies.*

A full solution for system pressure therefore depends on a specification for the rectifier and condenser sizes, efficiencies, heat transfer characteristics, and the sink temperature, together with simultaneous solution of the these relations with a solution for the vapour production rate of the boiler feeding the rectifier. A convenient simplification is to adopt independent values for rectifier exit temperature (T7) and condensing temperature. The supposition then is that the physical characteristics of the components are adjusted to maintain these values. In the present study this

simplification for T_{con} is maintained until section 3.12 when it becomes a dependent variable. In the case of T7 the simplification is maintained throughout.

Given independent values for T7 and T_{con}, the iterative solution adopted for system pressure and simultaneously for condensate purity is shown in fig 3.2.1.

3.3. Approximate solution for absorption phase

Conditions during the desorption phase are influenced strongly by the solution concentration which is the product of the preceeding absorption phase. The concentration achieved is determined by the pressure of the system and the solution temperature at the end of the absorption phase, as described in section 1.2. The total cooling effect, or heat extracted by the evaporator (Q_{ev}), is the result of the particular response of the evaporator, as investigated in chapter 4 and Appendix A. For the present purposes an estimate of the cooling effect is made by assuming the use of a dry expansion evaporator and assuming that a constant pressure is maintained during absorption (P_{ab}), which is determined by the prescription of the evaporating temperature desired, seen as the equilibrium temperature occuring at point 10, immediately downstream of the expansion valve. A schematic diagram of the evaporator is provided in figure 3.3.1. The evaporating temperature desired is assumed constant throughout the process, so that the process is being modelled as similar to that occuring in a continuous cycle device (fig 1.3.1). The analysis here draws on the work of Stoecker (1971) in steady state modelling of such devices.

The operation of the evaporator is complicated by the presence of unrectified water in the refrigerant. Fig 3.3.1 illustrates schematically the distribution of water in the evaporator. The sharp pressure drop across the expansion valve causes some liquid to flash to vapour. The liquid-vapour ratio is determined by the isenthalpic nature of the flashing at an overall enthalpy of $h_{L9}=h_{(total)10}$. The liquid remaining at point 10 is rather stronger in water since the more volatile ammonia preferentially vapourises. As the two-phase mixture is forced through the evaporator it draws heat from the tube walls and continues to vapourise at constant pressure, implying that the equilibrium temperature is rising, since the liquid will continue to become stronger in water. At the temperatures and pressures considered there will in fact be no significant evaporation of

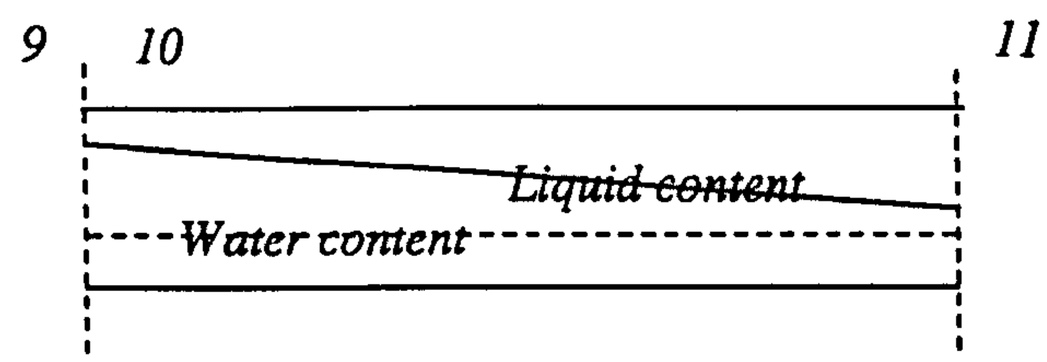

Fig 3.3.1 *Schematic of the evaporator showing that the water component of refrigerant does not evaporate; the refrigerant is weaker in ammonia at the evaporator exit.*

water. The residual water will be driven out of the evaporator in a solution the concentration of which is determined by the size of the evaporator and the cooling load. These may for instance cause sufficient vapourisation to occur such that the concentration reduces to a value of around 0.9. If the expansion valve is set to hold a pressure of for instance 3 bar, in order to induce cooling at -10 degC at the expansion valve, then the temperature at the exit of the evaporator, T11, is approximately -7 degC. It is evident therefore that no danger exists of ice forming in the evaporator tubing and either blocking it or reducing the internal heat transfer coefficient. Reference to figure 1.2.5 indicates that a solution of concentration 0.9 will have a freezing point no higher than -70 degC.

In practice a pressure drop exists over the evaporator tube, so that the pressure at point 10 is greater than the absorption pressure in the reservoir; neglecting this, the absorption pressure can be written

$$P_{ab}=\text{function}(x_{L10},T10)$$

where T_{ev} = T10, and is prescribed. P_{ab} can now be found by solving iteratively for the value of x_{L10}, following the code illustrated in fig 3.3.2. The mass fraction of vapour at 10 (VF10), can be found by taking an energy balance

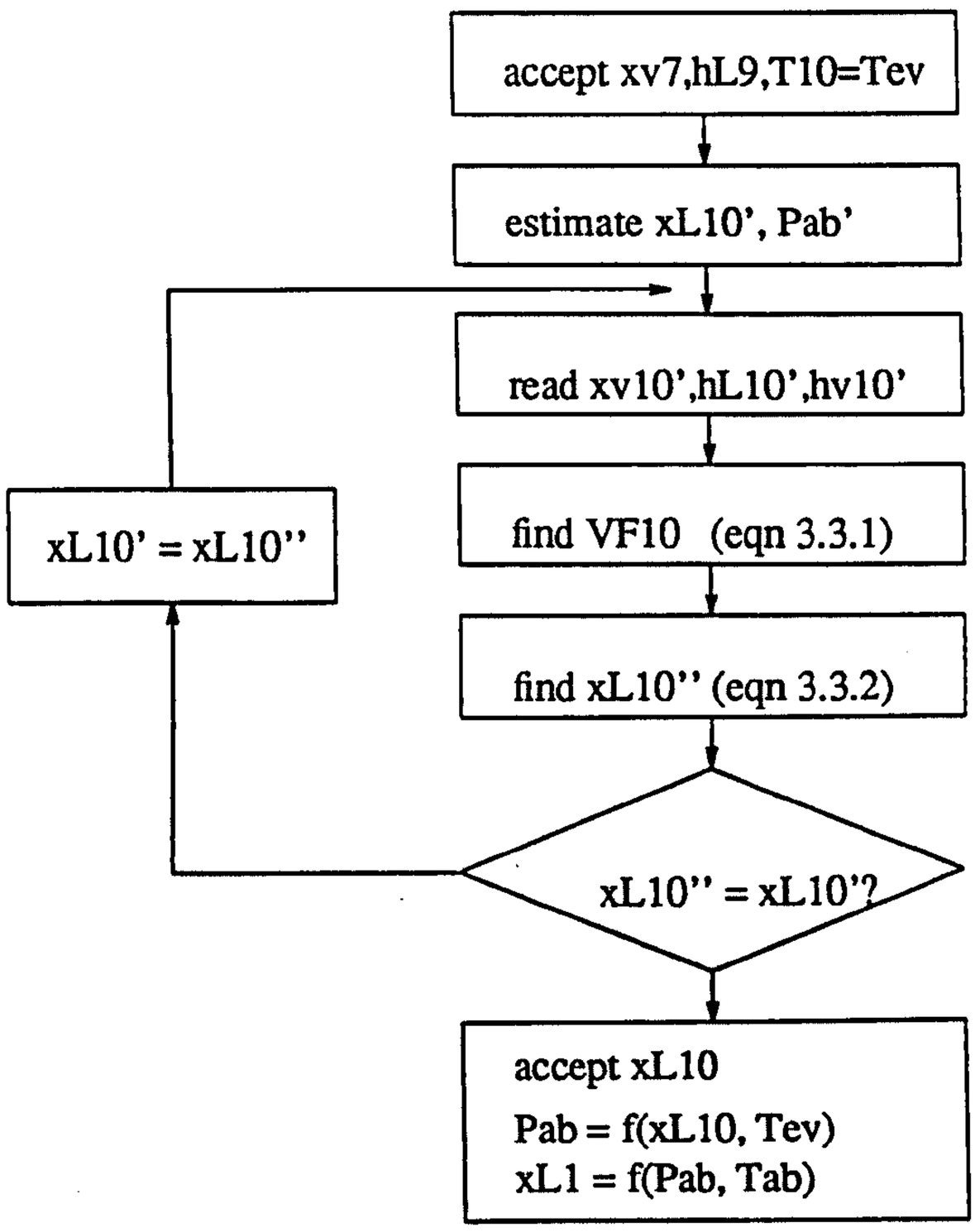

Fig 3.3.2 *Iterative solution for rich solution concentration* (x_{L1}) and absorption pressure (P_{ab}) based on a given value of evaporating temperature. Refrigerent concentration (X_{v7}) is calculated by the code shown in fig 3.2.1.

$$h_{(total)10}=VF10.h_{v10}+(1-VF10).h_{L10}$$

such that:

$$VF10=\frac{h_{(total)10}-h_{L10}}{h_{v10}-h_{L10}} \qquad (3.3.1)$$

It can be assumed that no water vapourises at 10 and that therefore

$$x_{L10}=1-\frac{(1-x_{L9})}{(1-VF10)} \qquad (3.3.2)$$

x_{L10} can be found by simultaneous solution of these two equations and the equation $h_{(total)10}=h_{L9}$.

In order to estimate the enthalpy of the refrigerant as it leaves the evaporator, it is neccessary firstly to solve for the distribution of liquid and vapour at the outlet:

$$\dot{m}_{L11}=\dot{m}_{L9}-\dot{m}_{v11}$$

$$x_{L11}\dot{m}_{L11}=x_{L9}\dot{m}_{L9}-x_{v11}\dot{m}_{v11}$$

$$\dot{m}_{v11}=\dot{m}_{L9}\frac{(x_{L11}-x_{L9})}{(x_{L11}-x_{v11})}$$

where conditions at point 11 are found as equilibrium functions of P_{ab} and T11. The final enthalpy of the refrigerant (h_{v11}) is then

$$h_{v11}=\frac{h_{l11}\dot{m}_{L11}+h_{v11}\dot{m}_{v11}}{\dot{m}_{v11}+\dot{m}_{L11}}$$

The total heat extracted by the evaporator during the absorption phase can then be evaluated as

$$Q_{ev}=\int(\dot{m}_{ref}h_{L9}-(\dot{m}_{L11}h_{L11}+\dot{m}_{v11}h_{v11})$$

If the assumption is made that the evaporator area is sufficiently large then the expression can be simplified:

$$Q_{ev}=\int\dot{m}_{ref}(h_{L9}-h_{v11})dt$$

The definitions for cycle internal efficiency and solar efficiency, and COPs, given in chapter 1, are valid here.

3.4. Mass flows

Fig 3.4.1 shows the control volume 1-4-6. In order to find an expression which gives the rate of vapour generation,$\dot{m}_{v6}$, in terms of $\dot{m}_{L1}$, mass balances can be taken of ammonia and solution across the boundries of the control volume. $\dot{m}_{L6}$ refers to the portion of the condensate collected inside the rectifier which trickles back into the separator. $\dot{m}_{L4}$ is the poor solution leaving the separator and entering the return path of the solution heat exchanger. $\dot{m}_{sep}$ is the rate at which the mass of solution stored in the separator decreases as generation of vapour progresses. The rate

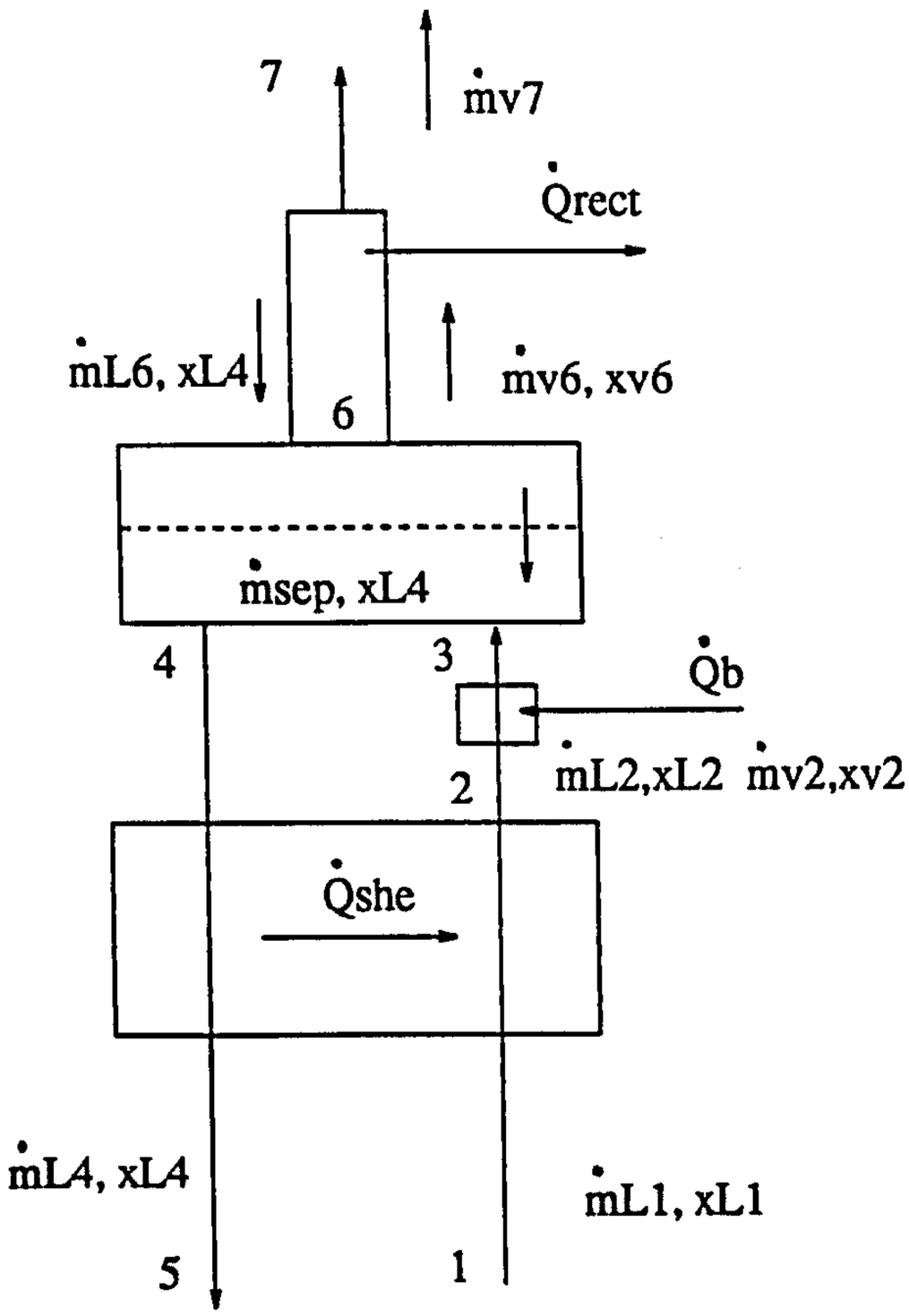

Fig 3.4.1 *Detailed view of generator, showing station points and heat flows. The total heat of desorption or "generation" ($\dot{Q}_{gen}$) is the sum of boiler heat input from the solar collector ($\dot{Q}_b$), and heat transferred effectively by the solution heat exchanger ($\dot{Q}_{she}$, or Q_{12})*

of decrease is here treated as having a positive sign. The separator is assumed to be small enough and well insulated enough for a uniform temperature at equilibrium conditions to obtain throughout, such that T3 = T4 = T6. This implies that the vapour flow $\dot{m}_{v6}$ is already fully formed at the exit of the boiler (point 3) and neither it nor its concentration (x_{v6}) is affected by passage through the separator. The liquid concentration will then also be uniform throughout the separator

(x_{L4}), and because the conditions in the rectifier are also equilibrium conditions, the concentration of the returning rectifier condensate is also x_{L4}.

Conservation of solution mass:

$$\dot{m}_{sep}=\dot{m}_{v6}+m_{L4}-m_{L1}-m_{L6} \tag{3.4.1}$$

Conservation of ammonia mass:

$$x_{L4}.\dot{m}_{sep}=x_{v6}.\dot{m}_{v6}+x_{L4}.\dot{m}_{L4}-x_{L1}.\dot{m}_{L1}-x_{L4}.\dot{m}_{L6}$$

Solving:

$$\dot{m}_{v6}=\dot{m}_{L1}\frac{(x_{L4}-x_{L1})}{(x_{L4}-x_{v6})} \tag{3.4.2}$$

Expressions can be found for $\dot{m}_{L6}$ and the mass flow of vapour leaving the rectifier ($\dot{m}_{v7}$) by considering the control volume 6-7 for the rectifier. Equilibrium obtains at point 7 so that the concentration of yielded vapour is known (x_{v7}). Taking mass balances:

$$\dot{m}_{v7}=\dot{m}_{v6}-\dot{m}_{L6} \tag{3.4.3}$$

$$x_{v7}.\dot{m}_{v7}=x_{v6}.\dot{m}_{v6}-x_{L4}.\dot{m}_{L6}$$

Solving:

$$\dot{m}_{v6}=\dot{m}_{L6}\frac{(x_{v7}-x_{L6})}{(x_{v7}-x_{v6})} \tag{3.4.2.1}$$

Solving equations 3.4.2 and 3.4.2.1, and remembering that $x_{L6} = x_{L4}$:

$$\dot{m}_{L6}=\dot{m}_{L1}\frac{(x_{L4}-x_{L1})(x_{v7}-x_{v6})}{(x_{L4}-x_{v6})(x_{v7}-x_{L4})} \tag{3.4.4}$$

The mass flow rate of weak solution returning to the reservoir through the heat exchanger ($\dot{m}_{L4}$) is found by considering the overall control volume 5-1-7 in fig 3.1.1. In the case of the FVR system (where the volume of liquid held in the reservoir is constant), the relationship between mass outflow and inflow is due only to density differences. If the increase in density of the return liquid from point 4 to point 5 is considered insignificant, then:

$$\dot{m}_{L4}=\dot{m}_{L1}\frac{\rho_5}{\rho_1} \tag{3.4.5.1}$$

In the case of the VVR system (where the reservoir has a variable volume), the change in solution mass in the separator can be very small compared to the change in mass in the reservoir. The separator mass contraction can be neglected and a mass balance across the control volume becomes:

$$\dot{m}_{L4}=\dot{m}_{L1}-\dot{m}_{v7} \qquad (3.4.5.2)$$

3.5. Energy flows

3.5.1. Generator

Referring again to fig 3.4.1 an energy balance can now be made over the control volume 1-4-6. Specific enthalpies are known as functions of concentration and temperature. The flow conditions are non-steady since the separator is emptying as generation proceeds. Velocity and piezometric head terms can be considered negligible. Insulation inhibiting heatflow from any of the components in this control volume is assumed to be perfect. If we examine a short time period dt conservation of energy demands that:

$$dQ-(dW+dm_{v6}p_{v6}v_{v6}+dm_{L4}p_{L4}v_{L4}-dm_{L1}p_{L1}v_{L1}-dm_{L6}p_{L6}v_{L6})$$

$$=dE+(dm_{L6}u_{L6}+dm_{v6}u_{v6}-dm_{L1}u_{L1}-dm_{L4}u_{L4})$$

Therefore

$$dQ=dE+dm_{L4}h_{L4}-dm_{L1}h_{L1}-\dot{dm}_{L6}h_{L6}+dm_{v6}h_{v6}$$

The internal energy stored in the separator dE decreases because of the decrease of mass stored at the rate $-dm_{sep}$. If we use the subscripts i and f to denote the start and finish of the generation period respectively, then

$$dE=U_{Lf}-U_{Li}$$

$$dE=(H_{Lf}-P_{Lf}v_{Lf})-(H_{Li}-P_{Li}v_{Li})$$

Allowing v to be negligible, and accepting that the state of the liquid in the separator does not alter during the period considered:

$$dE=H_{Lf}-H_{Li}$$

$$dE=-dm_{sep}h_{L6}$$

Therefore

$$dQ=-dm_{sep}h_{L6}+dm_{L6}h_{L6}-dm_{L1}h_{L1}-dm_{L6}h_{L6}+dm_{v6}h_{v6}$$

We can now divide through by dt and define dm/dt as $\dot{m}_v$ or $\dot{m}_L$, specific enthalpies as h_L or h_v (remembering that since temperature is assumed uniform throughout the separator state 6 equals state 4), and dQ/dt as $\dot{Q}_{gen}$, or the sum of $\dot{Q}_{she}$ and $\dot{Q}_b$:

$$\dot{Q}_{gen}=-\dot{m}_{sep}h_{L4}+\dot{m}_{L4}h_{L4}-\dot{m}_{L1}h_{L1}+\dot{m}_{v6}h_{v6}-\dot{m}_{L6}h_{L6} \qquad (3.5.1.1)$$

Although this expression is valid strictly for both circuits it is possible to simplify it in the case of the VVR system on the premise that separator mass contraction is designed to be a negligible proportion of the total mass contraction. In this case, for the VVR system:

$$\dot{Q}_{gen}=\dot{m}_{L4}h_{L4}+\dot{m}_{v6}h_{v6}-\dot{m}_{L6}h_{L6}-\dot{m}_{L1}h_{L1} \qquad (3.5.1.2)$$

3.5.2. Solar collector

The function of the solar collector is to transfer heat into a section of pipework which acts both as a generator and as a vapour lift pump. Both flat plat and concentrating parabolic trough collector designs are suitable for this, but neither would normally concentrate their power output into as small a surface area as can evacuated tube collectors (ETCs). The use of ETCs allows a relatively short generator tube length to be used, so minimising the thermal mass of steel and liquid in the generator and collector. A limiting factor in the reduction of surface area for heat transfer is the inverse relationship of temperature difference between collector and solution temperature and surface area for a given heat transfer. According to Holman (1981) the heat transfer performance of two stainless steel surfaces in contact is in the order of 3000 watts/m^2K, implying that the temperature difference can be reduced to less than three degrees centigrade. This difference is neglected in the present analysis. Performance tests on the Thermomax THS300 evacuated tube collector (Mahjuri, 1986) show that its performance can be adequately modelled by the

equation:

$$\eta_{coll}=\alpha\tau-\frac{1}{G}(\sigma\varepsilon(T_c^4-T_{amb}^4)+U_m(T_c-T_{amb})) \qquad (3.5.2.1)$$

where η_{coll} is the efficiency of the collector, $\alpha\tau$ is the absorption - transmittance product, $\dot{G}$ is the insolation rate measured in watts/m^2, σ is the Stefan-Boltzman constant, ε is the emissivity of the collector, U_m is the manifold heat loss coefficient, and T_c is the temperature of the condensing head of the collector. The parameter values chosen are:

$$\alpha\tau=0.8$$

$$\varepsilon=0.15$$

$$U_m=1.0W/m^2K$$

Since the temperature difference bettween collector and generator is neglected, T_c becomes T4. For a given collector area A_{coll} the heat delivered to the generator is:

$$\dot{Q}_b=\eta_{coll}\dot{G}A_{coll} \qquad (3.5.2.2)$$

3.5.3. Solution heat exchanger

Referring to fig 3.4.1, $\dot{Q}_{gen}$ is composed normally of two inputs, firstly the heat transferred in the solution heat exchanger from the return liquid flow to the incoming rich flow ($\dot{Q}_{she}$ or $\dot{Q}_{12}$), secondly the heat delivered by the solar collector ($\dot{Q}_b$), such that:

$$\dot{Q}_{12}=\dot{Q}_{gen}-\dot{Q}_b \qquad (3.5.3.1)$$

It is not conceivable that any vapour should exist at point 1 but it is possible that boiling is taking place at some point along the heat exchanger feed leg, in which case conservation of energy demands that

$$\dot{Q}_{12}=\dot{m}_{v2}.h_{v2}+\dot{m}_{L2}.h_{L2}-\dot{m}_{L1}.h_{L1} \qquad (3.5.3.2)$$

Where boiling is taking place in the feed leg the simultaneous solution of ammonia and solution mass balances gives an expression for the relative flow rates:

$$\dot{m}_{v2}=\dot{m}_{L1}\frac{(x_{L1}-x_{L2})}{(x_{v2}-x_{L2})} \qquad (3.5.3.3)$$

$$\dot{m}_{L2}=\dot{m}_{L1}-\dot{m}_{v2} \qquad (3.5.3.4)$$

The temperature at the exit of the heat exchanger feed leg (T2) is found by simultaneously satisfying the energy and mass flow equations. This is done with the iterative loop shown on fig 3.5.3.1.

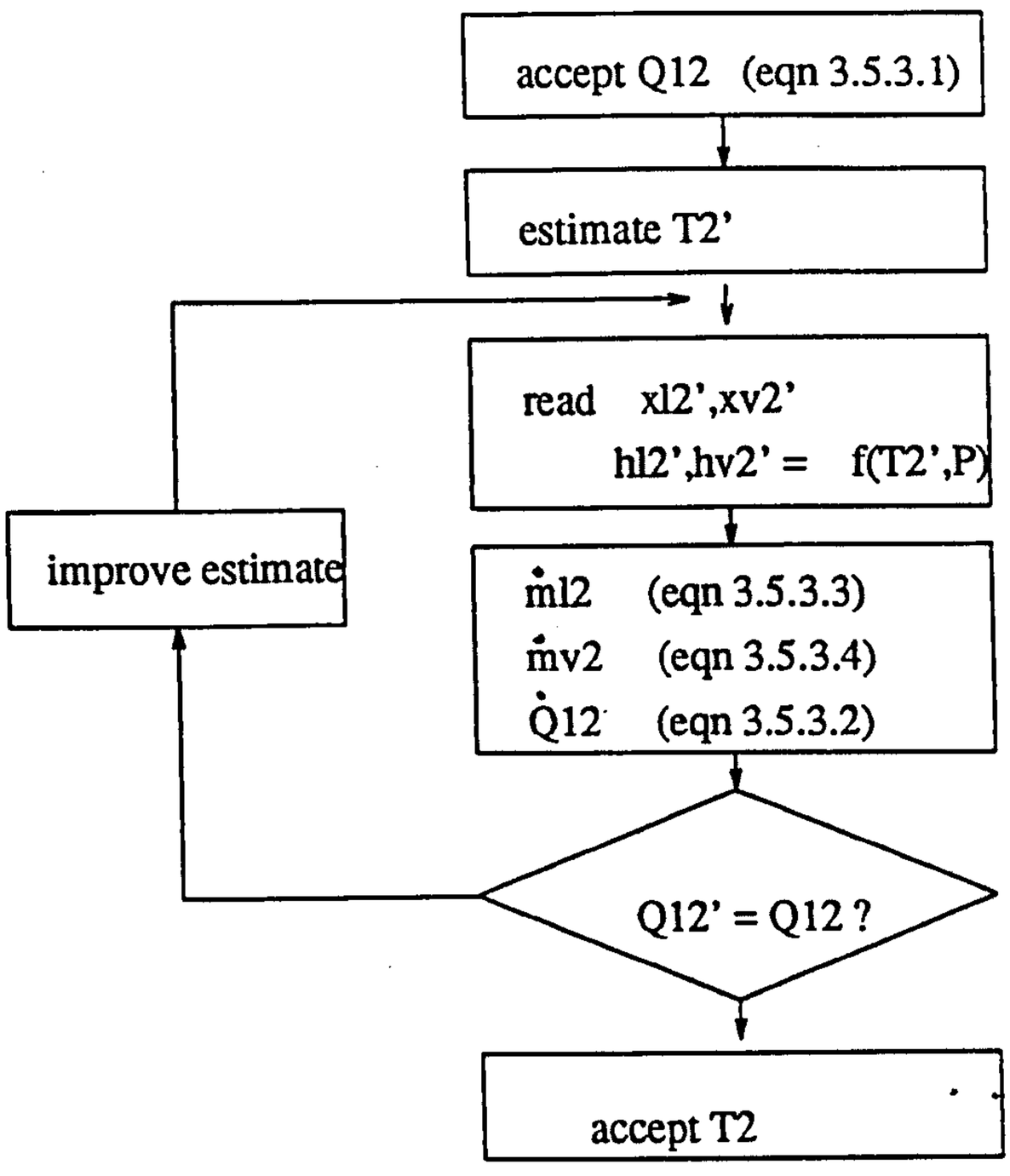

Fig 3.5.3.1 *Iterative solution for T2 based on the calculated value of* $\dot{Q}_{12}$.

On the assumption that the heat exchanger is perfectly insulated so that the heat removed from the return leg ($\dot{Q}_{45}$) is equal to the heat received by the feed leg, the specific enthalpy of the return stream as it exits the solution heat exchanger is:

$$h_{L5}=h_{L4}-\frac{\dot{Q}_{12}}{\dot{m}_{L4}}$$

The temperature of the stream at point 5 is given by the function

$$T5=function(x_{L4},h_{L5},P_{con})$$

In practice the liquid enthalpy can be considered invariate with pressure, so that a good approximation for T5 is found by:

$$T5=function(x_{L4},h_{L5})$$

If it is assumed that changes in thermal capacity in any one of the two streams are negligible, then the log mean temperature difference between the streams can be used to predict the heat transfer:

$$T_{out}=T5-T1$$

$$T_{in}=T4-T2$$

$$LMDT=\frac{(T_{out}-T_{in})}{\ln(\frac{T_{out}}{T_{in}})} \qquad (3.5.3.5)$$

If we make the assumption that the heat transfer coefficients for convection are constant throughout the heat exchanger, then the heat transferred is given by:

$$\dot{Q}_{she}=UA_{she}LMDT \qquad (3.5.3.6)$$

3.5.4. Rectifier

The heat absorbed in generation, Q_{gen}, is partially wasted in the production of the water vapour which is mixed with refrigerant vapour leaving the separator. The function of the rectifier is to return this water to the separator by forming a water-rich condensate. The rate at which heat is rejected by this condensation process is given by:

$$\dot{Q}_{rect}=\dot{m}_{v6}.h_{v6}-\dot{m}_{v7}.h_{v7}-\dot{m}_{L6}.h_{L6}$$

3.5.5. Condenser

The condenser receives superheated vapour from the rectifier and therefore rejects a quantity of sensible heat in addition to the heat of condensation. These quantities can be taken together in evaluating the rate of heat rejection by the condenser:

$$\dot{Q}_{con}=\dot{m}_{v7}(h_{v7}-h_{L8})$$

The condenser can be sized if the Fourier expression governing the heat flow is considered:

$$\dot{Q}_{con}=\left[\frac{1}{\Sigma\frac{1}{h_nA_n}}\right](T_{con}-T_{amb})$$

where n thermal resistances are present. Conductances are considered of insignificant magnitude relative to the convective heat transfer coefficients. A representive value of $\dot{Q}_{con}$ can be taken as 200 watts. The use of a heat pipe circuit for the removal of absorption heat is discussed in chapter 4; this can be brought into use for the rejection of condensation heat in the arrangement shown in figure 3.5.5.1. Three of the six interfaces are between two-phase fluids and their adjacent walls. The heat transfer coefficients are therefore high and little error is incurred if they are neglected altogether. The two interfaces present inside the reservoir vessel can be treated together since they share a common fluid. Heat transfer by mass transport and convective mixing in the reservoir and in the heat pipe passage can be considered perfect, although in practice thermal lag effects in the reservoir will alter the condenser dynamic characteristic. A further complication is that properties of the solution in the reservoir will change with decreasing concentration as generation progresses. An intermediate value of concentration is adopted here. The Nusselt number for each of the two surfaces is found from the empirical correlation of McAdams (1954) for isothermal horizontal cylinders in conditions of free convection:

$$Nu=0.59(PrGr)^{0.25}$$

which is valid for 10E4<PrGr <10E9 as in all the cases investigated here. For small temperature differences between solution and tube wall (ΔT) and for condensation occuring at 45 degC the value of the Grashof number becomes:

$$Gr=22E9\times\Delta Td^3$$

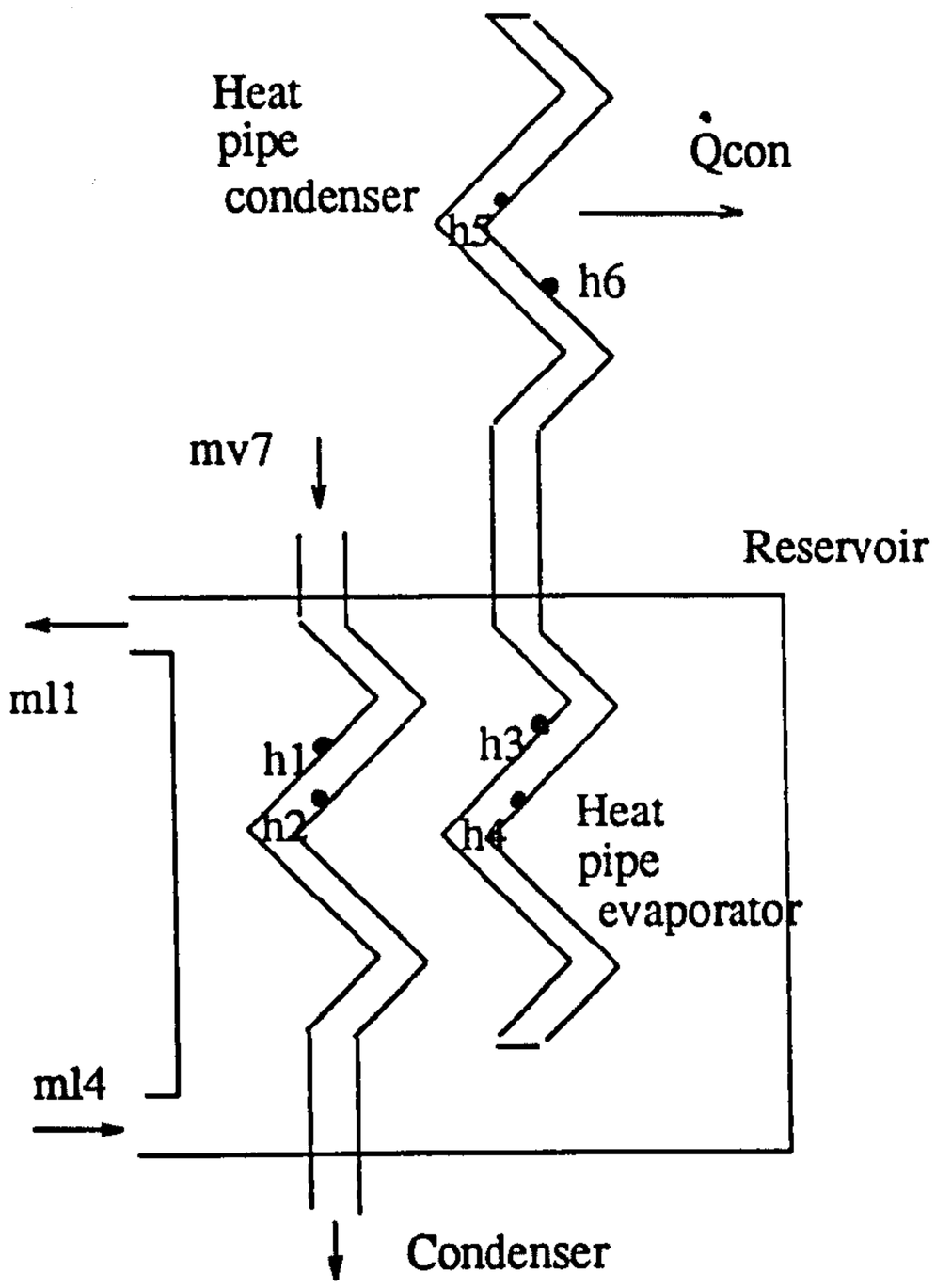

Fig 3.5.5.1 *Condenser heat exchanger as a single length of pipe wound spirally inside the reservoir. A second immersed spiral pipe is used to remove reservoir heat, and therefore condensation heat, to ambient via a heat pipe arrangement. Six surfaces with heat transfer coefficients of interest are marked as 'h'.*

where d is the assumed common diameter of each tube. The property values adopted for a calculation of condenser size are given in table 3.5.5.1.

A tube diameter of 12mm and a temperature difference of 1 degC will result in a Grashof number of 3.8 E4. The required length of tube will be

$$L=\frac{\dot{Q}_{con}}{Nuk_o\pi\Delta T}$$

condensing temperature	T_{con}	45	degC
solution bulk concentration	x_{L1}	0.41	kg/kg
solution bulk temperature	T_{res}	44	degC
Solution properties at 44 degC:			
density	ρ	820	kg/m^2
volume coefficient of expansion	β	1.37E-3	K^{-1}
viscosity	ν	640E-6	m^2/sec
thermal conductivity	k_o	0.56	W/m.degC
specific heat	c_p	4.8E3	kj/kg.degC
Prandtl no	Pr	5.5	
Grashof no	Gr	$22E9.\Delta t.d^3$	

Table 3.5.5.1 *Parameter values adopted for calculation of condenser size. The condenser arrangement is illustrated in fig 3.5.5.1.*

which for a heat removal rate of 200 watts is 9 metres. This is just practical. Assuming both tubes immersed in the reservoir are of this length and diameter the temperature of the heat pipe condenser wall, delivering heat to air at ambient temperature, will be approximately 2 degrees below the refrigerant condensing temperature T_{con}. If it is desired to limit T_{con} to 10 degC above ambient then sufficient area must be exposed to air cooling to allow 200 watts to flow over a temperature drop of 8 degC. A proprietry finned tube manufacturer (Integron, 1987) provides information on the heat tansfer characteristic of its product which indicates that the coefficient "k" in the expression

$$\dot{Q}=kA\Delta T^{1.25}$$

would take the value 1.68. Tests by Van Paassen (1986) on an alternative design of finned heat exchanger demonstrated that this efficiency is practible at reasonable cost. Given this characteristic the necessary area of the heat pipe condenser (A_{HPC}) will be 9 m^2, according to the relation

$$A_{HPC}=\frac{\dot{Q}_{con}}{k_{HPC}\Delta T^{1.25}}$$

The method described has a beneficial effect on the efficiency of generation in that the rich

solution has absorbed a portion of the energy dissipated in condensation. The condensation heat rejection rate, and consequently the area required, is reduced by the rate at which warm solution is transported out of the reservoir and the rate at which the reservoir itself dissipates heat to ambient.

3.5.6. Insulation

It is of some value to write approximate heat loss equations to model leakage through the insulation surrounding the hot side components. A UA value can be calculated from the Fourier equation for the separator and another for the solution heat exchanger, although in practice it was found preferable to establish the values experimentally, by plotting measured temperatures against measured heat flow through the insulation. The generator heat loss can be treated as a manifold loss in the solar collector performance characterisation.

$$\dot{Q}_{b(net)}=\dot{Q}_b-(UA)_{sep(loss)}(T4-T_{amb}) \qquad (3.5.6.1)$$

and

$$\dot{Q}_{45(net)}=\dot{Q}_{12}-UA_{she(loss)}\left[\frac{\frac{T4+T2}{2}-\frac{T1+T5}{2}}{\ln\frac{\frac{T4+T2}{2}-T_{amb}}{\frac{T1+T5}{2}-T_{amb}}}\right] \qquad (3.5.6.2)$$

The computer code can be modified by the introduction of the two UA_{loss} values drawn from experimental evidence, and then by replacing $\dot{Q}_b$ and $\dot{Q}_{45}$ with their net values.

3.6. Computer model

A number of methods are possible for the solution of the equations governing cycle performance. Three iterative calculations, solving for P_{gen}, T2, and T_{ab}, have been described already. These are solved sequentially without undue sacrifice of computing speed. A minimum solution for cycle performance is then achieved by forming a further iterative loop which solves for the generating temperature, T4. This approach is illustrated in fig 3.6.1, which lists the input parameters required by the calculation and the resulting solution for steady state performance

parameters. The minimum version of the model encompasses in addition a calculation which takes into account transient energy losses as described in the next section.

3.6.1. Transient effects

An allowance for the sensible heat load during the pressurisation phase Ia of the solution contained initially in the generator, and the steel content, is made by first applying the code of fig 3.6.1 to calculate steady state performance parameters for a given heat input. During pressurisation the solution concentration remains unchanged. If the subscript f is used to denote the final conditions of the phase, then

$$h_{L(sep)f}=f(T4,x_{L1})$$

An estimate of the enthalpy of the liquid contained in the solution heat exchanger can be made by assuming a mean temperature

$$h_{L(she)f}=f(\frac{T4+T1}{2},x_{L1})$$

The sensible heat requirement, Q_{sen}, is then:

$$Q_{sen}=M_{L(sep)}(h_{L(sep)f}-h_{L_{(T_{amb},x_{l1})}})+M_{L(she)}(h_{L(she)f}-h_{L_{(T_{amb},x_{l1})}})+(M_{st(she)}+M_{st(sep)})c_{p(st)}(T4-T_{amb})$$

Given that the proposed model assumes a steady heat input $\dot{Q}_b$ continuing for a specified period Δt_I, an expression can be written for the nominal period (Δt_{sen}) consumed by the sensible heating and pressurisation process:

$$\Delta t_{sen}=\frac{Q_{sen}}{\dot{Q}_b}$$

The net yield of condensate (M_{ref}) recovered at the end of the generation phase can then be written:

$$M_{ref}=\dot{m}v7(\Delta t_I-\Delta t_{sen}) \qquad (3.6.1)$$

This estimate of yield allows the weight ratio (WR) of the device to be calculated. The weight ratio is a useful indicator of the weight, cost, and bulk of the device, referred to the mass of solution required to produce a given output. The mass of solution circulated during the generation

process is

$$M_{circ}=\dot{m}_{L1}(\Delta t_I-\Delta t_{sen})$$

If the initial solution masses in the generator and, where the VVR circuit is concerned, the transfer tank, are denoted by the subscripts gen(i) and tt(i), then the weight ratio is written

$$WR=\frac{M_{circ}+M_{gen(i)}+M_{tt(i)}}{M_{ref}}$$

For present purposes it is sufficient to evaluate M_{tt} as equal to M_{ref} so idealising the size of the transfer tank. In practice it would be sized to contain a mass of solution equal to the maximum yield expected of the device.

3.6.2. Application of computer model

The model is mounted in three modes as shown in fig 3.6.3. The first mode applies the model in the form so far described to the tasks covered in sections 3.7 and 3.8, of sizing the solution heat exchanger and displaying the system response to vaying input parameters. These tasks allow some analytical investigation of the cycle to be made. The second mode allows the flow response of the circuit to be characterised, as described in section 3.9. To this end the code is modified to include as an input a function which defines the flow resistance of the circuit repreesnted here as the constant K; it is an external parameter, being adjustable by the system manufacturer or operator. The third mode involves a modification of the code such that the condenser area, expressed as a heat pipe condenser area A_{HPC}, and the overall condenser heat transfer characteristic k_{HPC} are taken as external inputs. Additionally a representitive function relating G to time, whether season or year, is included as an external input. Initially a sine function is considered adequate, which together with an expected peak value of $\dot{G}$ nominally describes the solar climate.

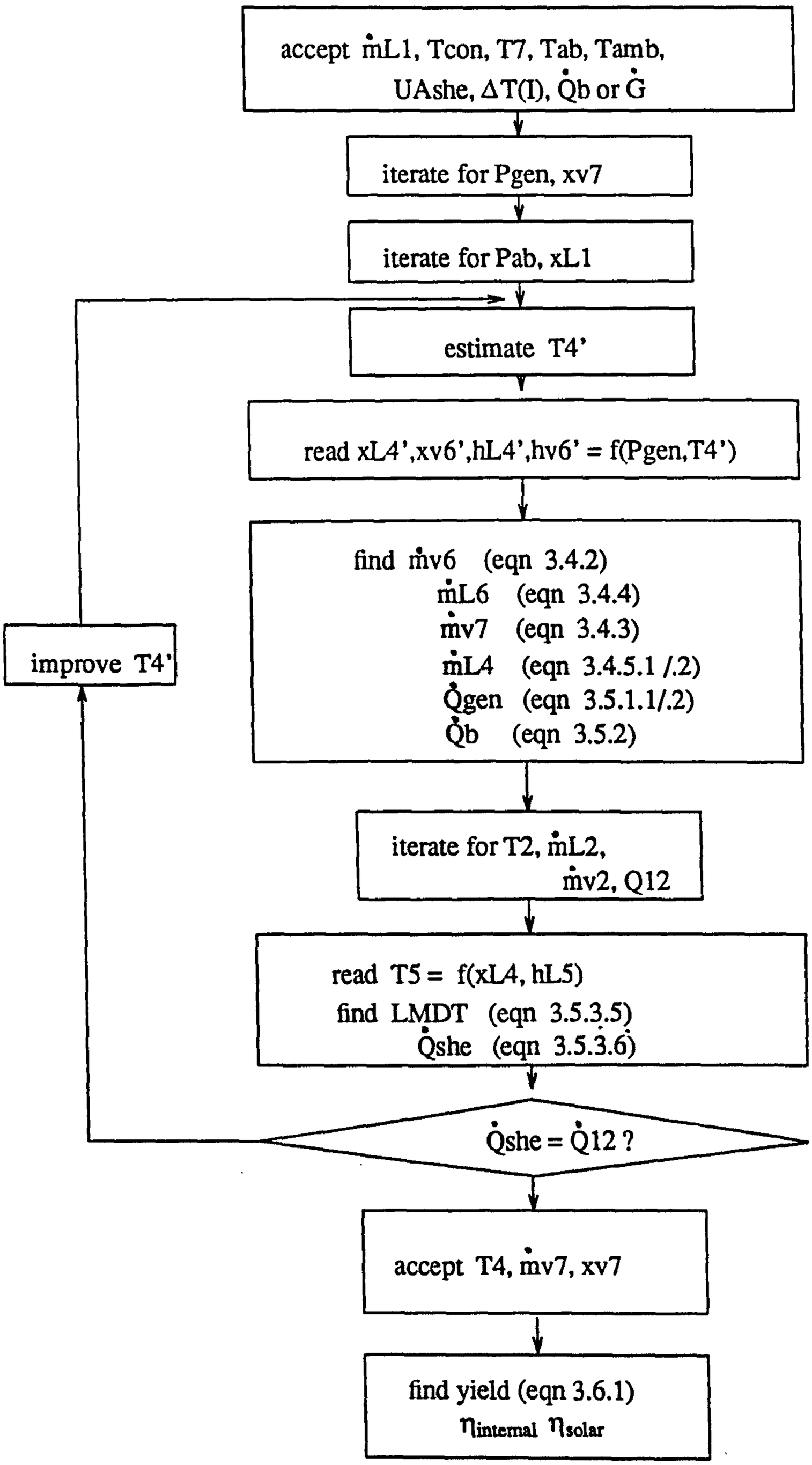

Fig 3.6.1 *Iterative solution for steady state performance*

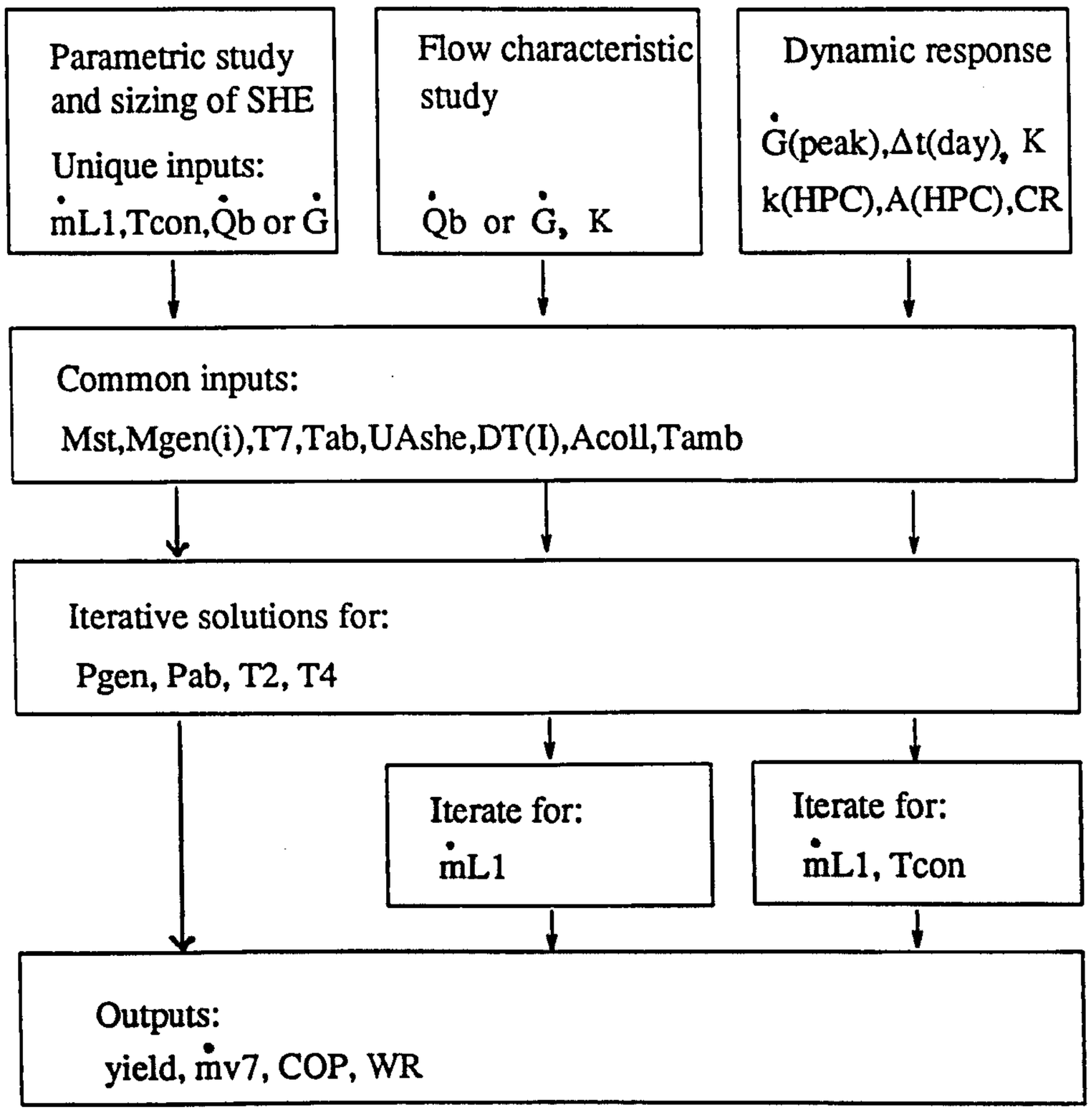

Fig 3.6.3 *The computer model is run in the three modes shown, each one represented by a vertical stream of boxes. These three modes are described in section 3.6.2.*

3.7. Sizing of solution heat exchanger

The simulation of steady flow conditions can first be applied to the case of a VVR system absorbing 300 watts as a steady generator heat input ($\dot{Q}_b$), and operating under the conditions detailed in table 3.7.1. A generation period of 8 hours is arbitrarily chosen, such that the bulk energy absorbed in the boiler is 8.64 MJ. The climatic conditions and operating parameters chosen are identical to those adopted in chapter 1, so allowing comparison. The rich solution

concentration is calculated to be 0.45 mass fraction of ammonia and the system pressure is 17.7 bar absolute. The refrigerant purity is 0.990. These internal parameter values depend on the values of T_{con}, T7, T_{ab}, and T_{ev}, all of which retain in the course of the discussion of this chapter the single values displayed on table 3.7.1, except where explicitly stated otherwise.

$\dot{Q}_b$	300	watts	UA_{she}	na	watts/K
G	na	watts/m^2	$M_{gen(i)}$	2.5	kg
$\dot{m}_{L1}$	na	mg/sec	M_{st}	1.4	kg
T_{con}	45	degC	Δt_I	8	hours
T7	75	degC	T1	$=T_{con}$	degC
T_{amb}	35	degC	T_{ab}	30	degC
T_{ev}	-10	degC	A_{coll}	1	m^2

Table 3.7.1

Values adopted for parameters in calculating IR performance for a range of solution heat exchanger "UA" values, as shown in fig 3.7.1.

The condensate yield (M_{ref}) is plotted against rich solution mass flow rate on figure 3.7.1 (a) for a range of heat exchanger sizes, expressed as the product UA_{she}. The heat exchanger effectiveness is plotted for the same range of sizes as shown in figure 3.7.1 (b). The two plots indicate that as size rises beyond 50 watts/K the gain in performance becomes very slightly less in proportion to further increase in size and cost. As the thermal mass of the feed stream reduces with flow reduction, the number of heat transfer units (NTUs) increases and effectiveness tends to one in theory.

Costing considerations, and practical considerations concerning ease of fabrication and the requirement for a compact device, also effect the choice of size for the solution heat exchanger, so that it is necessary to investigate the actual physical configuration necessary to realise an effectiveness of this order. This is done in the following sections. It is concluded in section 3.7.3 that a heat exchanger designed for a UA_{she} value of 50 watts/K is physically as large as can be accommodated conveniently. This taken together with the conclusion drawn from fig 3.7.1(a) leads to the decision to model the IR device on a UA_{she} value of 50 watts/K.

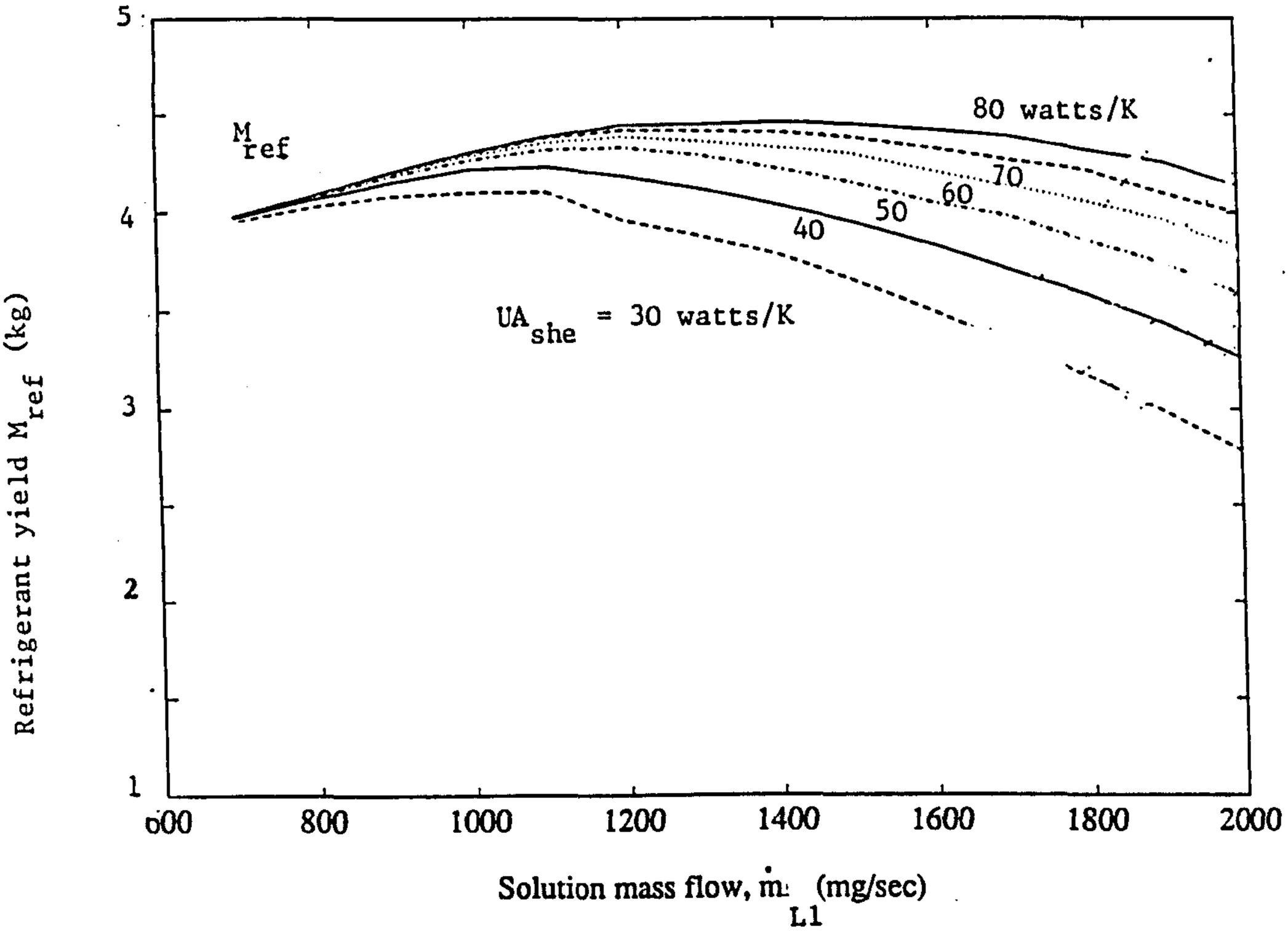

Fig. 3.7.1(a) Refrigerant yield (M_{ref}) plotted against solution mass flow rate for a range of solution heat exchanger sizes (UA_{she}) ranging from 80 to 30 watts/K. Operating conditions on Table 3.7.1.

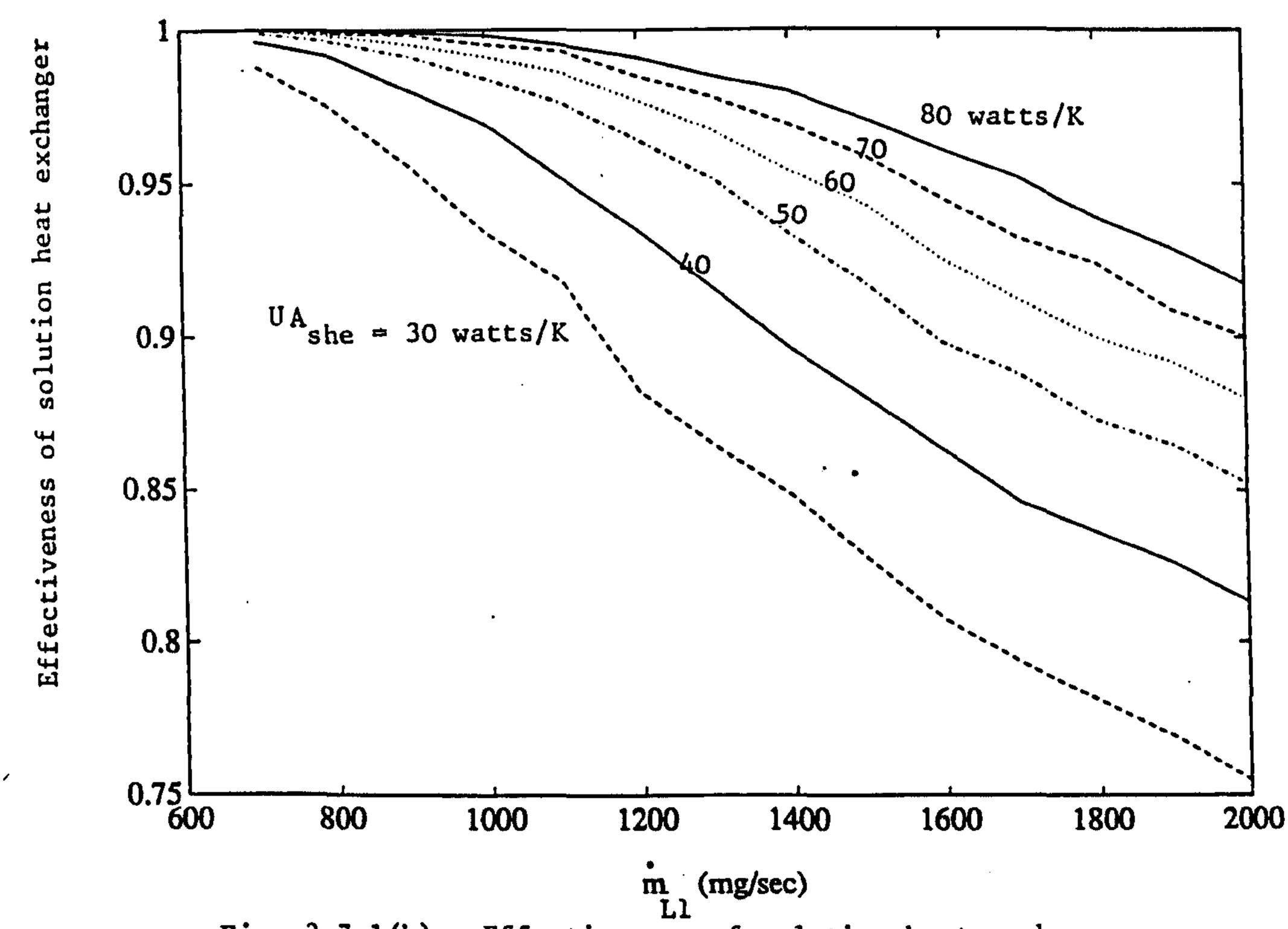

Fig. 3.7.1(b). Effectiveness of solution heat exchanger plotted against mass flow rate for a range of heat exchanger sizes. Operating conditions on table 3.7.1.

The solution heat exchanger is most conveniently manufactured in shell and tube form. Variation of the number of tubes will allow the overall exchanger length to be kept within desired limits. The shell and tube configuration is illustrated on figure 3.7.2 (a); a view of the two fluid streams is given in figure 3.7.2 (b), and a cross-section of a tube bundle element is given on fig 3.7.2 (c).

For the sake of a comparison with the IB system described in chapter 1, the code was also run for a UA_{she} value of zero, with the result that an optimum internal efficiency of 0.28 was shown to occur at a solution flow rate of 400 mg/sec.

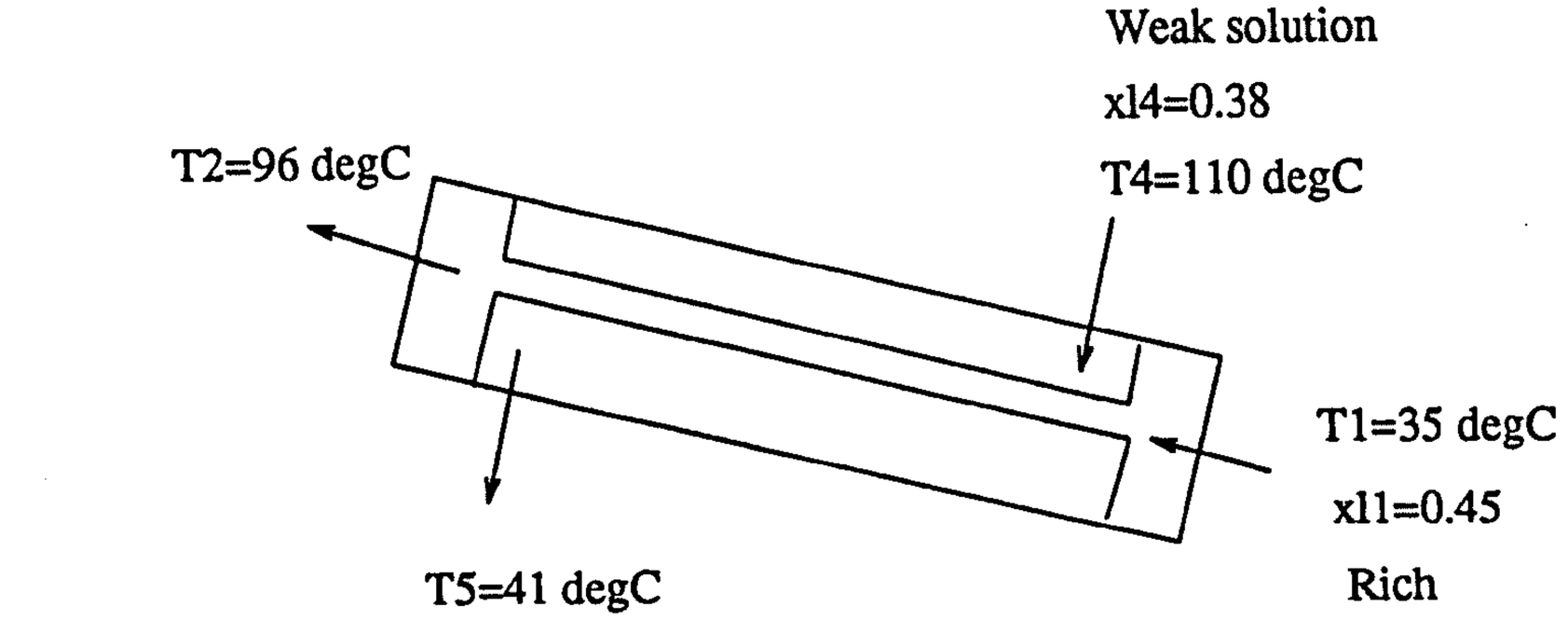

Fig 3.7.2 (a)

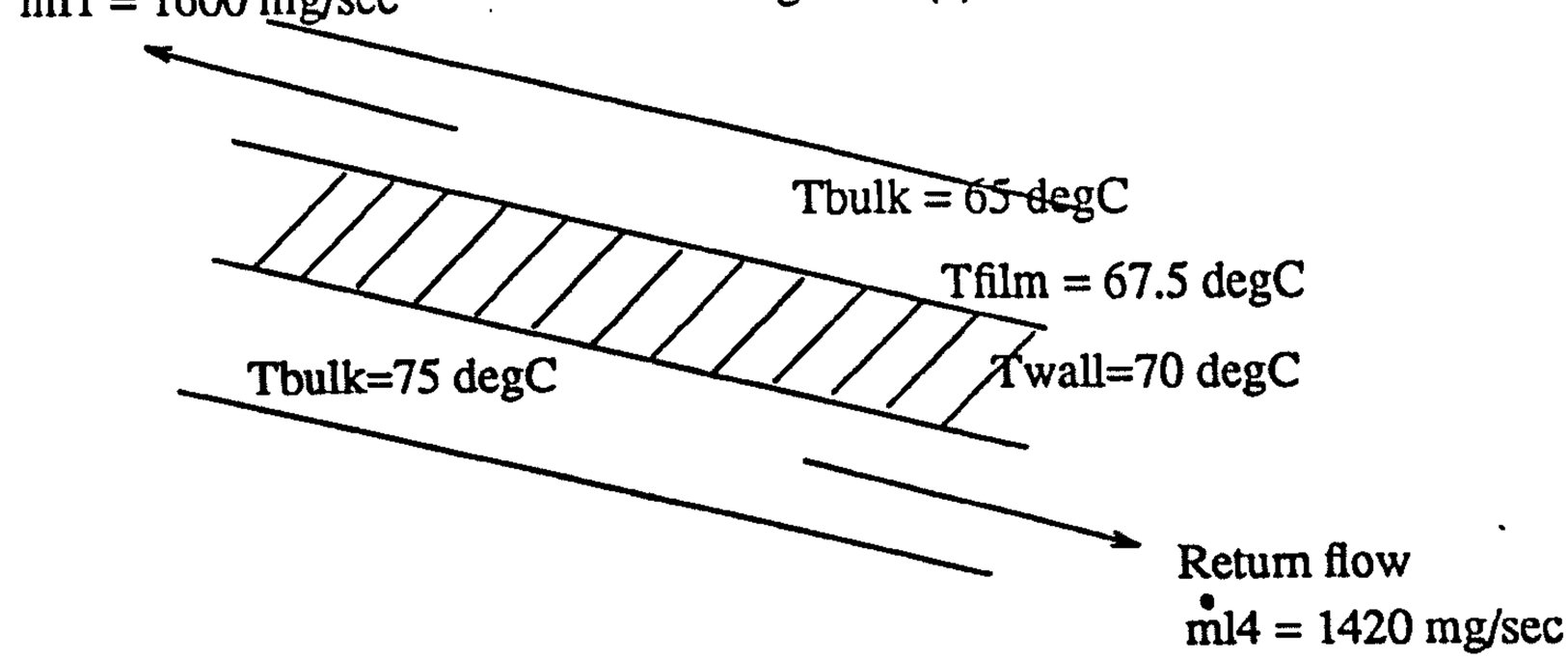

Fig 3.7.2 (b)

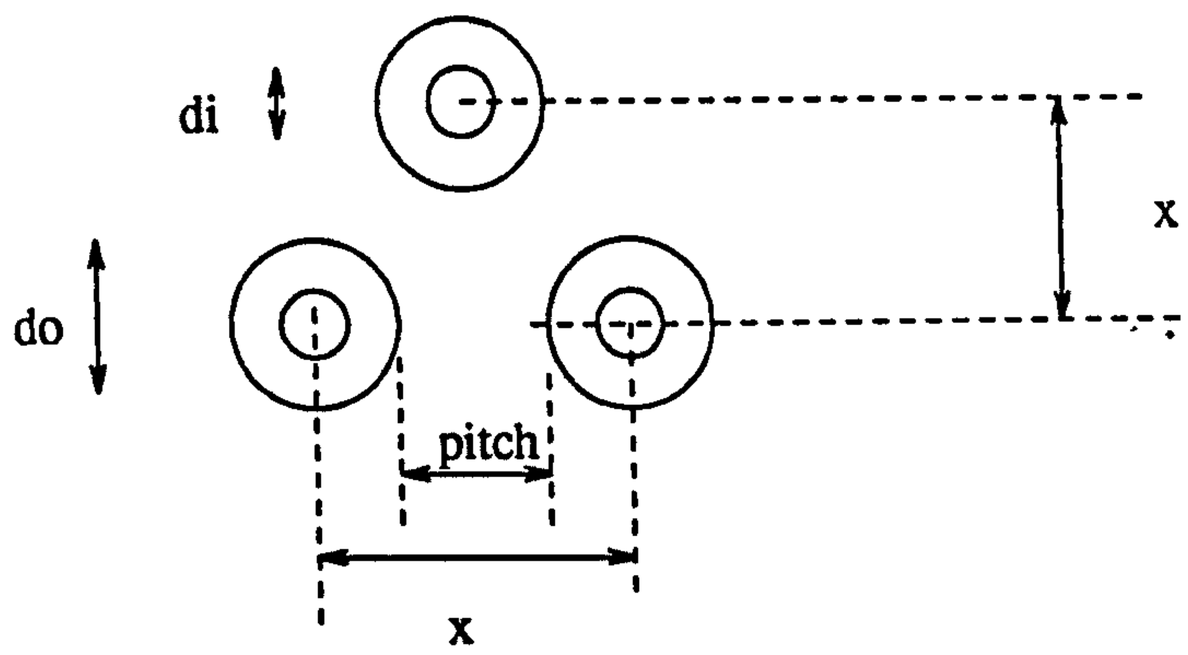

Fig 3.7.2 (c)

Fig 3.7.2 *Solution heat exchanger in shell and tube form showing the parameter values used in sizing calculation.*

The proposed geometry of the tube bundle is given on the figure. The solution heat exchanger is shown offset from the horizontal to allow vapour forming in the feed leg to escape. Although boiling will in practice take place the analysis here assumes the heat transfer characteristic of the feed tube can be treated as a constant determined by single phase liquid convection only.

$\dot{Q}_b$	na	watts	UA_{she}	50	watts/K
$\dot{G}$	700	watts/m^2	$M_{gen(i)}$	2.5	kg
$\dot{m}_{L1}$	1600	mg/sec	M_{st}	1.4	kg
T_{con}	45	degC	Δt_I	8	hours
T7	75	degC	T1	$=T_{con}$	degC
T_{amb}	35	degC			
T_{ev}	-10	degC	A_{coll}	1	m^2
T_{ab}	30	degC	$\dot{m}_{L4}$	1420	mg/sec
x_{L4}	0.38		x_{L1}	0.45	
T4	110	degC	T2	96	degC
T5	41	degC			

Table 3.7.1 *Parameter values adopted (together with those shown on table 3.7.2) for calculation of solution heat exchanger dimensions. Results are shown on table 3.7.3.*

Since the fluid properties vary considerably with changing temperature along the exchanger length an analysis of heat transfer can be undertaken by considering finite elements of length individually. The benefit of doing this is offset by uncertainty as to the characterisation of the heat transfer performance on the shell side. Instead the fluid properties are evaluated at a single bulk temperature for each stream. A log mean temperature difference approach to the overall heat transfer can then be adopted on the assumption that the specific heats of the two streams can be treated as constants. Because the temperature difference between the streams does not vary greatly the heat transfer is considered as taking place under conditions of uniform heat flux along the exchanger length. The bulk temperatures taken are means of the entry and exit temperatures. The dividing wall is assumed to experience no significant temperature drop, its temperature being estimated as mid-way between the two stream temperatures. This approximation is later justified when it is established that the values of the heat transfer coefficients on either side are of similar

magnitude.

		Rich stream	
Bulk temperature	T_b	65	degC
Film temperature	T_f	67.5	degC
Wall temperature	T_{wall}	70	degC
Viscosities	μ_b	421E-6	Pa-sec
	μ_f	387E-6	Pa-sec
	μ_w	353E-6	Pa-sec
Coeff thermal exp	β_f	1.4E-3	K^{-1}
Thermal cond	k	0.56	watts/m.K
Density	ρ	820	kg/m^3
Specific heat	c_p	5.1	kj/kg
Wall thickness	wt	1	mm

Table 3.7.2 *Parameter values adopted (together with those on table 3.7.1) for calculation of solution heat exchanger dimensions. Results are given on table 3.7.3.*

Fluid property values are given in table 3.7.2. The values for solution viscosity and thermal conductivity are found from the graphs published by Niebergall (1959) after the work of Pinewitsch and Koch respectively. The low temperature feed flow is assumed to flow inside the tubes.

3.7.1. Feed flow, interior of tubes

The bulk flow velocity, u_m, in each tube is

$$u_m = \frac{4\dot{m}_{L1}}{\rho \pi d_i^2 n_t}$$

where n_t is the number of tubes in the bundle. The Reynolds number is given by

$$Re = \frac{u_m d_i \rho}{\mu_b}$$

Kays (1966) shows that the hydrodynamic entry length, x, is given by

$$x = d_i \frac{Re}{20}$$

A friction factor f can be defined in terms of the wall shear stress τ_w and the pressure difference across the tube ends as

$$\tau_w=\frac{f\rho u_m^2}{8}=\frac{\Delta p d_i}{4L}$$

where L is the tube length. This allows the pressure drop along the tube to be written

$$\Delta p=\frac{f\rho u_m^2 L}{2d_i}$$

Where the flow is laminar the friction factor is

$$f=\frac{64}{Re}$$

Because the flow rates considered here are very small turbulent flow can only be induced if extremely small tube diameters are employed. These diameters are typically less than 1.5mm and give rise to excessive pressure drops, as well as inviting problems with blockage and capillary action. Accordingly only larger tubes are considered and laminar flow regimes are experienced.

The Reynolds number decreases in size as larger tube diameters or a greater number of tubes are employed. This has the effect of decreasing the significance of forced convection effects and increasing the effect of free convective heat transfer between the tube wall and the bulk of the fluid in the tube. The difference between film and bulk temperatures is in the order of 2.5 degC, and the wall to bulk difference is in the order of 5 degC. Where bouyancy effects are insignificant, the correlation for heat transfer performance developed by Sieder and Tate is relevant:

$$Nu_d=1.86\left[RePr\left(\frac{d_i}{L}\right)\right]^{1/3}\left[\frac{\mu_b}{\mu_w}\right]^{0.14}$$

where Pr is the Prandtl number. The Sieder Tate equation is useful where the tube length is not long enough for the temperature profile to fully develop. In the constant heat flux case the Nusselt number has been shown by Holman (1981) and others to take the value 4.364 when the temperature profile is fully developed.

The magnitude of the buoyancy effect is expressed in terms of the Grashof and Prandtl numbers:

$$Gr=\frac{\rho^2 g\beta(T_w-T_b)d_i^3}{\mu_f^2}$$

$$Pr=\mu_f\frac{c_p}{k_f}$$

The volume coefficient of expansion, β, is defined by

$$\beta=\frac{dv}{vdT}$$

and is found for aqua ammonia solution from tabulated values of solution density at the relevant concentration and pressure. Holman states that free convection effects dominate the heat transfer mode when $Gr/Re^2>1$. This approximate guide indicates that free convection is of greater significance in all the practical solution heat exchanger sizes considered here. Metais and Eckert (1964) present accumulated experimental evidence of free, forced, and mixed convection regimes in horizontal tubes. They distinguish the regimes in terms the relative magnitudes of GrPr(d/L) and Re. Following their guidance it is apparent that almost all the solution heat exchanger sizes considered give rise to mixed convection regimes. Holman recommends that in these instances the Nusselt number is found from the correlation developed by Brown and Gauvin (1965):

$$Nu=1.75\left[\frac{\mu_b}{\mu_w}\right]^{0.14}\left[Gz+0.012(GzGr^{1/3})^{4/3}\right]^{1/3}$$

where the Graetz number, Gz, is defined by

$$Gz=RePr\frac{d}{L}$$

The Graetz number is independent of tube diameter. For a given tube length the Nusselt number and internal heat transfer characteristic can be evaluated:

$$h_i=Nu_i\frac{k}{d_i}$$

The calculated hydrodynamic entry lengths are consistently less than 10% of the overall tube length calculated. The pressure drops imposed by tube diameters of greater than 2 mm are very

small for the lengths calculated.

3.7.2. Return flow, shell side

The Reynolds number, Nusselt number, and Grashof number are evaluated for the flow cross section shown in fig 3.7.1 in terms of the hydraulic diameter d_h:

$$d_h=\frac{4\times FlowArea}{Perimeter}$$

The outer diameter of the tubes is taken to be always 1mm greater than the internal diameter in this discussion. No pressure difference exists across the tube walls indicating that thin walled tubes are desirable to reduce thermal mass and bulk.

The Nusselt number can be calculated following the equations presented above. The tubes are taken to be spaced apart with either 2 or 3 mm pitch. Large values of Gr arise but the final Nu numbers are similar to those found on the inside of the tube, because of the reduction in Re caused by the relatively large hydraulic diameter. Considerably larger values of Nu are calculated if the external tube diameters are considered as convecting in an unenclosed mode. These values appear to be more accurate in the light of experimental investigation, if the supposition is made that the internal heat transfer is adequately modelled. The heat transfer coefficient is evaluated in terms of the external tube diameter:

$$h_o=Nu_o\frac{k}{d_o}$$

As in the case of internal flow the pressure drops experienced on the shell side are insignificant for the dimensions considered here.

3.7.3. Sizing of solution heat exchanger

In order to see whether the requirement for a specified exchanger UA value is satisfied the physical dimensions and heat transfer characteristics of the exchanger are written:

$$UA=\frac{n_t L\pi}{\frac{1}{h_i d_i}+\frac{1}{h_o d_o}}$$

Table 3.7.3 gives the heat exchanger lengths required for a range of parameter values, based on a UA_{she} value of 50 watts/K.

The case where the solution heat exchanger is mounted vertically differs in that mixed convection is either aided by gravity or hindered. In the present case both effects will exist since the two streams are in counterflow.

d_i		4	5	6	7	8	9
n_t	pitch						
51	3	.53	.51	.49	.47	.45	.44
51	2	.58	.55	.53	.51	.49	.46
41	3	.65	.62	.60	.58	.56	.54
41	2	.77	.71	.68	.65	.63	
36	3			.71	.68	.65	
36	2			.80	.77	.71	

Table 3.7.3
Solution heat exchanger tube lengths (meters) as a function of the number of tubes (n_t), the gap between the tubes (pitch, mm), and the tube internal diameter (d_i, mm). Dimensions are illustrated on fig 3.7.2.

3.8. Parametric Study - Fixed volume reservoir (FVR) system

The reader is reminded that two versions of the IR system are proposed, as shown in figure 3.1.1 and discussed in section 3.1. The version without a transfer tank has a fixed volume reservoir (FVR) and a large separator which accommodates the change in solution mass during absorption. The variable volume reservoir (VVR) version has a transfer tank which accommodates this change in mass while the separator is physically small. The advantage of the VVR system is that less thermal mass exists in the generator, so giving a more rapid response to heat input. Further, the sizing of the separator in the FVR system is critical, since too small a separator will dry out of solution on a hot day and so cause desorption to stop. Too large a separator will have a hot residue of solution at the end of the day, representing wastage of incoming energy in sensible heating, and so loss of potential refrigerant yield.

Because the VVR system is an improvement, most of the parametric study in Chapter 3 is devoted to it. The trends followed by the FVR system are similar, so that results obtained for the VVR system can be taken as a guide to trends experienced by the FVR system.

This section presents selected results of the computer model for the FVR system in order to illustrate the essential characteristic of critical separator sizing mentioned above. Results are also presented in order to characterise the FVR cycle and allow comparisons to be made with the VVR parametric study following, and with experimental results presented in Chapter 6. The operating conditions adopted for the calculation are given in table 3.8.1.

Fig 3.8.1 (a) shows the variations of temperatures in the machine run at different flow rates at a steady heat input of 300 watts. Each flow rate represents a different frictional resistance to flow of the solution circuit. It is apparent that high separator (T4) and heat exchanger exit (T2) temperatures are achieved at low flow rates, while heat exchanger hot side exit temperature (T5) increases at high flow rate. The increase in T5 is due to worsening effectiveness in the solution heat exchanger; the reduction in effectiveness is illustrated in fig 3.8.1 (c). Fig 3.8.1 (b) shows the final mass of refrigerant yielded given that the boilder heat input is taken to endure for a period (Δt_I) of 8 hours. The yield is seen to peak at an optimum flow rate at 3.8 Kg of refrigerant. The amount of vapour produced inside the heat exchanger (m_{v2}) is seen to decline, indicating a reduction in effectiveness as flow rate rises. The exit vapour flow rate or desorption rate (m_{v7}) is seen to peak at values of the order of 200 mg/sec. The separator is seen to run dry at top desorption rates. At lower desorption rates hot solution (''Sep residue'') is seen to remain used at the end of the day in the separator. These results are obtained with the generator initially charged with 6 Kg (Mgen(i)) of solution. When charged with more solution, the yield is found to reduce due to greater residual mass.

Fig 3.8.1 (c) shows the cycle internal efficiency, η_i , which is defined in Chapter 1, section 1.2, plotted against solution flow rate. A peak value of 0.5 is achieved under the specified conditions.

Looking ahead to figure 3.9.1 (d), it will be seen that the steady state yield rate, $\dot{m}_{v7}$, is considerably greater for the FVR system than for the VVR system, although the net yields are

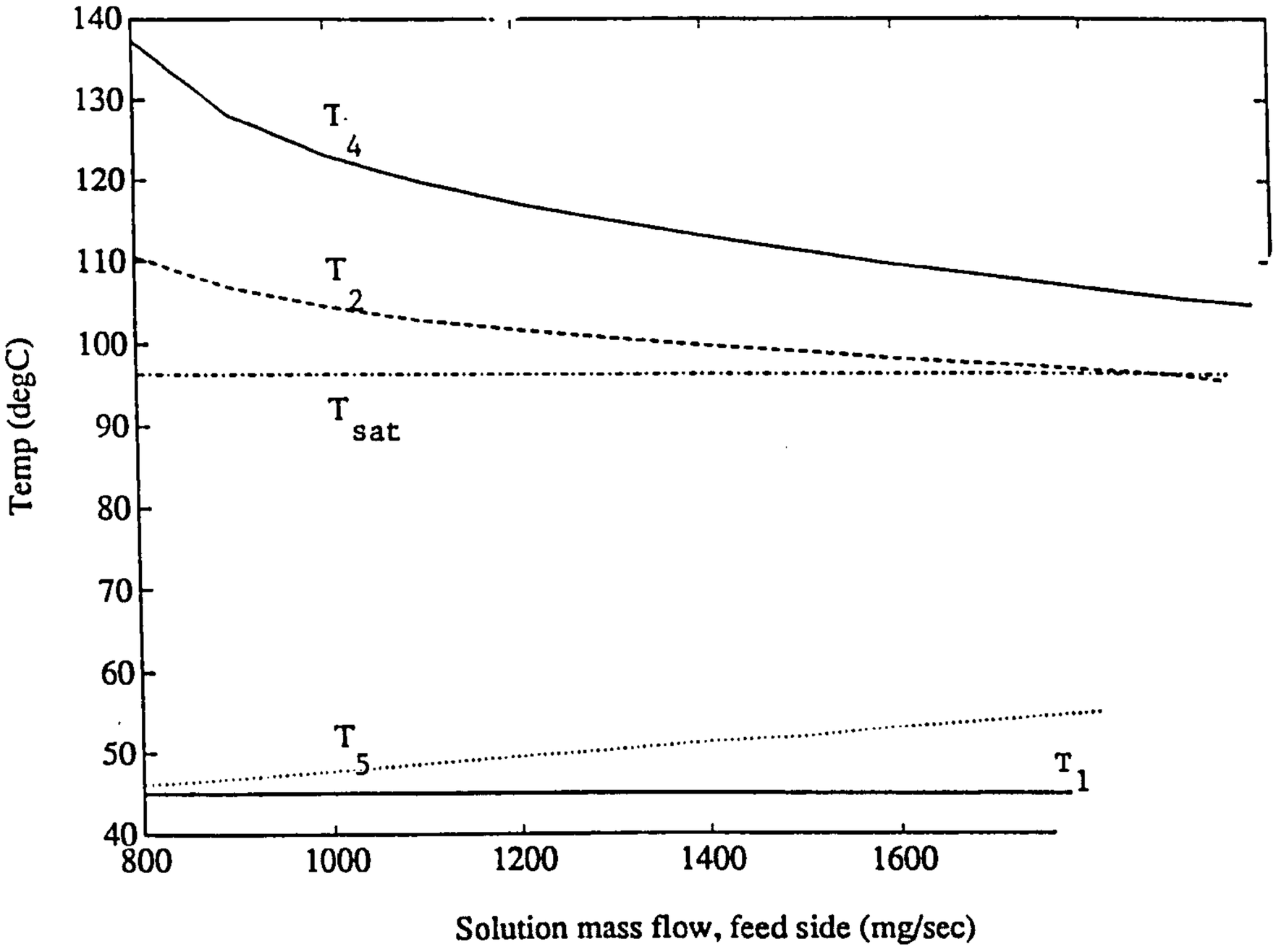

Figure 3.8.1(a). Temperature response of FVR system to solution flow rate. Operating conditions on Table 3.8.1. T_{sat} is the temperature at which boiling starts within the heat exchanger.

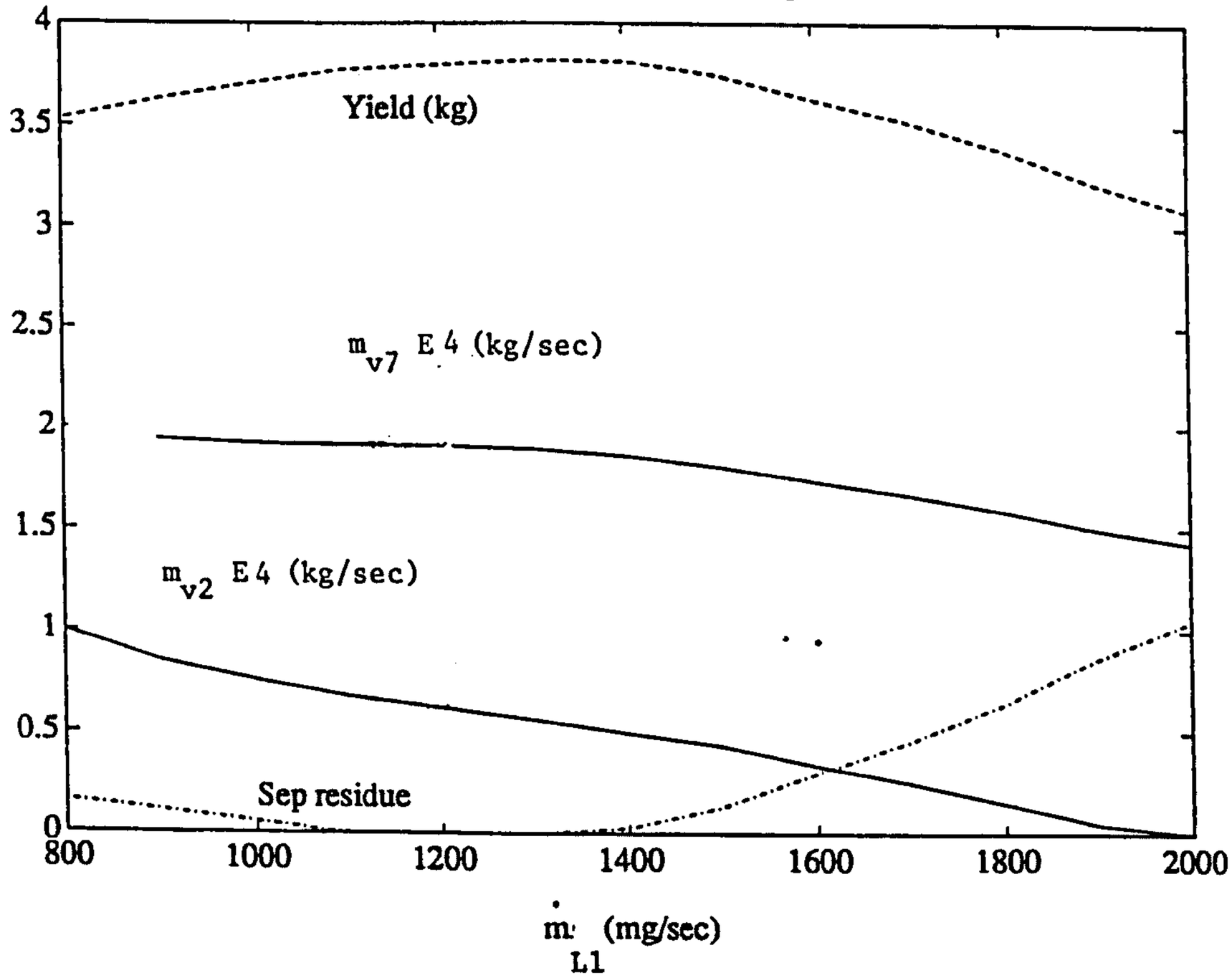

Fig. 3.8.1(b). Final yield of FVR system and mass flow rates of vapour at points 2 (exit of heat exchanger) and 7 (rectifier exit), for different flow rates. The graph also shows the mass of hot solution remaining in the separator at the end of the desorption phase. Operating conditions on Table 3.8.1.

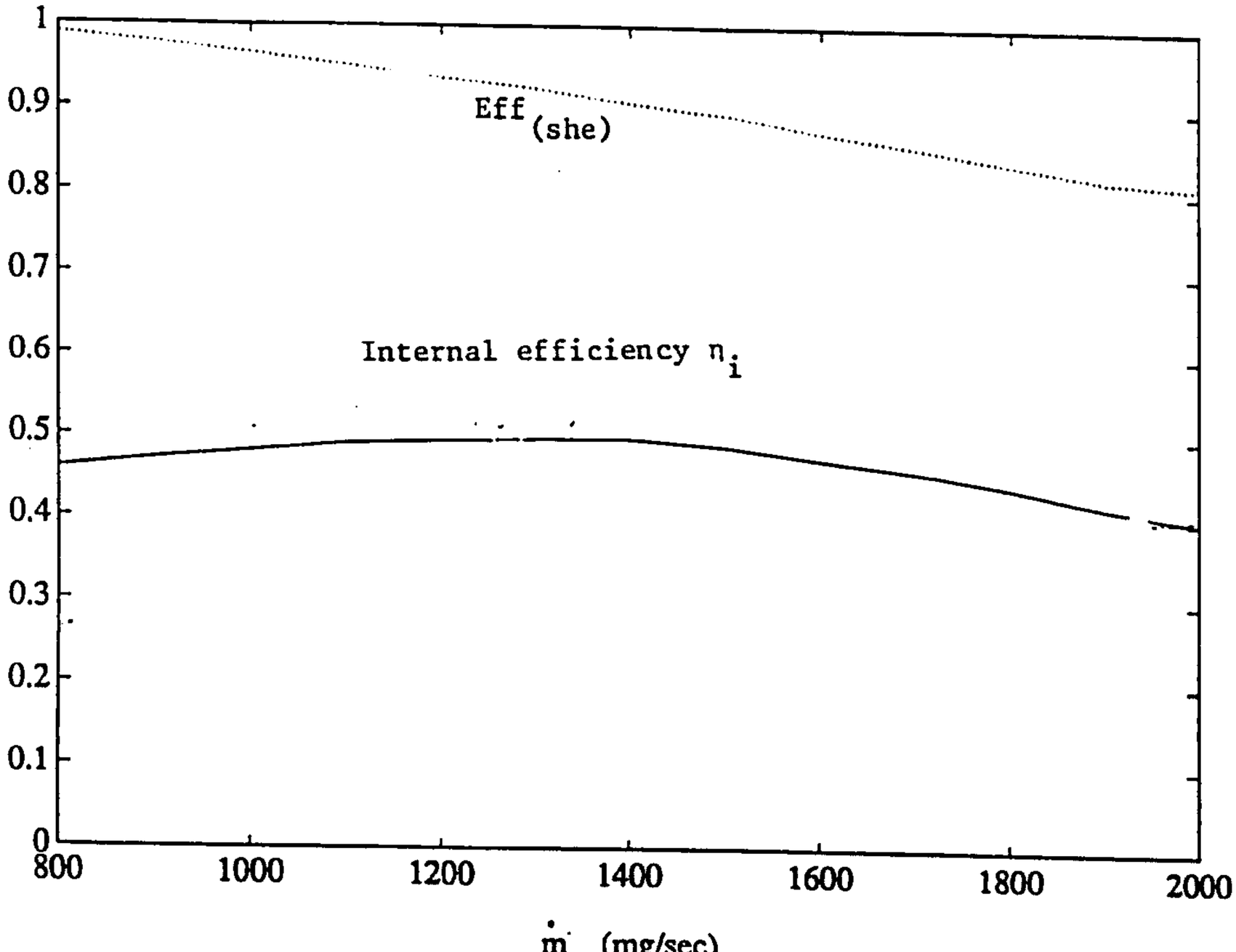

Figure 3.8.1(c). Cycle internal efficiency and heat exchanger effectiveness for the FVR system against solution mass flow rate. Operating conditions given on Table 3.8.1.

$\dot{Q}_b$	300	watts	UA_{she}	50	watts/K
$\dot{G}$	na	watts/m^2	$M_{gen(i)}$	0.6	kg
$\dot{m}_{L1}$	na	mg/sec	M_{st}	6.0	kg
T_{con}	45	degC	Δt_I	8	hours
T7	75	degC	T1	$=T_{con}$	degC
T_{amb}	35	degC	T_{ab}	30	degC
T_{ev}	-10	degC	A_{coll}	1	m^2

Table 3.8.1
Parameter values adopted for characterisation of the fixed volume reservoir (FVR) system as illustrated in fig 3.8.1. The FVR system is illustrated in fig 3.1.1.

comparable, only differing by virtue of the separator residual mass characteristic of the FVR system. The reason is that the greater sensible heating delay (Δt_{sen}) associated with the FVR system reduces its net yield, while the stored heat in the separator mass increases the steady state vapourisation rate. This feature constitutes in some circumstances a second draw back of the FVR system; in climatic conditions where clear skies appear only for short periods it is possible that the FVR system will produce considerably less yield because of the delay in separator heating.

3.9. Parametric study - Variable volume reservoir (VVR) system

Study of system response is now made with reference to the variable volume reservoir (VVR) system only. One aspect of VVR performance which is not illustrated here is that it is capable of producing yield in response to boiler heat relatively rapidly, since it does not have a significantly large separator thermal mass.

Fig 3.9.1 shows the VVR response to a boiler heat input of 300 watts for the operating conditions listed in table 3.9.1. Fig 3.9.1 (a) and (b) show the specific enthalpies of the working fluid at the various circuit stages, plotted against the vapour and liquid concentrations associated with a range of rich solution mass flow rates. The figures can be compared with the enthalpy-concentration chart of fig 1.2.5, the system pressure being 17.7 bar absolute. Boiling in the solution heat exchanger at low solution flow rates is evident from the variation shown in enthalpy of

$\dot{Q}_b$	300	watts	UA_{she}	50	watts/K
$\dot{G}$	na	watts	$M_{gen(i)}$	2.5	kg
$\dot{m}_{L1}$	na	mg/sec	M_{st}	1.4	kg
T_{con}	45	degC	Δt_I	8	hours
T7	75	degC	T1	$=T_{con}$	degC
T_{amb}	35	degC	T_{ab}	30	degC
T_{ev}	-10	degC	A_{coll}	1	m^2
T_{ab}	30	degC	M_{tt}	$=M_{ref}$	Kg

Table 3.9.1 *Parameter values adopted for characterisation of the variable volume reservoir (VVR) system as illustrated in figs 3.9.1 to 3.9.7*

fluid exiting the solution heat exchanger (h_{L2}). Fig 3.9.1 (c) shows the temperature response; where T2 is greater than T_{sat} boiling is taking place in the solution heat exchanger feed leg. The low values of T5 at low solution flow rates indicate high solution heat exchanger effectiveness. The assumption of a constant heat transfer characteristic in the solution heat exchanger independent of mass flow rate is conservative, in that the presence of boiling in the solution heat exchanger will tend to enhance the characteristic. Fig 3.9.1 (d) shows that yield for these conditions is considerably greater than for the FVR system. Weight ratios of the order of 8 are apparent, implying a solution charge in the order of 40 kg is necessary. Fig 3.9.1 (e) shows shows that the peak η_i is in the order of 0.55, comparable with the CP system investigated in chapter 1.

Fig 3.9.2 (a) and (b) show the response of the system to various levels of boiler heat input. Fig 3.9.2 (a) shows that the optimum solution flow rate increases as boiler heat input increases. Peak efficiences are in the order of 0.56. Fig 3.9.2 (b) shows that change in boiler heat significantly affects separator temperature. Fig 3.9.3 shows the response to varying levels of solar insolation. Fig 3.9.3 (a) shows that solar efficiency (defined in section 1.2) reduces significantly as heat input reduces. Peak solar efficiencies vary between 0.13 and 0.32 and occur at higher flow rates for higher heat input rates. Fig 3.9.3 (b) shows the collector response, the occurrence of high generating temperatures at low solution flow rates clearly having the effect of reducing collector efficiency. The drop in solar efficiency at low insolation is due to the

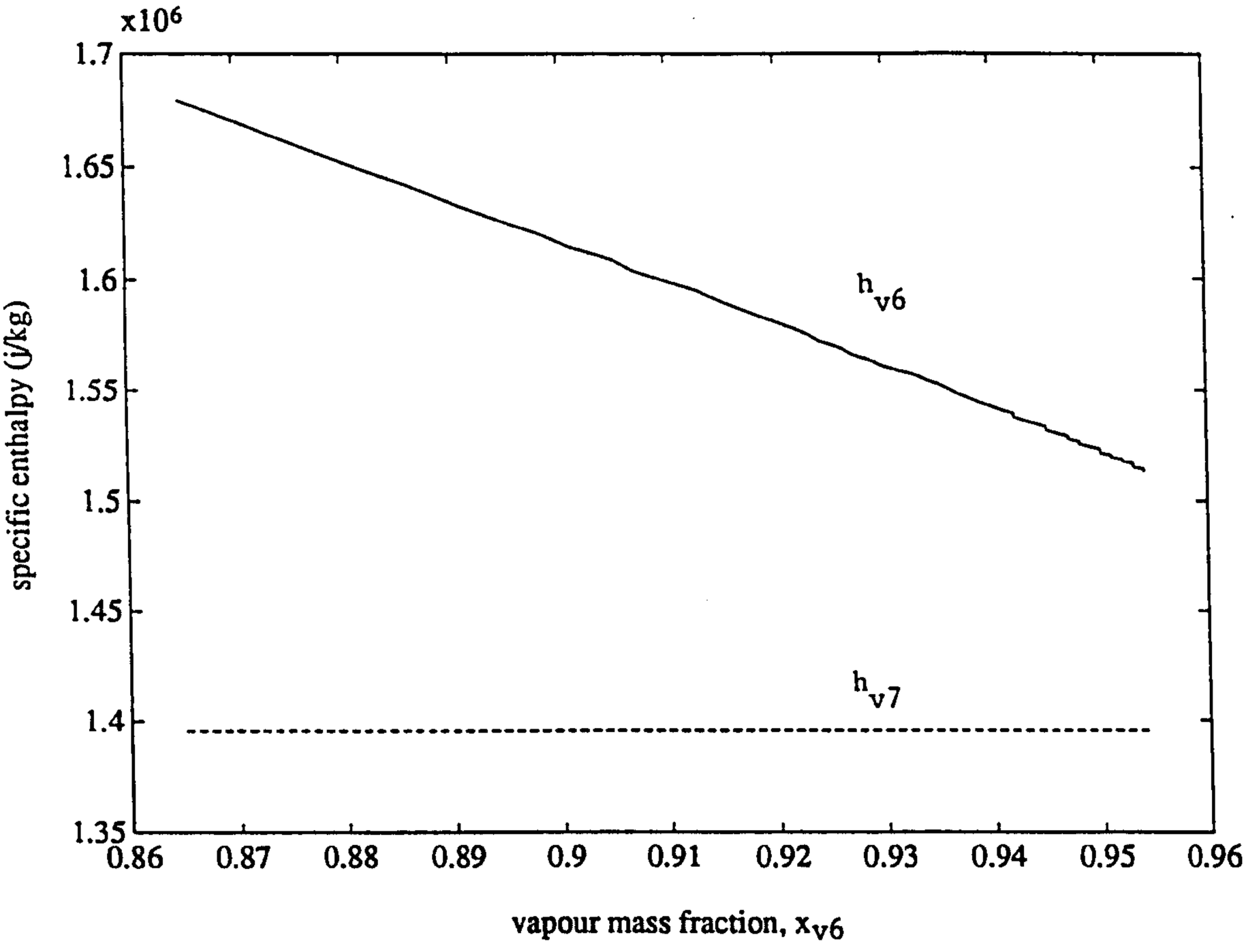

Fig.3.9.1(a). VVR system response to conditions listed on Table 3.9.1. Vapour enthalpies at points 6 and 7 (see Figure 3.1.1) are plotted against concentration at point 6, concentrations varying due to variations in solution flow rate.

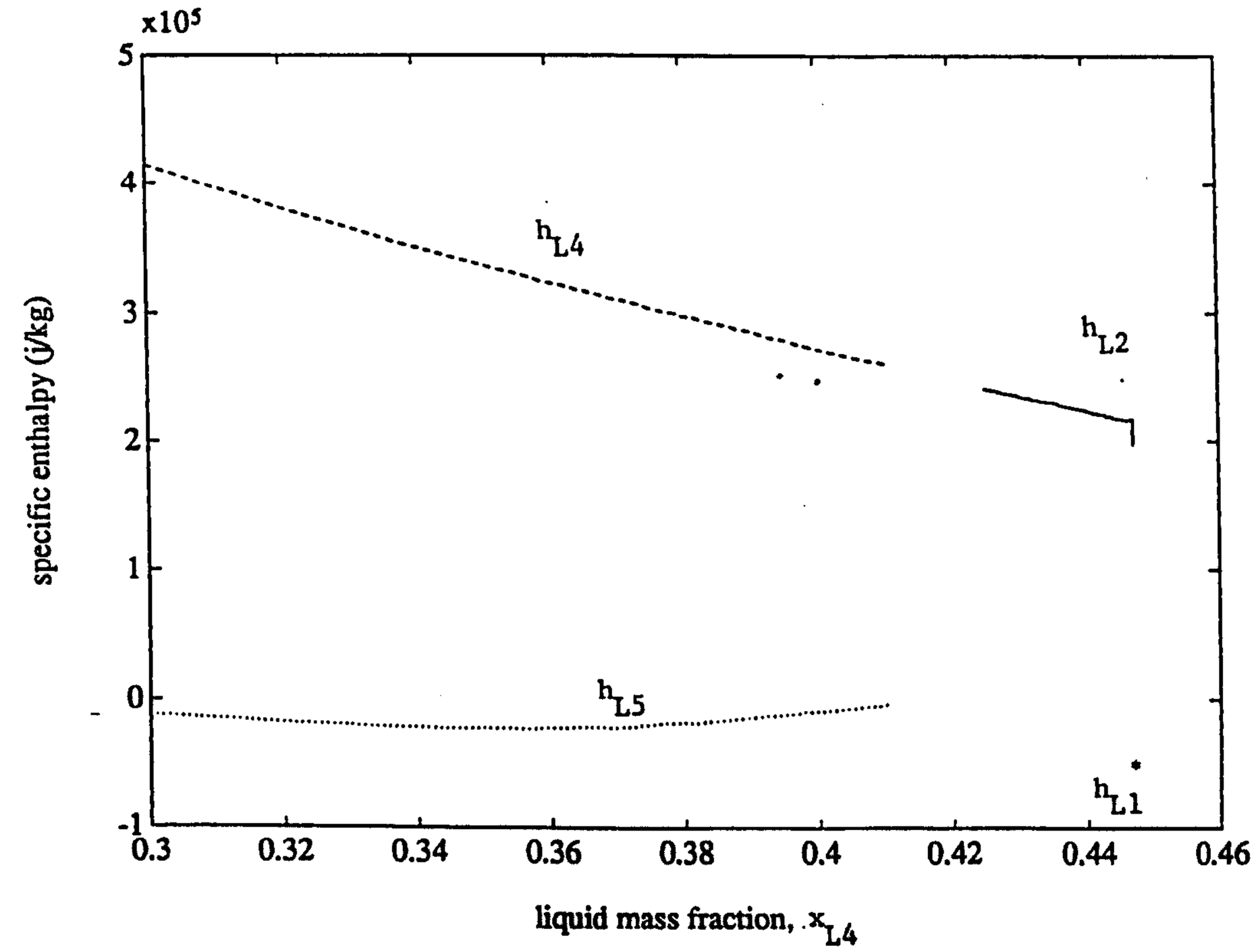

Fig. 3.9.1(b). VVR system response to conditions listed on Table 3.9.1. Liquid enthalpies in the generator are plotted against final solution concentration variations associated with variations in solution flow rate.

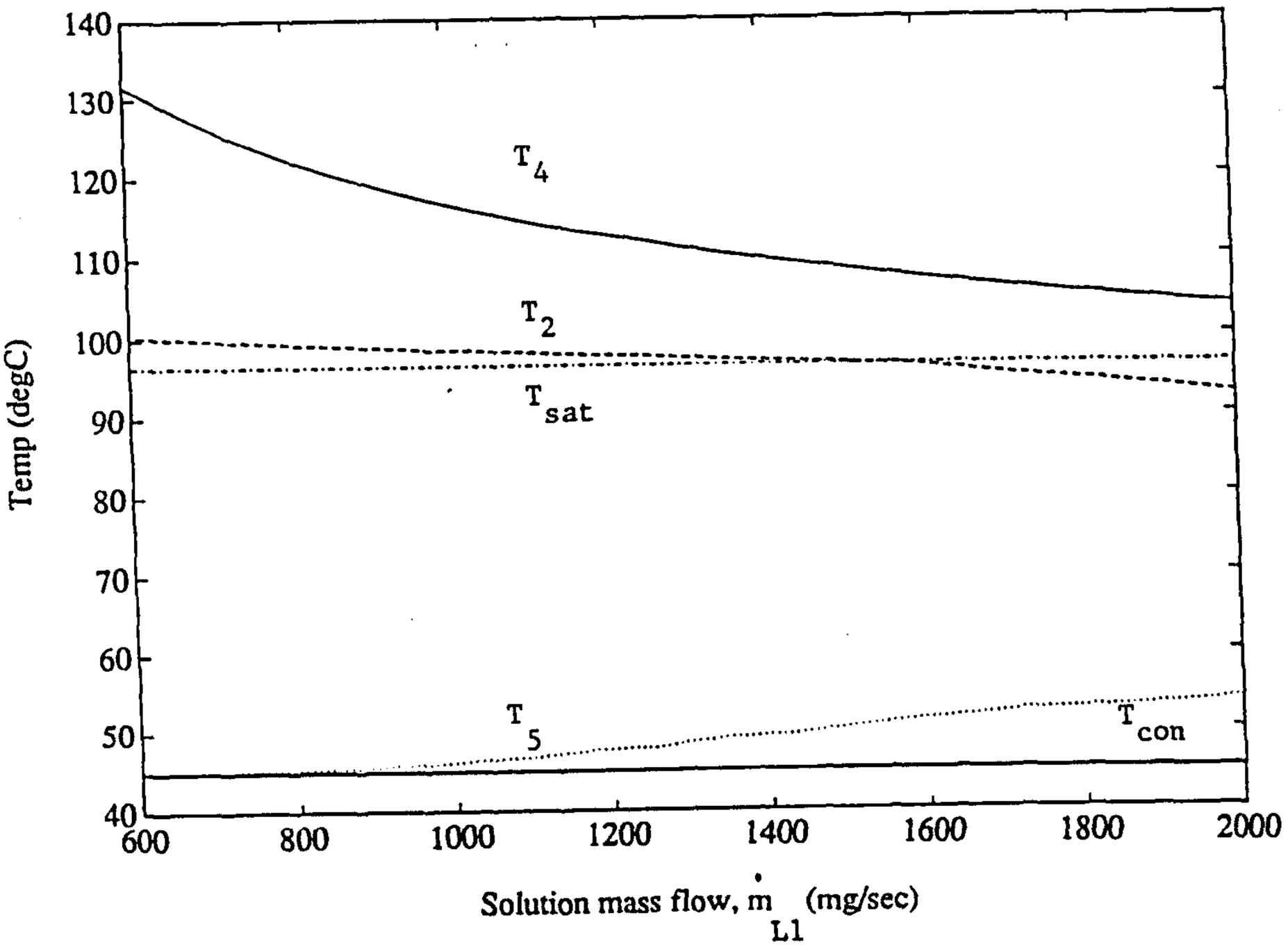

Fig. 3.9.1(c). VVR system response to conditions listed on Table 3.9.1. Temperatures (see Fig. 3.1.1) are plotted against solution mass flow rate. Saturation temperature T_{sat} is the boiling point of the solution in the heat exchanger.

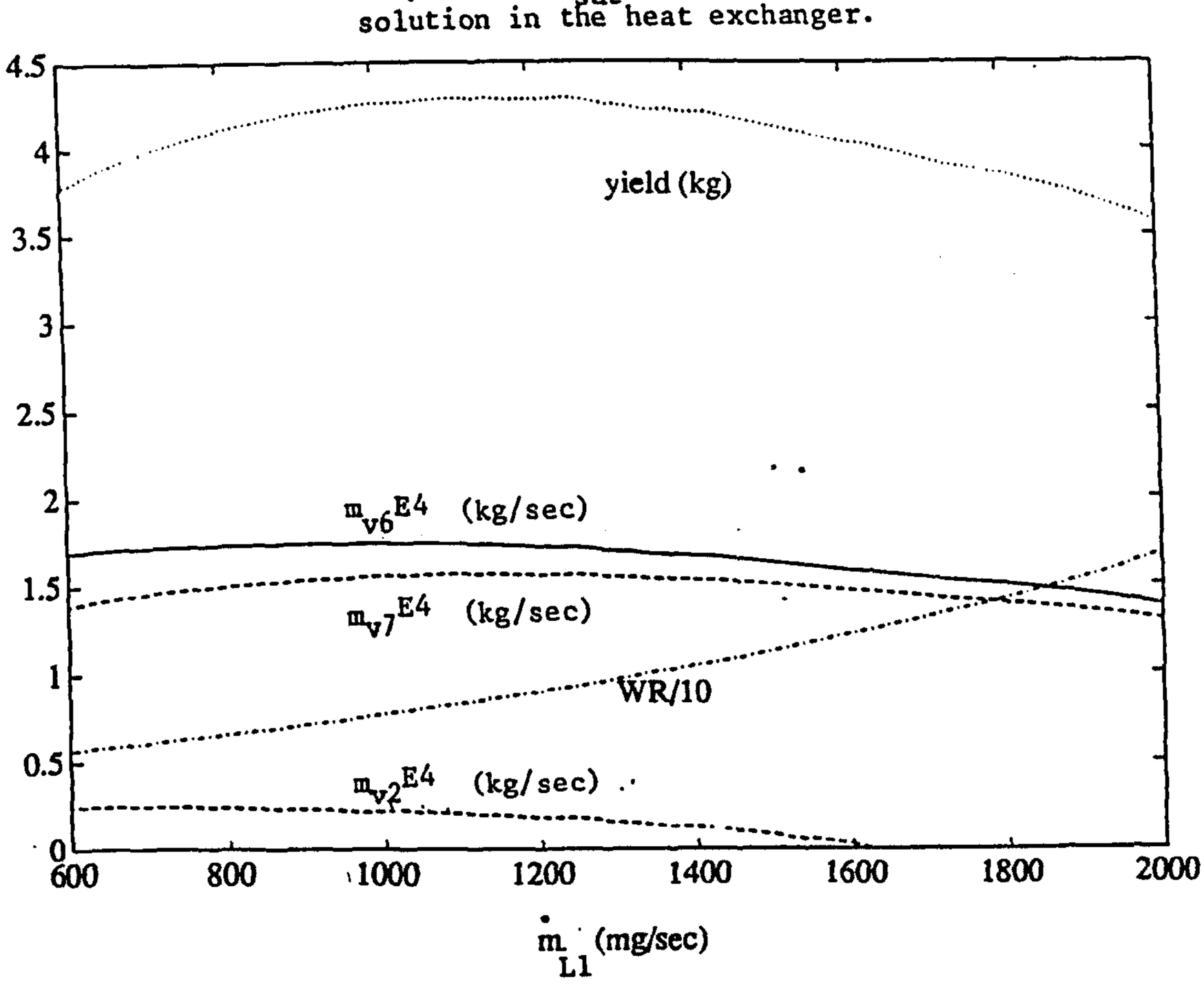

Fig. 3.9.1(d). VVR system response to operating conditions listed on Table 3.9.1. Refrigerant yield, weight ratio, and vapour mass flow rates at points 2, 6 and 7 (see Figure 3.1.1) are plotted against solution mass flow rate.

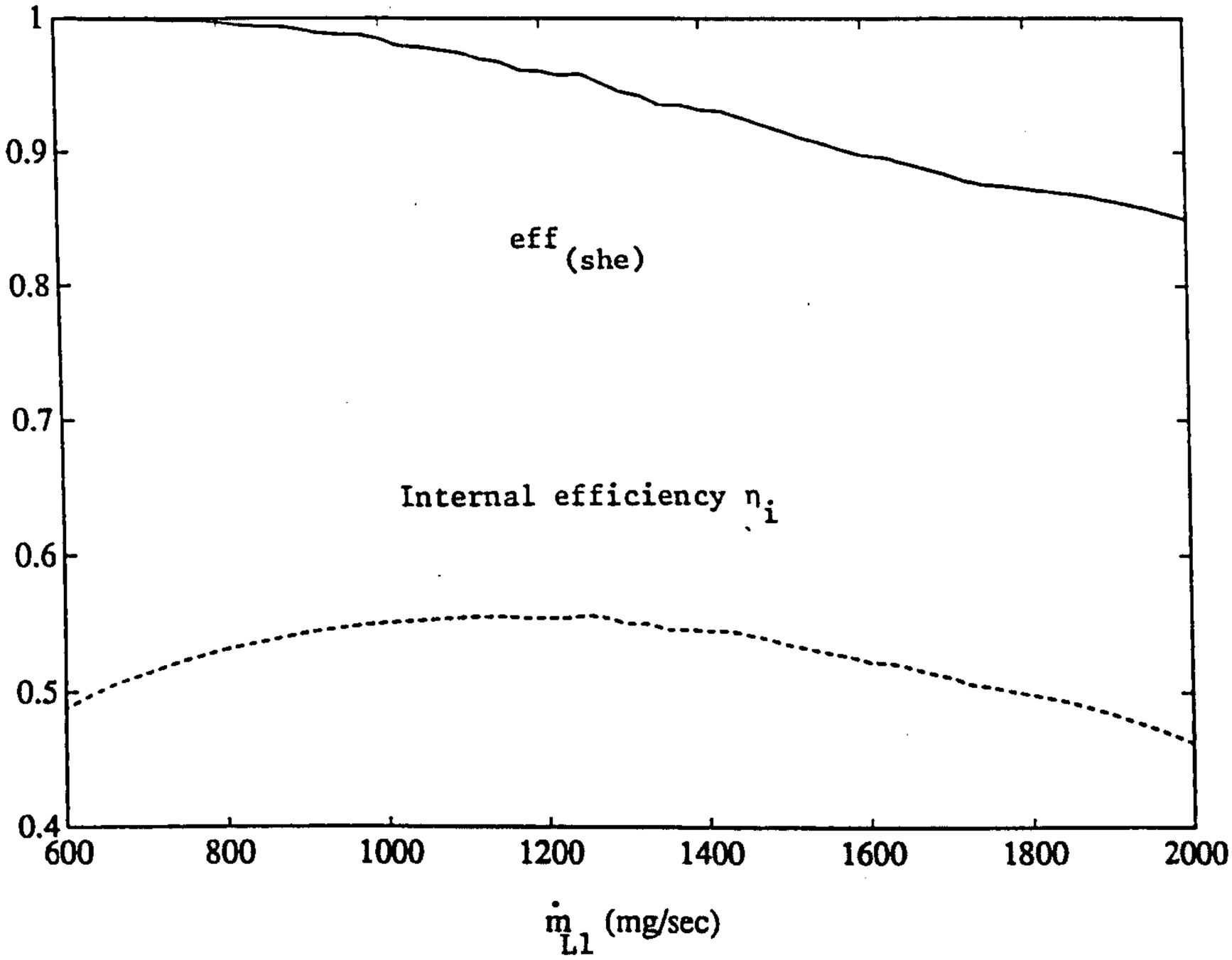

Fig. 3.9.1(e). VVR system response to operating conditions listed on Table 3.9.1. The solution heat exchanger effectiveness and the internal efficiency of the cycle is plotted against solution mass flow rate.

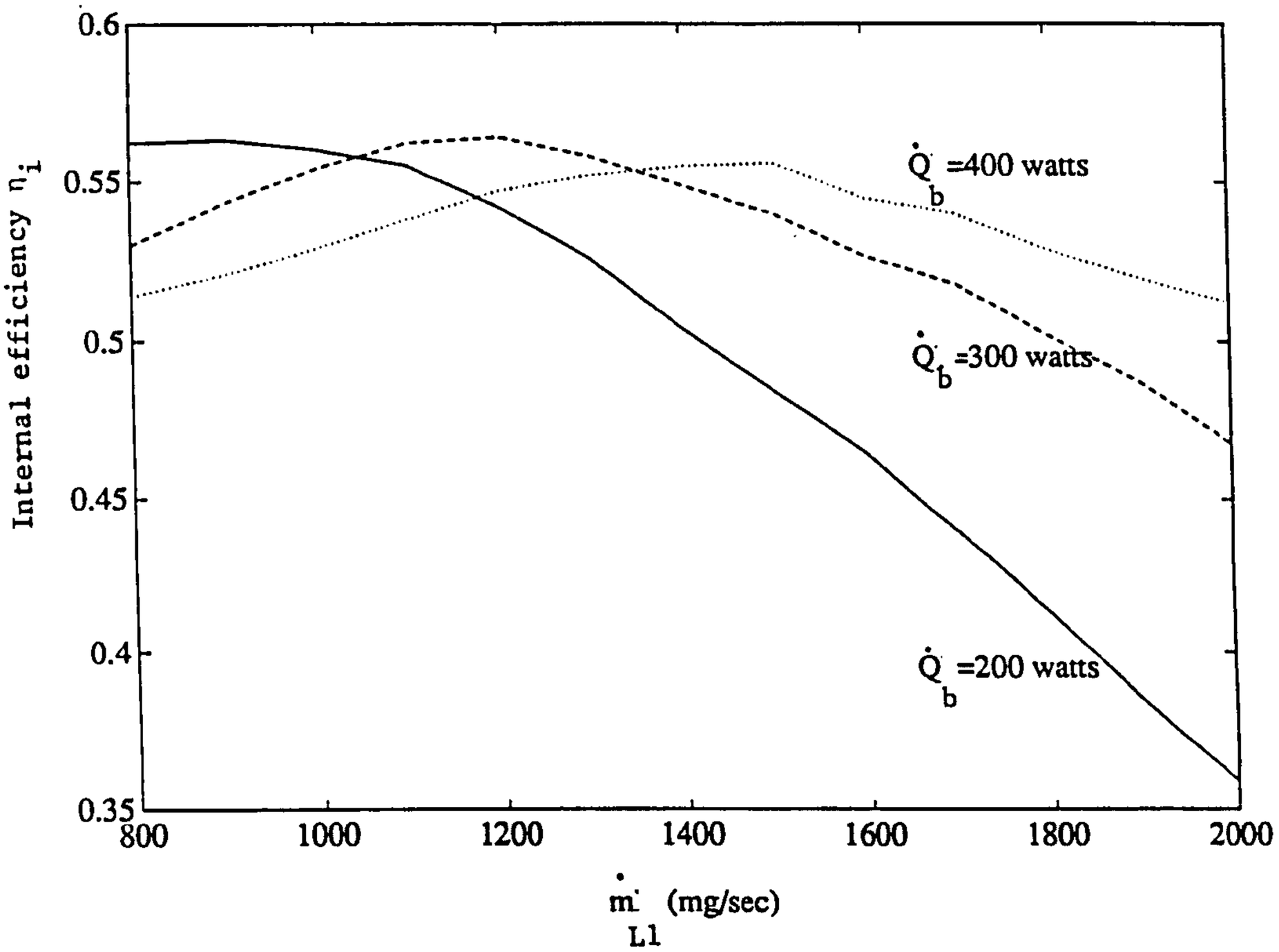

Fig. 3.9.2(a). VVR response to operating conditions listed on Table 3.9.1 for three separate boiler heat flow rates (Q_b). The internal efficiency of the cycle is plotted against solution mass flow rate.

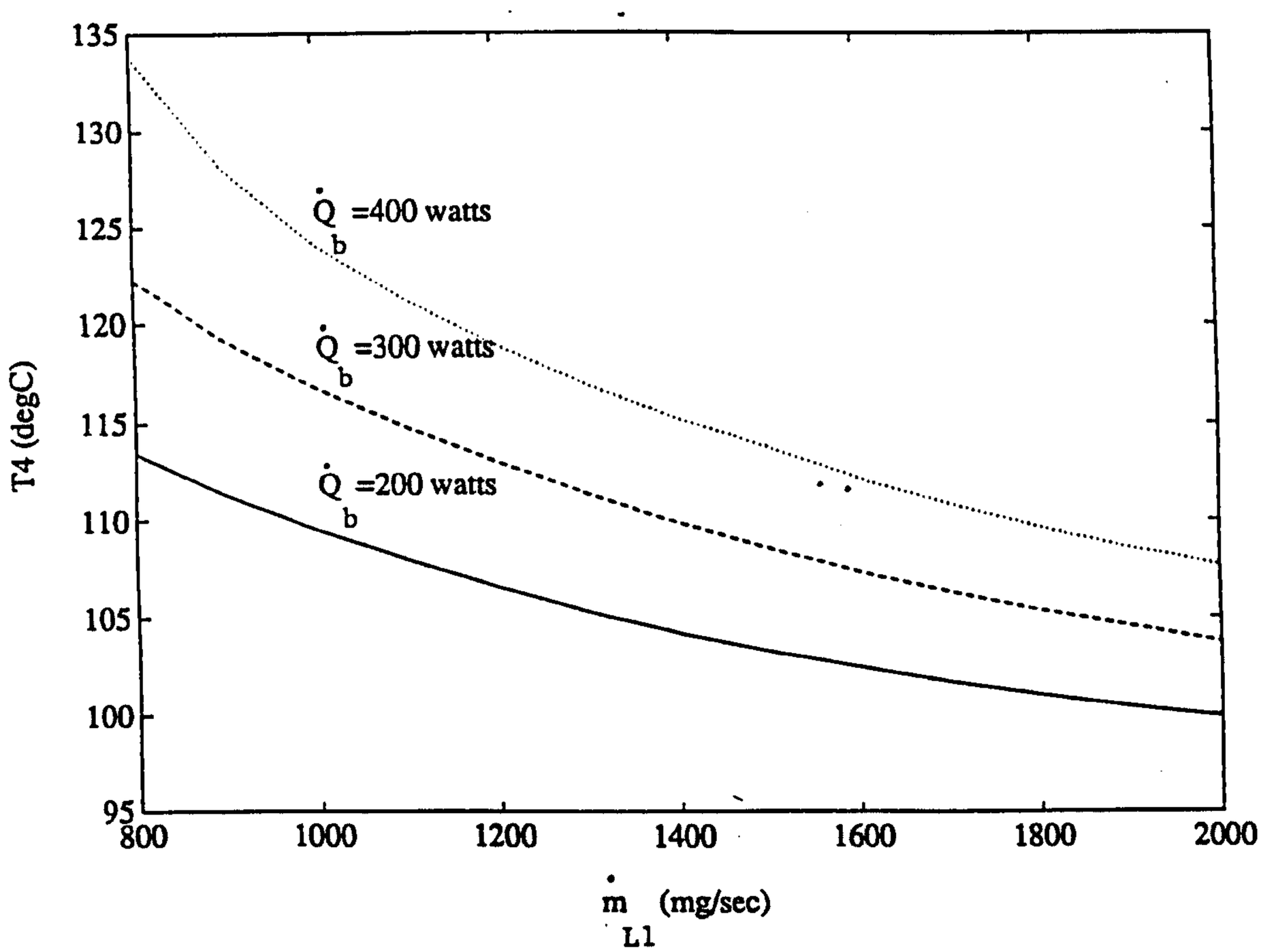

Fig. 3.9.2(b). VVR response to operating conditions listed on Table 3.9.1 for three boiler heat flow rates. Separator temperature T_4 is plotted against solution flow.

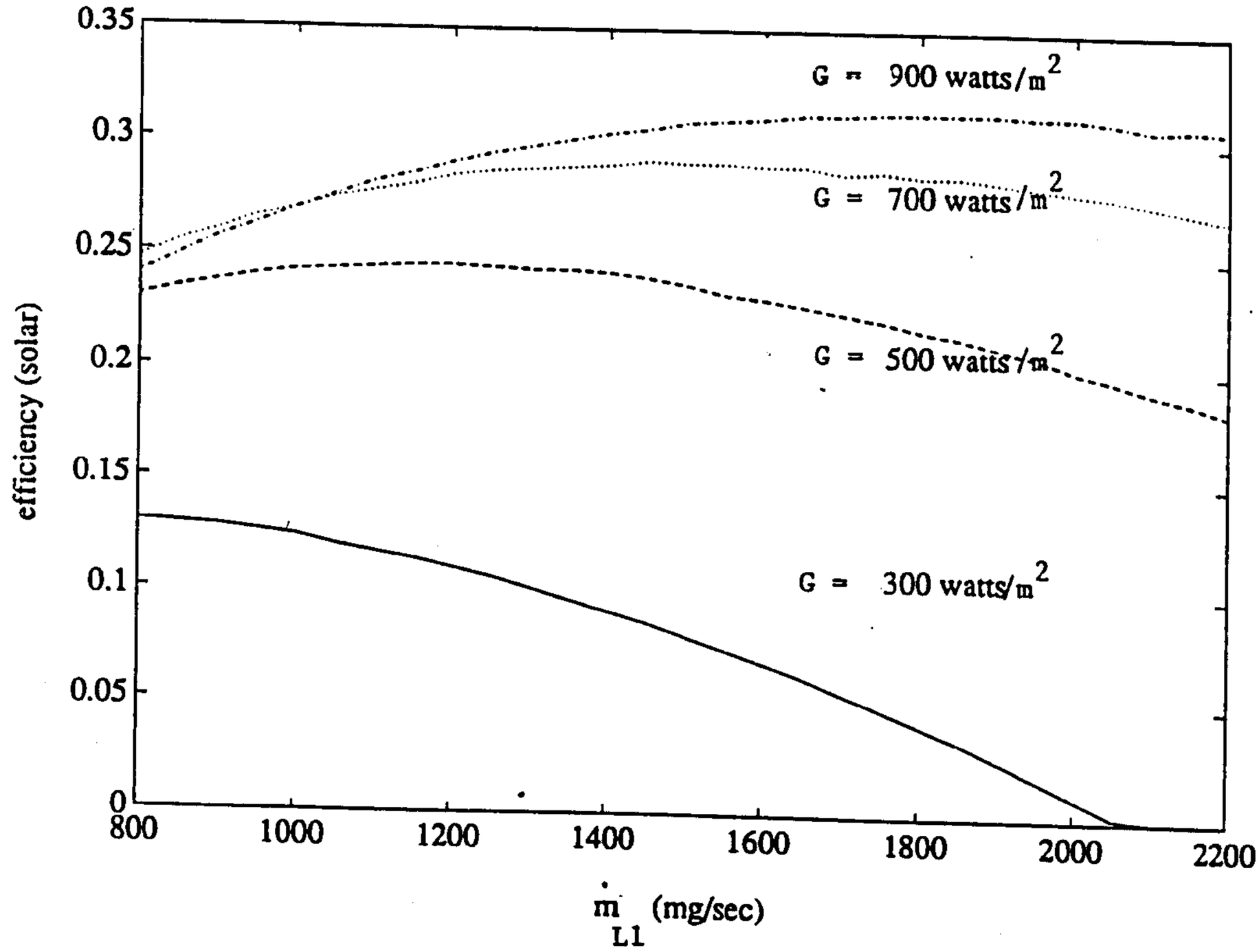

Fig. 3.9.3(a). VVR system response to operating conditions listed in Table 3.9.1 for four values of solar insolation. Solar efficiency is plotted against solution flow rate.

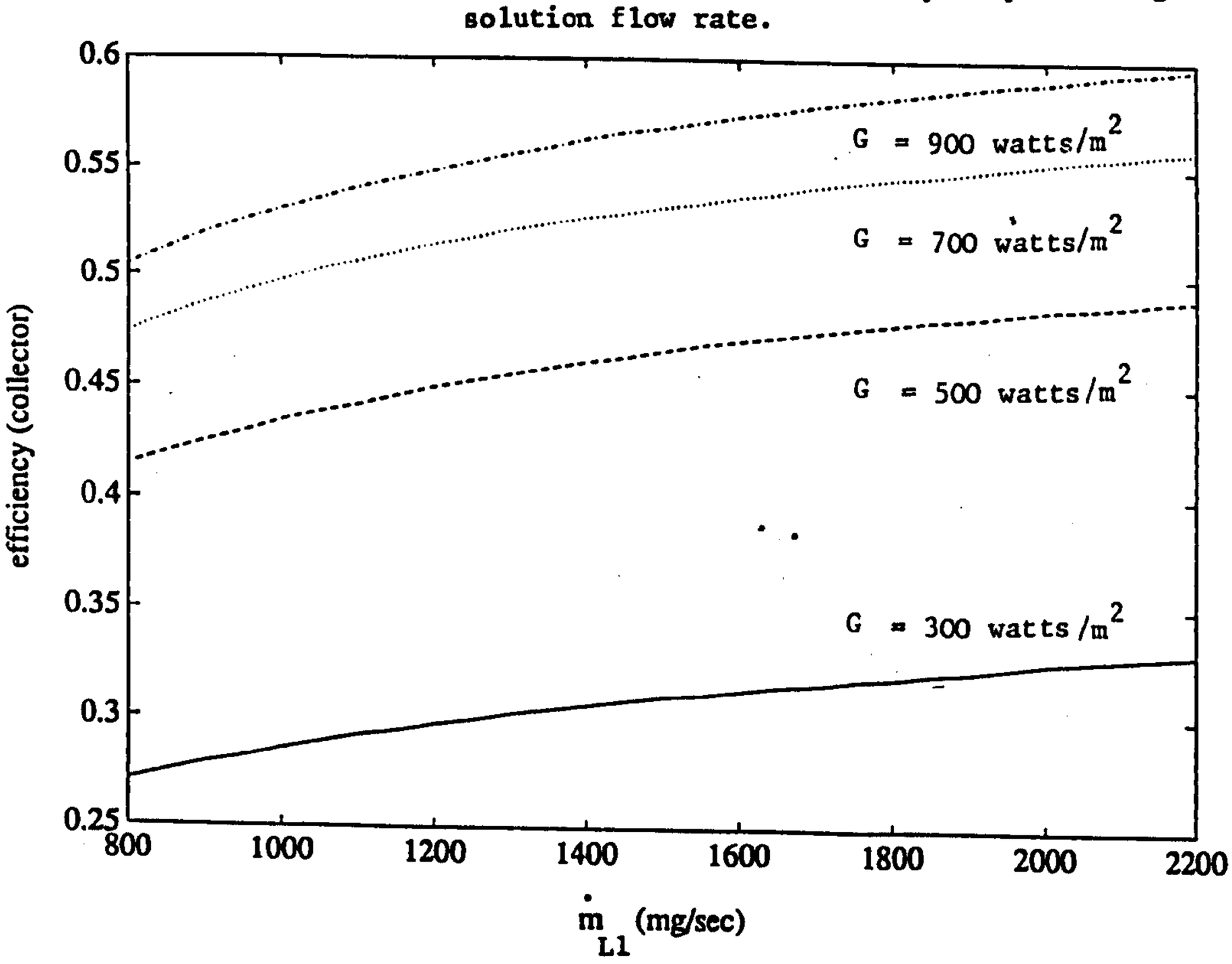

Fig. 3.9.3(b). VVR system response to operating conditions listed on Table 3.9.1. Collector efficiency is plotted against solution flow rate.

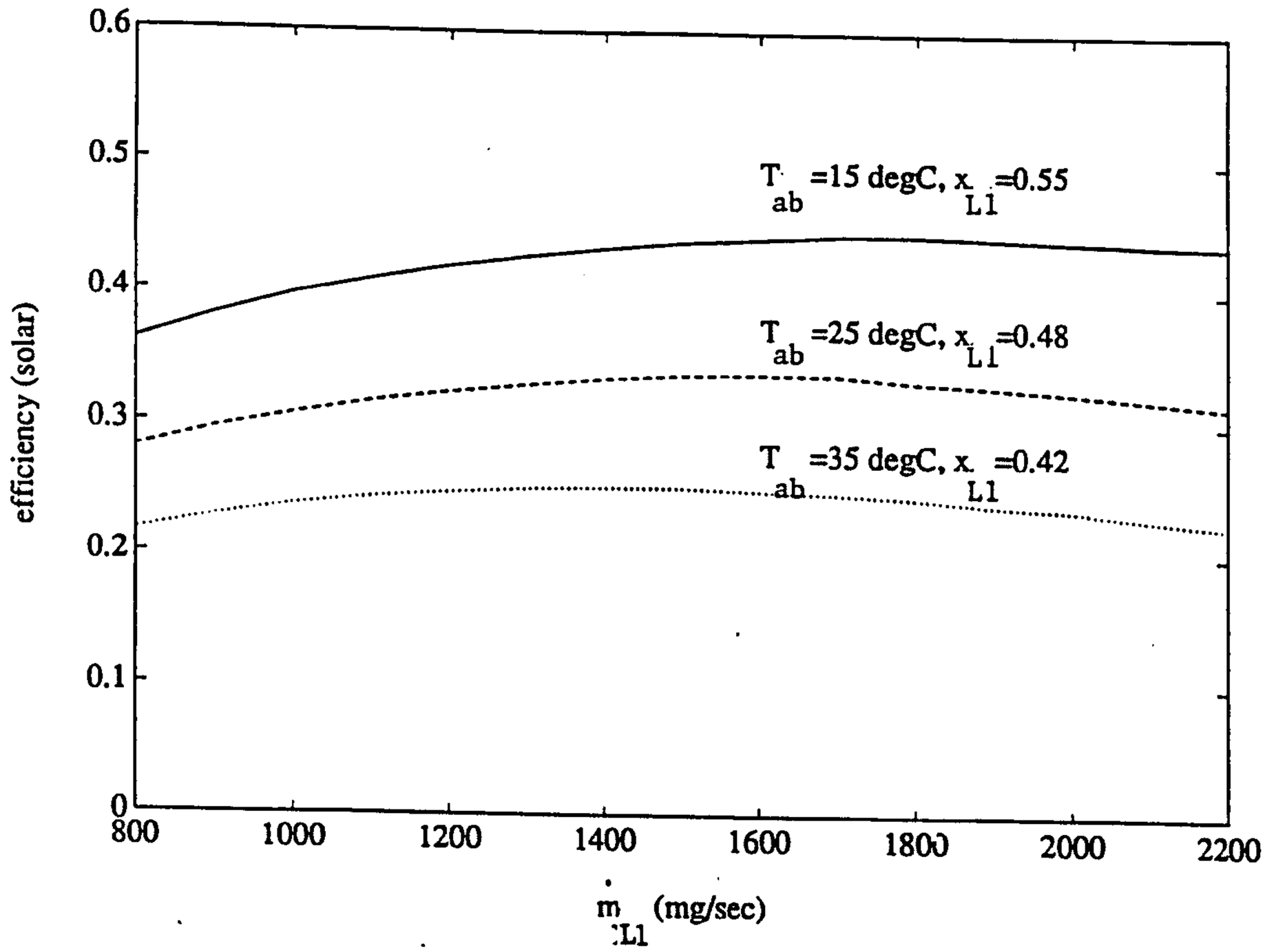

Fig. 3.9.4(a). VVR system response to operating conditions listed on Table 3.9.1, for range of values of absorption temperature T_{ab}. Each absorption temperature corresponds to a rich solution concentration x_{L1}. The solar efficiency of the cycle is plotted against solution flow rate.

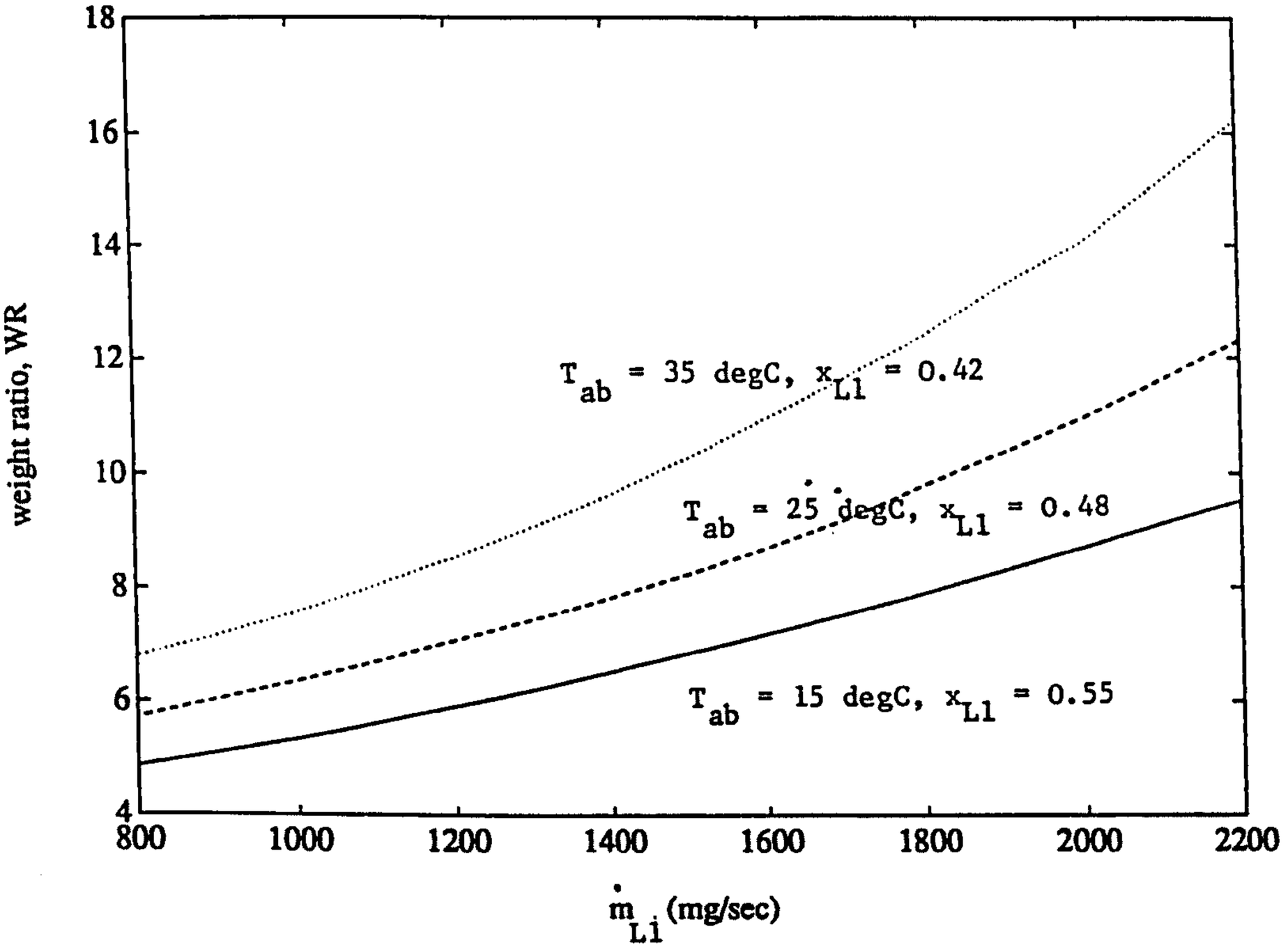

Fig. 3.9.4(b). VVR system response to operating conditions listed on Table 3.9.1. Weight ratios (WR) are plotted against solution flow rate.

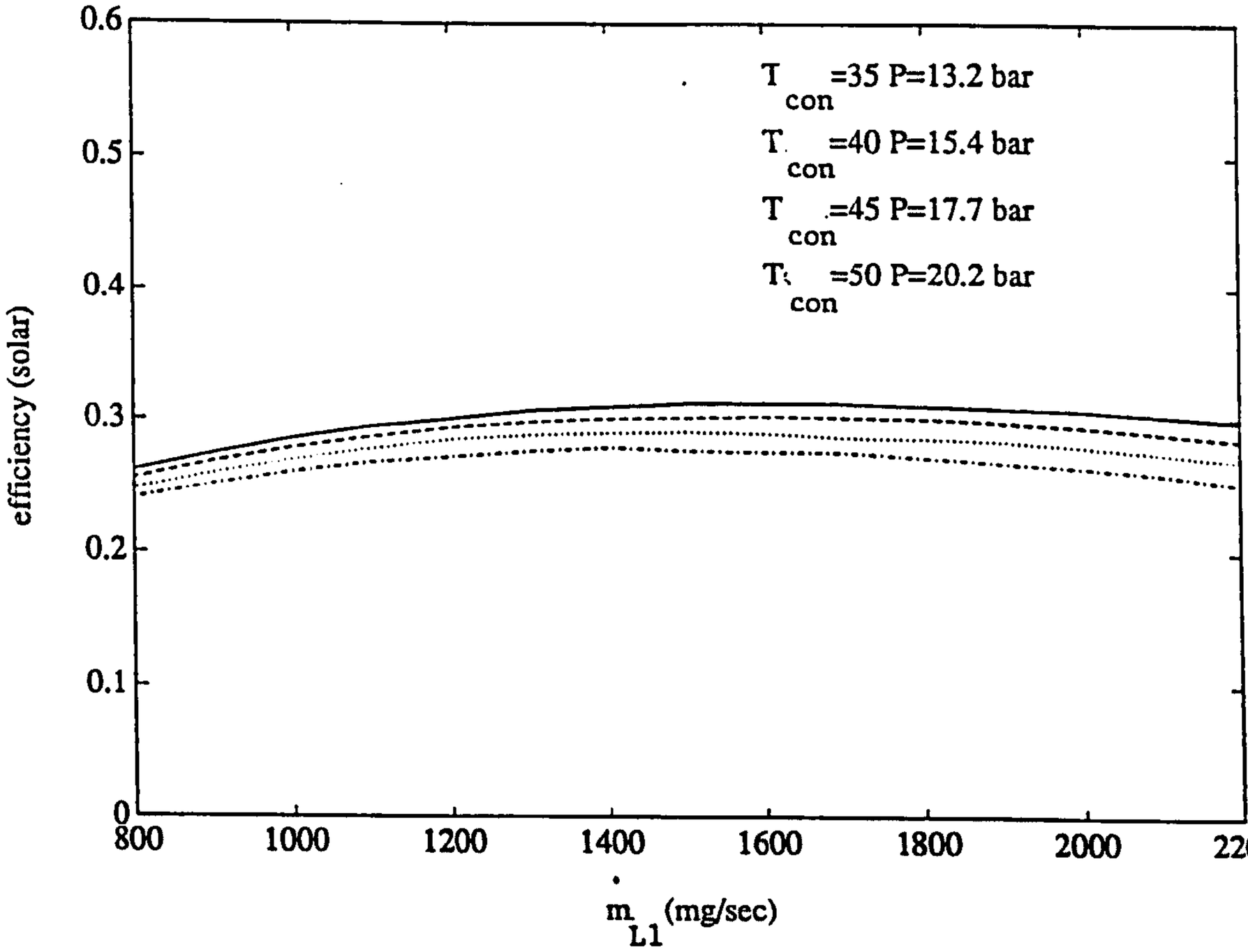

Fig. 3.9.5 VVR system response to the operating conditions listed on Table 3.9.1 for a range of condensing temperatures and system pressures. Solar efficiency is plotted against solution flow rate.

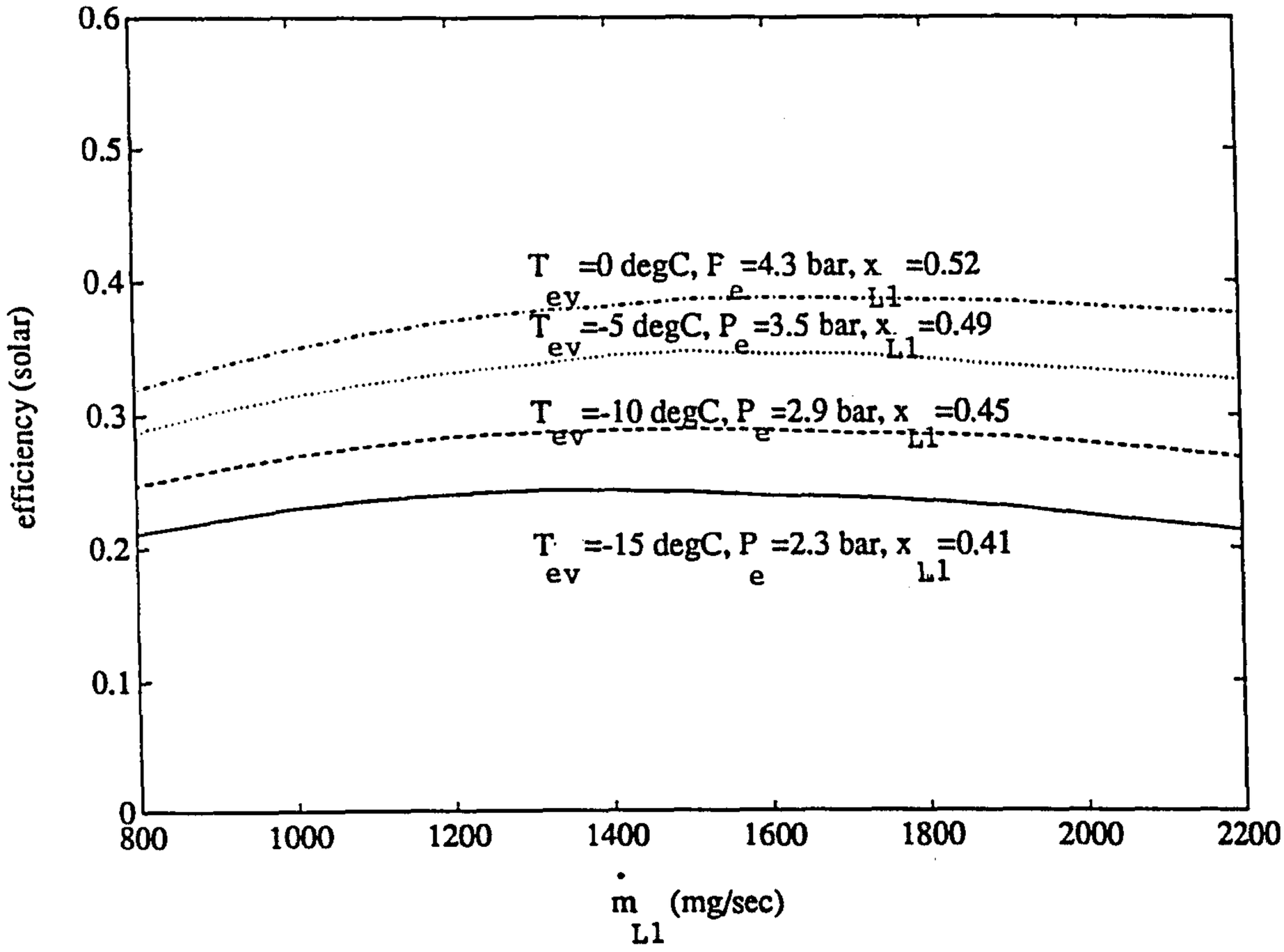

Fig. 3.9.6(a). VVR system response to variations in evaporating temperature, noting the effect of evaporating temperature on absorption/evaporation pressure (P_e), and on solution concentration (x_{L1}). Solar efficiency is plotted against rich solution flow rate (m_{L1}). Operating conditions are listed on Table 3.9.1.

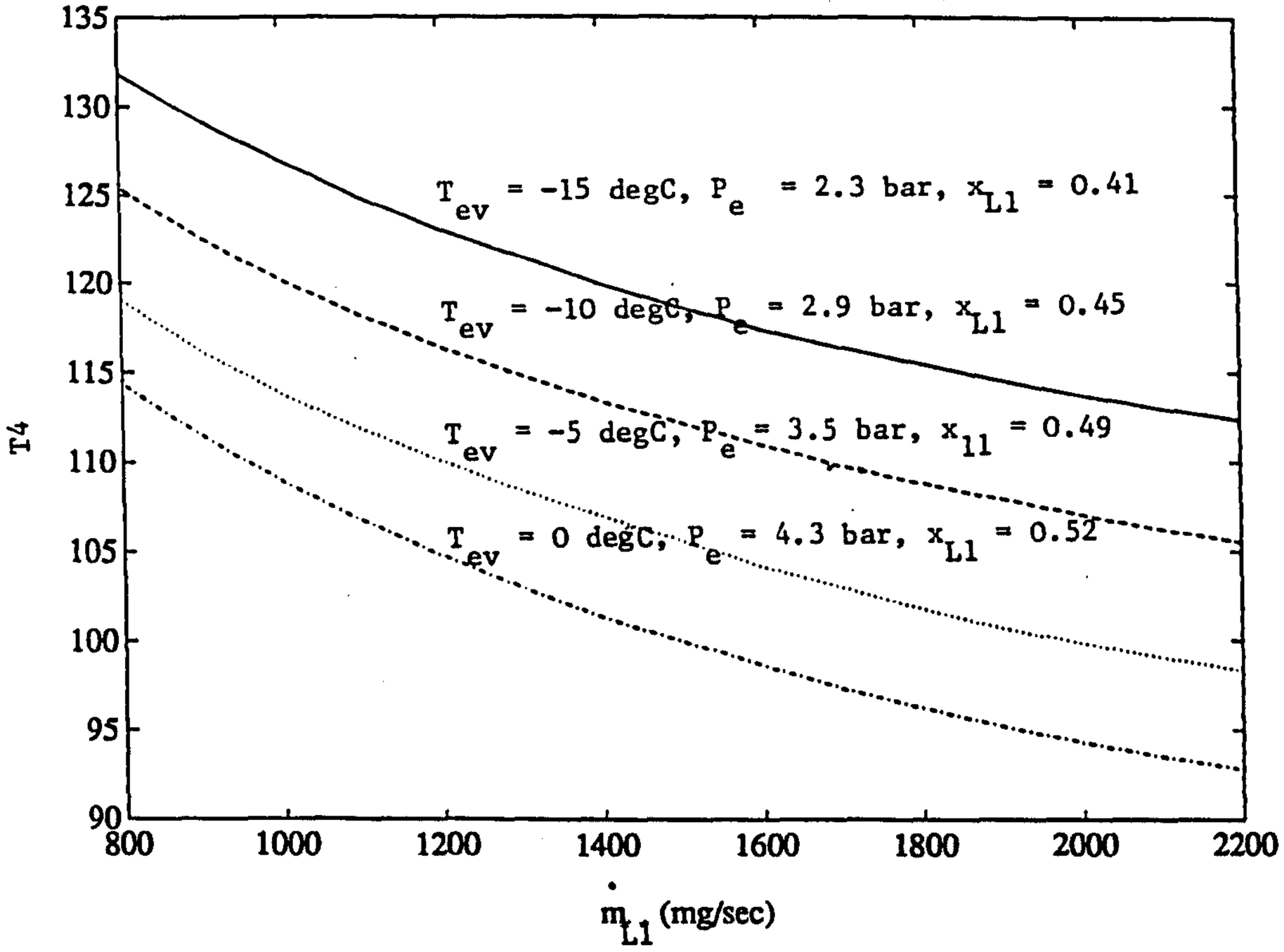

Fig. 3.9.6(b). VVR system response to variations in evaporating temperature. Separator temperature is plotted against rich solution flow rate. Operating conditions are given on Table 3.9.1.

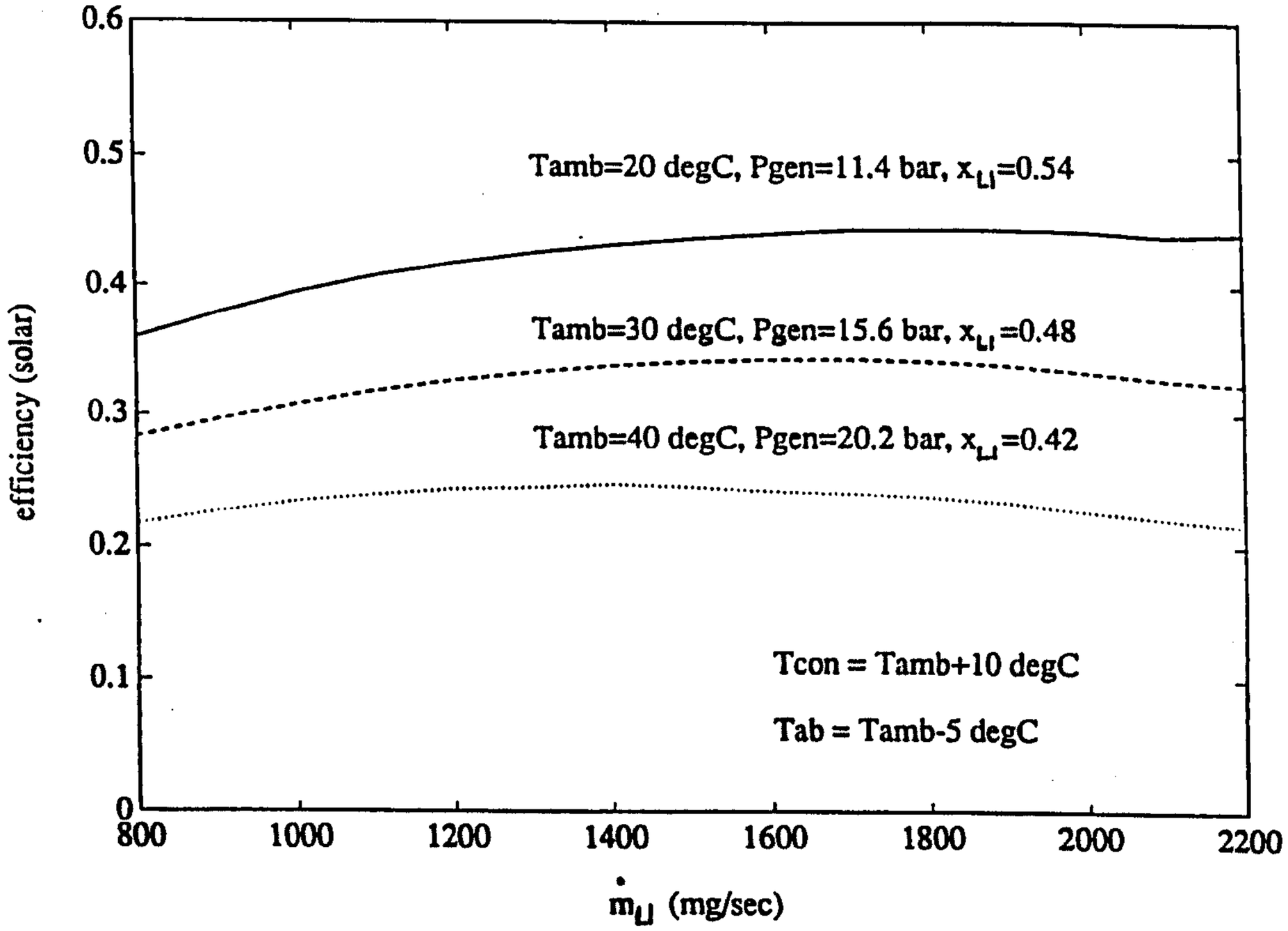

Fig 3.9.7 VVR system response to variations in day-time ambient temperature, assuming that night absorption and condensing temperatures rise with ambient. Solar efficiency is plotted against rich solution flow rate. In practice the assumption is not applicable to many dry climates where low night temperatures are associated also with high day temperatures; in these climates low absorption temperatures will raise efficiency.

increased proportion of heat loss (a function only of temperature and not insolation) to heat transferred. It is observable that the temperature sensitivity of the collector has had the effect of reducing the refrigeration efficiency markedly without pushing the range of solution flow for optimum performance very significantly beyond the limits seen previously in figure 3.9.2 (a). This is fortunate since high flow rates will imply the use of an over large reservoir.

The weight ratios resulting from the conditions examined is shown in fig 3.9.4(b) for a solar insolation value of 700 watts/m^2 and for a range of absorption temperatures. Fig 3.9.4 (a) shows the effect of absorption temperature on solar efficiency, while maintaining the operating conditions listed on table 3.9.1. The low solution concentrations resulting from high absorber temperatures are seen to markedly depress the cycle efficiency. This is expected since the proportion of ammonia mass vapourised in the boiler is a direct outcome of the concentration depletion effected in the boiler, which is limited by the generation temperature achieved and the richness of the concentration fed to the boiler. The effect of low feed concentrations is then to produce high generator temperatures, implying inefficient collector response, and vapours rich in absorbent. The cycle can be expected to perform dissapointingly in climates where high night temperatures will have this effect.

Fig 3.9.5 shows the system performance in response to varying condensing temperatures and system pressures. The system pressure is observed to rise markedly with condensing temperature indicating that safety considerations impose an upper limit on condensing temperature of the order of 50 degC. The plot indicates that overall ("solar") efficiency can be improved by reducing the condenser pressure, which is done by increasing the condenser area or decreasing the sink temperature. The indication is that the improvements achieved in this way are less worthwile than those achieved in reducing absorber temperature.

Variations in evaporating temperature, which imply corresponding variations in absorption pressure, have essentially the same marked effect on performance as absorption temperatures, since solution concentration is a function of absorption pressure. These effects are shown on fig 3.9.6 (a), together with the resulting variations in generator temperature, shown on (b). Low feed solution concentrations are observed to give rise to high generating temperatures, an expected

result since application of the same heat of generation will result in a swing to lower final solution concentrations.

Fig 3.9.7 indicates the effects of varying day-time ambient temperatures, supposing that absorption temperatures fall below the day temperature by 5 degC, and condensing temperatures are expected to be 10 degrees above day time ambient temperatures. The effect shown is clearly a combination of the effects previously considered. The marked variation in solar efficiency with ambient temperature is due to the effect of absorption temperature variation, which has been noted already.

In general the parametric study has demonstrated that the overall (solar) efficiency of the system is very sensitive to changes in absorption temperature, insolation, and evaporating temperature. Ambient temperature also affects the efficiency of the system in so far as it affects absorption temperature. In contrast the effect of condensing temperature is less significant and greater care is needed to providing a large absorption heat rejection flow than a large condenser.

The requirement for optimised solution flow rates in the face of varying insolation is seen in fig 3.9.3 (a) to be more critical than it is in the case of variations in any of the temperatures. These maintain relatively flat efficiency curves with respect to solution flow rate.

3.10. Flow characteristic

Possible practical geometrical arrangements for the FVR and VVR systems are indicated in fig 3.10.1. The distinction between these systems is explained in chapter 1, section 1.6. Fig 3.10.1 (a) shows the FVR circuit without vapour leaving the separator; this is because for the purposes of the present liquid flow analysis vapour flow and release of separator stored mass can be cosidered to cancel each other out leaving equal liquid flows either side of the separator. Fig 3.10.1 (b) shows vapour flow and transfer tank flow (Q7). Since these interact with the circuit at different locations they affect the relative flows in and out of the separator and so are shown.

It is assumed that all external heat is applied to a boiler tube and none to the separator. The maximum vapour mass flow, $\dot{m}_{v3}$, is therefore produced at point 3. This vapour flow reduces the density of the fluid on the supply side of the separator relative to the fluid on the return side.

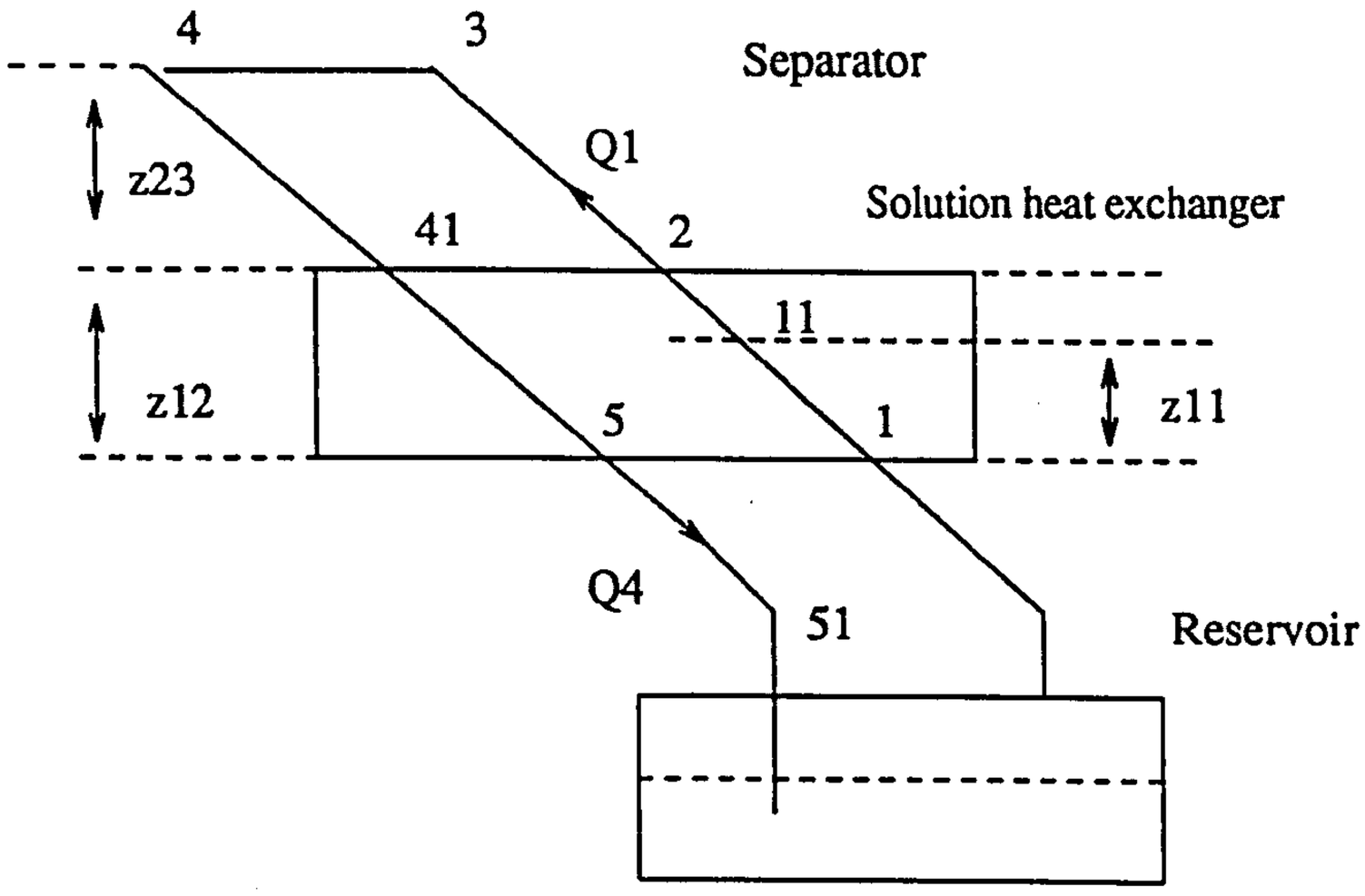

Fig 3.10.1 (a) *The fixed volume reservoir circuit showing vertical heads between numbered stations. No vapour flow is shown leaving the separator because this flow is balanced by a reduction in stored liquid in the separator, with the result that the flow marked Q1 entering the separator is equivalent to Q4 leaving the separator.*

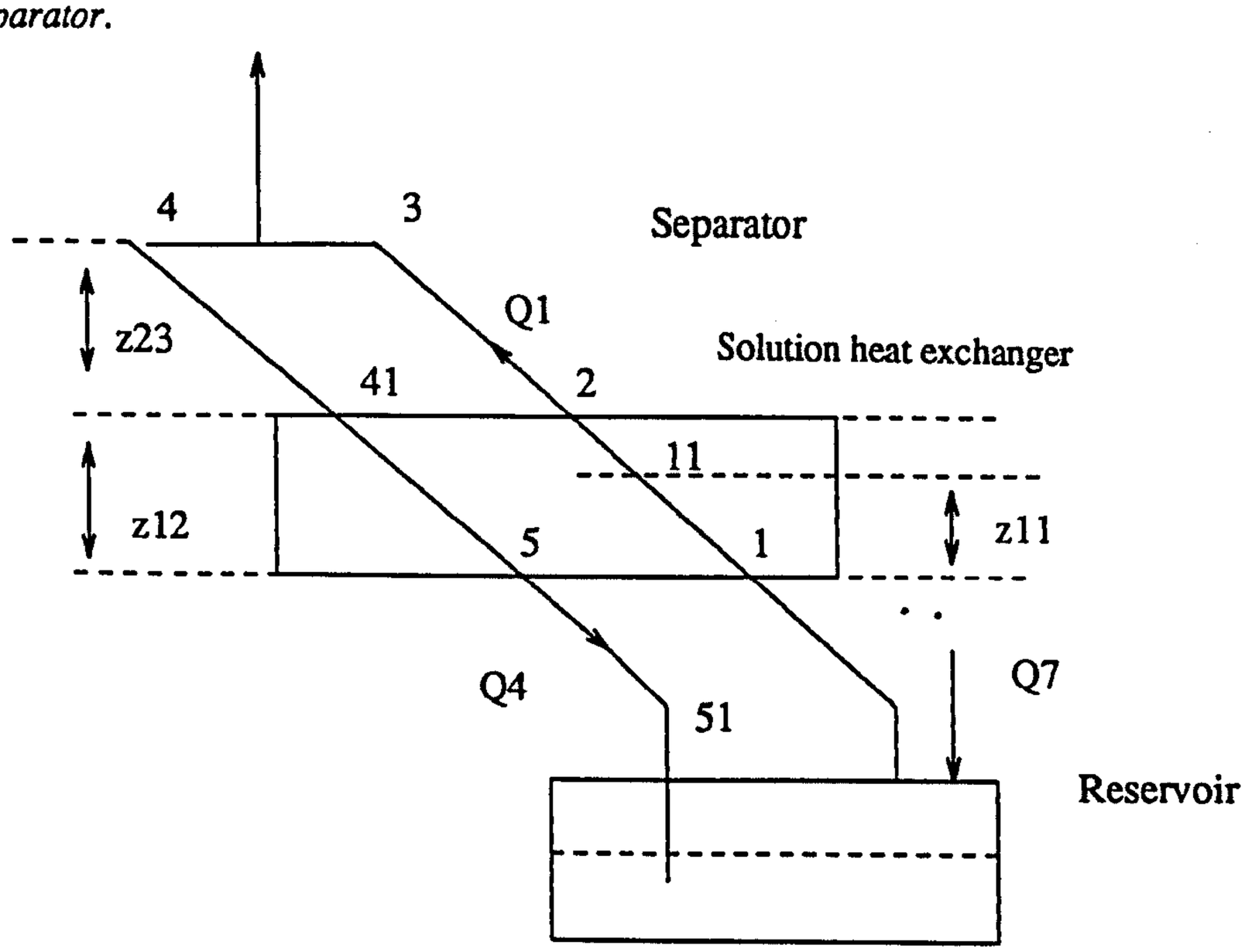

Fig 3.10.1 (b) The variable volume reservoir (VVR) circuit showing vertical heads between numbered stations. The flow marked Q7 is the solution fed to the reservoir from the transfer tank. The mass flow of vapour leaving the separator is shown by an unmarked arrow; this flow balances the transfer tank flow Q7. The shematic diagram shows that Q1 = Q4 + Q7.

Because boiling can sometimes take place in the solution heat exchanger feed leg, a significant density difference can be produced by the solution heat exchanger as well as by the generator. The effect of vapour in altering gross fluid density is large compared to the effect of changes in liquid concentration and temperature. Consequently, density differences on the reservoir side of points 5 and 1 are not considered here. Bernoulli's equation of energy conservation along a streamline can be applied to the points 2 and 3 in the diagrams. The equation is adapted to allow for the energy loss due to frictional pressure drop incurred by the solution flow. Points 1 and 5 can be considered a potential energy datum.

$$p_3+\frac{1}{2}\rho_3 v_3^2+\rho_{13}gz_{13}=p_1+\frac{1}{2}\rho_1 v_1^2+\rho_{45}gz_{13}+LOSS_{13}$$

The difference in kinetic energy per unit volume is considered here to be insignificant. The term Δp is used to describe the net driving pressure causing circulation of solution in the circuit, and is equal to the energy loss in conditions of steady flow.

$$\Delta p=z_{13}g(\rho_{45}-\rho_{13})$$

If k_{13}andk_{45} are circuit resistances as defined by the Hagen-Poiseuille equation for steady and uniform laminar flow in circular tubes (Douglas, 1979), and if Q is the volumetric flow of solution, then

$$\Delta p=k_{13}Q_1+k_{45}Q_4 \qquad (3.10.1)$$

The friction characteristic of the pipework is then a linear function of the Reynolds number where a laminar flow regime exists, such that where

$$Re=\frac{4Q\rho}{\pi d\mu}<2300$$

then

$$\Delta p=kQ=\left[\frac{128\mu l}{d^4\pi}\right]Q$$

In the circuit of fig 3.10.1 (a) (the FVR system) supply and return volume flows can be considered equal:

$$Q_1=Q_4=\Delta p\left(\frac{1}{k_{13}+k_{45}}\right)$$

In the circuit of fig 3.10.1 (b) (the VVR system) the continuity equation is:

$$Q_1=Q_4+Q_7$$

where Q_7 is the liquid volume flow from transfer tank into the resevoir. In the same way that Δp is dependent on the cycle performance so is the volumetric circulation ratio, which is defined as

$$CR_v=\frac{Q_1}{Q_7}$$

Therefore

$$Q_4=Q_1\left(1-\frac{1}{CR_v}\right)$$

Returning to equation (1):

$$\Delta p=k_{13}Q_1+k_{45}Q_1\left[1-\frac{1}{CR_v}\right]$$

Therefore

$$Q_1=\Delta p\left[\frac{1}{k_{13}+k_{45}\left(1-\frac{1}{CR_v}\right)}\right]$$

The driving pressure, Δp, is composed of the sum of the pumping effects in both the generator and solution heat exchanger:

$$\Delta p=\Delta p_{she}+\Delta p_{gen}=z_{23}g(\rho_{4,41}-\rho_{23})+z_{12}g(\rho_{4,15}-\rho_{12})$$

The effective density in the boiler feed path can be estimated by integrating along its length. This is simplified if it is assumed that heat is supplied uniformly along the length such that fluid enthalpy increases linearly with height. By calculating ratios of liquid and vapour flow the enthalpies at a series of ten even temperature steps (dividing the difference between T_2 and T_3)can be found. By linear interpolation the fluid densities at the temperature boundries can be converted to densities at the boundries of equal enthalpy. Bulk boiler density is then calculated as the mean of densities of fluid at a series of ten even enthalpy steps.

The liquid density in the return pipework 4 to 41 (ρ4,41) can be assumed constant since changes in temperature are negligible and concentration is constant. An accurate estimate of

density difference in the solution heat exchanger would be complex, since the heat transfer rate increases along its length both as a function of increasing temperature difference and variations in the heat transfer coefficient. The coefficient will increase as boiling starts to take place in the feed leg. An approximate estimate can be made by assuming that the temperature difference between the streams increases linearly with height. The height (z_{11}) at which the cumulative heat transfer, considered only as a function of varying temperature difference and constant single phase heat transfer, is sufficient to cause boiling can then be identified. Overall densities of the two streams can then be expressed as averages:

$$\rho_{12}=\left(\frac{\rho_2+\rho_{11}}{2}\times\frac{z_{12}-z_{11}}{z_{12}}\right)+\left(\frac{\rho_1+\rho_{11}}{2}\times\frac{z_{11}}{z_{12}}\right)$$

$$\rho_{41,5}=\frac{\rho_4+\rho_5}{2}$$

For both the FVR and VVR systems,

$$\dot{m}_{L1}=\rho_1 Q_1=\rho_1\Delta p \qquad (3.10.2)$$

Figure 3.10.2 shows the result of running the VVR code in two different modes. Firstly the rich solution flow rate ($\dot{m}_{L1}$) is treated as an independent parameter and the program run for various values of solar insolation, $\dot{G}$. Solar efficiency (η_{solar} is taken as the output parameter, so that the ideal flow characteristic of the circuit is represented by the curve joining the points of optimum performance. Secondly the VVR code is run with $\dot{m}_{L1}$ as an internal parameter, defined by the function:

$$\dot{m}_{L1}=\rho_1\Delta p\left[\frac{1}{k_{13}+k_{45}\left(1-\frac{1}{CR_v}\right)}\right]$$

The error introduced by assuming a constant value for CR_v is less than 4% and has an insignificant effect on η_{solar}. The function can therefore be approximated to become the same as that derived for the FVR circuit. The approximate function is adopted for the computer model:

$$\dot{m}_{L1}=\rho_1\Delta pK$$

where K is the appropriate composite constant for the resistance of the circuit to fluid flow. The

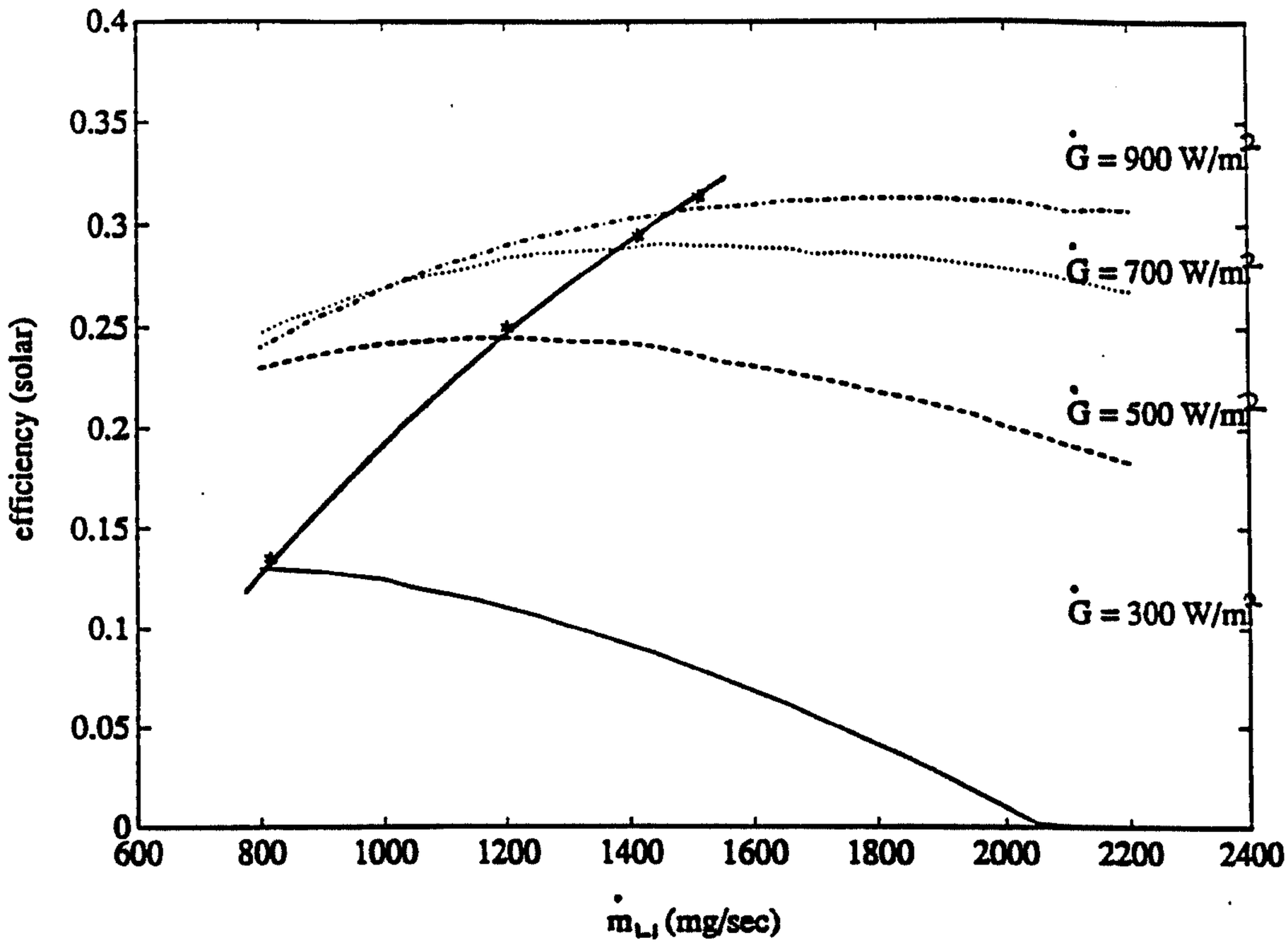

Fig. 3.10.2. Solar efficiency of the VVR system plotted against rich solution flow for a range of constant insolation values. Operating conditions are given on Table 3.9.1. The solid line connecting stars represents the operating curve of a machine with one fixed characteristic of frictional resistance (K) to solution flow. A real machine will always have one resistance characteristic, though this may be tuned with a throttle to position the operating curve as desired. A value of K is adopted here to optimise performance under varying insolation conditions, while also remembering that a lower value of K is desirable to reduce the weight ratio or solution bulk.

circuit can be imagined to include a flow restricting component such as a needle valve which will allow the overall conductance to be tuned to any value considered to optimise performance. K is therefore treated as an input parameter, and figure 3.10.2 shows a flow characteristic curve for one value of K. It should be appreciated that a small value of K is to be preferred on the basis that it implies a low weight ratio and therefore less overall bulk and weight. Since the ideal curve and the function curves have similar tendencies the circuit can be described as in principle self-tuning to climatic conditions. The same conclusion applies to the FVR circuit.

3.11. Dynamic response of VVR circuit

The computer code used to simulate the dynamic response of the VVR circuit has been presented schematically in figure 3.6.3, the proceedure for solving for P_{gen} and T4 being identical to that used in the steady state simulation and described by figure 3.6.1. The code solves for steady state conditions for finite time steps (dt) on the basis of a given condenser heat transfer area (A_{HPC}) and heat transfer coefficient (k_{HPC}), taking into account the thermal lag effects of the generator. The input parameters used by the code are listed in table 5.3.11 together with values used as standard in the execution of the code here.

A simple model of the sensible heating process taking place in the generator at the start of the day consists of treating it as a single lumped thermal mass experiencing no circulation of solution. Its heat capacity is then given by:

$$\dot{M}c_{p(gen)}=M_{L(sep)}c_{p(sep)}+M_{L(she)}c_{p(she)}+(M_{st(she)}+M_{st(sep)})c_{p(st)}$$

where $c_{p(sep)}$ is evaluated as $\delta h/\delta T$ for a concentration of x_{L4} and $c_{p(she)}$ is evaluated similarily for the mean value of x_{L1} and x_{L4}. For the generator size considered in section 3.6 (Table 3.7.1), containing 2.5 kg of liquid in 1.4 kg of steel, the thermal capacity of the generator $Mc_p(gen)$ is calculated to be in the order of 5 MJ/K. The dynamic model presented here treats $Mc_{p(gen)}$ as a single input parameter. The rise in separator temperature (T_{gen}) during a short time period dt in response to heat input to the generator is given by:

$$T_{gen_t}=\frac{\dot{Q}_b dt}{Mc_{p(gen)}}+T_{gen_i}$$

In practice the bubble point in the generator is reached soon after sunrise because of the low thermal inertia of the generator tube and heat pipe collectors. This will cause circulation, most of the circulated heat being retained by virtue of the solution heat exchanger. Heat distribution to the separator is by vapourisation and condensation, and is therefore effective. The lumped thermal mass model is therefore justified.

Condensation of refrigerant is assumed to start only once the solution bubble point temperature, T_{sat}, is reached. The system pressure which determines this point is found by assuming that condensation takes place initially at a temperature just greater than T_{amb}. Thereafter steady flow conditions can be calculated from energy and mass balances for each successive finite element of time. Transient effects due to changing solar irradiance can be adequately modelled by calculating for each time period the sensible heat lost to increased generator temperature or gained through declining separator temperature, and normalising this energy component to allow the net yield (M_{ref})for each time element to be expressed:

$$M_{ref}=\dot{m}_{v7}(dt-dt_{sen})$$

where dt_{sen} is calculated from the enthalpy change resulting from varying generator temperature:

$$dt_{sen}=\frac{1}{Q_b}M_{L(sep)}(h_{LA_t}-h_{LA_t})+M_{L(she)}(h_{L(she)_t}-h_{L(she)_t})$$

$$+M_{st(sep)}c_{p(st)}(T_{gen_t}-T_{gen_t})+M_{st(she)}c_{p(st)}(T_{she_t}-T_{she_t})$$

The dynamic code makes use of a simplified function to characterise the rate of rich solution flow ($\dot{m}_{L1}$), which expresses the solution flow as linearly proportional to the refrigerant yield rate ($\dot{m}_{v7}$) using a constant value for circulation ratio (CR) which is based on the experimental observations recorded in chapter 6. It remains in accordance with the function described in section 3.10 and shown in figure 3.10.2. A value is chosen which results in a device characterisation which is optimised both for energy efficiency and for a low solution storage requirement.

Hirschmann (1974) shows that the sine function can be used to model solar insolation on a clear sunny day. The topic is discussed further by Brinkworth (1972). In this case study of measured insolation patterns on clear days allow the following function to be derived:

$$\dot{G}=\frac{\dot{G}_{max}}{2}\left[1+\sin\left[\frac{2\pi}{\Delta t_{day}}(t-dt)-\frac{\pi}{2}\right]\right]$$

where Δt_{day} is the period between sunrise and sunset. Figs 3.11.1 (a) and 3.11.2 (a) show the two cases where the peak value reached at midday is 600 and 900 watts/m^2 respectively. An equatorial diurnal period is assumed such that Δt_{day} is 12 hours. The two cases are nominal; although a clear day is modelled with acceptable accuracy by the 900 watts/m^2 case, the reduced case is less likely to resembled closely in practice. Nevertheless it serves as an initial model of a cloudy or broken day where the diffuse component of irradiation is significant.

Figures 3.11.1 and 3.11.2 show the response of the VVR circuit to the simulated insolation on the assumption of a constant ambient temperature of 30 degC.

CR	7.27		UA_{she}	50	watts/K
Δt_{day}	12	hours	$M_{cp(gen)}$	5	MJ
A_{HPC}	7	m^2	k_{HPC}	1.68	watts/K
T7	75	degC	T1	$=T_{con}$	degC
T_{amb}	30	degC	T_{ab}	30	degC
T_{ev}	-10	degC	A_{coll}	1	m^2
dt	10	mins			

Table 3.11.1 *Parameter values adopted for dynamic characterisation of VVR system, as shown on figures 3.11.1 and 3.11.2.*

The yield calculated for a cloudy day of 600 watts/m^2 peak insolation is 2.9 kg as shown on fig 3.11.1(a). The energy received by the collector during the full day is calculated to be 13.0 MJ. An approximate estimate of the energy of evaporation of the refrigerant at a nominal evaporating temperature of -10 degC is 1.16 MJ, so that the daily COP, as defined in section 1.2, is calculated to be 0.26. In the case of the clear day modelled as having a peak insolation of 900 watts/m^2, the yield is 4.9 and the received energy is 19.4 MJ, resulting in a daily COP of 0.29. The mass of solution which has been processed by the end of the day is 25 kg in the first case and 41 kg in the second case.

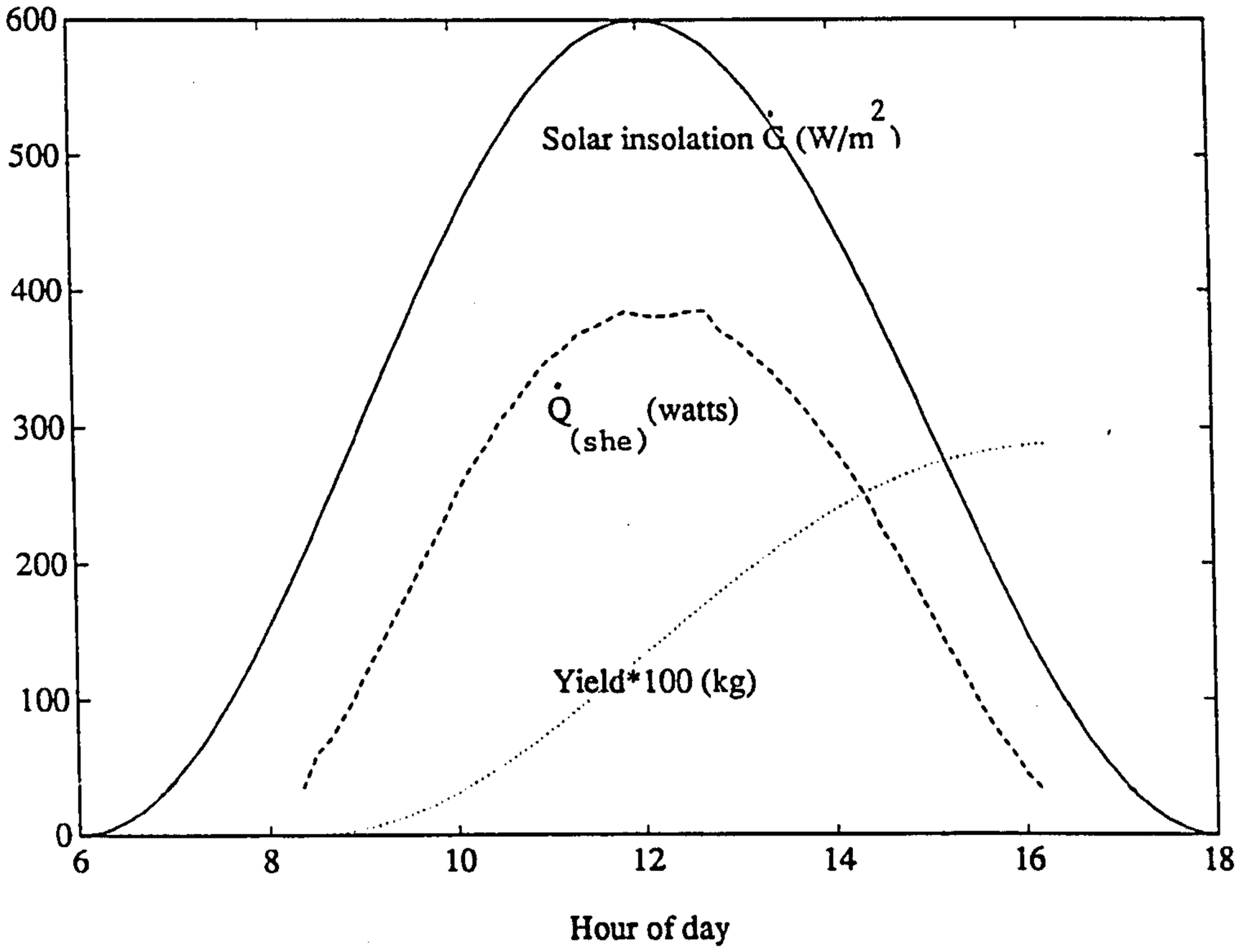

Fig. 3.11.1(a). Dynamic response of the VVR circuit to a simple sine function simulation of a slightly overcast day, solar insolation peaking at 600 W/m^2 at mid-day. Computer code is run for the operating conditions given on Table 3.11.1. Accumulated refrigerant yield is plotted against hour of day, and heat transferred within the solution heat exchanger (Q_{she}).

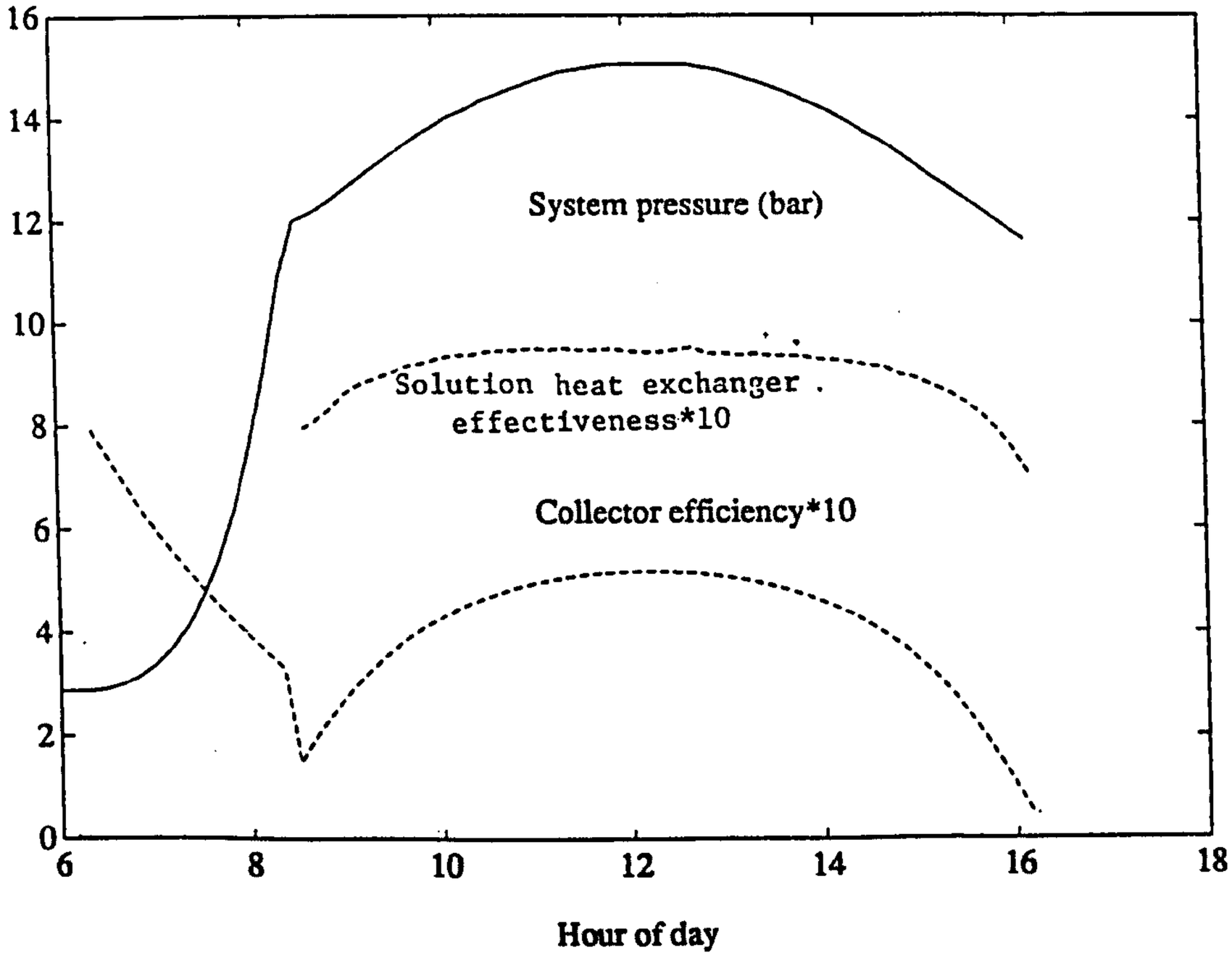

Fig. 3.11.1(b). Dynamic response of the VVR circuit as in Figure 3.11.1(a). System pressure, solution heat exchanger effectiveness, and collector efficiency are plotted against time of day.

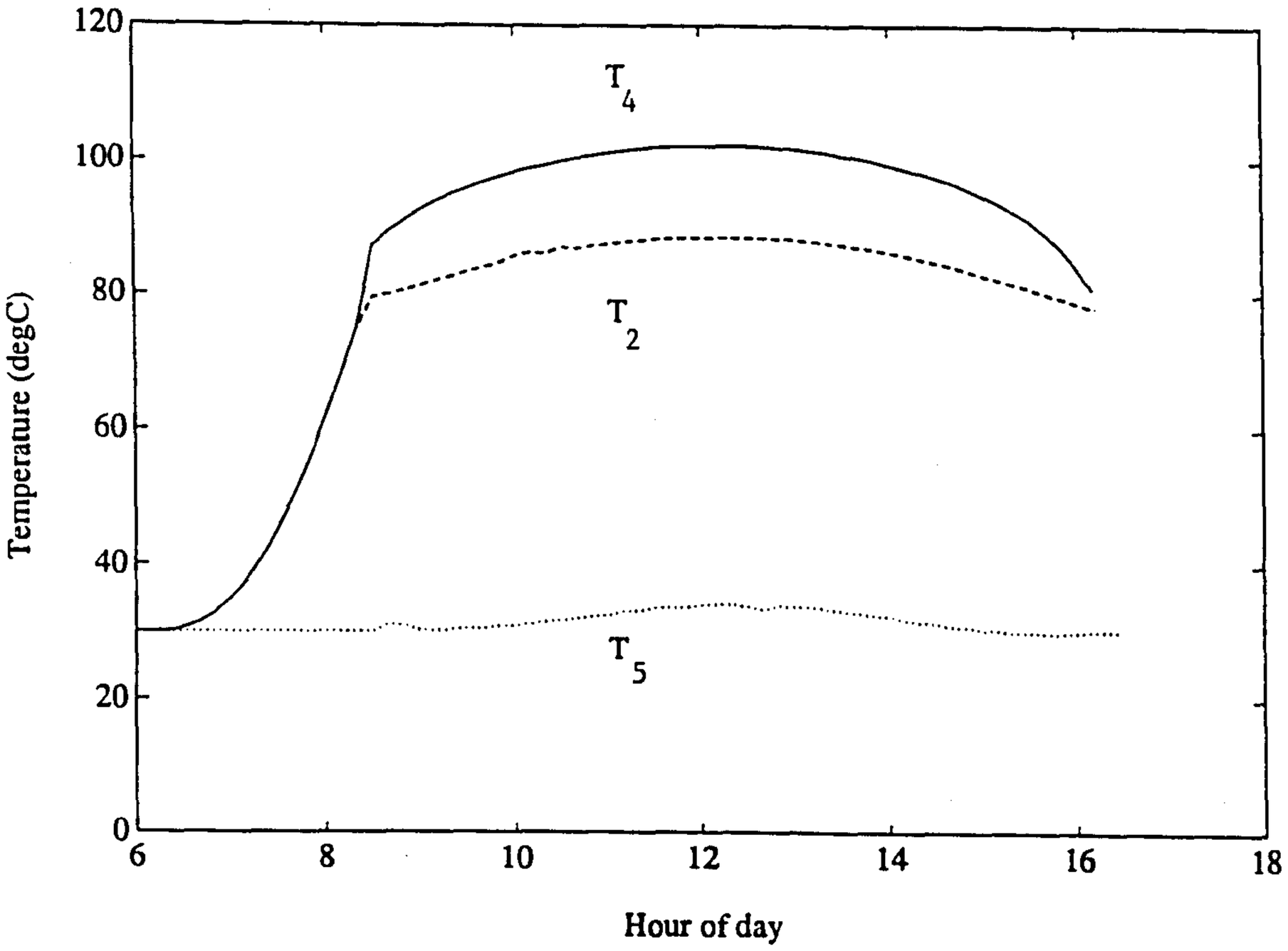

Fig. 3.11.1(c). Dynamic response of the VVR circuit as in Figure 3.11.1(a). Separator temperature (T_4), boiler feed temperature (T_2) and solution heat exchanger return flow exit temperature (T_5) are plotted against time of day.

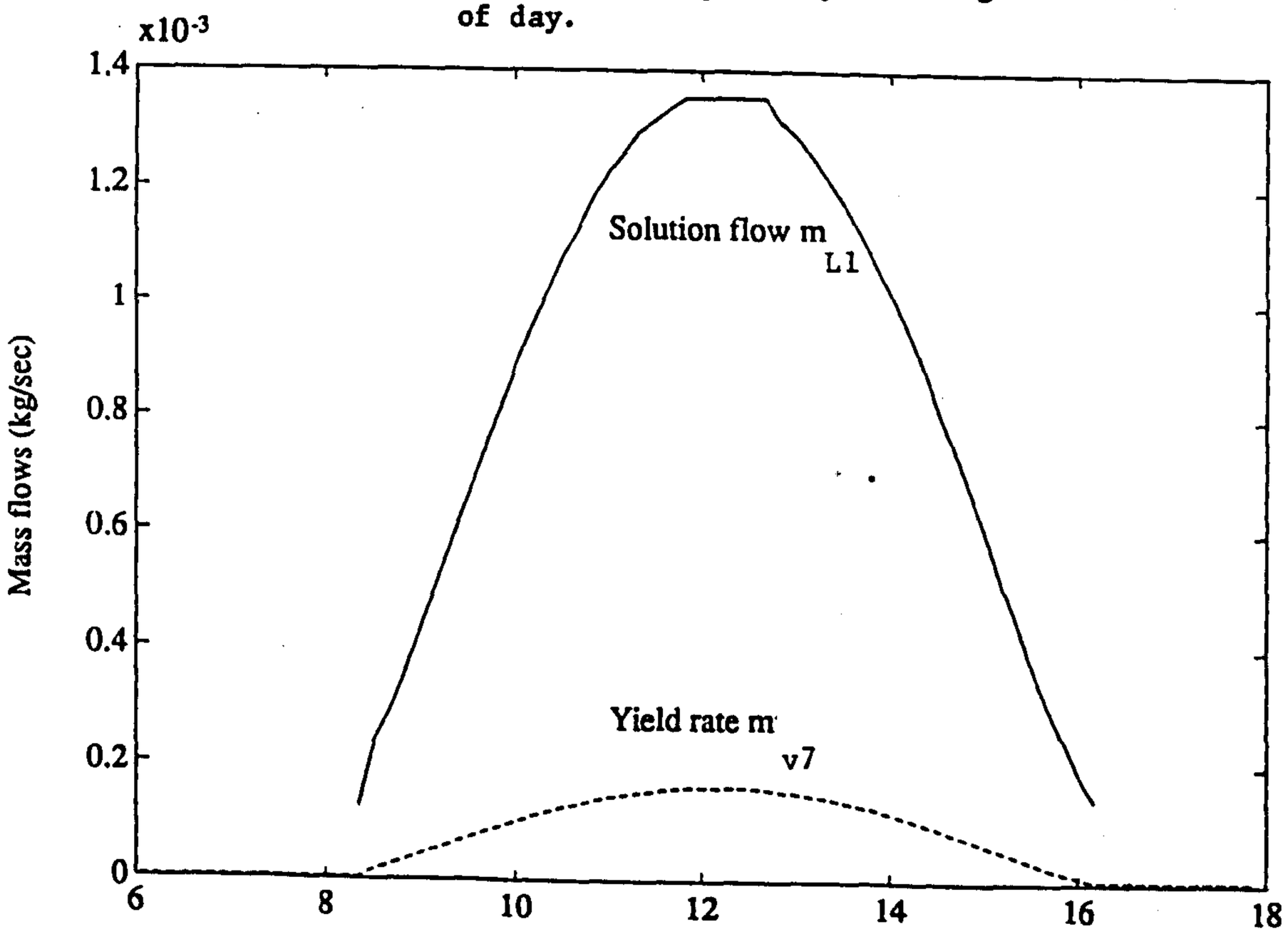

Fig. 3.11.1(d). Dynamic response of the VVR circuit as in Figure 3.11.1(a). Rich solution mass flow (m_{L1}) and condensate yield rate (m_{v7}) are plotted against time of day.

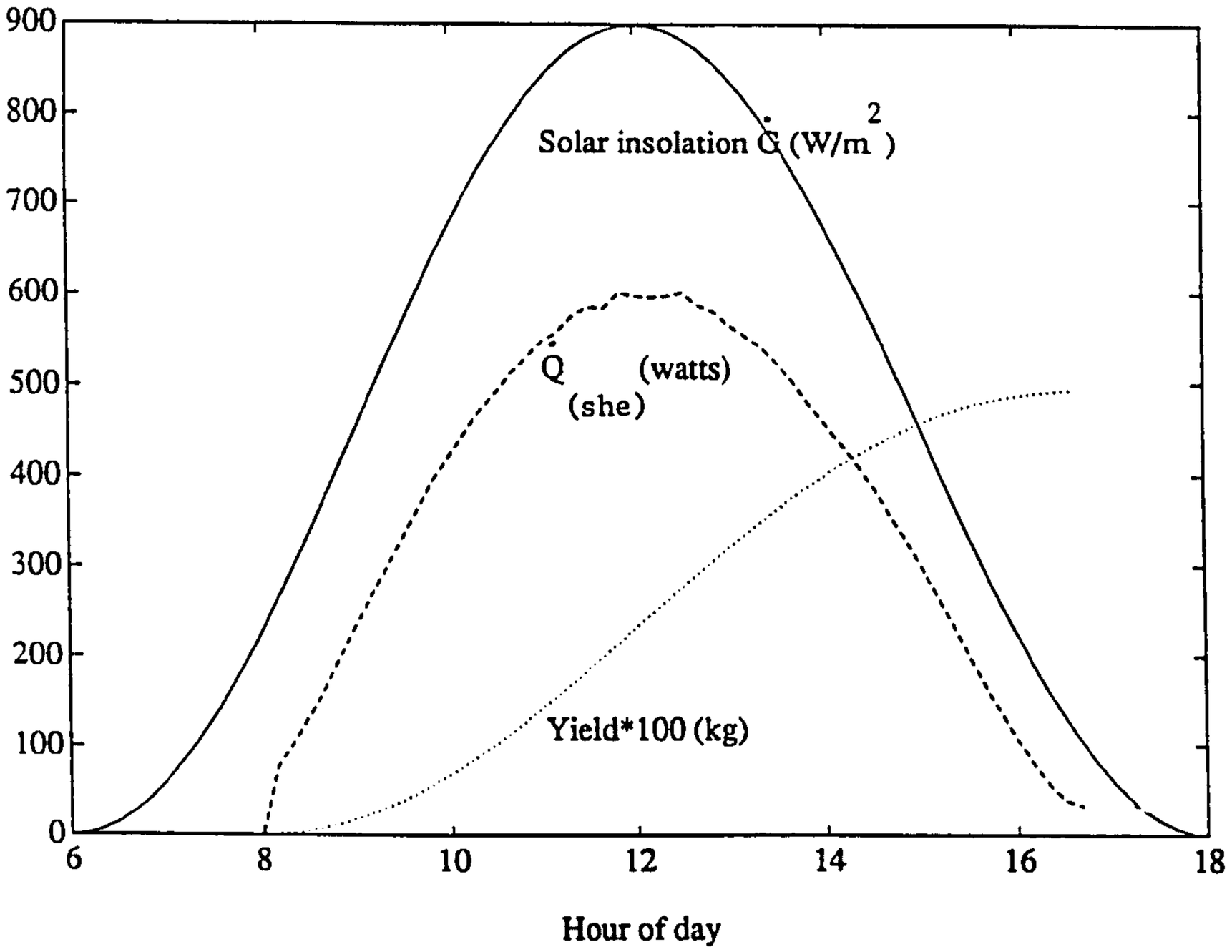

Fig. 3.11.2(a). Dynamic response of the VVR circuit to a simple sine function simulation of a clear sunny day, insolation peaking at 900 W/m^2 at midday. The computer code is run for the operationg conditions given on Table 3.11.1. Accumulated refrigerant yield is plotted against hour of day, and heat transferred within the solution heat exchanger (Q_{she}).

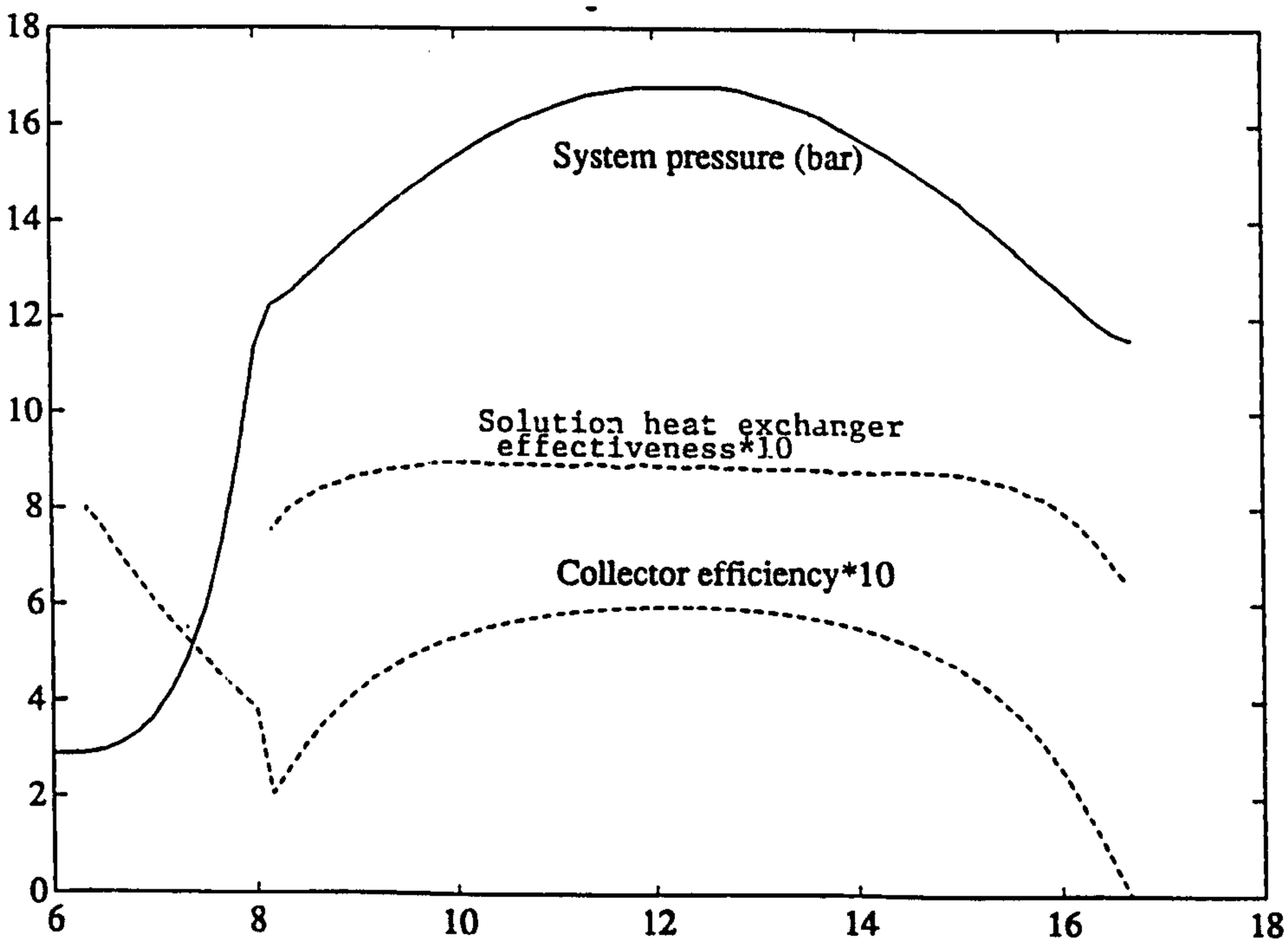

Fig. 3.11.2(b). Dynamic response of the VVR circuit as in Figure 3.11.2(a). System pressure, solution heat exchanger effectiveness, and collector efficiency are plotted against time of day.

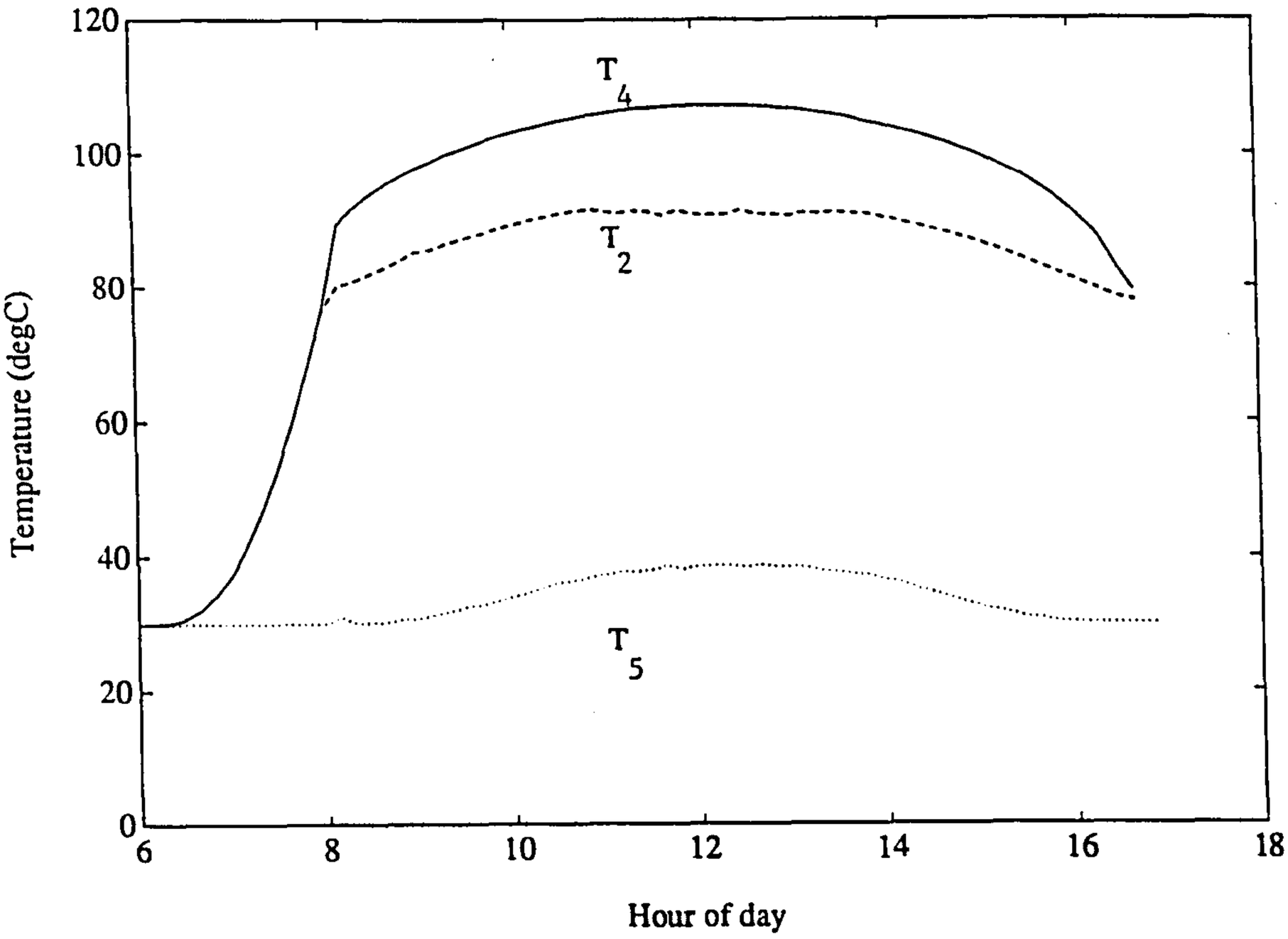

Fig. 3.11.2(c). Dynamic response of the VVR circuit as in Figure 3.11.1(a). Separator temperature (T_4), boiler feed temperature (T_2) and solution heat exchanger return flow exit temperature (T_5) are plotted against time of day.

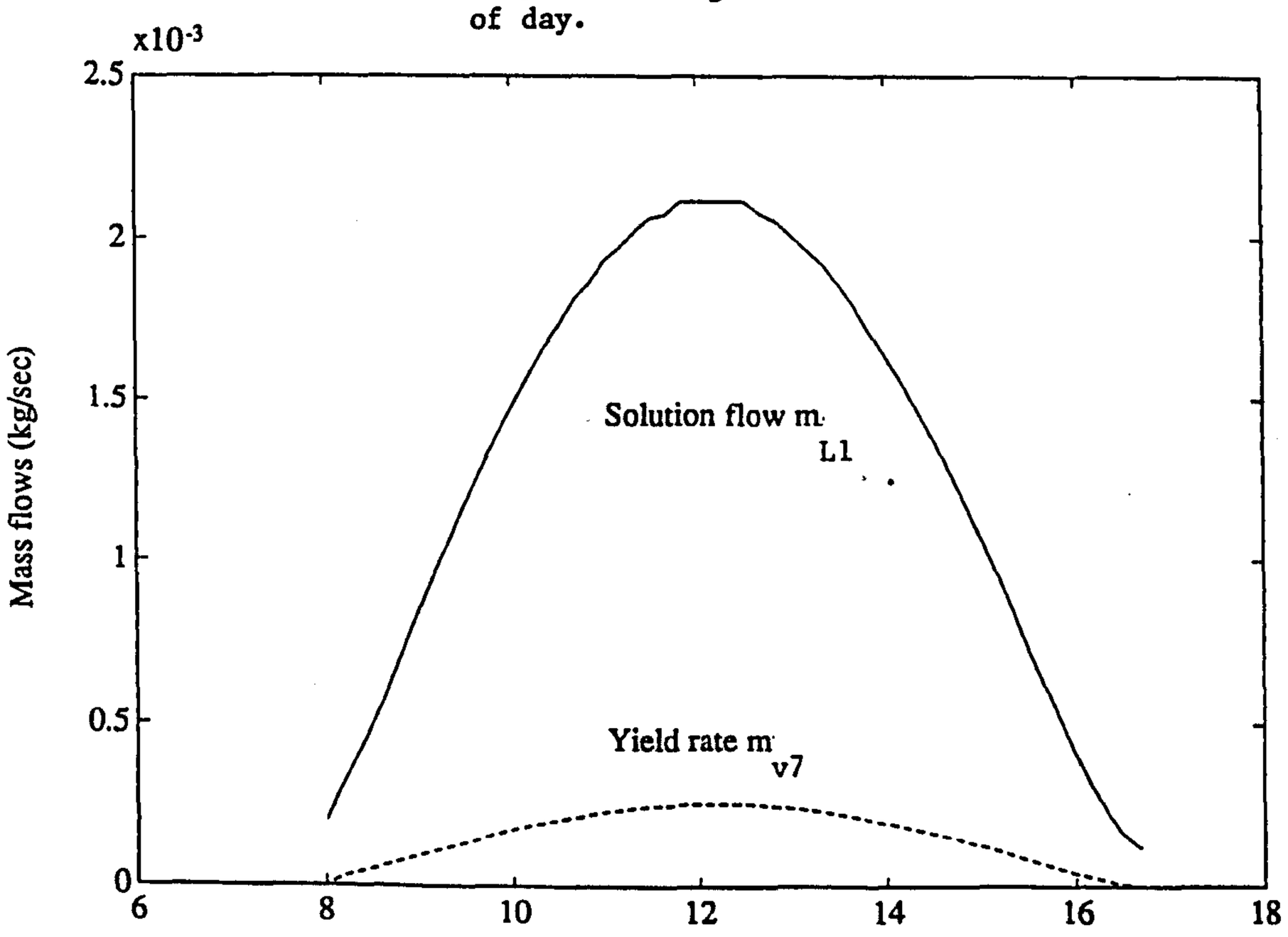

Fig. 3.11.2(d). Dynamic response of the VVR circuit as in Figure 3.11.1(a). Rich solution mass flow (m_{L1}) and condensate yield rate (m_{v7}) are plotted against time of day.

Some limited parametric study has been made on the basis of the dynamic model. If the final absorption temperature (T_{ab}) is considered to be 15 degC, resulting in a rich solution concentration of 0.55 (as opposed to 0.45 achieved when T_{ab} is 30 degC), the final yield for the simulated clear day becomes 6.8 kg, implying a daily COP value of 0.39.

3.12. Summary

The computer simulation has been useful in a number of ways. It has allowed examination of all the special features of the IR circuit which were outlined in the introduction to the chapter. Taking these features in turn:

High solar efficiency values are predicted for the standard set of operating conditions used also in chapter 1 in modelling of alternative cycles. The IR system has internal efficiencies in the order of 0.55, and solar efficiencies in the range 0.14 to 0.32 depending on the solar insolation rate (Fig 3.9.3(a)). These figures are obtained by modelling of the solar day as an eight hour period of constant wattage insolation. Just as in the continuous pumped (CP) system, these efficiencies are only achieved at optimum flow rates, which vary with insolation rate. A study of the flow response of the system has shown that the IR unit automatically maintains optimum flow at all insolation rates. The benefit of this feature is demonstrated in section 3.11 which calculates the IR performance in response to a sinusoidal model of two solar days. The values calculated for solar COP (net performance) are very close to those calculated when the solar day is modelled as a step function of constant wattage over eight hours. The implication is that the steady state model is an adequate guide to COP.

The exercise of section 3.11 (which models the solar day as a sinusoid) not only functions to validate the steady state model, but also is a useful tool for use at a later date to for more accurate modelling of the device in specific climatic regimes, providing the basis for economic projections.

Performance is found to be significantly improved by low absorption temperature, implying that an advantage of the IR system is that it operates at high efficiency in climates with low night temperatures and clear days.

The simulation has allowed some component sizing calculations to be made. The solution heat exchanger has been sized, and the condenser has been sized. In both cases the sizing decisions are specific to a particular solar collector area, in this case 1 m^2.

Chapter 4 Absorption phase of intermittent regenerative (IR) system

The absorption and evaporation processes of the IR system demand further attention, because difficulties in these areas can raise the cost and complexity of the system beyond cost effective limits. The analysis and computer model of Chapter 3 characterised the evaporation/absorption processes in a manner suitable for the evaluation of the desorption phase, but not in terms of anticipation of detailed design difficulties. The details of a study made of the processes are recorded in Appendix A. The conclusions of the study are presented here.

Firstly, a specialised component required during the absorption phase is a valve placed between the rectifier and condenser which stops vapour from returning through the rectifier to the separator during absorption. This could be a manual valve or an automatic check valve. The danger posed by either is an unreliable operation in the long term. A "solid-state" solution, involving no moving parts, is the use of a liquid seal. Practical tests with a check valve reported by Van Paasen (1986) indicated reliable operation, while reports from Exell (1984) on the liquid seal did not recommend its reliability.

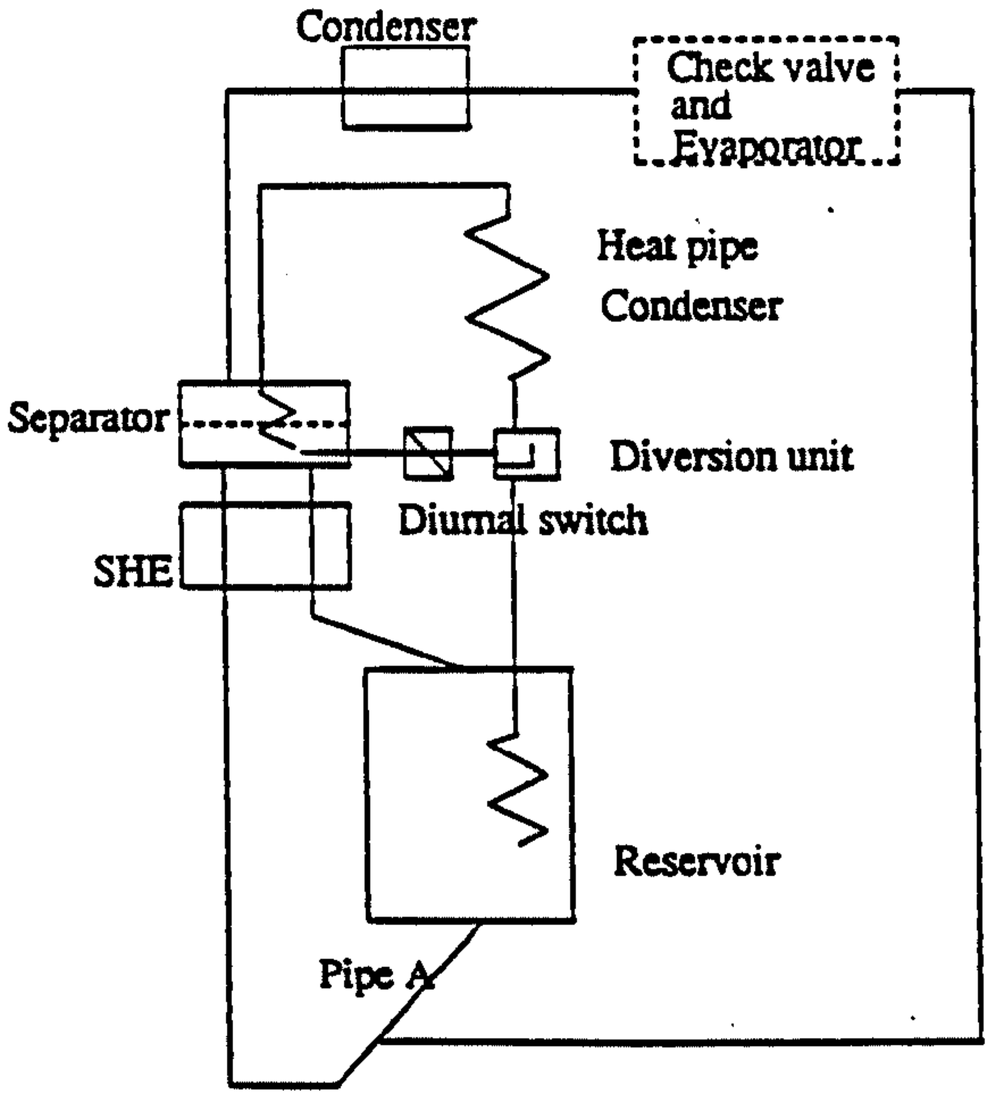

Fig. 4.1. *The proposed separator, condenser, and absorber heat pipe cooling circuit for the IR system.*

In section A.3 of Appendix A it is concluded that a heat pipe cooling circuit is required to remove heat from the reservoir during the night. Fig. 4.3.1 shows the proposed heat pipe arrangement. This doubles as a condensation heat rejection path during the day. The arrangement has already been described in part in Section 3.5.5 with respect to condenser cooling.

The heat pipe cooling circuit is expected in addition to perform a third task, which is to remove sensible heat from the solution remaining in the separator at the end of the desorption phase. Only if the separator liquid is cooled rapidly can low temperature evaporation start taking place early on in the absorption phase.

The disadvantage of this additional branch to the heat pipe is that it must be opened only at the end of the desorption phase, at dusk, and closed again at dawn. Consequently a diurnal valve is required, either manually operated, or automatically operated by the presence and absence of solar irradiation. Although this is possible in practical terms (conventional central heating thermostatic valves can be used, since the heat pipe circuit is not necessarily a high pressure ammonia circuit) the long term reliability of such a device is questionable.

It is possible that the adoption of the transfer tank principle (the VVR or "variable volume reservoir" system) will make this additional branch of the heat pipe unnecessary, because the separator is radically reduced in size.

The remainder of Appendix A is devoted to a detailed study of the relative merits of two different types of evaporator, the gravity circulating ("flooded") evaporator, and the dry expansion evaporator. Computer modelling of the absorption phase in each case shows that the two evaporator types are theoretically equally efficient, both converting 1 kg of refrigerent into 2.5 kg of ice. Figure A.7.4(b) shows that the gravity

circulating design converts slightly faster requiring 6½ hours to make 13 kg of ice with a heat pipe condenser (the absorption/condensation heat radiator) area of 7m², at an ambient temperature of 20 degC. The dry expansion design requires in contrast 8½ hours for the same duty (figure A.6.8.2(b)). Both designs incorporate valves. In the case of the gravity circulating evaporator a valve is needed to drain accumulated water-rich residues from the evaporator. This needs to be opened every five days or so. In the case of the dry expansion evaporator a pressure regulating expansion valve is required to maintain a pressure drop between the receiver and the evaporator.

While both valves introduce complexity, expense, and unreliability into the system, the design of an automatic expansion valve is more critical and it is likely to be the more expensive and more unreliable component. The sizing of the expansion orifice becomes impracticable in practical terms on small refrigerator units. In both cases the valves can be either manual or automatic. In the case of a manual drain valve on a gravity-circulating evaporator, there is a danger that periodic use leads to physical deterioration of the valve or increased forgetfulness, since incorrect use only lowers cooling output gradually rather than dramatically. The option exists of manual pressure regulation in the dry expansion case.

It is concluded that the automatic version of the dry evaporator is not recommended for practical reasons, although it is sound in theory. Comparing the manually regulated dry expansion option and the gravity circulation option no strong indication decides the issue either way. Both systems require a manual input, although in the case of the gravity circulated system less attention is needed and several days of forgetfulness can be accommodated for. For small units of a capacity of less than 100 kg of ice per day, a dry evaporator is not an option, unless a capillary tube is used in conjunction with the valve, an option likely to lead to

further unreliability. It is conceivable that a reliable automatic version of the drain valve for gravity circulating systems could be devised, but none is known of to date. Failing this, the best option for further development is conversion to a non-volatile absorbent and the use of a gravity circulating evaporator, which then does not suffer the problem of collecting absorbent or condensate.

Chapter 5 Initial Experimentation

Early experiments were conducted with the help of a bench top version of the fixed volume reservoir (FVR) circuit. Photographs are placed at the end of the chapter. A circuit schematic is given in figure 5.1. The total solution mass used was 5 kg. Absorption was expected to take place in a tube leading into the reservoir, rather than in the reservoir itself. No evaporator circuit was connected to the condenser.

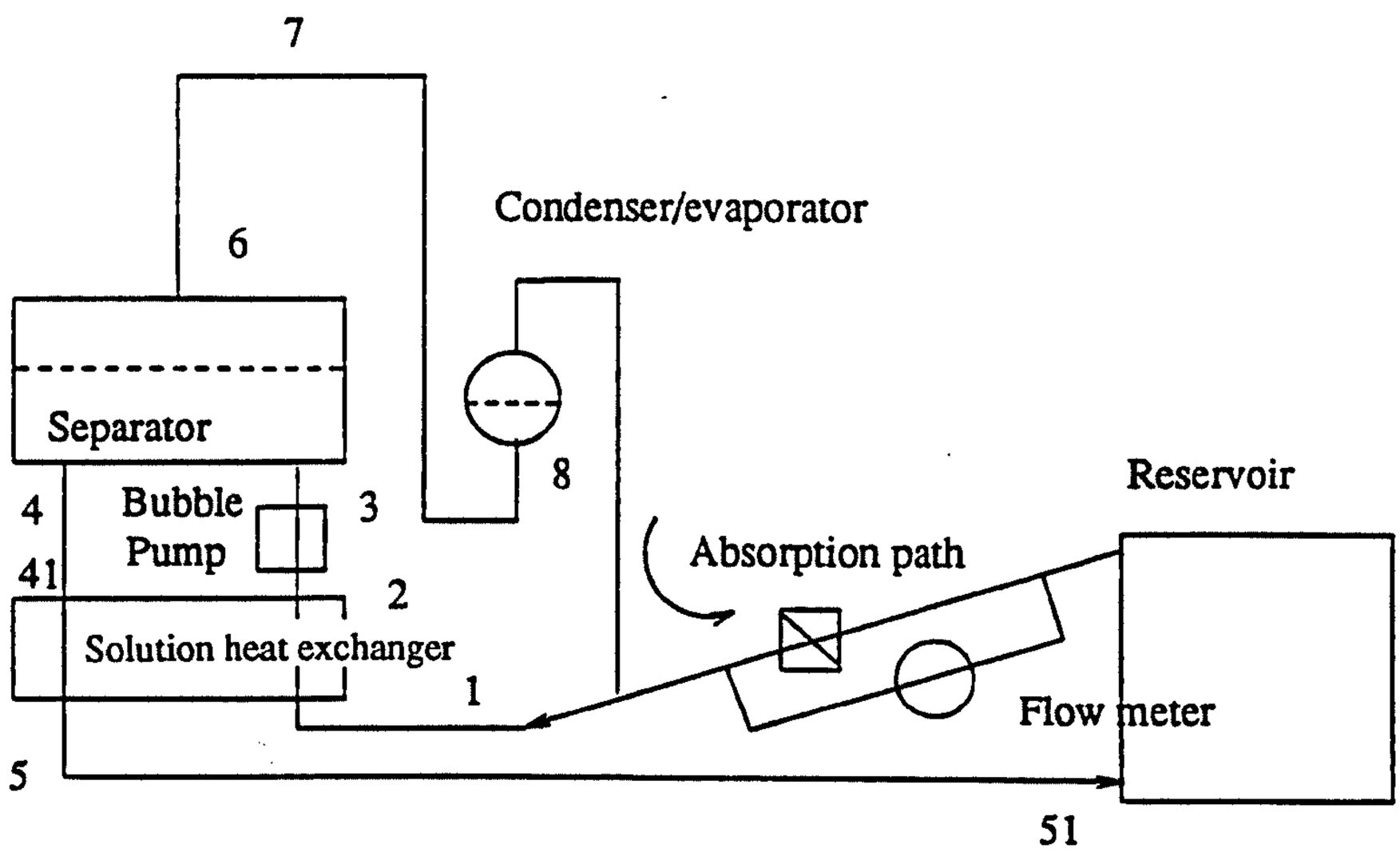

Fig. 5.1. *Schematic diagram of the experimental apparatus used for initial tests of IR system.*

The tests conducted were revealing in a number of ways and pointed the way toward the more developed experimental apparatus described in Chapter 6. The high desorption rate obtained proved that high COPs were obtainable. Cycle efficiencies in the order of 0.5 were measured. The solution heat exchanger was proved to be effective. Pressure oscillations in the circuit during desorption were shown to be due to the boiler/bubble pump tube being too small in internal diameter. Evidence of variations in

rich solution concentration indicated that the horizontal orientation of the reservoir was inadequate. Heat losses through the insulation on the generator side constituted a large proportion of the heat transfer within, indicating that a larger experimental unit was necessary for accurate monitoring of heat quantities. Absorption behaviour was not fully monitored, although the need for separator cooling to reduce the duration of the absorption phase became apparent. In practice absorption occurred successfully in part in the inclined tube in circulating solution, and in part in the reservoir, the inclined tube then being full of vapour.

The achievement of high cycle efficiencies indicated that further development of cycle was worthwhile. The construction of a larger unit of revised design was considered necessary for several reasons. Firstly, measurement of very low solution mass flows (in the order of 0.15 grams/sec in this case) had proved excessively difficult. Flows of eight times this amount were necessary for accurate measurement with the instrumentation available. Secondly, internal heat flows could be measured more accurately in a larger unit where losses would constitute a small proportion of heat flow. A larger unit would be nearer to a size of practical usefulness, so would more easily give an indication of the economic and practical viability of the device. Finally, a second apparatus would allow a revised design to be implemented and an evaporator to be incorporated.

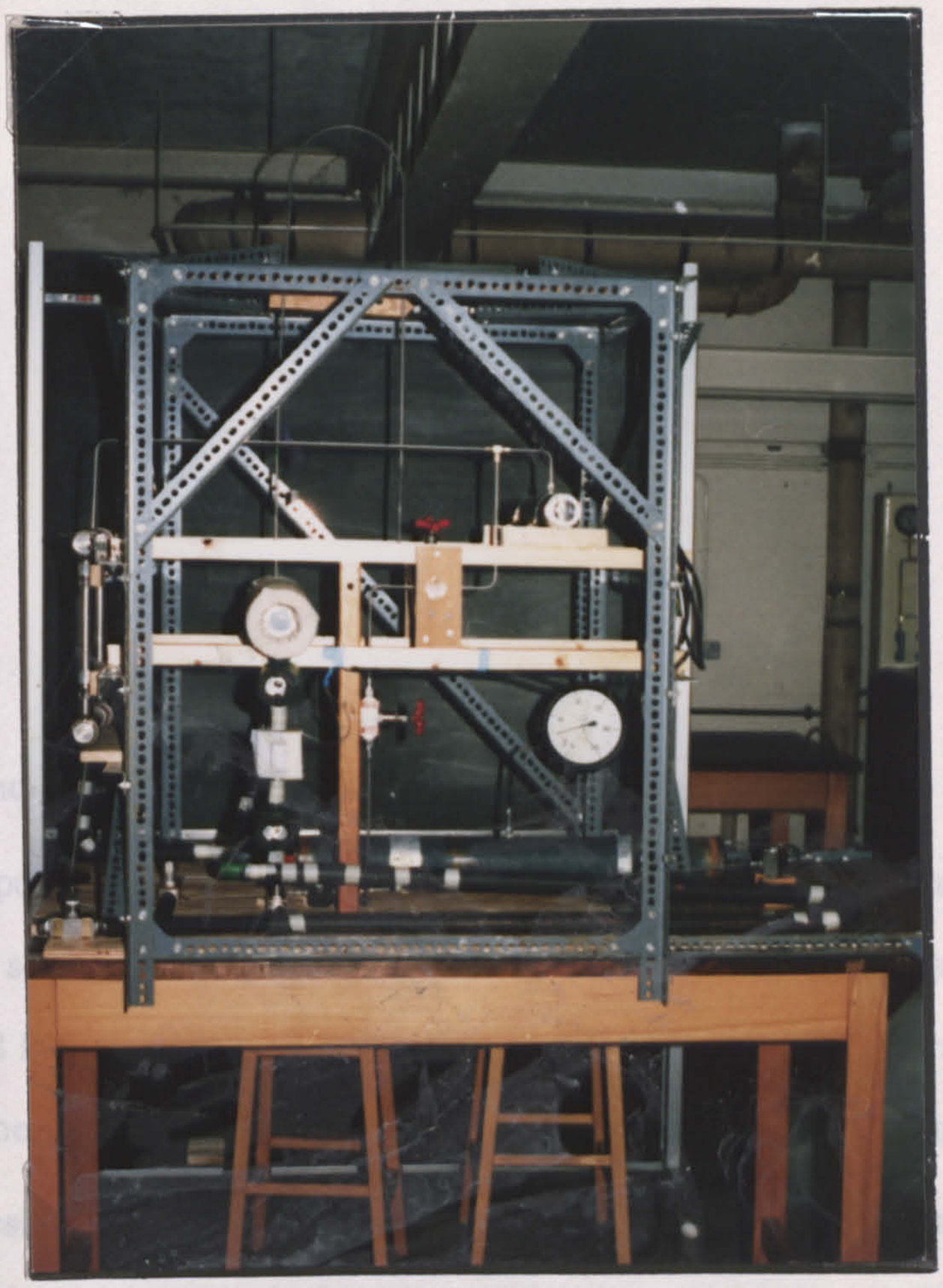

Fig 5.2 *Initial experimental apparatus. Top: Apparatus showing separator end on at mid height at left, and receiver end on at a higher level on the right. The tube rising above the separator is the rectifier. The long horizontal cylinder at base level at the back is the reservoir. Bottom: The solution heat exchanger without insulation. At the top left, the resistance heating element acting as a boiler heat source.*

Chapter 6: Experimental results

6.1. Introduction

For experimental purposes the fixed volume reservoir (FVR) circuit was constructed in the form shown schematically in figure 6.1.1. Photographs are provided as fig 6.1.2. The apparatus contained 33 kg of solution, all the components being contained in a frame of approximately 0.8 x 1.2 x 0.8 metres. Solution flows were expected to be in the order of 1 to 2 grammes/sec.

The design allowed the full boiler heat input to be applied to the inclined tube supplying the separator; this tube acted both as a vapour lift pump and a boiler. A diameter of 25 mm internal and 30mm external was chosen on the grounds that smaller diameters caused large temperature drops between the fluid and heat source, while larger diameters would raise the liquid content of the generator and threaten to produce an ineffective bubble pumping action. Electrical resistance heating elements in the form of flexible tapes were wound around both the generator and boiler tube, so that application of a divided heat flow was possible. Sight glasses were placed in the positions indicated. The frictional characteristic of the solution flow path was altered during experimentation by a throttling valve, or a flow metering valve, as indicated on the diagram.

Heat of condensation of the refrigerant was rejected into the reservoir contents by way of a 6 meter long coil of 4mm id tubing. This heat then served to raise the temperature of solution entering the solution heat exchanger while also being absorbed by a flow of water in a second coil incorporated into the reservoir, which approximately simulated the heat pipe evaporator envisaged in a stand-alone solar refrigerator. No direct measurement of the heat transferred to the cooling water was made. The pressure at which desorption proceeded during tests was regulated by appropriate alteration of the cooling water flow rate, so that all the tests could be directly compared in terms of condensing temperature and system pressure. In practice some variation of pressure proved unavoidable, but remained within tolerable limits.

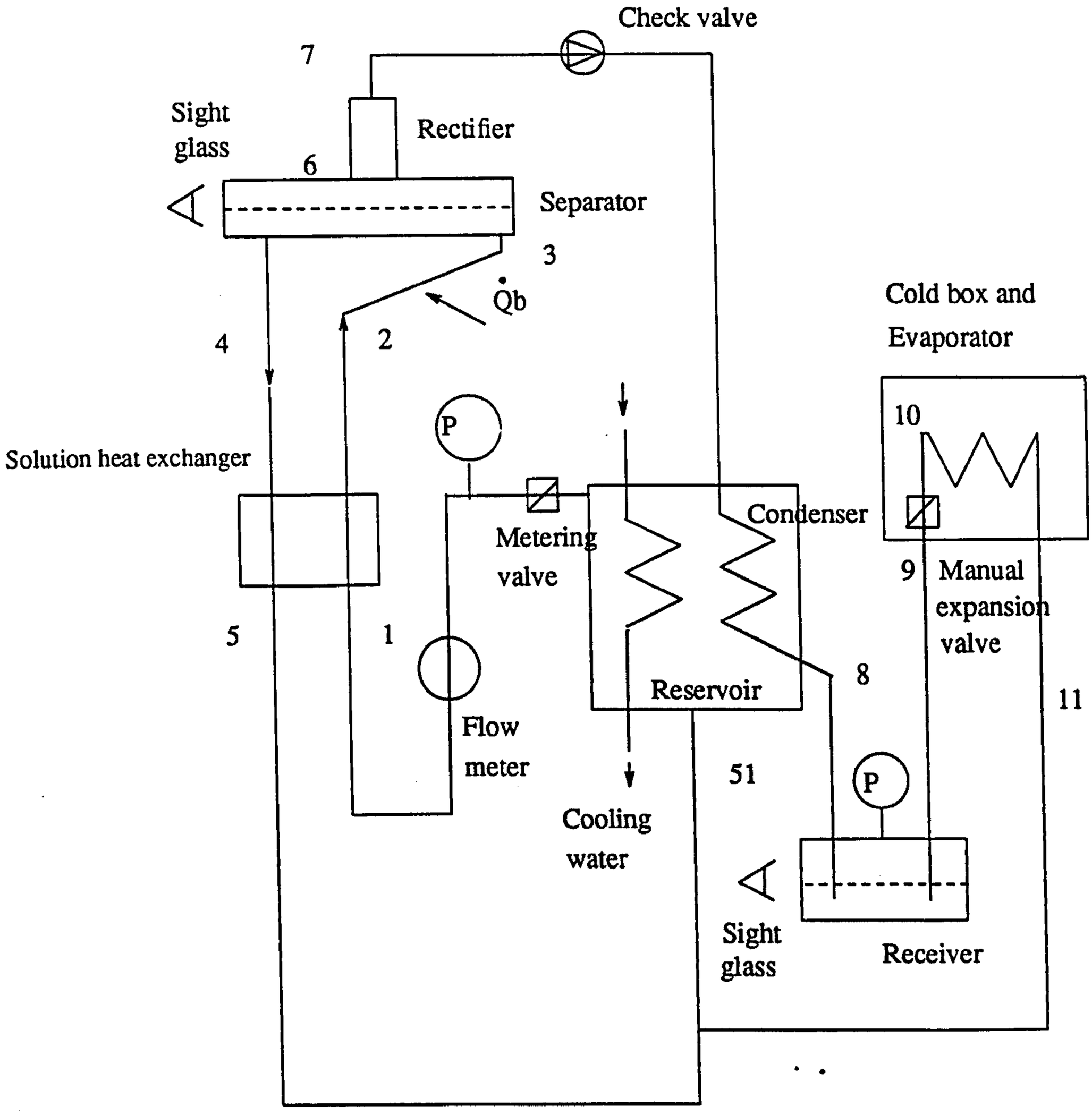

Fig 6.1.1 *Circuit of experimental unit. Of the two pressure gauges (marked "P") one monitors desorption and absorption pressures, the other receiver pressure during the absorption phase.*

No provision was made for separator cooling, since the primary concern of the experiments was to investigate the practical efficiency characteristic of the desorption phase. The separator was allowed to cool slowly by heat leakage through its insulation overnight, so that the

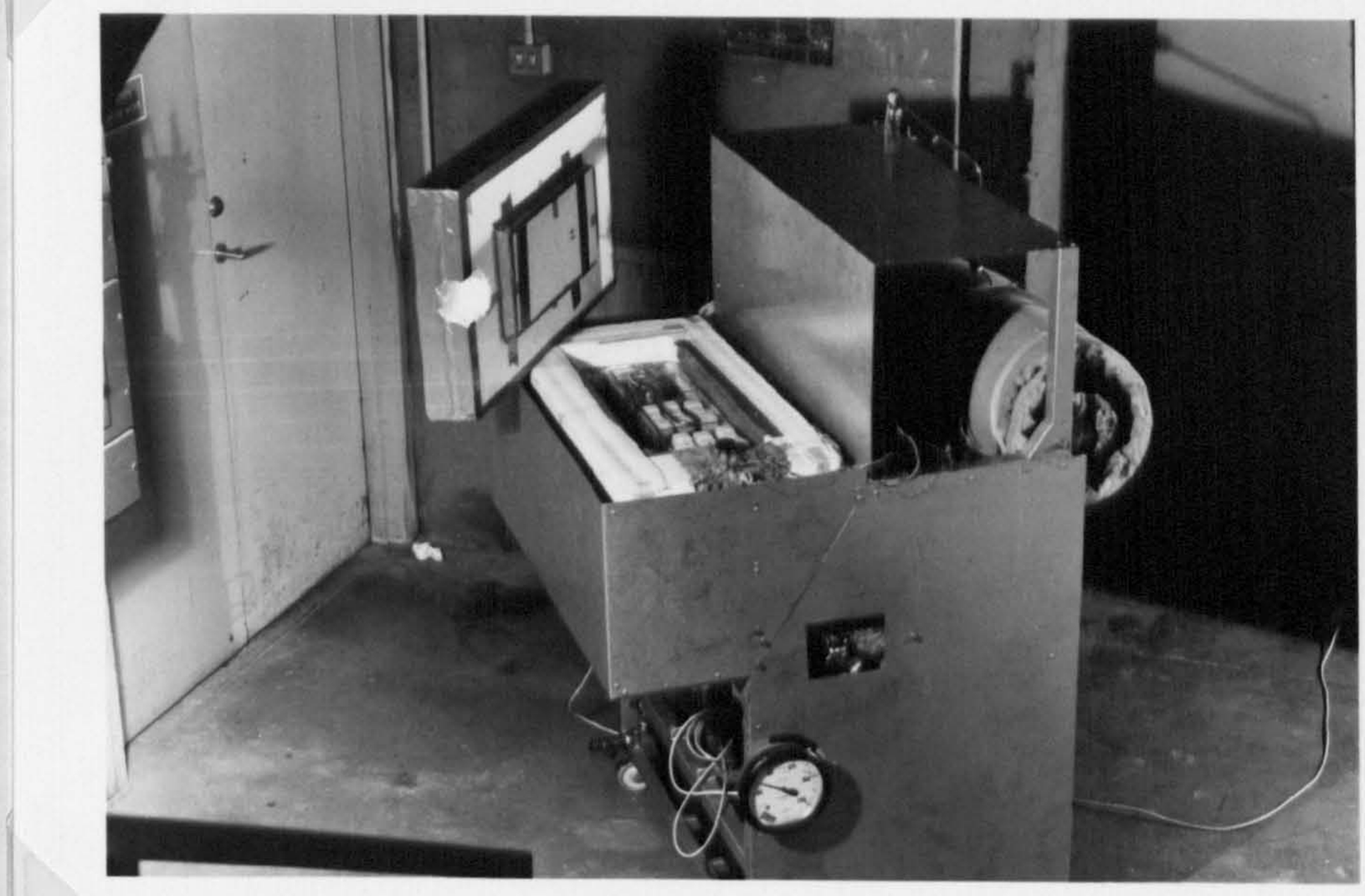

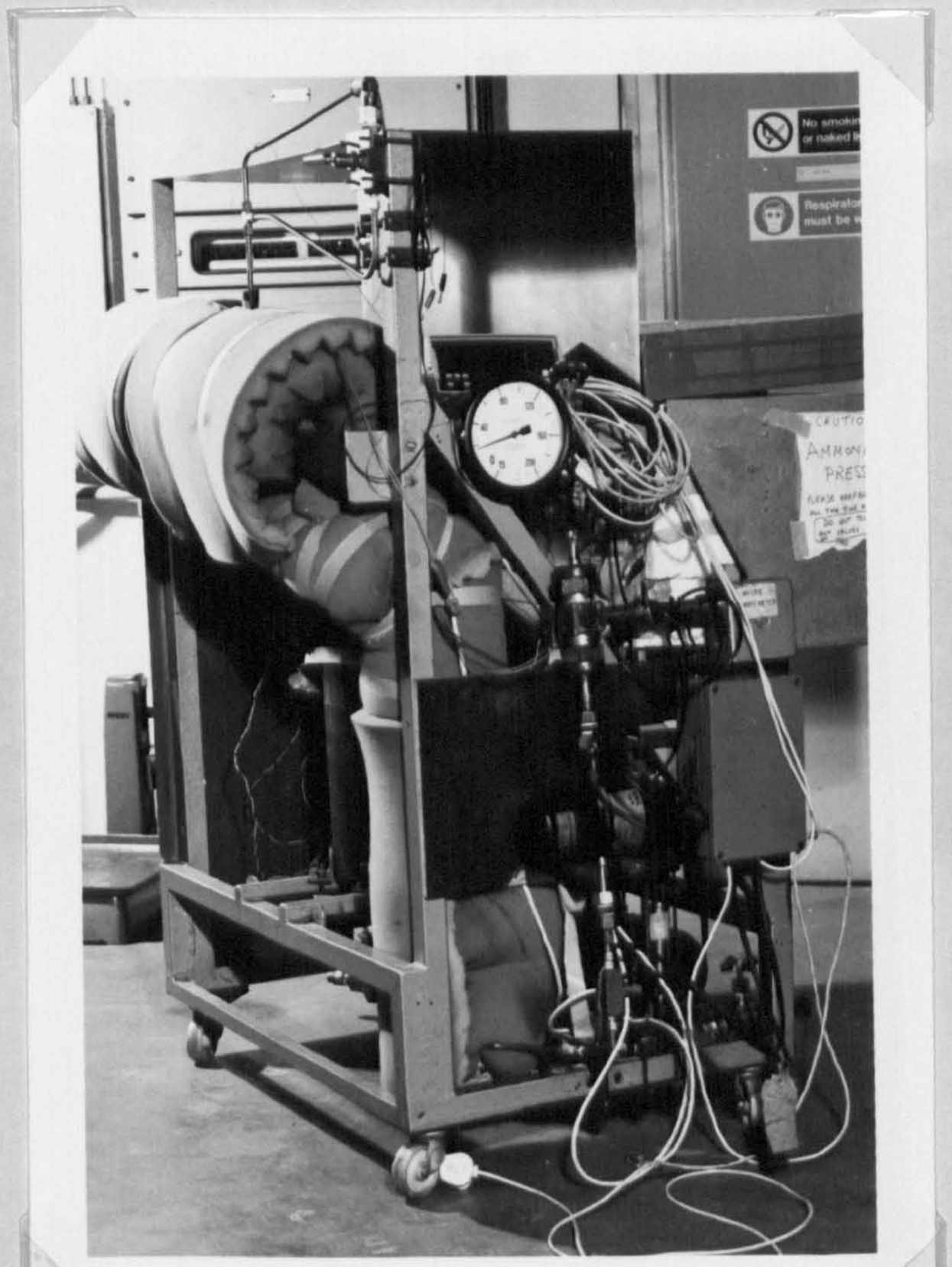

Fig 6.1.2 *Experimental apparatus Top: Experimental unit showing cold chest opened; separator is top right contained in roll of insulation; the gauge monitors receiver pressure. Bottom: Unit showing magnetic induction mass flow meter in foreground. The solution heat exchanger is contained in the insulation roll standing vertically behind the board. The gauge monitors reservoir pressure.*

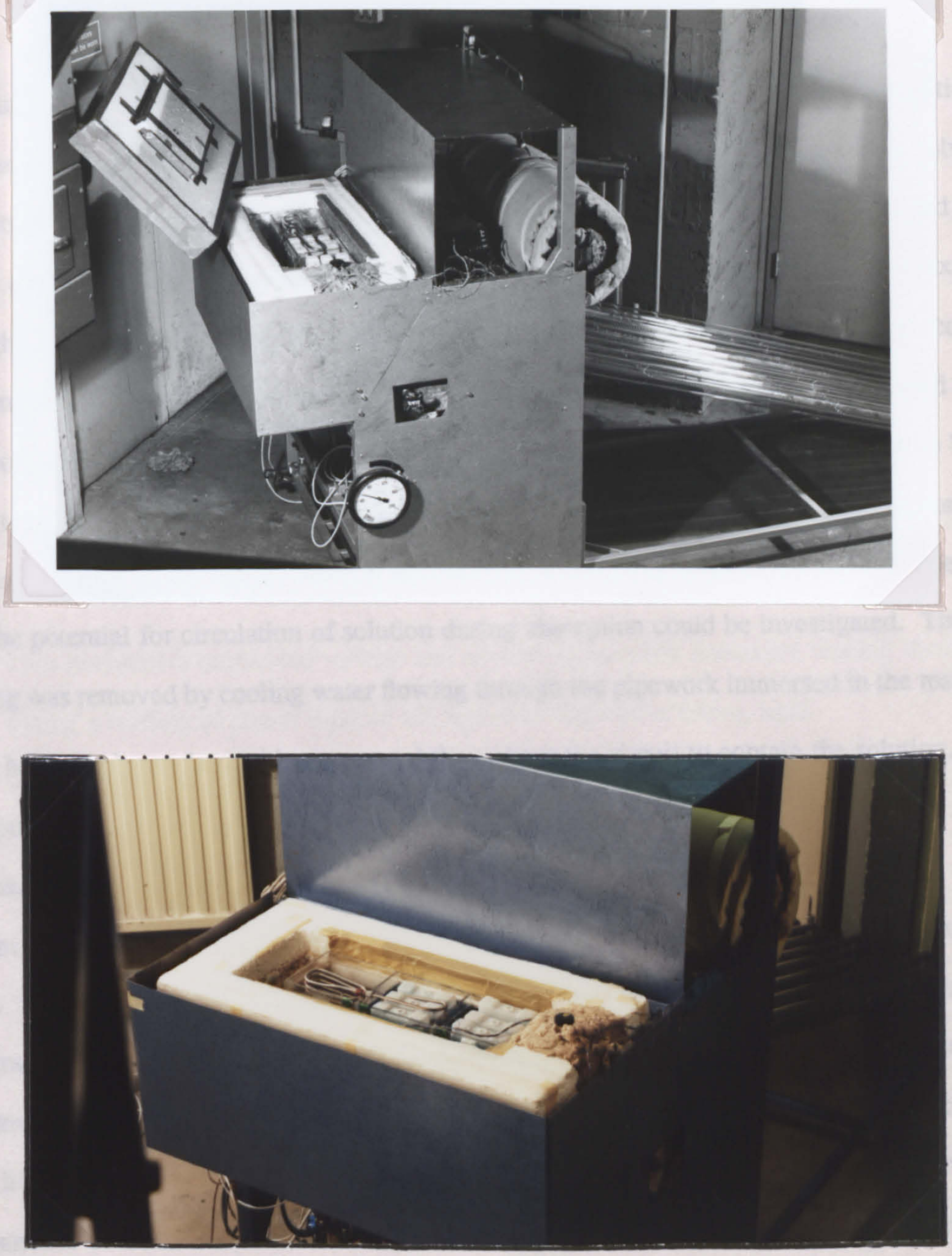

Fig 6.1.2 (continued) *Top: Unit showing intended position of solar collector array. For experimental purposes the array was substituted with electrical resistance heating tape wound round the boiler tube. Bottom: Cold chest interior showing evaporator tube and ice packs.*

absorption process could be observed in the morning before initiation of a further desorption test. In order to reduce the number of uncertainties effecting initial experiments, the check valve indicated in the diagram was replaced by a manual valve, closed at the end of desorption and opened on the commencement of the succeeding desorption phase. Evaporation was by dry expansion through a hand operated metering valve. This was opened when the separator had cooled to ambient temperature, and closed when the receiver contents had been fully re-absorbed into the reservoir solution. The use of a manual expansion valve allowed the absorption rate to be regulated to obtain a constant pressure process. The circuit was designed to allow absorption to proceed by entry of the evaporated gas into the tubing returning solution flow to the reservoir, so that the potential for circulation of solution during absorption could be investigated. The heat of mixing was removed by cooling water flowing through the pipework immersed in the reservoir.

Mild steel seamless tubing was used throughout the circuit to contain the solution, with the exception of the evaporator coil which was formed from stainless steel. The reservoir was constructed from a seamless tube of internal diameter 254mm and height 633mm, of wall thickness 10mm, and closed by discs welded either end. The separator was constructed in a similar way from 130mm i.d. tubing of length 315mm. Two "bull's eye" sight glasses were fitted to the separator to allow empty and full conditions to be registered. The receiver was constructed from 130mm i.d. tubing of length 530mm. It was fitted with a vertical tube sight glass which allowed the liquid level to be directly monitored. The level indicator was calibrated in terms of the volumetric contents of the receiver vessel. The solution heat exchanger was sized according to the design process described in section 3.7 and following table 3.7.3. The inner diameter of the tube forming the shell measured 56mm, the shell length being 460mm. 37 tubes, 28 of which were 6.3mm o.d. and 9 of which were 6mm o.d., all of wall thickness 1mm, were assembled in the shell. The complete tube length was 17 meters and the total heat exchange surface area was $0.52m^2$.

The rectifier consisted of an inclined tube of 4mm i.d and 6mm o.d., of length 0.6 meters and rising to a height of 10 cm. The condenser consisted of a 6 meter length coil of tube of the same cross-sectional dimensions. The coil carrying cooling water for rejection of both absorption

and condensation heat consisted of 22mm o.d/20mm i.d tube of 3.6 meters length.

The mass of steel incorporated into the generator was measured before installation, the separator and boiler tube together weighing 7.7 kg while the solution heat exchanger weighed 11.9 kg. In construction of the generator components the tubing wall thicknesses specified were excessive in terms of the pressure handling duty expected but were available ex stock.

6.2. Instrumentation

The performance of the unit was recorded from readings manually logged from the following instruments:

1) Two Avometers monitored voltage and current across each resistance heating element, providing a reading of power input to the separator and boiler during tests.

2) Comark K-type (Nickel-Chrome and Nickel-Aluminium) thermocouples were used at the locations indicated in fig 6.1.1. These were calibrated before use with ice at melting point and saturated steam at atmospheric pressure. Their accuracy was estimated at +/- 0.5 degC.

3) Two compound pressure gauges of the Bourdon tube type was used to measure the pressures in the reservoir and receiver respectively. Their positions are marked on fig 6.1.1.

4) Solution volumetric flow rate was measured in the position shown on fig 6.1.1 with a electromagnetic induction type flowmeter, specifically chosen for the purpose because its placement in circuit produced no significant pressure drop. The unit was a Veriflux Flowmeter type VSC, made by Brown Bovari. Accuracy was +/- 1% error at 10% of full scale deflection; in the experiments the minimum flow measured was in excess of 20% of full scale deflection. Calibration tests were made on the unit with weak ammonia-water solution before installation, in order to confirm the calibration constants provided by the manufacturers. Volumetric flow readings were converted to mass flow on the assumption that solution of undepleted concentration flowed in all cases from the upper portion of the reservoir into the flow meter. Together with the maintenance of a steady ambient temperature this allowed an estimate to be made of the solution density as it passed through the flowmeter.

5) Measurement of the refrigerant collection rate in the receiver was accomplished by periodic logging of the liquid level as observed through the the sight glass fitted to the receiver. The relationship between liquid level and volume of liquid in the cylindrical receiver had been previously measured and plotted. Calibration equations were then derived so allowing conversion of a liquid level reading to a volume and thence to a mass by division by the density of pure ammonia at ambient temperature.

6.3. Commissioning

The unit was charged from a mixing tank into which carefully weighed amounts of ammonia and distilled and de-ionised water had been introduced. A 0.1% weight addition of potassium dicromate was made to the water charge in order to protect mild steel components from internal corrosion. The mixing tank was fitted with a Bourdon tube pressure gauge so that the bulk solution concentration as measured by weight could be checked against the concentration implied by readings of pressure and temperature. These checks led to the discovery of an inert gas presence, which had the effect of raising the vapour pressure beyond that indicated by weight measurements of concentration. The foreign vapour could be separated by absorption of the mixing tank vapour in a tank of water open to atmospheric pressure and containing an immersed upturned jar in which the inert gas could be trapped. No analysis or precise measurement of the quantity of the foreign vapour were made; it was considered likely to be air driven from the water during the absorption of ammonia. The vapour pressure of the solution mixed was reduced to a value commensurate with the prevailing temperature and concentration by bleeding of the mixing tank vapour. The solution concentration was estimated to be 0.47 once this process was complete, in the case of refrigerator charge used for the tests described in sections 6.4 and 6.5 below. During the testing process itself some minor inadvertent leaks developed and were rectified, such that the concentration of the solution for the final four or five tests was indeterminate, though estimated to be approximately 0.46.

No density measuring or concentration measuring device was fitted to the circuit to allow concentration localising effects to be monitored.

The reservoir was sized to contain a volume of 32.6 litres of solution, corresponding to a charge of mass 27.4 kg for solution of concentration 0.47 kg ammonia in unit total mass, which has a specific volume at 20 degC of 1.19 litres/kg. Once the apparatus was charged with a total solution mass of 33 kg, the generator components taken together contained by subtraction a mass of 5.6 kg with the separator liquid levelled to a reference mark on the sight glass. This corresponded to a volume of 6.7 litres. Previous calibrations of component volumes had indicated the separator to contain, when showing the referenced liquid level, 4.7 litres of solution, corresponding to a separator initial liquid mass of 3.9 kg.

Given these mass contents note could be made in advance of experiments. as to the capacity of each component for full content replacement times. For solution flow rates in the range 500 to 2000 mg/sec the liquid replacement time for the separator would vary by a linear function between 2.2 and 0.4 hours, while the cycle time of the reservoir would be between 15 and 3 hours.

6.4. Heat loss characteristic

The electrical resistance heating tapes attatched to the separator and generator components, together with one temporarily applied to the solution heat exchanger, allowed the heat leakage through the lagging of the generator to be calibrated. The solution heat exchanger and boiler heat loss was found to be in the order of 11 watts for a 40 degree temperature difference between the mean solution heat exchanger and boiler temperature and ambient. This indicated the use of a $UA_{she(loss)}$ value of 0.28, as defined by equation 3.5.6.2. Similarly tests on the separator indicated a value of 0.15 for $UA_{sep(loss)}$ as defined by equation 3.5.6.1.

6.5. Performance observations

Figs 6.5.1 (a), (b),and (c) show the time response of various parameters measured during tests with boiler heat inputs of 200, 350 and 500 watts input respectively, given various settings of the flow metering valve. The figures only show response in the period of the desorption phase, when condensate is observed to be collecting in the receiver.

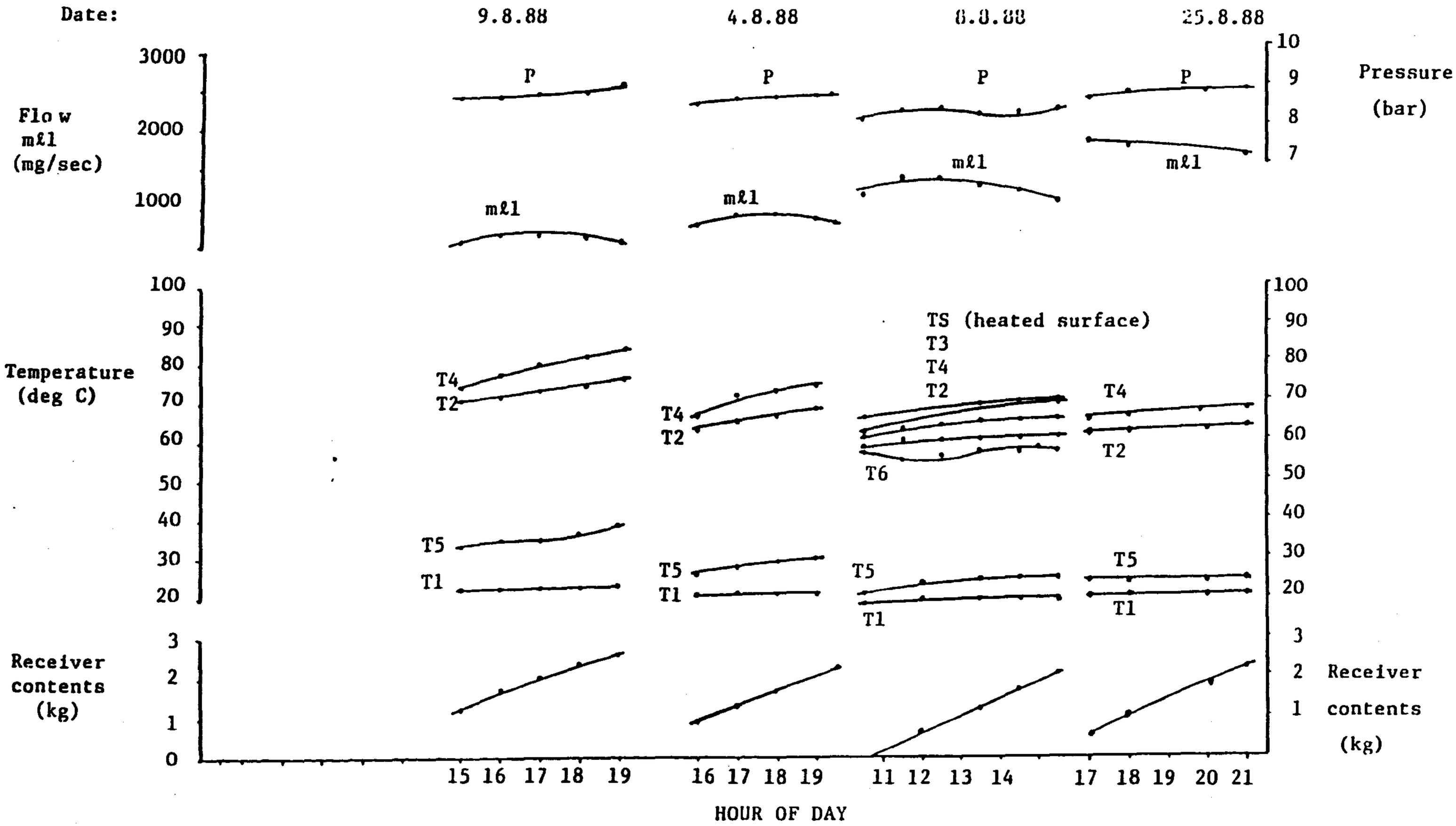

Figure 6.5.1(a). Laboratory experiments conducted with Boiler Heat Rate (Q_b) = 200 watts. Each test corresponds to a particular rich solution flow (m_{L1}) characteristic, induced by resetting of the flow metering valve.

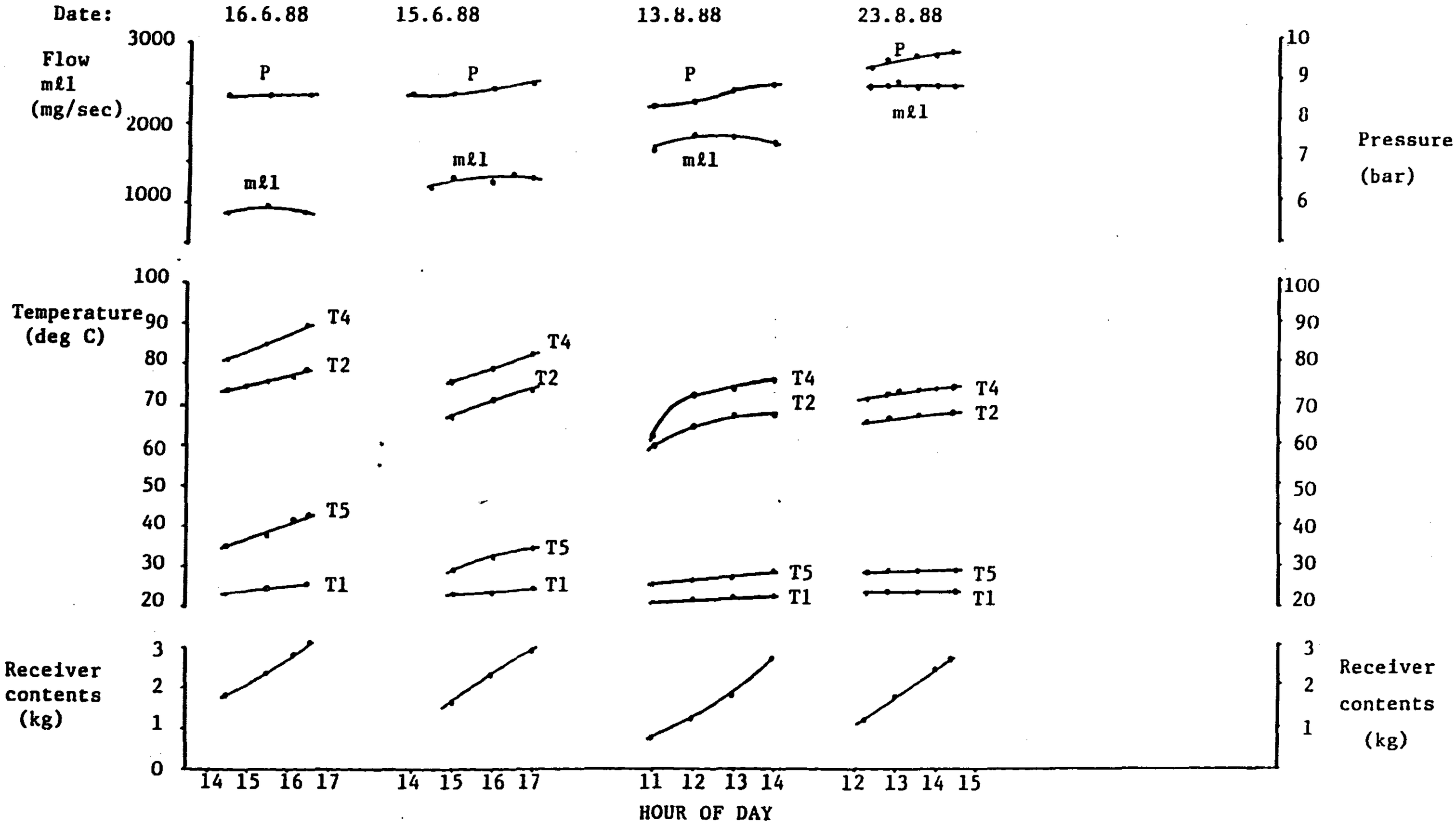

Figure 6.5.1(b). Laboratory experiments conducted with Boiler Heat Rate (Q_b) = 350 watts. Each test corresponds to a particular rich solution flow (m_{L1}) characteristic, induced by resetting of the flow metering valve.

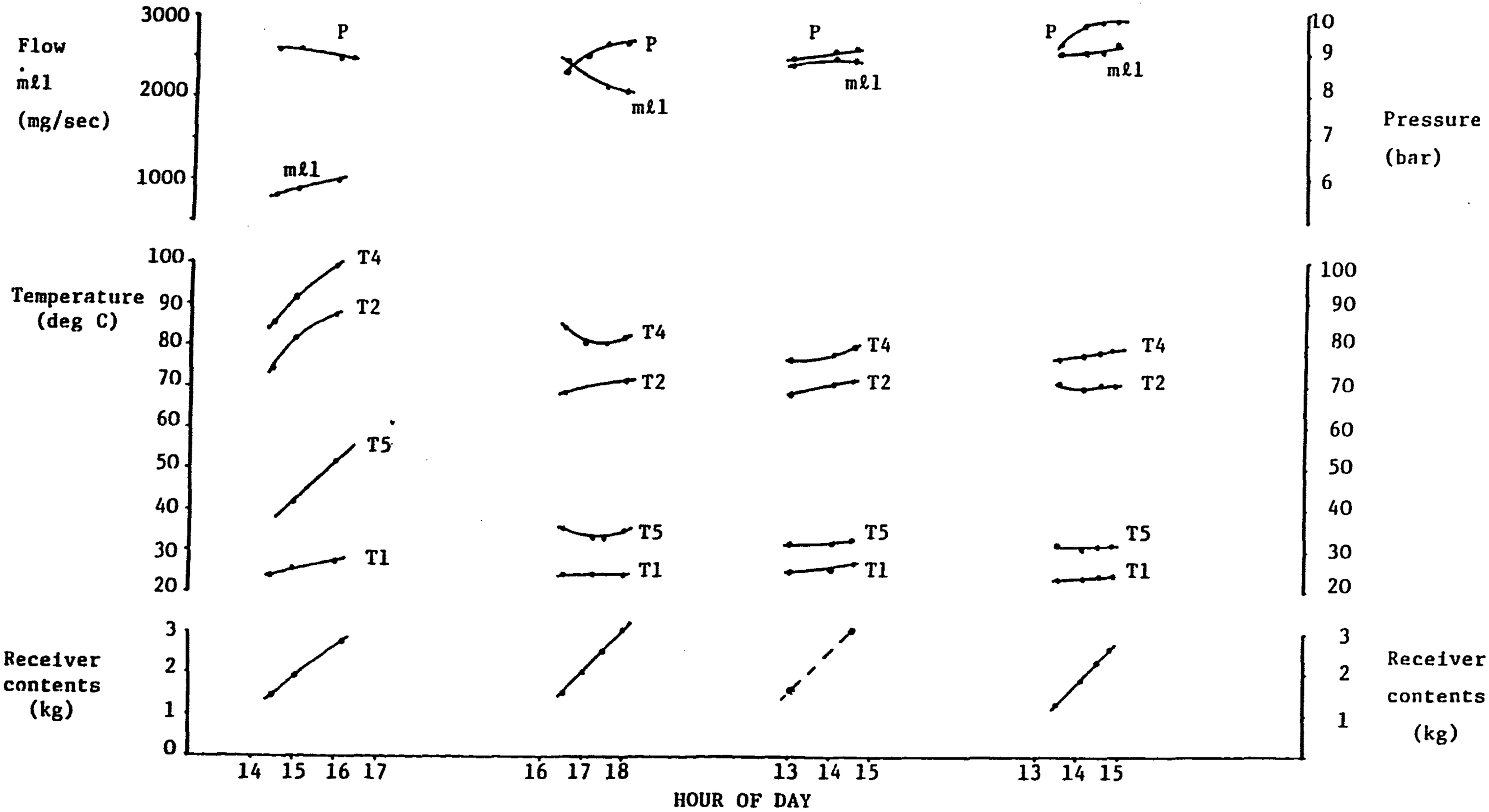

Figure 6.5.1(c). Laboratory experiments conducted with Boiler Heat Rate = 500 watts.
Each test corresponds to a particular rich solution flow (m_{L1}) characteristic, induced by resetting of the flow metering valve.

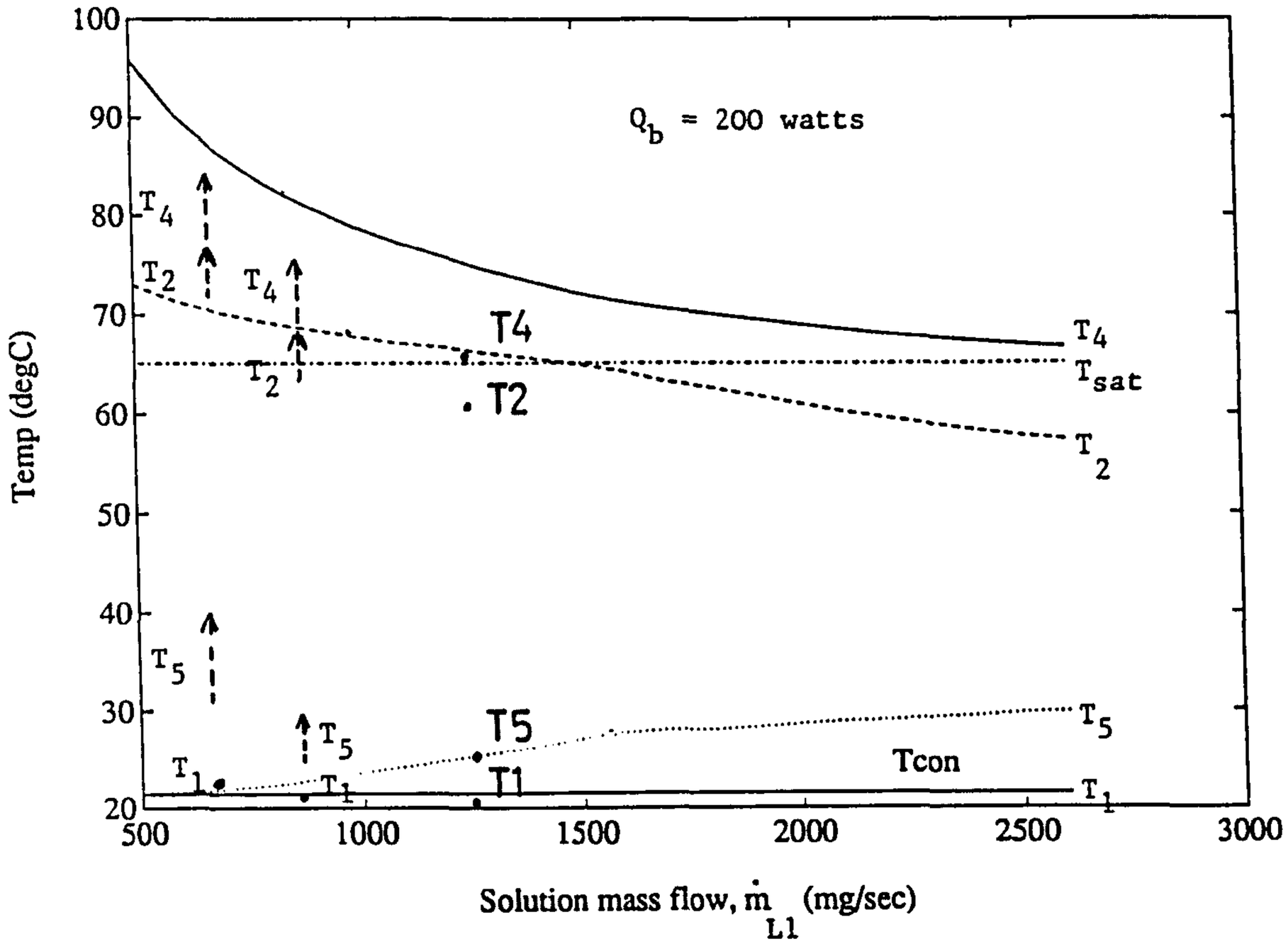

Fig. 6.5.2. FVR cycle with boiler heat input of 200 watts. Comparison of temperatures predicted by computer modelling, shown by continuous lines, and measured temperatures for three solution mass flow settings. Broken lines with arrows show range and direction with time of temperature change in experiments where performance was non-steady. Operating conditions for both theoretical calculation and laboratory experiment are listed on Table 6.5.1.

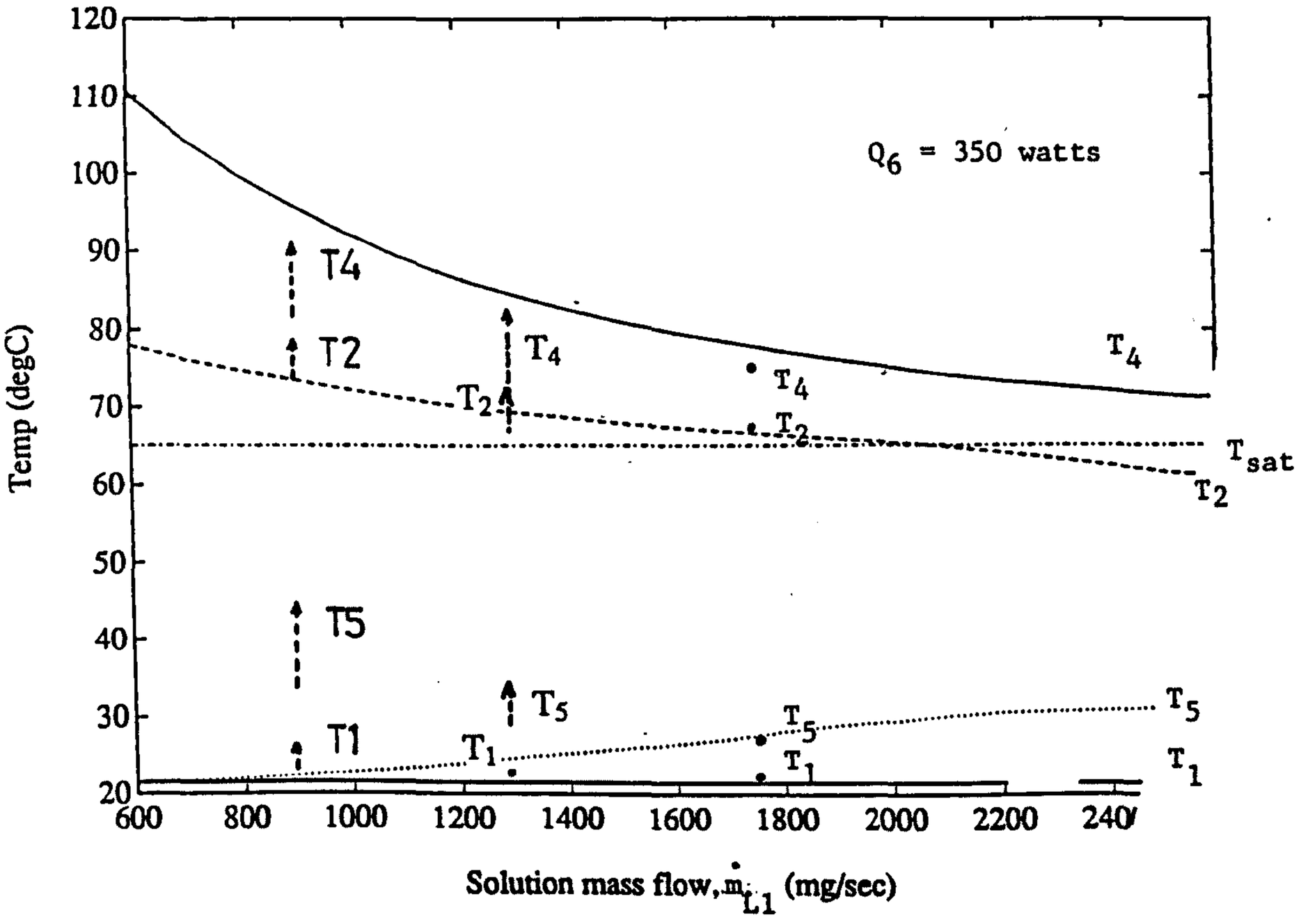

Fig. 6.5.3. FVR cycle with boiler heat input of 350 watts as described by caption to Figure 6.5.2.

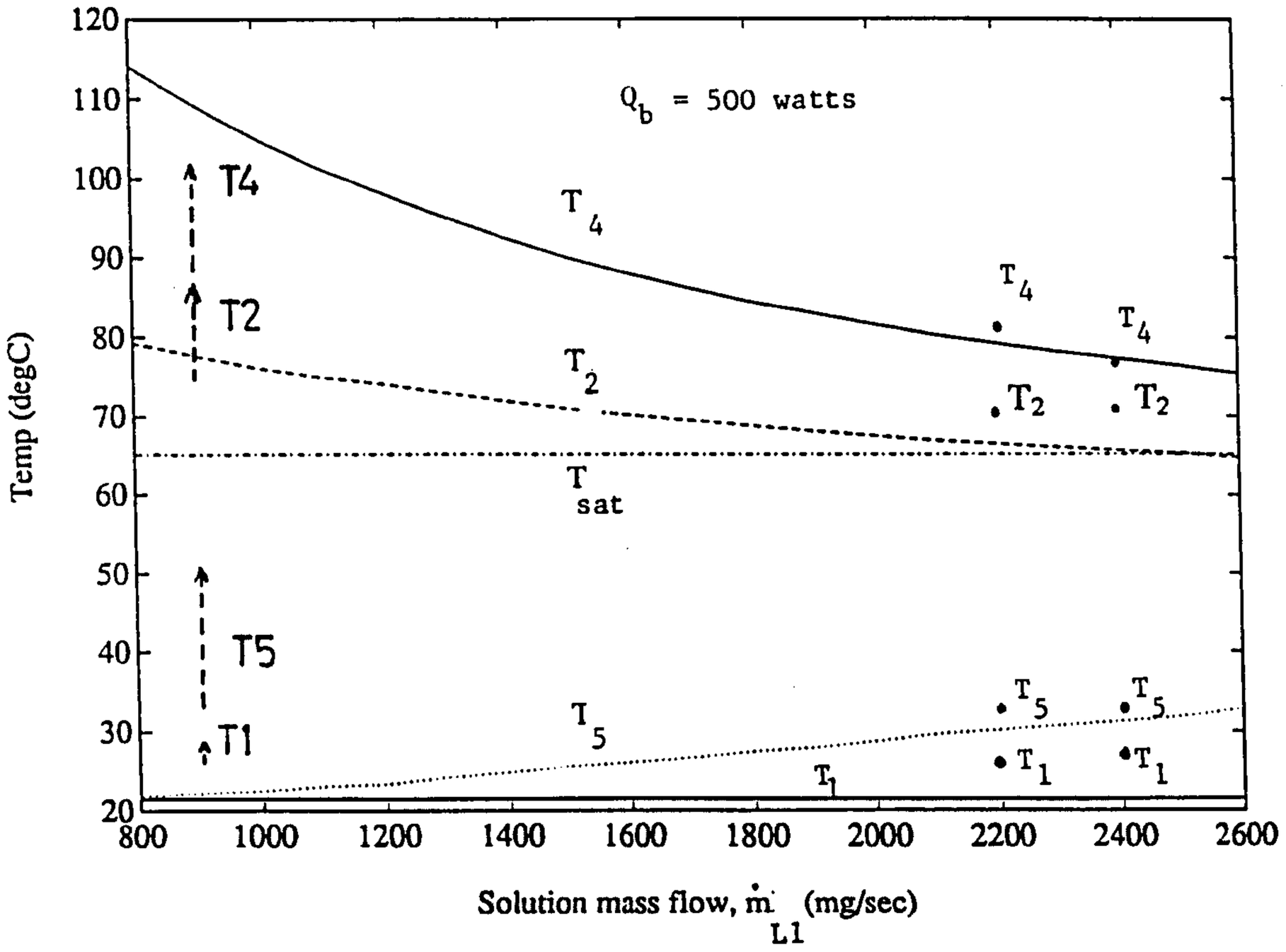

Fig. 6.5.4. FVR cycle with boiler heat input of 500 watts. As described by caption to Figure 6.5.2.

Figs 6.5.1(a) to (c) show that steady state operating conditions were not achieved at low solution flow rates, while improved stability of operating temperatures was obtained at higher flow rates. The mass flow rate of solution, in all cases except where active regulation was applied, showed a tendency to rise and then fall. Condensate yield rates proved to be relatively steady.

Q_b	na	watts	UA_{she}	50	watts/m^2
$\dot{G}$	na	watts/m^2	$M_{gen(i)}$	5.6	kg
$\dot{m}_{L1}$	na	mg/sec	M_{st}	19.6	kg
T_{con}	22	degC	Δt_I	na	hours
T7	70	degC	T1	22	degC
T_{amb}	18	degC	T51	=T1+5	degC
T_{ev}	-10	degC	A_{coll}	na	m^2
T_{ab}	26	degC			

Table 6.5.1 *Parameter values used for computer simulation of experimental conditions. Results are shown in figs 6.5.2 to 6.5.5 and 6.6.1.*

Figs 6.5.2, 6.5.3, and 6.5.4 show, for each boiler heat input, the temperature profiles as functions of solution mass flow predicted for the apparatus by the FVR computer model, set against the temperatures measured during experimentation. The parameters used for simulation of laboratory conditions are given on table 6.5.1. The non-steady temperatures are represented by vectors indicating their measured range during test and and their direction with time. Although at faster flow rates the temperatures T4, T5, and T1 tend to approximate toward predicted values, certain departures from predicted performance are immediately apparent. The spread between T4 and T2 is smaller than predicted throughout the tests, although a tendency for spreads corresponding to the theoretical may be indicated at high solution flow rates. The non-steady cases are characterised by rising temperatures in the separator (T4 rising). (A glance at fig 6.1.1 at the start of this chapter will help the reader; T4 is both the separator and the hot solution temperature as it returns to the heat exchanger.) The implication of rising T4 is that solution is progressively weakening as time goes on, at the same time as circulating slowly. This implies that the large separator of the apparatus is acting in part in a similar manner to the boiler or generator of the intermittent basic (IB) system.

Figures 6.5.5 (a) and (b) show experimental results compared with computer simulations calculated for the laboratory conditions. Turning attention first to 6.5.5 (b), two problems are evident. Firstly the heat exchanger effectiveness is poor at low flows, and is better than predicted by the simulation at higher flow rates. Secondly, at low flow rates, the effectiveness decreases with time in any particular test. This is indicated by broken lines, the arrow heads indicating direction with time. Since the thermal mass of the fluid on the feed side of the heat exchanger is greater, effectiveness is taken as the ratio (T4-T5)/(T4-T1).

In the case of the four points measured for the 350 watts test, a tendency for effectiveness to begin to fall again at high solution flow can be detected. Since theory strongly indicates that this will occur curves are drawn through all three constant-heat sets of tests showing a fall in effectiveness at high flow rate. Unfortunately the apparatus was incapable of producing high flow rates in order to confirm this tendency experimentally.

At low flow rates it is not possible to explain the observed low and unsteady values of effectiveness. These are functions of of fluid flow patterns and heat transfer mechanisms that could not be observed directly or even indirectly in the experiment. It is possible that much more extensive temperature and flow instrumentation within the exchanger would be helpful. Modelling with an equivalent water-water heat exchanger would be easier to undertake in practice.

Although the model of heat exchanger performance is clearly not sophisticated enough to predict the flow rate giving optimum effectiveness, it is of interest that measured effectiveness rises to peak values of around 0.85 which correspond well to expectations based on experience. Values of 0.85 were measured by Van Paasen (1986).

Figure 6.5.5 (a) shows the effect of the behaviour described above on desorption yield rate, or refrigerant vapour production rate, $\dot{m}_{v7}$. As in figure 6.5.5 (b), speculative curves have been drawn to link measured points. These indicate the existence of a peak in yield rate since this is strongly indicated by theory, although the experimental apparatus could not be run for higher flow tests in order to confirm the exact positions of the peaks.

The discrepancy between the yield rate characteristic predicted by computer simulation and that measured experimentally is explained by the measured heat exchanger characteristic shown

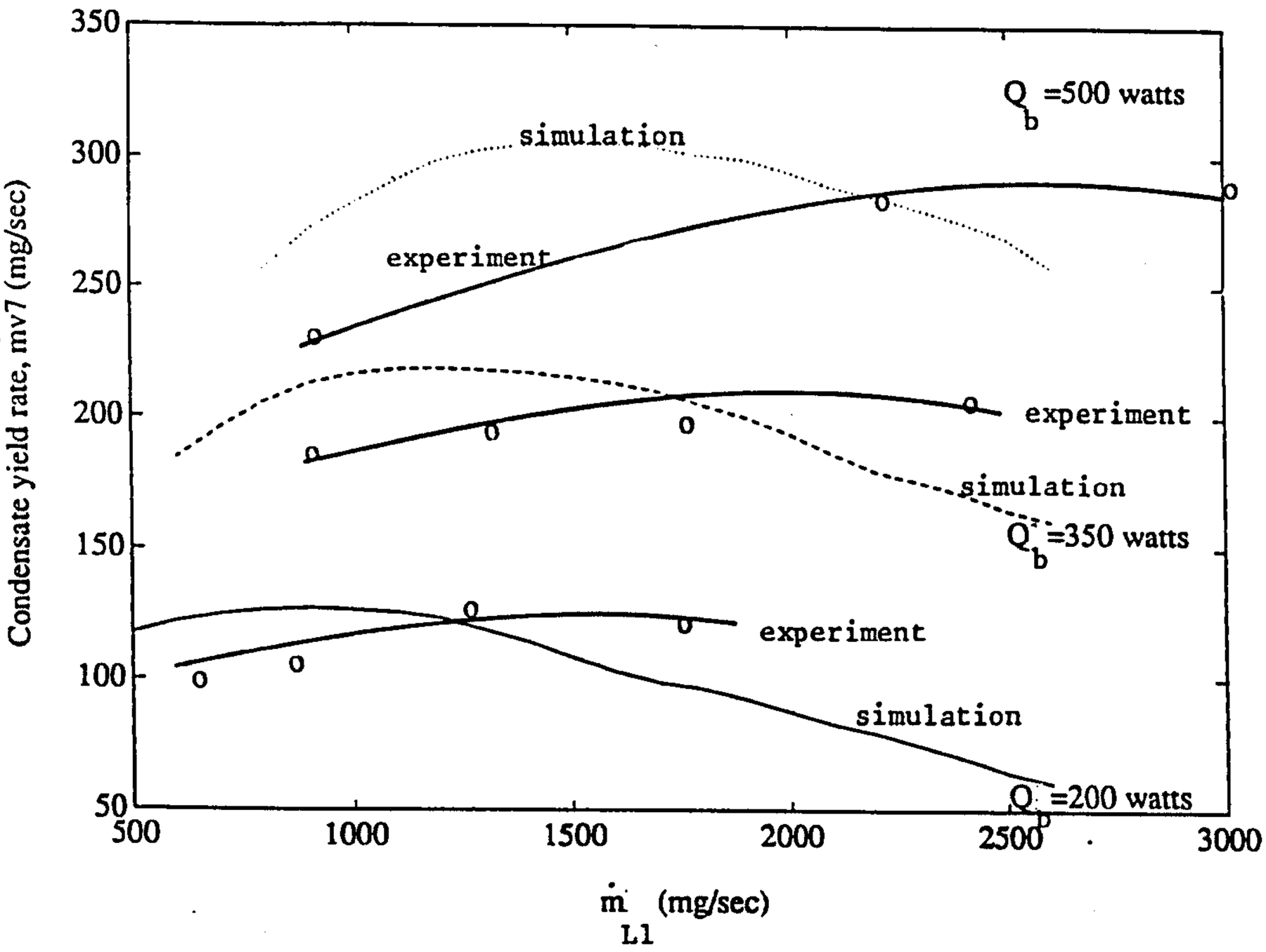

Fig. 6.5.5(a). Comparison of theoretical and experimental FVR cycle response to boiler inputs of 500, 350, and 200 watts. Condensate yield rate is plotted against rich solution flow rates. Experimental results are marked 'O'. Curves linking experimental points are shown to peak in relation to variation in flow rate because of the strong indication from theory that this occurs. Operating conditions for both the computer simulation and experiments are given on Table 6.5.1.

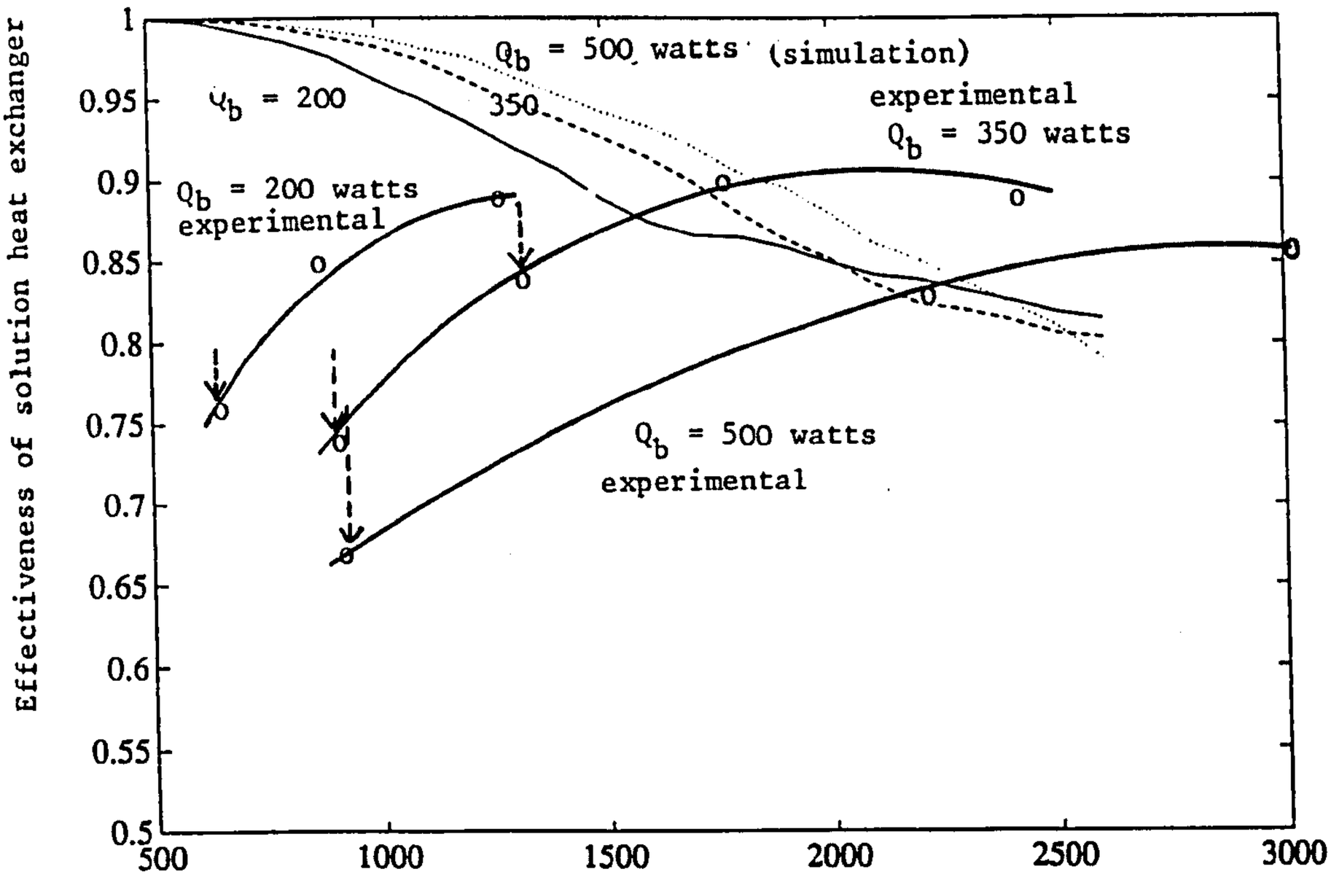

Figure 6.5.5(b). Comparison of theoretical and experimental values of solution heat exchanger effectiveness in the FVR cycle. Experimental results are marked 'O' Broken lines with arrows indicate the range and direction with time of change in effectiveness while cycle operation is unsteady.

in fig 6.5.5 (b). At low flows actual effectiveness is lower than predicted, causing yield rate to be lower than predicted. At high flow rates actual effectiveness is higher than predicted so causing higher yield rates than predicted. It is interesting to note that the peak yield rate values measured correspond to those predicted, so validating the computer model in one essential respect. The optimum flows at which these peaks occur are wrongly predicted, implying that the modelling of the heat exchanger needs to be refined. Since low optimum flow rates are required to keep the weight ratio of the device low, attention should be paid first to revision of the actual heat exchanger design in order to encourage high effectiveness at the lowest possible flow rates. This is an important conclusion arising from the experimental work.

The term "COP" (coefficient of performance) is reserved in this study for daily or yearly net performance under conditions of varying insolation. Since the experiments were conducted at constant boiler heat input rate the term "internal efficiency" is used instead of internal or cycle COP in order to make this distinction. Internal efficiency and internal COP are defined as the ratio of energy absorbed by the boiler to useful cooling energy present in the collected refrigerant. The experimental apparatus allowed the evaporator performance to be tested, so that the useful component of the energy contained in the refrigerant could be measured. Once these measurements are reported (in section 6.8) it is possible to calculate the measured internal efficiency (in the subsequent section) as the ratio of measured energy input and measured cooling energy.

6.6. Flow as function of heat input

The flow characteristic of the experimental unit is plotted for three of the tests in fig 6.6.1, in comparison with the predicted yield rates and flow response. The three tests chosen are all reasonably good confirmations of the simulation in all other respects. Fig 6.6.1 shows lines of constant circuit flow resistance, and indicate that the unit responds to variations in heat input in a way which maintains its efficiency near to the optimum efficiency as determined by flow rate. This figure should be compared with figure 3.10.2, which shows the flow response of the unit according to the computer model. The confirmation through experimental work of the predicted

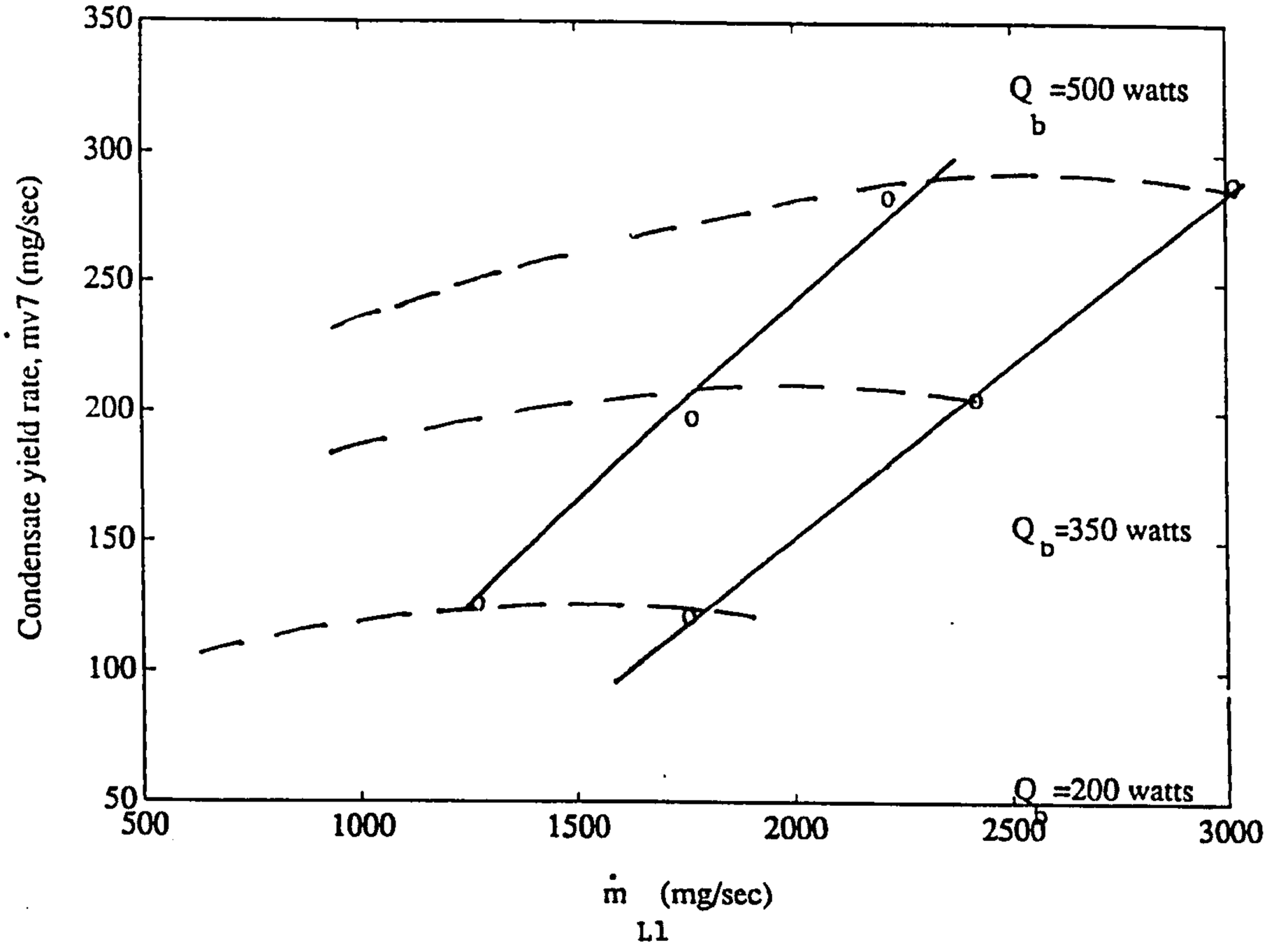

Fig. 6.6.1. The experimentally observed automatic flow regulation characteristic of the FVR cycle is shown by the two solid lines joining the experimentally measured points marked 'O'. Each line represents the fixing of the flow metering valve on the apparatus at a set position, so that the circuit behaves as it would in the field. The broken lines joining the experimental points are the experimentally inferred performance characteristic.

"self-tuning" characteristic of the IR system is one of the major outcomes of the experimental work.

6.7. Construction of evaporator

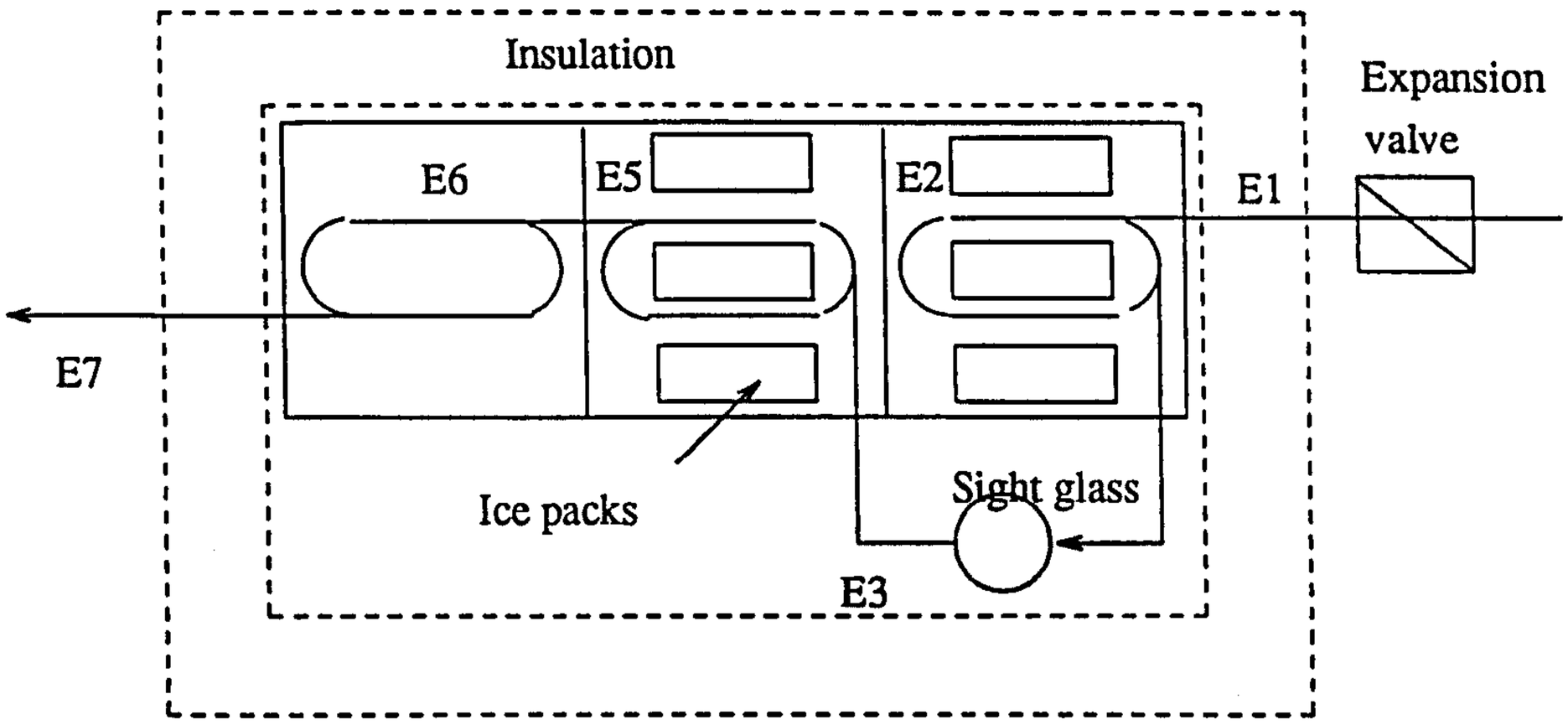

Fig 6.7.1 *Plan view of evaporator, which consists of a single stainless steel tube wound into three coils placed in series. Six ice packs surrounded by anti-freeze are shown; the third coil in the sequence is surrounded by water for freezing.*

The evaporator consisted of three coils of stainless steel tubing each of 5 meters length and connected to each other for series flow of the refrigerant, as shown schematically in the plan view fig 6.7.1. A manual needle valve, which served to expand the refrigerant, was placed immediately upstream of the coils. The internal diameter of the tubing was sized to obtain a sufficiently high gas velocity to entrain the liquid contents of the coils. This allowed the flow path to be led against gravity so simplifying the construction of the evaporator. A sight glass was placed at the lowest point in the flow path so that any collection of liquid could be observed. Tubing with an internal diameter of 4mm was found to produce "dry" evaporation conditions as desired. The

choice of narrow bore tubing resulted in a pressure drop across the evaporator tube ends of between 1.5 and 2 bar, implying a degree of inefficiency in the system.

Each of the three evaporator coils were designed to provide cold sources for separate compartments each sized to contain three standard ice-packs immersed in ethylene glycol solution. The ice packs were lozenge shaped, 34mm by 115mm by 180mm, each holding 0.58 litres of water. During tests only six packs were used, filling the first two compartments, while the third compartment was filled with 2.9 kg of tap water in direct contact with the evaporator tubing. The compartments were surrounded with polyurethane foam insulation of thickness 15 cm on six sides, the top section being removable as a lid. A storage volume of 3 litre capacity to one side of the compartments was left empty during tests. Approximately 3 litres of air space remained below the lid. 3.5 kg of ethylene glycol solution, mixed with water in a 30% weight concentration, were used in the first two compartments.

6.8. Absorption and evaporation processes

Date	Time	T0	E1	E2	E3	E5	E6	E7
25.8.87	8.30	19	13	6	6	7	6	19
	8.50		-11	7	4	8	6	8
	10.00	29	-14	-9	-9	-3	6	6
	11.00	30	-9	-10	-10	-4	5	-3
	12.00	21	-8	-5	-7	-5	1	13
	13.00	19	-2	-5	-7	-3	0	13
26.8.87	10.10	18	10	0	-1	2	1	18

Table 6.8.1 *Measurements against time of temperatures achieved in the cold chest. TO is the reservoir/absorber temperature. Other temperature stations are given on figure 6.7.1.*

Table 6.8.1 shows the time response of the experimental apparatus during a representitive absorption phase. Before the start of the process the system pressure was allowed to drop to 2.9 bar, and ambient temperature was measured as 19 degC. The insulated components of the generator circuit

retained temperatures between 22 and 25 degC, while the exposed portions of the apparatus were in equilibrium with ambient. As a result of previous use of the apparatus the contents of the cold chest were below ambient temperature at the start of the present test, as indicated in the table.

The receiver contained 2 kg of refrigerant before the start of the test, at a pressure of 8.24 bar, indicating a concentration value of 0.981. The in-line sight glass showed the presence of solution in the evaporator tubing. At 8.47 a.m. the expansion valve was opened manually to a postion one turn from closed. This had no visible effect. At 8.50 a.m the valve was opened a further turn, which had the effect of clearing the solution from the tubing within 30 seconds, and causing the temperatures measured along the tube wall to drop markedly. No cooling water flow was provided during this test until 11.20 a.m. The expansion valve was maintained at a setting of one turn open until 11.20 a.m. when it was closed down by a half turn in order to slow the absorption rate and regulate the system pressure. At 12 a.m. no refrigerant could be observed in the sight glass connected to the receiver, implying the mass held had diminished to a value below 0.3 litres. The receiver maintained a consistent pressure throughout the test which was observed to persist at 12.30 p.m. At 1.00 p.m a fall off in pressure to 5 bar was observed, indicating complete exhaustion of the contents of the receiver.

Inspection of the cold chest at 1.50 p.m. revealed that approximately 90% of the contents of the ice packs were frozen, while 65% of the contents of the third compartment was frozen. The total ice yield was estimated to be 5 kg, which represented a heat of freezing of 1.67 MJ. No attempt was made to measure the heat distribution in the cold chest accurately. By assuming that the water content of the cold chest was subject to a nominal overall temperature drop of 6 degC, and that the glycol content was subject similarily to a drop of 10 degrees, the load due to sensible cooling of liquids was estimated to be 250 KJ. A theoretical calculation of the heat transfer characteristic of the cold chest insulation indicates a UA value in the order 0.2 watts/K, implying a leakage rate of 5 watts and the loss of approximately 90 KJ of cooling energy in five hours. The 2 kg of refrigerant evaporated had a net energy of evaporation of approximately 1.16 MJ/kg, implying an energy extraction of 2.32 MJ. It can be assumed that the bulk of the 320 KJ not yet accounted for travelled with the refrigerant vapour exiting the cold chest, as indicated by the

temperatures measured at point 7. A portion of this energy will have been consumed in sensible cooling of the solid materials present in the cold chest, and in sub-cooling of the ice formed. The ratio of refrigerant evaporated to ice produced (2:5) which was measured on this occasion proved to be repeatable, as long as care was exercised in the setting of the manual expansion valve. Set to a small orifice size the evaporation process became marginally more efficient while the time taken for absorption increased. As expected reduced evaporating temperatures were more easily obtainable, while the absorber cooling water flow was able to maintain a low value of system pressure. Set to a larger aperture the temperature at point E7 became as low as E1 implying a considerable wastage of refrigerant. System pressure and evaporator temperatures rose under these conditions.

The conclusion reached as a result of observations of the evaporator performance was that the ice-making and cold storage aspects of the design were working according to expectation, and that the refrigerant:ice ratio achieved was the maximum that could expected of a practical system operating under normal conditions.

6.9. Internal Efficiency and COP

The COP of a refrigeration device is the ratio of its useful cooling energy output to the energy input. In the case of a solar driven device, the energy input is insolation which varies in intensity during the day and through the year. It has been demonstrated in Chapters 1 and 3 that this variation in insolation gives rise to inefficiencies in the refrigeration circuit as well as the collector itself, and that the performance response to varying insolation of one type of machine is different to that of another. Consequently solar-driven machines can be compared by measuring their net performance at the end of the day, or better at the end of the year. If they are compared in terms of their response to a theoretical constant power input, incorrect conclusions result. For this reason the term 'COP' is reserved for true net performance, the product of collector and refrigerator COP (''solar COP'') or only refrigerator COP (''internal COP''). The terms ''internal'' and ''solar'' efficiency are used to describe performance at constant rate of heat input.

Because the experimental program was not extensive enough to include measurements with collector fitted, no direct measurements of solar COP were possible. Neither were any attempts made to vary boiler heat input in a single test as an approximate simulation of typical conditions during a solar day. Instead only internal efficiencies were measured. Nevertheless the work of chapter 3 allows inferences to be made from these results which indicate net performance, or COP.

The measured internal efficiency is given by the equation

$$\eta_i = \frac{\text{Yield} * L_{ref}}{\dot{Q}_b * \Delta t_I}$$

where Δt_I is the full duration of Phase I, including both sensible heating and pressurisation (Phase Ia) and then desorption (Phase Ib). L_{ref} is the useful energy of evaporation of the refrigerant, which was confirmed by the measurements recorded in the previous section to be 1.16 MJ/Kg. The Yield is the measured quantity of refrigerant collected at the end of Phase I. $\dot{Q}_b$ is 200 watts, 350 watts, and 500 watts in successive sets of tests. The internal efficiences measured for each of the tests are plotted against solution mass flow rate on figure 6.9.1. Since practical and theoretical efficiencies are related to yield rate in the same way, the correspondence of yield rates shown for each heat input value in fig 6.5.5 applies equally well to the correspondence of theoretical and practical efficiencies. Peak values are very close to each other, but the experiment shows that optimum efficiency occurs at higher mass flow rate than predicted.

Solar efficiencies are calculated for the peak yield rates measured in the three tests, and noted on figure 6.9.1. In each test a particular value of heat input $\dot{Q}_b$ applies, and a particular value of T4 is attained, so implying a certain value of solar insolation $\dot{G}A_{coll}$ as indicated by the collector efficiency and heat flow equations:

$$\eta_{coll} = 0.8 - \frac{1.9(T4 - T_{amb})}{\dot{G}}$$

$$\dot{Q}_b = 0.8\dot{G}A_{coll} - 1.9(T4 - T_{amb})$$

The collector characteristic used above differs from the version given in section 3.5.2 only in so far as it has been simplified to become a linear characteristic, the error in the area of interest

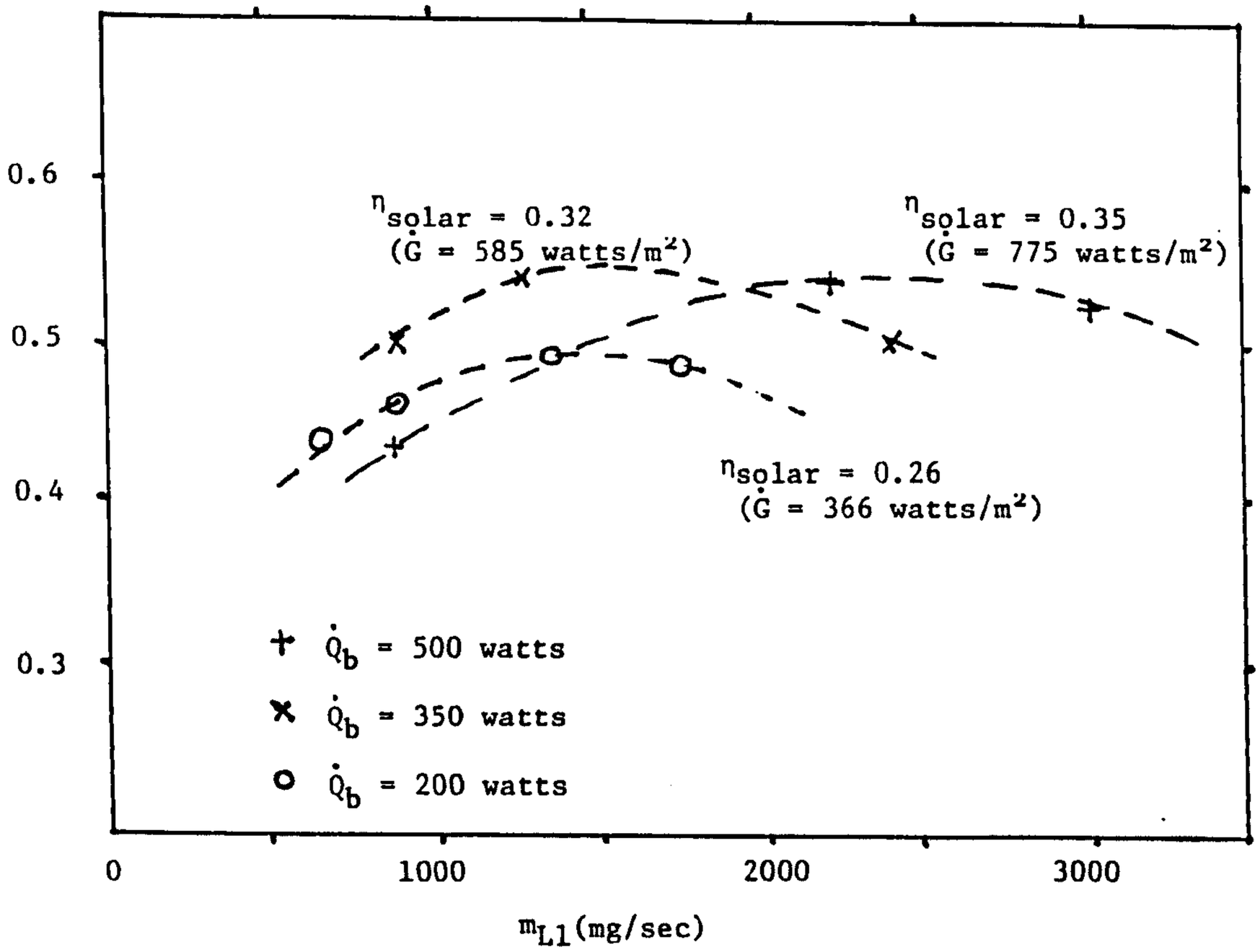

Fig. 6.9.1. Internal and solar efficiencies calculated from observed performance of the experimental apparatus are plotted against rich solution flow rate for a range of boiler heat input ($\dot{Q}_b$) values. Solar efficiency values are calculated for 3 tests, each associated with an implied value of solar insolation $\dot{G}$. As elsewhere a collector area of $1m^2$ is assumed. Collector efficiencies are calculated from ($T4-T_{amb}$) temperature differences measured in the laboratory from each test, using the simplified collector characteristic, ($\eta_{coll} = 0.8 - 1.9 (T4 - T_{amb})/\dot{G}$), which approximates with reasonable accuracy to the full characteristic given in section 3.5.2. Collector efficiencies are 0.6, 0.65 and 0.54 for the $\dot{Q}_b$ = 350 watts, 500 watts and 200 watts respectively.

being negligible. The experimental apparatus is sized for connexion to a collector area (A_{coll}) of 1 m^2, which is the collector size assumed for theoretical work in Chapter 2 and 3. Given the calculated value of $\dot{G}$ solar collector efficiency η_{coll} can then be found. Solar efficiency is the product of η_{coll} and the η_i value observed for a particular test. All solar efficiency values inferred from fig 6.9.1 are therefore linked to particular values of solar insolation, $\dot{G}$. The values range between 0.26 for a low insolation (366 W/m^2) and low measured internal efficiency (0.49) to 0.35 for high insolation (775 w/m^2) and high internal efficiency (0.54). This spread is as expected from the computer simulation results of Chapter 3 (fig 3.9.3(a)) and the associated discussion.

It is useful to compare these findings and the experimental results of Van Paasen (1986) with respect to his testing of a flat plate collector version of the IR device. His report is discussed in Chapter 2. The two major reasons why he obtains a lower solar COP value (measured over a day of real varying insolation) of 0.1 are (a) the flat plate collector has an efficiency of around 0.3, as opposed to the 0.5 to 0.65 efficiency of evacuated tube collectors, and (b) the collector/generator has excessive thermal mass. Results are recorded only for clear days, the collector/generator efficiency and thermal mass having the effect of significantly impeding performance on days with intermittent cloud cover. This implies that yearly net solar COP figures would tend be lower than 0.1. The separator dries out in the early afternoon, between 2 and 3 pm, and even lower solar COP is calculated if the whole days insolation rather than the insolation up to separator emptying time, is taken into account. The use of a large separator would increase the desorption period but also increase generator thermal mass. Many of the design features of the IR system developed in this study overcome these problems; the use of evacuated tubes, for instance, gives higher collector efficiency and allows the incorporation of a low thermal mass generator.

Chapter 7: Study of implementation

7.1. Introduction

In order to provide the ground work for a full assessment of the IR system the present chapter addresses itself to the question of what role the device might be expected to play in an economic and social environment. The specific environment chosen for a case study is the fish trading economy of Zambia. The examination of the technical performance limits undertaken in previous chapters provides data for an economic assessment, although a number of assumptions have had to be made as to technical performance which have not yet been validated.

7.2. Summary of implementation study

The fishing economy of Zambia is chosen as the subject of an implementation study. Hayward (1983) and Subramaniam (1985) have established that the expansion of fish production is both important and possible in Zambia, and that a major and necessary aid to expansion will be the provision of reliable cooling to reduce post-harvest losses. Such cooling will increase the marketing of both dry and fresh fish, and in so far as it promotes the consumption of fresh fish, it will satisfy a growing demand for fresh fish which already exists.

The study made of the potential role of the IR system concentrates on the trade in fresh fish. The IR system is first costed conservatively on the basis of the performances predicted in chapter 3 and allowing ample financial incentive for a manufacturer to commence production. A value is calculated for the cost per unit mass of ice sold by operators of the IR device in rural areas. Although this cost is considerably greater than the cost of ice produced in urban areas by conventional machinery, it is nevertheless found that the profits of "small and medium capital" traders - the dominant categories of traders - transporting fish on road to the urban markets will be increased by the availability of ice at remote locations. This can be expected to lead to an

increase in the number of active traders. The availiability of ice at remote locations would also be complementary to the emergence of boat collection services on the lakes of Zambia, on a larger scale than they exist already. Such services and autonomous icemakers will have a very important part to play in increasing the number of remote artisanal fishing communities with good access to large markets. The incentives, in the form of profit and attractive pay-back periods, existing for potential purchasers of solar ice-making equipment are found to be very substantial. The assumption that permanent dwellers of remote artisanal fishing communities will be purchasers is not made; the conservative assumption is made that icemaking machinery will normally be leased for use. Nevertheless it is argued that the availiability of ice in remote communities could raise the economic power of those communities and cause them to receive a greater share of the trading returns than they presently receive. The reason for this is that they would be in a position to store their catches. It is suggested that the fish-handlers tend traditionally to be responsible members of the community whose earnings are spent constructively increasing the productivity of the community and its vigour, and that it is therefore conceivable that the increase in returns on fish trading will benefit the under-capitalised sectors of the rural economy.

Although the question of wealth distribution is speculative, the study finds with some certainty that conditions exist in Zambia for the spontaneous uptake the solar cooling technology without public sector intervention. The possible re-introduction of mains electricity driven refrigeration plant at major fish landing sites will not alter the attractiveness of autonomous icemaking very significantly, given the particular geographical conditions surveyed.

7.3. The demand for cooling

The consumption of fish provides 50% of the protein in the Zambian diet (Ministry of Agriculture and Water Development, 1983), considerably higher than the proportion for Africa as a whole. The total catch is around 55-65,000 tonnes per year, comparing favourably with some African coastal countries. 35% of this catch is consumed fresh as opposed to frozen, dried, canned, smoked, salted, or otherwise preserved (Hayward, 1983). A proportion is consumed at the lake shore without a preservation process being required. If solar ice-making technology

proves economic and is convenient, it will therefore process some 20%-30% of the nation's catch under current consumption conditions. If solar ice-makers are sized to process one tonne of fish per day, one unit will process 365 tonnes per year. The total number of units in use in the nation as a whole would be between 30 and 50.

In 1976 the per capital supply of fish was 12.8 kg per year while imports of fish and fish products were 10,200 tonnes and exports were negligible. It has been suggested that because of the increase in population since 1976 per capita consumption is now lower and considerable demand exists for more fish supply in the country. It is also observed (Subramaniam, 1985) that the market trend at present is a steep increase in appetite by urban consumers (constituting half the Zambian population of 5 million) for fresh fish, as opposed to the traditional dried fish, although the latter retains its popularity amongst both urban and rural consumers. It should be noted that although dry fish is an important protein resource for rural dwellers and poor people in general, because it can be stored and eaten in small quantities continuously, it has the disadvantage of lacking some of the nutritional content present in fresh form (National Academy of Sciences, 1978). The appetite for fresh fish is most clearly shown by the very high prices charged by urban retailers. While consumer prices are high fishermen are still receiving very low prices for landed fish, and very large profits are being made by traders.

Zambian inland lake fisheries could provide double the current total catch. The FAO/World Bank identification mission in 1979 concluded that the potential was for 100,000 tonnes/year. Estimates from other sources (Hayward 1983, Subramàniam 1985, Pearce, 1985) of the potential yield of each major fishery compared to present production are given on Table 7.3 and the fisheries of Zambia are illustrated on Figure 7.1. There exist therefore, two possible effects which would increase the demand for ice plant installations: the potential increase of the total catch to 100,000 tonnes/year and a growing preference in the towns for fresh fish. An upper limit for demand considering the first effect would then be for between 20,000 and 30,000 tonnes of fresh fish per year, requiring between 55 and 82 ice-making units. An estimate can also be made by imagining that Zambia's urban and peri-urban population of 3 million are content to consume no more than half their fish in fresh form, a reasonable conclusion considering the convenience of

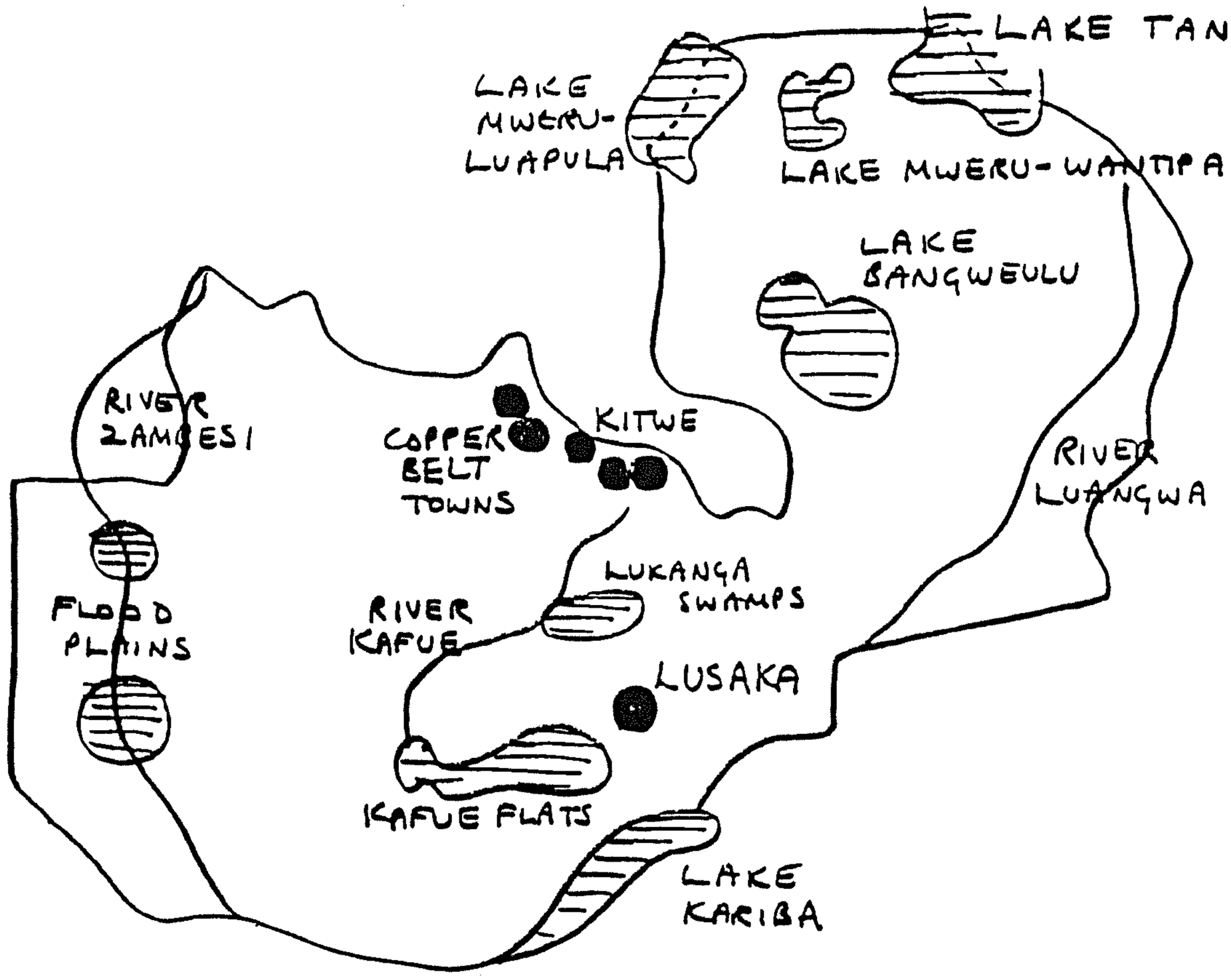

Fig 7.1 *Major fisheries and urban centers of Zambia*

dry fish. If the per capita consumption is 20 kg per year, the total urban demand for fresh fish will be 30,000 tonnes, requiring 82 ice-making units in the nation.

The reasons for the shortfall between current and potential national catch area given by Haywood and Subramaniam (1983, 1985) as:

(a) lack of adequate fishing equipment

(b) insufficient facilities for collection, storage, distribution

(c) presence of unfished remote areas.

It is also generally accepted that facilities for the enforcement of stock management legislation are inadequate. With respect to (b) the researchers point to the lack of provision for supply of ice and chill rooms at collection and distribution points. It is noted that any future planning must

guard against the breakdowns experienced up to now in fishing boats, ice plants and refrigerated vehicles. Attempts to set up large ice-making facilities run either by diesel generators or by mains electricity have failed, and expensive plants in 3 locations now lie idle, as shown in Figure 7.2. The reasons are various but are all associated with the need in remote areas for specialised technical skills, organisational input and regular fuel or power supply. The contribution that maintenance-free solar coolers could make to fisheries development in Zambia is therefore very significant.

7.4. Fishing techniques

The most common fishing methods in Zambia are gill netting and light fishing. Gill netting is most commonly done by artisanal fishermen setting nets in the evening and returning for the catch at dawn. The larger fish, mostly breams, are caught in this way. Boats and nets are commonly owned by proprietors who retain a proportion of the catch. Other fish of major importance in Zambia are the small sardine-like kapenta, or chisense, which are suitable for both drying and freezing. These are caught using light attraction techniques at night, mainly on Lakes Tanganyika, Kariba, and Mweru-Luapula. Fishing operations are organised in various ways. Individual fishermen may be self-employed, own only two or three nets and a dug out canoe, and mix subsistence fishing, cash fishing, and agricultural activities in varying degrees. They may sell to traders directly or they may act as an independent supply source to a local fishing company with its own trading arrangements. Alternatively fishermen act as manual labourers employed by a proprietor of nets and boats. In small businesses payment will be by division of the catch so that the terms of employment approximate to those of a partnership. Artisanal fishing is an umbrella term covering both individual fishermen and both small and larger businesses involved in marketing and employing up to twenty waged employees; it accounts for 97% of the total catch in Zambia (Hayward, 1983), industrial fishing being limited to about 10 companies operating 40-tonne purse-seiners in the central waters of Lake Tanganyika.

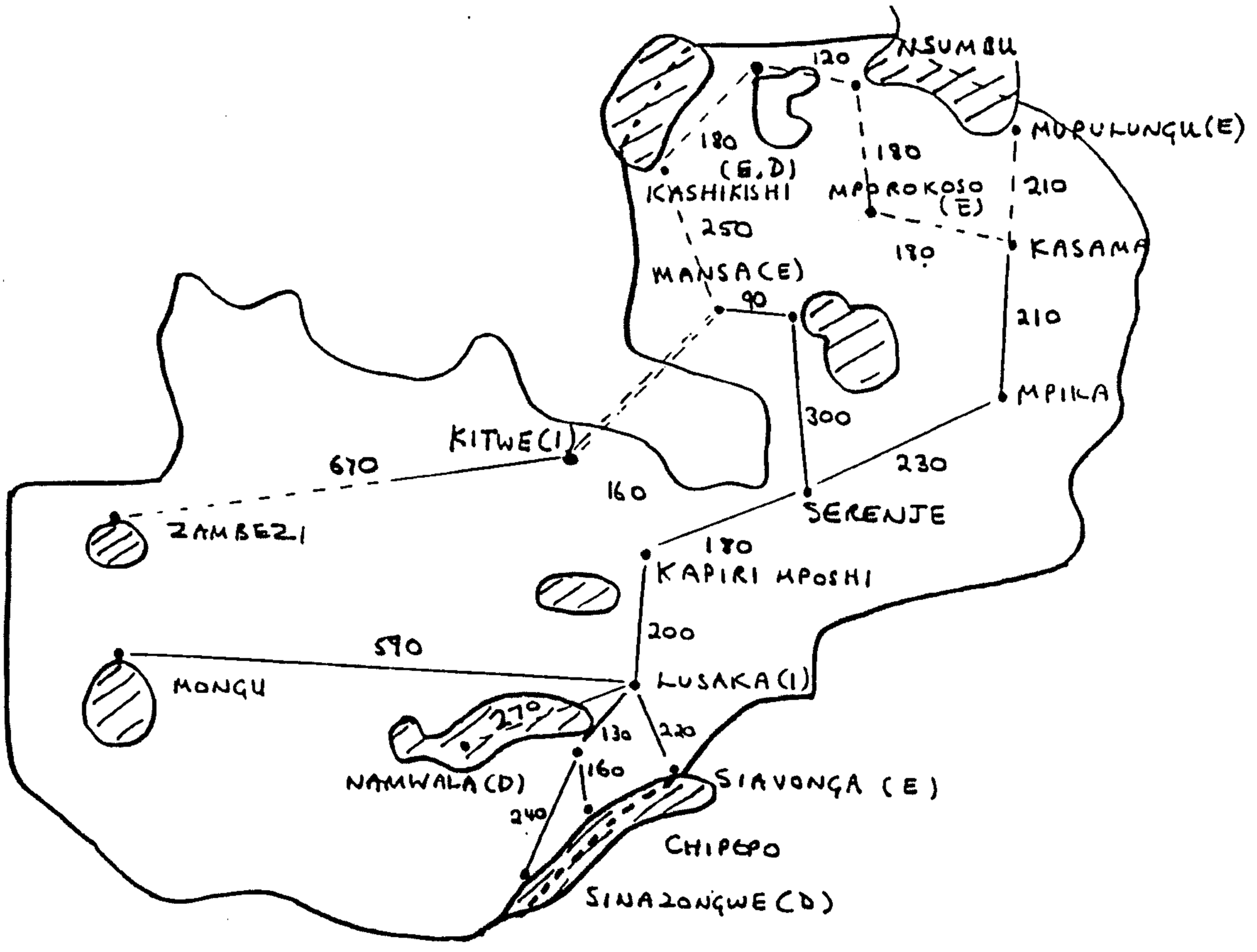

Key:

Solid line: Sealed road, approximate distances in km

Broken line: Graded or unsurfaced road

Double broken line: Road sometimes inaccessible and subject to delay

(E): Mains electricity available

(I): Ice commercially available, produced by electrical plant

(D): Defunct ice plant, previously diesel or mains driven

Fig 7.2 *Approximate distances between urban markets and fisheries*

7.5. The marketing chain

Figure 7.3 (a) shows a simple model of marketing flows for fresh and dry fish. The figure indicates the variety of scales of capitalisation that exist both in the field of transport and fishing.

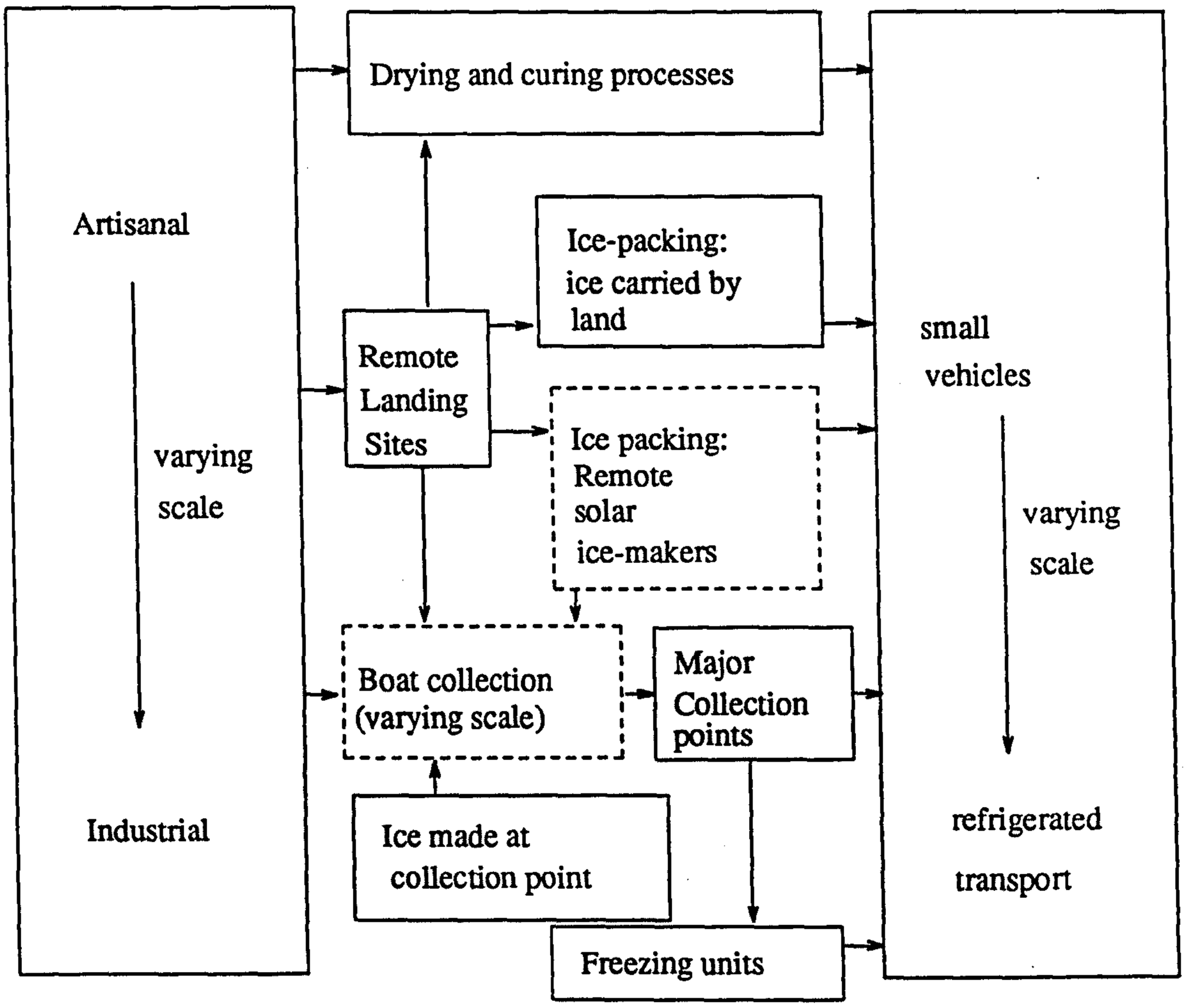

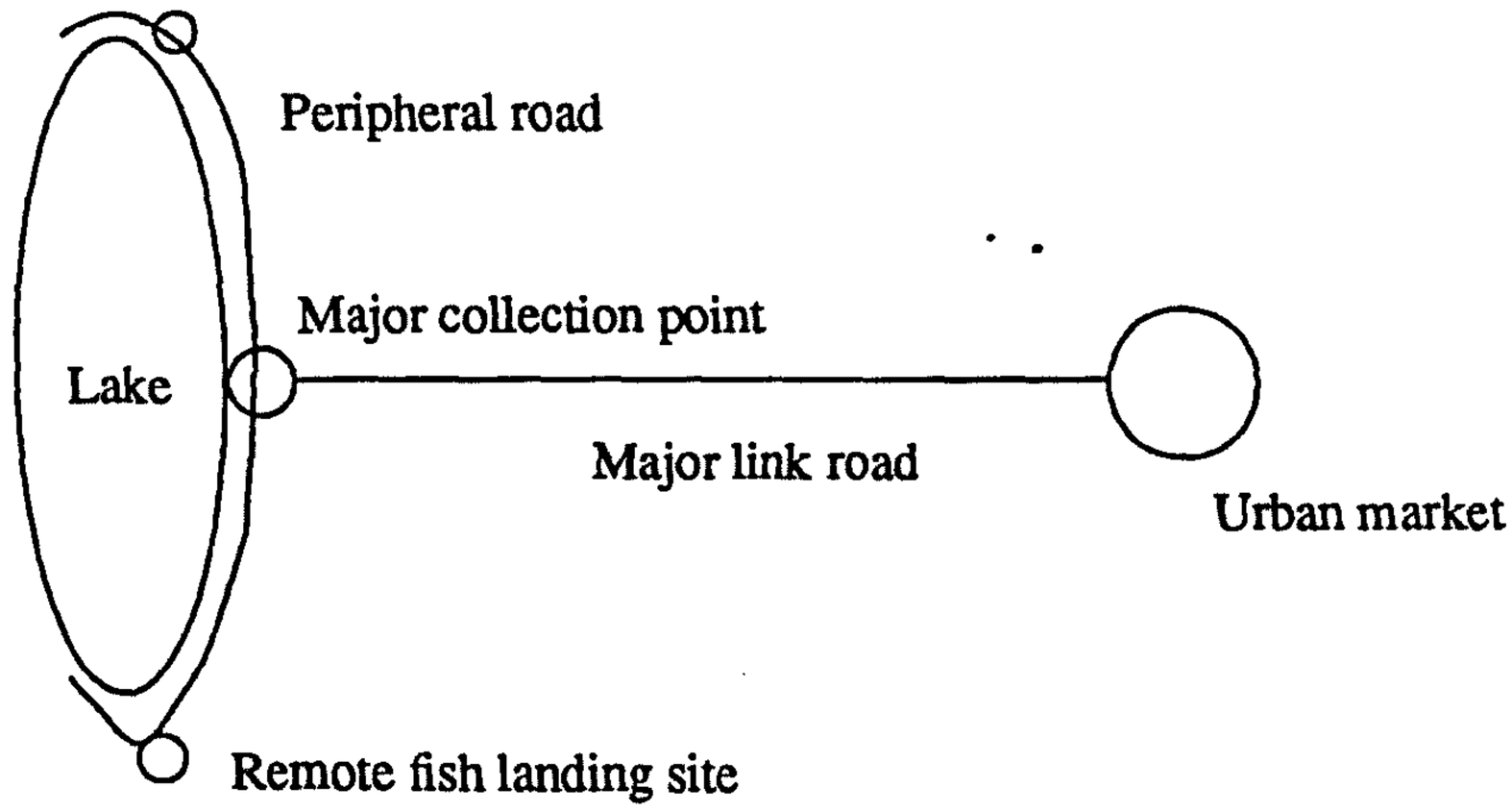

Fig 7.3 (a) *Marketing flows*, (b) *Schematic fishery*

Boxing with broken lines indicate the activities which are recommended for expansion by fishery researchers or which are considered here as candidates for expansion, these being boat collection and solar ice packing respectively. The figure indicates the space for integration of both of these activities in improving the marketing flow. Figure 7.3 (b) shows schematically a fishery in order to clarify terminology. The need for improved road access is not shown but must be assumed.

Figures 7.4, 7.5, and 7.6 show the three fisheries mainly considered here. It can be seen that recent road building by Canadian aid has improved the road access to the northern lakes considerably. There are no sealed roads west of Tanganyika and market link roads to collection centres on Mweru-Wantipa and Mweru-Luapula are still not yet provided. It is assumed in this discussion that collection points have mains electricity and freezing plant, although in most cases installation and rehabilitation work still needs to be carried out.

The question is raised whether ice making plant is useful in expanding the market outlet capacity of the fisheries, and whether it is useful or feasible for it to be located at the remote landing sites. It is assumed here that diesel generation has already proved itself inappropriate in practice. It is clear from Figure 7.2 that the establishment of freezing and icemaking sites at major collection points could have a significant effect in improving the market outlet for fresh fish. If ice is on sale to the public then both land traders and boat traders can carry the ice to remote sites. Similarly the presence of remotely located solar ice plant would be complementary to land and boat trade of fresh fish. It is quite likely that both facilities can coexist and minor collection sites based on solar ice-making facilities can emerge where the geography of a lake encourages this. It is possible that greater financial incentive exists for the various members of the chain to adopt one or other course of action, if a simple economic choice is open to them; the financial incentives open to manufacturers, ice-plant equipment owners, boat traders are therefore considered in turn below. Finally the implications in terms of the interests of artisanal and capitalised fishermen are considered.

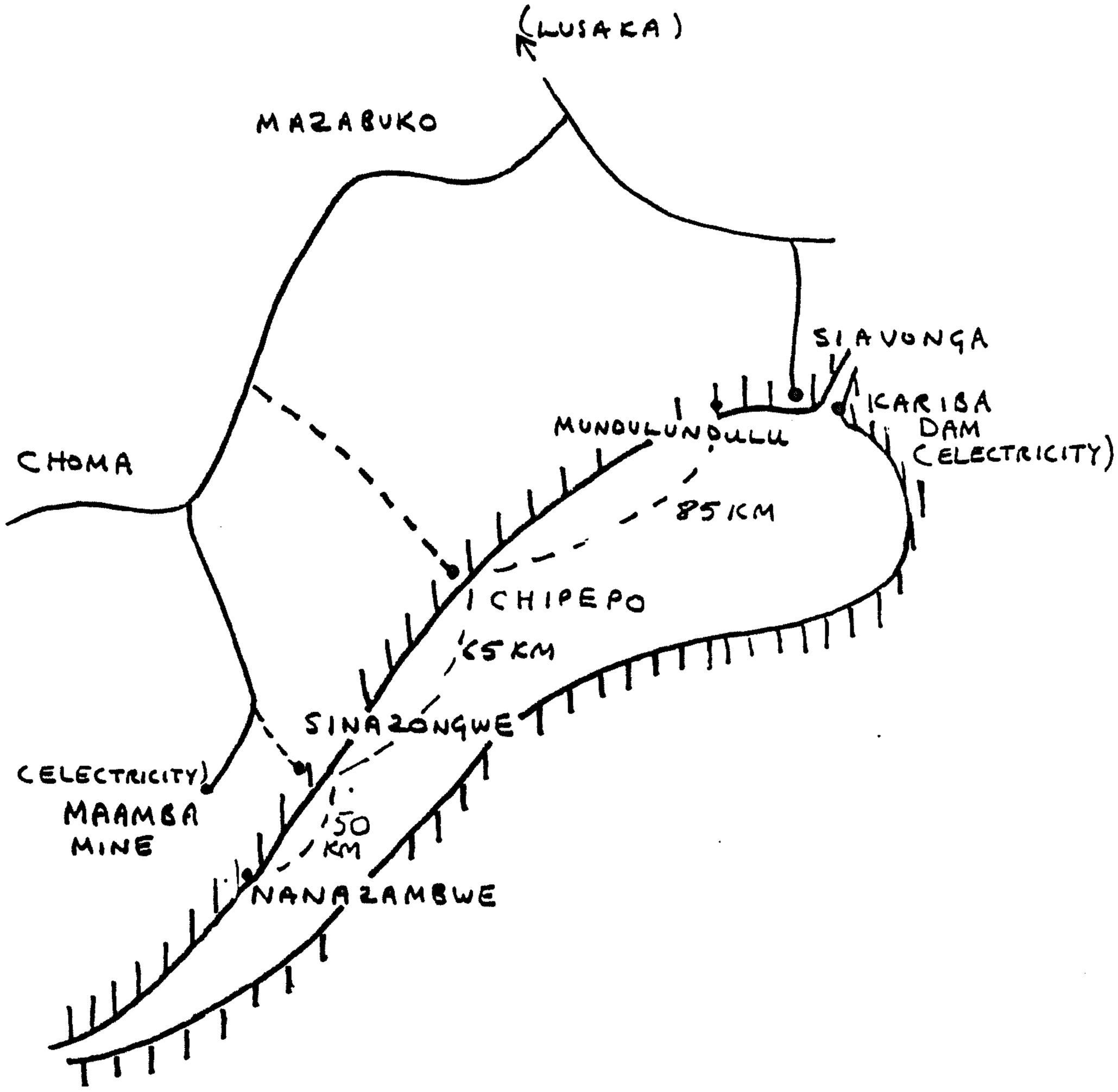

Fig 7.4 *Lake Kariba, showing approximate distances by water*

7.6. Ice as a storage medium

Discussion with traders in Zambia revealed some information on the use of ice to preserve fish (Hutchinson, 1985, and annex F). The technique is to make chippings from a large block. The chippings are used to cover successive layers of fish and will pack in well if sufficiently small. The thickness of ice applied is about one inch. A five hour vehicle or boat journey in very hot conditions such as encountered at Lake Kariba (which is well below the relatively cooler plateau altitudes of most of Zambia), using poorly insulated containers, will cause sheets of ice of approximately half an inch thickness to form between the layers of fish. After this melt loss is

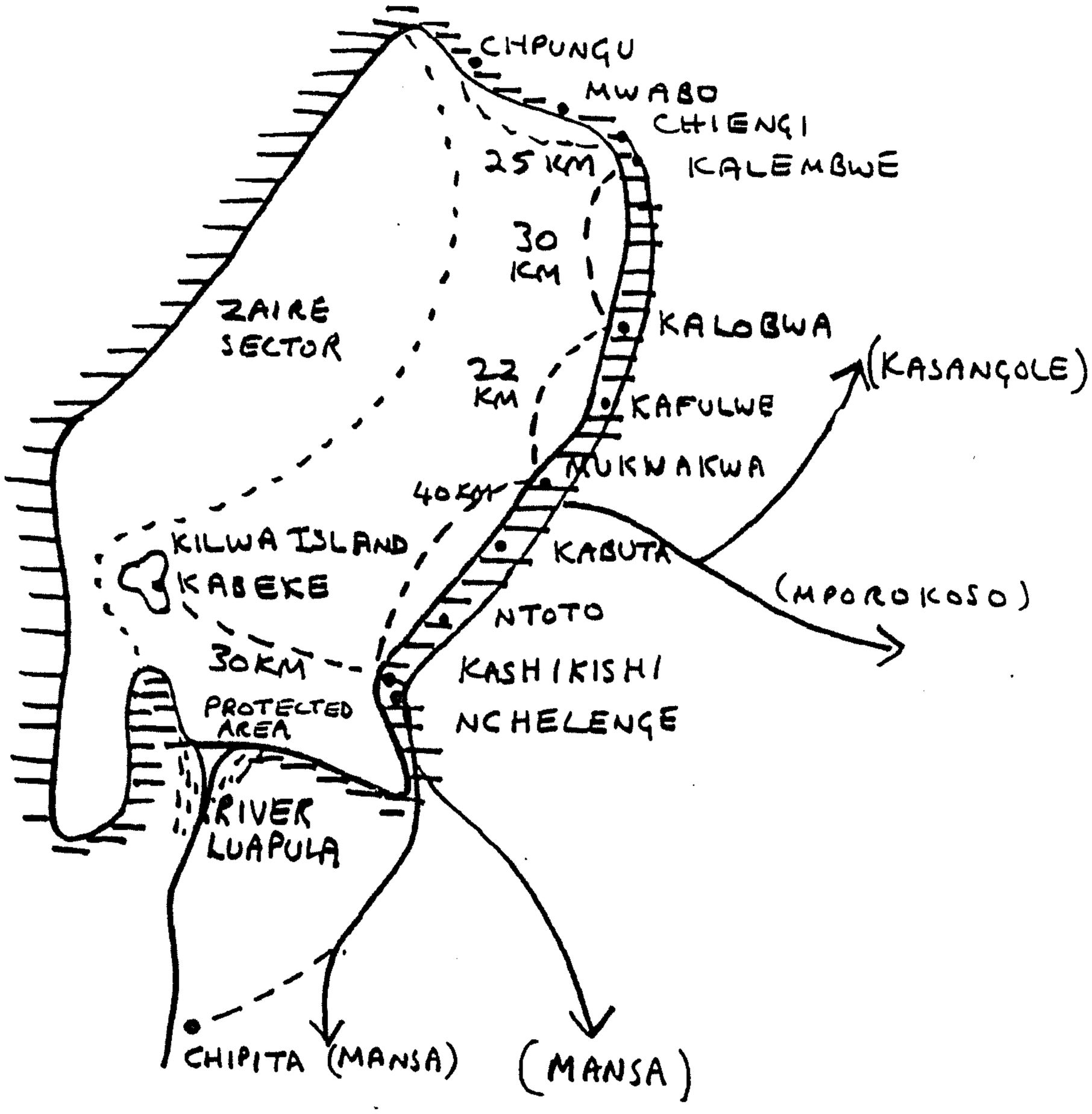

Fig 7.5 *Lake Mweru-Luapula, showing approximate distances by water*

slower and storage or transport for up to 4 days is possible.

The fish sizes will be a mixture of 1-kg to 3-kg specimens of, typically, breams, with a few larger predators present. Refrigeration literature indicates that to reduce the temperature of 1 kg of fish at 20 degC by 20 degC will require the melting of 0.2 kg of ice, if done in a perfectly insulated container. Kept at 2 to 5 degC the fish will keep for 5 days, which will require only some 10 kg of ice in a well insulated box which could hold 100 kg of fish. The implication is that 1 kg of ice is ample given rough handling and insulation to preserve 1 kg of fish.

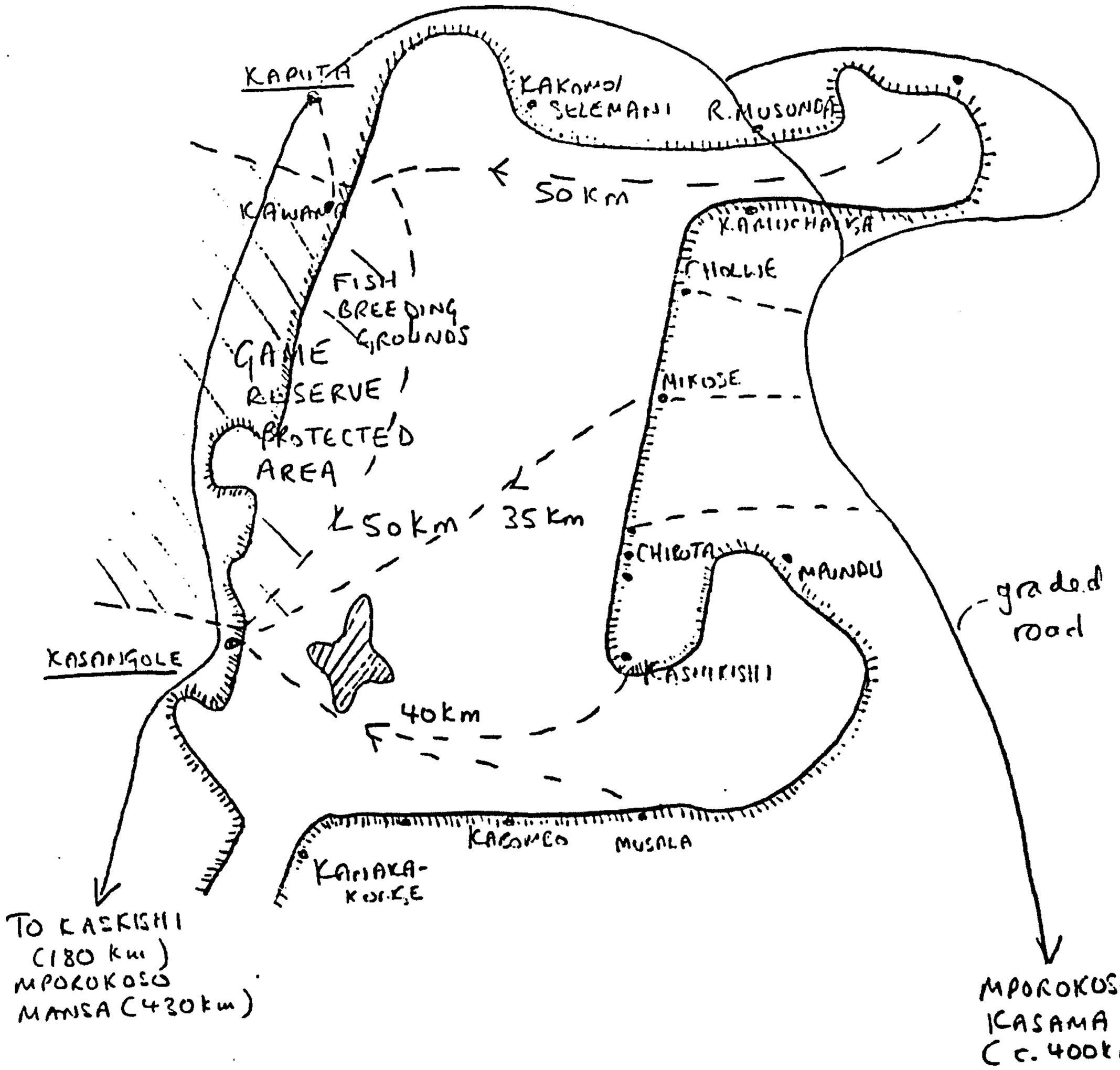

Fig 7.6 *Lake Mweru-Wantipa, showing approximate distances by water*

7.7. The capital cost of icemakers

A breakdown of production costs for the solar refrigeration plant is suggested in Annex B. This includes a sizable return on investment for the manufacturers. The resulting retail price of a 1-tonne per day ice making unit is taken to be 300,000 Kwacha (KW). At the time of writing (March 1986) the exchange rate is 10 KW to £1.

7.8. Ice plant owners: the cost of solar ice

A clear profit incentive of 50 KW/day (1800 KW per year), over and above running costs and capital repayment, can be assumed to be sufficient incentive for an entrepreneur to purchase and operate a solar ice-making machine. It is assumed that the owner employs two staff to attend to the day to day running of the machine, which should involve no skills at all, but consist primarily of unloading ice, collecting water from the lake for recharging, and caretaking. Interest rates on loans are at present set at 25% by the Agricultural Development Bank of Zambia. The repayment required on loads can be expressed in terms of a constant annual repayment sum over a specified loan payback period, as shown in Annex C. The repayment factor calculated in Annex C is defined as:

Constant annual repayment sum over specified period

= repayment factor x original face value of capital sum.

The calculation as to the likely production and retail costs of solar ice is shown on Table 7.1. Site costs are assumed to be low because traditional village building techniques can be used for mounting of collectors and fencing. Lake water can either be pumped or carried; again very cheap methods are likely to be most practical. The salaries allowed for 2 caretakers are about three or four times average rural earnings and commensurate with skilled fishermen's earnings and other respected members of a local community.

The estimate of 300 solar days allows for poor ice production during the rainy season months. In areas where the fresh fish catch experiences an off-season it is assumed that the sale of ice continues because other uses are found for it. The retail price arrived at on Table 7.1 compares poorly with the retail cost of ice bought at present in the urban centres. In February 1986 this varied between 0.17 and 0.25 KW/kg in Lusaka and Mazabuko. The extra cost penalty of solar ice does not necessarily threaten its viability for use in the marketing chain, as the advantages of ready availability in remote locations outweigh this. Certainly transport costs in Zambia tend often to be reflected in 60% of prices of goods sold in rural areas (Hutchinson, 1985).

The projection of a single entrepreneur owning a single ice-making machine may be quite different from reality. An entrepreneur running several units would stand to make greater profits,

		thousand KW	KW/Kg
(C)	Capital cost of 1 tonne ice/day unit	300	
(i)	Annual interest: 25%		
(n)	Loan repayment period: 10 years		
(M)	Capital repayment factor:		
	$M=i(1+i)^n/(1+i)^{n-1} = 0.28$		
(Y)	Constant annual loan repayment = M.C	84.0	
	Site costs:		
	(a) two caretakers at 400 KW/month each	9.6	
	(b) chill room construction, fencing,	5	
	maintenance, water collection		
(S)	Total site costs	14.6	
(A)	Total annual costs = S + Y	98.6	
(Q)	Quantity of ice produced in 300 solar days: 300 tonnes		
(P)	Production cost of solar ice = A/Q		0.33
(I)	Profit incentive of 50 KW/day for owner	18.5	
(R)	Retail cost of solar ice = (A + I)/Q		0.39

Table 7.1 *Cost of Solar Ice*

but may have difficulty in controlling the earnings of his machines. Local ownership by permanent local residents would suit the need for constant supervision; it is quite likely that the women working at present on fish drying, agriculture, and domestic duties, would be most capable of embracing the tasks of retailing ice and packing and selling iced fish. The cash earnings would possibly then be spent more on community benefits than otherwise.

Financial incentive is then better looked at in terms of payback period. Table 7.2 indicates the cost of solar ice if short payback periods are considered the incentive necessary to promote the uptake of the technology. A three year payback at interest rates of 25% implies a cost of 0.56 KW/kg.

Lower interest rates are also shown on Table 7.2. Most officials consulted in Zambia considered that the loans offered under the World Bank Fisheries Development Project should be at lower interest rates than currently available from the Agricultural Credit Bank.

Interest Rate	15%	20%	25%
Payback Period			
10 years	0.25	0.29	0.33
3 years	0.49	0.52	0.56
2 years	0.66	0.70	0.74

Table 7.2 *Production Costs (KW/kg) for short payback periods*

7.9. Fish Wholesalers

7.9.1. Land Traders

99% of the distribution of fish in Zambia is accomplished by the informal sector (Hayward, 1983). Fresh fish are transported in lorries, vans and pick-ups. which carry ice from urban centres to remote fish landing sites. Figures 7.1 and 7.2 show schematically the major fisheries of Zambia and their distances on road to the urban markets. Existing ice plants, where traders can purchase ice, are shown; points at which mains electricity is available are also shown, implying that ice is privately produced and marketed in a limited manner.

The traders spend some days buying fish and packing it for the return journey to the urban market. The economic incentive for this activity has increased with the urban appetite for fresh fish, but decreased with the difficulty of vehicle maintenance on rough roads over long distances. Ice melt loss on outward journeys is a limitation, particularly since breakdowns are common. The loss of carriage space to ice on the outward journey is also an economic limitation as it can be used as source of earnings. A major problem is uncertainty as to the length of time required to collect a full load. Since the time available is restricted by the melting of ice, returns are often made with partial loads. Traders therefore make poor financial returns on some trips, hoping they will be compensated for on further, more successful trips. The existence of ice available at very remote fish landing sites (where mains electricity or reliable diesel generating plant are not feasible alternatives) would reduce these risks. The economic incentives for the present day trader making a successful trip using urban-bought ice, as compared to one where solar-ice is bought, are compared in Annex D. These calculations show that solar-made ice would be preferred by traders, though it will sell at a higher price than urban-bought ice. The calculations clearly show that the most important disincentives to traders under present conditions are the long collection periods required to collect a load, and the likelihood of being forced to return under capacity because of the time restriction imposed by ice melting loss. These conclusions were also reached by Beatty in 1965. The disincentives are removed if ice is available at landing sites. Other factors in the calculation, such as the higher cost of solar ice, have a far less significant effect on earnings.

Trader earnings depend on the size of vehicle used and its age. The calculations show that for relatively small vehicles the use of solar ice can at best raise the earnings of the vehicle from 689 KW/day to 1,733 KW/day. Assuming trips are always successful and 10 days are spent each month travelling, the rate of earnings of the vehicles are 6,900 KW/month if urban ice used and 17,000 KW/month if solar ice is used. If the vehicle proprietor is content with 3,000 KW/month return (100 KW/day) then each member of a 3-men crew is earning 1,300 (urban ice) or 5,100 KW/month (solar ice). At worst the use of solar ice will secure the same returns as are achieved at present, although with the important advantage of less risk of returning with partial load.

In practice journey failures, most often due to mechanical breakdown, reduce the earnings, particularly in cases where urban-bought ice is relied on. Because trader profits are high it might fairly be assumed that traders rather than customers will pay for any elevated fish price due to the possible use of ice-storage in the landing villages. At the same time the more reliable local supply of ice-packed fish or further ice supply for packing will probably increase the amount of trading activity, so that the competitive effect will also reduce trader profits.

7.9.2. Boat collection services

Boat collection services have been suggested as a viable solution to the problem of providing a market outlet for artisanal fishermen working at some distance from land transport routes. Boats of the common cargo size, 500 kg to 1 tonne capacity, are used for the collection and marketing of dry fish on Tanganyika (traders commonly buy the sacks while wading thigh deep), for the purchase of dry and fresh fish by Zaireans on Lake Mweru-Luapula, and for fresh fish collection by a company ("Family Farms") on the Kafue flood plains, to name some examples of present practice.

The increased use of boat collection is envisaged as a necessary measure additional to the increased use of road transport on the lake shores. Boat collection services are assumed to be the most feasible short term method of extending the transport link beyond the collection centres to all points along the lake shores. The requirement for increased collection activity presuppposes that the fisheries succeed in producing catches nearer their estimated yield limits. This will only occur when finance is available to allow effective enforcement of legislation protecting fish breeding and to allow more appropriate equipment and techniques to be taken up. Present World Bank loans are designed to provide this finance, which includes provision for loans to large scale commercial fisherman to fish central lake waters as well as to artisanal fishermen to buy better equipment. Table 7.3 summarises current and potential yield estimates for the major fisheries and indicates where boat collection services are considered practical (Subramaniam, 1986, Pearce, 1986).

	Current Yield *1000 tonnes	Potential Sustainable Yield *1000 tonnes	Practicality of Boat Collection
Tanganyika	9	12-20	Yes. Same current practice
Mweru-Wantipa	9	20	Yes. Considerable need
Mweru-Luapula	9	20	Yes. Considerable need
Kariba	9	12	Yes. Some previous practice
Kafue	5	7	Yes. Some current practice
Bangweulu	11	32	Dubious. Flat bottom boats
Itezhi-tezhi	0.8	2	Yes
Lukanga	1.2	2	Not investigated
Upper Zambezi	4	5.5	Not investigated
Others	0.6	2	Not investigated
Total	58.6	102-110	

Table 7.3 *Yields of Major Fisheries*

Some of the huge potential outputs listed on Table 7.3 will be marketed in dry form. The discussion here assumes that a high proportion will be sold to satisfy the large consumer demand for fresh fish.

The viability of boat collection services as a means of handling these catches may be affected by the presence of remotely produced solar ice as postulated. To some extent the question as to the usefulness of solar ice to boat collectors shares the same ground as the question asked about land traders. Both are wholesalers of fresh fish packed in ice, and both must choose between the options:

(a) To carry ice with them on an outjourney, collect fish and pack it wherever it seems available or where prearranged, and return the iced fish.

(b) To make an arrangement with local fishermen or an agent to take delivery of a store of ice, and to use it to pack the catch over the next 2 or three days. The wholesaler then reappears to pick up the iced fish while dropping off the next consignment of ice, and does not need to

spend time locally collecting. The local agent is busy collecting from a surrounding area while the trader is travelling.

If locally made solar ice is available, the local operators have the chance of acting autonomously, especially if they are also proprietors of the equipment, and so a very different kind of situation arises. Assuming for the moment that the ice plant is owned by the wholesaler, a third option can be considered:

(c) To carry goods other than ice on the outjourney; to pick up iced fish which has been collected by the local agent as in (b).

The disadvantages of (a) have already been discussed and apply equally to boat and land traders. A relevant case example is mentioned below with reference to Lake Kariba (Annex F). In the case of (b) the trading cycle is constrained to stick to a tight time table, imposed by the melting rate of the ice. Agreements between partners must be watertight. The occurence of delay or vehicle/boat mechanical breakdown could result in spoilt fish and disastrous financial loss. The total travelling time must be not more than 3 days. If fish supply is at a low ebb, the collecting period cannot be extended but partial return loads must be suffered with attendent financial loss. Case (c) does not suffer from these risk elements and allows flexibility as to where and when a collecting visit is made. It also allows more use of the hold to carry commercial goods on the outward journey, or the first few legs of the journey if many collection points are visited.

In practice the choice between (b) and (c) will depend on particular conditions. The disadvantages of (b) mentioned probably apply more to land traders than boat traders, since a boat collection service may well be content with a strict time table of visits. It is open to question whether boat holds would be needed for carriage of goods on the early parts of a journey. In some cases (b) may be the preferred option of boat collection services, especially where mains electricity operated ice makers are available at their base stations.

From the point of view of fishing village inhabitants, it is possible that the existence of local solar ice makers will be preferred. Local ownership of the plant will mean that iced fish can be sold to whichever wholesaler offers the best price, whether a land trader or water trader. The traders may be in a position to act as importers of supplies to the village.

Boat trading can be shown to be economically viable for cargo boats of 2 tonnes capacity and upwards. Interviews with a fishing company on Lake Kariba were helpful in establishing the potential for small boat trading on that lake, as described in Annex F. Fishery authorities are eager to encourage boat collection on Mweru-Wantipa and Luapula in order to encourage improved fishing by providing improved market outlet facilities. The suggestion was made that the running of one or two large (50 tonne) boats on these lakes might be more economic than the running of a much greater number of small boats. The economics of a large boat collection service are roughed out in Annex E. The calculation assumes a collection of 3,000 tonnes of fish per year. A typical round trip would take 3 days picking up 30 tonnes from about 10 landing sites each producing on average of 1 tonne of fish per day. (Figures 7.5 and 7.6). On average 20 tonnes of ice would be used to preserve 30 tonnes of fish. Fish kept for a full three day period would require a fish:ice ratio of 1:1 while fish picked up at later stations would require lower ratios. The use of solar ice-makers at remote landing sites would suit this type of collection and could be initially purchased and then hired out to villages by the boat company. Because of the high returns the incentive for the uptake of the technology would be considerable. Certainly there may be a preference on the part of a boat company to make ice centrally and carry it out (option (b) above) but government authorities could intervene to allow greater independence and trading power to villages by insisting on local ice plant. The high returns calculated in Annex E (over 1 million Kwacha per year clear of costs and repayments for a payback period of 3 years) imply that local villages would be in a position to obtain higher prices for their fish than at present and effectively share some of the wholesaling mark-up.

Similar arguments would apply to the use of many smaller collection boats on the lakes. Although overall costs would be considerably higher the possible increased frequency of activity, transport possibilities, and import as well as export trade open to the villages, may have greater benefits.

7.10. Community Benefits

Locally owned and operated ice plant will put the community in a strong position to take a much larger share of the very high profits accruing from the fish trade. Because women traditionally are active in fish preservation and processing and because they are stable members of the community, it is possible that they would play an important role in ice-packing and trading, with the result that earnings are more likely to be spent constructively on welfare needs, for instance nutrition. A research study (Allen, 1986)) has contrasted the itinerant behaviour and non-social expenditure of male fishermen with the marketing, cash earning, agricultural and child-rearing responsibility of women.

7.11. Artisanal Fishermen

Some posible effects of the availability of solar ice locally can be considered:

(a) One of the serious problems reducing both dry and fresh fish consumption in Zambia is loss during the fishing operation. Fish caught at night will degrade until landed in early part of the day. Deterioration of gilled fish under water cannot easily be avoided but retention in boats after pulling and during transportation to shore involves even higher temperature and worst deterioration. In the case of kapenta fishing there is marked tendency for the first hauls taken at night to be spoiled by the time the catch is landed in the morning. Some companies are considering the possibility of overcoming this problem by returning to shore during the night to unload into freezers or into night driers should the necessary equipment be available. One at least already does this(Brignot, 1986)). It is considered an important potential contribution of solar ice that a relatively small amount of chilling on board a kapenta rig during the night would have a significant economic impact(Subramaniam, Brignot). An estimated total of 10-15% of all fish caught in Zambia are spoilt in this way together with losses due to poor handling, transport, and beetle infestation of dry fish. It is not clear what proportion is due to night time losses but if a guess is taken that they account for 4% of total national loss, then the annual saving potential due to use of ice at night time would be 2,400 tonnes annually. In the case of kapenta and chisense cooling, where the fish

are delicate and will tend to fragment if mixed with chipped ice, the use of plastic ice packs placed in the packing crates may well provide a cheap method of cooling, and easy loading and unloading of a solar ice maker. For two to eight hours cooling a fish: ice ratio of 4:1 is adequate implying an increase in cost of the salvaged fish of 0.1 KW/kg. This would be more than compensated for by the value of the increased yield, at 2.0 KW/kg in the case of fresh fish.

The price of fresh fish (destined both for drying and fresh consumption) at landing depends largely on the remoteness of the landing site and the type of fish. Proximity to local markets can raise the price to 3 KW/kg whereas at remote sites 1 KW/kg can be found. The most common prices are between 1.5 and 2.0 KW/kg at present. Fish now sold at 1.75 KW/kg would cost 2.0 KW/kg if 0.7 kg of solar ice is used to preserve 1 kg of fish, a desirable ratio for periods of up to 1 to 3 days (depending on the type of fish). A price of 2 KW/kg is taken as standard for fresh fish in the present discussion.

(b) Proprietors of solar ice makers, whether doubling as fishermen or not, may decide to retail ice freely to any customers. The fishermen in principle would then be able to manage a store of iced fish without constraint to sell to first buyer, but with some freedom to hold out for a higher price. This would increase their earning power. The opinion of at least one research officer is that in practice this in unlikely to happen, since entrenched habit dictates that fishermen will only be interested in immediate cash earnings on the point of landing, and will not organise their own stores and follow-up operations. If they were interested in doing so, the argument goes, they would by now have proved it by involving themselves in the drying process, which in practice they abstain from. An alternative scenario is that the proprietors of local ice-making equipment would buy from fishermen and act as local wholesalers of fish. They would be the ones benefiting from an increased bargaining power vis-a-vis traders, because of the 2 to 3 day storage period available to them. In this case it can be argued that rural dwellers of another sort would benefit from increased income, and posibly the village economy would benefit as a whole, in a spin-off effect. The collective management of ice plant by villagers has also been discussed and is feasible in some

locations due to the sustained success of co-operatives on Lake Mweru (Lester, 1985). In this case the potential spin-off effects of ice plant availability can be clearly seen since the aim of the co-operatives in question has been to raise the village's power to buy in from the urban areas needed goods and infrastructural equipment of common importance.

It is possible that ice plant would be operated locally but owned by absentee proprietors, for instance well-off fish traders. This arrangement would be unlikely to work in practice since the nature of the equipment is such as to demand close local control and ownership, but nevertheless should be anticipated.

7.12. Conclusions

The conclusions drawn from the study are summarised above in section 7.2.

7.13. Acknowledgement of sources

In addition to Dr S P Subramaniam, to whom special thanks is given for advice and encouragement, and for helpful comments on reading an early draft of this chapter, thanks is due to a number of individuals who provided information and guidance either in discussion or in written form. These individuals are listed here. The studies are also the result of interviews and continued contact with traders and fishermen, amongst whom special thanks is due to Sidi Sokoni, and of observations made directly in a number of visits to Lakes Kariba, Tanganyika, Mweru-Wantipa and Mweru-Luapula. An itinerary of these visits is provided in annex A.

E. Muyanga, Director of Fisheries, Chilanga

S.P. Subramaniam, Chief Fisheries Research Officer, Chilanga

M.J. Pearce, Fisheries Research Officer, Mupulunga

D.D. Tapiador, National Co-ordinator, World Bank Fisheries Project

D. Shikoswe, Fisheries Research Officer, Nchelenge

D. Lulemba, World Bank Sub Zonal Officer, Nsumbu

P. Fernandez, Agricultural Development Officer, SIDA, Mansa

B. Lester, Project Co-ordinator, Luapula Fishermen's Co-operatives Project, Mansa

P. Hayward, Institute of African Studies, Lusaka

J. Hutchinson, Director, Lakar Fisheries, Sinazongwe

L.G. Avila, Director of Operations, Zambia Agricultural Development Bank

Chapter 8 Conclusions

8.1 Introduction

In Chapter 1 a number of criteria are proposed for the evaluation of remote solar ice making systems. The four most useful ones are repeated and explained briefly here:

Supportability A particular system is supportable if the kind of maintenance operations it requires for reliable performance are readily obtainable in the remote location. Devices which incorporate moving parts, such as rotating element pumps, are unlikely to be supportable. The inclusion in the device of a check valve, which may in time fail to operate, reduces its supportability. This is because any device containing pressurised ammonia solution will require personnel with specialised skills to undertake replacement of a component.

Solar COP A high solar COP implies the use of smaller solar collectors for the same duty. This implies lower overall, less maintenance, and greater portability.

Component cost A device incorporating a large number of components with interlinking plumbing will tend to be more expensive than a simple device. For example a device requiring twice the air-cooled radiator area of another device

which is otherwise similar will be more expensive, since radiator area constitutes a high proportion of overall cost. Moving parts requiring special materials and precision engineering, such as check valves, will raise the overall cost.

Weight

A device which is too heavy to transport by normal methods will incur the extra expense of needing to be commissioned and maintained on site. This problem may be avoidable to an extent if the device is broken into separate, transportable modules. A non-portable device will also have less capacity to draw revenue in situations where the market for cooling shifts seasonally.

A convenient way to evaluate the novel intermittent regenerative (IR) system is to consider it in relation to each of these criteria in turn. This is done below in sections 8.2 to 8.5 with reference to the proposed IR system above. Section 8.6 then draws comparisons on the basis of these criteria with the alternative systems considered in Chapters 1 and 2. A summary of key points made is given on Tables 8.6.1 and 8.6.2. Section 8.7 draws general conclusions from the study as a whole, and section 8.8 makes recommendations for further work.

8.2 Supportability of the IR device

The IR design proposed here is illustrated by figure 3.1.1, at the start of Chapter 3. If initially the transfer tank component is overlooked, the circuit is the "fixed volume reservoir" version. The evaporator shown is the dry expansion type. The heat pipe cooling

circuit, which is necessary for absorption, condensation, and separator heat removal, is not shown on figure 3.1.1 but is shown separately on figures 4.1 and A.3.1. Taken as a whole the device contains three moving parts: the check valve, the expansion valve, and the valve or "diurnal switch" for separator cooling. All three valves can be either conventional manually operated valves or automatic devices. If manually operated, the device is only as reliable as the operator. Successful operation of the ice-maker will depend on the operator closing the check valve at dusk, opening the separator cooling valve, and regulating the setting of the expansion valve during absorption. Experience of manual operation during laboratory tests showed that expansion valve regulation would in practice be convenient, consisting of no more than one or two manipulations in the evening, led by the need to avoid wastage indicated by frosting of the evaporator tube as it exits the cold chest. Since the operator would in most cases be economically motivated to secure successful ice-production, and his or her presence is required in any case for ice removal and water replenishment, the dependency is acceptable and the machine can be considered "supportable" on this count. Unfortunately experience has shown that manually operated valves often have a limited life before developing leaks, at which point glands must be tightened with great care to avoid rapid deterioration in the performance of the valve. Life times of between 2 and 5 years can be expected depending on the skills applied in valve maintenance. Since the device should perform for at least twenty years, this implies the involvement of well equipped and skilled technicians in decommissioning, valve maintenance, and recommissioning, several times in the life of the unit. A manually operated unit is therefore not easily supported in many remote locations where the availability of such technicians usually cannot be

relied on over the years. Many other locations do exist, of course, where this approach is acceptable.

The use of automatic valves presents similar difficulties. The present study has not investigated the reliability of such devices over periods of longer than two years, and no data has been found on this. Van Paasen (1986) experienced severe difficulties in the design of an automatic expansion valve. Although his check valve operated successfully in the field, test data does not exceed two years. On this basis it must be concluded for the present that the device requires support in the form of skilled technical maintenance.

The replacement of the dry expansion evaporator with a gravity circulating type removes the need for a expansion valve. This removes the difficulty of designing an automatic version, and removes the need for operator input in the case of a manual version. The gravity circulating evaporator requires instead a drain valve for watery residues in the evaporator. This poses the same problems mentioned above. The possibility exists of eliminating this valve through the use of a less volatile absorbent than water, such as sodium thiocyanate.

The conversion of the unit to operation with a small separator and a transfer tank (the "variable volume reservoir", or VVR, version) makes some difference to the number of moving parts. The evaporator drain valve or evaporator expansion valve is still needed, and the check valve is still needed, but the separator cooling valve could be removed. Because the separator container and liquid content has small thermal mass, it can be cooled by natural convection to ambient by the simple expediency of removing a piece of insulation which is later replaced. This requires operator input but the mechanical arrangement does not affect the ammonia plumbing and so can be maintained locally in any location and therefore is "supportable". The

transfer tank does introduce into the system a further moving part, which is a flexible membrane inside the tank, most conveniently in the form of bellows. Degradation of the bellows material over long period may be a problem.

The supportability of the novel IR device is also affected by the proposed use of evacuated tube collectors. Their fragility suggests that occasional replacements will be required. Fortunately the connection between collector condensers and the boiler tubes is conveniently arranged to be indirect, with the condensers clamped to the outside of the boiler tube. Removal and replacement is then a task which can be undertaken by local personnel; no skilled work involving contact with the working fluid of the refrigerator is necessary. The loss of one or two collectors reduces heat input and cooling output but does not stop the refrigerator working. The fragility of the evacuated tubes is therefore a shortcoming but is not critical; the major problem posed is that the refrigerator users cannot fabricate collectors themselves but must order replacements from afar. This is a serious constraint in many locations, and limits the number of remote locations in which the IR device as proposed is supportable. The problem can be avoided by the use of non-evacuated tube collectors which can be locally fabricated.

In other respects the device can be said to be supportable in remote areas. Over-pressure testing during the fabrication stage is necessary to ensure that leaks do not develop during the working life of the unit. The working fluid is stable over the long term under the conditions of use, as has been demonstrated in years of experience with aqua-ammonia refrigerator devices, and there is no evidence of corrosion being a long term problem. The long-term reliability of the

bubble-pump is also suggested by the performance of Electrolux-type refrigerators over the years.

8.3 Solar COP of the IR device

The solar COP of the IR device is the ratio of useful cooling energy available from the refrigerent to the solar radiation absorbed by the collector. In Chapter 3 a computer model is developed which predicts solar COP under a range of operating conditions. In Chapter 6 experimental results are reported which give the internal efficiency of the device; the internal efficiency is the ratio of useful cooling energy available from the refrigerent to energy absorbed by the boiler/bubble pump. The tests are conducted at constant heat input to the boiler. The reality of solar insolation is that it varies in intensity through the day and through the year. The term "COP" is reserved for realistic conditions of varying insolation, such as the sine wave approximation used in section 3.11. The COP found in section 3.11 is therefore a "24 hour COP"; an extended simulation to take long periods into account is also possible, giving rise to an even more useful indices of real performance, such as "yearly COP" or "worst season COP", "best season COP", etc. The work of Chapter 3 established that the solar efficiencies calculated on the basis of constant insolation rate could be taken as approximate guides to daily solar COP values. The simulation showed that under typical operating conditions solar COPs of the order of 0.25 and above are theoretically obtainable by the novel IR device.

The practical tests reported in Chapter 6 showed that a peak internal efficiency (again, because tests were conducted at constant boiler heat, the term "efficiency" is used) of the order of 0.5 is obtainable. Since the efficiency characteristic of the solar collector is

based on practical tests made by the manufacturer, then the inference that solar COPs of 0.25 and above are obtainable in typical climates is also based soundly on experiental evidence.

The price of the collector is likely to be approximately half the total production cost of the machine. The use of evacuated tube collectors, which are bought in small modules suggesting that collector costs rise proportionately with total area, indicates that doubling of the system efficiency (or a halving of collector area) is an improvement of 25% in cost. The evidence of this study is that the proposed IR system can achieve improvements of this order and greater over alternative pumpless systems.

8.4 Component cost

The heat pipe cooling circuit discussed in Chapter 4 allows condenser and absorber heat to be rejected by a single air-cooled heat exchanger, the "heat pipe condenser". Because absorption and condensation heat rejection does not occur simultaneously, the rate of heat removal is considerably lower than is possible in a continuous system. Consequently the surface area required for heat rejection radiators is less. Since radiator cost is likely to be one quarter of total unit cost and rise approximately proportionately with size, the 50% reduction in size achieved here will reduce overall cost by 12%.

A number of precisely engineered components are incorporated in the design, most particularly the active components mentioned in the section above on supportability. Valves suitable for use with ammonia under pressure are expensive, whether manual or automatic. The bellows required for the transfer tank is likely to require an expensive material, such as a specialist synthetic rubber, if it is to be proof to degradation over twenty and more years.

Otherwise component cost is based on the price of mild steel tubing. Fabrication of circuit is fairly complex, requiring a large number of pressure-proof welds.

8.5 Weight

The weight of the IR unit affects its usefulness in the field and its market appeal.

There are two main reasons for this. One is maintenance; as noted in the section above on "supportability", specialist technical support is likely to be needed every two years or so in valve maintenance. A low-weight machine is more conveniently transported to town where such a service may be available. Further, a low-weight machine can be initially commissioned the factory and transported as a sealed unit to site, without any need for engineers to travel to site.

The second reason a low weight design would extend the market for the device is that ice-making applications are sometimes peripatetic. For instance, an ice vendor selling for domestic use may prefer to move his machinery between sites through the year. Fishing activities in some cases shift ground once or twice a year as fish congregations move seasonally, as noted in Chapter 7. In this last case it may be convenient to transport machinery capable of making as much as 1 ton of ice per day or more. The IR device is predicted by computer simulation in Chapter 3 to have a "weight ratio" (WR) of between 7 and ll. Between 7 and ll kg of solution are needed to produce one kg of refrigerent, which in turn produces in practical terms 2 kg of ice in tropical conditions. Higher optimum flow rates than predicted were observed by experiment, indicating that weight ratios of l0 could be expected. This implies that a machine making 50 kg of ice per day would contain 250 kg of solution. Although such a size unit could be

carried by a pick up truck it would not be in practice be convenient to transport. Any serious commercial ice making unit would produce between 100 kg and 1 ton of ice per day. Even if it consisted of small ice maker modules each producing 250 kg, the transport difficulties would be prohibitive.

The indication very clearly is that IR units would normally be commissioned on site or maintained on site. The cost difficulties and delays involved in getting specialist engineers to remote places are well known. They are, indeed, the main reason why diesel generators linked to conventional compressor-driven ice makers have not proved reliable over the years in remote locations. In conclusion the high weight ratio of the IR unit combined with the need for maintenance severely limits its application in remote locations.

8.6 Comparative evaluation

This section discusses the IR system's merits and demerits in comparison with the alternative systems described in Chapters 1 and 2. The four criteria dwelt on above are taken in turn in the following four paragraphs, and then some general comparisons are made. The abbreviations IB, CP and DA, are used as in Chapter 1 for, respectively, the intermittent basic, continuous pumped, and diffusion absorption (or Platen-Munters, as developed by Electrolux and other firms) systems. Much of the discussion in this section is summarised in Tables 8.6.1 and 8.6.2.

The IB system could be fitted with the same number and types of valves as the IR system, and the same comments made on the supportability of valves in section 8.2 above apply to it. The CP system incorporates a solution circulation pump which will also require specialist maintenance. It is likely that the power source driving the

pump will need maintenance as well. The DA system is unique in respect of the supportability criterion, in that it contains no moving parts. In non-solar form it is a tried and tested technology in remote areas. A solar driven version promises full reliability since the problems experienced with DA units always associated with the boiler heater assembly rather than the refrigeration circuit. In terms of supportability, then, the DA system is ideal, and the IR system cannot be said to be an improvement on the other systems, except the CP system. It is certainly inferior to the DA. system.

In terms of solar COP, the IB system is low-efficiency with a solar COP of the order of 0.1. The DA system produces solar COPs lower than 0.1 because of the limited flexibility of the evaporator to changing heat input rates. In addition the DA system is unsuitable as an ice maker, because of the temperature gradient of the evaporator, and taken as an ice maker solar COPs are considerably lower still. The CP system has high efficiency if absorption temperatures are low, but because absorption is required during the day when temperatures are high, the solar COP is affected and is not likely to rise above 0.2. Higher COP can be obtained by increasing heat transfer area or introducing a cooling water circuit, but these options add expense and in the second case introduce unreliability. The IR system is a significant improvement on all these alternatives, having a solar COP of 0.25 and above, with the potential to reach values of COP of the order of 0.35 in climates which feature low night temperatures and clear days.

In terms of component cost the two intermittent systems, the IB and IR, have the advantage of rejecting heat during the night, as well as during the day, and so benefit from smaller overall radiator size and cost. In the case of the IB system either the collector can double

as an absorber radiator, or the condenser and absorber can share one radiator as proposed for the IR system. The continuous DA and CP systems reject absorption and condensation heat simultaneously and so require greater and therefore more costly radiator area.

The CP system suffers the disadvantage of requiring a costly solution pump and a separate power supply to drive the pump. In a fully solar driven unit the pump power can be drawn from photovoltaic cells which would introduce further expense. In the case of the DA system the extra complexity in plumbing introduced by the inert gas circuit raises the cost, as does the extra component involved, the gas heat exchanger. Nevertheless it is conceivable that the DA system can be built for only marginally more than the IR system, in the order of 15% or 20% more. The IB system will tend to be cheaper than the IR and the other two systems since it would normally use a flat plate collector, whereas the alternatives would normally use evacuated tubes. The CP will be more expensive than the IR, which promises overall to be a low–cost system in relation to its performance. It is unlikely to be as much as 2.5 times more expensive than the IB system, despite the use of evacuated tubes, although it is found to give 2.5 times the efficiency. Its cost effectiveness is therefore superior to those of the alternative cycles, given that the CP and IB systems also are likely to incur maintenance costs, and the DA system has very low efficiency, especially in ice making. The cost effectiveness of the IR system is nevertheless severely contrained by the high cost of evacuated tubes, and their replacement by less efficient but much cheaper heat pipe collectors could raise its cost effectiveness significantly.

In terms of weight the impracticality of transporting IR units has been pointed out earlier. The problems associated with on–site maintenance and commissioning in remote locations by specialist

engineers, or engineers with access to specialist resources such as pressurised containers of ammonia, are well known. The IB unit suffers the same constraint. The continuous DA and CP systems have considerably lower weight ratios: whereas a 50 kg of ice per day IR unit requires 250 kg of solution, a CP unit requires something in the order of 60 kg of solution, and is therefore very much more convenient to transport. A DA unit cannot make ice effectively but in terms of cooling energy provided at a range of temperatures, similar lightweight units are possible. Units with even smaller solution charges are conceivable at higher cost, given careful design of bubble pump and absorber arrangements to allow rapid process times.

Some attempts have been made to develop novel designs where absorption and desorption take place simulatenously – these are surveyed in Chapter 2, under the heading of Pumpless Continuous or Semi-continuous (SC) Systems. In all 3 cases, Chung, Zhang and Chinappa designed circuits without solution pumps in order to increase reliability and independence from auxiliary power sources. Although this end was achieved the practical experiments demonstrated low overall COPs in comparison to the IR system. Absorption heat rejection occurs during day-time in these systems. The number of components, implied overall cost, and the number of valves and moving parts is in all cases greater than those of the IR system. One possible advantage of these cycles is their lower weight, since unlike the intermittent systems, they require no reservoir of solution large enough to provide one cycle per day. In practice because of the use of transfer tank methods, greater solution charges are necessary than in the CP and DA systems, so weight reduction is not as great and no claim is made for portability.

System	Supportability	Solar COP	Component cost	Weight
IB	-active components: check valve, valve for nightly release of absorption heat (manual or automatic) expansion valve or drain valve depending on type of evaporator	-less than 0.12 since not flexible to variations in $\dot{G}$	-Aab low since integral collector and absorber -reduced cooling surface since Qcon and Qab out of phase	WR=7
CP	-active components: solution pump expansion valve regulating expansion valve if dry expansion evaporator used evap purging if gravity circulating evaporator used -day and night running possible with auxiliary heat source	0.2 day absorption at high temperature no self regulation of flow	-separate pump power supply -larger cooling surface since Qcon and Qab in phase	WR=2.5 less solution charge cost
DA	No active components day and night running possible with auxiliary heat source	less than 0.07 since evaporator matching suspect uneven Tev may limit application	additional component: gas heat exchanger plumbing more complex larger cooling surface since Qcon and Qab in phase	WR=2.5 less solution charge cost
IR (present study)	Identical to IB Active components: check valve, separator cooling valve, expansion valve or drain valve depending on evaporator type	-0.25 (better than CP since absorption governed by lower night temperature) -desorption phase flexible to variations in $\dot{G}$ -low separator thermal thermal mass possible (VVR) / analysis and rectification heat reclaim possible (VVR)	reduced cooling surface area since Qcon and Qab out of phase	WR: 7-11

Table 8.6.1 *Comparison of the aqua-ammonia systems studied. This comparison is based on applying standard operating conditions to all the systems, so that solar COP figures can be directly compared.*

	Reference Section	COP theoretical	COP practical	Description
IB	Williams (57) 2.2.1	int 0.37	int 0.36 sol 0.15	non-dedicated collector considerable manipulation no moving parts minimum complexity domestic scale
	Chinnappa (61) 2.2.3	int 0.3	int 0.26	
	Exell (81) 2.2.4		sol 0.09-0.14	flat plate collectors hourly adjustment of mirrors 60% of cost in collectors small scale
	Exell (84) 2.2.4		sol 0.11	scaled for 100 kg ice per day automatic except for water purging
CP	Sloetjes (88) 2.3.1		sol 0.08-0.15	3 KW continuous (24 hr) cooling rate pumped cooling water collectors: ETCs
DA	Hinotani (83) 2.4.2		sol 0.05	fully automatic collectors: ETCs
SC	Chung (61) 2.5.1	int 0.47 sol 0.2		continuous for 23 hours manual transfer switching complex
	Zhang (82) 2.5.2	sol 0.17	sol 0.15	pumped cooling water complex
	Chinnappa (84) 2.5.3	int 0.39	sol 0.13 η_{coll} 0.35	fully automatic complex
IR	Van Paassen (86) 2.6.2	int 0.6	sol 0.1	fully automatic problems with expansion valve inefficient flat plate collector excessive thermal mass
	Harvey (88) (in present study)	int 0.5 sol 0.25	int 0.5	fully automatic collectors: ETCs

Table 8.6.2 *Comparison of COP figures reported by various researchers including the present study. The figures given cannot strictly be compared because of variations in operating conditions and assumptions, but nevertheless are an indication of relative performance.*
Key: int = internal ; sol = solar.
ETC = Evaccuated tube collector. SC = semi-continuous systems

A final point of comparison is worth noting. The IB and IR systems are simpler to fabricate than the other systems described. Steel tubing and appropriate valves (if manual) can be bought readily by provincial fabricators. Skilled welding is generally available. The DA system is more complex, and requires a third working fluid; the CP system requires a pump. The greatest difficulty met in the fabrication of the IR system is the procurement of evacuated tube solar collectors, which are expensive and made by very few suppliers.

8.7 Conclusions

The study reported in the preceding chapters has established a number of things.

Firstly, the investigation of the market demand for remote ice makers has uncovered a very strong economic incentive (in the realm of inland fishing in Africa with implications for other areas, notably Pacific islands) for pursuing their design and development. It has shown that remotely placed devices could make a significant difference to the economic situation of people living in remote areas. By showing how such devices would be used from the economic point of view, a firm basis is laid which allows any persons concerned with rural development to devise strategies for channeling the expected economic benefits equitably.

Secondly, the study devises in detail a new absorption ice making cycle (the IR cycle) which promises to be a significant improvement on existing cycles. Several new discoveries and departures are made in design. While regeneration improves desorption efficiency by around 100%, the discovery is made that the regenerator (solution heat exchanger) impedes transfer from desorption to absorption phases. To overcome this separator cooling is needed. A novel method is devised

to provide separator cooling while also providing condenser and absorber cooling; this is the 3-branched heat pipe cooling circuit. A separate problem is identified, which is that both the finite quantity and the thermal mass of the separator fluid is a constraint on cycle efficiency, and a method is invented of removing this constraint. This is the transfer tank or 'VVR' (variable volume reservoir) method. Apart from improving desorption efficiency this design feature also promises to remove the need for a separate separator cooling circuit and diurnally switched valve.

Thirdly, the study develops a computer model of the cycle. The computer model predicts the efficiency of the cycle and is checked against an experimental study which confirms that the predicted efficiencies are obtainable in practice. The experimental study investigates the responsiveness of the system to changing heat input and confirms the predictions of the simulation. Experiments also establish the validity of evaporator performance predictions made in subsidiary computer models. The main computer model is useful in allowing the IR unit's performance to be predicted for different regions with different metereological conditions. For instance, a unit destined for the Sahara Desert will be shown to have a very different COP to one destined for the climate of Thailand. The computer model therefore allows economic feasibility studies to be made separately for different regions.

The computer model also allows specific components to be sized, for instance the solution heat exchanger, reservoir, condenser, separator and collector. It allows critical dimensions or settings to be decided, for instance the bubble pump height or circuit resistance constants. A second model of the absorption characteristic of the cycle allows the heat pipe condenser area and evaporator area to be sized, and the

spring setting distance on an expansion valve to be decided. The model can be run for different climates allowing specific sizing decisions to be made.

Fourthly, extensive building of experimental apparatus has been undertaken, and tests conducted. These have allowed both calibration of the computer model, and close experience of the fabrication constraints of the IR unit to be gained. This has indicated that construction of such apparatus with simple techniques and tools (welding, straight for work machining, pipe bender, vice, etc.) is possible and that therefore manufacture in provincial towns in developing countries is possible. The task of handling and mixing ammonia-water solution, and the task of dealing with entrained gases, proved possible with simple equipment.

Finally, the study has allowed the promise of the IR cycle to be fully evaluated. The cycle proves to be the most efficient of the aqua-ammonia cycles considered, in terms of year round performance. Because it relies on expensive evacuated tube collectors, much of the advantage of the high efficiency is lost, but the indication is strongly that it is the most cost-effective of the cycles considered. Unfortunately it is demonstrated also that the cycle falls badly on two further counts which determine whether or not it is in practice suitable as a technology for remote areas. It is found to be too cumbersome for transport, on the one hand, and dependent on maintenance of moving parts (valves), on the other hand. The methodology devised for evaluation is useful, and these conclusions are useful in that they point the way ahead toward improving the technology. In comparison with the three alternative cycles considered, the IR system, though far from the perfect answer, remains nevertheless an improvement. The DA system is too inefficient and inflexible to be economic; as a solar

driven unit; the CP and IB systems have similar or worse maintenance requirements than the IR system while having lower cost-effectiveness.

8.8 Further Work

Various design options for the intermittent regenerative (IR) system have not yet been tested. The transfer tank and small separator which constitute the variable volume reservoir (VVR) option shoulld be incorporated into a modified version of the experimental apparatus. This should preferably be done before testing of the apparatus under varying heat input regimes, or before fitting of the apparatus with solar collectors.

The heat pipe cooling circuit should then be tested, with and without a separator cooling branch. The possibility of depressurisation or separator cooling by simple manual removal of separator insulation could then also be tested. A further design option which should be built and examined experimentally in the IR circuit is the bubble pump design proposed by Hinotani; its performance at low flow should in particular be investigated, with a view to overcoming the failure of the present apparatus to achieve steady state operation at low flow as reported in Chapter 6. It should also be examined with a view to improving its design to raise system efficiency by virtue of analysis and rectification heat exchange.

Some redesign of the solution heat exchanger is indicated by the experimental results achieved to date. A heat exchanger of better effectiveness at low flow than realised to date should be devised. It may be worthwhile to initiate work on this by conducting extensively instrumented tests of a shell and tube heat exchanger of the kind used in the experiment, operating with water first as a working fluid. First priority in further work should be given to exchanger design aimed at

achieving high effectiveness at low flow, since this will result in a machine with less overall weight and smaller separator size. The comparison of theoretical and practical results presented in Chapter 6 also indicates that the computer simulation should be refined with respect to solution heat exchanger performance in relation to solution flow, since the prediction of optimum flow was found to be at variance with actual optimum flows. There is a clear need for collecting a larger number of practical test results in order to characterise performance at higher flow rates. Tests should also be conducted with varied parameter values, for instance different solution concentrations (reflecting different absorption temperatures) and different condensation temperatures, in order to calibrate the computer simulation fully. Having done this the computer simulation in its dynamic form can be run for yearly or seasonal climatic regimes, in simplified form, of specific locations. This work will allow economic projections to be made for those locations.

Earlier sections of this chapter evaluated the IR device in general terms, and identified several major problems which affect its suitability as a remote solar cooling device. The use of valves in the IR circuit is a case in point, and a priority area in further development is the removal of these valves. The use of a gravity-circulating evaporator is recommended since it does not require the expansion valve of the dry expansion evaporator. The expansion valve is a complex and expensive component, potentially unreliable, and can seemingly only be substituted by alternatives (such as capillary tubes) which are similarly undesirable. The gravity-circulating evaporator requires a drain valve (or evaporator purging valve) only because the absorbent envisages here is water. Accordingly the IR cycle should be tested with a non-volatile absorbent, the recommended option being sodium

thiocyanate (NaSCN). Research into use of the NaSCN–NH_3 pair in IB cycles has proved it to be as efficient or more efficient than H_2O–NH_3 without any serious practical constraints being imposed, in tests made with the IB cycle. It is possible that NaSCN–NH_3 crystallisation conditions will occur in an IR cycle, freezing the solution circulation. Apart from this possibility, no major design changes are implied in making the substitution and it is likely that it will remove the need for an evaporator purging valve.

The possibility of substitution of the check valve by a liquid seal has already been discussed. It is likely that further work on the development of the liquid seal will make this a reliable alternative.

The removal of the separator cooling valve may be an outcome of successful incorporation of the variable volume reservoir design option. This replaces the large separator with a transfer tank and small separator, such that separator cooling can very likely be achieved by naturally convected heat loss. The valve would be replaced by manual removal of separator insulation each evening.

A large proportion of the cost of the solar IR device is in evacuated tube collectors. Development of low cost alternatives is also a priority. This work would also be directed at local fabrication of the collectors, and the use of collectors more robust than the evacuated tubes.

The weight and bulk of solution charge required by the IR device has been identified as a major problem. Only radical redesign can remove this, shifting the design philosophy toward the 'continuous' or 'semi–continious' cycle options where desorption and absorption occur concurrently. An example of a possible direction here is the development of a system where two or more small intermittent systems operate on a fast cycle, with small reservoirs, out of phase

with other. The disadvantage of continuous options such as these have been pointed out – twice the heat rejection radiator area is needed, and absorption takes place at daytime temperatures, unless provisions are made to store night temperatures for use in the day.

The collector cost of the IR system can be reduced significantly if efficiency during low insolation periods (morning, evening, cloud) is raised. Auxiliary heating from, for instance, an open biomass burner circulating steam to the refrigerator boiler tube, could be arranged to add power at these times.

The rejection of solar heating altogether as a design option is a possibility deserving serious investigation. The present study has demonstrated in many ways the disadvantages of the solar element – these are high cost, and poor efficiency during low insolation periods giving rise to low year round efficiency. Local fabrication of advanced collectors is difficult, and imported evacuated tubes are fragile and difficult to replace when broken. In contrast an open biomass stove can be fabricated locally at low cost and does not suffer a significant fall in efficiency when solution is boiled to optimum temperature. Consequently low flow rates, which are achieved at higher temperatures, are permissible and less solution charge is required, resulting in the convenience of a lighter and more compact IR unit.

References

Backstrom, 1965, "Kaltetechnik" G Braun, Karlsruhe

Borseau P, Bugarel R, 1986, "Refrigeration par cycle a absorption-diffusion: comparaison des performance des systemes NH3-H2O et NH3-NaSCN" International Journal of Refrigeration Vol 9 pp 206-214

Bosnjakovic F, 1937, "Technische Thermodynamik" transl. P.L.Blackshear, 1965, Holt Reinhart & Winston, New York

Brinkworth, B J, 1972, "Solar Energy for Man" Compton Press, London and Halstead Press, New York

Chinnappa J C V, 1961, "Experimental study of the intermittent vapour absorbtion refrigeration cycle employing the refrigerant-absorbent systems of ammonia water and ammonia lithium nitrate" Solar Energy Vol 5 pp 1-18

Chinnappa J C V, 1962, "Performance of an intermittent refrigerator operated by a flat-plate collector" Solar Energy Vol 6 No 4 pp 143-50

Chinnappa J C V, Kok P L, 1986, "A continuous cycle ice plant" Proceedings of Solar Cooling Workshop 1984: Active solar cooling systems, ISBN 0 86443 201 1, Indian Institute of Technology Madras India and James Cook University of North Queensland Australia

Chung R, Duffie J A, 1961, "Cooling with solar energy" New Sources of Energy: Proceedings of the United Nations conference (Rome) Vol 6 pp 20-28

Crees M R,1986, "State equations for ammonia-water mixtures" Proceedings of Solar Cooling Workshop 1984: Active solar cooling systems, ISBN 0 86443 201 1, Indian Institute of Technology Madras India and James Cook University of North Queensland Australia

Douglas J F, Gasiorek J M, Swaffield J A, 1979, "Fluid Mechanics" Pitman, London

Eisenstadt M, Flanigan F, Farber E, 1959, "Solar air conditioning with an ammonia-water absorption refrigerating system" ASME Paper 59-A-276

Exell R H B, 1978, "Using the sun to power a refrigerator" Appropriate Technology, Vol 5 No 3, pp 4-6

Exell R H B, Komsakoo S, Oeapipatanakul S, Chanchaona S, 1984, "A village-size solar refrigerator" Bangkok: Asian Institute of Technology. Research report no 172

Exell R H B, Kornsakoo S, 1981, "Design and testing of a solar powered refrigerator" Bangkok: Asian Institute of Technology. Research report no 126

Gosney W B, 1982, "Principles of refrigeration" Cambridge University Press

Green, 1985, private communication, Electrolux, Luton, U.K.

Gutierrez F, 1988, "Behaviour of a household absorption-diffusion refrigerator adapted to autonomous solar operation" Solar Energy Vol 40 No 1, pp 17-23

Harvey A B, 1987, "Performance of an intermittent regenerative cycle for solar cooling" Proceedings Solar World Congress Hamburg, Pergammon Press, Oxford

Haseler L E, Robertson J M, 1978, "Absorbtion cycle heat pumps for domestic heating" (Harwell: AERE - G 1049)

Heywood H, 1953, "Solar energy: past present and future applications" Engineering Vol 176, Pt 4573/4, pp 377-380 and 409-411

Hinotani K, Kanatani K, Osumi M, Moroto M, 1984, "Development of a solar absorption refrigeration system" in Szokolay S V (editor) Solar World Congress Pergammon Press Oxford pp 507-531

Hirschmann J R, 1974, "The cosine function as a mathematical expression for the processes of solar energy" Solar Energy Vol 16, pp 117-124

Holman J P, 1981, "Heat transfer" McGraw-Hill International, Singapore

Integron: IMI Yorkshire Alloys Ltd, 1987, private communication, Leeds, U.K.

International Institute Refrigeration, 1976, "Refrigeration techniques in developing countries", Paris

Jain P C, Gable G K, 1971, "Equilibrium property data equations for aqua-ammonia mixtures" ASHRAE trans.

King G R, 1971, "Modern Refrigeration Practice" McGraw Hill Book Co, New York

Mahjuri, 1986, private communication, Thermomax, Bangor, N. Ireland

Merrick R H, 1960, "An air-cooled absorption cycle" ASHRAE trans Vol 66 pp 339-346

Monsoori G A Patel V, 1979, "Thermodynamic basis for the choice of working fluids for for solar absorption cooling systems" Solar Energy Vol 22, pp 483-491

Moore G L, Farber E A, 1967, "Combining the collector and generator of a solar refrigeration system" ASME paper 67-WA/sol 4

Niebergall W, 1959, "Sorptions-Kaltemaschine" in "Handbuch der Kaltetechnik" Vol 7, ed R Plank, Springer, Berlin

National Academy of Sciences, 1978, "Post-harvest food losses in developing countries", Washington, U.S.A

Persson S, Svensson O, 1982, "Solar refrigeration to deepfreezing temperatures with the absorbtion process" Lund: Lund Institute of Technology, Sweden

Saunier G Y, Reddy T A, 1986, "Multi-fuel ice-making machine" (Bangkok: Asian Institute of Technology. Research report no 190)

Scratchard G, Epstein L F, Warburton Jr J, Cody P J, 1947, "Thermodynamic properties of saturated liquid and ammonia-water mixtures" Refrigeration Engineering, May 1947, pp 413-419 and 446-452

Shiran Y, Shitzer A, Degani D, 1982, "Computerised design and economic evaluation of an aqua-ammonia solar operated absorption system" Solar Energy Vol 29 No 1 pp 43-54

Sloetjes W, Haverthals J, et al, 1988, "Operational results of the 13 KW/50 m^3 solar driven cold store in Khartoum, The Sudan" Solar Energy Vol 41 No 4 pp 341-347

Stoecker W F, Reed L D, 1971, "Effect of operating temperatures on the coefficient of performance of aqua-ammonia refrigerating systems" ASHRAE trans., Vol 77 pt 1 pp 163-70

Svensson O, Hansson H, 1979, "A survey of existing solar powered refrigeration systems for food storage and a method for calculation for a solar powered Platen-Munters system" (Lund: Lund Institute of Technology, Sweden)

Swartman R K, et al, 1975, "Comparison of ammonia-water and ammonia- sodium thiocyanate as the refrigerant-absorbent in a solar refrigeration system" Solar Energy Vol 17 pp 123-27

Trombe F, Foex M, 1957, "The production of cold by means of solar radiation" Solar Energy Vol 1 No 1 pp 51-52

Van Paassen J P, 1986, "Testing of a solar powered refrigerator" Delft: Delft University of Technology, Netherlands

Whitlow E P, 1976, "Relationship between heat source temperature, heat sink temperature and coefficient of performance for solar powered absorption air conditioners" ASHRAE trans., Vol 82 pt 1 pp 950-8

Williams D A, Chung R, Lof G O G, Fester D A, Duffie J A, 1957, "Intermittent absorption cooling systems with solar regeneration" Paper No 57-A-60 ASME

Zhang Zhi-jing, 1982, "A study on pumpless circulating ammonia water absorption solar refrigeration system" Zhileng. Xllebao No 2 pp 28-36

References particular to implentation study

Food Strategies Study, 1983, Ministry of Agriculture and Water Development .IP

Subramaniam, S.P., 1985, "Recent Trends in Fish Utilization in Zambia", Department of Fisheries, Zambia. Also discussion.

Hayward, P., 1983, "Production in Zambian Fisheries", Institution of African Studies, University of Zambia. Also discussion.

Tapiador, D.D. 1986, Project Co-ordinator, World Bank Fisheries Development Project. Discussion.

McVeigh J C, 1983, "Sunpower" Pergamon Press, Oxford

Pearce, M.J. 1986, Fisheries Research Officer, Mpulungu. Discussion.

Beatty D, 1969, "Results of a Fish Marketing Survey in Zambia 1964-65", Ministry of Rural Development, Department of Wildlife and Fisheries

Hutchinson J, Director, Laker Fisheries, Sinazongwe, Lake Kariba. Discussion

Brignot C. 1986, Director, Cape Kaches, Nsumbu, Lake Tanganyika. Discussion.

Lester B, Project Co-ordinator, Luapula Fishermen's Co-operative Project, Mansa.

Allen M C, 1986, "The Unbaptised: Farming in a fishing economy - the case of the Mweru-Luapula Lakeshore, Zambia", Rural Research Station, Mansa. Advanced Research Planning Team, Lusaka.

Annexes to implementation study

Annex A

Itinerary of visits made in Zambia (1986)

January 21-24	Lusaka	Department of Fisheries: Dr. Subramaniam Inst. African Studies: Dr. P. Haywood
January 25-29	Kariba	Local fish-traders and fishermen, near Siavonga
January 30-April 4	Lusaka	Local fish-traders and ice retailers. Technology Development Advisory Unit: M Tembo. UNICEF: Y Mesfin
April 5-8	Nyanje	District hospital and rural health clinics
April 13-14	Lusaka	Zambia Steel and Building Supplies Mr. Shankar, Nitrogen Chemicals Mr. Mack, Director, BMS Engineering
April 17-21	Mupulungu	M. Pierce (Fisheries Research Officer) Sopelac (para-statal purse seining company) Mr. Gondwe (fishing proprietor)
April 23-25	Nsumbu	C. Brignot, Director, Kape Kaches Fishing Co. Mr. Lulemba, World Bank Zonal Office Mr. Kasambala, Fisheries Officer
April 27	Nsama	Mr. Sichona, Asst. Research Officer for Lake Mweru-Wantipa
March 1-4	Kaputa	Kawama fishing village: fishermen, traders Rural health clinics
March 6	Nchelenge	Luapula Co-op at Ntoto village P. Shikoswe; Research Officer for Make Mwera-Luapula

March 8, 22	Mansa	Luapula fishing co-operative, B. Lester Ministry of Agric: P. Fernandez (IRDP, SIDA) ONV (Dutch aid): M. Reile (Regional director) T. de Kuyer (IRDP, Engineer)
March 11-14	Lusaka	EEC Delegation, Mr. Loher, (Agricultural Advisor)
March 15-16	Kariba	Lakar Fishing Co. Director, J. Hutchinson
March 18-20	Lusaka	Zambia Co-op Federation, Agric. Dev. Bank: L. Avila (Director Operations) Fisheries Dept: E.Muyanga (Director) Meteorological Office

Annex B

Retail Cost of Solar ice-making device

Specification of unit: One tonne of ice per day,
300 days per year in Zambian insolation conditions.

	KW
Steel tubing and NH3	25,000
Overheads and wages	25,000
Collectors (2000 at KW100 each)	200,000
Manufacturer's mark up	50,000
Retail price	300,000

Annex C

Loan repayment calculations

Following McVeigh (1977) a constant annual repayment can be calculated by expressing the outstanding balance on a capital loan (C) after a repayment (Y) as an algebraic equation referring to the year of payment, e.g the m th year. If the interest rate is i where i is a fraction (ie 10% interest is an i of 0.1), then the outstanding balance at the end of the first year once a repayment of Y is made, is :

$$C(1+i)-Y$$

The debt owed is C + Ci but the repaid quantity is Y. Y is a constant repayment quantity made each year. At the end of the m th year the outstanding balance is:

$$C(1+i)^m-\frac{Y(1+i)^m}{i}+\frac{Y}{i}$$

If the debt is paid off in n years then:

$$C(1+i)^n-\frac{Y(1+i)^n}{i}+\frac{Y}{i}=0$$

Therefore:

$$\frac{Y}{C}=\frac{i(1+i)^n}{(1+i)^n-1}$$

Therefore if effective interest is 20% and n is 10 years, the capital repayment factor Y/C is 0.238.

If n is 5 years, the repayment factor is 0.343. If n is 3 years, the repayment factor is 0.475.

Annex D

Fish trading profits

The following is an attempt to provide a simple but hopefully adequate analysis of data on fish trade practice and market conditions. By formulating the information in the following way some prediction can be made as to the likely behaviour of fish traders should new opportunities, such as the availability of solar made ice at fish collection points, be made available to them at given prices.

Since fish traders undertake collection journeys of variable lengths under variable conditions (of market price, fish type available, climate. etc.) a great many possible calculations based on a considerable amount of data should be made; consequently an algebraic approach is suitable:

Distance covered by journey (km)	D
Out journey period (days)	NO
Collection period (days)	NC
Return journey (days)	NR
Total period (days)	N
Vehicle costs per km (KW/km)	
(including fuel and capital depreciation)	VC
Travel costs per day (KW/day)	
(including food and accommodation)	TC
Calculate total overheads for complete trip (KW):	(TC.N + VC.D)
Going rate for passenger carriage per km (KW/km)	E
No. of passengers taken	G
Total distance over which passengers taken (km)	DP
Calculate total earnings from passenger carriage:	DP.E.G
Melt rates assume standard insulation (sawdust packing):	
Melt loss (Melt fraction x no. of days x original mass of ice):	
Melt fraction on out journey (kg/kg.day)	MRO

Melt fraction on return journey (kg/kg.day) MRR

Ratio of quantity of fish/quantity of ice required to successfully complete return journey (function of NR, MRR, but often on practice known directly from experience for typical return journey durations. A value of one is recommended by government authorities for typical journeys, a value of 1.5 - 2 is often used in practice, leading to poor quality fish found in the market R

Amount of ice required to be bought (kg) IB

Quantity of ice remaining for preservation of fish (kg) QI

Express QI in terms of ice bought minus melt loss

$$QI = IB (1 - MRO. (NO + NC/2))$$

Quantity of fish returned QF

Quantity of fish returned as determined by amount of ice available and ice: fish ratio demanded by return

$$QF = R.QI$$

Going price of ice (KW/kg) I

Total price paid for ice on journey (KW) I.IB

Buying price of fish (KW/kg) BF

Selling price of fish (KW/kg) SF

Total mark-up on fish sale QF.(SF-BF)

Total revenue from journey summing fish mark-up and passenger earnings:

QF. (SF - BF) + DP.E.G

Total journey costs (overheads plus cost of ice): (TC.N + VC.D) + I.IB

Total journey profit: QF.(SF-BF) + DP.E.G. - (TC. N + VC.D) + I.IB

Profit per day (P):

$$P = 1/N\ (QF.\ (SF - BF) + DP.E.G. - (TC.N + VC.D) - I.IB)$$

where $QF = R.IB.\ (1 - MR0.\ (NO + NC/2))$

A disadvantage suffered by urban ice buyers is that they cannot predict exactly what quantity of fish they will find and how long it will take to collect a full load. It is safe to assume that they will buy enough ice to cover them for a full return load. They therefore stand either to lose some investment in ice if they return under load, or they stand to lose the freshness of the fish found if they spend too long collecting a full load. A solar ice buyer does not suffer this disadvantage since the ice necessary to return the fish fresh can be supplemented by buying ice at the final collection point, before setting out on the return journey.

If the full load capacity of the vehicle is C, then

$$C = QF+QI = QF + QF/R = QF\ (R+1)/R$$

$$QF = R\ C\ /\ (R + 1) \text{ and}$$

$$IB = QI/(1 - MRO(N0 + NC/2))$$

$$IB = (C - QF)/(1 - MRO(N0 + NC/2))$$

The urban ice buyer in principle uses this equation to calculate the amount of ice needed to return a full load, hoping that the guess as to collection time (NC) is correct.

Comparison (1)

Following is a numerical comparison (using the above equations) between a typical journey practised at present, and a speculative one utilising solar-made ice marketed at distribution points. The vehicle is a 2-tonne truck ; the journey is Kitwe to the Mweru area and back.

The assumption is that the urban ice buyer guesses perfectly the time required for collection, and so returns with a full load, but note is made as to possible loss due to poor matching with supply conditions, which could lead to return under load.

Calculation of the price at which solar ice is sold is made elsewhere. Here it is assumed to be considerably more expensive, 0.5 KW/kg as compared to 0.15 KW/kg in town.

URBAN ICE	SOLAR ICE
C = 2000 kg	same
D = 1000 km	same
N0 = 2 days	same
NC = 6 days	same
NR = 2 days	same
N = 10 days	same
VC = 1.5 KW/km	same
TC = 20 KW/day	same
E = 7.5E-2 KW/km	same
G = 0	10
DP = 0 km	500
MRO = 0.125 kg/kg day	0
R = 1.5 (fish:ice ratio)	same
BF = 2 KW/kg	same
SF = 8 KW/kg	same
I = 0.15 KW/kg	0.5 KW/kg

(1.1) Urban-ice buyer:

Quantity of fish ideally returned as determined by capacity of truck

$QF = RC / (R + 1) = (3/5)\, C = 1200$ kg

$IB = (C - QF)/(1 - MR0\ (NO + NC/2))$

$IB = (2000 - 1200)/(1 - 0.125\ (2 + 3)) = 2133$ kg

The urban ice buyer is therefore constrained to bring back less fish because his truck will not carry enough extra ice to compensate for the melt loss. (Alternatively he may raise R and risk bringing back fish further deteriorated). By constraint of truck capacity, IB = 2000 kg.

Ice surviving melt loss:

QI = IB(1 - MRO (NO + NC/2) = 2000 (1 - 5/8) = 750 kg

Quantity of fish actually bought and marketed:

QF = R.QI = 1.5 x 750 = 1125 kg

Revenue from sales: QF (SF - BF) = 1125 (8-2) = 6750 KW

Passenger earnings : nil.

Vehicle and travel costs:

(TC.N + VC.D) = 20 x 10 + 1500 = 1700 KW

Cost of ice bought: I.IB = 0.15 x 2000 = 300 KW

Profit per day: P = 1/10 (6750 - 1700 - 300) = 475 KW/day

The prospect of this profit is much reduced by the risk of the ice and fish purchases being mismatched. The "trader" may of course be a group of 2 persons or more between whom the profit is shared.

(1.2) Solar-ice buyer

Fish bought: (QF . R . C) / (R + 1) = (3/5) C = 1200 kg

Ice bought: IB = (C-QF) = 800 kg

Revenue from sales: QF (SF - BF) = 1200 (8-2) = 7200 KW

Passenger earnings: DP.E.G = 10 x 7.5 x 5 = 375 KW

Vehicle cost = 1700 KW as before

Cost of ice bought: I.IB = 0.5x800 = 400 KW

Profit per day: P=0.1 x (7200+375-1700-400) = 577 KW/day

In contrast to the case of the urban-ice buyer the prospect of this profit is not reduced by a risk of mis-match of fish and ice purchases. This is the major benefit of solar ice purchase, but is not reflected in the present calculation. It is noticeable that the opportunity to fill the truck to full capacity increases revenue more than the decrease due to purchase of ice at a higher price. The

opportunity to earn from carriage also compensates for the increase in price of the ice.

Comparison (2)

It is safe to predict that the availability of solar ice locally will result in fish being more readily available at the lake shore in larger quantities, since fisherpeople will be able to store and greater incentive will exist to pull larger yields. The collection period (NC) can then become considerably shorter. The profit of a trader in this case, following the same conditions as described in comparison (1), can be calculated.

If the parameter values taken above are repeated, excepting that NC = 1, N = 5, and D becomes 900km as an estimate of saving on distance travelled, then the profits of traders buying solar ice are considerably improved:

Vehicle end travel costs: (TC.N + VC.D) = 20.5 +1350 = 1550 KW

Profit per day: 0.2 x (7200+375-1550-400) = 1205 KW/day

The reality would possibly be an increase in the price of fish at the point of landing, due to the local storage facility, so that effectively a portion of the profit calculated here would be retained by the fisherpeople.

Comparison (3)

One journey discussed detail with one group of traders in Lusaka is from Lusaka to Chipepo on the Kariba shore. Most of the data used here is provided verbally by the traders and not checked against any other source. The landrover used could carry 1.3 tonnes of fish and ice together. The ice was bought in Mazabuka for 0.15 KW/kg and packed with sand in 2 sheet metal boxes roughly insulated with 2'' thick polystyrene. The profit calculation based on collected data is first presented, and then compared with a speculative calculation involving solar ice. The comparison illustrates the point that the availability of cheap urban ice near to fish landing sites does not alter the economic advantage of using solar ice.

Profits of interviewed traders

Overall distance (D) = 700 Km

Distance travelled on out journey (Do) = 300Km

Distance ice transported on out journey (Di) = 150 Km

Time for which ice transported (Di/Do).NO + NC/2

NO = 1, NC = 3, NR = 2, N = 5

VC = 1 KW/km (oil cost 100KW and diesel 230KW for whole journey)

TC = 10 KW/day

QI = 300 Kg (traders estimate very approximate)

QF = 700 Kg (ditto)

BF = 2 KW/Kg on average

SF = 8 KW/Kg

Revenue from sales = QF(SF - BF) = 4200KW

Vehicle and travel costs = TC.N - VC.D = 5 x 10 + 700

Ice bought = IB = QI/(1-MRO((Di/Do) NO + NC/2)) = 300/(1-0.125 x 2)=400 kg

Cost of ice bought = 60 KW

Passenger earnings (5 passengers) = ((Do-Di)/100) x 7.5 x 5 = 56 KW

Profit for whole journey = 4200 + 56 - 750 - 60 = 3446 KW

Profit per day = 3446/5 = 689 KW

The traders stressed that more often than not they experienced a mechanical breakdown and lost money on such a trip. They also said that fish were picked up in small quantities from fishermen at different sites to which access was difficult and slow. The following calculation shows the effect of loading the vehicle to full capacity should ice be available locally. Solar ice is assumed to cost 0.5 KW/Kg:

Speculative profits with solar ice

If the conservative assumption is made that solar ice use does not improve the fish:ice ratio, and does not lead to earnings from carriage, nor to a reduction in the collecting period and total distance travelled, then the only advantage is the return of a greater load:

C = QI + QF = 1300 kg (fish and ice together)

QF = R . QI = 7/3 QI = 2.33 QI

QI = 1300/(1 + 2.33) = 558 kg

QF = C - QI = 1300 - 558 = 742 kg

Cost of ice bought = 0.5 x 558 = 279 KW

Revenue from sales = 6 x 742 = 4452 KW

Vehicle and travel costs as before = 750 KW

Profit for the whole journey = 4452 - 750 - 279 = 3423 KW

Profit per day = 3423/5 = 684 KW

The extra 42 kg of fish returned does not compensate for the higher price of solar ice. If this price is 20% less (near to the price calculated as a retail price in Table 7.1) the daily profit rises only to 696 KW/day.

The calculation can be repeated assuming the ratio of fish to ice is higher, say R=3, since given the availability of solar ice the second half of the collecting period is shorter. D is reduced to 600 km. N is reduced to 3.

C = QI + QF = 1300 kg (fish and ice together)

QF = R . QI = 3 . QI

QI (1 + 3) = 1300 kg

QF = 975 kg

Cost of ice bought = 0.5 x 325 = 162 KW

Revenue from sales = 975 x 6 = 5850 KW

Passenger earnings possible on the out journey (5 passengers) = 112 KW

Vehicle costs VC.D = 600 KW

Travel costs TC.N = 30 KW

Profit for the whole journey = 5200 KW

Profit per day = 5200/3 = 1733 KW/day

Added to this possible incentive is the the security of finding fish and ice together, although this may also imply a higher buying price. At present this group of traders is forced spread the finance from successful trips to cover unsuccessful ones.

Annex E

1. NET REVENUE

	thousands KW
50 tonne boat and engine	500
30 tonne freezer capacity at base (mains electricity)	300
Total	800
Constant Annual Repayment at interest rate	
of 25%, 10 years payback (reduce capital by repayment	
factor 0.28, annex C)	224
Yearly Running Costs	
Freezer site overheads, maintenance, electricity	20
Boat diesel consumption (3 day trip of 250 km consumes	
600 litres at 2 KW per litre; 100 trips per year)	120
Oil consumption (50% diesel cost)	60
Boat overheads, maintenance (10% of capital)	50
Crew cost (2 skilled crew at 600 KW/month, 3 unskilled	
handlers at 600 KW/month)	21.6
Wages onshore	20
Total running costs per year	291.6

Fish buying price 2 KW/kg.

Competition between land and boat buyers and the use of solar ice may raise this price further which will reduce town trade profits, at present very high, rather than

boat collection company profits .

Fish sold to traders at 3 KW/Kg. Boat collection service mark up is therefore 1 KW/Kg. (Fishery research officers agree that this is a conservative estimate).

Turnover is 3,000 tonnes of fish per year.	millions KW
Gross revenue	3

Fish : ice ratio is on average 3:2

(1:1 is sufficient to store fish for 3 days; some of the fish require less storage time). Quantity of ice used each year is 2 Million Kg.

(a) Cost of ice depends on whether boat collection company owns the ice-makers or not. Assuming they do then production cost of 0.33 KW/Kg is paid.

Cost of ice per year:	0.66
In summary : gross revenue/year	3
cost of ice/year	0.66
capital repayment/Year	0.22
running costs/year	0.29
Net revenue/year	1.83

(b) If ice makers are owned by independent entrepreneurs the company will pay a retail cost of 0.39 KW/Kg (annex I). Cost of ice per Year retail: 0.78

In summary : gross revenue/year	3
cost of ice/Year	0.78
capital repayment/Year	0.22

running costs/year	0.29
Net revenue/Year	1.71

2. SHORT PAY-BACK PERIODS

In both cases the above calculation implies that loan payback times of less than 3 years are possible. For a 3 year loan at 25% effective interest, the capital repayment factor is 0.51 (annex C). For the boat collection service the yearly repayment is therefore 0.4 million KW. The cost of solar ice in case (b) would raise to 0.62 KW/Kg.
(Payback for ice plant owners is also reduced from 10 to 3 years).

In summary : gross	revenue/year	3
	cost of ice/year	1.2
	capital repayment/year	0.4
	running costs/year	0.29
	Net revenue/year	1.11

Annex F

Road access to most of the shore of Lake Kariba in limited (Figure 7.4). The Zambian fisheries research department looks upon boat collection services on the lake as very promising (Subramaniam, 1985). The output of Lake Kariba is mostly of small kapenta which are dried. Some kapenta are marketed frozen but they are not suitable for preservation over long periods with ice due to their physical delicacy. The lake also produces larger fish which are mostly consumed fresh; these are bream and to a lesser extent tiger fish, bottle nose and cornish jack. The sustainable potential of the lake is for an extra 2000 tonnes a year of these larger fish. It is quite likely that these fish are not caught and marketed only because of the lack of a transport route. The illegal practice of beach seining, which on other lakes tends to reduce the bream population due to nesting-site disturbance and landing of juveniles, does not occur on Kariba because of the presence of vegetation and trees below the water surface. (Gill netting fishermen on Kariba spend as much as half their labour time on net repairs). Certainly the operators of boat collection services stand to make considerable profits.

An interview with Lakar Fisheries on Kariba (Hutchinson, 1986) clarified the difficulties. In addition to Kapenta fishing, drying, and marketing, Lakar also buy bigger fish from local gill netters to freeze and market in fresh form. They are exceptional in having access to mains electricity because of a loan of Maamba Mine premises. For a period they sent a boat of 500 kg capacity 50 km down the lake to collect from a fishing crew of their own stationed near Nanazambwe. (Figure 7.4). Ice was carried in sawdust insulation and stored on arrival in a commercial freezer container acting as a cold box with 2" polystyrene insulation complete with sealing door. The melt rate experienced was between 10% and 15% of original weight per day. In 4 days 400 kg of ice in 25 kg blocks would reduce to 200 kg. The collection of fish from local gill-netters, dispersed along the shore, was very time consuming and in spite of the presence of a local crew the melt loss of ice forced return with a partial load. This caused the operation to become uneconomical and the project was abandoned. It was considered that a larger capacity was required, and that local production of ice would provide a good solution to the problem of melt loss. The mark up on fresh fish bought from fishermen and sold in market is 2.5 KW/kg. Ice is

required in a 1:1 ice:fish ratio if it is transported directly to market or a 1.5:1 ratio if the total storage period is as long as 6 days. The cost of using solar ice would therefore reduce the mark up to around 2 KW/kg, but would nevertheless result in very high revenue compared to the costs of the operation. (The cost of running the ice plant is included in the estimate of solar ice cost of 0.5 KW/kg). The length of time needed to collect from dispersed fishermen would cease to be a problem, and it is likely that local fishermen would be encouraged to transport their catches themselves to ice plant site. Fish would then be collected and packed while the collection boat was travelling to the company's base and back.

Appendix A: Study of the absorption phase of the IR System

A1. Introduction

The present appendix develops a dynamic model of the absorption and evaporation processes. The model allows the useful output of the refrigerator to be calculated, and allows the sizes of the absorber and evaporator heat exchangers to be calculated. Consideration is given to the design of all the components necessary for the absorption process. Both the gravity-circulating and pressure-regulated modes of evaporation are modelled in order to compare their suitability for use in the IR system.

A2. Non-return valve

The ammonia-water intermittent system is open to the possibility of vapour resorbing into the surface layer of the solution in the separator and so causing a high system pressure to be maintained which will prevent further absorption from occuring. To avoid this a non-return valve is placed downstream of the rectifier, as shown in the circuit depicted in fig 3.1.1. An alternative device is the liquid seal arrangement proposed by Williams (1957) and proved by Exell (1984). Fig A.2.1 shows the liquid seal in circuit and its method of operation. For the seal to function successfully sufficient pressure difference between the evaporator and the separator is needed to pump vapour to the lower end of the reservoir where it is absorbed. This pressure difference is $\rho_1 g z_1$, where $\rho_1$is the density of the solution in the reservoir. An equivalent head of solution, made up of solution of trapped in the liquid seal of density ρ_2, is required to balance the pressure difference. The concentration of the trapped solution will normally stabilise at a value close to the weak solution concentration, since the seal will normally be at a temperature close to separator temperature. It will be able to absorb ammonia from the vapour generated and simultaneously receive weak condensate forming on its upper walls, which act as a rectifier. Consequently the

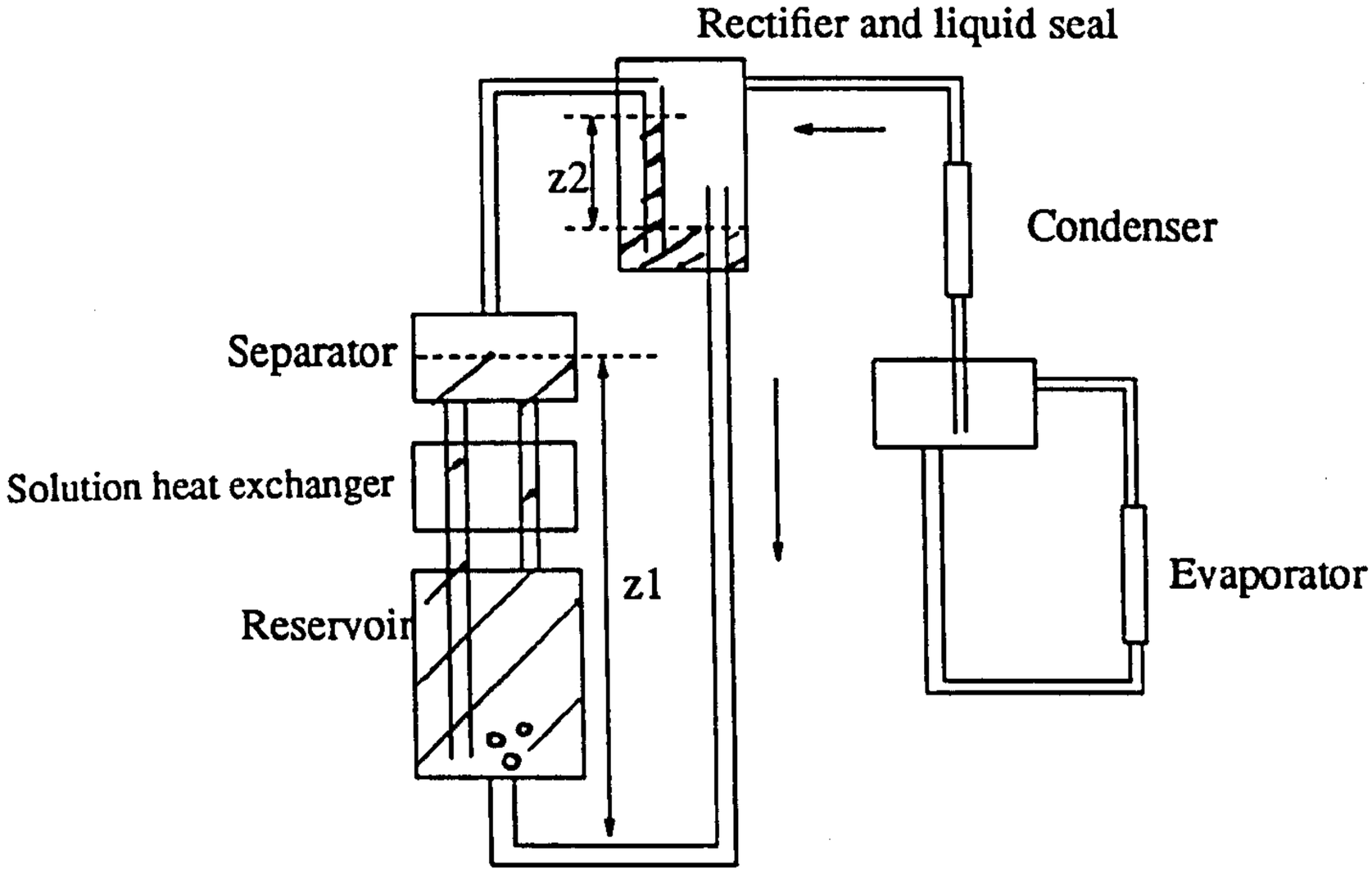

Fig A.2.1 *Liquid seal during absorption*

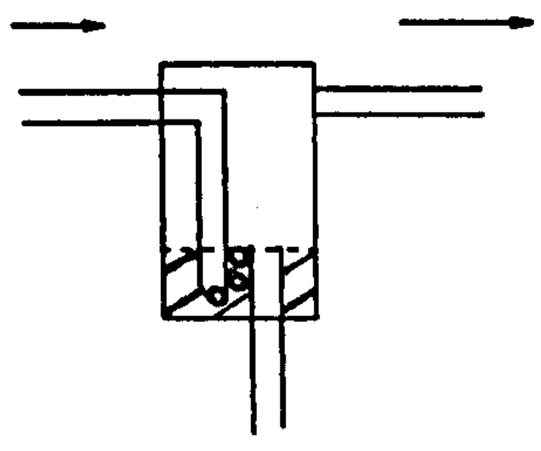

Fig A.2.1 (b) *Liquid seal during generation*

value of z_2 will be of the same order as z_1. The disadvantage of the liquid seal can be seen to be its bulk, which can only be minimised by reduction of reservoir and generator height to a minimum. Exell (1984) experienced practical difficulties with the operation of the liquid seal.

A3. Heat removal

Once the generation phase is ended rapid cooling of the all the generator is required, since evaporation of the refrigerant at low temperature is not possible until the system pressure is reduced. The temparature of the free surface of liquid in the separator is the primary determinant of system pressure, so that some method for reducing this temperature must be provided. Delay in separator cooling will reduce the period of time available for absorption heat rejection so raising the area required for heat rejection. This is undesirable since the cost of providing surface area for absorption heat rejection is high.

A number of methods of aiding separator cooling can be considered. The circulation of solution through the separator will carry away its heat only to the extent that the solution heat exchanger is ineffective. In order to make use of this method the solution heat exchanger will have to be by-passed, but the switching in of any such bypass for the absorption phase alone introduces an extra complexity. The use of a separate cooling fluid or heat pipe to transport the separator heat also involves a switch so that the cooling circuit or heat pipe is disabled during generation.

The removal of the heat of absorption does not present the problem of diurnal switching since in the IR system the absorber/reservoir remains close to ambient temperature during generation, and so can be fitted with a heat rejection method that operates continuously throughout the cycle. It is evident that if absorption heat is removed from some part of the circuit other than the separator, the question is raised as to what then determines the separator temperature and hence the system pressure, which continues to be governed by the free liquid surface in the separator. Since the system pressure determines the evaporating temperature it is of paramount importance.

In order to maintain a low evaporating temperature it may be expected that a high rate of separator cooling is desirable in order to minimise system pressure. The system pressure in this case would follow the path marked "s" in the pressure-temperature-concentration (p-t-x) plot given on figure A.3.1. Unfortuneately the rate of cooling of the reservoir, if this is acting as an absorber as shown, may be insufficient to restrain the solution temperature from rising above the bubble point determined by the separator pressure, as shown by the path "a". In this case vapour

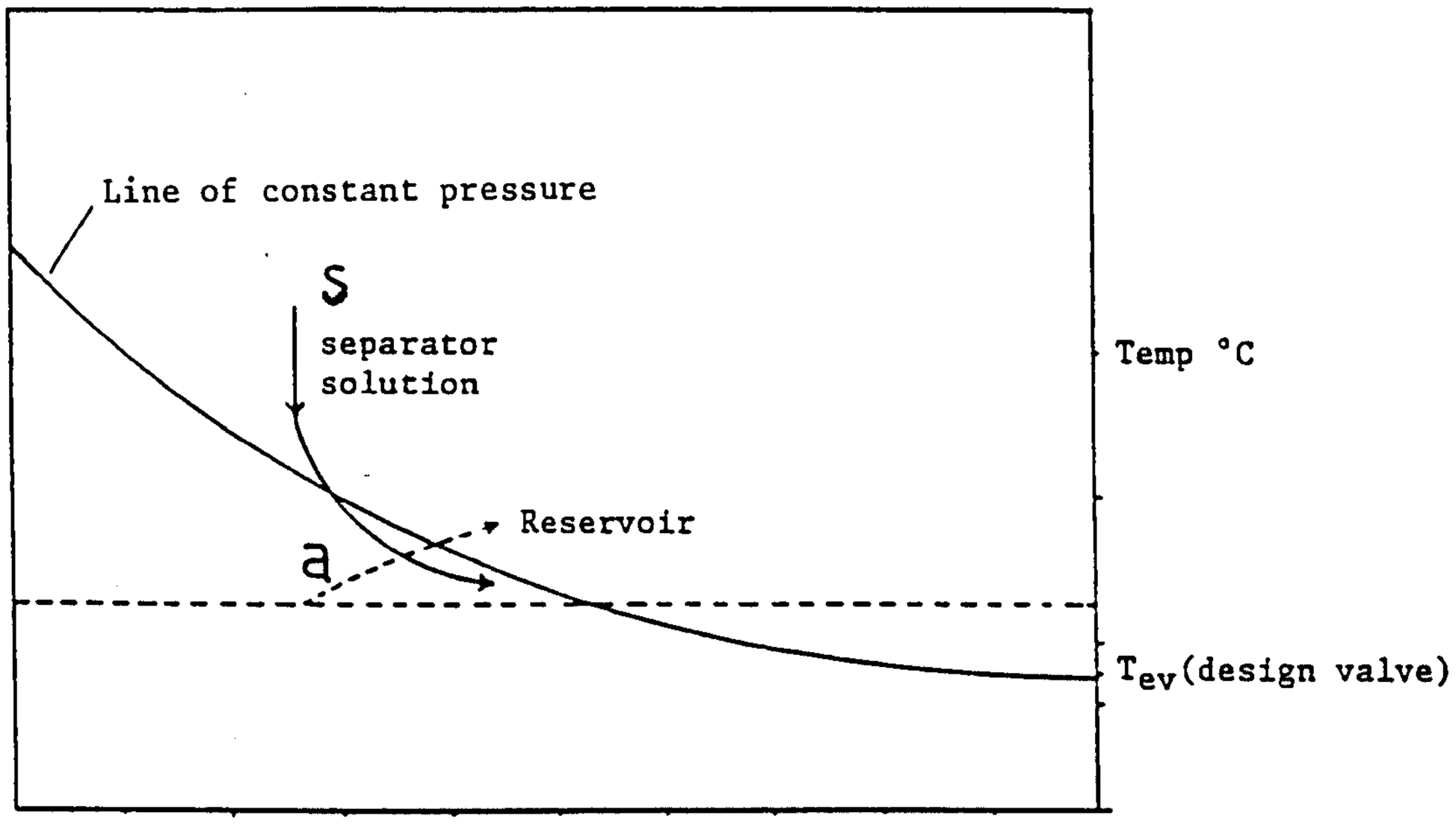

Fig. A.3.1. A schematic pressure-temperature-concentration plot showing the temperature of the solution in the separator (path marked 's') and the temperature of the solution in the absorber/reservoir (path marked 'a'). It is intended that 's' falls below or follows the constant pressure line corresponding to the evaporating temperature (T_{ev}) desired. But if absorption heat is not rejected rapidly enough at the same time, 'a' will move above the constant pressure line, and the absorption/evaporation process will be unsuccessful. The steeper the path of 's', the more danger of 'a' rising too rapidly.

would cease to absorb and would collect in the reservoir, in the worst instance displacing solution in the separator and so flooding the receiver irretrievably.

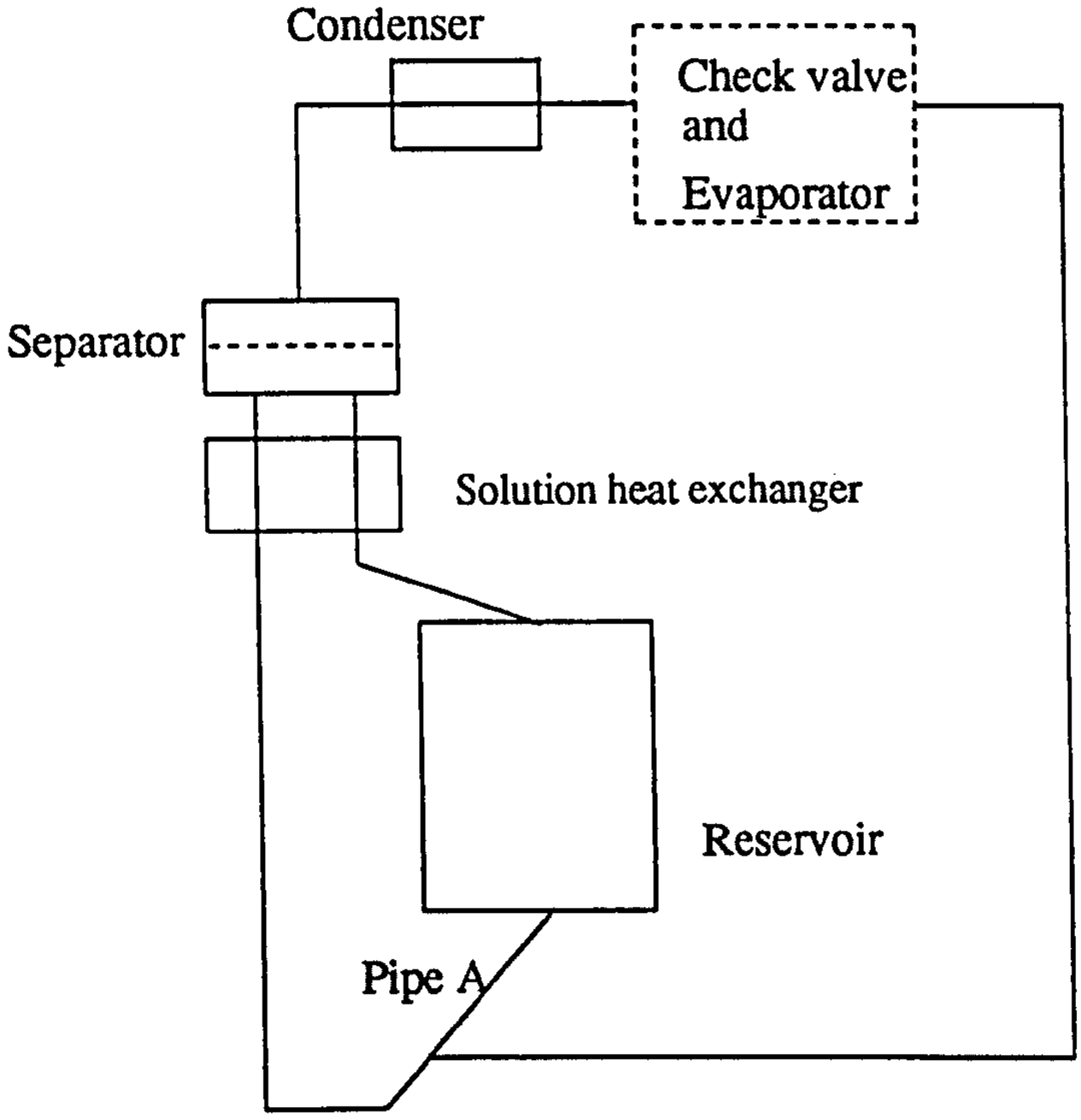

Fig A.3.3 *IR circuit shown with the solution heat exchanger positioned above the reservoir in order to avoid the danger posed by vapourisation occurring in the reservoir. Fig A.3.5 shows a preferred design.*

The careful positioning of the separator and solution heat exchanger shown in figure A.3.3 allows a flow of vapour to pass from the reservoir to the separator. Mass transfer of solution can be supposed to occur by the thermosyphon action caused by solution density reducing in the reservoir as concentration increases. It should be recognised that the solution heat exchanger still acts to decouple the temperatures of the two vessels. The use of a line to bypass the solution heat exchanger, mentioned earlier with respect to methods of providing separator cooling, will recouple the temperatures of the fluids in both vessels, and also provide a vapour path. This is shown on fig A.3.4. Circulation of solution is then by thermosyphon action caused by

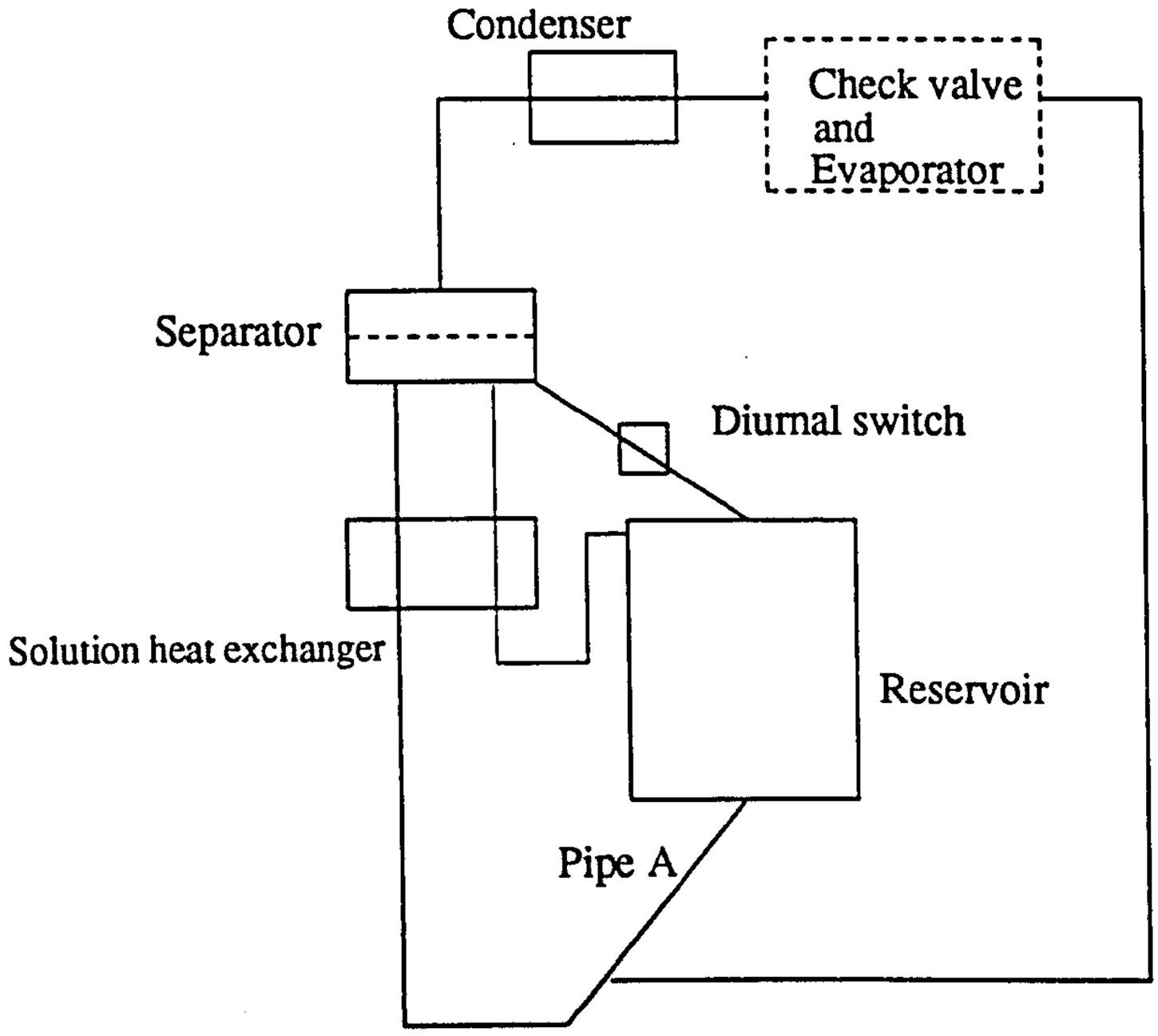

Fig A.3.4. *IR circuit shown with pipework bypassing the solution heat exchanger in order to promote rapid sepatator cooling between desorption and absorption phases. Fig A.3.5 shows a preferred design.*

concentration difference. In all cases circulation can be promoted by the provision of vapour lift in pipe A.

Another method of equalising temperatures is to allow both vessels to be cooled by a single heat pipe circuit, as shown in figure A.3.5. A clear advantage of this arrangement is that the heat pipe condenser can be used both during the separator cooling period and the absorption period. Under this arrangement only the warmer vessel will reject heat, since it will tend to raise the pressure inside the heat pipe beyond the equilibrium point of the other, cooler, heat pipe evaporator. Consequently reservoir temperature and separator temperature will be equalised once the separator is cooled initially from the final generation temperature of the day.

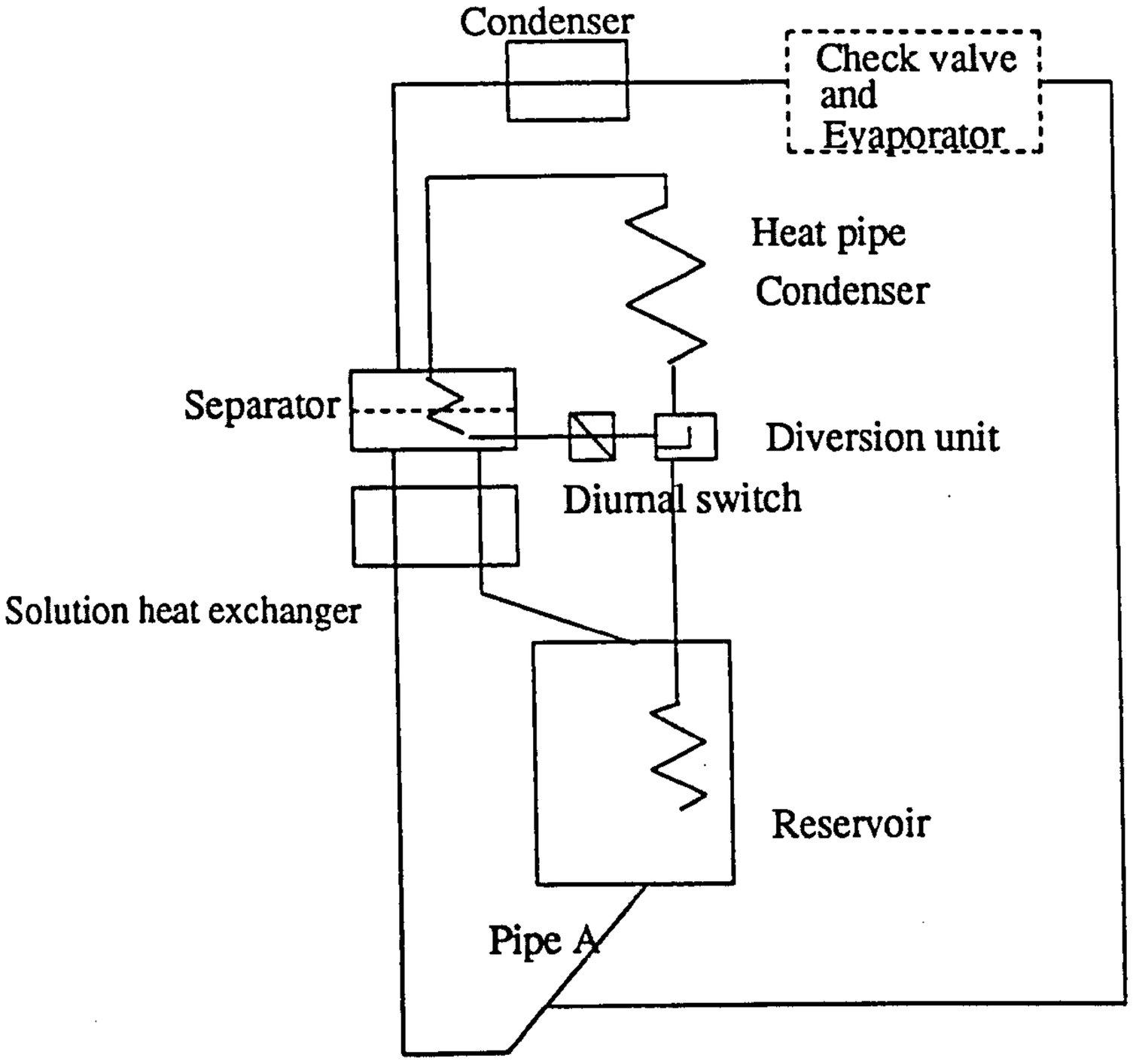

Fig A.3.5 *The IR circuit shown with the preferred separator and absorber cooling circuit. The advantage of this arrangement is that rapid separator cooling is accomplished by a heat pipe circuit together with absorber and condenser cooling, so minimising overall radiator cost. The reader is reminded of fig 3.5.5.1 which shows the condenser in relation to the cooling circuit.*

Overall costs are further reduced if the same heat pipe condenser is used during the generation phase for removal of heat of condensation. The diurnal switch shown on fig A.3.5 would then be closed during the day, and a portion of the heat available for generation would be devoted to vapourising the contents of the cooling coil located in the separator. With a condenser coil immersed in the reservoir as shown in fig 3.1.1 the remaining components of the cooling circuit would remove condensation heat. At nightfall the diurnal switch would open and the component

marked "diversion unit" would serve to supply a constant head of working fluid to the separator cooling coil, while additional condensate from the heat pipe condenser continued to supply the reservoir cooling coil.

A4. Choice of evaporator: gravity circulated or dry expansion

Figures 3.1.1 illustrates the circuit fitted with a dry expansion type evaporator. The major disadvantage of the dry expansion type is that it requires a valve which may be a source of unreliable operation or may invite blockage. In the case of a refrigerator sized for use with a $1m^2$ collector, the capacity of the valve is too small for the necessary orifice size to be manufacturable. To ease this problem the valve may be used in conjunction with a capillary tube. In contrast to this the gravity circulating evaporator as illustrated in figure A.2.1 contains no delicate parts, and is cheaper as a result, but has the major disadvantage of allowing the water content of the refrigerant to accumulate. A cost effective rectifier can at best (Gosney, 1982) only be expected to attain a refrigerant purity of 0.997, implying an accumulation of water of the order of 12 grams per day in a refrigerator producing a yield of 4 kg per day. Refrigerant purity will then reduce to 0.97 after 10 days, so beginning to affect evaporator performance. It will therefore be necessary to either return to manual operation, and expect the water to be periodically drained, or to incorporate an automatic purging action at increased complexity and cost. The conventional method used in large continuous aqua-ammonia devices, whereby a portion of evaporator liquid is bled to the absorber, would be uneconomic in a small system, particularly if rectification performance is poor.

A further disadvantage of the gravity fed evaporator is that the receiver vessel is necessarily cooled to evaporating temperature, implying that both its contents and its mass will consume some of the energy available for cooling. During generation the vessel is warmed by condensate and initially acts as a condenser itself, so delivering some heat to the insulation material surrounding it. Any refrigerant held in it which is not evaporated is unnecessarily cooled, in contrast to the case of a dry expansion system. This is a disadvantage because it is preferable to store surplus refrigerant in the receiver so that the final solution concentration achieved at the end of

absorption is maximised. Where night temperatures vary considerably throughout the year this surplus is a significant quantity.

Sections A.6 and A.7 below investigate each type of evaporator in detail.

The preference for a particular mode of expansion will be based on how well it satisfies the following requirements given the wide range over which ambient temperatures will vary with siting and season.

1. Minimum cost and size of heat rejection assembly.

2. Close-off during generation phase and bulk of separator cooling phase.

3. Minimum wastage of refrigerant given a range of evaporator loading conditions and an economic evaporator size. Wastage occurs in two ways. In the case of the dry expansion evaporator insufficient evaporator area or excessive resistance to evaporation heat transfer results in liquid refrigerant passing into the absorber. In addition, low flow rates will result in available refrigerant not being utilised within the time available.

5. A desirable but not indispensible feature of an evaporator is that it gives a measure of cold box temperature control.

A5. Evaporator model

The instantaneous rate of heat extraction by the evaporator, $\dot{Q}_{ev}$, is determined by the relations:

$$\dot{Q}_{ev}=U_{ev}A_{ev}(T_o-T_{ev}) \qquad (A.5.1)$$

and, in the case of the dry expansion evaporator,

$$\dot{Q}_{ev}=\dot{m}_{ref}\Delta h \qquad (A.5.2)$$

where $\dot{m}_{ref}$ is the refrigerant mass flow rate and Δh is its enthalpy change between entrance and exit. A_{ev} is the evaporator surface area. A one dimensional model for the calculation of progressive ice thickening during evaporation is illustrated in figure A.5.1. The figure shows a configuration where ice is formed in removable containers, the containers and evaporator tubes

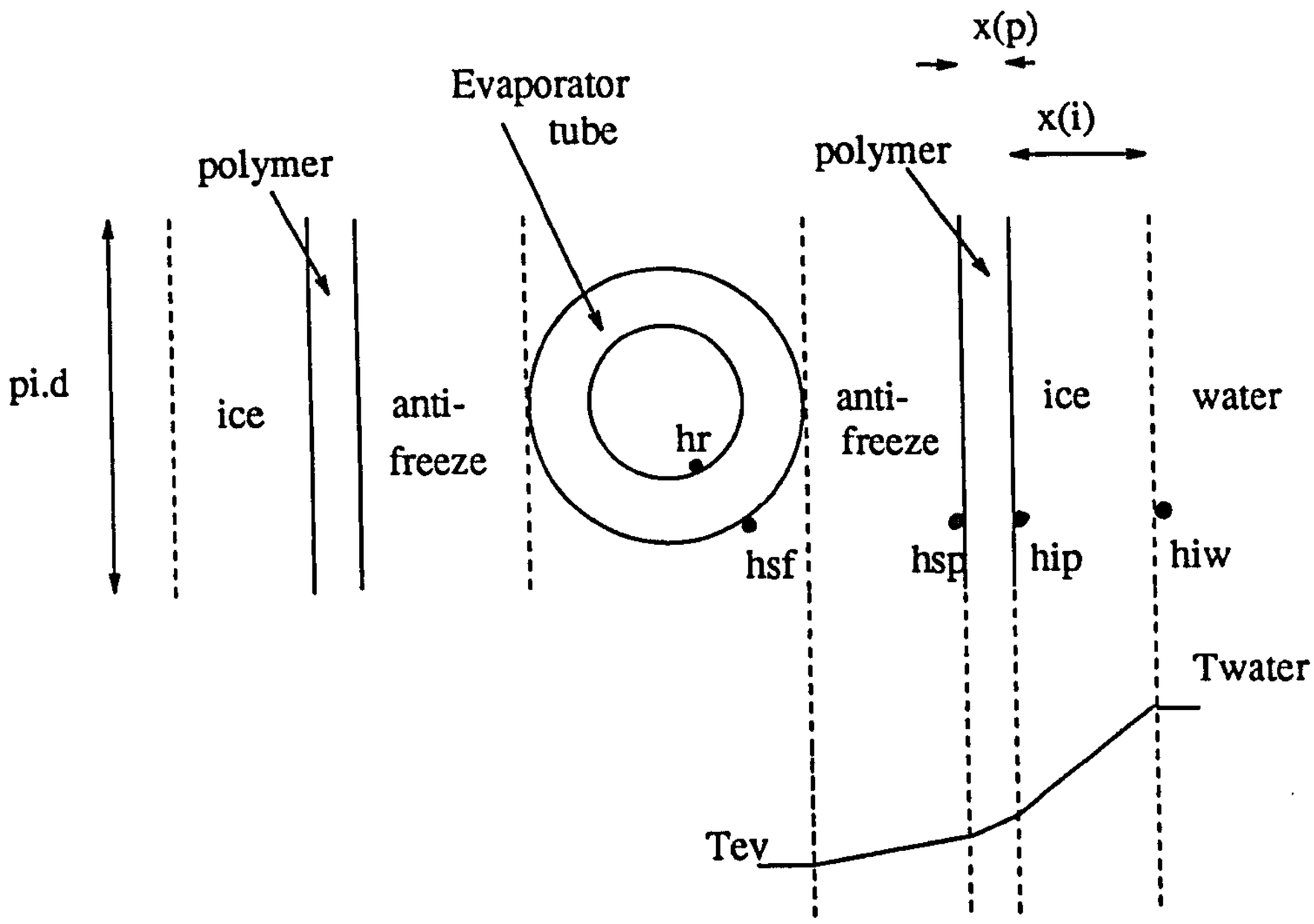

Fig A.5.1 *Cross-section of evaporator tube immersed in a low freezing temperature fluid. Ice is formed in plastic containers which are placed in the anti-freeze solution. Heat transfer surfaces of interest are shown marked "h" and a temperature profie is drawn.*

being immersed in an intermediate fluid with a freezing point below the minimum expected evaporator temperature. For the present the fluid is imagined to be ethylene glycol; its relevant properties and those of the ice container, which is imagined to be moulded from a polymer material, are given on table A.5.1.

The ice formation is assumed to take place by uni-directional heat flow, rather than radial, toward the evaporator tubes, each tube offering a plane area of $\pi dL/2$ to each of the ice layers forming on either side. This model is justified by the anticipation that the tubes in successive turns of a coil will be close to each other. U_{ev} in equation (A.5.1) is composed of the sum of resistances to heat transfer in the evaporator, the primary ones being:

Heat transfer coefficients:			
ice to water	h_i	548	W/m^2K
Thermal conductivities:			
Ethylene glycol	k_f	0.16	W/mK
Polymer	k_p	0.25	W/mK
Ice	k_i	2.2	W/mK

Table A.5.1 *Parameter values adopted for sizing and characterisation of the evaporator. Results are given on figures A.6.8.1, and A.6.8.2, and A.7.3.*

$$\frac{1}{U_{ev}}=\frac{1}{h_r}+\frac{1}{h_{sf}}+\frac{x_f}{k_f}+\frac{1}{h_{fp}}+\frac{x_p}{k_p}+\frac{1}{h_{ip}}+\frac{x_i}{k_i}+\frac{1}{h_{iw}}$$

An estimate of U_{ev} can be made by assuming that heat transfer by convection does not occur to a significant extent. The surface coefficients are therefore discounted, except h_i which is given the value 5 48 W/m^2K following the recommendation of Backstrom (1965). Values adopted for the remaining parameters are included on table A.5.1. From these it is estimated that U_{ev} will have a value of 114 W/m^2K before the ice layer begins to form, while x_i is zero. The equation then simplifies:

$$\frac{1}{U_{ev}}=\frac{1}{114}+\frac{x_i}{k_i} \qquad (A.5.3)$$

Although this estimate applies to the case of ice-pack freezing, it is used here also as a conservative estimate for the portion of the cold box where irremovable ice is made for cold holdover purposes. The useful cooling produced by the evaporator can be conveniently treated for the present in terms only of ice production. Heat entry from outside the cold box is by leakage through the insulation and during door opening. Door opening losses are not accounted for here; for the size of refrigerator considered (having a nominal ice production of 10 $kg/day.m^2$) in conditions of careful usage they will result in a loss of less than 1/5 kg of ice per day. Calculations and experimentation show that a reasonable estimate of insulation loss given a cost effective cladding thickness will be approximately

$$\dot{Q}_{ev(loss)}=0.2(T_{amb}-T_{ev})$$

The ratio of ice produced to refrigerant expended will be sensitive to oversizing of the cooled space and overloading with either antifreeze or unfrozen water. If the mass of water initially loaded into the cold box is M_w, then assuming energy expended in subcooling ice is small, the mass of ice (M_i) produced (up to the point at which all the water is frozen) is:

$$M_i = \frac{Q_{ev} - \int \dot{Q}_{ev(loss)} dt - (M_f c_{p_f} \Delta T_f)}{M_w (c_{p_w} \Delta T_w + h_{fg(w)})}$$

where Q_{ev} is the heat extracted by the evaporator, $h_{fg(w)}$ is the heat of freezing of water at atmospheric pressure, $M_w c_{p_w} \Delta T_w$ and $M_f c_{p_f} \Delta T_f$ are the sensible cooling energies of water and antifreeze respectively. The sensible cooling of antifreeze is estimated to displace the freezing of approximately 3% of the mass of ice otherwise produced.

A6. Pressure regulated evaporation

A6.1. Evaporator tube sizing

In the case of a dry expansion evaporator the tube diameter is kept sufficiently small so that residual liquid is entrained in the vapour flow. The velocity of vapour in the tube increases along the length as evaporation progresses. A conservative estimate of pressure loss is therefore obtained by taking the maximum flow rate. This is found to result in pressure losses of less than 0.3 bar when a tube of inner diameter of 4mm is used, for a maximum practical length of 30 meters. The effect of the pressure drop is to reduce the pressure at the evaporator exit relative to the entrance. The tendency for this to be reflected in a difference in temperatures is neglected here, partly because the effect is offset by other factors, as discussed in the next section.

A6.2. Heat extracted by the evaporator

The behaviour of the dry evaporator with respect to the presence of unrectified water in the refrigerant has already been described, in section 3.3. In order to to maintain clarity in seeking out other characteristics of the absorption phase the present treatment will assumes the refrigerant is uncontaminated, and has a concentration of 1. (The code described by figure 3.3.2 in principle applies here as a method of calculation, altough in this case an iterative solution for evaporating temperature would be found from the instantaneous value of absorption pressure). The rate of heat extraction ($\dot{Q}_{ev}$), is expressed:

$$\dot{Q}_{ev}=\dot{m}_{ref}(h_{v11}-h_{L9})-\dot{Q}_{ev(loss)}$$

given the assumption of complete vapourisation of refrigerant in the evaporator tube. The absorption pressure is assumed to be unaffected by frictional resistance in the tube, and is determined by the instantaneous concentration and temperature of the solution in the separator. This pressure, together with the assumption of pure refrigerant, determines the value of the vapour enthalpy at the evaporator exit, h_{v11}. The initial liquid enthalpy of the refrigerant is given by the assumption that the receiver finds equilibrium with ambient temperature.

A6.3. Separator cooling

Given the integrated cooling assembly the heat pipe condenser area available for separator cooling is substantial. A problem arises with providing sufficient area for the evaporator end. A small area here will result in a temperature drop between the solution and the heat pipe fluid, resulting in turn in a reduction in the available temperature difference between the condenser and ambient. No attempt is made here to model the heat pipe assembly in detail, or to size the evaporator immersed in the separator. Instead it is assumed that the separator cooling characteristic "k'" in equation (A.6.3) has a value 25% of the value calculated for k for reservoir cooling where a fully sized heat pipe evaporator can be provided. In this way a pessimistic estimate is made of the performance of the separator cooling circuit, allowing confidence that the physical design to meet this specification will be feasible. If the thermal mass of the hot side (or generator) components are treated in lumped form, such that all internal conductances and heat transfer

coefficients are considered small compared to the final interface between the heat pipe and ambient, and assuming perfect insulation, then the Fourier and Newton equations governing the cooling rate can be equated:

$$hA(T-T_{amb})=-Mc_{p(gen)}(\frac{dT}{dt})$$

where h is the heat transfer coefficient between the heat pipe condenser surface (HPC) and ambient, T is the temperature of the generator and $Mc_{p(gen)}$ the composite thermal mass, given by

$$Mc_{p(gen)}=M_{L(sep)}c_{p(sep)}+M_{L(she)}c_{p(she)}+(M_{st(she)}+M_{st(sep)})c_{p(st)}$$

where $c_{p(sep)}$ is evaluated as $\frac{\delta h}{\delta T}$ for a concentration of x_{L4} and $c_{p(she)}$ is evaluated similarily for the mean value of x_{L1} and x_{L4}. The thermal mass of the FVR system will be approximately twice the magnitude of that of the VVR system, and will be greater when generation is incomplete and excessive liquid remains in the separator. The Fourier expression given above can be rewritten on the assumption that the heat transfer coefficient for natural convection will always take the form

$$\dot{Q}=kA\Delta T^{1.25}$$

which is in agreement with McAdam (Holman, 1981) for 1E4<GrPr<1E9. The energy transfer equation can then be integrated to give

$$T_f=T_{amb}+\left[(T_i-T_{amb})^{0.25}+(\frac{A_{HPC}k'_{HPC}dt}{.4Mc_{p(gen)}})\right]^{-4} \qquad (A.6.3)$$

where T_f and T_i are final and initial hot side temperatures occurring over a small period dt. A_{HPC} is the area of the heat pipe cooling surface and $A_{HPC}k_{HPC}$ is the heat transfer characteristic of the heat pipe corrected to become $A_{HPC}k'_{HPC}$ to allow for the undersized evaporator at the separator end.

A6.4. Cooling of refrigerant

Heat is lost to ambient by the refrigerant in the receiver (Q_{8-9}), since it can be supposed to have cooled from its condensation temperature (T_{con}, or T8) to ambient temperature before entering the expansion valve. (The heat lost by the steel mass of the receiver due to the diurnal temperature variation, as with other steel masses outside the solar heated assembly, can be assumed to be balanced by corresponding gains and so ignored). An estimate of the heat lost by the refrigerant can be made by treating it as a function of the instantaneous value of condensing temperature during absorption and the initial value of refrigerant temperature at the start of absorption:

$$Q_{8-9}=M_{ref}-\int \dot{m}_{ref}(h_{L8}-h_{L9})dt$$

where the subscript L8 refers to the refrigerant condensing state during generation and L9 to the refrigerant in the receiver as it is absorbed. The yield rate during generation is $\dot{m}_{ref}$. Liquid enthalpy is assumed independent of pressure such that

$$h_{L8_t}=\text{function}(x_{L8},T_{con_t})$$

and

$$h_{L9}=\text{function}(x_{L8},T_{amb})$$

The reclaim of some of the heat of evaporation lost in further sensible cooling of the refrigerant as it reduces to evaporating temperature is a possibility. Precooling can be accomplished by heat exchange with the vapour leaving the evaporator, but is likely to be only marginally cost-effective, if at all, because a relatively large area is needed for heat transfer to a gas. Nevertheless this option should be investigated; it is not evaluated here.

A6.5. Heat gain

During absorption the heat released tends to raise the solution temperature and pressure. If a mass of refrigerant vapour dm_{ref} enters the reservoir in time dt, possessing a specific enthalpy h_{v11}, then the final state of the reservoir can be expressed as

$$(M_{sol(i)}+dm_{ref})u_{Lf}=dm_{ref}h_{v11}+M_{sol(i)}u_{Li}-\dot{Q}_{amb}dt$$

where u_{Li} and u_{Lf} are initial and final specific internal energies of the solution, and $\dot{Q}_{amb}$ is any heat flowing out of the reservoir to ambient. Since internal energy is approximately equal to enthalpy in the case of liquids,

$$(M_{sol(i)}+dm_{ref})h_{Lf}=dm_{ref}h_{v11}+M_{sol(i)}h_{Li}-\dot{Q}_{amb}dt \qquad (A.6.5.1)$$

$M_{sol(i)}$ is the initial mass of solution; the determination of the mass flow rate of the refrigerant (dm_{ref}/dt) is a topic which will be dealt with below. The absorption process will raise the solution concentration according to the expression:

$$x_{Lf}=\frac{(x_{Li}M_{sol(i)}+dm_{ref})}{(x_{Li}M_{sol(i)}+dm_{ref})+M_w} \qquad (A.6.5.2)$$

where M_w is the mass of water present in the solution. The final temperature to which the solution rises can therefore be evaluated as a function of concentration and enthalpy:

$$T_f=\text{function}(x_{Lf},h_{Lf})$$

During separator cooling the heat pipe evaporator placed inside the reservoir will remain inactive. Some cooling of the reservoir contents will nevertheless take place since the drum is not insulated and is not hindered from cooling by free convection to ambient from the external surfaces of its walls. It is in fact possible that finning of the reservoir walls could increase this effect economically and save on heat pipe condenser area. The reservoir dimensions are assumed to satisfy the condition

$$D/L\geq\frac{35}{Gr_L^{0.25}}$$

such that the vessel behaves like a vertical flat plate with respect to free convection (Holman, 1981). The Nusselt number can then be expressed in the form

$$Nu=C(Pr_fGr_f)^m$$

where m takes the value 0.25 and C the value 0.59 when Pr_fGr_f is in the range 10^4–10^9. This range is applicable to the reservoir geometry and temperature drops considered here. Consequently in the period when the separator is cooling and absorption is occurring, the term $\dot{Q}_{amb}$ in the heat gain equation (2) is evaluated as:

$$\dot{Q}_{amb}=A_{res}k_{res}(T_{res}-T_{amb})^{1.25} \qquad (A.6.5.3)$$

where A_{res} is the surface area of the reservoir and k_{res} is the characteristic constant for heat transfer.

The heat gain equation can be solved iteratively for T_{res} in finite time steps.

A6.6. Absorption cooling

Once the separator and reservoir temperatures equalise the heat pipe evaporator immersed in the reservoir becomes active. The heat loss rate now is augmented by the heat pipe transfer rate, so that

$$\dot{Q}_{amb}=(A_{res}k_{res}+A_{HPC}k_{HPC})(T_{res}-T_{amb})^{1.25} \qquad (A.6.6)$$

The heat gain equation applies equally well to these circumstances, and is solved in the same way as in the combined separator cooling and absorption mode.

The final mode experienced in the absorption process occurs when the mass flow of refrigerant stops due to the receiver contents being exhausted. In this case the heat gain equation is evaluated with $\dot{m}_{ref}$ equal to zero. No positive heat gain now exists, and the reservoir cools toward ambient temperature. It is possible that this mode will not normally occur in practice, because the receiver preferably contains surplus refrigerant at all times, in order that the final concentration achieved at the end of absorption is maximised.

A6.7. Flow characteristic

Fig A.6.7.1 shows a constant pressure expansion valve design in which the areas A_d and A_o are equal, so that the orifice position, defined by dx, is independent of upstream pressure. The orifice position is determined by vertical resolution for equilibrium and depends on a number of parameters. These are the values of the two spring constants (k_{s1} and k_{s2}) and their accompanying free lengths (XF and YF), threshold values of spring extension applying when the valve is just closed (XT and YT), and the reference position at which the adjustable spring Y is set (S). For equilibrium of forces,

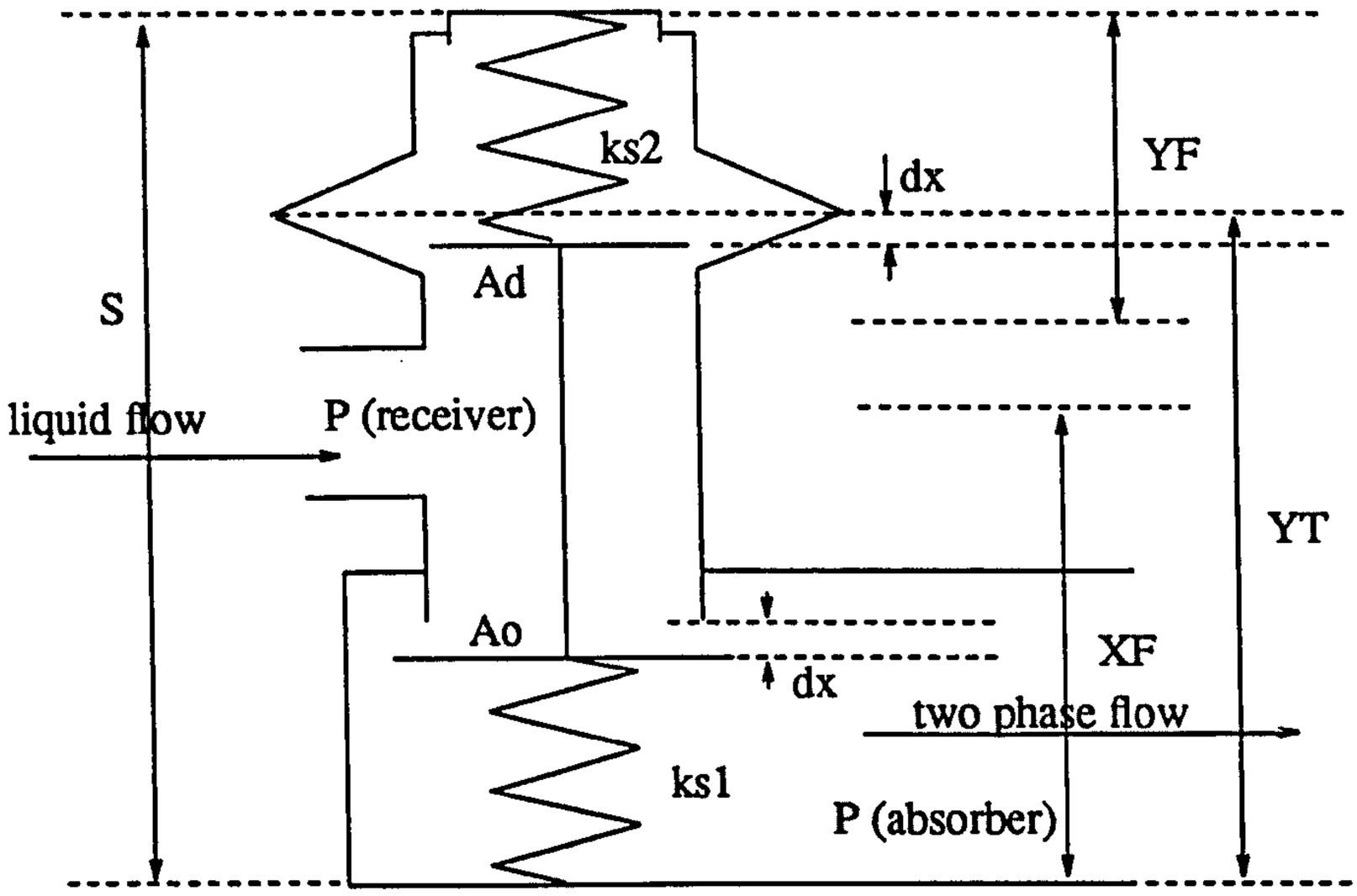

Fig A.6.7.1 *Constant pressure expansion valve. The absorber pressure, and therefore the evaporator temperature, is regulated to a desired value by manual setting of the distance S, and is independent of receiver pressure.*

$$k_{s2}(YT-\Delta x-S+YF)-k_{s1}(XF-XT+\Delta x)=A_o(P_{ab}-P_{atmos})$$

so that

$$\Delta x=k_1-k_2P_{ab}$$

where k_1 and k_2 are constants. The equation for refrigerant flow ($\dot{m}_{ref}$) can then be written

$$\dot{m}_{ref}=C_d\pi d_o(k_1-k_2P_{ab})[2(P_{rec}-P_{ab})\rho]^{1/2}$$

The discharge coefficient C_d can be assumed to have a constant value for the orifice profile so that the equation becomes

$$\dot{m}_{ref}=(k_{O1}-k_{O2}P_{ab})(P_{rec}-P_{ab})^{1/2} \qquad (A.6.7)$$

where k_{O1} and k_{O2} are constants describing the valve characteristic. It can be supposed that the two springs have the same stiffness k_s and the same free length. The two constants are then

defined by the expressions:

$$k_{O2}=\frac{C_d(A_o 8\pi\rho)^{½}A_o}{2k_s}$$

and

$$k_{O1}=\frac{(YT+XT-S)}{2}C_d(A_o 8\pi\rho)^{½}+k_{O2}P_{atmos}$$

A6.8. Performance simulation

Mass of water in cold box	M_{water}	15	kg
Temperature of water	$T_{box(i)}$	$=T_{amb}$	degC
Surface area of reservoir	A_{res}	0.6	m^2
Heat transfer	k_{HPC}	1.68	W/m^2K
	k'_{HPC}	1.68/4	W/m^2K
	k_{res}	1.63	W/m^2K
Concentration of refrigerant	x_{L9}	0.990	
Initial receiver contents	$M_{rec(i)}$	5.0	kg
Initial concentration in res	$x_{L(res)}$	0.377	
Generator thermal capacity	$Mc_{p(gen)}$	20	kJ/kg
Initial temp of generator	$T_{gen(i)}$	90	degC
Valve characteristics			
Spring setting	S	114	mm
Spring constant	k_{02}	184	mm

Table A.6.8.1 *Parameter values adopted for characterisation of the dry expansion evaporator as shown on figs A.6.8.1. and A.6.8.2.*

The plots given on figure A.6.8.1 show the absorption process occurring for the flow characteristic described. A basic set of parameter values is given on table A.6.8.1. The temperature of solution in the separator is represented throughout the process as T_{ab}. The decline of T_{ab} from an assumed final generating temperature of 90 degC (point A) to the temperature represented by point B is calculated according to equation (A.6.3) above.

The reduction in separator temperature is accompanied by a reduction in system pressure, P_{ab}. The pressure at which the expansion valve begins to open is given by solving the valve

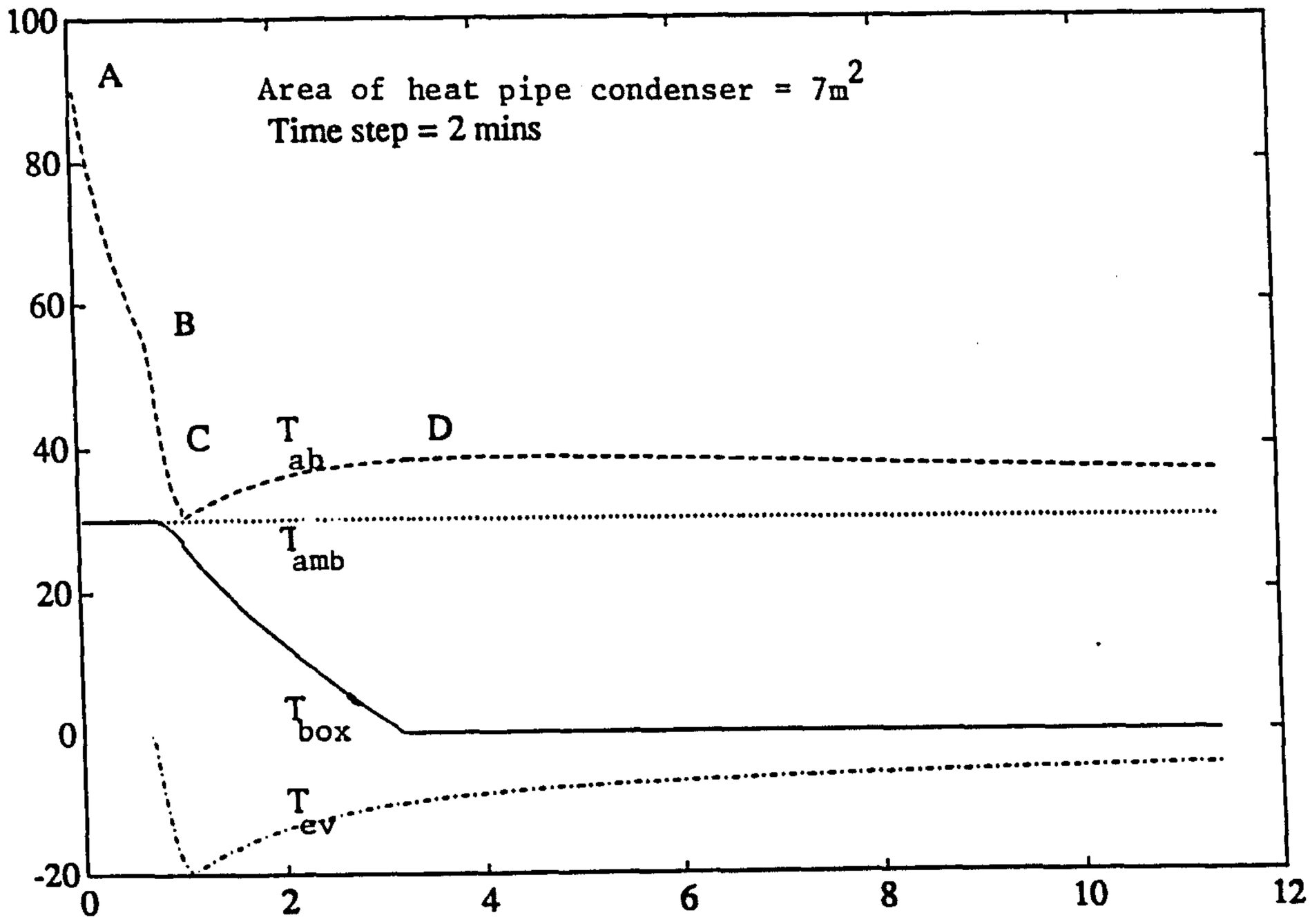

Fig. A.6.8.1(a). Temperature parameters of a pressureregulated evaporation/adsorption process as described in Section 4.6. Operating conditions are listed on Table 4.6.8.1 and given on the graph. Ambient temperature is fixed at 30°C.

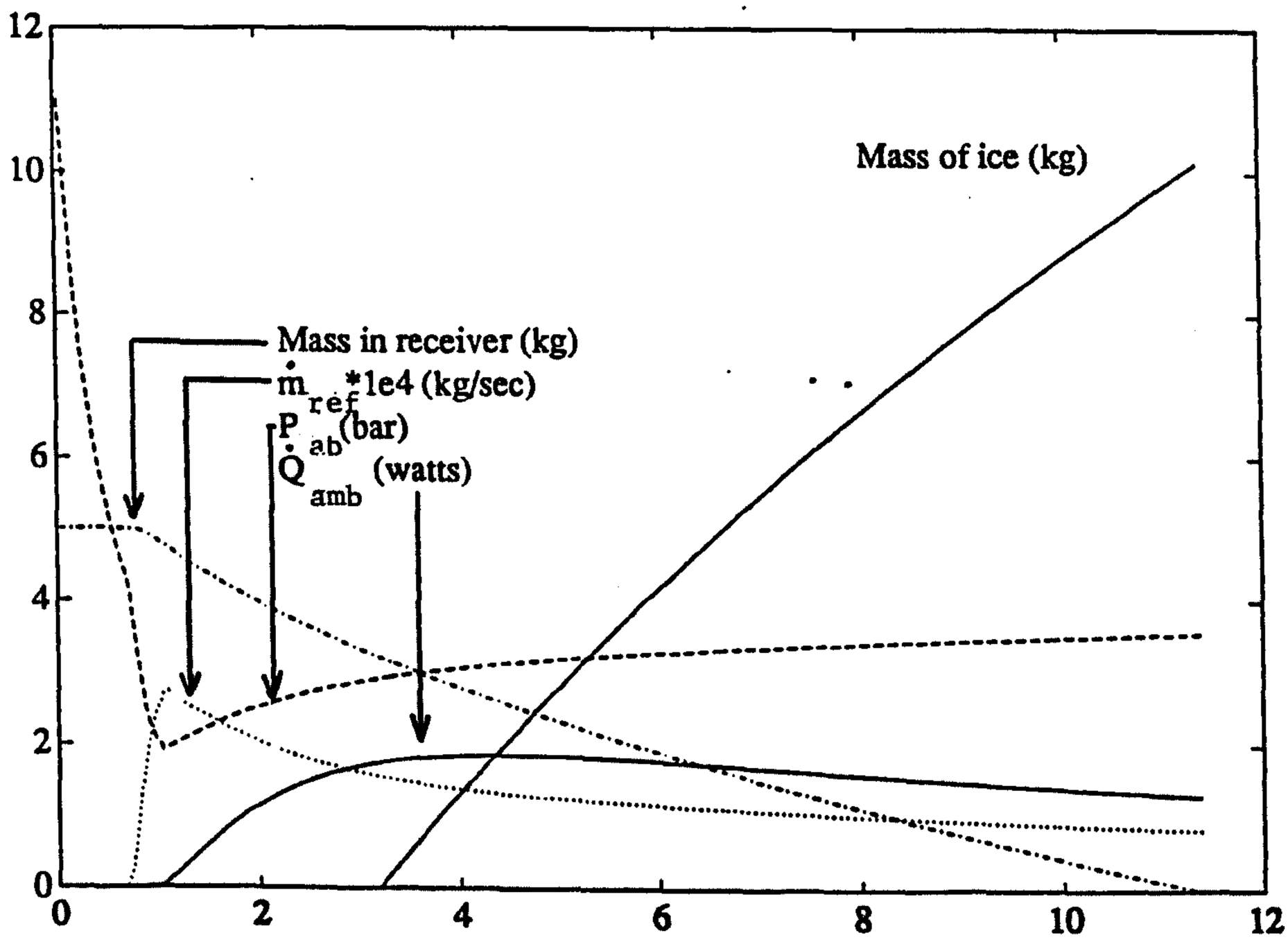

Fig. A.6.8.1(b). Parameters associated with the pressure-regulated evaporation/adsorption process as described in Section 4.6. Operating conditions listed on Table 4.6.8.1 and given on Figures 4.6.8.1(a). Ambient temperature is 30°C.

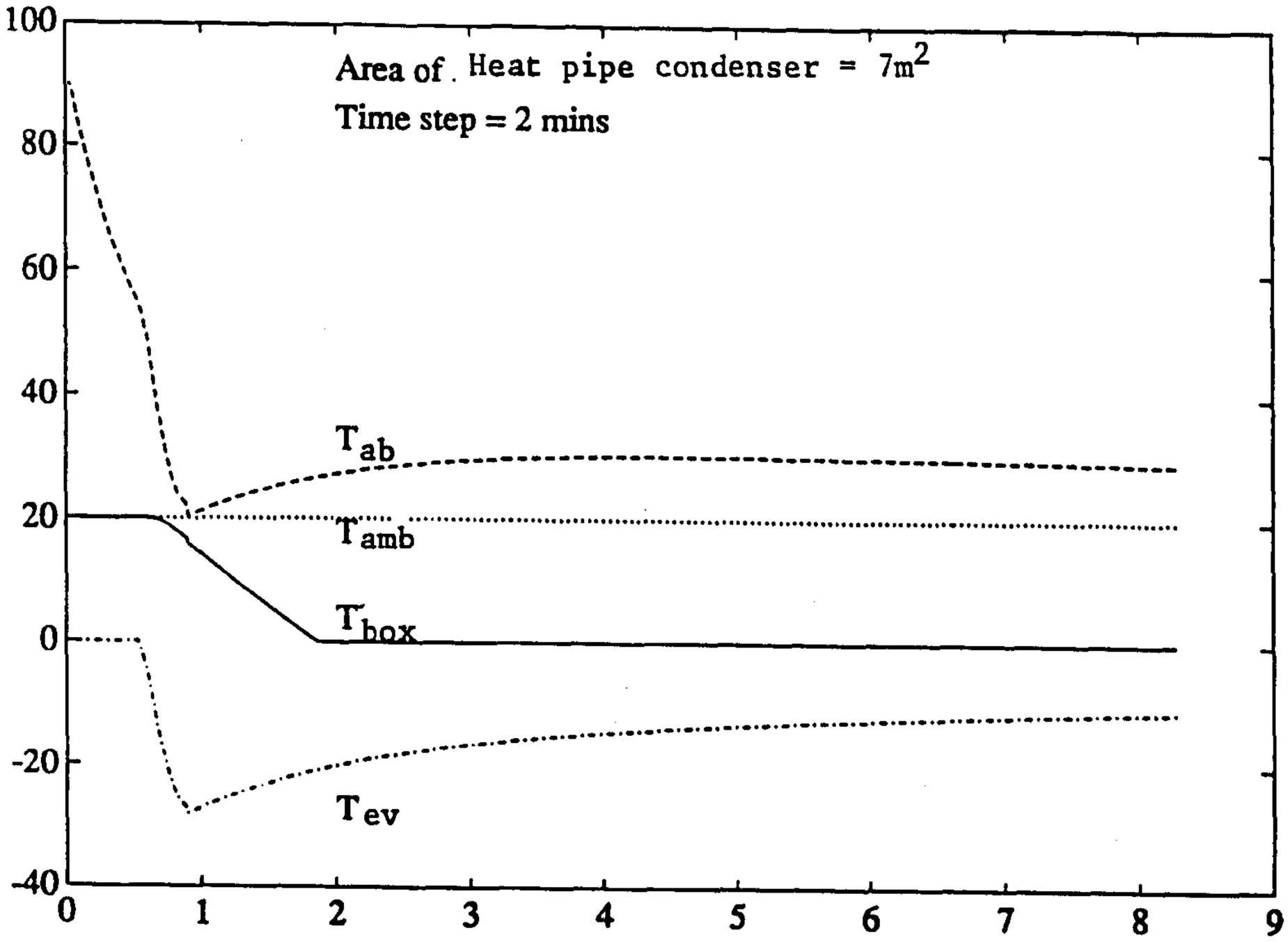

Fig. A .6.8.2(a). Temperature parameters of a pressure-regulated evaporation/absorption process as described in Section 4.6. Operating conditions are listed in Table 4.6.8.1 and given on the graph. Ambient temperature is fixed at 20°C.

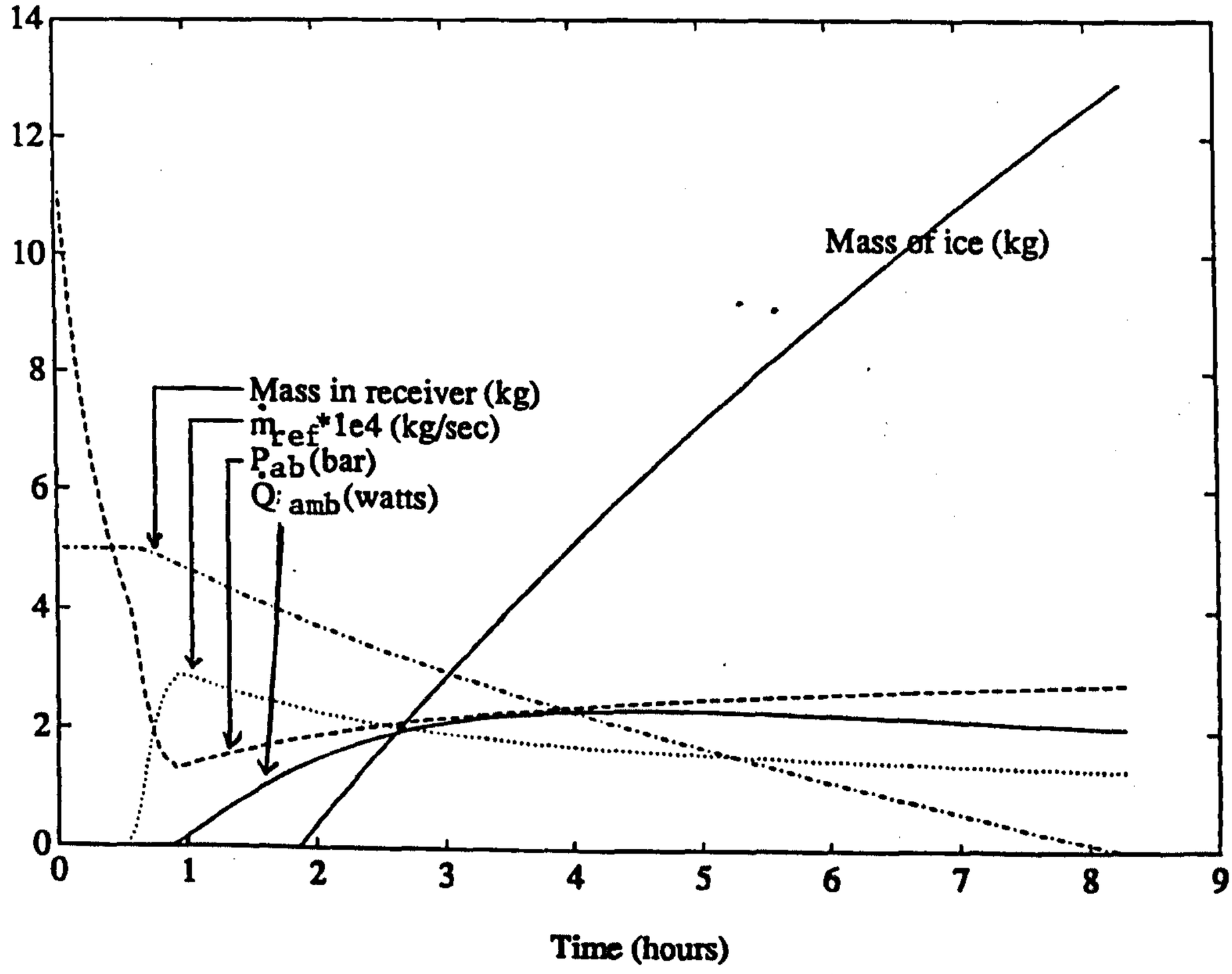

Fig. A.6.8.2(b). Parameters associated with the pressure-regulated evaporation/absorption process as described in Section 4.6. Operating conditions listed on

equation for zero flow:

$$P_{ab}=\frac{k_{O2}}{k_{O1}}$$

The continuing cooling of the separator causes further lowering of system pressure so that the mass flow of refrigerant becomes significant soon after point B, and evaporation is sub zero.

At this stage the refrigerant vapour flow is causing circulation of solution by a vapour lift effect in the absorber entry pipe. The rate of heat removal from the generator thermal mass is therefore increased, the plot showing the trend if an increase of 50% is assumed. Simultaneously the concentration of the solution in both reservoir and separator is increasing with the absorption of refrigerant vapour. The continuing reduction of pressure is therefore increased by accelerated temperature reduction, following equation (A.6.3), and decreased by increasing concentration. Evaporation temperature drops with declining system pressure, tending toward the limit governed by the exponential decay in separator temperature. Ambient temperature is assumed to remain constant throughout the separator cooling process, which is limited finitely in time because simultaneously the absorption process is generating heat in the reservoir, according to equation (A.6.5.1). This heat is partly stored and partly lost to ambient by radiation and free convection effects from the reservoir wall, the net effect being a small rise in reservoir temperature.

Point C represents the point in time at which reservoir and separator temperatures equalise. The temperatures will remain equalised for the remainder of the process because of the action of the integrated heat pipe; they are therefore collectively described as T_{ab}. The effect of absorption heat gain is now to raise T_{ab} since it is initially stored faster than it is rejected. The rejection rate (Q_{amb}) is as given in equation (A.6.6). The increase in T_{ab} increases absorption pressure (P_{ab}) so causing the evaporation temperature (T_{ev}) to increase. The progressive rise in solution concentration has the effect of causing T_{ab} to decline after the maximum (point D) so decreasing the temperature difference available for heat loss. (The calculations assume that all the solution is initially at the weakest separator concentration, x_{L4}, implying the reservoir is perfectly sized for the generation flow considered). $\dot{Q}_{amb}$ correspondingly declines, and similarily P_{ab} rises at a reduced rate. The refrigerant flow responds inversely to P_{ab} and so continues to decline although less

rapidly. The declining flow implies a reduced rate of generation of absorption heat, which combines with the effect of increasing concentration to reduce solution temperature T_{ab}.

Fig A.6.8.2 shows the absorption process investigated above taking place under conditions of reduced night temperature. It can be seen that the effect is that T_{ev} is lowered to a more satisfactory value, because of effective absorber cooling at lower P_{ab}. It is also noticeable that the reduction in P_{ab} is allowed despite the intended pressure regulating effect of the expansion valve. This is because $\dot{Q}_{amb}$ increases as a power function of 1.25 with the temperature drop to ambient, so restraining the expected rise in reservoir temperature due to increased mass flow, while the mass flow decreases as a root function of the pressure difference across the valve ($P_r - P_{ab}$), but is nevertheless restrained significantly because of the reduction in receiver pressure with colder ambient conditions.

Because mass flow is greater at low night temperature larger quantities of refrigerant can be absorbed within the period available. If it is assumed that surplus refrigerant is available then the concentration will rise beyond the value obtained by mixing of the yield generated. Clearly it is also possible to take advantage of reduced night temperatures by decreasing the size of the heat pipe condenser.

A6.9. Ice production and evaporator size

In both the plots shown ice production ceases when the receiver runs dry of refrigerant. Ice production is calculated here as a simple function of the useful energy of evaporation of the refrigerant (net of its sensible self-cooling load) diminished by the leakage of heat energy through the cold box insulation, and the sensible load of cooling all the water in the cold box to zero and then freezing it. At higher ambient temperature the conversion ratio between refrigerant consumed and and ice made is worse, since the longer absorption period has resulted in greater loss. In practice the loss will be less rather than more in this case since the temperature difference causing the loss is less and the period of which the loss is experienced is always the same, since the cycle is governed by the diurnal period.

Calculation of evaporator tube length is complicated by the development of an ice layer of non uniform thickness, implying a non uniform heat transfer resistance along the length. Because the evaporator is relatively inexpensive it can be oversized to a certain extent to tolerate off-design operating conditions. An estimate of the area required can be made by considering the instantaneous heat transfer rate in the cold box:

$$\dot{Q}_{ev}=\dot{m}_{ref}(h_{v11}-h_{L9})=U_{ev}A_{ev}(T_o-T_{ev})$$

where the subscripts refer to the stages shown on fig 3.3.1. The largest areas are required when conditions force T_{ev} high and when the maximum ice thickness is formed. T_o can be taken as water on the point of freezing, and is therefore 0 degC. Given a 6mm evaporator tube diameter, it is apparent that conditions where T_{ev} is greater than -4 C result in impractical evaporator lengths of more than 30 metres. In these conditions an inefficiency in cooling, due to unevaporated refrigerant entering the absorber, must be expected. The effect is less in conditions of less efficient generation, when yields are smaller. The greater the extent to which cold box dimensions inhibit the fully formed ice profile the greater the wastage of refrigerant in adverse conditions. The calculation of cold box dimensions which reflect the tapering characteristic of the freely formed ice is outside the scope of the present study.

A7. Gravity-circulating evaporator

The evaporation and absorption process by gravity circulation is described for a basic intermittent system (IB) in section 1.2.2 and the p-t-x plot of fig 1.2.3. The process is identical for the IR system. A dynamic computer model is developed here with reference to the schematic diagram of fig A.7.1. This arrangement differs from the pressure regulated expansion system in that the separator and absorption pressure affects the receiver as well as the evaporator tubing, so implying a uniform temperature thoughout both receiver and evaporator. This leads to two possible sources of inefficiency not experienced by valve operated expansion systems. Firstly, during each cycle the receiver container must be brought to evaporating temperatures from condesing temperature so consuming a proportion of the available latent energy of cooling. Approximate calculations reveal that the loss incurred here is likely to be less than 3% of the energy available;

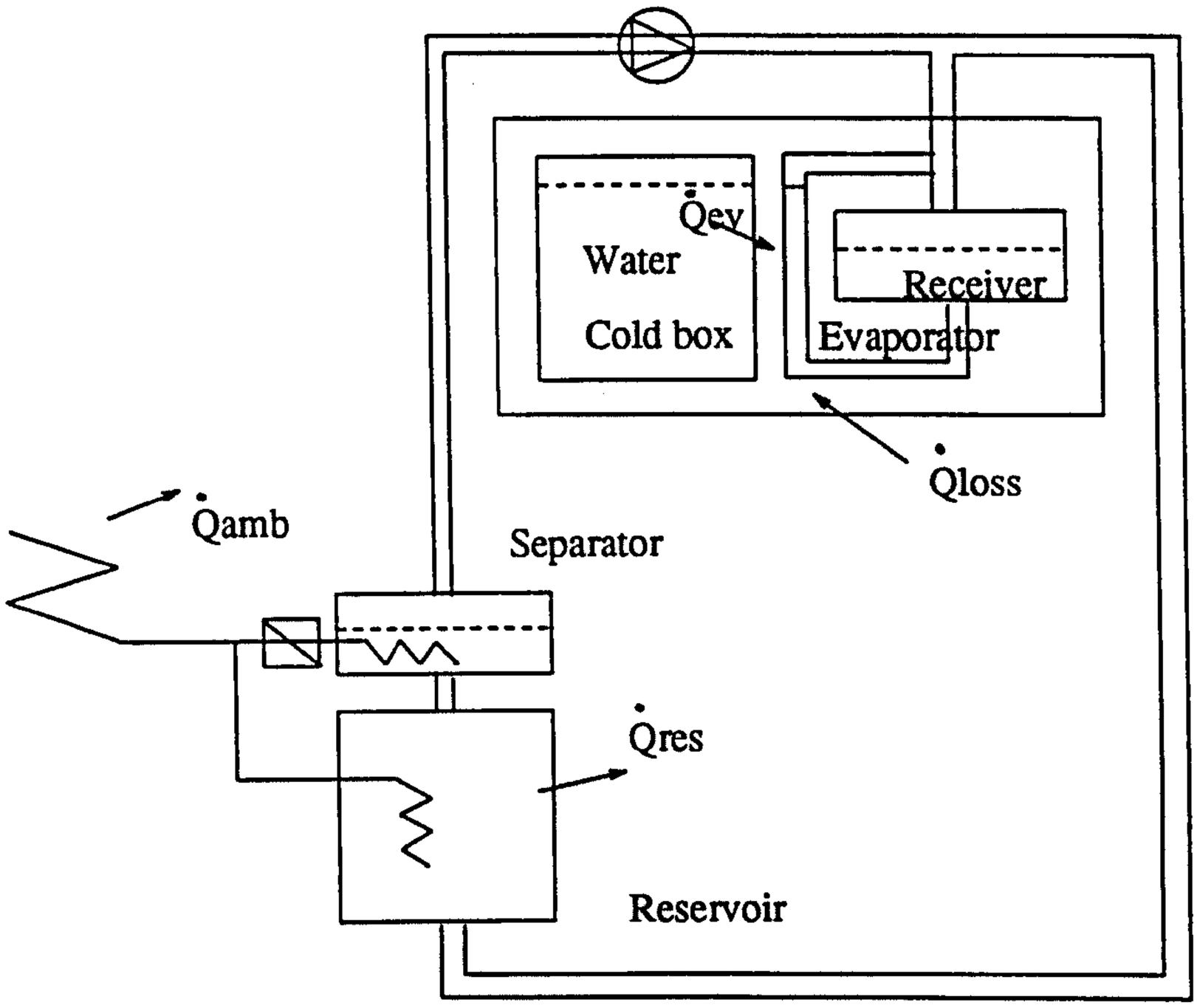

Fig A.7.1 *The gravity circulating evaporator shown in an IR schematic which includes the heat pipe cooling circuit discussed in section A.3.*

no further accounting for this loss is made here. A second inefficiency stems from the sensible cooling of the receiver liquid contents. Unlike the dry expansion evaporator system the complete contents are cooled, so that any surplus which is not evaporated by the end of the process constitutes a potential thermal loss. Some surplus may be required to fill the evaporator tubing during generation in order to avoid the passage of condensation heat to the cold box, and a surplus is useful to accomodate seasonal fluctuations in minimum absorption sink temperatures. In so far as the cold box is insulated, so that cold surplus refrigerant does not significantly warm as a result of heat leakage, it provides the first cold sink available to the desorbed refrigerant vapour in the following generating phase, so encouraging a low pressure start to generation and returning the energy invested in it usefully. Fig A.7.2 shows the computer code which simulates the absorption

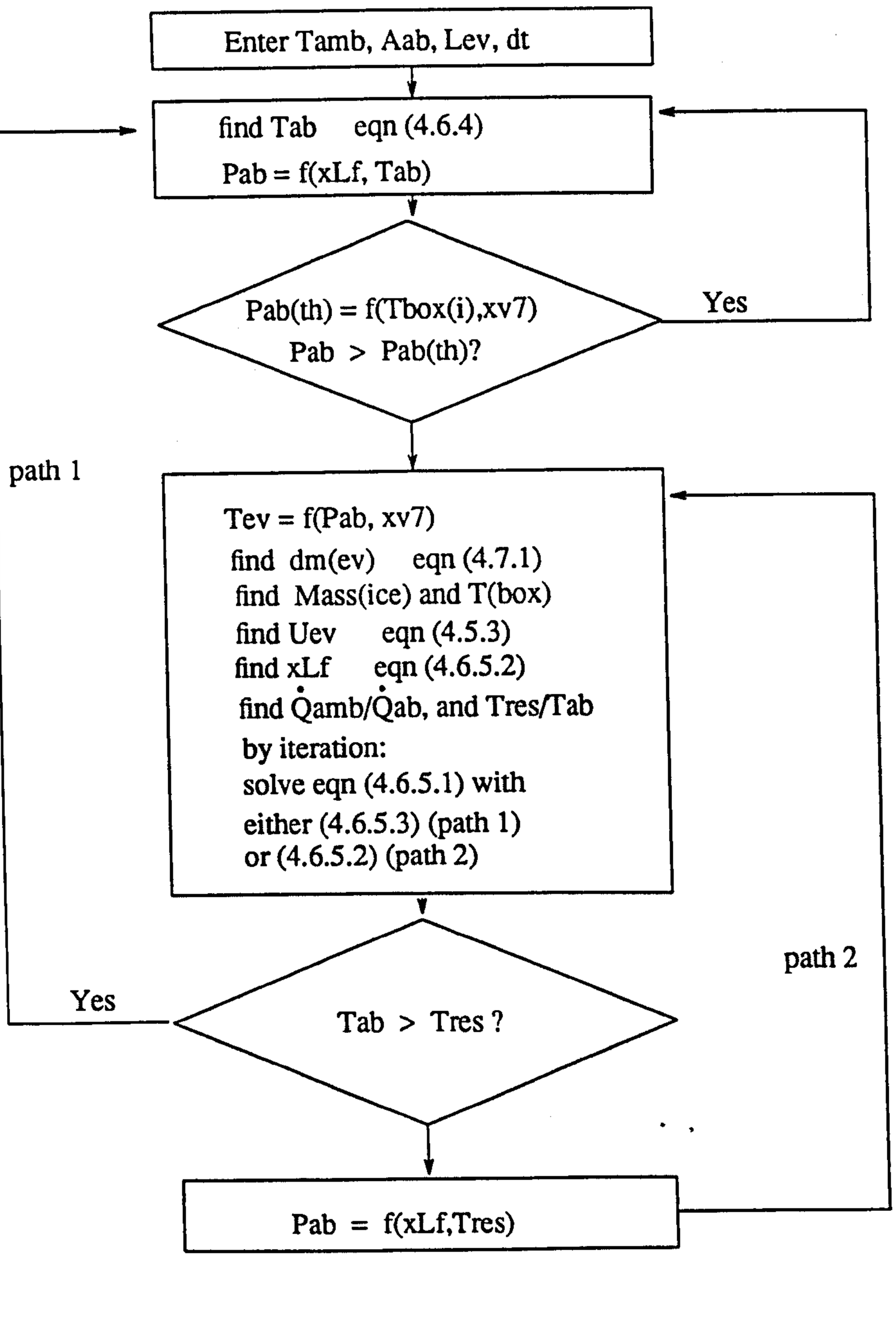

Fig A.7.2 *Computer code used to model the IR absorption phase including separator cooling, or depressurisation, phase.*

phase. The first process is that of separator cooling. Absorption then occurs while the separator cooling characteristic continues to determine the system pressure and now also the evaporating

temperature. During this period the reservoir warms, as it is unable to efficiently reject heat, until the separator temperature has reduced to an equivalent value and the reservoir cooling circuit becomes active. In these respects the system behaves in the same way as the dry expansion evaporator system described above.

The passage of heat (Q_{ev}) from the "cold box" containing water to be frozen is governed by equation A.5.1. The heat of evaporation of refrigerant in the evaporator tube and receiver is the sum of this heat, heat entering through the receiver insulation from the surroundings (Q_{loss}), and the sensible heat of cooling of the refrigerant in the receiver. For a given drop in system pressure the reduction of evaporating temperature is known, so that the various heats can be calculated for a finite step in time. The mass evaporated in time dt is therefore calculated:

$$dm_{ev}=\frac{Q_{ev}+Q_{loss}+M_{ref}(h_{L9i}-h_{L9f})}{h_{v9f}-h_{L9i}} \qquad (A.7.1)$$

where M_{ref} is the instantaneous value of receiver liquid contents. The value of U_{ev} taken to calculate Q_{ev} (equation A.5.1) is a function of the thickness of the ice layer forming around the evaporator tube, as given by equation A.5.3. The mass of ice formed and the temperature of the cold box at any instant is known by the extent to which Q_{ev} extracts from the water in the cold box first sensible heat, then the heat of freezing, and finally the sensible heat of cooling of the ice formed. An assumption of uniform temperature throughout the cold box is made. The rate at which evaporation can take place is in practice also controlled by the frictional resistance characteristic of the pipe-work connecting the receiver to the absorber; the model assumes a large conduit which offers no resistance.

Figs A.7.3, 4, and 5 show the results of running the code. In figure A.7.3 (a) a sharp drop in the temperature difference governing heat flow ($\dot{Q}_{ev}$) between the the cold box and the evaporator is brought about when the heat pipe condenser is connected directly to the reservoir, so causing the system pressure and T_{ev} to stabilize. This causes the refrigerant flow to drop sharply, which in turn implies a sharp drop in demand on receiver sensible heat. Shortly after this the cold box begins to form ice so increasing the heat transfer coefficient governing Q_{ev}, and also causing the cold box temperature to stabilize at 0 degC. The previous effect has the dominating influence,

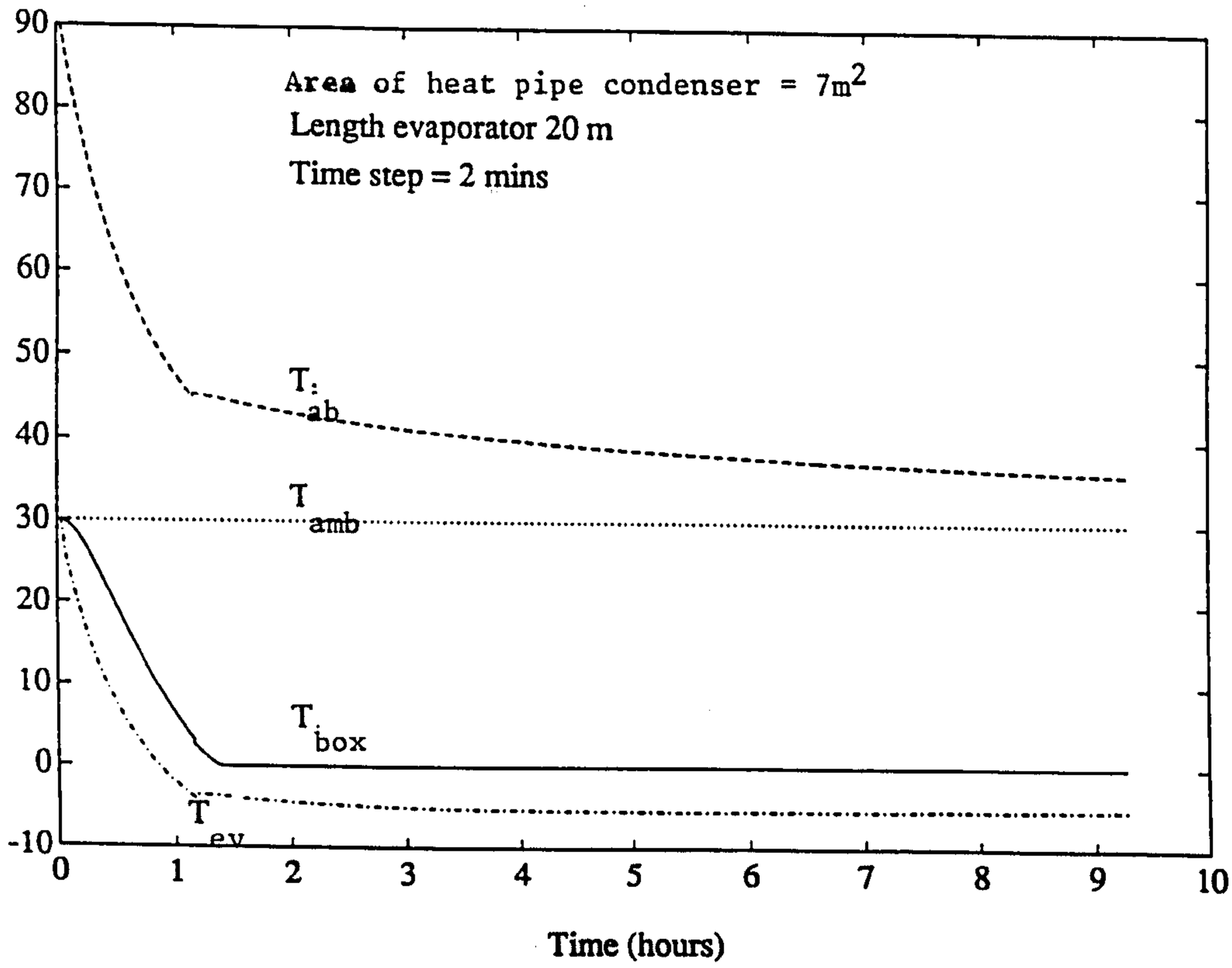

Fig. A.7.3(a). Temperature parameters of a gravity-circulating evaporation/absorption process as described in Section 4.7. Operating conditions are given on the Figure. Ambient temperature is 30°C.

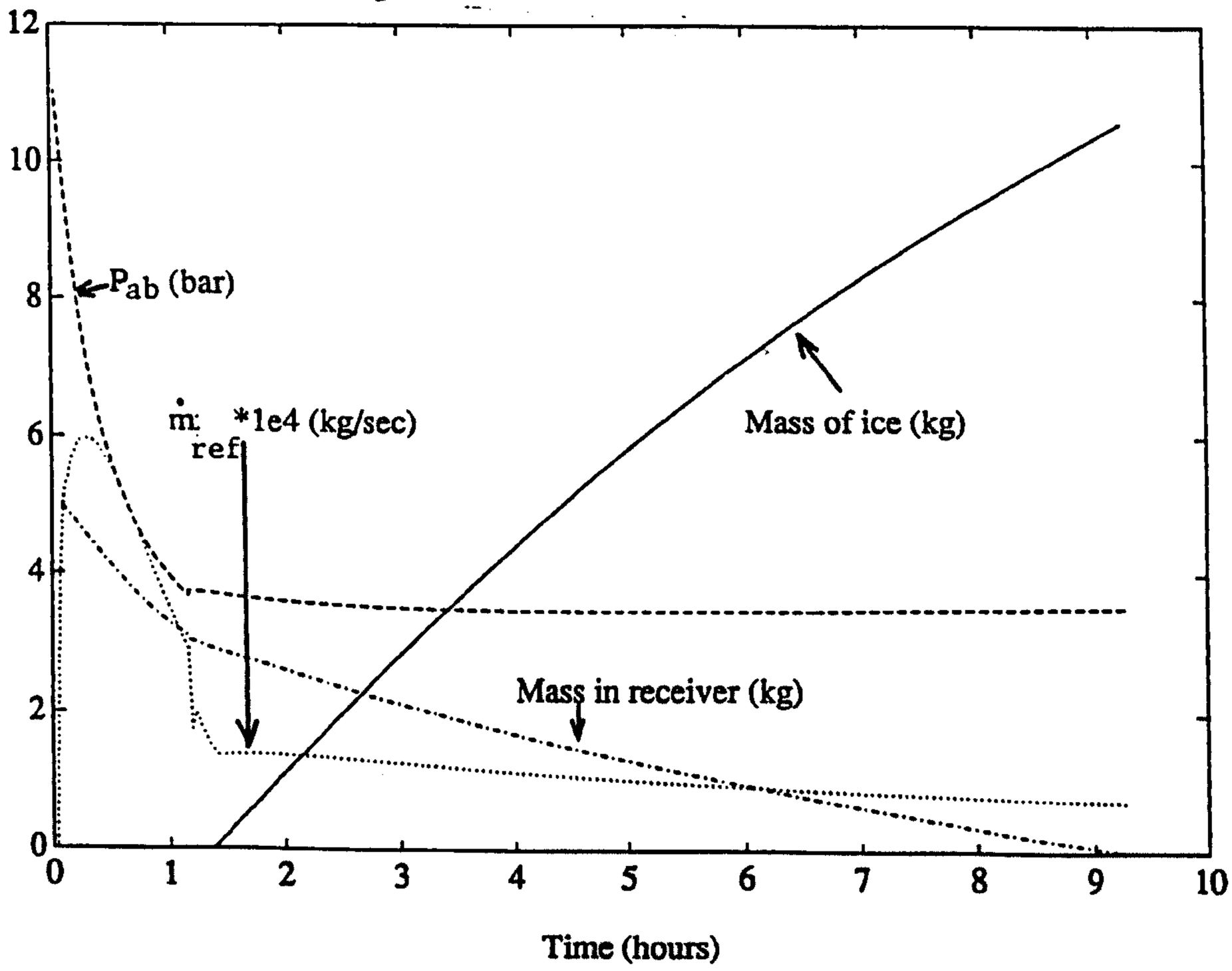

Fig. A.7.3(b) Parameters associated with a gravity-circulating evaporating/absorption process as described in Section 4.7.3(a). Operating conditions are given on the Figure 4.7.3(a).

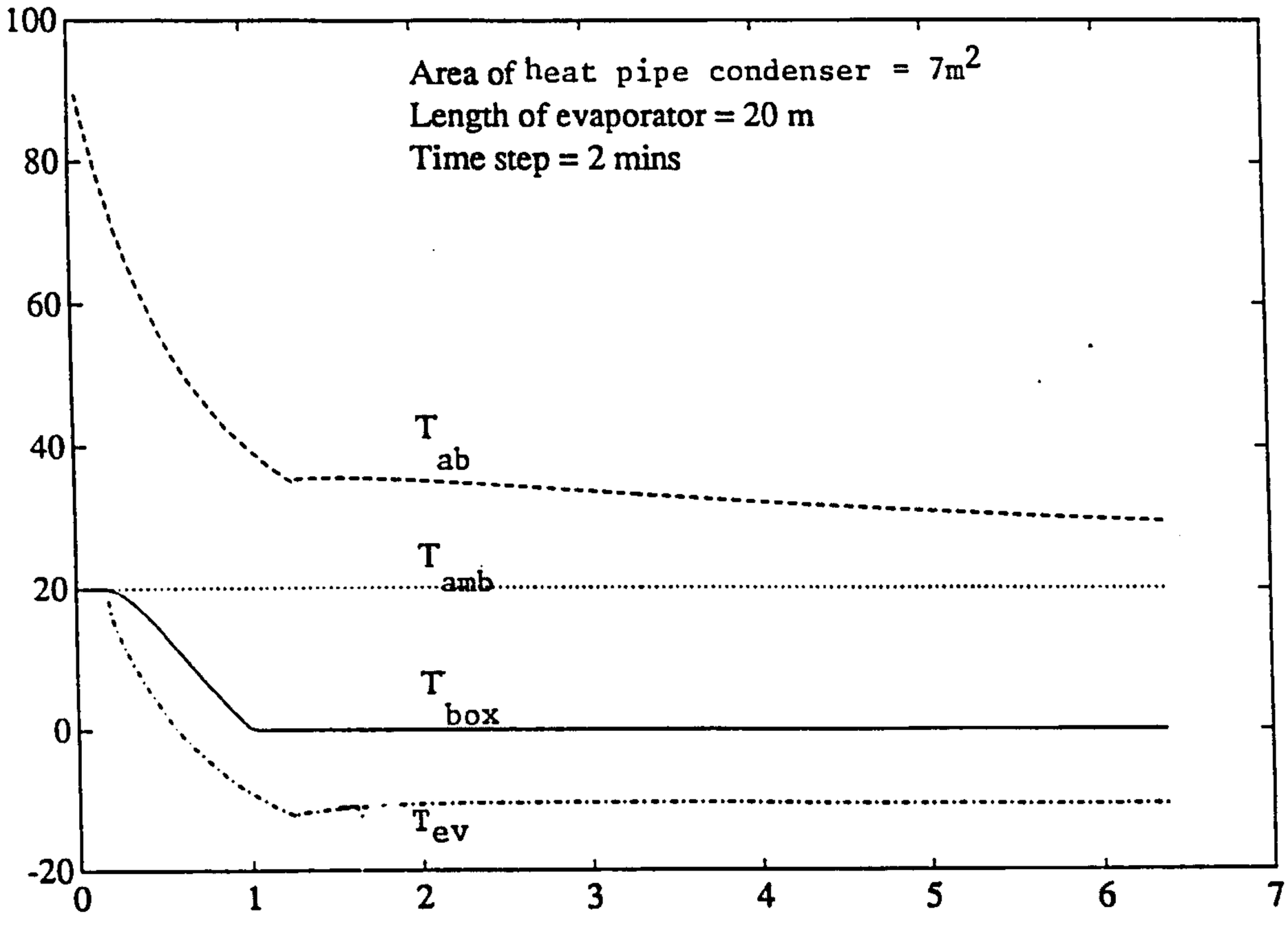

Fig. A.7.4(a). Temperature parameters of a gravity-circulating evaporation/absorption process as described in Section 4.7. Operating conditions are given on the Figure. Ambient temperature is 20°C.

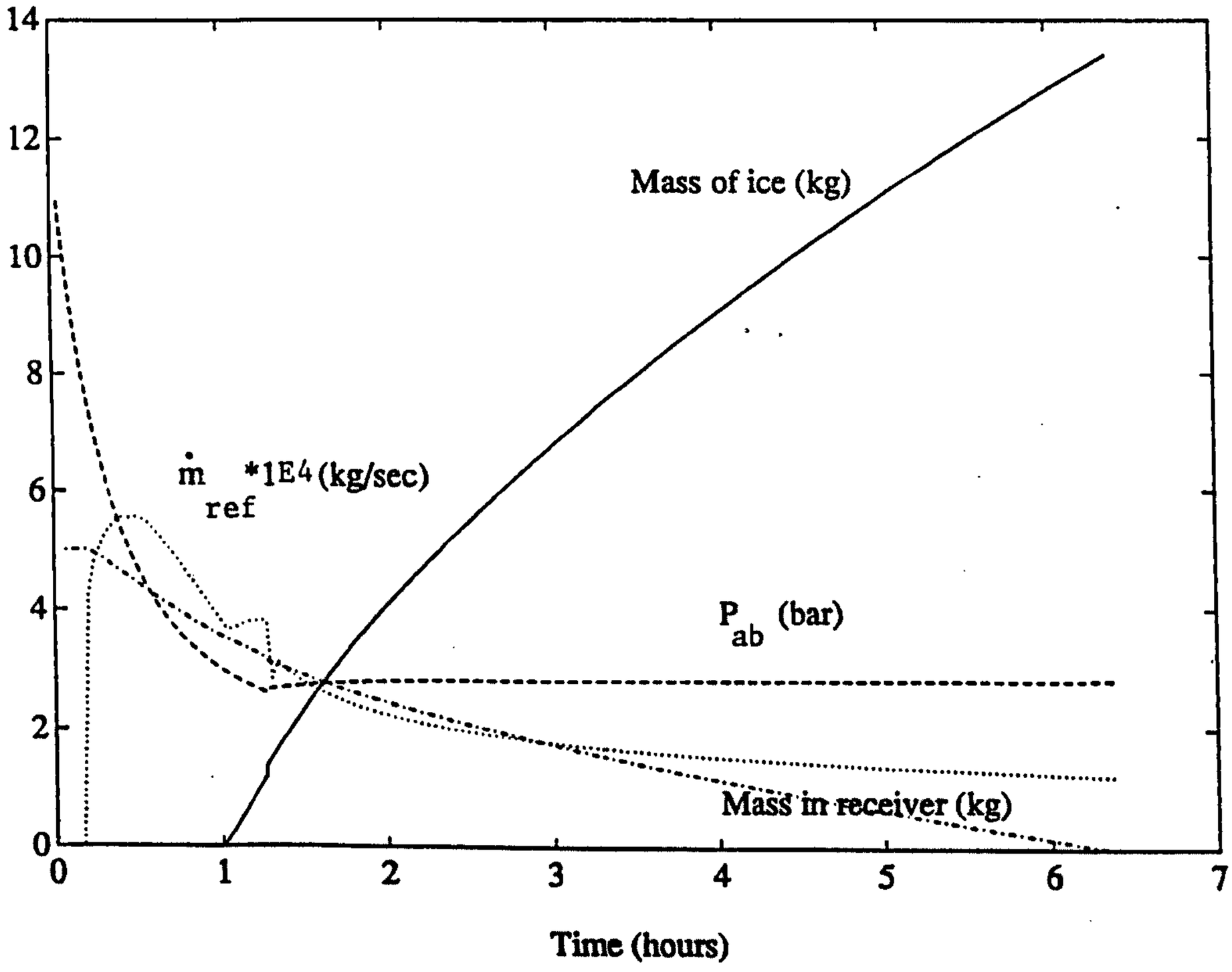

Fig. A.7.4(b) Parameters associated with a gravity-circulating evaporating/absorption process as described in Section 4.7.4(b). Operating conditions are given on the Figure 4.7.4(a)

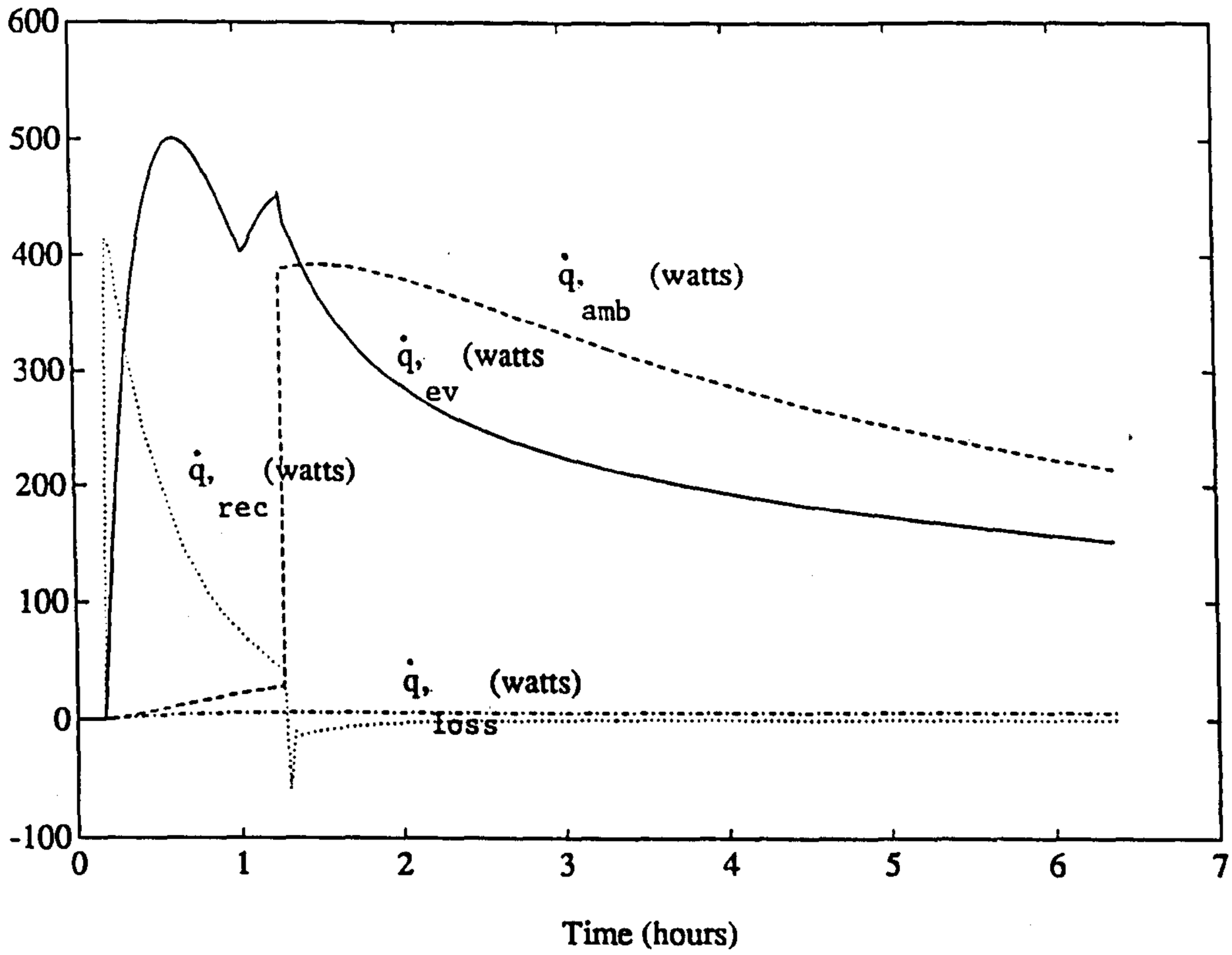

Figure A.7.4(c). Parameters associated with a gravity-circulating evaporating/absorption process as described in Section 4.7.4(b). Operating conditions are given on the Figure 4.7.4(a).

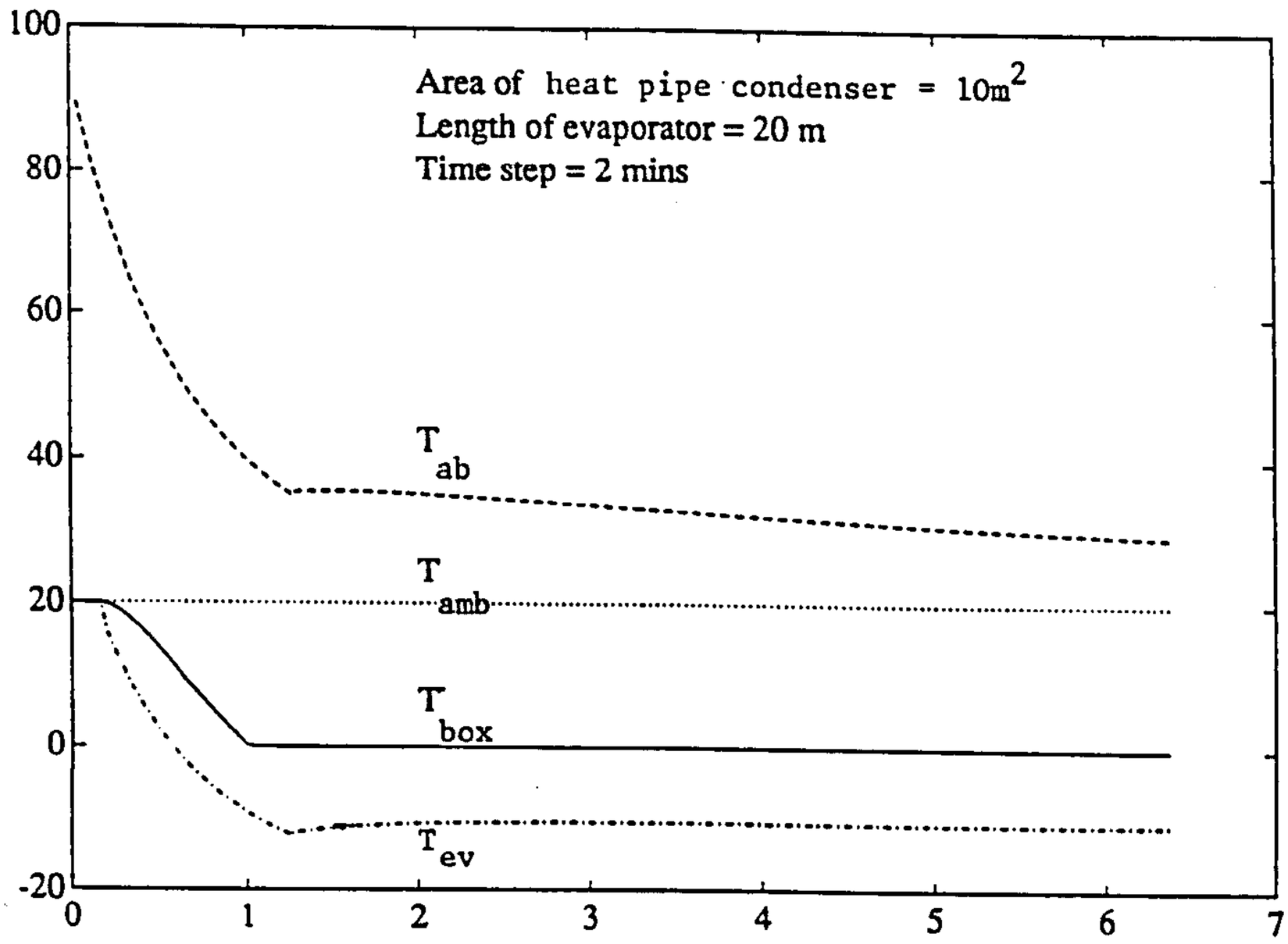

Fig. A.7.5(a). Temperature parameters of a gravity-circulating evaporating/absorption process as described in Section 4.7. Operating conditions are given on the Figure. Ambient temperature is 20°C, as in Figure 4.7.4. In this case the area of the heat pipe condenser is increased to 10m^2.

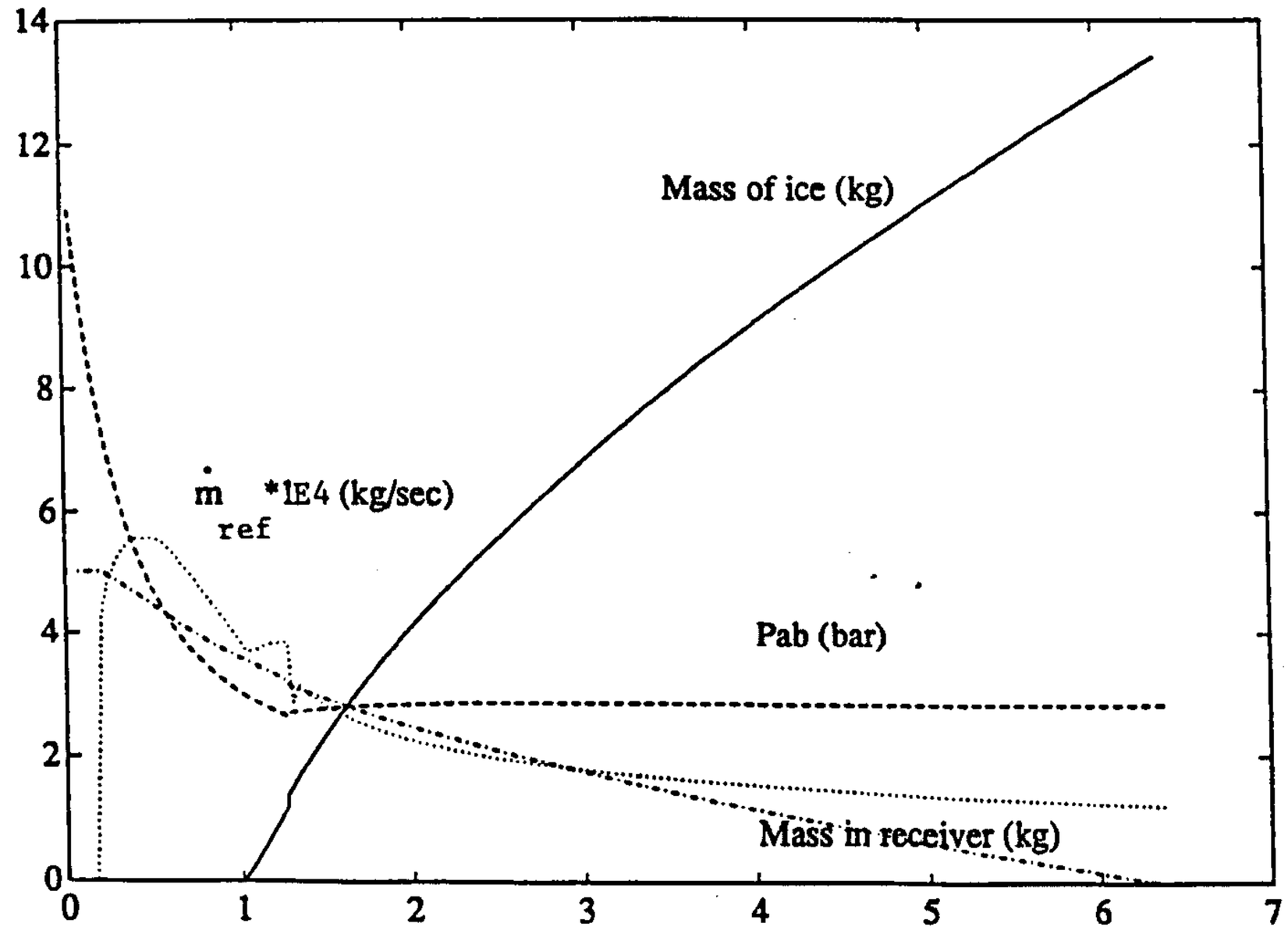

Fig. A.7.5(b). Temperature parameters of a gravity-circulating evaporating/absorption process as described in Section 4.7. Operating conditions are given on the Figure. Ambient temperature is 20°C, as on Figure 4.7.5(a). In this case the area of the heat pipe condenser is increased to 10m^2.

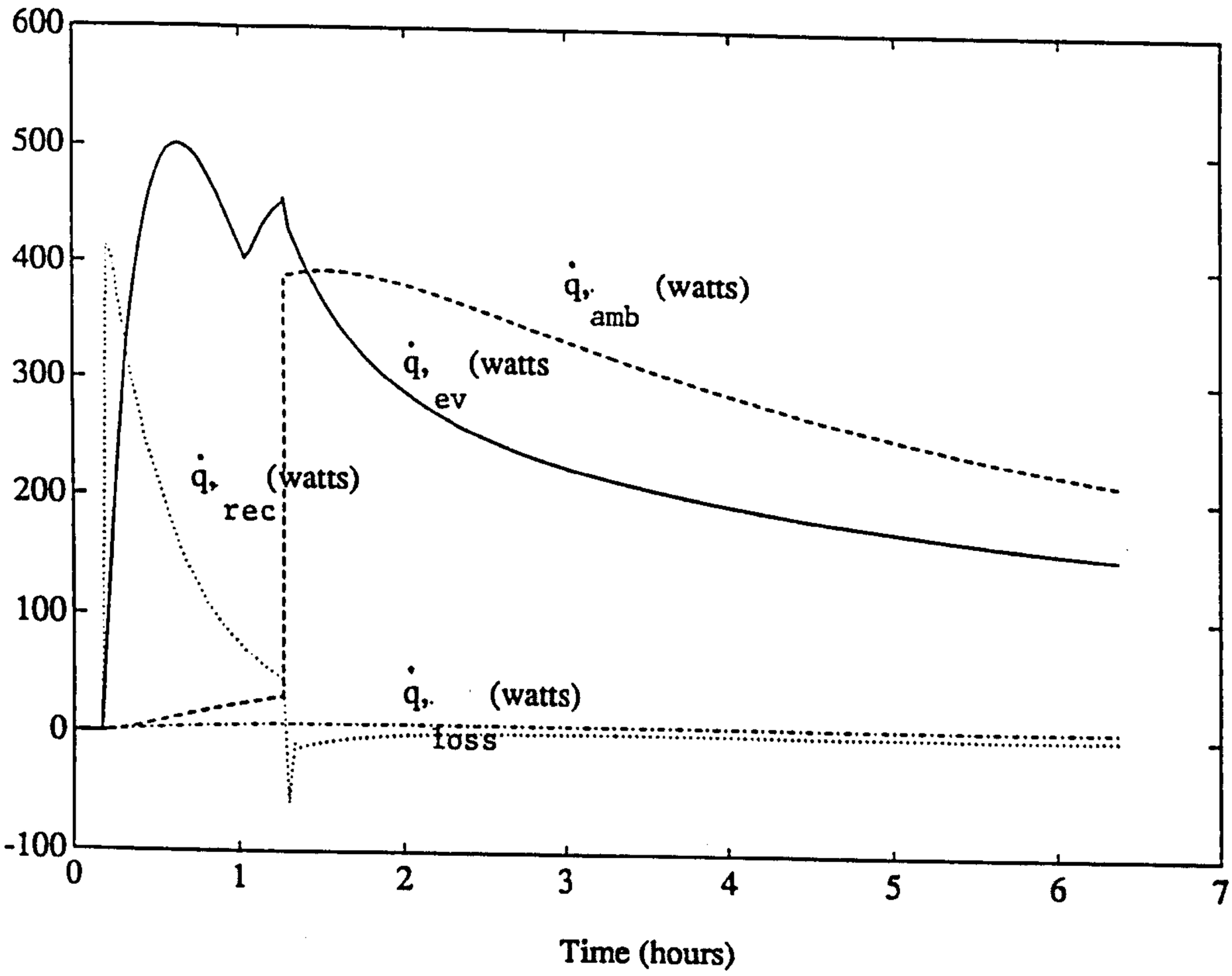

Figure A.7.5(c). Temperature parameters of a gravity-circulating evaporating/absorption process as described in Section 4.7. Operating conditions are given on the Figure. Ambient temperature is 20°C, as on Figure 4.7.5(a). In this case the area of the heat pipe condenser is increased to 10m^2.

causing the temperature difference to increase again, so that $\dot{Q}_{ev}$ rises. The balancing of cooling rate and heat gain in the absorber then stabilizes the process, the gradual fall-off in performance being due to the thickening of the ice formed in the cold box increasing resistance to heat extraction from the cold box.

Fig A.7.4 shows the effect of a reduced night temperature, which results in faster ice production and a better final refrigerant:ice ratio. In this case the cold box reaches 0 degC while the separator cooling circuit is still governing system pressure and T_{ev}, so causing a temporary rise in the refrigerant flow rate.

Fig A.7.5 shows the effect of an increase in the size of the heat pipe condenser (HPC), given a low night temperature. The effect is to speed ice production to a small extent, without improving the refrigerant:ice ratio achieved.

A8. Assessment of absorption modes

The pressure regulating valve shuts flow effectively whenever P_{ab} is greater than the threshold value. P_{rec} never drops below its value at minimum ambient temperature.

The pressure regulating valve passes refrigerant at a rate which is independent of of evaporator loading conditions. Therefore if the evaporator is already fully laden with ice at the start of absorption the evaporator area will be insufficient and refrigerant will enter the absorber largely as liquid. This may be a disadvantageous characteristic in a climate where a bright day is likely to followed by a dull day, since the wasted refrigerant is not stored for use on the succeeding day.

The tapering formation of ice has an advantage where the cold box is used for ice making, or partly for ice removal and partly for space cooling. It is predictable that ice will be fully formed at the valve end of the evaporator, and that temperatures will decrease toward the further end, to an extent depending on climatic conditions. This means that the operator will find more thoroughly frozen ice packs at the valve end rather than a large quantity of packs partially frozen to the same degree. It also means that the design lends itself to compartmentalisation, with ice making occurring at the valve end and less severe space cooling duties met at the further end.

Unfortunately this would not provide temperature regulation of the warmer end since the variation in conditions would mean that on occasion the full evaporator length would be under used. Better temperature regulation could be obtained by referencing the regulated space to the cold end, where a more predictable heat extraction regime would prevail.

Comparison of figures A.6.8.2 and A.7.5, which model the two evaporation modes for the same size of heat pipe condenser, indicates that the full ice yield of 13 kg can be obtained more rapidly by the flooded evaporator system. In the case of the expansion valve system the assumption is made that the ideal evaporator length is used, so reinforcing the indication of inferior dry expansion evaporator economic performance. It should be stated that no firm conclusions as to the comparative performances of the two systems are drawn at this stage, the models being in a stage of development useful mostly in revealing the trends described in the figures. It is noticed that the refrigerant:ice ratio indicated by the simulation (2:5) corresponds well with practical results achieved during experimentation with a manually pressure-regulated dry expansion system, as described in chapter 6.

The relative merits of the two types of evaporator under inspection are discussed in section A.4. The gravity circulating evaporator has two useful features which are not shared by the pressure regulated system. The first is that it suitable for use in machines with modest cooling capacity, the threshold for practical construction of the regulating expansion valve being in the order of 20 MJ per day in an ammonia machine. The second is that it is a "solid state" system without moving parts, and so can be expected to be more reliable. One disadvantage associated with it is that it does not automatically clear itself of small quantities of residual absorbent carried over by the refrigerant during desorption, but requires a drain valve for this purpose.

APPENDIX B

(1) VVR code listing

```
      REAL ML1,ML2,ML4,ML5,ML6,MV6,MV7,MV2,LMDT,NUSS,KH,INIT,NTUBES,
     CCK4,KAMB,LHX,K2,JCOOL,MSEP,MOGEN,MORES,MST,ICE,ICEM2,MMEM,
     CCMHE,MV11,MCIRC,MLIT,MSST,MOSEP,INC51,MOTOTAL,MSEPR,MTT
      REAL TG(11),XLG(11),HLG(11),HVG(11),DLG(11),DVG(11),DG(11)
      REAL QG(11),MVG(11),MLG(11),QGREF(11),DGREF(11),DM(50),ML(50)
      REAL VOLL(11),VOLV(11),QHX(51)
      DIMENSION XAX(50)
      DIMENSION YAX(50)
      DIMENSION ZAX(50)
      DIMENSION TEMP4(50)
      DIMENSION DIFFQ(50)
      DIMENSION TEMP2(50)
      DIMENSION QDIFF(50)
      DIMENSION V(24)
      CHARACTER*32 FULOUT
      CHARACTER*32 NUMOUT
      CHARACTER*6 NAME(24)
      EQUIVALENCE(ML1,V(1))
      EQUIVALENCE(TEV,V(2))
      EQUIVALENCE(T7FL,V(3))
      EQUIVALENCE(QIN,V(4))
      EQUIVALENCE(TCON,V(5))
      EQUIVALENCE(UAGS,V(6))
      EQUIVALENCE(UAOHX,V(7))
      EQUIVALENCE(TAB,V(8))
      EQUIVALENCE(G,V(9))
      EQUIVALENCE(HOURS,V(10))
      EQUIVALENCE(T7,V(11))
      EQUIVALENCE(MST,V(12))
      EQUIVALENCE(TAMB,V(13))
      EQUIVALENCE(DKSET,V(14))
      EQUIVALENCE(TCONFL,V(15))
      EQUIVALENCE(TABFL,V(16))
      EQUIVALENCE(MV7,V(17))
      EQUIVALENCE(MOGEN,V(18))
      EQUIVALENCE(T2,V(19))
      EQUIVALENCE(T4,V(20))
      EQUIVALENCE(UASHE,V(21))
      EQUIVALENCE(T1,V(22))
      EQUIVALENCE(T1FL,V(23))
      EQUIVALENCE(INC51,V(24))

      DV(P,T)=(P*17.03*100000)/((T+273)*8314.4)

      DATA(V(I),I=1,9)/1000.0,-10.0,1.0,0.0,0.0,0.0,0.0,0.0,700.0/
      DATA(V(I),I=10,24)/8.0,0.0,2.5,35.0,2.0,1.0,1.0,
     C0.0,1.4,0.0,0,50.0,0,1.0,2.0/
      DATA (NAME(I),I=1,6)/'ML1 ','TEV','T7FL','QIN','TCON','UAGS'/
      DATA (NAME(I),I=7,12)/'UAOHX','TAB','G','HOURS','T7','MST'/
      DATA (NAME(I),I=13,24)/'TAMB','DKSET','TCONFL','TABFL','MV7',
     C'MOGEN','T2','T4 ','UASHE ','T1','T1FL','INC51'/

0     DO 10 N=1,8
        WRITE(6,5)N,NAME(N),V(N),N+8,NAME(N+8),V(N+8),N+16,
     C NAME(N+16),V(N+16)
        FORMAT(1X,I2,A7,F9.3,6X,I2,A7,F9.3,6X,I2,A7,F9.3)
)     CONTINUE
      READ *, I
      IF (I.EQ.88) GO TO 27
```

```
      IF (I.GT.24) GO TO 70
      READ *, V(I)
      GO TO 60
70    DO 20 N=1,I/1000
       READ *,V(N)
20    CONTINUE
      GO TO 60
      READ *,J,JZ
      K=17
      READ *,A,B,C
      READ *,AZ,BZ,CZ

      OPEN (8,FILE='mv7.mat',STATUS='MODIFY')
      OPEN (9,FILE='ovt.mat',STATUS='MODIFY')
      OPEN (10,FILE='ovq.mat',STATUS='MODIFY')
      OPEN (11,FILE='ovy.mat',STATUS='MODIFY')
      OPEN (12,FILE='effc.mat',STATUS='MODIFY')
      OPEN (13,FILE='ovr.mat',STATUS='MODIFY')
      OPEN (14,FILE='t4.mat',STATUS='MODIFY')
      OPEN (15,FILE='yield.mat',STATUS='MODIFY')
      OPEN (16,FILE='copc.mat',STATUS='MODIFY')
      OPEN (17,FILE='cops.mat',STATUS='MODIFY')
      OPEN (18,FILE='ml1.mat',STATUS='MODIFY')
      OPEN (20,FILE='cr.mat',STATUS='MODIFY')
      OPEN (21,FILE='conc1.mat',STATUS='MODIFY')
      OPEN (22,FILE='conc2.mat',STATUS='MODIFY')
      OPEN (23,FILE='qan.mat',STATUS='MODIFY')
      OPEN (24,FILE='conc.mat',STATUS='MODIFY')
      OPEN (25,FILE='enth.mat',STATUS='MODIFY')
      OPEN (26,FILE='x14.mat',STATUS='MODIFY')
      OPEN (27,FILE='uashe.mat',STATUS='MODIFY')
      OPEN (28,FILE='effhx.mat',STATUS='MODIFY')
      OPEN (29,FILE='dtsen.mat',STATUS='MODIFY')
      OPEN (30,FILE='t7.mat',STATUS='MODIFY')

      DO 65 NF=1,8
     C NAME(NF+16),V(NF+16)
65    CONTINUE

      IFL=2
      IF(ML1.LT.1E-4)THEN
      IFL=1
      ML1=1000.0
      END IF

      L=0
      DO 29 I=A,B,C
      L=L+1
      XAX(L)=I
      V(J)=XAX(L)

      LZ=0
      DO 18 IZ=AZ,BZ,CZ
      LZ=LZ+1
      ZAX(LZ)=IZ
      V(JZ)=ZAX(LZ)

      KM=0
93    IM=IM+1
619   ML1=ML1/1000000
      MV2=0.0
      ML2=ML1
      IF(TCONFL.GT.0.5)TCON=TAMB+10
      IF(T7FL.GT.0.5)T7=75
      IF(TABFL.GT.0.5)TAB=TAMB-5
      TNIGHT=TAB-5
```

```
      IF(T1FL.GT.0.5)T1=TCON
      T51=T1+INC51
      T2=TCON
      NTUBES=10.0
      ACC4=0.04
      IF(T1+3.LE.TAMB)T1=TAMB-2

C     1 Find pressure (P) and concentration of condensate (XV7) for
c     given rectification temperature (T7)

       CALL CONC7(TCON,T7,XL7,P,XV7,HV7)
C     Night receiver conditions: iterate to find value
c     of PE and then XL1

      XL8=XV7
      XL9=XL8
      T10=TEV
      CALL RHL(XL9,TNIGHT,HL9)

      XL10=0.95
732   CONTINUE
      CALL RHL(XL10,T10,HL10)
      CALL RXVPX(PE,XL10,XV10)
      CALL RHV(XL10,T10,HV10)
C     Assume isenthalpic expansion. VF is vapour fraction of total mass.
      HTOT10=HL9
      VF=(HL10-HTOT10)/(HL10-HV10)

C     Water remains liquid so recalculate XL10
      XL101=XL10
      XL10=1-(1-XL9)/(1-VF)

      IF((XL101-XL10)*(XL101-XL10).GT.1E-6) GOTO 732
      CALL RP(XL10,T10,PE)
      CALL RXL(PE,TAB,XL1)

C     2 Find temp at which initial concentration (XL1) is
c     saturated (TSAT)

      CALL RTXP(XL1,P,TSAT)

C     3 Find initial and revised T4 value

      N=0
      T4=TSAT+5
850   N=N+1
      N5=0
877   CONTINUE
      IF (T4.GT.250) GOTO 313
      CALL RXL(P,T4,XL4)
      CALL RHL(XL4,T4,HL4)
      HL6=HL4
      CALL RXVPX(P,XL4,XV6)
      CALL RHV(XL4,T4,HV6)
      CALL RHL(XL1,T1,HL1)

      X1=(XL4-XL1)/(XL4-XV6)
      X2=(XV7-XL4)/(XV7-XV6)
      ML6=ML1*X1/X2
      MV6=ML1*X1
      MV7=MV6-ML6
      CALL DENL(XL4,T51,DL51)
      CALL DENL(XL1,T1,DL1)
: SPECIFIC TO VVR SYSTEM
:     If sep is 30mm id vol decrease is 1% mmem so ignore msep
      ML4=ML1-MV7
```

```
c SPECIFIC ENDS

C      5 Find net heat (QGSUA=QINS-QGSL) into generator and separator
c      QGSUA is heat lost through separator insulation. Collector has
c      radiative loss and convective loss from collector manifold/generator.
c      Collector specification includes emissivity (EPS), manifold U
c      value (UM), absorbtive area of each tube, glass transmittance/
c      coating absorbtivity product (ALPTAU)
       DTGS=T4-TAMB
       AREAT=0.1
       IF (QIN.GT.0.01) THEN
       QINS=QIN
       EFFC=0
       GO TO 1143
       END IF
       ALPTAU=0.8
       EPS=0.15
       UM=1.0
       K4=T4+273
       KAMB=TAMB+273
       EFFC=ALPTAU-(5.669E-8*EPS*(K4*K4*K4*K4-KAMB*KAMB*KAMB*KAMB)
      C+UM*(T4-TAMB))/G
       QINS=EFFC*G*AREAT*NTUBES

1143   QGSL=UAGS*DTGS
       QGSUA=QINS-QGSL

C      6 Find total heat between 1 and 4 and subtract input heat (QGSUA)
c        to find heat exchanger contribution (Q12)

C ******SPECIFIC TO VVR SYSTEM****
       QTOTAL=ML4*HL4+MV6*HV6-ML6*HL6-ML1*HL1
C *****SPECIFIC ENDS**************

       Q12=QTOTAL-QGSUA
       IF (Q12.LT.0.0) THEN
       T4=T4+10
       GO TO 877
       END IF

C      7 Find T2 assuming not boiling and test

       HL2=(Q12/ML1)+HL1
       IF (HL2.GT.365000) THEN
       T2=TSAT+10
       ELSE
       CALL RTXH(XL1,HL2,T2)
       END IF
C      COULD USE T2.LT.TSAT AS A TEST FOR BOILING
       CALL RXL(P,T2,XL2)
       IF (XL2.GT.XL1) THEN
       XL2=XL1
       XV2=0.0
       ML2=ML1
       MV2=0.0
       HV2=0.0
       GOTO 40
       END IF

C      Skip this section if not boiling
C      8 Find boiling conditions and T2
       M=0
       TGES2=TSAT
 73        M=M+1
           CALL RXL (P,TGES2,XL2)
           CALL RXVPX(P,XL2,XV2)
```

```
X3=(XV2-XL1)/(XV2-XL2)
ML2=ML1*X3
MV2=ML1-ML2
CALL RHL(XL2,TGES2,HL2)
CALL RHV(XL2,TGES2,HV2)
Q12G=ML2*HL2+MV2*HV2-ML1*HL1
QD=Q12-Q12G
DIFFT2=TGES2-TEMP2(M-1)
OPPT2=TGES2*TEMP2(M-1)
IF (QD.LT.3.0.AND.QD.GT.-3.0) THEN
      GOTO 64
      ELSE IF (DIFFT2*DIFFT2.LT.0.25.AND.OPPT2.LT.0) THEN
      GOTO 64
      END IF
QDIFF(M)=QD
      TEMP2(M)=TGES2
         IF (M.EQ.1) THEN
         TGES2=TGES2+2
         GOTO 73
         END IF
      Z=(TEMP2(M)-TEMP2(M-1))/(QDIFF(M-1)-QDIFF(M))
      TGES2=TEMP2(M-1)+Z*QDIFF(M-1)
      GOTO 73


64        T2=TGES2

C     9 Find LMDT and the heat exchanger UA value

40    CONTINUE
      TH=(T4+T2)/2
      TL=T1+3
      LMDTO=(TH-TL)/LOG((TH-TAMB)/(TL-TAMB))
      QHXL=UAOHX*LMDTO
      Q45=Q12+QHXL
      HL5=HL4-(Q45/ML4)
      IF (HL5.GT.365000) THEN
      HL5=365000
      END IF
      IF (XL4.GT.9.0.OR.XL2.GT.9.0) THEN
      V(K)=0
      MV7=0.0
      T2=0.0
      T4=0.0
      T5=0.0
      EFFHX=0.0
      COPC=0.0
      COPS=0.0
      COPCL=0.0
      COPSL=0.0
      YIELD=0.0
      GOTO 917
      END IF
      CALL RTXH(XL4,HL5,T5)

      TOUT=T5-T1
      IF(TOUT.LE.0.0)THEN
      N5=N5+1
      IF (N5.GT.10) GOTO 313
      T4=T4-(T4-TEMP4(N-1))/2
      GO TO 877
      END IF
      N5=0
      TIN=T4-T2
      LMDT=(TOUT-TIN)/LOG(TOUT/TIN)
      IF(LMDT.LE.0)THEN
```

```
      END IF

      KH=0.465
      VIS=0.000648
      DHX=0.00623
      LHX=16.28
      REYNO=(4.0*ML4)/(3.1416*DHX*VIS)
      IF (REYNO.GT.2000) THEN
      END IF
      UHX=(KH*4.364/DHX)/2.0
      AHX=3.1416*DHX*LHX
      TUAHX=UHX*AHX
      UAIHX=UASHE

C     10 Find heat exchanger heat transfer from UA (QUA) and compare with Q1
c      Difference QUA-Q12 (DQ) decreases with rising T4

      QUA=UAIHX*LMDT
      DQ=QUA-Q12

c     Balance can be either by heat or insignificant error in T4 (0.2 deg)
      DIFFT4=T4-TEMP4(N-1)
      OPPT4=T4*TEMP4(N-1)
      IF (DQ.LT.(ACC4*QINS).AND.DQ.GT.-(ACC4*QINS)) THEN
               GOTO 514
               ELSE IF(DIFFT4*DIFFT4.LT.0.04.AND.OPPT4.LT.0) THEN
               GOTO 514
      END IF
      DIFFQ(N)=DQ
      TEMP4(N)=T4

C          If first iterative step return to calculate a second DQ
           IF (N.EQ.1) THEN
           T4=T4+10
           GOTO 850
           END IF

313   IF(N.GT.15.OR.N5.GT.10.OR.T4.GT.250) THEN
      MV7=0.0
      T2=0.0
      T4=0.0
      T5=0.0
      EFFHX=0.0
      COPC=0.0
      COPS=0.0
      COPCL=0.0
      COPSL=0.0
      YIELD=0.0
      GOTO 917
      END IF

      W=(TEMP4(N)-TEMP4(N-1))/(DIFFQ(N-1)-DIFFQ(N))
      T4=TEMP4(N-1)+W*DIFFQ(N-1)
      IF (T4.EQ.TEMP4(N).AND.DIFFQ(N).GT.0.0) T4=T4+0.1
      IF (T4.EQ.TEMP4(N).AND.DIFFQ(N).LT.0.0) T4=T4-0.1

      GOTO 850

514   CONTINUE


      QSEN=ML1*HL4-ML2*HL2
      QVAP=QINS+MV2*HV2-QSEN
      XB=X1/X2

      EFFHX=(T4-T5)/(T4-T1)
```

```
C      MSEP is rate of decrease of mass in the separator
C      EMPHRS is the sep emptying time from start of steady state
C  PROPORTIONS HERE RELATE TO PRODUCTION DESIGN
C  EXPERIMENTAL SET UP is 0.7, 0.39

C *****SPECIFIC TO VVR SYSTEM*******
       MOSEP=0.1
       MSST=0.3*MST
       EMPHRS=10000.0
C ***SPECIFIC ENDS****

       CALL RHL(XL1,T4,HLSEPF)
       CALL RHL(XL1,TAMB,HLAMB)
       SNSLIQ=MOSEP*(HLSEPF-HLAMB)
       SNSST=MSST*450*(T4-TAMB)
       THE=(T4+T1)/2
       XLHE=(XL1+XL4)/2
       CALL RHL(XLHE,THE,HLHE)
       SENHEG=(MOGEN-MOSEP)*(HLHE-HLAMB)+(MST-MSST)*450*THE
       QWU=SNSST+SNSLIQ+SENHEG
       TW=QWU/QINS
       TWH=TW/3600

       GENHRS=HOURS-TWH
       YIELD=MV7*(GENHRS*3600)
       YDID=MV7*HOURS*3600*1E-6
       YSS=MV7*HOURS*3600
       MSEPR=MOSEP-MSEP*3600*GENHRS
       ESIGN=0.0

       MCIRC=ML1*GENHRS*3600
       MTT=YIELD
       CR=(MCIRC+MOGEN+MTT)/YIELD

C      Find conditions at exit of evaporator
       T9=TNIGHT
       XL9=XL8
       CALL RHL(XL9,T9,HL9)
       T11=T10+5
       CALL RXLPT(PE,T11,XL11)
       CALL RHL(XL11,T11,HL11)
       CALL RXVPX(PE,XL11,XV11)
       CALL RHV(XL11,T11,HV11)
       RATIO=(XL11-XL9)/(XL11-XV11)
       MV11=YIELD*RATIO
       HTOT11=(MV11*HV11+(YIELD-MV11)*HL11)/YIELD

       QEV=YIELD*(HTOT11-HL9)

C      Energy balance
       QSOL=G*AREAT*NTUBES*HOURS*3600
       QGEN=QSOL*EFFC
       IF (QIN.GT.0.00000001) THEN
          QGEN=QINS*HOURS*3600
          END IF
       QCL=(1-EFFC)*QSOL
       QIL=(QHXL+QGSL)*GENHRS*3600
       QV6=MV6*HV6
       QL6=ML6*HL6
       QV7=MV7*HV7
       QRL=(MV6*HV6-MV7*HV7-ML6*HL6)*GENHRS*3600
       CALL RTXP(XL4,PE,TAB1)
       CALL RHL(XL4,T51,HL51)
       CALL RHL(XL4,TAB,HLAB)
       CALL RHL(XL4,TAB1,HLAB1)
```

```
CALL RHL(XL8,TCON,HL8)
Q551=ML4*(HL5-HL51)*GENHRS*3600
QCON=(HV7-HL8)*YIELD
QREF8N=YIELD*(HL8-HL9)
RLIQ=MOGEN-YIELD
IF (RLIQ.LT.0.0001) RLIQ=0.0
SNSLIQ=RLIQ*(HL4-HLAB1)
SNSST=MST*450*(T4-TAB1)
SENHGN=SENHEG*(T4-TAB1)/(T4-TAMB)
QWD=SNSLIQ+SENHGN+SNSST
QHS2=QWD*(TAB1-TAB)/(T4-TAB1)
QN=(MORES-YIELD)*HLAMB
QN4=ML4*GENHRS*3600*HLAB
Q11=YIELD*HTOT11
Q1=MORES*HL1
      QAB=QN+Q11-Q1
      QSUMI=QSOL+QEV
C NOTE THAT RESERVOIR AND RECEIVER ASSUMED TO
C  START AND FINISH AT SAME MASS, CONC
      QSUMO=QCL+QIL+QRL+Q551+QCON+QREF8N+QWD+QHS2+QAB
      IF (QIN.GT.0.00000001) THEN
         QSUMI=QGEN+QEV
         QSUMO=QIL+QRL+Q551+QCON+QREF8N+QWD+QHS2+QAB
         END IF
      QSHE=Q12*GENHRS*3600
      QGS=QGSUA*GENHRS*3600
      QWUPC=QWU*100/QGEN
      QRLPC=QRL*100/QGEN
      Q551PC=Q551*100/QGEN
      Q12PC=QSHE*100/QGEN
      QGSPC=QGS*100/QGEN

      IF (QIN.GT.0.0001) THEN
      COPCL=QEV/QGEN
      COPSL=0.0
      ELSE
      COPSL=QEV/QSOL
      COPCL=COPSL/EFFC
      END IF

      TPEN=YIELD/YSS
      COPC=COPCL/TPEN
      COPS=COPSL/TPEN

      ICE=QEV/(335000+2110*TAMB)
      ICEM2=ICE/(AREAT*NTUBES)
      COST=(200+NTUBES*14)/(ICE*365*15)

      IF (IFL.NE.1.0) GOTO 917
c       Find density differences (DRO) and driving pressures
C       GENHEI in cms

        GENHEI=10.0
        CALL DENL(XL2,T2,DL2)
        CALL DENL(XL4,T4,DL4)
     ZTOT=0.58
     CALL DENL(XL1,T1,DL1)
     CALL DENL(XL4,T5,DL5)
     CALL RHL(XL1,TSAT,HL2SAT)
     CALL DENL(XL1,TSAT,DL2SAT)

     TG(N)=T2+(N-1)*(T4-T2)/10.0
     CALL RXL(P,TG(N),XLG(N))
     IF(XLG(N).GT.XL1) XLG(N)=XL1
     CALL RHL(XLG(N),TG(N),HLG(N))
     CALL RHV(XLG(N),TG(N),HVG(N))
```

```
      CALL DENL(XLG(N),TG(N),DLG(N))
      IF(XLG(N).GT.1.0.OR.HVG(N).EQ.9.99.OR.HLG(N).EQ.9.99) THEN
      DRIVEP=0.0
      DPK=0.0
      GOTO 917
      END IF
      DVG(N)=DV(P,TG(N))
      MVG(N)=ML1*(XL1-XLG(N))/(1-XLG(N))
      IF(TSAT.GE.TG(N))MVG(N)=0.0
      MLG(N)=ML1-MVG(N)
      VOLV(N)=MVG(N)/DVG(N)
      VOLL(N)=MLG(N)/DLG(N)
      DG(N)=ML1/(VOLV(N)+VOLL(N))

      QG(N)=(MVG(N)*HVG(N)+MLG(N)*HLG(N))-(ML2*HL2+MV2*HV2)
      QGREF(N)=(N-1)*(QGSUA)/10.0

134   CONTINUE

      DGTOT=0.0
      DO 135 N=1,11
      DGREF(N)=((DG(N)-DG(N+1))*(QG(N+1)-QGREF(N))/(QG(N+1)-QG(N)))
     C+DG(N+1)
      DGTOT=DGTOT+DGREF(N)
135   CONTINUE

      DO 136 N=1,11
136   CONTINUE
      DO 137 N=1,11
137   CONTINUE
      DO 139 N=1,11
139   CONTINUE

      DGMEAN=DGTOT/11.0
      DRO=DLG(11)-DGMEAN
      DPGEN=9.81*(GENHEI/100)*DRO

C     Heat exchanger thermosyphon effect gives a driving pressure (DPHX)

      IF(TSAT.GE.T2) THEN
      Z11=ZTOT
      DL11=DG(1)
      GOTO 251
      END IF
      DL11=DL2SAT
      HL11=HL2SAT
      QHXSEN=ML1*(HL11-HL1)
      QHXBL=Q12-QHXSEN
      QHXTOT=0.0
      DO 523 N=1,61
      QHX(N)=(((T4-T2)-(((T4-T2)-(T5-T1))/60)*(N-1)))*UAIHX)/60
      QHXTOT=QHXTOT+QHX(N)
      IF (QHXTOT.GT.QHXBL) GOTO 623
523   CONTINUE
623   N=REAL(N)
      Z11=ZTOT-(N/60.0)*ZTOT
251   DCLDHX=((DG(1)+DL11)*(ZTOT-Z11)+(DL1+DL11)*Z11)/(2*ZTOT)
      DHOTHX=(DL4+DL5)/2
      DPHX=9.81*ZTOT*(DHOTHX-DCLDHX)

      DRIVEP=DPGEN+DPHX
      DPK=(ML1*1000000)/DRIVEP

917   CONTINUE
      YAX(L)=V(K)
```

```
      MV7=MV7*1000000
      ML1=ML1*1000000

      IF(IFL.NE.1)GOTO 919

      IF (SKIP.GT.0.5) GOTO 6119
      MLIT=DRIVEP*DKSET
      DM(IM)=MLIT-ML1
      DIFFM=ML1-ML(IM-1)
      OPPDM=DM(IM)*DM(IM-1)
      IF ((DM(IM)*DM(IM)).LT.100) THEN
      SKIP=1.0
      GOTO 6119
      ELSE IF (DIFFM*DIFFM.LT.100.AND.OPPDM.LT.0
     C.AND.DM(IM)*DM(IM).LT.10000) THEN
      SKIP=1.0
      GOTO 6119
      END IF
      ML(IM)=ML1
      IF (IM.EQ.1) THEN
      ML1=ML1+500
      GOTO 93
      END IF
      ZM=(ML(IM)-ML(IM-1))/(DM(IM)-DM(IM-1))
      ML1=ML(IM)-ZM*DM(IM)
      GOTO 93

 6119 FLR=1-(1/CR)
      DK13=1/(DKSET*2)
      DK45=DK13/0.85
      DKO=1/(DK13+(DK45*FLR))
      MLIT=DRIVEP*DKO
      DM(IM)=MLIT-ML1
      DIFFM=ML1-ML(IM-1)
      OPPDM=DM(IM)*DM(IM-1)
      IF (KM.LT.0.5) THEN
      ML1=ML1+100
      KM=KM+1
      GOTO 93
      END IF
      IF ((DM(IM)*DM(IM)).LT.100) THEN
      GOTO 6120
      ELSE IF (DIFFM*DIFFM.LT.100.AND.OPPDM.LT.0
     C.AND.DM(IM)*DM(IM).LT.10000) THEN
      GOTO 6120
      END IF
      ML(IM)=ML1
      ZM=(ML(IM)-ML(IM-1))/(DM(IM)-DM(IM-1))
      ML1=ML(IM)-ZM*DM(IM)
      KM=KM+1
      GOTO 93

      DO 61 N=1,8
      WRITE(6,57)N,NAME(N),V(N),N+8,NAME(N+8),V(N+8),N+16,
     C NAME(N+16),V(N+16)
   61 CONTINUE


      DO 63 N=1,8
     C NAME(N+16),V(N+16)
   63 CONTINUE

      IF (COPSL.LT.0.001)COPSL=0
      IF (YIELD.LT.0.001)YIELD=0
      IF (MV7.LT.0.1E-8) MV7=0.0
      MSEPR=0.0
```

```
      IF (CR.GT.990) CR=0.0
      WRITE(10,426)
      WRITE(11,427)MV6*1E4,MV7/100.0,YIELD,CR/10.0,MSEPR,MV2*1E4
      WRITE(13,428)COPCL,COPSL,EFFHX,XL4,EFFC
      WRITE(21,430)XL1,XL4,XV6,XV7,XV7-XL4,XV6-XL4
      WRITE(22,431)XV7-XV6,XL1-XL4,X1,X2/100,XB*10
      WRITE(23,432)ML2*HL2,ML1*HL4*1E-6,(HV6-HL4)/10000,QINS+MV2*HV2,
     cQSEN,QVAP
      WRITE(24,433)XL1,XL2,XL4,XL4,XV6,XV6
      WRITE(25,434)HL1,HL2,HL4,HL5,HV6,HV7
426   FORMAT(1X,5F9.2)
427   FORMAT(1X,6F6.3)
428   FORMAT(1X,5F9.3)
429   FORMAT(1X,4F9.3)
430   FORMAT(1X,6F6.3)
431   FORMAT(1X,5F6.3)
432   FORMAT(1X,6F9.3)
433   FORMAT(1X,6F7.3)
434   FORMAT(1X,6F10.1)

      WRITE(8,526)MV7
      WRITE(14,526)T4
      WRITE(12,526)EFFC
      WRITE(15,526)YIELD
      WRITE(16,526)COPCL
      WRITE(17,526)COPSL
      WRITE(18,526)ML1
      WRITE(20,526)CR
      WRITE(26,526)XL4
      WRITE(27,526)UASHE
      WRITE(28,526)EFFHX
      WRITE(29,526)TWH*3600
      WRITE(30,526)T7

526   FORMAT(1X,F14.3,$)

18    CONTINUE
      WRITE(8,'(/)')
      WRITE(14,'(/)')
      WRITE(12,'(/)')
      WRITE(15,'(/)')
      WRITE(16,'(/)')
      WRITE(17,'(/)')
      WRITE(18,'(/)')
      WRITE(20,'(/)')
      WRITE(26,'(/)')
      WRITE(27,'(/)')
      WRITE(28,'(/)')
      WRITE(29,'(/)')
      WRITE(30,'(/)')
29    CONTINUE
      CLOSE(6)
      CLOSE(8)
      CLOSE(9)
      CLOSE(11)
      CLOSE(12)
      CLOSE(13)
      CLOSE(14)
      CLOSE(15)
      CLOSE(16)
      CLOSE(17)
      CLOSE(18)
      CLOSE(19)
      CLOSE(20)
      CLOSE(26)
      CLOSE(25)
```

```
      CLOSE(27)
      CLOSE(28)
      CLOSE(29)
      CLOSE(30)

57    FORMAT(1X,I2,A7,F9.3,6X,I2,A7,F9.3,6X,I2,A7,F9.3)

      STOP
      END
```

```
C  PROGRAM AP.F
   This program simulates the dry expansion evaporator (DEE)

      REAL ML1,ML2,ML4,ML5,ML6,MV6,MV7,MV2,LMDT,NUSS,KH,INIT,NTUBES,
     CK4,KAMB,LHX,K2,JCOOL,MSEP,MOSEP,MST,MLIQ,ICE,ICEM2,MMEM,
     CMHE,MV11,MSO,MLIT,MAB,MR,MW,MSI,MABT,MICE,KICE,MIC,LEV,MWA
      REAL MCPHS,MLS,MABAV,MABD,MREF,MREFI
      REAL QABD(50),TEMPF(50)

      OPEN (8,FILE='OAPF',STATUS='MODIFY')
      OPEN (13,FILE='aptemp.mat',STATUS='MODIFY')
      OPEN (14,FILE='ap1.mat',STATUS='MODIFY')
      OPEN (15,FILE='ap2.mat',STATUS='MODIFY')
      OPEN (16,FILE='time.mat',STATUS='MODIFY')

      READ *,AAB,TR,TAMB,TNI,OKS,SET
      OKS=OKS*1000.0
      SET=SET/1000.0
      OK2=6.48/OKS
      OK1=((0.12-SET)*0.02)+OK2
      DRAM=12000
      TINT =TAMB
      TRESI=TINT
      QAMB=0
      MAB=0.0
      TEV=0.0
      TEVD=-10
      CALL RP(XV7,TEVD,PABD)
      PABTHA=OK1/OK2
      RESK=1.63
      RESA=0.6
      ABK=1.68
      ASEPK=1.68/4.0
C     U VALUE FOR 2mm GLYCOL, PLASTIC, ICE/WATER(580)
      UFIX=114
      UEV=UFIX
      KICE=2.2
      TBOXI=TAMB
      TBOX=TBOXI
      YIELD=5.0
      MREF=YIELD
      MREFI=YIELD
      DH=1.15E6
      MABD=YIELD/36000
      MWA=15.0
      MIC=0.0
      HFGWA=333000
      CPICE=2040
      CPWA=4200
      QSEN=TBOX*MWA*CPWA
      QFRZ=-1*MWA*HFGWA
      QLOSS=0.0
      QREC=0.0
      XM=0.035
      DEV=0.006
      UEVF=1/((XM/KICE)+(1/UEV))
      SUMTR=0.0
      XL4=0.377
      XL1=0.449
      MSI=YIELD*(1-XL1)/(XL1-XL4)
      MW=MSI*(1-XL4)
      XLF=XL4
      MLS=2.0
      MCPHS=20000.0
      TR=TR*60
      ACC=(TR/10000)*(TR/10000)
```

```
      MABT=0
      T4=90
      XLI=XL4
      TI=TAMB

----------------
1ST SEP COOLING MODE
----------------

100   CONTINUE
      TF=TAMB+1/((1/(T4-TAMB)**0.25)+((AAB*ASEPK*SUMTR)/(4.0*MCPHS)))**4
      CALL RP(XL4,TF,PAB)
      SUMTR=SUMTR+TR
      IF (PAB.GT.PABTHA) GOTO 100
      ENDS1=SUMTR

C     ---------------------------------
C     2ND SEP COOLING MODE
C     ---------------------------------
C     FIRST ESTABLISH RES TEMP RISE

      SUMTR2=TR
200   CONTINUE

      CALL RHV(XV7,TEV,HVF)
      CALL RHL(XV7,TINT,HL9)
      CALL RP(XV7,TINT,PR)
      QLOSS=0.2*(TINT-TEV)*TR

C code to find TBOX, MIC, XIC
C note that QEV is useful latent heat
c taking self cooling into account
      QEV=MR*(HVF-HL9)-QLOSS
      QSEN=QSEN-QEV
c remains liquid
      IF (QSEN.GT.0.00001) THEN
      TBOX=QSEN/(MWA*CPWA)
      MIC=0
      XIC=0
c partially freezes
      ELSE IF (QSEN.GT.QFRZ) THEN
      MIC=-QSEN/HFGWA
      XIC=MIC/(916.6*AEV)
      TBOX=0
c fully frozen, ice below zero
      ELSE
      MIC=MWA
      XIC=MIC/(916.6*AEV)
      TBOX=(QSEN-QFRZ)/CPICE
      END IF

      MAB=(OK1-OK2*PAB)*((PR-PAB)**0.5)
      IF (MAB.LT.0) MAB=0.0
      MR=TR*MAB
      XLF=(XLI*MSI+MR)/((XLI*MSI+MR)+MW)
      TRESF=TRESI+1
      NT=0

187   NT=NT+1
      CALL RHL(XLI,TRESI,HLI)
      CALL RHL(XLF,TRESF,HLF)
      QAB=((HLF*(MSI+MR))-(HLI*MSI)-(HVF*MR))/TR
      QAMB=RESK*RESA*((TRESF-TINT)**1.25)
      QAD=QAMB+QAB
      TEMPF(NT)=TRESF
      QABD(NT)=QAD
```

```
      IF (NT.EQ.1) THEN
      TRESF=TRESF+1
      GO TO 187
      END IF
      DTRESF=TRESF-TEMPF(NT-1)
      OPPQAD=QAD*QABD(NT-1)
      IF(QAD*QAD.LT.ACC) THEN
      GOTO 197
       ELSEIF(DTRESF*DTRESF.LT.0.0001.AND.OPPQAD.LT.0) THEN
       GOTO 197
      END IF
       IF ((QABD(NT-1)-QABD(NT))**2.LT.0.0001) THEN
        GO TO 197
        END IF

      ZT=(TEMPF(NT)-TEMPF(NT-1))/(QABD(NT-1)-QABD(NT))
      TRESF=TEMPF(NT-1)+ZT*QABD(NT-1)
      GOTO 187

197   CONTINUE
C     ESTABLISH REDUCED SEP TEMP

      CON=1/(TF-TINT)**0.25
      TER1=(1.5*AAB*ASEPK)/(4.0*MCPHS)
      TER2=TER1*SUMTR2
      TER3=1/((CON+TER2)**4)
      TF=TINT+TER3
      CALL RP(XL4,TF,PAB)
      CALL RTXP(XLF,PABD,TABD)
      CALL RTP(PAB,TEV)
      IF (TEV.GT.999) TEV=-18
      SUMTR2=SUMTR2+TR
      SUMTR=SUMTR+TR

      TRESI=TRESF
      MSI=MSI+MR
      MREF=MREF-MR
      XLI=XLF

      IF(TF.GT.TRESF) GOTO 200
      ENDS=SUMTR

C     ---------------
C     ABSORBTION MODE
C     ---------------

107    CONTINUE
      CALL RHV(XV7,TEV,HVF)
      TINT=TNI
      IF(SUMTR.LT.ENDS+DRAM) THEN
      TINT=TAMB-((SUMTR-ENDS)*(TAMB-TNI)/DRAM)
      END IF
      CALL RHL(XV7,TINT,HL9)
      CALL RP(XV7,TINT,PR)
      MAB=(OK1-OK2*PAB)*((PR-PAB)**0.5)
      IF (MAB.LT.0) MAB=0.0
      MR=TR*MAB
      QLOSS=0.2*(TINT-TEV)*TR

code to find TBOX, MIC, XIC
QEV is useful latent heat
      QEV=MR*(HVF-HL9)-QLOSS
      QSEN=QSEN-QEV
remains liquid
      IF (QSEN.GT.0.00001) THEN
      TBOX=QSEN/(MWA*CPWA)
```

```
      MIC=0
      XIC=0
c partially freezes
      ELSE IF (QSEN.GT.QFRZ) THEN
      MIC=-QSEN/HFGWA
      XIC=MIC/(916.6*AEV)
      TBOX=0
c fully frozen, ice below zero
      ELSE
      MIC=MWA
      XIC=MIC/(916.6*AEV)
      TBOX=(QSEN-QFRZ)/CPICE
      END IF
      XLF=(XLI*MSI+MR)/((XLI*MSI+MR)+MW)
      TF=TI+0.05
      NT=0

87    NT=NT+1
      CALL RHL(XLI,TI,HLI)
      CALL RHL(XLF,TF,HLF)
      QAB=((HLF*(MSI+MR))-(HLI*MSI)-(HVF*MR))/TR
      QAMB=(ABK*AAB*((TF-TINT)**1.25))+(RESK*RESA*((TF-TINT)**1.25))
      QAD=QAMB+QAB
      TEMPF(NT)=TF
      QABD(NT)=QAD
      IF (NT.EQ.1) THEN
      TF=TF+1
      GO TO 87
      END IF
      DIFFTF=TF-TEMPF(NT-1)
      OPPQAD=QAD*QABD(NT-1)
      IF(QAD*QAD.LT.ACC) THEN
      GOTO 97
       ELSEIF(DIFFTF*DIFFTF.LT.0.00001.AND.OPPQAD.LT.0) THEN
       PRINT *,'**JUMP OUT TF NOT CHANGING ***'
       GOTO 97
      END IF
       IF ((QABD(NT-1)-QABD(NT))**2.LT.0.0001) THEN
       PRINT *,'**JUMP OUT QAD NOT CHANGING ***'
       GOTO 97
       END IF
      ZT=(TEMPF(NT)-TEMPF(NT-1))/(QABD(NT-1)-QABD(NT))
      TF=TEMPF(NT-1)+ZT*QABD(NT-1)
      GOTO 87

97    CONTINUE
      CALL RP(XLF,TF,PAB)
      CALL RTXP(XLF,PABD,TABD)
      CALL RTP(PAB,TEV)
      IF (TEV.GT.999) TEV=-18
      TINT=TAMB
      PAB=PAB

126   FORMAT(1X,4F9.3)
127   FORMAT(1X,5F9.3)
128   FORMAT(1X,4F9.3)

      SUMTR=SUMTR+TR
      MABT=MABT+MR
      IF(MABT.GE.YIELD) THEN

      IF (SUMTR.GE.43200.0) THEN
      GOTO 117
      END IF

      XLI=XLF
```

```
      MSI=MSI+MR
      MREF=MREF-MR
      TI=TF
      GOTO 107

117   CONTINUE
      LEV=QEVAV/(UEVF*3.14*DEV*(-1*TEV))
      GOTO 451
      CLOSE (19)
      CLOSE (8)
      CLOSE (13)
      CLOSE (14)
      CLOSE (15)
      CLOSE (16)
      STOP
      END
```

```
c       PROGRAM AF.F
c       This program simulates the gravity circulated evaporator (GCE)

        REAL ML1,ML2,ML4,ML5,ML6,MV6,MV7,MV2,LMDT,NUSS,KH,INIT,NTUBES,
       CK4,KAMB,LHX,K2,JCOOL,MSEP,MOSEP,MST,MLIQ,ICE,ICEM2,MMEM,
       CMHE,MV11,MSO,MLIT,MAB,MR,MW,MSI,MABT,MICE,KICE,MIC,LEV,MWA,
       CMSTR,MWR,MAR,MREF
        REAL QABD(50),TEMPF(50)

        OPEN (8,FILE='OABF',STATUS='MODIFY')
        OPEN (13,FILE='aftemp.mat',STATUS='MODIFY')
        OPEN (14,FILE='af1.mat',STATUS='MODIFY')
        OPEN (15,FILE='af2.mat',STATUS='MODIFY')
        OPEN (16,FILE='time.mat',STATUS='MODIFY')

        READ *,TAMB,AAB,TR,LEV

C       U VALUE FOR 2mm GLYCOL, PLASTIC, ICE/WATER(580)
        UFIX=114
        UEV=UFIX
        KICE=2.2
        TEV=TAMB
        TEVI=TEV
        TBOX=TAMB
        YIELD=5.0
        MREF=YIELD
        MWA=15.0
        HFGWA=333000
        CPICE=2040
        CPWA=4200
        QSEN=TBOX*MWA*CPWA
        QFRZ=-1*MWA*HFGWA
        MSTR=2.0
        DEV=0.006
        XM=MWA/(916.6*3.14*DEV*LEV)
        AEV=LEV*3.14*DEV
        SQEV=0
        SMQMR=0
        SMQSTR=0
        CALL RHL(XV7,TAMB,HL9I)
        CALL RHV(XV7,TAMB,HV9)
        TR=TR*60
        ACC=(TR/10000)*(TR/10000)
        XL1=0.449
        XL4=0.377
        MSI=YIELD*(1-XL1)/(XL1-XL4)
        SUMTR=0
        SUMMR=0
        MW=MSI*(1-XL4)
        XLI=XL4
        TI=TAMB

C -------------------------------
C IST SEP COOLING MODE, NO ABSORPTION
C -------------------------------

        MCPHS=20000
        T4=90.0
        CALL RP(XV7,TAMB,PABTHA)
        HTFRES=1.63
        ARES=0.6
        HTFAB=1.68
        HTFABS=1.68/4.0
1119    CONTINUE
        TF=TAMB+1/((1/(T4-TAMB)**0.25)+
       C((AAB*HTFABS*SUMTR)/(4.0*MCPHS)))**4
```

```
      CALL RP(XL4,TF,PAB)
      SUMTR=SUMTR+TR
      TBOX=TI
      PR=PAB
      QAMB=0.0
      QEV=0.0
      QWW=0.0
      XLF=XLI
      MAB=0.0
      IF (TBOX.LT.0.0) TBOX=0.0
      IF(PAB.GT.PABTHA) GOTO 1119

C ---------------------------------------
C IST ABSORPTION COOLING MODE, SEP COOLING
C ---------------------------------------

      CALL RTP(PAB,TEV)
      TRESI=TAMB
19    CONTINUE
      PRINT *, 'TBOX,TEV',TBOX,TEV
      QLOSS=0.2*(TAMB-TEV)*TR
      QEVW=(UEV*(TBOX-TEV)*AEV)
      QEV=QEVW*TR
      CALL RHL(XV7,TEV,HL9F)
      CALL RHV(XV7,TEV,HV9)
      QREC=MREF*(HL9I-HL9F)
      PRINT *, 'QREC',QREC
      MR=(QEV+QREC+QLOSS)/(HV9-HL9I)
      MAB=MR/TR

C code to find TBOX, MIC, XIC
      QSEN=QSEN-QEV
c remains liquid
      IF (QSEN.GT.0.00001) THEN
      TBOX=QSEN/(MWA*CPWA)
      MIC=0
      XIC=0
c partially freezes
      ELSE IF (QSEN.GT.QFRZ) THEN
      MIC=-QSEN/HFGWA
      XIC=MIC/(916.6*AEV)
      TBOX=0
c fully frozen, ice below zero
      ELSE
      MIC=MWA
      XIC=MIC/(916.6*AEV)
      TBOX=(QSEN-QFRZ)/CPICE
      END IF
      UEV=1/((1/(UFIX))+(XIC/KICE))
      SQEV=SQEV+QEV

C CALCULATE ABSORBER TEMP RISE THEN SEP TEMP DROP
C----------

      SUMTR2=TR

      XLF=(XLI*MSI+MR)/((XLI*MSI+MR)+MW)

      TRESF=TRESI+1
      NT=0

87    NT=NT+1
      CALL RHL(XLI,TRESI,HLI)
      CALL RHL(XLF,TRESF,HLF)

      QAB=((HLF*(MSI+MR))-(HLI*MSI)-(HV9*MR))/TR
```

```
      QAMB=HTFRES*ARES*((TRESF-TAMB)**1.25)

      QAD=QAMB+QAB
      TEMPF(NT)=TRESF
      QABD(NT)=QAD
      IF (NT.EQ.1) THEN
      TRESF=TRESF+1
      GO TO 87
      END IF
      DTRESF=TRESF-TEMPF(NT-1)
      OPPQAD=QAD*QABD(NT-1)
      IF(QAD*QAD.LT.ACC) THEN
      GOTO 97
      END IF
      ZT=(TEMPF(NT)-TEMPF(NT-1))/(QABD(NT-1)-QABD(NT))
      TRESF=TEMPF(NT-1)+ZT*QABD(NT-1)
      GOTO 87

97    CONTINUE
C     ESTABLISH REDUCED SEP TEMP

      TF=TAMB+1/((1/(T4-TAMB)**0.25)+
     C((AAB*HTFABS*SUMTR)/(4.0*MCPHS)))**4
      CALL RP(XLF,TF,PAB)
      CALL RTXP(XLF,PABD,TABD)
      CALL RTP(PAB,TEV)
      IF (TEV.GT.999) TEV=-18
      SUMTR2=SUMTR2+TR
      SUMTR=SUMTR+TR
      SUMMR=SUMMR+MR
      IF (TBOX.LT.0.0) TBOX=0.0

449   CONTINUE
      TRESI=TRESF
      TEVI=TEVF
      HL9I=HL9F
      HLI=HLF
      HV9=HV9
      XLI=XLF
      MSI=MSI+MR
      MREF=MREF-MR
      IF(TF.GT.TRESF) GOTO 19
      ENDS=SUMTR

C     ---------------
C     ABSORPTION MODE
C     ---------------

119   CONTINUE
      PRINT *, 'TBOX,TEV',TBOX,TEV
      QLOSS=0.2*(TAMB-TEV)*TR
      QEVW=(UEV*(TBOX-TEV)*AEV)
      QEV=QEVW*TR

      CALL RHL(XV7,TEV,HL9F)
      CALL RHV(XV7,TEV,HV9)

      QREC=MREF*(HL9I-HL9F)
      PRINT *, 'QREC',QREC
      MR=(QEV+QREC+QLOSS)/(HV9-HL9I)
      MAB=MR/TR

C code to find TBOX, MIC, XIC
      QSEN=QSEN-QEV
c remains liquid
      IF (QSEN.GT.0.00001) THEN
```

```
      TBOX=QSEN/(MWA*CPWA)
      MIC=0
      XIC=0
c partially freezes
      ELSE IF (QSEN.GT.QFRZ) THEN
      MIC=-QSEN/HFGWA
      XIC=MIC/(916.6*AEV)
      TBOX=0
c fully frozen, ice below zero
      ELSE
      MIC=MWA
      XIC=MIC/(916.6*AEV)
      TBOX=(QSEN-QFRZ)/CPICE
      END IF
      UEV=1/((1/(UFIX))+(XIC/KICE))
      SQEV=SQEV+QEV

C---------
C CALCULATE ABSORBER TEMP RISE
C----------

      SUMTR2=TR

      XLF=(XLI*MSI+MR)/((XLI*MSI+MR)+MW)

      TRESF=TRESI+0.05
      NT=0

187    NT=NT+1
      CALL RHL(XLI,TRESI,HLI)
      CALL RHL(XLF,TRESF,HLF)
      QAB=((HLF*(MSI+MR))-(HLI*MSI)-(HV9*MR))/TR
      QAMB=((HTFRES*ARES)+(HTFAB*AAB))*((TRESF-TAMB)**1.25)
      QAD=QAMB+QAB
      TEMPF(NT)=TRESF
      QABD(NT)=QAD
      IF (NT.EQ.1) THEN
      TRESF=TRESF+1
      GO TO 187
      END IF
      DTRESF=TRESF-TEMPF(NT-1)
      OPPQAD=QAD*QABD(NT-1)
      IF(QAD*QAD.LT.ACC) THEN
      GOTO 197
      END IF
      ZT=(TEMPF(NT)-TEMPF(NT-1))/(QABD(NT-1)-QABD(NT))
      TRESF=TEMPF(NT-1)+ZT*QABD(NT-1)
      GOTO 187

197    CONTINUE
      TF=TRESF
      CALL RP(XLF,TF,PAB)
      CALL RTXP(XLF,PABD,TABD)
      CALL RTP(PAB,TEV)

326   FORMAT(1X,4F9.3)
327   FORMAT(1X,4F9.3)
328   FORMAT(1X,4F9.3)

      SUMTR=SUMTR+TR
      SUMMR=SUMMR+MR
      IF (MREF.LT.0.001) THEN
      GOTO 117
      END IF

      IF(SUMTR.GE.43200.0) GOTO 117
```

```
      TI=TF
      TRESI=TRESF
      TEVI=TEVF
      HL9I=HL9F
      HLI=HLF
      HV9=HV9
      XLI=XLF
      MSI=MSI+MR
      MREF=MREF-MR

      GOTO 119

117   CONTINUE
      GOTO 451
      CLOSE (8)
      STOP
      END
```